MODELLING FOR THE OPERATIONAL CONTROL OF THE OXIDATION DITCH PROCESS

P. MARKANTONATOS, C. Eng., MSc.

A report submitted in partial fulfilment of the
requirements for the degree of Doctor of Philosophy
in the University of London

Department of Civil Engineering,
Imperial College of Science and Technology

November 1988

to my father's memory

ABSTRACT

A study of the oxidation ditch process was undertaken with the objective of developing mathematical models to predict process performance and operating cost. Such models could be employed for the derivation of operating policies which minimize cost and improve process performance and reliability. Process measurements from a full-scale oxidation ditch plant were used for the calibration and validation of the models.

The work focused on modelling the carbonaceous and nitrogenous kinetics in the aeration tank, as well as the thickening function of the final clarifiers. The various process models previously developed for the activated sludge were classified and discussed. Systems analysis techniques were employed for model structure identification and parameter estimation. Model simulations and statistical techniques were employed to assess the performance of the models developed. A dynamic model was constructed which adequately simulated the process during the selected period, however validation using data from a different operating period was less successful.

The importance of the oxygen uptake rate as a process indicator for on-line monitoring was investigated and a simple model for predicting the daily oxygen demand developed. A procedure to estimate the oxygen uptake rate from on-line dissolved oxygen measurements in an operating activated sludge plant was developed and implemented on- site.

The oxidation ditch model was applied both as a means to simulate the process under different operating conditions and as the basis for designing operational control strategies. A simple running cost model was also developed, based on aeration, pumping and sludge disposal costs, in order to investigate the effect of operating conditions upon operating cost. Nitrification was used as the most critical performance indicator, while mixed liquor concentration was identified as the key variable determining the cost of operation. Initially an optimum mixed liquor level was established for minimum cost operation, which satisfied the various physical and effluent quality constraints taking account of the long term behaviour of the inputs. This was accompanied by the formulation of control strategies for the recycle and surplus sludge flows to achieve the above operating objectives. Adaptive feedback control based on one- step-ahead predictions was found to be an efficient controller.

Simulation results illustrated that the proposed control strategies produced potential reductions in running cost by operating at an optimum mixed liquor level which was generally lower than the normal operating level. In addition, process reliability and nitrification performance were improved by maintaining an adequate autotrophic population in the reactor and by avoiding total oxygen demand in excess

of the plant capacity. Finally, the potential benefits of using on-line measurements for control purpose were discussed and recommendations for further research made.

ACKNOWLEDGEMENTS

I would like to express my gratitude to my supervisor Dr. J.P. Lumbers for his ideas, criticisms and his enthusiasm throughout this project. I am also grateful to Dr. S.C. Cook for his valuable advice and guidance in the early stages of the work.

I wish to thank Thames Water Authority for their co-operation and assistance during experiments at one of their wastewater treatment plants. Thanks also go to my colleagues M. von Sperling and S.J. Wishart for their helpful discussions on the work.

Contents

Abstract 2
Acknowledgments 4
Contents 5
List of Tables 11
List of Figures 13

1 Introduction **19**
1.1 General 19
1.2 Wastewater treatment systems 20
1.2.1 The activated sludge process 20
1.2.2 The oxidation ditch process 21
1.3 Application of modelling 23
1.4 Outline of approach to model development 24
1.4.1 General 24
1.4.2 Definition of goals and objectives 25
1.4.3 Conceptualization 25
1.4.4 Selection of model type 26
1.4.5 Model formulation 26
1.4.6 Experimental design 27
1.4.7 Model calibration (parameter estimation) and verification . . . 27
1.4.8 Model validation 28
1.4.9 Sensitivity analysis 28
1.5 Specific objectives of the study 28
1.6 Structure of the thesis 29

2 Final Clarifier Modelling **31**
2.1 Objectives 31
2.2 Review of final clarifier models 31
2.2.1 Introduction 31
2.2.2 Theory of sedimentation 32
2.2.3 Models for the thickening process 35
2.2.4 Models for the clarification process 39
2.3 General assessment of plant performance and operational data 41
2.3.1 Introduction 41
2.3.2 Description of the Cirencester plant 42

2.3.3 Experimental data - monitoring program 43
2.3.4 Assessment of plant performance 44
2.3.5 Time-series data analysis 47
2.3.6 Conclusions 49
2.4 Modelling the clarification function 49
2.5 Modelling the thickening function 52
2.5.1 General 52
2.5.2 Applicability of solids flux theory to Cirencester clarifiers . . . 52
2.5.3 Development of a simple model 54
2.5.4 Need for a dynamic model 57
2.5.5 Development of a dynamic model 57
2.5.6 Performance comparison between pseudo steady-state and dynamic models 60
2.5.7 Model validation 61
2.5.8 Effect of diurnally varying inputs 62
2.5.9 Sensitivity analysis 63
2.6 Conclusions 34
Figures from Chapter 2 66

3 Modelling the Oxidation Ditch Process 91
3.1 Introduction 91
Part I. Review on kinetics and modelling approaches 92
3.2 Carbonaceous oxidation process 92
3.2.1 General 92
3.2.2 Kinetics of carbonaceous oxidation 92
3.2.3 Reactor biomass structuring 95
3.2.4 Organic substrate structuring 96
3.2.5 Substrate storage and utilization concept 97
3.2.6 Endogenous respiration of biomass 100
3.2.7 Environmental effects 101
3.3 Nitrification process 102
3.3.1 Reactions of nitrification 102
3.3.2 Kinetics of nitrification 103
3.3.3 Environmental effects 104
3.4 Denitrification process 106

3.5 Mass transport mechanism 107
3.6 General assessment of process models 109
3.6.1 Introduction 109
3.6.2 General comments on models 110
3.7 "Black-box" (input-output) models 110
3.7.1 Discussion 111
3.8 Steady-state models 112
3.8.1 Discussion 113
3.9 Dynamic process models 113
3.9.1 General 113
3.9.2 Marais model 114
3.9.3 Other dynamic models 116
3.9.4 Simple dynamic models 117
3.10 Stochastic-dynamic, low-order models 118
3.10.1 Discussion 120
Part II. Modelling the oxidation ditch process 122
3.11 Objectives of modelling 122
3.12 Model-type selection 122
3.13 Model development stages 123
3.14 Transportation mechanism 123
3.14.1 Model formulation 123
3.14.2 Results and discussion 125
3.15 Artificial aeration mechanism 128
3.16 Carbonaceous oxidation modelling 129
3.16.1 Main Processes 129
3.16.2 Formulation of a structured biomass model 130
3.16.3 Model calibration (parameter estimation) 134
3.16.4 Parameter estimation approach 136
3.16.5 Model results and discussion 137
3.17 Simple carbonaceous model 140
3.17.1 Model formulation 140
3.17.2 Parameter estimation — discussion 141
3.17.3 Model verification 143
3.17.4 Adaptive estimation 144

3.17.5 Results and discussion 146
3.17.6 Conclusions 148
3.18 Nitrification-denitrification modelling 149
3.18.1 Introduction 149
3.18.2 Model development 150
3.18.3 Parameter estimation 153
3.18.4 Discussion of results 155
3.18.5 Adaptive parameter estimation 157
3.18.6 Conclusions 159
3.19 Integrated process model 159
3.20 Sensitivity analysis 160
3.20.1 Discussion 162
3.21 Model validation 162
3.21.1 Discussion 164
3.22 Summary 164
Figures from Chapter 3 165

4 Modelling and Real-Time Estimation of Oxygen Demand 193
4.1 Monitoring of wastewater treatment plants 193
4.1.1 Current practices of monitoring 193
4.1.2 Advantages of "on-line" monitoring 194
4.2 The oxygen utilization rate as a process indicator 195
4.3 Oxygen transfer in wastewater treatment 196
4.3.1 Oxygen transfer mechanisms 196
4.3.2 Determination of oxygen supply at Cirencester plant 199
4.4 Modelling the oxygen demand in the oxidation ditch process 201
4.4.1 Components of oxygen demand 201
4.4.2 Estimation of oxygen yield coefficients 204
4.4.3 Discussion of results 207
4.4.4 Recursive parameter estimation 209
4.4.5 Conclusions 211
4.5 Methods for the estimation of K_{LA} and OUR coefficients 212
4.5.1 Models for the dissolved oxygen dynamics 212
4.5.2 Non-adaptive estimation techniques 214

4.5.3 Adaptive estimation techniques 216
4.6 Estimation of K_{LA} coefficient from on-line DO measurements 217
4.6.1 Experimental programme 217
4.6.2 Estimation of K_{LA} and OUR coefficients 218
4.6.3 Relation between K_{LA} and air-flow rate 224
4.7 Estimation and importance of real-time OUR 225
4.7.1 Real-time OUR estimation 225
4.7.2 Importance of OUR for process monitoring 226
4.8 Summary 228
Figures from Chapter 4 229

5 Cost-Related Operational Control Strategies for the Oxidation Ditch Process 245

5.1 Introduction 245
5.2 Review of control strategies for the activated sludge process 246
5.2.1 Introduction 246
5.2.2 Design characteristics of control systems 247
5.2.3 Control systems for effluent variability 249
5.2.4 Control systems for solids management 252
5.2.5 Control systems for the nitrification-denitrification processes . 254
5.2.6 Control systems based on oxygen uptake rate 255
5.2.7 Applicability of control systems to the oxidation ditch process . 257
5.3 Development of an operational cost model 258
5.3.1 Formulation of the operating cost relationships 258
5.3.2 Operating cost at Cirencester plant 260
5.3.3 Sensitivity analysis of the cost model 261
5.3.4 Effect of variable thickened sludge concentration 262
5.3.5 Evaluation of running cost under different operating conditions 263
5.4 Transient response of the oxidation ditch system 265
5.4.1 Introduction 265
5.4.2 Response to a pulse in the recycle flow 266
5.4.3 Response to a pulse in the surplus sludge flow 267
5.4.4 Comparison of the transient responses 267
5.5 Analysis of operational control problem for the oxidation ditch process 268
5.5.1 Definition of control objectives 268

5.5.2 Frequency of control application 269
5.5.3 Determination of the desired operating $MLSS$ 269
5.5.4 Determination of the maximum operating $MLSS$ 270
5.5.5 Determination of a minimum operating $MLSS$ 271
5.5.6 Discussion 276
5.6 Design of control systems for the oxidation ditch process 276
5.6.1 Main control methods 276
5.6.2 Available measurements for process control 280
5.6.3 Simplified process model for solids control 280
5.6.4 Constant-gain proportional feedback control systems 282
5.6.5 Adaptive, prediction-error feedback control systems 286
5.6.6 Iterative feedback control system 288
5.6.7 Adaptive-gain feedback control system 290
5.6.8 Comparison of adaptive feedback control systems 292
5.7 Design and comparison of alternative operational control policies . . . 295
5.7.1 Policy 1 296
5.7.2 Policy 2 298
5.7.3 Policy 3 300
5.7.4 Policy 4 300
5.7.5 Conclusions 301
5.8 Topics for future research 302
Figures from Chapter 5 304

6 Conclusions **335**
6.1 Process modelling 335
6.1.1 Final clarifier modelling 335
6.1.2 Oxidation ditch modelling 335
6.2 Real-time OUR estimation 335
6.3 Operational control 336

References **339**
APPENDIX 1 360
APPENDIX 2 362
APPENDIX 3 366

List of Tables

2.1. Relationships between hindered settling velocity and concentration
2.2. Design parameters for Cirencester plant
2.3. Monitored variables at Cirencester S.T.P. and their notation
2.4. Average operating conditions for the period 13/3/79 – 20/12/79
2.5. Correlation among input and output variables at lag zero for the selected study period
2.6. Correlation of SSe with the clarifier operating variables
2.7. Performance of simple models for effluent SS prediction
2.8. Operating conditions of Cirencester clarifiers (1979 period)
2.9. Performance of pseudo steady-state model for the $RASS$
2.10. Models studied for simulating the underflow concentration
2.11. Dynamic model performance for the thickener
2.12. Basic statistics and model performance during validation
2.13. Dynamic model performance with diurnally varying inputs
2.14. Sensitivity trajectories of $RASS$ for 10% change in inputs

3.1. Hydraulic model performance (basic statistics)
3.2. Hydraulic model with return liquor (basic statistics)
3.3. Typical parameter values for heterotrophic biomass kinetics
3.4. Parameter & initial values for structured biomass model
3.5. Structured biomass model performance
3.6. Parameter & initial values for carbonaceous oxidation model
3.7. Carbonaceous oxidation model performance
3.8. Carbonaceous oxidation model with temperature effect
3.9. Recursive estimation with non-dynamic parameters
3.10. Recursive estimation with additive noise in the parameters
3.11. Typical parameter values for nitrification - denitrification kinetics
3.12. Parameters & initial state values
3.13. Performance of nitrification-denitrification model
3.14. Recursive estimation with non-dynamic parameters
3.15. Sensitivity coefficients (mean) and sensitivity ranking of parameters
3.16. Modification in model parameters during validation
3.17. Model performance during validation

4.1. Proposed values for oxygen yield coefficients
4.2. Block estimation of oxygen yield coefficients
4.3. Block estimation of oxyegn yield coefficients (period d. 95-126 excluded)
4.4. Recursive estimation of coefficients by Kalman filter

4.5. Experimental conditions during the 'on-line' aeration trials
4.6. Simultaneous bloch estimation of K_{LA} and OUR
4.7. Independent estimation of OUR by simple least squares
4.8. Estimation of K_{LA} for a fixed OUR by optimization
4.9. Relationship between K_{LA} and air-flow rate

5.1. Linear model performance for pumping energy requirements
5.2. Typical values of inputs/parameters for sensitivity analysis
5.3. Models for the thickened sludge concentration
5.4. Average daily cost and main process variables at different operating conditions
5.5. Percent contribution of initial value (I.V) and steady-state value (S.V.)
5.6. Determination of gains in the single-loop FB controller
5.7. Estimation of gains in the two-loop FB controller
5.8. Comparison of performance of models for process input forecasting
5.9. Summary statistics of adaptive control systems performance under variable input conditions
5.10. Performance comparison of alternative operational control policies

List of Figures

Fig. 1.1. Model development procedure (Fig. 2.2 from Beck 1983)
Fig. 2.1a. Typical variation of hindered settling velocity with solids concentration
Fig. 2.1b. Experimental determination of settling velocity relation with concentration
Fig. 2.2. Schematic representation of a final clarifier
Fig. 2.3. Variation of solids flux with concentration
Fig. 2.4. Schematic representation of the Cirencester oxidation ditch plant
Fig. 2.5a. Crude sewage BOD_5 concentration
Fig. 2.5b. Crude sewage SS concentration
Fig. 2.5c. Crude sewage COD concentration
Fig. 2.5d. Crude sewage $NH_3 - N$ concentration
Fig. 2.5e. Crude sewage $NO_3 - N$ concentration
Fig. 2.5f. Crude sewage $NO_2 - N$ concentration
Fig. 2.6a. Final effluent BOD_5 concentration
Fig. 2.6b. Final effluent SS concentration
Fig. 2.6c. Final effluent COD concentration
Fig. 2.6d. Final effluent $NH_3 - N$ concentration
Fig. 2.6e. Final effluent $NO_3 - N$ concentration
Fig. 2.6f. Final effluent $NO_2 - N$ concentration
Fig. 2.7a. Mixed liquor suspended solids
Fig. 2.7b. Recycle activated sludge solids
Fig. 2.7c. Settleability of mixed liquor (Stirred specific volume index)
Fig. 2.8a. Crude sewage flow rate
Fig. 2.8b. Recycle sludge flow rate
Fig. 2.8c. Surplus sludge flow rate
Fig. 2.8d. Return liquor flow rate
Fig. 2.9a. Thickened sludge concentration
Fig. 2.9b. Tankered sludge volume per day
Fig. 2.10a. Mixed liquor temperature
Fig. 2.10b. Rainfall at Cirencester
Fig. 2.11a. Percent removal of organic substrate BOD_5
Fig. 2.11b. Percent of COD removal
Fig. 2.11c. Percent removal of ammonia ($NH_3 - N$) (nitrification)
Fig. 2.11d. Percent removal of measured nitrogenous compounds (denitrification)
Fig. 2.12a. Autocorrelogram of input BOD_5
Fig. 2.12b. Autocorrelogram of input flow rate
Fig. 2.12c. Autocorrelogram of input $NH_3 - N$
Fig. 2.12d. Autocorrelogram of input SSi
Fig. 2.13a. Autocorrelogram of output BOD_5
Fig. 2.13b. Autocorrelogram of output SS
Fig. 2.13c. Autocorrelogram of output $NH_3 - N$
Fig. 2.13d. Autocorrelogram of output $NO_3 - N$
Fig. 2.14a. Cross-correlogram between input & output BOD_5
Fig. 2.14b. Cross-correlogram between input & output SS
Fig. 2.14c. Cross-correlogram between input & output $NH_3 - N$
Fig. 2.14d. Cross-correlogram between input & output COD

Fig. 2.15a. Cross-correlogram of $BODi$ against Qi
Fig. 2.15b. Cross-correlogram of $NH3i$ against Qi
Fig. 2.15c. Cross-correlogram of $NO3i$ against Qi
Fig. 2.15d. Cross-correlogram of $NO2i$ against Qi
Fig. 2.16a. Steady-state model based on solids load : $SSe_t = a \cdot G_F + b$
Fig. 2.16b. Steady-state model based on effluent BOD : $SSe_t = a \cdot BODe + b$
Fig. 2.16c. Autoregressive model performance: $SSe(t) = a \cdot SSe(t-1) + b \cdot G_F + c$
Fig. 2.17a. Applied – predicted limiting solids flux ($Vo = 5.18$, $K = 0.38$)
Fig. 2.17b. Applied – predicted limiting solids flux ($Vo = 6.50$, $K = 0.35$)
Fig. 2.17c. Observed $RASS$ – predicted limiting concentration ($Vo = 5.18$, $K = 0.38$)
Fig. 2.18a. Predicted – observed underflow concentration from steady-state model
Fig. 2.18b. Prediction error in $RASS$ from steady-state model
Fig. 2.18c. Autocorrelogram of error in $RASS$
Fig. 2.19. Performance of autoregressive model : $RASS(t) = a \cdot RASS(t-1) + b$
Fig. 2.20. Schematic representation of clarifier for modelling a. single CSTR, b. 2-CSTRs, c. sludge blanket modelling
Fig. 2.21a. Predicted – observed underflow concentration from dynamic (1 CSTR) model
Fig. 2.21b. Predicted sludge blanket level
Fig. 2.21c. Prediction error in $RASS$ from dynamic model
Fig. 2.21d. Autocorrelogram of error in $RASS$
Fig. 2.22a. Predicted – observed $RASS$ from dynamic model during validation
Fig. 2.22b. Predicted sludge blanket level
Fig. 2.22c. Prediction error in $RASS$ during validation
Fig. 2.22d. Autocorrelogram of error in $RASS$
Fig. 2.23. Typical standardized diurnal variation of Qi and $MLSS$
Fig. 2.24a. Performance of dynamic model with diurnally varying inputs (1979 set)
Fig. 2.24b. Performance of dynamic model with diurnally varying inputs (1980 set)
Fig. 2.25. Change in $RASS$ concentration due to 10% change in the inputs

Fig. 3.1a. Output response due to a "delta" input of a conservative substance
Fig. 3.1b. Output response due to a "step" input of a conservative substance
Fig. 3.1c. Output response due to a " step " input of a non-conservative substance
Fig. 3.2. Radioactive tracer output from an oxidation ditch plant
Fig. 3.3. Schematic representation of the oxidation ditch plant
Fig. 3.4a. Predicted – observed $MLSS$ from hydraulic model
Fig. 3.4b. Predicted – observed $RASS$ from hydraulic model
Fig. 3.4c. Prediction error in $MLSS$
Fig. 3.5a. Predicted – observed $MLSS$ incorporating return liquor stream
Fig. 3.5b. Predicted – observed $RASS$ incorporating return liquor stream
Fig. 3.6a. Sensitivity of $MLSS$ due to 10% increase in flow rates
Fig. 3.6b. Sensitivity of $RASS$ due to 10% increase in flow rates
Fig. 3.7a. Simulated diurnal variation of $MLSS$
Fig. 3.7b. Simulated diurnal variation of $RASS$
Fig. 3.8. Typical DO profile in an oxidation ditch reactor

Fig. 3.9. Representation of the aerobic-anoxic zones in the oxidation ditch
Fig. 3.10. Main processes for the removal of organic substrates
Fig. 3.11. Assumed structure of crude sewage for carbonaceous oxidation modelling
Fig. 3.12. Schematic representation of structured biomass model for carbonaceous oxidation
Fig. 3.13a. Predicted – observed $MLSS$ from structured biomass model
Fig. 3.13b. Predicted – observed $RASS$ from structured biomass model
Fig. 3.13c. Predicted active, inactive and inert mass from structured biomass model
Fig. 3.13d. Predicted – observed effluent soluble organic substrate
Fig. 3.13e. Predicted – observed cumulative net biomass growth
Fig. 3.13f. Autocorrelogram of error in $MLSS$
Fig. 3.13g. Autocorrelogram of error in $RASS$
Fig. 3.14. Schematic representation of simple carbonaceous model
Fig. 3.15a. Predicted – observed heterotrophic biomass ($MLSS$) from carbonaceous model
Fig. 3.15b. Predicted – observed recycle heterotrophic biomass ($RASS$) from carbonaceous model
Fig. 3.15c. Predicted – observed effluent soluble organic substrate
Fig. 3.15d. Predicted – observed cumulative net biomass growth
Fig. 3.16a. Autocorrelogram of error in $MLSS$
Fig. 3.16b. Autocorrelogram of error in $RASS$
Fig. 3.16c. Autocorrelogram of error in $BODe$
Fig. 3.16d. Autocorrelogram of error in daily net growth
Fig. 3.17a. Estimated trajectory of μ_{max} (as non-dynamic state)
Fig. 3.17b. Estimated trajectory of Kd (as non-dynamic state)
Fig. 3.17c. Estimated trajectory of Ysx (as non-dynamic state)
Fig. 3.18a. Estimated trajectory of μ_{max} (with additive noise)
Fig. 3.18b. Estimated trajectory of Kd (with additive noise)
Fig. 3.18c. Estimated trajectory of Ysx (with additive noise)
Fig. 3.19. Main processes in the biochemical transformation of nitrogenous compounds
Fig. 3.20. Schematic representation of nitrification-denitrification model
Fig. 3.21a. Predicted – observed effluent ammonia concentration
Fig. 3.21b. Predicted – observed effluent nitrate concentration
Fig. 3.21c. Predicted nitrifier concentration in M.L.
Fig. 3.21d. Predicted denitrifier concentration in M.L.
Fig. 3.21e. Predicted nitrifier concentration in recycle
Fig. 3.21f. Predicted denitrifier concentration in recycle
Fig. 3.22a. Autocorrelogram of error in $NHse$
Fig. 3.22b. Autocorrelogram of error in $NOse$
Fig. 3.23a. Estimated trajectory of μ_{Nmax}
Fig. 3.23b. Estimated trajectory of Kdb
Fig. 3.23c. Estimated trajectory of μ_{Dmax}
Fig. 3.23d. Estimated trajectory of Kdb
Fig. 3.24a. Predicted effluent ammonia from adaptive simulation
Fig. 3.24b. Predicted effluent nitrates

Fig. 3.24c. Predicted nitrifier concentration in A.T.
Fig. 3.24d. Predicted denitrifier concentration in A.T.
Fig. 3.25. Parameter sensitivity results
Fig. 3.26a. Predicted – observed $MLSS$ concentration during validation
Fig. 3.26b. Predicted – observed $RASS$ concentration during validation
Fig. 3.27a. Predicted effluent BOD in validation
Fig. 3.27b. Predicted – observed effluent NH_3 concentration during validation
Fig. 3.27c. Predicted – observed effluent NO_3 concentration during validation
Fig. 3.27d. Predicted nitrifier-denitrifier concentration in the mixed liquor
Fig. 3.27e. Predicted recycle nitrifier-denitrifier concentration

Fig. 4.1a. Aeration efficiency against aerator submergence (from Rachwal et al. 1983)
Fig. 4.1b. Power drawn against aerator submergence (from Rachwal et al., 1983)
Fig. 4.1c. Oxygenation capacity against aerator submergence (from Rachwal et al., 1983)
Fig. 4.2. Average daily power drawn per aerator during selected operating period
Fig. 4.3. Average daily immersion depth of aerators during selected operating period
Fig. 4.4. Standard & actual oxygenation capacity
Fig. 4.5. Standard & actual oxygenation efficiency
Fig. 4.6. Observed and predicted energy consumption (Case 1)
Fig. 4.7. Typical diurnal variation of aerator submergence, and DO (from Rachwal et al., 1983)
Fig. 4.8. Observed and predicted aeration energy (Case 2)
Fig. 4.9. Adaptive estimation of oxygenation coefficient $'a'$
Fig. 4.10. Adaptive estimation of oxygenation coefficent $'b'$
Fig. 4.11. Air-flow rate profile during the experiments
Fig. 4.12. On-line measurements of DO concentration (smoothed) for three locations
Fig. 4.12a. First deoxygenation trial (Exp. 1)
Fig. 4.12b. First reoxygenation trial (Exp. 2)
Fig. 4.12c. Second deoxygenation trial (Exp. 3)
Fig. 4.12d. Second reoxygenation trial (Exp. 4)
Fig. 4.12e. Experiments 5 to 7
Fig. 4.13a. Calibration curve for Probe 2
Fig. 4.13b. Calibration curve for Probe 3
Fig. 4.13c. Calibration curve for Probe 2
Fig. 4.14. Schematic representation of the activated sludge reactor
Fig. 4.15. Off-line DO monitoring for OUR determination
Fig. 4.16. Relationship between K_{LA} and air-flow rate :
a. For probe 2 b. For probe 3 c. For probe 4
Fig. 4.17a. DO profile during 25/5/85
Fig. 4.17b. DO profile during 26/5/85
Fig. 4.17c. DO profile during 27/5/85
Fig. 4.18a. Effect of oxygen mass-transport upon the OUR estimates
Fig. 4.18b. OUR estimates from a dynamic and non-dynamic DO model
Fig. 4.18c. OUR estimates from the linear and non-linear dynamic DO model

Fig. 4.19a. Estimated OUR profile during 25/5/85
Fig. 4.19b. Estimated OUR profile during 26/5/85
Fig. 4.19c. Estimated OUR profile during 27/5/85
Fig. 4.20. OUR profile in the reactor during 26/5/85

Fig. 5.1. Observed and predicted energy for crude sewage pumping
Fig. 5.2. Observed and predicted energy for return sludge pumping
Fig. 5.3. Effect of $MLSS$ level on total operating cost
Fig. 5.4. Effect of $MLSS$ level on Energy cost
Fig. 5.5. Sensitivity of total cost to process inputs : (a. Input flow Qi (m^3/d), b. Recycle flow Qr (m^3/d) c. Input SSi (mg/l), d. Organic load $(kgBOD/d)$, e. Ammonia load $(kg\ NH_3 - N/d)$, f. Denitrified mass $(kgNitrogen/d)$
Fig. 5.6. Sensitivity of total cost to model parameters : a. Oxygenation parameter a $(kgO_2/kgBOD)$ b. Oxygenation parameter b $(gO_2/kgSS \cdot hr)$, c. Biomass yield, d. Biomass decay rate (d^{-1}), e. Thickened sludge concentration (kg/m^3)
Fig. 5.7. Sensitivity of total cost to unit cost prices : (a. Electricity cost (pence/kWh), b. Sludge disposal cost $(£/m^3$ sludge)
Fig. 5.8. Observed and predicted thickened sludge concentration
Fig. 5.9. Relationship between operating conditions $(RASS, Qw)$ and thickened sludge
Fig. 5.10. Relationship between disposal cost and $RASS$
Fig. 5.11. Effect of variable thickened sludge on Total cost
Fig. 5.12. Effect of operating $MLSS$ on average daily cost under real input conditions
Fig. 5.13. Effect of operating $RASS$ on average daily cost
Fig. 5.14a. Generated pulse in the recycle flow
Fig. 5.14b. Generated pulse in the surplus sludge flow
Fig. 5.15. Transient response of $MLSS$ to a pulse in control inputs
Fig. 5.16. Transient response of $RASS$ to a pulse in control inputs
Fig. 5.17. Transient response of soluble effluent BOD_5 to a pulse in control inputs
Fig. 5.18. Transient response of effluent $NH_3 - N$ to a pulse in control inputs
Fig. 5.19. Transient response of effluent $NO_3 - N$ to a pulse in control inputs
Fig. 5.20. Transient response of nitrifiers to a pulse in control inputs
Fig. 5.21. Transient response of denitrifiers to a pulse in control inputs
Fig. 5.22. Transient response of sludge blanket level to a pulse in control inputs
Fig. 5.23a. Schematic representation of a proportional-error FB control system
Fig. 5.23b. Schematic representation of an adaptive prediction error FB control system
Fig. 5.23c. Schematic representation of a combined FB/FF control system
Fig. 5.24. Performance of a single-loop FB control with constant gain: a. $MLSS$ b. $RASS$
c. Recycle flow d. Surplus sludge flow
Fig. 5.25. Performance of a two-loop FB control with constant gains: a. $MLSS$ b. $RASS$ c. Recycle flow d. Surplus sludge flow (Case 1)

Fig. 5.26. Performance of a two-loop FB control with constant gains with modified objective function: a. $MLSS$ b. $RASS$ c. Recycle flow d. Surplus sludge flow (Case 4)
Fig. 5.27a. Autocorrelogram of input BOD load
Fig. 5.27b. Autocorrelogram of input ammonia load
Fig. 5.28. Performance of the 'adaptive-gain' Feedback system to a pulse in the $MLSS$ set-point (with $BL = 0.90 - 1.10$): a. $MLSS$, b. Sludge blanket level, c. Recycle flow, d. Surplus sludge flow
Fig. 5.29. Performance of the 'iterative' Feedback system to a pulse in the $MLSS$ set-point (with $w_1/w_2 = 1/12.5$ & $BL = 0.9 - 1.10$):
a. $MLSS$ concentration, b. Sludge blanket level, c. Recycle flow,
d. Surplus sludge flow
Fig. 5.30. Performance of the 'adaptive-gain' Feedback system under variable input conditions (with $BL = 0.90 - 1.10$): a. $MLSS$, b. Sludge blanket level, c. Recycle flow, d. Surplus sludge flow
Fig. 5.31. Performance of the iterative Feedback system under variable inputs (with $BL = 0.90 - 1.10$, $w_1 = 20, w_2 = 1000, w_3 = 0.002$ & $w_4 = 0.2$) :
a. $MLSS$, b. Sludge blanket level, c. Recycle flow, d. Surplus sludge flow
Fig. 5.32. Performance of controlled system under Policy 1 : a. $MLSS$, b. Sludge blanket level, c. Recycle flow, d. Surplus sludge flow, e. Effluent ammonia, f. Nitrifier concentration, g. Effluent nitrate, h. Denitrifier concentration
Fig. 5.33. Excess ammonia load versus input flow rate
Fig. 5.34. Frequency distribution of excess ammonia load a. For Qi above 10,000 m^3/d b. For Qi below 10,000 m^3/d
Fig. 5.35. Performance of controlled system under Policy 2
Fig. 5.36. Performance of controlled system under Policy 3
Fig. 5.37. Performance of controlled system under Policy 4

1 Introduction

1.1 General

The ever increasing use of river water for potable water supplies and other related uses in densely populated catchments has increased the need for maintaining high water quality in the river systems. The purpose is to protect primarily the human health, but also the aquatic life and the surrounding environment. The quality of water is measured by the value of certain parameters representing the concentration of various pollutants. Preservation of a high water quality according to its intended uses, has been traditionally implemented by imposing limits to the quality parameters, known as water quality standards or consent conditions.

The application of water quality standards imposes constraints on the quality of discharges into a river system, which represent the main source of water pollution. As a result, a set of effluent discharge standards were imposed on all discharges, which were designed to prevent deterioration of surface water quality beyond an acceptable level. The oldest and most commonly quoted discharge standard is the 20/30 for BOD/SS, applied to discharges into non-tidal river systems assuming a dilution of 8:1. This was proposed by the Royal Commission on Sewage Disposal in 1912. More recently there has been greater concern to further reduce river pollution by revising the discharge standards and by relating them to the current and potential uses of river water (NWC, 1978). The revision of consents resulted in the establishment of more stringent standards for the majority of discharges and particularly for those located in areas where high water quality was to be maintained (Thames Water, 1979). It is important to note that the revised standards were particularly stringent with respect to effluent ammonia concentration, because they appreciated the marked effects that ammonia can have on the oxygen demand downstream of the discharge, the problems created during the water treatment and its toxicity to fish.

The natural response of the water industry to the more stringent discharge standards, was to upgrade existing works by adding tertiary treatment facilities, or to select other treatment processes that can achieve higher quality. Furthermore, the need to improve the performance and efficiency of existing works became of paramount importance in recent years. This was further motivated by the desire of the water industry to reduce manning levels and operating costs of medium and large size works (DoE/NWC, 1981). Increased mechanization and automation of the works, combined with better monitoring of the process was considered the only way to improve effluent quality and reduce manpower and operating costs.

The growing need to improve the efficiency of treatment works has motivated

a lot of research towards a better understanding of wastewater treatment processes, which is vital for developing more efficient and low-cost means of operation. Furthermore the importance of improving process monitoring, by developing more reliable on-line sensors and the potential benefits from the application of operational control, were recognized in the four IAWPRC Workshops held between 1973 and 1985. These Workshops aimed at assessing the current state of the art in instrumentation, process control and automation and consolidate the effort in this area.

1.2 Wastewater treatment systems

Wastewater treatment systems have been used for almost a century for the purpose of reducing the pollution load from domestic sewage and industrial effluents discharged into natural watercourses. Their role consequently is of paramount importance for the control of surface water quality. Wastewater treatment processes are broadly subdivided into "fixed-film" and "suspended-growth" processes, with their main representatives being the trickling filter and the activated sludge respectively. In fixed-film processes the microorganisms responsible for the biochemical reactions are attached to some inert medium, while in suspended-growth processes the microorganisms are maintained in suspension within the liquid. The activated sludge process has gained increased popularity because of the smaller land requirements per volume of sewage treated and the greater flexibility to cope with a large number of treatment problems.

1.2.1 The activated sludge process

The activated sludge, is an aerobic biological oxidation process, in which sewage is aerated in the presence of a flocculant mixed microbial culture. The main features of the process are the aeration tank, in which raw or settled incoming sewage is thoroughly mixed with the activated sludge and an abundant supply of dissolved oxygen is provided. The mixture, which is known as the mixed liquor, is then passed into a final clarifier for separating the activated sludge from the treated effluent. The majority of the thickened sludge is then returned back to the aeration tank, while a small part of it is removed from the process in order to maintain the solids concentration at the desired level.

The efficient operation of the process depends on the amount and consistency of sludge in active microorganisms. This is a function of the solids retention time in the system which can be positively controlled by the operator. A unique feature of the activated sludge process, compared with other biological processes, is that it is amenable to much closer control and hence there is scope for improved performance.

The activated sludge process is very flexible and can be adapted to almost any type of biological waste treatment problem. Various modifications have been developed, which although they retain most of the main features of the process, vary significantly in their design, operational characteristics and area of application. The most commonly used modifications are :

- Conventional activated sludge
- High-rate process
- Extended aeration
- Tapered aeration
- Stepped-aeration
- Pure oxygen activated sludge
- Contact stabilization
- Oxidation ditch

In the search to find a process retaining the principles of the activated sludge, but with potential of achieving higher performance to cope with the more stringent standards, the oxidation ditch process is a strong candidate. This process combines a number of desirable features, such as a high degree of nitrification and nitrogen removal, substantial attenuation of input load fluctuations and simplicity of operation. Oxidation ditch plants are therefore suitable for small and medium size communities where high effluent quality is required. For this purpose a closer study of the process was undertaken.

1.2.2 The oxidation ditch process

The oxidation ditch is an extended aeration process in which the mixed liquor is recirculated into a long continuous channel. The oxidation ditch process was initially devised as a simple, low- maintenance treatment unit for small and medium-size communities. For this purpose no primary sedimentation was provided, while the operating long sludge retention times (SRT) aimed at producing a minimum quantity of sufficiently stable sludge which would not require further treatment. A direct consequence of the long SRT is the realization of high degree of ammonia oxidation to nitrates (nitrification), while the long hydraulic retention time made the process less sensitive to input load fluctuations. Aeration and mixing of the mixed liquor was provided either by brush or cage aerators located near the end of the channel in the early versions. The non-uniform air supply assists in the formation of aerobic and

anoxic zones in the reactor, which promote the reduction of nitrates to nitrogen gas (denitrification). As a result a substantial reduction in the nitrogen content of the treated wastewater is accomplished.

The ability of the oxidation ditch to both nitrify and denitrify, made the process particularly attractive in cases where control of nitrogen level in the receiving waters is of primary importance. In addition the overall simplicity and reliability of the process favoured its wider application for larger communities. However, an often claimed disadvantage of the process is the higher cost of operation compared to the conventional activated sludge. This is due to the high energy consumption per unit mass of substrate removed, as a result of the prolonged aeration of the mixed liquor in the reactor. This energy, which is normally in the form of electricity, must be supplied externally since anaerobic digestion for power generation is not possible. Nevertheless, the apparently high cost for aeration is partly offset by the lower and more stable sludge production which, after thickening, can be directly disposed off to land. Additional benefits are gained from the denitrification reaction, by which substantial quantities of chemically bound oxygen are released, offering an appreciable reduction in energy consumption and nitrogen content of the effluent.

Nevertheless the efficient and reliable operation of an oxidation ditch cannot be guaranteed a priori, since this is directly affected by the operating conditions of the plant. A recent survey of small-size ditches in the U.K., showed that their effluent quality exhibited large variability, particularly with respect to the effluent ammonia concentration (Forster 1983). The nitrification performance was frequently found to fluctuate randomly with time, while the denitrification performance was largely affected by the prevailing dissolved oxygen profile in the reactor. Taking into account that many of the surveyed plants were unmanned, it can be suggested that without proper supervision the previously discussed benefits of the process cannot be fully realized.

Oxidation ditches have been extensively used for small plant applications in the U.K. over the past 25 years, however they have only been used for larger works for about a decade. One of the reasons is that earlier aeration systems required shallow channels (below 1.5 m) and hence large ditches were uneconomical to built. The development of the 'Carrousel' system, in which air is supplied by cone aerators, can cope with deeper channels of 2-3.5 m, therefore reducing the size of the works.

The use of oxidation ditches for large wastewater treatment applications, involves high operating costs, which is contrary to the water industry policy to reduce cost. However due to the flexibility of the process, it is possible to reduce its running cost without affecting its performance, by operating the process more efficiently. Efficient operating strategies can be derived from a rigorous study of the process and can be

implemented through better monitoring and closer operational control.

The oxidation ditch process has not been adequately studied regarding the cost reductions that can be achieved through better monitoring and operational control. Therefore a study on the application of efficient operating strategies to the process was considered essential for demonstrating the potential benefits regarding reduction in cost and improvement in performance. However such a study requires substantial knowledge of the process and a suitable mathematical representation. This area is also poorly covered in the literature as discussed later in Chapter 3 and therefore process modelling was initially undertaken.

1.3 Application of modelling

The use of models for the study of an engineering system is common practice. Among the various types of models (physical, mathematical, conceptual), the mathematical models have gained popularity because they are easier and less expensive to develop than physical models and more applicable for quantifying the behaviour of a system than conceptual models. Mathematical models have been applied to a large variety of systems with considerable success especially for the "well-defined" systems in which the uncertainty regarding their internal mechanisms is minimal. However, environmental systems are classified as "poorly-defined" systems because of the uncertainty surrounding the physical and biochemical processes involved.

As a result the application of mathematical models to environmental systems cannot achieve the same degree of success as for well- defined systems. Nevertheless there are major benefits to be gained which justify the application of models in most cases. Firstly, mathematical models are commonly used for the design of wastewater treatment systems, assisting the optimum dimensioning of the unit operations, although for this purpose simple model structures usually suffice. However more important benefits can be realized during the operation of the process, where mathematical models can be used for a variety of purposes such as :

- They assist in the description of the complex biochemical reactions in a wastewater treatment process and quantification of the effects of external factors and operating conditions upon the system behaviour.
- They provide an alternative source of information to experimentation on the real system, which is generally too costly and often not feasible.
- They can be used for predicting both measurable and unmeasurable process variables.
- They provide a basis for selecting minimum cost operating policies able to

achieve certain performance targets.

- They can be used for designing an efficient control system.

Research into the modelling of suspended-growth systems has been conducted in excess of twenty years, however the developed models show considerable differences among them. The reason for such discrepancy is the different purpose that each model serves and the various process modifications. Nonetheless it also shows the considerable uncertainty and even controversy that still exists regarding the description of the internal process mechanisms. The successful application of an existing mathematical model to a particular system cannot be guaranteed a priori, even if it was shown to perform well on another system. In most cases the application of a model would require at least a re-calibration of its parameters, in order to account for the characteristics of the particular system. However, in case where an in-depth study into a system is intended, such as for the purpose of improving its performance and designing operating strategies, a separate model development exercise should be undertaken. Next, an approach to developing a mathematical model for a system is outlined.

1.4 Outline of approach to model development

1.4.1 General

There is no universal systematic procedure for developing a model for a given system and several model development techniques have been used by analysts. However, a step-wise procedure has become widely acceptable as a good guide for the development and testing of models. This approach, which represents the state of the art in Systems Analysis, is briefly described herein, since it was employed for analyzing the oxidation ditch system and for developing models in this study.

At this stage there is an important distinction to be made with respect to the available knowledge about the system to be modelled. Initially, before any experimental observations are available, some a priori (theoretical) knowledge may exist about the basic laws that govern the system, which may be sufficient to define the structure of the system. Then, after experimental work has been carried out, more information become available which assists in refining the initial model and assessing its performance under a wide range of conditions related to its future applications. This represents the a posteriori measurement knowledge.

The model building exercise is ideally based on both the a priori and a posteriori knowledge, but it can also be based on one of them only. According to Beck (1983a)the first approach associated with a priori structural knowledge only is a

deductive reasoning procedure, whereby from a general theory one can deduce the model relationships. The second approach associated with a posteriori knowledge is an inductive procedure, assuming no a priori knowledge and attempts to develop the model from the available experimental data. The main steps of the modelling procedure are shown in Figure 1.1 and are briefly described below.

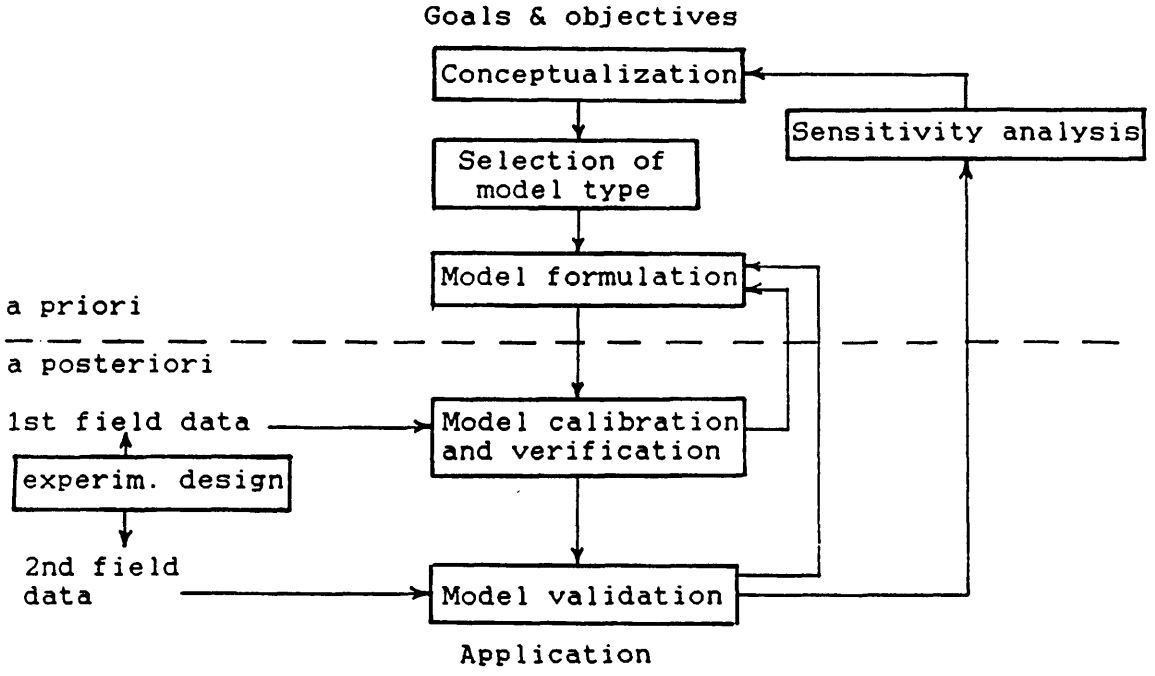


Fig. 1.1. Model development procedure (Fig. 2.2 from Beck 1983)

1.4.2 Definition of goals and objectives

This primarily intends to define the purpose of the modelling exercise and its future application area. It forms the basis upon which the model selection and development is to be decided and determines the need and type of experimental work to be conducted.

1.4.3 Conceptualization

At this stage the nature of the physical system must be defined and the key variables and interactions identified and classified according to their importance for the modelling exercise. Here, the complex physical system may be decomposed into smaller components for individual analysis. Furthermore the inputs and outputs of the system must be identified, as well as, the state variables to be modelled.

1.4.4 Selection of model type

The selection of the model type for a particular system must be related to the objectives of modelling and its future application. The selection also depends on the dynamic characteristics of the system and the available knowledge of its internal mechanisms. In addition the feasibility to identify and validate the model from any available or planned experimental observations must be also considered. The main features which define the model type are discussed below :

internally descriptive/black-box (input-output) : Internally descriptive models exploit most of the available a priori information for describing the phenomena which determine the system behaviour. On the contrary, black-box models require no a priori knowledge and are only based on a posteriori information obtained usually from input and output observations of the system.

dynamic/steady-state : In a dynamic model the variables change with time, while in a steady-state model they are independent of time.

lumped/distributed parameter : In a distributed parameter model the variations of one or more vectors of inputs, outputs, states or parameters are distributed in an infinite dimension vector space. In a lumped parameter model the above variables are considered uniform and independent of their position within a defined volume.

stochastic/deterministic : In a stochastic model, random input and system disturbances, as well as, measurement errors are taken into account while in a deterministic model such disturbances are negiected.

time variant/time invariant (parameters) : This is related to the time variation of the model parameters.

linear/non-linear : The linearity of a model is determined by the order of the variables.

continuous/discrete time : In continuous models the time is a continuous function, while in discrete models the time takes only discrete values.

1.4.5 Model formulation

This is the main stage in the development of internally descriptive models for a physical system. For this purpose as much a priori information as possible must be collected describing the internal mechanisms of the system. The model structure is usually expressed by a set of mathematical equations, which will then be solved through analytical or numerical techniques. The mathematical formulation also depends on the selected model type and the necessary complexity for describing the

system, which are related to the initial objectives of modelling. In practice however, a trade-off is usually made between model complexity and computational load for solving the mathematical equations. Furthermore, in poorly-defined systems a trade-off is also made between the expected model performance and the available observations on the system for the calibration and validation of the particular model.

1.4.6 Experimental design

The experimental design aims at providing the 'a posteriori' information on the system behaviour, through collection of experimental observations. Therefore, a well planned and conducted experimental design is very important for the acquisition of useful information about the particularities of the system or its response under extreme conditions. A priori knowledge is necessary to determine important aspects of the experimental design such as, major process time constants, sampling frequency, duration of experiments, choice of input test signal, noise levels and process nonlinearities (Gustavsson 1975). In this study most of the experimental observations concerning the oxidation ditch system were made available. Experiments however were conducted for another exercise involving the modelling of dissolved oxygen dynamics and estimation of its parameters. In that case the process time constants and measurement noise had to be considered for the selection of sampling frequency and duration of experiments.

1.4.7 Model calibration (parameter estimation) and verification

Following the model formulation, it is necessary to estimate parameter values which will enable the model to simulate the reality when the inputs to the system are known. The performance of the model is usually assessed from the difference between simulated and observed system variables, known as error. A selected function of these errors constitutes the objective function of the calibration problem which must be minimized, in a broad sense, by selecting an optimum parameter set. In this study the sum of square errors was chosen in most cases as the error function to be minimized. The model performance was then assessed by the statistical properties of the error and the correlation between predicted and observed states. At this stage modifications to the initially developed model structure can be justified, since more information about the process behaviour become available. The complexity of the model plays an important role in the calibration process, since complex models with a large number of parameters are more difficult to calibrate than simpler ones.

The next step is to verify that the calibrated model correctly describes the real system on the basis of the available observations. This requires that the assump-

tions made about the error sequences be valid, suggesting that they should possess certain statistical properties, and in particular those of 'white' noise. Should the error sequences not conform with their desired properties, this indicates that the model does not characterize well the observed system behaviour and possible restructuring is necessary (Beck 1983a).

1.4.8 Model validation

Validation is the procedure of testing the adequacy of the model against a second independent data set. For this purpose a new set of experimental observations is necessary and the model verification must be repeated. It is of course difficult to prove that the model is valid under any conditions. Thus many analysts have suggested that at this stage statistical hypothesis testing could be used to indicate that the developed model is valid on the basis of the available observations and the chosen test of statistics (Beck, 1983a).

1.4.9 Sensitivity analysis

This analysis aims to test the sensitivity of the model state variables to changes in the parameter or input values and can be applied at various stages of the development procedure. During model formulation a preliminary sensitivity analysis detects if any of the parameters affect significantly the model, cause instability or they do not affect it at all, which may lead to restructuring the model. At the parameter estimation stage the sensitivity coefficient can be calculated, which assist for sensitivity ranking of the parameters and for assessing if some of them are not identifiable or cause instability. Finally, after the validation stage the a posteriori sensitivity analysis can be used to examine the possible distribution of model responses given the distribution of the estimated parameter values.

1.5 Specific objectives of the study

The aim of the study was to model the oxidation ditch process and subsequently use the model to design operating policies aiming at minimizing running costs and improving process performance. A number of sub-objectives were eventually established :

- Collection of a priori information from the literature, on the internal mechanisms of the activated sludge and more specifically of the oxidation ditch process.

- Collection of experimental observations from a full-scale oxidation ditch plant.
- Development of a simple model to simulate the thickening and clarification functions of the final clarification stage.
- Development of a model for the oxidation ditch reactor to simulate the main processes, such as mass-transport, carbonaceous oxidation, and nitrification-denitrification.
- Development of a simple running cost model for assessing optimum levels of the main process variables leading to lower cost operation.
- Determination of the operating conditions for achieving the desired process performance.
- Design and application of a control system to the oxidation ditch process and evaluation of its performance under naturally varying input conditions.
- Investigation of the use of on-line (monitored) process indicators for a more efficient process monitoring and control.

1.6 Structure of the thesis

The structure of the thesis is directly related to the previous objectives. Mathematical models were developed for predicting both performance and operating cost of the oxidation ditch process and measurements from a full-scale oxidation ditch plant were used for calibration and validation of the models.

The thesis consists of five chapters. After the introduction the problem of modelling the final clarification stage was considered in Chapter 2, because its function is often disregarded when modelling a wastewater treatment system. Steady-state and dynamic models, as well as, the applicability of hindered settling theory were examined for modelling the thickening function. Also in this chapter the available experimental observations were presented and evaluated.

Chapter 3 focuses on modelling the carbonaceous and nitrogenous kinetics in the oxidation ditch reactor, which was combined with the final clarifier model to produce a comprehensive model of the process. A literature survey was undertaken and the various models developed for the activated sludge were classified and discussed. Systems analysis techniques were employed for the identification and calibration of a simple but sufficient model of the process. The model development exercise was based on both existing knowledge and information contained in real process observations. Model simulations and statistical techniques were used to assess the performance of the developed models, while the validation of the model was based on data from a

different operating period.

In Chapter 4 the importance of the oxygen uptake rate as a process indicator for on-line monitoring was investigated and a simple model for predicting the daily oxygen demand developed. A practical application of a procedure to estimate the oxygen transfer coefficient and oxygen uptake rate from on-line dissolved oxygen measurements in a full-scale activated sludge plant was described and discussed.

Finally, in Chapter 5 the developed process model was applied both for simulating the process under various conditions, and as a basis for the design of operational control policies aiming to reduce operating cost and achieve a desired level of performance and reliability. A simple running cost model was developed based on aeration, pumping and sludge disposal costs, in order to investigate the effects of operating conditions upon cost. A two-level hierarchical control was postulated. In the higher level rational operating policies were formulated for achieving the performance objectives. These policies considered the operational and effluent quality constraints imposed to the plant, as well as the seasonal pattern of the inputs. At the lower level a number of control systems were designed including adaptive and non-adaptive feedback controllers, to determine the necessary corrective action upon the manipulated process variables, and their performance was evaluated via simulations.

2 Final Clarifier Modelling

2.1 Objectives

The modelling of the oxidation ditch process focused initially on the final clarification stage, because of the important role it plays in the overall performance of the plant. In addition its function is often ignored when modelling a suspended-growth process or lumped with the aeration tank. This fact tends to impair overall performance of process models and reduce their ability to realistically reproduce the actual behaviour of the process, even when the biochemical reactions in the aeration tank are adequately described. Furthermore, the existing knowledge regarding the internal mechanisms of thickening and clarification processes is limited, and for this reason final clarifier models have often shown poor performance.

Therefore the objective of this chapter was to study the performance of full-scale clarifiers using operational data and develop a simple model that adequately describes their main functions. The final clarifier model is to be combined with a model for the aeration tank and finally used for process control.

2.2 Review of final clarifier models

2.2.1 Introduction

The importance of the final clarification stage in the overall performance of the activated sludge process has been emphasized by many investigators (Dick, 1970; White, 1975) who suggest that care must be taken in both the design and operation of final clarifiers. Inefficient operation of the clarifiers may lead either to loss of solids in the effluent, or to the production of a dilute underflow with adverse effects on solids recirculation and surplus sludge handling facilities. The final clarifiers play three major functions :

- Clarification function, for the separation of solids from the liquid phase and the production of an effluent which is relatively free of suspended matter.
- Thickening function, for the production of an underflow containing the settled solids in high concentration.
- Temporary storage of sludge, to cope with the wide variations of incoming solids load and sludge recycle requirements.

A large number of studies have been undertaken for modelling the behaviour of final clarification units. Such studies can be broadly subdivided into modelling the

clarification function with the main emphasis on simulating the effluent suspended solids concentration, and modelling the thickening function with emphasis on simulating the underflow concentration and sludge blanket level. A brief review of the theory that governs sedimentation of solids, as well as, of the main models developed for the clarification and thickening processes was initially undertaken.

2.2.2 Theory of sedimentation

Any particle dispersed in a fluid under quiescent conditions tends to settle, if its density is higher than the fluid. The behaviour of particles while settling depends largely on the concentration of the suspension and the tendency of particles to interact. Accordingly the following four types of settling have been identified:

- Discrete settling, where no interaction between particles occurs.
- Flocculent settling, where particles tend to adhere to each other as they settle.
- Hindered (or zone) settling, where particles settle together as a mass.
- Compression settling, where particles need compression for further settlement.

The settlement of discrete particles in a fluid has been successfully described by Stokes' law, where the settling velocity under laminar flow conditions is a function of particle and fluid characteristics :

$$Vs = \frac{g \cdot d^2}{18 \cdot \mu} \cdot (p_s - p_f) \qquad (2.1)$$

where; d : particle diameter $[L]$,
μ : fluid viscosity $[ML^{-1}T^{-1}]$,
p_s : particle density $[ML^{-3}]$,
p_f : fluid density $[ML^{-3}]$,
g : acceleration due to gravity $[LT^{-2}]$.

However, for the other three types of settling the above law cannot be applied, since additional forces due to particle interaction seriously affect their settling velocity. Kynch (1952) suggested that for concentrated suspensions the settling velocity of particles can be considered to depend only on the local concentration of the suspension. Dick & Ewing (1967) disputed the validity of the above assumption for flocculent particles found in the activated sludge, although other workers (Dick & Javaheri, 1972) confirmed that the assumption is valid. Furthermore, Bisogni & Lawrence (1971) found that the hindered settling velocity could be related to the sludge age of the biomass. In contrast, Tuntoolavest et al. (1982) reported insignif-

icant influence of the operating $MLSS$, aeration rate and recycle rate upon the hindered settling velocity.

The relationship between settling velocity and solids concentration under flocculent and hindered settling conditions is important for modelling the settling behaviour of solids in final clarifiers.Although such a relationship may be difficult to derive from theoretical considerations, it can be more easily determined experimentally from batch settling tests. A typical curve of this relation for activated sludge solids with good settling properties is shown in Fig. 2.1a. Several mathematical expressions have been proposed by different researchers to approximate the above relationship, some of which are presented in Table 2.1. The parameters in the equations characterize the settling properties of the particular suspension and are usually determined by regression analysis using observations from batch settling tests.

Equation		Reference
$Vs = Vo \cdot e^{-K \cdot C}$	(2.2a)	Vesilind (1968), White (1975), Johnstone et al. (1979)
$Vs = a \cdot C^{-n}$	(2.2b)	Dick & Young (1972)
$Vs = Vo \cdot (1 - K \cdot C)$	(2.2c)	Kynch (1952)
$Vs = a/(C - b)$	(2.2d)	Tracy & Keinath (1973)
$Vs = Vo \cdot (1 - C) \cdot e^{KC}$	(2.2e)	Petty (1975)
$Vs = a/(b + C^n)$	(2.2f)	Stehfest (1984)
$Vs = Vo \cdot (1 - C)^n$	(2.2g)	Richardson & Zaki (1954) from Handley (1974)

Table 2.1. Relationships between hindered settling velocity and concentration.

Johnstone et al. (1979), using a large number of hindered settling velocities from two oxidation ditch plants, found that the exponential form (equation 2.2a) gave the highest correlation with the measurements among other forms examined (Fig. 2.1b). They reported that the following values for the constants: $Vo = 5.18\ m/hr$, $K = 0.38\ l/g$, are applicable for a wide range of sludge characteristics. Marriot (1981), using daily measurements from settling tests at a pilot activated sludge plant, also fitted the exponential function and reported the following values: $Vo = 2.21\ m/hr$, $K = 0.211\ l/g$, for a wide range of $SSVI$ values, which are significantly different from those reported by Johnstone.

In a continuously operated final clarifier, shown schematically in Fig. 2.2, the total flux of transmitted solids (G_T) consists of two components (Dick 1970) :

- Gravity flux component (G_G), caused by the gravitational settlement of solids.

- Bulk flux component (G_B), caused by the downward movement of slurry as a result of the underflow withdrawal of sludge.

Hence:

$$G_T = G_G + G_B \qquad (2.3)$$

where; $G_G = Ci \cdot Vi$ (2.4a)

$G_B = Ci \cdot Qu/A$ (2.4b)

Ci : SS concentration in the sludge $[ML^{-3}]$,

Vi : settling velocity at concentration Ci $[LT^{-1}]$,

Qu : underflow rate $[L^3T^{-1}]$,

A : surface area of clarifier $[L^2]$.

Typical curves of the bulk, gravity and total flux variation with the concentration of suspended solids are illustrated in Fig. 2.3. The total flux curve exhibits a maximum point which is followed by a minimum at concentration C_L. It is interesting to note that operation of the clarifier at a solids flux below the minimum, results in a uniform concentration profile within the tank, where no thick blanket exists. However, in normal clarifier operation, where the sludge has to be thickened from the feed concentration C_F to a concentration higher than C_L, the value of the flux at the minimum determines the maximum solids handling capacity of the clarifier. (Dick 1970, 1972 ; Handley 1974 ; White 1975).

This is known as the limiting flux (G_L), and results in the formation of a thick sludge blanket with concentration C_L. Operation of the clarifier at a flux greater than the limiting results in accumulation of sludge and eventual loss of solids in the overflow. It follows that, for the successful operation of a thickener the applied solids flux should be restricted to the limiting flux. Both the limiting flux and limiting concentration depend on the underflow rate and the settling properties of the sludge. The limiting flux increases at higher underflow rates, however as the underflow increases, the maximum and minimum points in the flux approach each other until they merge at a critical underflow rate, above which the thickening function ceases to exist.

Finally, the formation of compression zones at the tank bottom through gradual elimination of water, is a process which depends both on time and depth of solids. For this reason several workers (Dick & Javaheri, 1972 ; George & Keinath 1978), have questioned the existence of compression zones in activated sludge clarifiers, because the depth of sludge and detention time is not sufficient to allow formation. However Hibbert & Jones (1974) found experimentally that for poorly settling sludges the underflow concentration increased with sludge depth implying the presence of compression zones.

2.2.3 Models for the thickening process

The majority of models in the literature, describing the thickening process, are based on the limiting flux concept. Some of their basic assumptions are :

- The flow entering the final clarifier splits into an overflow and an underflow stream.
- The solids flux theory can be applied throughout the settler.
- The solids concentration in any cross-section of the tank is uniform.
- The solids act as a conservative substance.

Bryant & Wilcox (1972) based their model on the continuity equation developed by Shannon & Tory (1965), which simulates the time and position dependence of total suspended solids concentration (TSS) in the thickening zone :

$$\frac{\partial\, TSS}{\partial t} = -\left(Vu + \frac{\partial\, Gs}{\partial\, TSS}\right) \cdot \frac{\partial\, TSS}{\partial z} \qquad (2.5)$$

where; Vu : underflow velocity $[LT^{-1}]$,
Gs : solids settling flux $[MT^{-1}L^{-2}]$,
z : depth $[L]$.

with the boundary condition: $\partial Gs/\partial z = 0$ at the bottom of the settler ($z = 0$), since the solids cannot settle through this physical barrier. In order to solve the above equation numerically, the thickener was divided into 20 completely-mixed layers, so that the partial differential equation 2.5 was replaced by a set of ordinary differential equations. It was assumed that the feed stream enters the lowest layer having TSS concentration less than or equal to the feed concentration. The performance of the model cannot be easily assessed from their simulation results since it forms a part of an integrated model for the activated sludge process.

Tracy & Keinath (1973) used the same continuity equation and made some additional assumptions :

- The solids inlet stream falls as a density current to the top of the blanket and then spreads out instantaneously to form a layer.
- The solids entering the thick blanket are concentrated instantaneously to the limiting concentration.
- The sludge blanket can be modelled as a series of variable volume completely-mixed reactors in series.

Further constraints were imposed to the model to ensure that the concept of limiting flux was not violated. Accordingly, the flux through each layer in the settler is checked and if it exceeds the maximum flux allowed for that layer its volume is increased. From simulations under step changes in feed solids concentration and underflow rate, they observed the formation of concentration discontinuities propagating through the blanket as distinct quantities, rather than adjusting to the new operating conditions. From experiments with an iron slurry they reported that the limiting-flux theory could be applied under most conditions, but they noticed departure from that theory whenever compression took place in the bottom of the tank.

Busby & Andrews (1975), used a similar model for the thickener to that of Tracy & Keinath in which they also assumed.

- the thickening zone consists of 10 CSTRs, from which the top nine are of variable volume while the bottom layer has a fixed volume.
- when the thickness of a layer decreases below 0.5 *cm* it disappears.
- the layer into which the solids stream enters, is at the limiting concentration determined by the operating conditions at the time.
- under transient conditions a new limiting concentration will occur at the layer being fed, which will propagate downwards at a rate equal to the total downward velocity.

The performance of this thickening model cannot be assessed separately as it forms part of an integrated activated sludge model, however its structure is generally complex and has the limitations of the Tracy & Keinath model.

George & Keinath (1978) did not observe concentration discontinuities as those predicted by Tracy & Keinath, based on experimental results under variable flow conditions. In addition they reported that the limiting concentration did not exist at the surface of the blanket, but within the blanket at a certain depth. On the basis of these observations they modified the continuity equation by introducing an upward velocity of the displaced fluid (Vw).

$$\frac{\partial C}{\partial t} = (Vs + Vw + Vu) \cdot \frac{\partial C}{\partial z} - C \cdot \frac{\partial Vs}{\partial z} - C \cdot \frac{\partial Vw}{\partial z} \qquad (2.6a)$$

The velocity of the displaced fluid was derived from a liquid mass-balance over an incremental volume:

$$\frac{\partial Vw}{\partial z} = \frac{-Vu}{C} \cdot \frac{\partial C}{\partial z} - \frac{1}{C} \cdot \frac{\partial C}{\partial t} \qquad (2.6b)$$

with the boundary condition, $\partial Vw/\partial z = 0$ at $z = 0$ (tank bottom).

The model performance was evaluated with data obtained from a laboratory-scale thickener using chemical slurries. The model was shown to predict satisfactorily the underflow concentration and sludge blanket level under transients between underloaded and overloaded conditions, except for the case of extreme overloading, where the model failed to predict the response accurately.

Johnstone et al. (1979) employed the limiting flux concept for predicting the maximum solids capacity of a clarifier for various operating conditions. The predictions were compared with the observed maximum capacity at which solids washout was encountered. They reported an over-estimation of both the actual clarifier capacity and the underflow concentration, which they partly explained by suggesting that significant part of the clarifier area remains ineffective for solids settlement.

Foster (1985), developed a similar model to that of Tracy & Keinath based on the limiting flux concept. Based on simulation results under transient operating conditions he reported that qualitatively the model performed similarly with other models. However when it was tested and calibrated using real observations its performance was substantially affected by the values chosen for the sludge settling constants. The best performance was obtained with values similar to those reported by Marriot (1981). Some of the reported drawbacks of the model were the underestimation of blanket rise during overloading and the neglected effects of the compression zone upon the underflow concentration.

Stehfest (1984), realizing the complexity of such distributed parameter models for on-line application, attempted to develop a simplified, lumped-parameter model with a small number of states. Using the method of characteristics for solving the partial differential equation 2.5, he simulated the complexity of concentration profiles resulting from changes in the feed solids load and underflow rate. He also reported the formation of concentration discontinuities inside the settler, which led him to propose a simpler representation using two zones of variable volume, separated by a discontinuity. He suggested therefore, that the necessary state variables were the mean solids concentration above and below the discontinuity and the sludge blanket height, while the underflow concentration could be calculated from mass-balance at the bottom of the settler.

Stehfest selected equation 2.2f to relate settling velocity with concentration, and estimated parameters a, b and n through least squares optimization. The model performed well over a 60-hour calibration and validation period, however for longer periods he suggested that an adaptive scheme should be used to update the parameters. The proposed model by Stehfest is the simplest among all the previous models, and as a result it would be the most applicable for process control. However further testing of the model seems necessary over longer operating periods in order to assess

its validity. Finally, an apparent drawback arising from the model structure, is that the model states are not defined under extreme conditions of the sludge blanket level ($h = 0$ and $h = h_F$ feed level).

Most of the models presented herein attempt a detailed description of the theoretical behaviour of an 'ideal' slurry under hindered settling conditions according to the principles of limiting-flux theory. However all these models, despite their complexity, have limitations in accurately predicting the settling behaviour of activated sludge solids which mainly arise from the following factors :

- the activated sludge is not an ideal slurry since its particles tend to coalesce as they settle.
- the settling characteristics of the sludge change continuously while most models assume a fixed settling velocity-concentration curve.
- specification of the solids settling behaviour from batch settling tests frequently over-estimates the maximum capacity of the clarifiers.
- the existence of a compression zone at the bottom of a settler and its effect upon the underflow concentration is usually neglected.

Furthermore, the complex structure of the above models requires substantial computing power for extended period simulations and also causes difficulties in their application for process control. For this purpose several workers have used simpler non-dynamic relationships to simulate the behaviour of the underflow concentration ($RASS$), ignoring the constraints dictated by limiting flux theory. Such models are usually based on solids mass balance over the final tanks, or on a fixed separation efficiency between the overflow and underflow streams, (Poduska & Andrews 1975; Ghobrial 1978; Beck 1981; Holmberg 1982; Cook 1983). Simplified relationships for the thickening function have the advantage of reducing the complexity of the overall model which is important for their application to other areas such as process control and optimization. However their is an imminent danger of obtaining unrealistic results, because such models do not consider the dynamic nature of the process and its thickening limitations.

Finally in many studies of process modelling the function of the clarifiers has been ignored, or lumped with the aeration tank and a constant underflow concentration is often assumed for the purpose of simulating the recycle solids mass, (Ekama & Marais 1977; Sincic & Bailey 1978; Marsili-Libelli 1980).

2.2.4 Models for the clarification process

Modelling of the clarification process has been the least satisfactory because the clarification process is substantially affected by several complex mechanisms, such as the fluid motion in the tank and the byoancy of low density suspended matter. Clarification takes place in the upper part of the tank referred to as the clarification zone, where the incoming solids settle out through discrete and flocculent settling leaving a relatively clear overflow. However the clarification performance, and hence the effluent SS concentration, can be seriously affected by operational problems related to the thickening process, such as those caused by solids overloading and bulking or rising sludge.

Traditionally, the clarification performance was thought to be governed by the hydraulic overflow rate ($Vc = Q/A$), so that any particle with settling velocity greater than Vc was removed from the overflow. However in activated sludge solids, the flocculent particles tend to coalesce during sedimentation which changes their size and creates difficulty in predicting their settling velocity without carrying out settling tests.

From experimental investigations a number of operating variables have been shown to affect the clarification performance and subsequently the effluent quality, such as :

- hydraulic detention time in the tank,
- solids and hydraulic loading rate of the tank,
- sludge blanket level,
- side water depth,
- depth of final tank,
- sludge settleability,
- mixed liquor temperature.

The models developed to simulate the clarification process can be broadly classified into the following types according to Foster (1985) :

- Pseudo steady-state models, where the effluent quality at any time is related to clarifier operating variables by a "steady-state" equation.
- Dynamic-mechanistic models, which attempt to simulate the dynamic behaviour of the clarification zone using a number of CSTRs in series.

- Stochastic models, derived by analysing the response of a clarifier to time-varying disturbances.

In the first category falls the expression proposed by Pflanz (1969), relating the effluent SS concentration to the applied solids load:

$$SS = Kp \cdot G_F \tag{2.7}$$

where; Kp : proportionality coefficient $[L^{-1}T]$,
$G_F = Q_F \cdot MLSS/A$, applied solids load to clarifier $[ML^{-2}T^{-1}]$,
Q_F : feed flow rate $[L^3T^{-1}]$.

Ghobrial (1978), based on experimental observations, emphasized the effect of sludge blanket on the effluent quality when it lies above a critical level, which he described by the following equation :

$$SSe = Kn \cdot G_F \cdot \frac{(Vs/V)}{(Vs/V)_{cr}} \tag{2.8}$$

where; (Vs/V) : ratio of accumulated sludge volume to total volume of settling basin [–],
$(Vs/V)_{cr}$: critical value of the above ratio [–],
Kn : constant $[L^{-1}T]$.

Chapman (1983), based on pilot-plant experiments and regression analysis, found that the feed flow rate, $MLSS$ and sidewater depth (SWD), accounted for 78% of the steady-state effluent SS variability through the following equation :

$$SSe = a_0 + a_1 \cdot MLSS + a_2 \cdot \frac{Q_F}{A} + SWD \cdot (a_3 - a_4 \cdot \frac{Q_F}{A}) \tag{2.9}$$

where; a_0, a_1, a_2, a_3, a_4 are coefficients to be determined.

In the second category fall dynamic representations like the one suggested by Bryant & Wilcox (1972), where the clarification zone is modelled by five CSTRs in series. However for circular tanks, the single CSTR representation has been commonly adopted (Foster 1985), so the model describing the effluent SS becomes :

$$\frac{dSSe}{dt} = \frac{Q_F}{V} \cdot (SS_F - SSe) \tag{2.10}$$

where; V : volume of the clarification zone $[L^3]$,
SS_F : SS of feed to clarification zone $[ML^{-3}]$.

The third class comprises models developed from statistical and time-series analysis of performance data from laboratory or full- scale clarifiers. Most of the models are simple stochastic expressions usually having an autoregressive structure relating the current effluent SS to its previous value and the current forcing functions, such as the model developed by Chapman (1985).

$$SSe(t) = a_0 + a_1 \cdot SSe(t-1) + u(t) \qquad (2.11)$$

where; $u(t) = b_1 \cdot Q_F(t) + b_2 \cdot MLSS(t)$, the forcing function at t $[ML^{-3}]$.
a_0, a_1, b_1, b_2, model parameters to be determined.

From the review of clarification process models it can be seen that most structures are based on empirical relationships involving certain process variables. Such models were derived through linear regression and a set of experimental observations, and no adequate mathematical description was found based on a rational approach.

2.3 General assessment of plant performance and operational data

2.3.1 Introduction

For the development, calibration and validation of a process model to describe a poorly-defined system, it is essential to have real process observations to assess the model performance and make any necessary modifications to its structure. In this study experimental data were made available by Thames Water Authority, regarding the "Carrousel" oxidation ditch plant located at Shorncote farm, serving the urban area of Cirencester and a few surrounding villages. The plant was commissioned in 1977 and was designed to treat mainly domestic sewage from a population equivalent of 25,000 inhabitants, although during the first years of operation it served a population of only 14,000. The dry weather flow (DWF) was estimated at 4,550 m^3/d, but the plant was designed to treat 8.8 times the DWF, because of extensive infiltration of surface waters into the sewerage system (Rachwal et al., 1983). The main design parameters of the plant are shown in Table 2.2. The Cirencester Works is located at the headwaters of the River Thames and is the first major sewage works discharging to the main river. As a result high effluent quality is required from the plant and this was specified by the 95 percentile limits for the effluent SS, BOD_5 and ammoniacal nitrogen shown in Table 2.2.

Parameter (units)	Value
DWF (m^3/d)	4,550
max. flow (m^3/d)	40,000
Sewage composition (mg/l)	
BOD	300
SS	350
NH_3-N	30
aeration tank vol.(m^3)	6,200
BOD load (kg/d)	1,375
sludge loading F/M	0.05
MLSS range (g/l)	3-5
nom. reten. time (hr)	33
max. aerator power (KWh/d)	1,820
nom. return rate (DWF)	1
final clarif. area (m^2)	1,510
final clarif. vol. (m^3)	3,290
clar. nom. ret. time (hr)	17
upflow velocity at DWF (m/hr)	0.13
Effluent quality (mg/l)	
BOD	10
SS	10
NH_3-N	5

Table 2.2. Design parameters for Cirencester plant (Rachwal et al. 1983)

2.3.2 Description of the Cirencester plant

The main units of the Cirencester plant are the inlet works, the aeration tank, the final clarifiers and the sludge thickening tanks, shown schematically in Fig. 2.4. The inlet works consist of a Screezer and a comminutor for the removal of coarse material and a Pista Grit trap for the removal of grit.

The incoming crude sewage passes through the inlet works into the main pumping station, where the flow is pumped by two Archimedian screw pumps into the aeration unit. The aeration tank has an external length of 91 m and is divided internally into four parallel interconnected channels, each 7 m wide. Oxygen is supplied to the tank by two vertical shaft Simcar surface aerators fitted with a variable level gearbox which allows for a maximum rise and fall of 400 mm.

The output from the aeration tank flows by gravity into the two final clarifiers. The clarified effluent overflows the tank weir, while the settled activated sludge is

withdrawn from the underflow and returned to the aeration unit via the pumping station. The rate of sludge withdrawal is kept at a pre-set level for low crude sewage flows, while for higher flows it is kept proportional to the incoming flow. Surplus sludge withdrawal is controlled by timers actuating the mono mutrator pumps and is directed into the two thickening tanks. The thickened sludge is then tankered on to farmland by road trucks, while the supernatant liquors and any other drainage liquors are returned to the aeration tank via the return liquor stream.

2.3.3 Experimental data - monitoring program

The experimental data supplied by Thames Water Authority (Cotswold Division), covered a 3-year period from 26/3/78 to 28/3/81 and is described by Cook (1983). Principal details are summarized as follows. The data consisted of daily measurements of influent and effluent characteristics, as well as, of operating variables of the Cirencester plant. The monitored variables are listed in Table 2.3 and the sampling points are shown in Figure 2.4.

Flow rates	(m^3/d)	input (Qi), recycle (Qr), surplus sludge (Qw), storm (Qst), return liquor (Qrl), disposed sludge (Qsl), flow to works $(Qworks)$.
Crude sewage	(mg/l)	BOD_5 $(BODi)$, COD $(CODi)$, SS (SSi), NH_3-N $(NH3i)$, NO_3-N $(NO3i)$, NO_2-N $(NO2i)$, PO_3-P $(PO3i)$, Cl (CLi).
Final effluent	(mg/l)	BOD_5 $(BODe)$, COD $(CODe)$, SS (SSe), NH_3-N $(NH3e)$, NO_3-N $(NO3e)$, NO_2-N $(NO2e)$, PO_3-P $(PO3e)$, Cl (CLe).
Operating variables		mixed liquor SS $(MLSS)$, return sludge SS $(RASS)$ thickened sludge SS (Csl), temperature $(Temp)$, $SSVI$.
Energy cons.	(KWh/d)	mains total (En), sewage pumps (Esp), return sludge pumps (Erp), aerators (Ea).

Table 2.3. Monitored variables at Cirencester S.T.P. and their notation in parenthesis.

All samples and instrument readings were collected every morning starting at 8am. The crude sewage samples were flow proportional composite samples bulked automatically, while the final effluent samples consisted of 24 hourly samples bulked manually. The solids concentration in the ditch and the recycle stream were monitored once per day by 'snap' samples. The disposed sludge was monitored by sampling each tanker and the individual samples were then bulked together for each day. Most

of the analyses were carried out using standard method procedures, while for the determination of NH_3-N, NO_3-N, NO_2-N and PO_3-P a Technicon auto-analyser was used. In the BOD test nitrification was suppressed with ATU. Finally, the various flow rates were measured continuously from the volume of pumped liquor using local dial gauges.

The frequency of monitoring the Cirencester plant for the purpose of assessing its performance was considered satisfactory for the size of the works, since only manual samples were collected. However under such monitoring frequency only average values of the process variables were obtained and hence the diurnal variation of inputs and their effect upon the plant performance cannot be assessed. Higher frequency of monitoring which would depict the diurnal pattern of the process operation, would require the use of adequate on-line instrumentation which was not available at the plant during the period of monitoring.

The available data set covered more than 1000 days of operation and was considered too long to be used as a whole during subsequent analyses. Furthermore, an inspection of the data revealed that there was a significant number of missing observations especially during the winter months. Thus the data set was split into smaller sub-sets, which in addition offered the potential of employing different subsets for the development and the validation of any model.

The subset covering a 283-day period from 13/3/79 to 20/12/79 was selected for the development of subsequent models, because it covered a sufficiently long operating period and contained a relatively small number of missing observations. Also during that period substantial variations in the inputs and operating conditions took place, which are of particular importance for any modelling exercise. The missing values were filled-in by linear interpolation between the two adjacent measured values. The data for the selected period are presented in graphical form in Figures 2.5-2.10.

An inspection of the data revealed some unexpected high or low values of certain variables for which there was no justification to discard. There was no information on the expected accuracy of the various measurements or on the instrument calibration and precision, so at this stage the data were considered of sufficient accuracy for subsequent analysis of the process. Finally there was no information on any operational problems experienced during the above period.

2.3.4 Assessment of plant performance

The overall high performance of the Cirencester Carrousel plant has been emphasized by Carmichael & Johnstone (1980) in their assessment of the first two years of plant operation. The plant also performed well during most of the selected study period,

with respect to effluent quality and removal efficiency of input pollutants. The average input and operating conditions over the study period are shown in Table 2.4. It is interesting to note that the plant was operating at well below its design capacity. The average input concentrations were much lower than the design values and the average BOD load accounted for only 50% of the design load, while the operating F/M ratio was only 0.03 on average.

The percent of organic substrate removal was very high with an average of 95.7% of BOD_5 and 88.8% of COD removed (Fig. 2.11a), resulting in a very low effluent organic concentration, which rarely exceeded the design value of 10 mg/l for the BOD.

The degree of nitrification calculated from the removal of ammonia was also high for most of the period. During the first 210 days of the study period the percent nitrification averaged 90.8% (Figure 2.11b), with an effluent ammonia concentration below the design value of 5 mg/l. However for the remaining period it averaged only 69.1% and the effluent ammonia exceeded its design value for a period of about 55 days. The period of poor nitrification coincided with a reduction in the recycle ratio which caused :

- low $MLSS$ concentration (2,400 mg/l on average),
- lower than average sludge age (22.5 days on average).

The removal efficiency of nitrogen from the crude sewage via denitrification was quite variable, but on average 51.2% of the input nitrogen was removed (Figure 2.11c), This was calculated from the reduction of all measured forms of nitrogen including ammonia, nitrate and nitrite. For the period between day 110 and 210 the percent denitrification averaged 76.3%, while for the remaining period it was only 37.2%. The poor denitrification performance corresponded with periods of :

- low mixed liquor temperature ($R = 0.678$),
- low hydraulic retention time ($R = 0.459$),
- low $MLSS$ concentration ($R = 0.26$),
- high input flow rate ($R = -0.57$),
- low sludge age ($R = 0.486$),
- low input $NH3 - N$ concentration ($R = 0.495$).

Parameter	Units	Mean	Std.dev.	Definition
Flow rates :				
Qi	m^3/d	8705.4	6378.2	
Qr	"	7472.3	4495.9	
Qw	"	202.0	70.8	
Qrl	"	219.6	198.3	
$Qworks$	"	9199.2	7472.2	
Input characteristics :				
$BODi$	mg/l	112.7	76.6	
SSi	"	179.7	92.0	
$CODi$	"	268.0	163.3	
NH_3i	"	18.15	9.13	
NO_3i	"	2.51	3.25	
NO_2i	"	0.29	0.41	
Effluent characteristics :				
$BODe$	mg/l	2.34	2.9	
SSe	"	5.03	3.34	
$CODe$	"	22.6	12.8	
NH_3e	"	2.99	3.59	
NO_3e	"	5.91	4.19	
NO_2e	"	0.42	0.46	
Operating conditions :				
$MLSS$	mg/l	3875.6	1279.8	
$RASS$	"	6902.5	2588.6	
$SSVI$	ml/g	73.2	19.0	
rec. ratio	$(\%\ Qi)$	100	48.8	$\frac{100}{N}\sum(Qr/Qi)_t$
BOD load	$kgBOD/d$	673.3	342.3	$\frac{1}{N}\sum(Qi \cdot BODi)_t$
F/M	$kgBOD/kgMLSS \cdot d$	0.0306	0.0186	$\frac{1}{N \cdot V}\sum(Qi \cdot \frac{BODi}{MLSS})_t$
sludge age	days	29.0	6.9	$\frac{1}{N}\sum[MLSS \cdot \frac{V+Vcl}{Qw \cdot RASS}]_t$
disp. sludge	kg/d	1375.7	1218	$\frac{1}{N}\sum(Qsl \cdot Csl)_t$
sludge conc.	kg/m^3	36.0	8.0	
sludge quant.	m^3/d	39.6	35.7	
Hydr. ret. time	hr	27.1	15.3	$\frac{1}{N}\sum(\frac{V}{Qi})_t$
clar. ret. time	hr	14.4	8.1	$\frac{1}{N}\sum(\frac{Vcl}{Qi})_t$
Temperature	oC	12.36	2.71	
Rainfall	mm	2.39	4.56	
Power consumption :				
total	KWh/d	1972.7	193	
aeration	"	1347.4	168	
sewage pump.	"	174.1	93.5	
ret. sl. pump.	"	137.5	45.5	

Table 2.4. Average operating conditions for the period 13/3/79 - 20/12/79.

where; $\sum(*)t$: denotes the sum of all data,
V : volume of the aeration unit $[L^3]$,
Vcl : volume of the final clarifiers $[L^3]$,
$N = 283$: total number of data.

where the figure in parenthesis denotes their correlation coefficient with percent of denitrification at lag zero.

The performance of the final clarifiers was also good, which is evident from the persistently low effluent suspended solids concentration, rarely exceeding the design value of 10 mg/l.

2.3.5 Time-series data analysis

An initial analysis of the operational data in the time-domain was performed, in order to evaluate their consistency and indicate potential relations between them. The autocorrelograms of the input and output series showed significant correlations at small lags, which decayed almost exponentially at higher lags (Figures 2.12 & 2.13). In particular, the input flow rate exhibited substantial autocorrelation which can be explained by the large infiltration of ground water into the sewerage system during 'wet' periods causing persistently high flows over a few weeks period (Rachwal et al., 1983). The input flow rate subsequently affects the incoming pollutant concentrations and partly explains their serial correlation. Furthermore a slight seasonal pattern with a period of one week can be observed in both influent and effluent series and particularly in the effluent ammonia and nitrate series.

The cross-correlation between input and output variables is generally poor especially for the BOD and SS series (Fig. 2.14a,b), while for the ammonia and COD series some correlation exists, which at lag zero is $R = 0.552$ and $R = 0.276$ respectively (Fig. 2.14c,d). The results clearly show that the process significantly attenuates the input variations, which is a common feature of extended aeration processes such as the oxidation ditch. The highest correlation between the two series is usually observed at lag zero indicating that any pure time- delays between inputs and outputs are short compared to the sampling interval of 24 hrs.

Among the input variables the most significant cross-correlations observed are presented in Table 2.5. Correlations among the input variables were expected, since the various quality parameters, such as the BOD_5, COD and SS measurements are directly inter-related. In addition the high correlation between input organics and ammonia can be attributed to the domestic nature of the crude sewage. The

correlation diminishes slowly with increasing lags which may be partly due to the autocorrelation of the individual series. Another point of particular importance is that the crude sewage flow rate shows substantial negative correlation with most of the input quality variables such as $BODi$ ($R = -0.63$), $CODi$ ($R = -0.59$), SSi ($R = -0.62$) and NH_3i ($R = -0.83$) which can be attributed to the dilution effect at high flows (Fig. 2.15a,b). On the contrary the input flow was positively correlated with NO_3i ($R = 0.713$) and NO_2i ($R = 0.672$), (Fig. 2.15c,d), which is a further confirmation of surface water infiltration from agricultural land, containing quantities of oxidized forms of nitrogen.

Input variables	R	Output variables	R
$BODi - SSi$	0.707	$BODe - SSe$	0.240
$BODi - NH_3i$	0.744	$BODe - NH_3e$	0.203
$BODi - CODi$	0.645	$NO_3e - NO_2e$	0.451
$CODi - SSi$	0.706	$CODe - NH_3e$	0.571
$NO_3i - NO_2i$	0.672	$NH_3e - NO_2e$	0.295
$NH_3i - NO_3i$	-0.615		

Table 2.5. Correlation among input and output variables at lag zero for the selected study period.

The correlation among the output variables is much poorer, shown in Table 2.5, which may be attributed to their low average levels and the high proportion of noise in their signal. The effluent ammonia, nitrate and COD concentrations, showed some correlation with the operating conditions of the plant such as the $MLSS$ concentration, sludge age, hydraulic retention time, recycle and surplus flow rates. However the effluent SS and BOD showed insignificant correlation with any of the above operating parameters, as a result of their persistently low levels throughout the period.

Examination of the influent and effluent concentrations showed a distinct difference in the behaviour of the two series. The influent series were highly variable as a result of the substantial input flow variation and the subsequent effects of dilution. On the contrary the effluent series did not follow a clear pattern of variation causing the poor correlation with the inputs. This can be attributed to the large buffering capacity of the oxidation ditch reactor which attenuates the input flow variations and leads to a stable effluent quality in the absence of any particular process failure. In addition the effluent series exhibited significant random variation which can be caused by external environmental factors, variability in the clarification performance of final tanks, and even by noise in the measurements.

The brief time-series analysis of the operational data showed that most of the

variables exhibit serial correlation and particularly the input variables. Less correlation however was observed between the output variables as a result of their random variability. In addition it was shown that the correlation between input and output variables was insignificant, indicating that the reactor behaves as a low pass filter, which precludes the development of simple transfer function models between inputs and outputs for simulating the process behaviour.

2.3.6 Conclusions

From the above presentation and brief analysis of the operational data, the following remarks can be made about their adequacy for studying the process mechanisms and developing a process model.

- the operational data cover the most important of the input, output and operating variables affecting the behaviour of the process. However some potentially useful variables for the development and evaluation of a process model were not monitored, among which are the dissolved oxygen concentration, sludge blanket level and the soluble component of effluent BOD.
- the measurements cover a sufficiently long period of plant operation under a variety of input and operating conditions, which is of great importance in any modelling exercise.
- the accuracy of measurements and instrument readings could not be assessed and therefore the existence of random or systematic measurement errors cannot be ruled out.
- the data had several missing observations in both the input and output variables. However this fact was not considered so important at this stage, as to prevent the use of the data set for process modelling.
- the measurements represent either daily average values or spot values, and no information existed on their diurnal variation.
- No information was available on any operating problems experienced.

2.4 Modelling the clarification function

In Section 2.2.4 it was discussed that models simulating the clarification function are mainly simple empirical, steady-state or dynamic relationships and have, in general, poor forecasting performance. Many of these models relate the effluent SS to the incoming $MLSS$ and flow rate, the underflow rate, the solids loading rate, the settleability of the sludge and even to the sludge blanket level. However analysis of the

available data from Cirencester showed that the effluent SS had very small or even negligible correlation with any of the above variables (Table 2.6), suggesting that a model of this kind would have a very poor predictive performance.

Oper. variable	Correl. with SSe
Qi	-0.147
Qr	-0.151
$MLSS$	-0.083
$Qi + Qr$	-0.158
$Qi \cdot MLSS$	-0.209
$(Qi + Qr) \cdot MLSS$	-0.189
$SSVI$	0.040
$RASS$	-0.065

Table 2.6. Correlation of SSe with the clarifier operating variables.

The effluent SS concentration for the whole study period was persistently very low, with an average of 5.03 mg/l and a standard deviation of 3.35 mg/l. A brief investigation into the operating conditions of the final clarifiers during that period, revealed that they were consistently underloaded. Typical operating parameters such as, the solids loading, surface loading and overflow rate, were well below recommended design and operating levels. Such conditions ensured high clarification performance and a very low effluent SS throughout the period despite the variability of the applied solids load to the tanks. As a result, the effluent SS series behaves like a random process rather than a structured series, without any periods of excitation, which hampers the identification of a successful model.

Using linear regression and the data from the selected study period several models were fitted, shown in Table 2.7 and Fig. 2.16. The model structures range from simple pseudo "steady-state" relationships (eq. 2.12a-e), to autoregressive structures with an added forcing function (eq. 2.12f-h) and include some of the models discussed in the review. The main variables considered, were those that are reported to affect the clarification performance such as, the applied solids load, the settleability of the sludge, the feed flow rate and concentration and the underflow load.

Model equation		Estimated param.		Correl.	C.O.D.*
$SSe_t = a \cdot GF_t$	(2.12a)	a=0.0645		-0.189	-0.676
$SSe_t = a \cdot GF_t + b$	(2.12b)	a=-0.0187	b=5.88	0.189	0.0359
$SSe_t = a \cdot GF_t + b \cdot SSVI_t$	(2.12c)	a=-0.0185	b=0.203E-2	0.190	0.036
$+c$		c=5.73			
$SSe_t = a \cdot GF_t + b \cdot Gu_t + c$	(2.12d)	a=-0.0927	b=0.0598	0.210	0.0441
		c=5.84			
$SSe_t = a \cdot BODe_t + b$	(2.12e)	a=0.277	b=4.39	0.240	0.0578
$SSe_t = a \cdot SSe_{(t-1)} + b$	(2.12f)	a=0.400	b=3.03	0.400	0.160
$SSe_t = a \cdot SSe_{(t-1)} + b \cdot QF_t$		a=0.3851	b=-3.02E-5	0.411	0.169
$+c \cdot MLSS_t + d$	(2.12g)	c=-2.49E-5	d=3.692		
$SSe_t = a \cdot SSe_{(t-1)} + b \cdot GF_t$		a=0.378	b=-0.0244	0.416	0.173
$+c$	(2.12h)	c=3.65			

* coefficient of determination

where; $GF_t = (Qi_t + Qr_t) \cdot MLSS_t/A$ applied solids load $(kg/d \cdot m^2)$

$Gu_t = (Qr_t + Qw_t) \cdot RASS_t/A$ underflow solids load $(kg/d \cdot m^2)$

eq. 2.12a proposed by Pflanz (1969)

eq. 2.12g proposed by Chapman (1985)

Table 2.7. Performance of simple models for effluent SS prediction.

It can be seen that the above models predict fairly well the average SS concentration, but are unable to simulate daily variations; hence the observed correlation coefficient and C.O.D. are generally poor. This can be explained by the fact that the performance of the clarification zone depends also upon several unmeasurable factors such as, the fluid motion in the tank, the amount of floating solids, the buoyancy of solids due to escaping nitrogen gas, the shape of the overflow weir and the speed and direction of wind. Furthermore, the constant term in the models is large compared to the mean of the SSe series, while the estimated parameters for the applied load are always negative, which is contrary to previous studies presented in the review (Section 2.2.4).

In the selected data set no significant loss of solids occurred so that any derived model would be valid only for the underloaded conditions prevailing during the selected period. It is obvious that such a model would not be able to predict the effluent solids during a clarification failure resulting from solids overloading, filamentous bulking, rising sludge, high sludge blanket or any other operating problem. For this reason the effluent solids concentration was not simulated in subsequent model developments, but it was treated as a known output term, in order to avoid any errors introduced by neglecting the solids mass lost in the effluent.

2.5 Modelling the thickening function

2.5.1 General

For the simulation of the settling and thickening functions a number of different models have been discussed ranging from simple steady- state relationships to complex, multi-layer dynamic models based on hindered settling theory (Section 2.2.3). The performance of each model depends largely on the validity of the underlying theory and accompanied assumptions for the specific case study, as well as, on the amount of information and process observations available for the calibration and validation of the particular model structure.

Thus, for the implementation of a multi-layer model based on solids- flux theory, an implicit assumption is that the thickener operates always under hindered settling conditions with no compression in the tank bottom and that the hydraulic regime can be represented by the selected multi-CSTR configuration. Furthermore it is essential to have accurate information on the relation between settling velocity and concentration for different sludge characteristics, which can only be determined from specifically designed settling tests. However, in the available data from Cirencester plant, the information on solids settling velocity and sludge characteristics was insufficient, since no regular settling tests were carried out apart from the $SSVI$ test. Consequently values from the literature had to be used and the values reported by Johnstone et al. (1979) were considered more appropriate, since they were derived from a similar oxidation ditch plant. However the limitations of using literature-based values must be recognized, since considerable error may be introduced from inaccurate specification of the sludge characteristics.

2.5.2 Applicability of solids flux theory to Cirencester clarifiers

In order to assess the applicability of solids flux theory to the Cirencester clarifiers, the operating conditions were examined throughout the study period and the results are summarized in Table 2.8. It can be seen that the average loading conditions were generally low compared with typical design values for oxidation ditch clarifiers reported by Metcalf & Eddy (1979). The limiting flux of the clarifiers during the selected operating period was predicted using the exponential function (eq. 2.2a) for relating settling velocity and concentration and a number of literature-based values for the parameters Vo and K. The predicted limiting flux was compared with the applied solids flux to the clarifiers and was found substantially higher throughout the period except for a very small number of days (Fig. 2.17a,b). Furthermore, the predicted limiting concentration was found to be higher than the observed underflow concentration for most of the period (Fig. 2.17c). The results indicate that through-

out the study period the final clarifiers were substantially underloaded, which was also evident from the consistently high clarification performance despite the large variability in the applied solids load (Section 2.4).

Determinant	Units	Mean	Std.dev.	Typical val.
Detention time	hr	7.40	4.82	> 3.0
Surface load	$m^3/m^2 \cdot d$	10.7	6.77	8.0 – 16.0
Overflow rate	$m^3/m \cdot d$	46.7	35.2	< 125
App. solid load	$kg/m^2 \cdot hr$	1.878	1.41	1.0 – 5.0
Estimation of limiting flux $(kg/m^2 \cdot hr)$				
Reference	Vo (m/hr)	K (l/g)	Lim. flux	
Johnstone (1979)	5.18	0.38	3.053±1.41	
"	6.50	0.35	3.496±1.643	
Marriot (1981)	2.21	0.21	4.075±1.44	
Foster (1985)	2.50	0.27	3.412±1.35	

Table 2.8. Operating conditions of Cirencester clarifiers (1979 period)

According to the solids flux theory, such prolonged underloading conditions would have caused the disappearance of the sludge blanket (Section 2.2.2). A uniform solids profile of low concentration would dominate in the tank with only a small layer near the bottom, where the concentration suddenly increases to the underflow concentration (Fig. 2.3)

The above hypotheses agree to some extent with observations made by Johnstone (1979), who reported that the sludge blanket at the Cirencester clarifiers was not very distinct. However the limitations of the solids flux theory to predict the formation of a dilute sludge blanket, having a concentration below the limiting (C_L), are also evident. The existence of a dilute blanket during underloaded periods agrees with experimental observations made by Hibbert & Jones (1974). They found that for flocculent suspensions like the activated sludge, the solids flux theory based on results from batch settling tests overestimates the handling capacity of the clarifiers; hence it cannot adequately simulate the sludge blanket variations. They attributed this discrepancy to the effect of partial support on the solids, which is transmitted from the tank bottom through the blanket and reduces their settling velocity from the 'ideal' value determined from settling tests. They also found that the effect of partial support is more pronounced at low underflow velocities and low blanket depths, which is normally associated with low loading rates. According to their observations a sludge blanket with a concentration gradient can exist, even if the applied flux is lower than the estimated limiting flux.

2.5.3 Development of a simple model

It was already shown that the final clarifiers were operating at a load below their predicted maximum capacity almost throughout the study period. Under these conditions the solids-flux theory was shown to have limitations in predicting the existence of a dilute sludge blanket. Hence the implementation of a complex, multi-layer model, such as those discussed in the review (Section 2.2.3), was not considered justifiable in this study, since simpler models could be investigated producing satisfactory results. However for the wider applicability of the model under any loading conditions of the clarifiers, their thickening limitations would need to be taken into consideration based on the concepts of solids-flux theory.

Examination of the data series serving as the inputs and outputs to the final clarifiers (Fig. 2.2), showed significant correlation between input and output mass of solids. Assuming that the solids in the clarifier act as conservative substances, the following relationship was derived based on mass-balance between input and output solids mass :

$$\text{Accum. in Clarifier} = \text{Input Mass} - \text{Output Mass}$$

$$\frac{dM}{dt} = (Qi_t + Qr_t) \cdot MLSS_t - [(Qr_t + Qw_t) \cdot RASS_t + (Qi_t - Qw_t) \cdot SSe_t] \tag{2.13}$$

where; dt : integration interval $[T]$,
M : mass of solids in final clarifiers $[M]$,
Qi_t : crude sewage flow rate $[L^3T^{-1}]$,
Qr_t : recycle sludge flow rate $[L^3T^{-1}]$,
Qw_t : surplus sludge flow rate $[L^3T^{-1}]$,
$MLSS_t$: mixed liquor concentration in the ditch $[ML^{-3}]$,
SSe_t : effluent suspended solids conc. $[ML^{-3}]$,
$RASS_t$: underflow concentration $[ML^{-3}]$.

Assuming that the accumulation of solids in the tank is negligible compared to the mass of solids passing through the clarifier over the simulation step of 1 day, the following pseudo steady-state equation was derived for predicting the underflow concentration :

$$\widehat{RASS}_t = \frac{(Qi_t + Qr_t) \cdot MLSS_t - (Qi_t - Qw_t) \cdot SSe_t}{Qr_t + Qw_t} \tag{2.14}$$

For the determination of $\widehat{RASS}$ the available measurements are average daily values of the flow rates and effluent SS and daily spot measurements of the $MLSS$.

The predicted daily $RASS$ from equation 2.14 was compared with the measured values from spot samples and the results are presented in Fig. 2.18 and Table 2.9. The observed and predicted series showed significant correlation, however there was a systematic difference between them, particularly in the second half of the simulation period, indicating a solids mass imbalance over the clarifier. Consequently the model performance was poor which is depicted by the negative coefficient of determination.

Prediction error (mg/l)		Predicted $RASS$ (mg/l)	
RMS error	2631	mean	8110
mean	-1208	std. dev.	2637
std. dev.	2341	variance	0.698E+7
variance	0.550E+7	coef. var.	0.325
sum square	0.196E+10	skewness	0.905
Correl. R	0.599	kurtosis	4.676
C.O.D.	-0.033		

Table 2.9. Performance of pseudo steady-state model for the $RASS$.

Potential causes of the observed mass imbalance can be :

1. Possibility of systematic error in the flow rate measurements.
2. Accumulation of solids in the final clarifiers (assumed negligible).
3. Systematic deviation of the spot measurements of $MLSS$ and $RASS$ concentrations from their daily average values.

The first source of error can be caused by incorrect calibration of the flow measuring instruments, but the existence of such error cannot be easily assessed, since no information about the accuracy of the instruments was available. In the recycle flow measurements, there were missing observations in the period between day 215 and 230 in which the model showed the poorest performance. The second source regarding the accumulation of solids in the clarifiers, may be significant over short time periods, however its effect is expected to be minimal over longer periods. It follows that, this source of error cannot explain the systematic deviation of predicted $RASS$ from the observed series. Finally, the third source of error, which can be attributed to the diurnal variation of $MLSS$ and $RASS$ concentrations caused mainly by the time-varying input flow, can significantly affect the model predictions. Unfortunately, no information on the diurnal variation of the above variables existed for testing this hypothesis.

Employing linear regression a number of other relationships were investigated, which might show better performance in predicting the underflow concentration and

are presented in Table 2.10.

Model equation		Estimated param.		R	C.O.D.	RMSe
$RASS_t = a \cdot \widehat{RASS}_t + b$	(2.15a)	a=0.588	b=2135	0.598	0.358	2069
$RASS_t = a \cdot \widehat{RASS}_t +$ $b \cdot SSVIt + c$	(2.15b)	a=0.585 c=2232	b=-1.11	0.598	0.358	2069
$RASS_t = a \cdot \widehat{RASS}_t +$ $b \cdot MLSS_t + c$	(2.15c)	a=0.311 c=995.8	b=0.873	0.682	0.465	1889
$RASS_t = a \cdot RASS_{ob(t-1)} + b$	(2.15d)	a=0.807	b=1346	0.806	0.650	1530
$RASS_t = a \cdot RASS_{ob(t-1)} +$ $b \cdot RASS_{ob(t-2)} + c$	(2.15e)	a=0.584 c=986	b=0.276	0.822	0.676	1473
$RASS_t = a \cdot RASS_{ob(t-1)} +$ $b \cdot \widehat{RASS}(t) + c$	(2.15f)	a=0.702 c=697.5	b=0.169	0.818	0.668	1489
where; $\widehat{RASS}(t)$ is given by equation 2.14						

Table 2.10. Models studied for simulating the underflow concentration.

Starting with the previous relationship (equat. 2.14) which was based on mass-balance, a constant term was added in order to account for the systematic error (eq. 2.15a). The estimated slope was much lower than unity, while the constant term represented a substantial proportion (31%) of the mean observed $RASS$ and reduced the RMS error by 21%. The incorporation of the sludge settling characteristics, expressed by the $SSVI$ value, as an additional term did not improve the fit (eq. 2.15b), while the incorporation of the $MLSS$ improved the fit slightly (eq. 2.15c).

In the above analyses the operating data for each day were treated as independent events. However, in reality the operating state of the plant on any particular day is influenced by the past operating conditions, and the magnitude of this effect depends on the time constants of the process. Since the nominal retention time in the clarifiers at DWF was 17 hr, then some influence from previous day operating conditions is expected. Such effect can be investigated through autoregressive models, in which past values of the particular variable are included in the model equation.

In the first-order autoregressive model the current $RASS(t_k)$ was expressed as a function of the previous day's measurement $RASS(t_{k-1})$, (eq. 2.15d). The model showed a substantial improvement in performance compared to all previous models judged by the higher correlation coefficient, C.O.D. and the lower RMS error (Fig. 2.19). The incorporation of a second-order autoregressive term $RASS(t_{k-2})$, improved the fit marginally (eq. 2.15e), implying that the effect of the second previous day was not important. In the first-order model, the addition of the current forcing function term, given by eq. 2.14, improved the performance marginally (eq. 2.15f).

This suggests that most of the variation in the observed $RASS$ was explained by the autoregressive term and only a small part was explained by the current loading of the clarifier.

From the brief investigation of pseudo-steady-state and autoregressive models, it is apparent that the process exhibits significant autoregressive structure, to the extent that process states can be better predicted from past values of that state than from rational input-output relationships. However, due to their structure autoregressive models have limited applicability for long-term forecasting and process control. This is because knowledge of the past state values is necessary for their implementation, and in addition they do not exploit the internal mechanisms of the process. The performance of the steady-state models was satisfactory over the first half of the simulation period, but systematic deviation was observed in most of the latter half. Among the possible causes discussed were limitations of the data used, such as missing observations and the use of spot measurements for $MLSS$ and $RASS$ instead of their daily average.

2.5.4 Need for a dynamic model

The models discussed so far, have used average daily values of the inputs to predict average (steady-state) daily concentrations of the underflow. These models cannot simulate the effect of transient behaviour upon the daily $RASS$ concentration resulting from changes in the input and operating variables. For this reason they could only be used for predicting average daily performance under relatively constant operation.

In this study, the developed models were used for predicting the plant performance under both constant and variable operating conditions. Consequently a model which accounts for the dynamic effects of instantaneous changes in the operating variables would be more appropriate.

2.5.5 Development of a dynamic model

It is well known that the hydraulic regime of a reactor affects significantly the processes involved. Between the two extreme cases of complete mixing and plug-flow conditions, there is an intermediate mixing regime. This can be described mathematically either by the introduction of a dispersion coefficient or by representing the reactor with a number of completely stirred tank reactors (CSTR) in series (Tomlinson & Chambers 1979). A single CSTR corresponds to the completely-mixed conditions, while as the number of tanks increases the hydraulic regime approaches plug-flow conditions. In order to assess the number of tanks that best describe a given hydraulic regime, the output response of the reactor to forced input signals has

to be determined and compared with theoretically derived curves.

Such studies were not undertaken for the Cirencester clarifiers. Therefore the representation of their hydraulic regime had to be conducted by analyzing their output response to the natural variation of the applied inputs. Initially the clarifiers were simulated as a single CSTR and then as two CSTRs in series. Larger number of CSTRs was avoided because the model becomes unnecessarily complex and the simulated hydraulic regime in the tank approximates plug-flow conditions, which were not expected due to the shallow tanks at the plant.

Another important assumption is the consideration of the clarifier as a flow splitting device, where the input flow splits into an overflow and an underflow stream. The former stream represents the clarified effluent containing very low solids concentration and moves upwards from the feed level towards the overflow weir. The latter stream containing the majority of the input solids, moves downwards through gravity and bulk settling and forms the sludge blanket. The model for the underflow concentration was based on solids mass balance according to eq. 2.13. For modelling purpose the tank representation by one and two CSTRs is shown schematically in Fig. 2.20a,b, assuming that the total volume of the CSTRs equals the total volume of the final clarifiers. The following equations were derived :

- Single CSTR :

$$Vcl \cdot \frac{dRASS_t}{dt} = (Qi_t + Qr_t) \cdot MLSS_t - (Qi_t - Qw_t) \cdot SSe_t - (Qr_t + Qw_t) \cdot RASS_t \quad (2.16)$$

- Two CSTRs in series :

$$\frac{Vcl}{2} \cdot \frac{dRASS1_t}{dt} = (Qi_t + Qr_t) \cdot MLSS_t - (Qi_t - Qw_t) \cdot SSe_t - (Qr_t + Qw_t) \cdot RASS1_t \quad (2.17a)$$

$$\frac{Vcl}{2} \cdot \frac{dRASS_t}{dt} = (Qr_t + Qw_t) \cdot (RASS1_t - RASS_t) \quad (2.17b)$$

where; Vcl : total volume of final clarifiers $[L^3]$,
$RASS1_t$: output sludge concentration from first CSTR $[ML^{-3}]$.

The performance of the above models was assessed from their ability to reproduce the $RASS$ observations and is summarized in Table 2.11 and Figure 2.21. Both models showed satisfactory performance, although there was a systematic overestimation of the $RASS$, particularly between days 150 and 260, producing a significant prediction error and a poor C.O.D. coefficient. The two dynamic models showed similar performance, indicating that variations in the hydraulic representation of the tanks did not significantly affect their dynamic behaviour. The performance of the

two-CSTR model was marginally superior, however such an improvement did not justify the additional complexity in its structure. Subsequently the single CSTR model was adopted for the sake of simplicity.

Determinant	pred. $RASS$ (mg/l)		obs. $RASS$ (mg/l)	Slud. Blan. (m)
	1 "CSTR"	2 "CSTR"		
mean	7999	7987	6902	0.784
std. dev.	2453	2467	2588	0.364
variance	0.604E+07	0.612E+07	0.672E+07	0.133
coef. var.	0.306	0.308	0.375	0.464
skewness	0.769	0.803	0.078	-0.252
kurtosis	4.12	4.29	2.086	2.08
RMS error	2331	2320		
Err. mean	-1097	-1084		
Err. std.dev.	2057	2051		
Err. variance	0.4248E+7	0.4222E+7		
R	0.668	0.671		
C.O.D.	0.189	0.196		

Table 2.11. Dynamic model performance for the thickening zone.

The sludge blanket level was considered not to affect the underflow concentration. Its variation was simulated as the volume occupied by the accumulated sludge, assuming that the contained solids concentration is uniform and equal to the underflow concentration. This assumption is rather crude and tends to underestimate the true sludge blanket level, because the solids concentration in the blanket is usually lower than in the underflow. In addition, a concentration gradient in the blanket has been reported from experimental observations in laboratory-scale clarifiers (Hibbert & Jones 1974 ; George & Keinath 1978). However this simulation intends only to give a rough estimate of the likely variations in its level, since no measurements of the blanket level were available for comparison and refinement of the model structure.

The model was based on solids mass-balance over the volume occupied by the sludge blanket shown schematically in Fig. 2.20c, where the tank shape was approximated to cylindrical having the average depth of 2.17 m. Hence :

$$\frac{d(V_{BL_t} \cdot C_{BL_t})}{dt} = Gi_t - Gu_t \qquad (2.18a)$$

$$\frac{dV_{BL}}{dt} \cdot C_{BL_t} + \frac{dC_{BL}}{dt} \cdot V_{BL_t} = Gi_t - Gu_t \qquad (2.18b)$$

Assuming that $C_{BL_t} = RASS_t$ at all times gives :

$$\frac{dC_{BL_t}}{dt} = \frac{dRASS_t}{dt} = \frac{Gi_t - Gu_t}{Vcl}$$

from equation 2.16. Substituting the above equation into 2.18b gives :

$$\frac{dV_{BL_t}}{dt} \cdot C_{BL_t} = (Gi_t - Gu_t) \cdot \frac{Vcl - V_{BL_t}}{Vcl} \qquad (2.18c)$$

But, $V_{BL_t} = Vcl \cdot BL_t / H_T$ and substituting into eq. 2.18c produces :

$$\frac{dBL_t}{dt} = (Gi_t - Gu_t) \cdot \frac{H_T - BL_t}{Vcl \cdot C_{BL_t}} \qquad \text{or}$$

$$\frac{dBL_t}{dt} = [(Qi_t + Qr_t) \cdot MLSS_t - (Qi_t - Qw_t) \cdot SSe_t - (Qr_t + Qw_t) \cdot RASS_t] \cdot \frac{H_T - BL_t}{C_{BL_t} \cdot Vcl} \qquad (2.18d)$$

where; C_{BL_t} : sludge blanket concentration $[ML^{-3}]$,
V_{BL} : sludge blanket volume $[L^3]$,
Gi_t : input solids load to sludge blanket $[MT^{-1}]$,
Gu_t : underflow solids load $[MT^{-1}]$,
$H_T = \frac{Vcl}{Acl}$: average depth of the tank $[L]$,
BL_t : sludge blanket level $[L]$.

The estimated sludge blanket level showed considerable variability and was predicted to fall to relatively low levels between days 120 and 265. However the model was expected to underestimate its level, as was previously discussed, but no observations existed for comparing the model predictions.

For the wider applicability of the thickening model under any operating conditions of the clarifiers, certain constraints have to be introduced to ensure that the maximum handling capacity of the tanks is not exceeded. It follows that the transmitted solids flux should be restricted by the limiting flux (G_L) and the sludge blanket concentration should be restricted by the limiting concentration (C_L). Thus equations 2.16 and 2.18 should be accompanied by the following constraints :

$$Gt_t = [(Qi_t + Qr_t) \cdot MLSS_t - (Qi_t - Qw_t) \cdot SSe_t]/Acl \leq G_L(Qr_t, Qw_t) \qquad (2.16a)$$

$$C_{BL_t} \leq C_L(Qr_t, Qw_t) \qquad (2.16b)$$

while equat. 2.18d takes the following approximate form, when its concentration is restricted by C_L :

$$\frac{dBL_t}{dt} = (Gi_t - Gu_t) \cdot \frac{H_T}{Vcl \cdot C_{BL_t}} - (C_{BL}(t_k) - C_{BL}(t_{k-1})) \cdot \frac{V_{BL}(t_{k-1})}{\Delta t} \qquad (2.18e)$$

2.5.6 Performance comparison between pseudo steady-state and dynamic models

The development of both the steady-state (eq. 2.14) and dynamic model (eq. 2.16) for predicting the $RASS$ concentration, was based on the principle of solids mass-balance

over the final clarifier. The main difference is that the dynamic model satisfies the solids balance at any time instant (in practice for very small time intervals), thus depicting the transient response between two different steady-state conditions. On the contrary, the steady-state model treats the daily measurements as independent events assuming implicitly that steady- state operating conditions are established, and in addition it does not account for the effect of sludge accumulation. The predictions of $RASS$ obtained from the dynamic model are generally less variable than those obtained from the steady-state model. This happens because the dynamic model predictions at the end of each simulation step, have not yet reached their steady-state values and also because the model accounts for the effect of temporary sludge accumulation in the clarifiers which tends to reduce the $RASS$ variability.

The performance of the two models was compared from their ability to reproduce the daily $RASS$ observations and was presented in Tables 2.9 and 2.11. It is apparent that the dynamic single-CSTR model performs better, judged by the higher C.O.D. and correlation coefficient between the observed and predicted series and the lower mean and RMS error. The performance comparison also shows that the dynamic nature of the process is important and as a result it cannot be adequately described by pseudo-steady-state models. Consequently the dynamic model (eq. 2.16 & 2.18) was selected for describing the thickening function of the final clarifiers.

2.5.7 Model validation

The dynamic model was validated using a different operating period in the data set. For this purpose the period between 9/5/1980 and 21/1/1981 was selected covering 258 days of operation. The above set covered similar period of the year with the previous data set and contained few missing observations, which were estimated by linear interpolation. The clarifiers were underloaded throughout the period and no incident of solids spillage in the effluent was experienced.

The dynamic model (eq. 2.16-2.18) performance using the new data set is shown in Table 2.12 and Fig. 2.22. The observed correlation between predicted and measured $RASS$ is higher than with the previous set. However a systematic error was observed between predictions and observations throughout the period and the predicted $RASS$ was 39% higher on average. This produced a very poor C.O.D. coefficient. For this purpose before deciding about the validity of the model the effect of diurnally varying inputs on the model performance was investigated, since this was identified as a potential source of error in Section 2.5.3.

Determinant	pred. *RASS*		obs. *RASS*	Sl. Blank.
	1 "CSTR"	2 "CSTR"		
mean (mg/l)	5970	5970	4281	1.194
std. dev.	1732	1743	1216	0.251
variance	0.301E+07	0.305E+07	0.148E+07	0.063
coef. var.	0.290	0.292	0.284	0.210
skewness	1.43	1.43	0.942	-0.199
kurtosis	5.55	5.56	4.05	3.118
RMS error	2025	2030		
Error mean	-1689	-1689		
std. dev.	1116	1125		
variance	0.125E+7	0.127E+7		
R	0.767	0.767		
C.O.D.	-1.781	-1.794		

Table 2.12. Basic statistics of model performance during validation.

2.5.8 Effect of diurnally varying inputs

In the available data there were no information regarding the diurnal variability of input flow and solids concentrations. Subsequently a typical daily profile of the input flow and $MLSS$ was assumed, found from a study at Leatherhead oxidation ditch plant (Wishart, 1986) during Dry Weather Flow conditions. Considering that the $MLSS$ spot measurements in the Cirencester monitoring programme were collected at 8am each day, then a set of hourly indices can be calculated, denoting the ratio of the hourly $MLSS$ values to the value at 8am. Similarly, hourly indices were calculated for the input flow, representing the ratio of the hourly flow values to the average daily value (Fig. 2.23) :

$$MLSS(ind)(t_k) = MLSS(t_k)/MLSS(8) \qquad (2.19a)$$

$$Qi(ind)(t_k) = Qi(t_k)/Qiav \qquad (2.19b)$$

These indices were then used to calculate the hourly input flow and MLSS values from the available daily values. Using these hourly values and neglecting any diurnal variation of the recycle flow, surplus sludge flow and effluent SS, the single CSTR model (eq. 2.16) was again employed to simulate the underflow concentration at 8am each day. The simulation results for both data sets are presented in Fig. 2.24 and Table 2.13.

Comparing the results with those obtained from constant inputs (Tables 2.11 & 2.12), it can be seen that although the correlation between predicted and observed

series has not improved, the prediction error is substantially reduced resulting in a higher C.O.D. coefficient. The improvement in performance was higher during periods of low input flow (DWF conditions), for which the above typical profile was observed. During the wet periods the diurnal variation is expected to deviate from that pattern due to the additional effect of surface runoff. The results indicate the importance of input variations upon the model performance, but also that the underlying structure of the model is adequate for describing the process dynamics. Hence the developed model was considered valid for the prevailing operating conditions of the clarifiers during the study period.

Determinant	1979 set	1980 set
RASS mean	6747	5099
std. dev.	1897	1413
variance	0.361E+7	0.200E+7
coef. var.	0.281	0.277
skewness	0.817	1.460
kurtosis	4.613	5.809
RMS error	2010	1241
Error mean	155	-818
std. dev.	2004	933
variance	0.403E+7	0.875E+6
R	0.640	0.758
C.O.D.	0.397	-0.042

Table 2.13. Dynamic model performance with diurnally varying inputs.

2.5.9 Sensitivity analysis

As it was discussed in the Introduction (Section 1.4.9) a sensitivity analysis examines the relative change in model predictions due to changes in the parameters or inputs of the model. The sensitivity is expressed by the sensitivity coefficient which is the ratio of state variation to the parameter variation as described in Appendix 3.

In the final clarifier model there are no parameters to be estimated, so the prediction error may be caused by either deficiencies in the model structure or measurement errors in the model inputs or both. Assuming that the given model structure is correct, then any discrepancy between predictions and observations is attributed to errors in the model inputs. Consequently, knowledge of the sensitivity coefficients may be helpful for the explanation of the above errors. The problem of solids mass-imbalance over the clarifier has already been discussed and various possible causes investigated. In addition, application of the model for two operating periods showed

different performance in reproducing the observed $RASS$ concentration. The above indicate that some external factors, such as an error in the inputs, significantly influence the model performance.

Consequently the sensitivity of the predicted underflow concentration to small deviations in the inputs from their nominal values was examined. The differential equation predicting the $RASS$ (eq. 2.16), is linear and its analytical solution is given by :

$$RASS_t = e^A \cdot RASS(t_0) + \frac{(Qi_t + Qr_t) \cdot MLSS_t - (Qi_t - Qw_t) \cdot SSe_t}{Qr_t + Qw_t} \cdot (1 - e^A) \quad (2.20)$$

where; $A = -(Qr_t + Qw_t) \cdot \Delta t / Vcl$

$\Delta t = t - t_0$

The inputs to the above model are the flows Qi, Qr, Qw and the solids concentrations $MLSS$ and SSe. Their sensitivity coefficients are given from the first derivative of equation 2.20, with respect to the particular input calculated at the nominal values (Fig. 2.25).

The sensitivity coefficients were calculated assuming a 10% deviation in each of the inputs from their nominal values. Their correlation with the prediction error in $RASS$ from the dynamic model (eq. 2.16) is significant for all the inputs, while in magnitude all the inputs except the surplus flow can seriously affect the $RASS$ concentration, shown in Table 2.14. In view of these results the possibility of error in any of the inputs exists.

Sens. traj.	Mean (mg/l)	Std.dev.	Correl. R
$Qi(s)$	433.6	206.1	-0.526
$Qr(s)$	-400.2	197.7	0.461
$Qw(s)$	-34.5	42.4	0.412
$MLSS(s)$	805.5	267.2	0.410
$RASS$ error	-1097.0	-1084.0	—

Table 2.14. Sensitivity trajectories of $RASS$ for 10% change in inputs.

2.6 Conclusions

From the study of the final clarification stage the following conclusions were reached :

- From the review on models of the thickening process it was found that most dynamic models are based on the limiting flux theory employing distributed-parameter structures, but despite their complexity they show limitations when applied to activated sludge thickeners. These mainly arise from the assumption of hindered settling of an 'ideal' slurry and the poor description of the sludge settling characteristics.
- The models developed to simulate the clarification process were mainly empirical, mechanistic relationships and no adequate mathematical description was found.
- The final clarifiers at the Cirencester plant performed well over the study period and no significant loss of solids in the effluent was experienced, which prohibited the identification of a suitable model to simulate the clarification function.
- For the underloaded condition of the clarifiers during the study period, the limiting flux theory was unable to predict the existence of a dilute sludge blanket in the tanks.
- A simple dynamic model was subsequently developed based on mass- balance, assuming that the clarifier is a flow-splitting device and representing its hydraulic regime by a single CSTR. This model was found adequate to simulate the underflow concentration under the prevailing underloaded conditions. However when tested against a different operating period its performance was poor.
- The effect of diurnal variation in the input flow and $MLSS$ concentration upon the model performance was studied by assuming a typical daily profile for those inputs. Consideration of the diurnal input variation improved significantly the model performance for both operating periods over that obtained with average daily values. In the light of these results the developed model structure was considered valid.
- For a wider applicability of the model under any loading conditions the thickening limitations of the clarifiers need to be considered along the principles of limiting flux theory. However regular settling tests are necessary for an accurate determination of the time varying settling properties of the sludge.

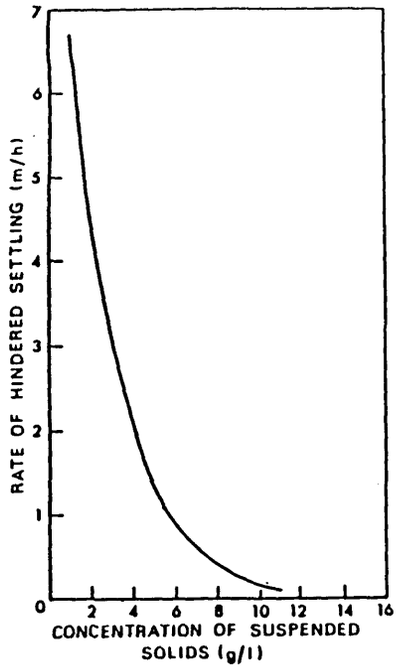


Fig. 2.1a. Typical variation of hindered settling velocity with solids concentration

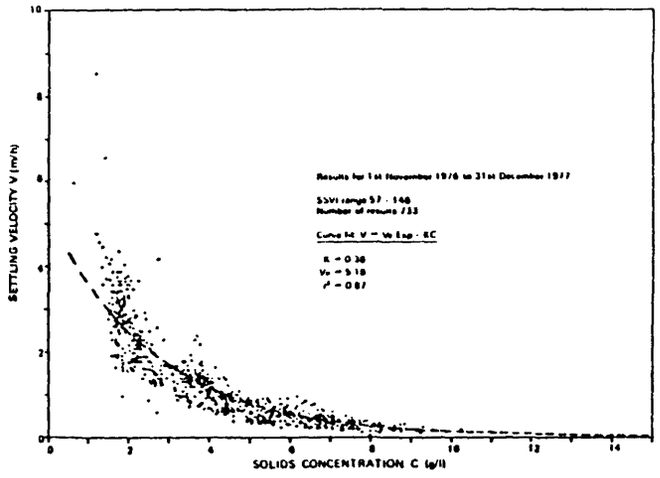


Fig. 2.1b. Experimental determination of settling velocity relation with concentration (Fig. 5 from Johnstone et al. 1979)

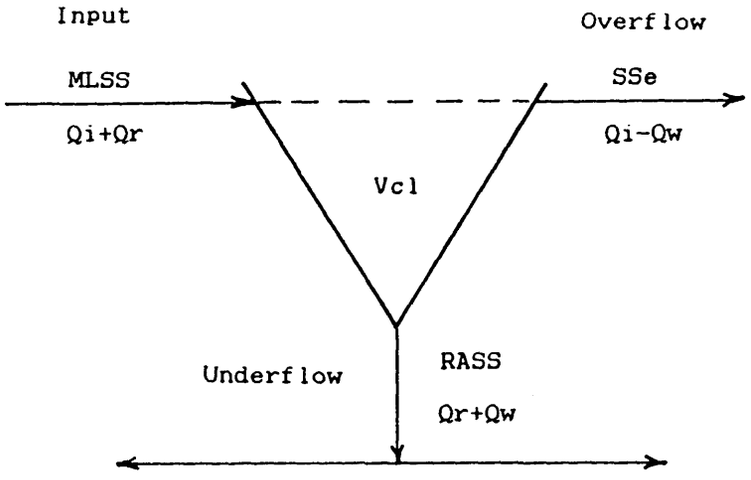


Fig. 2.2. Schematic representation of a final clarifier

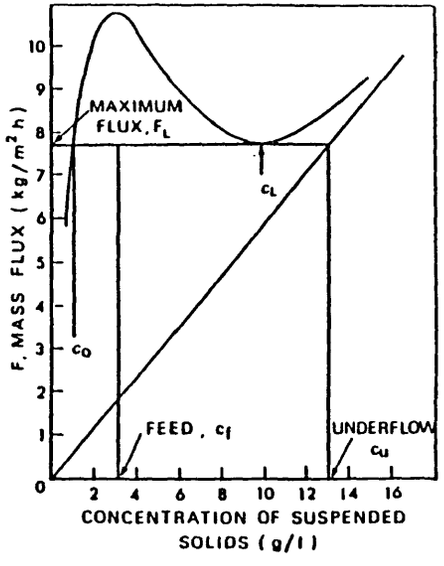


Fig. 2.3. Variation of solids flux with concentration

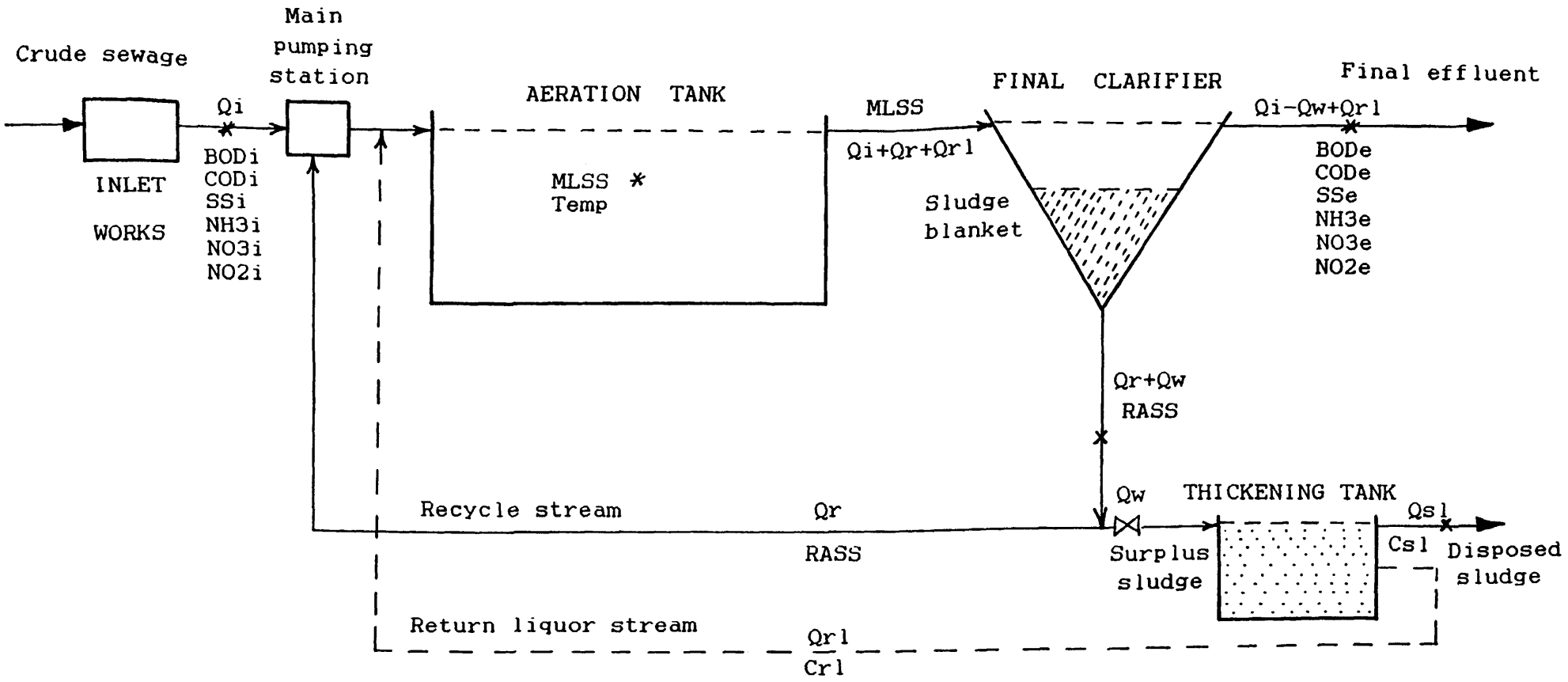


Fig. 2.4. Schematic representation of the Cirencester oxidation ditch plant with monitoring locations

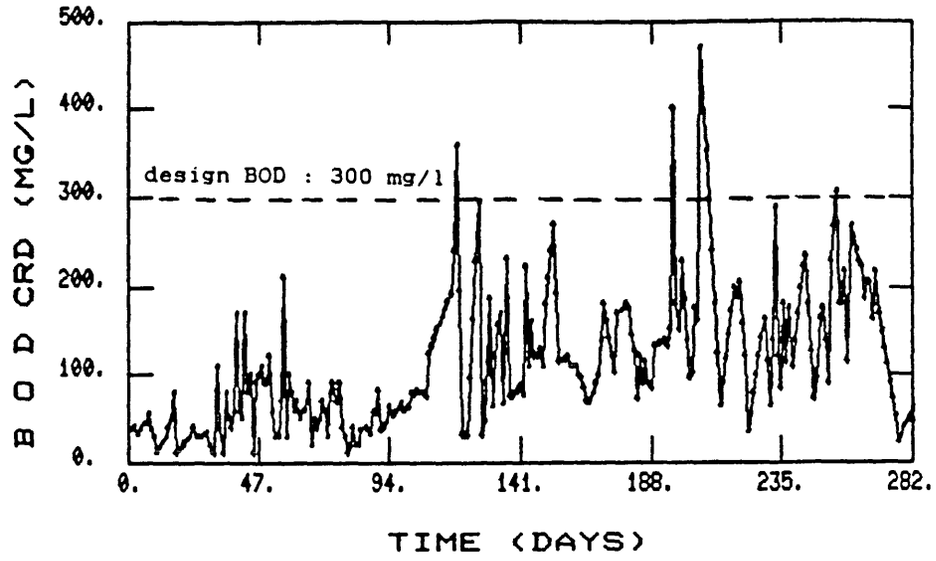


Fig. 2.5a. Crude sewage BOD_5 concentration

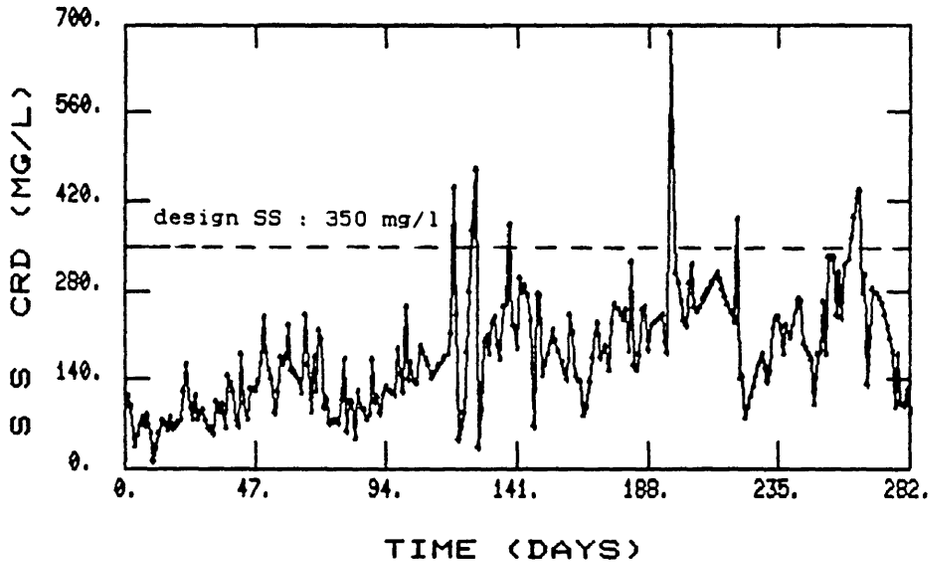


Fig. 2.5b. Crude sewage SS concentration

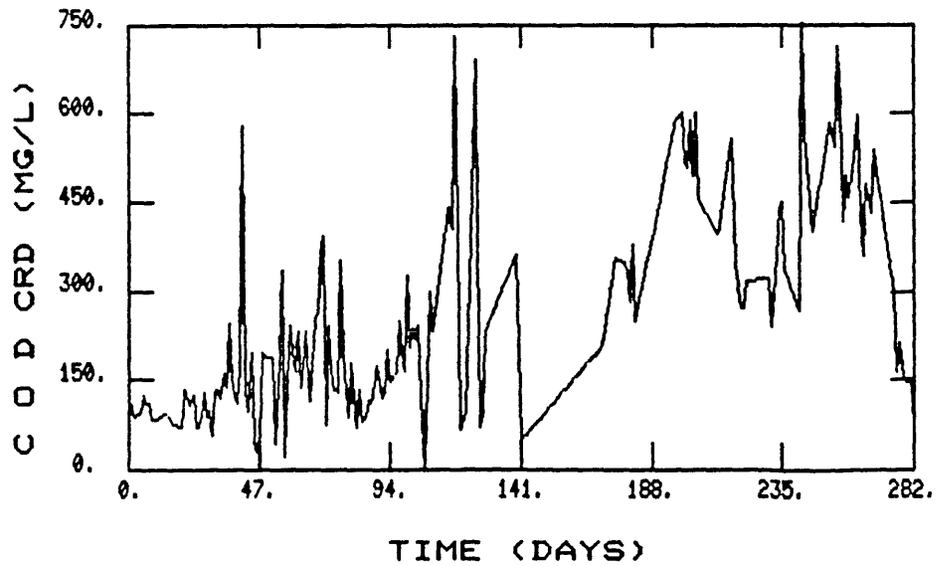


Fig. 2.5c. Crude sewage COD concentration

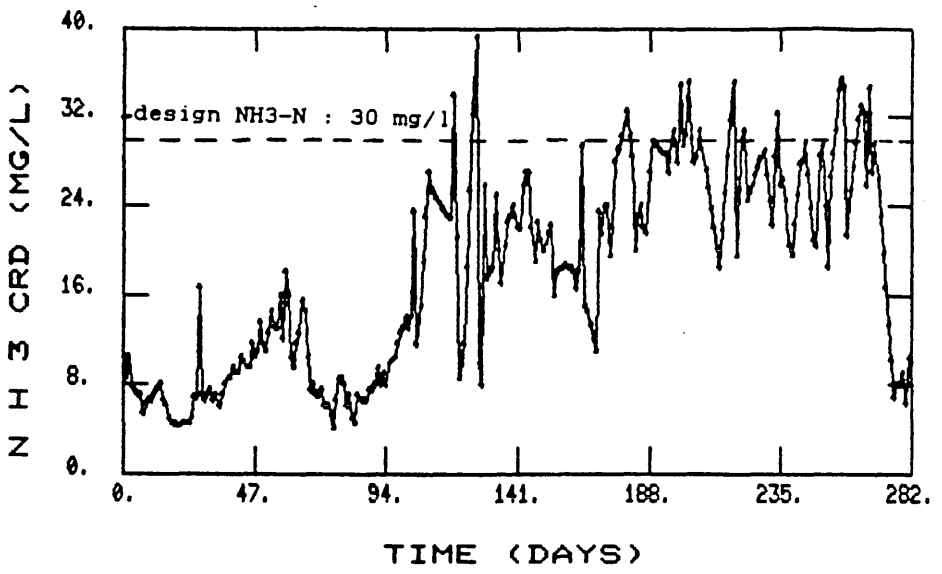


Fig. 2.5d. Crude sewage $NH_3 - N$ concentration

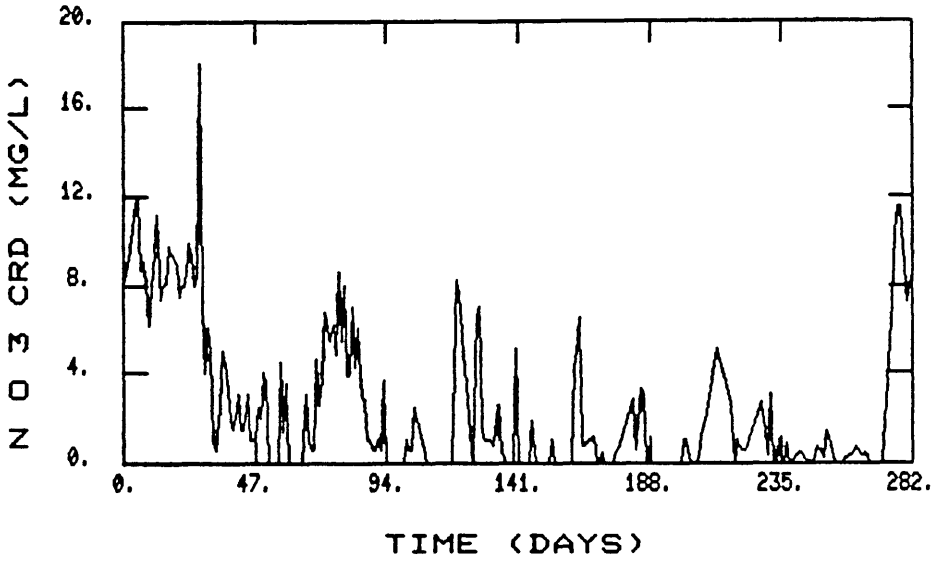


Fig. 2.5e. Crude sewage $NO_3 - N$ concentration

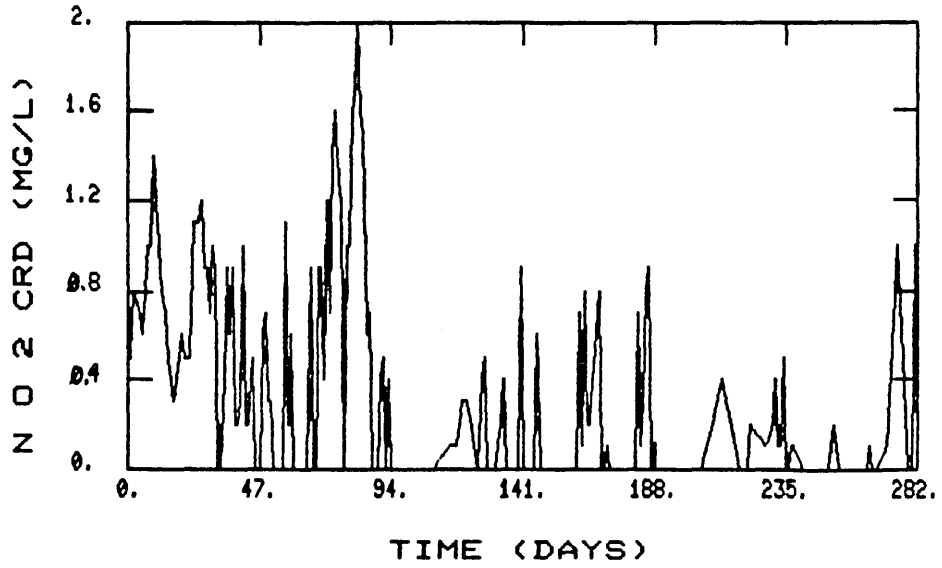


Fig. 2.5f. Crude sewage $NO_2 - N$ concentration

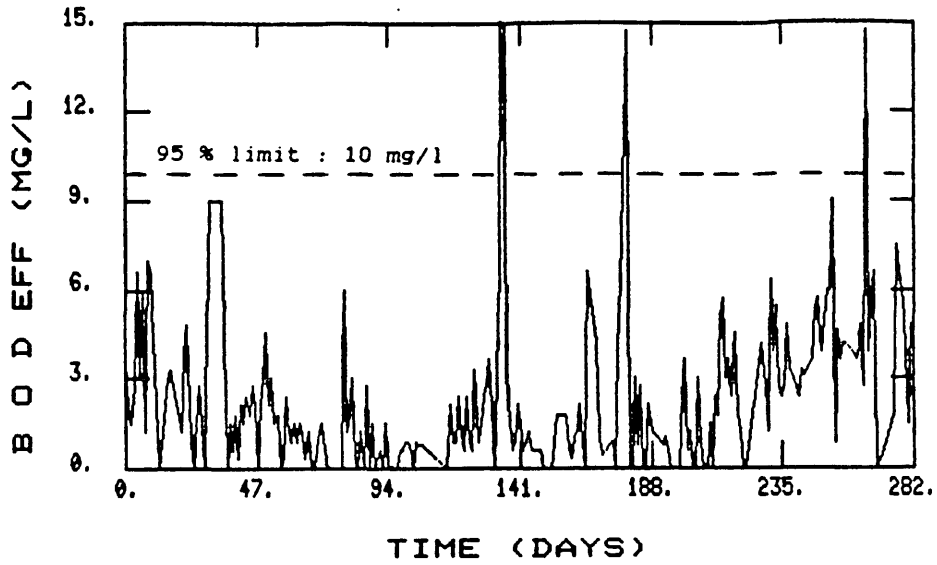


Fig. 2.6a. Final effluent BOD_5 concentration

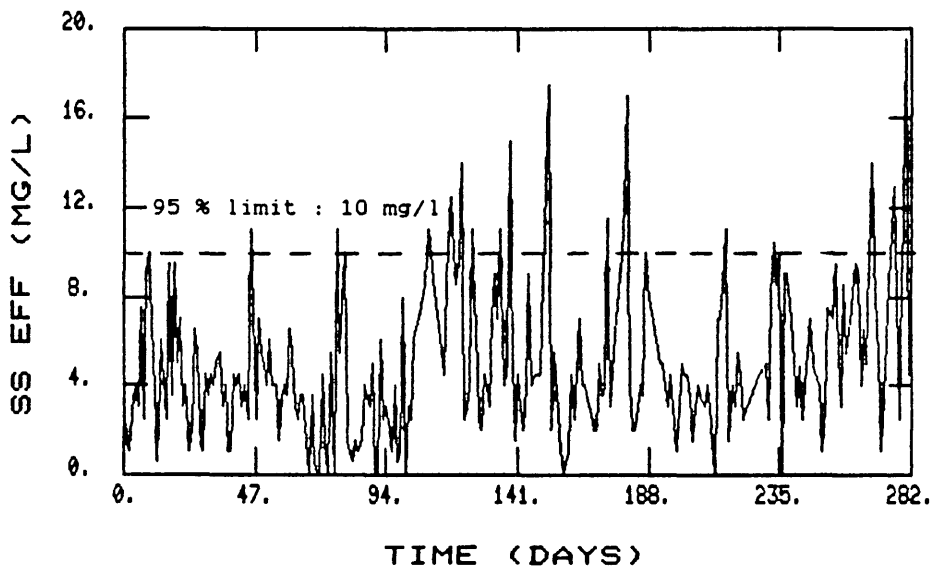


Fig. 2.6b. Final effluent SS concentration

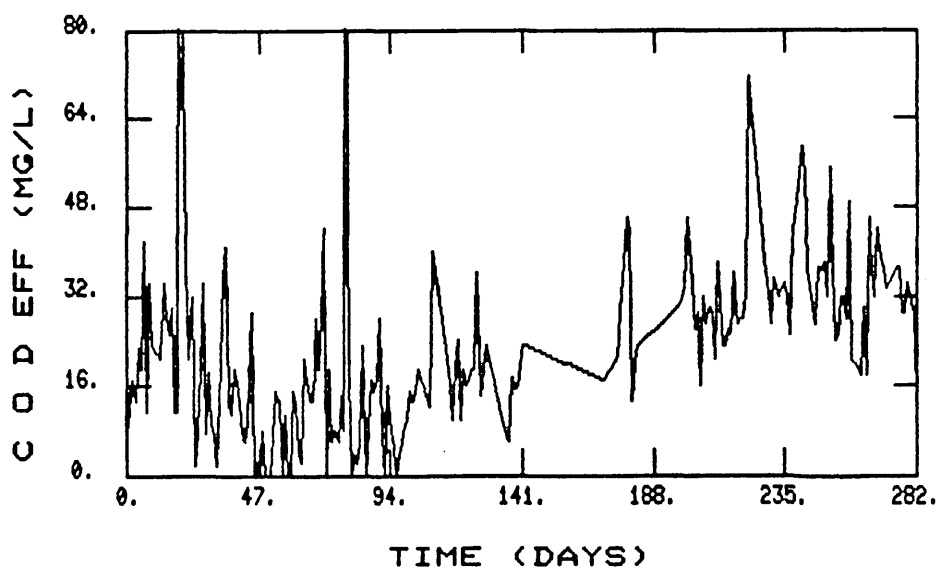


Fig. 2.6c. Final effluent COD concentration

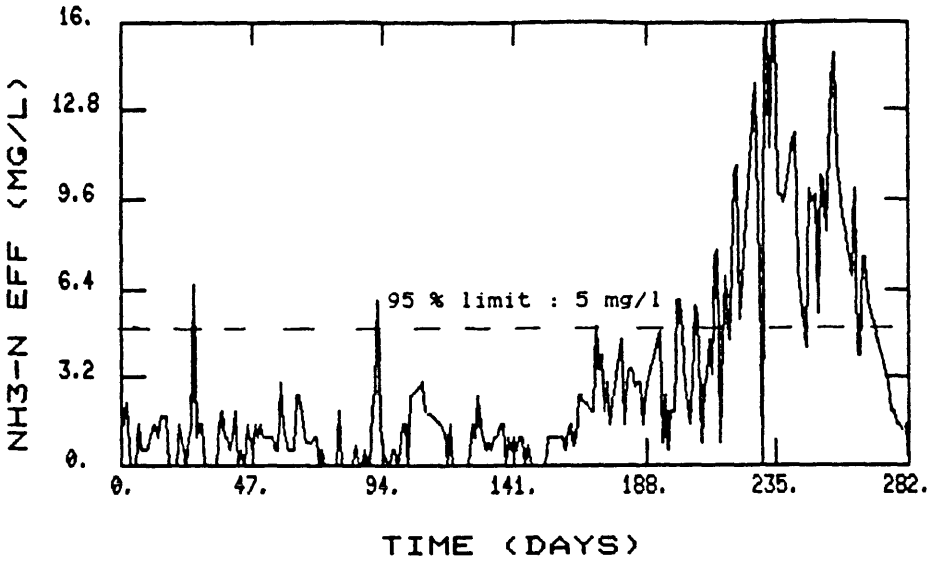


Fig. 2.6d. Final effluent $NH_3 - N$ concentration

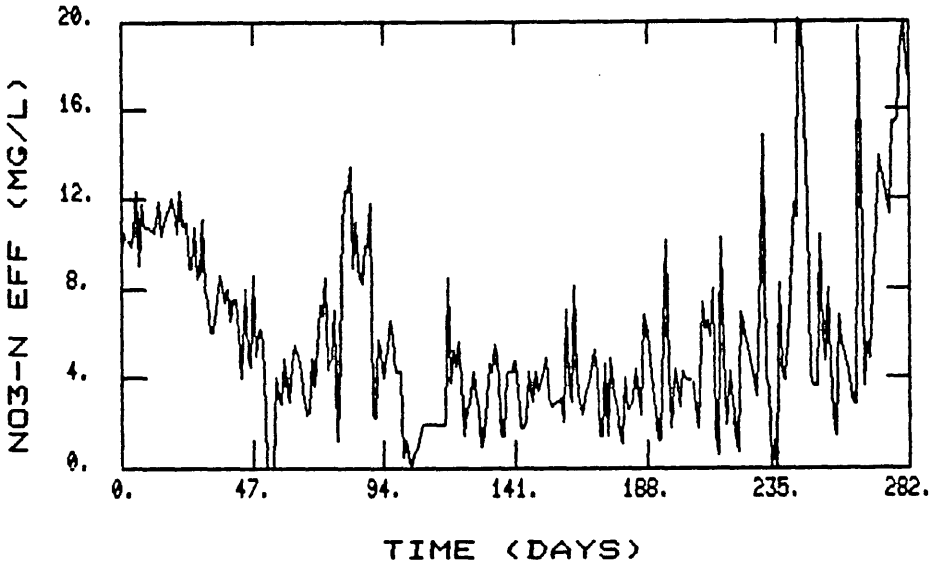


Fig. 2.6e. Final effluent $NO_3 - N$ concentration

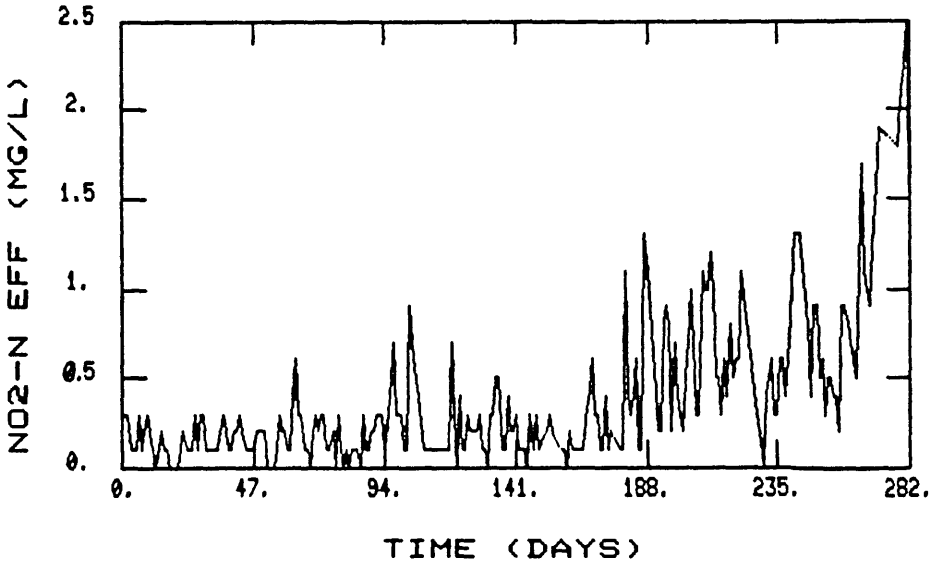


Fig. 2.6f. Final effluent $NO_2 - N$ concentration

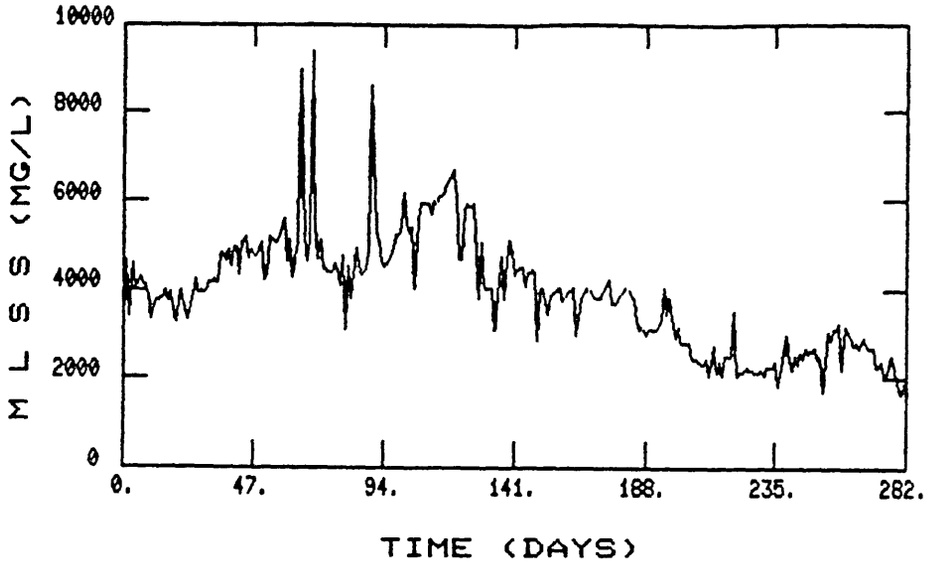


Fig. 2.7a. Mixed liquor suspended solids

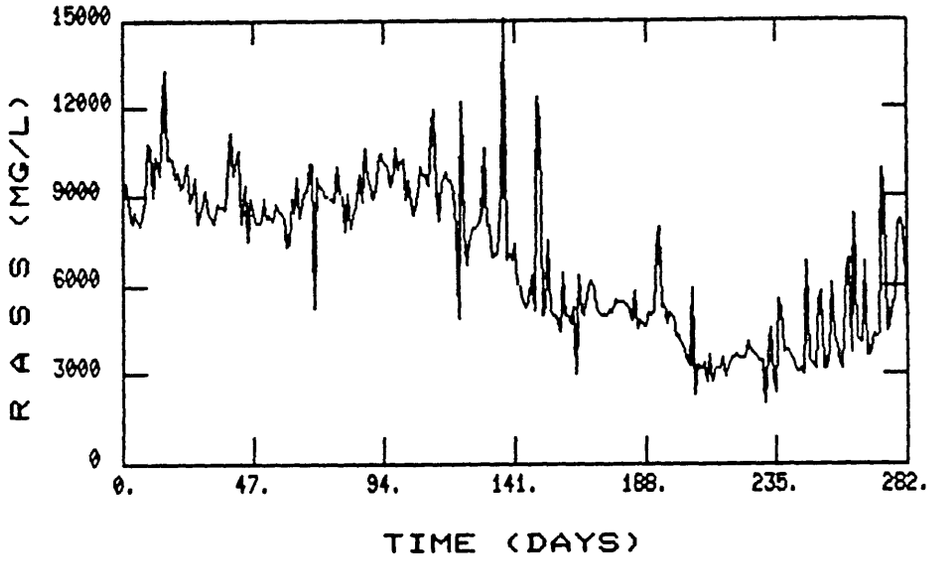


Fig. 2.7b. Recycle activated sludge solids

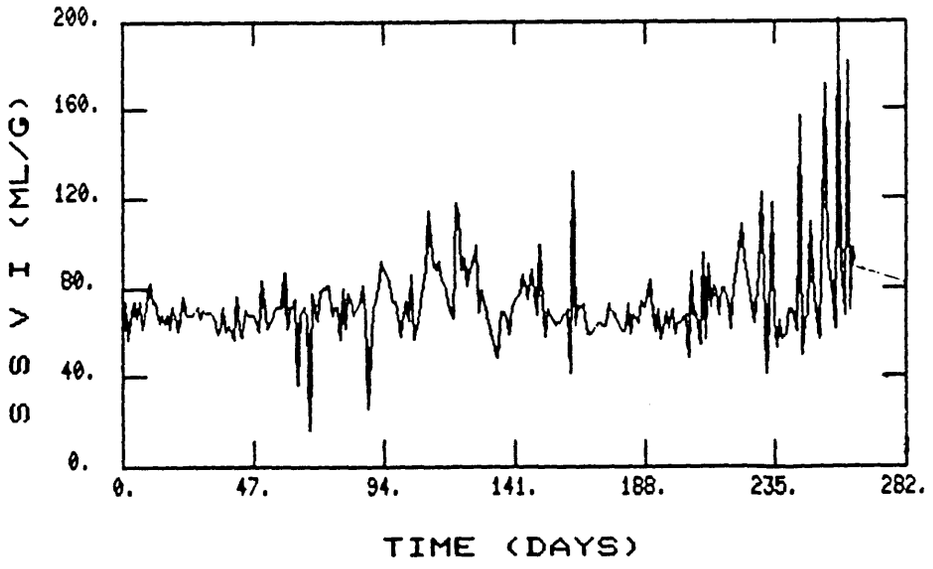


Fig. 2.7c. Settleability of mixed liquor (Stirred specific volume index)

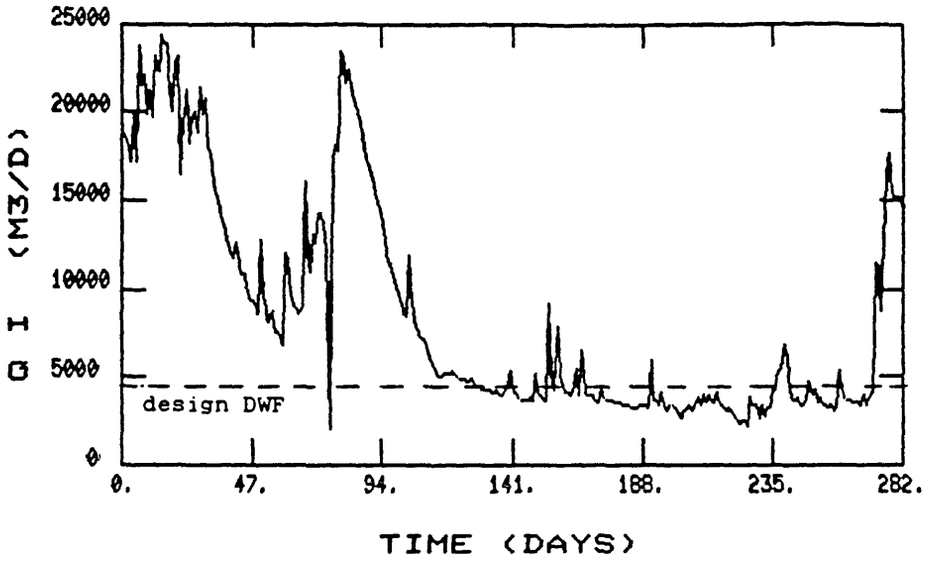


Fig. 2.8a. Crude sewage flow rate

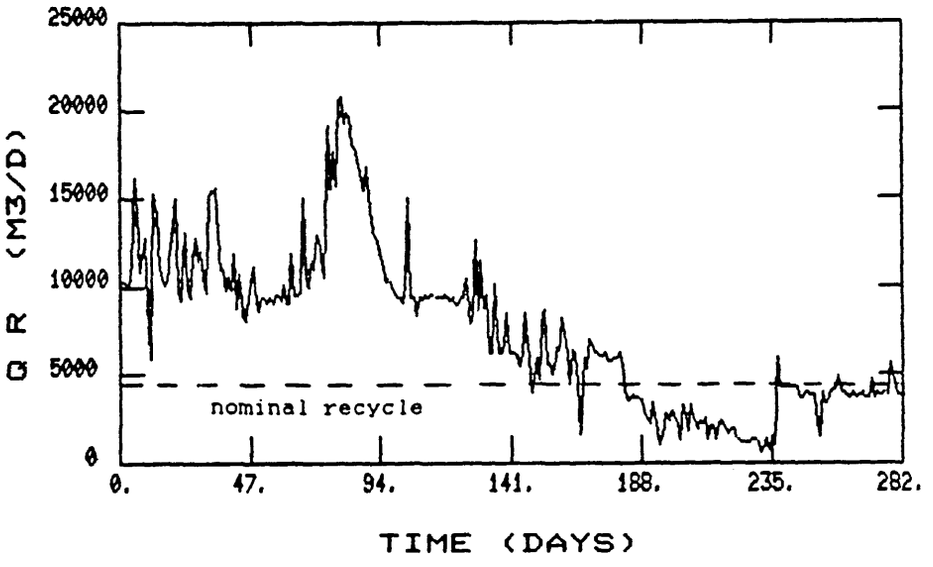


Fig. 2.8b. Recycle sludge flow rate

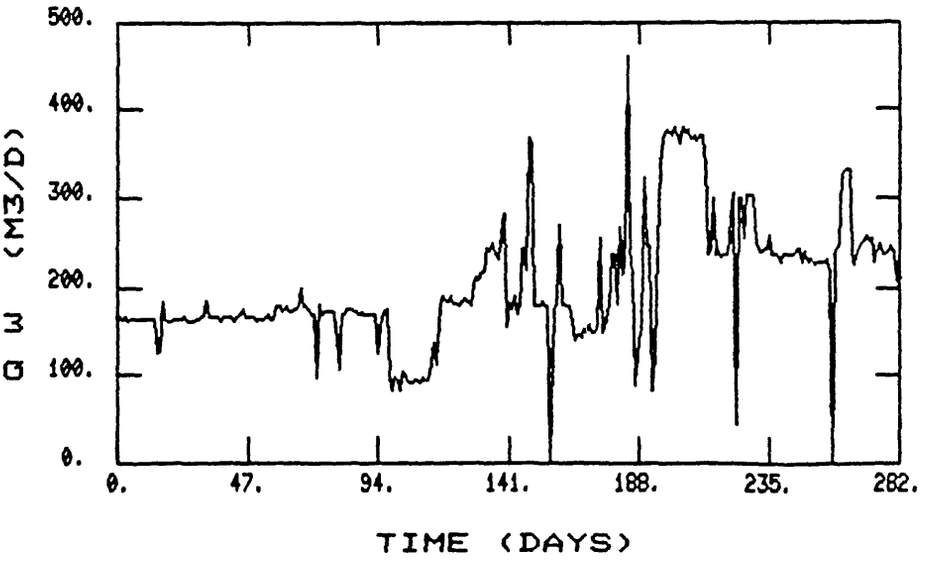


Fig. 2.8c. Surplus sludge flow rate

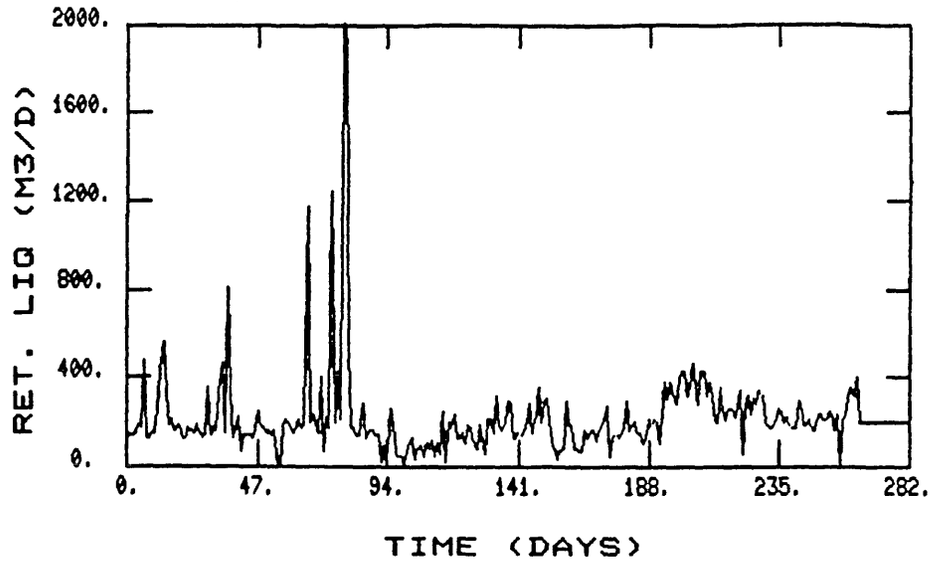


Fig. 2.8d. Return liquor flow rate

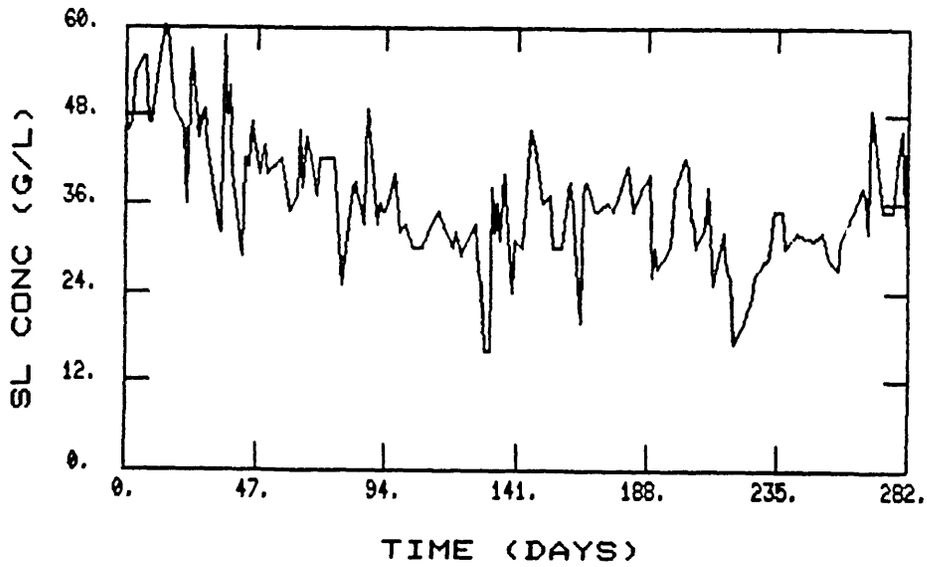


Fig. 2.9a. Thickened sludge concentration

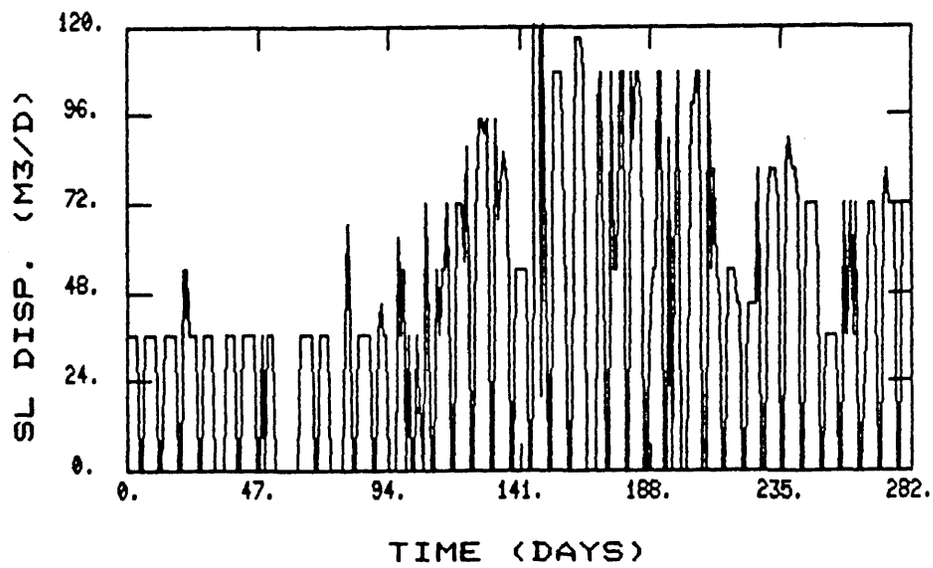


Fig. 2.9b. Tankered sludge volume per day

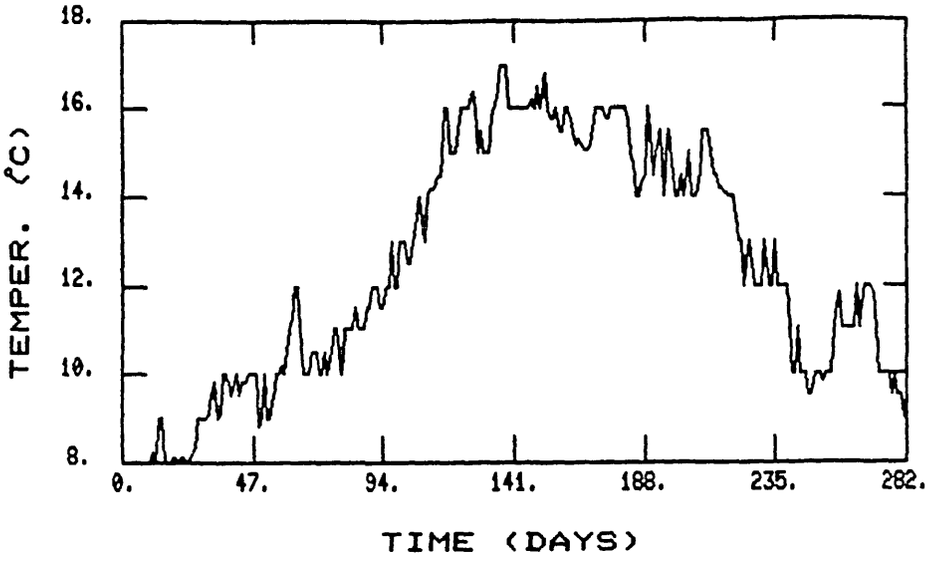


Fig. 2.10a. Mixed liquor temperature

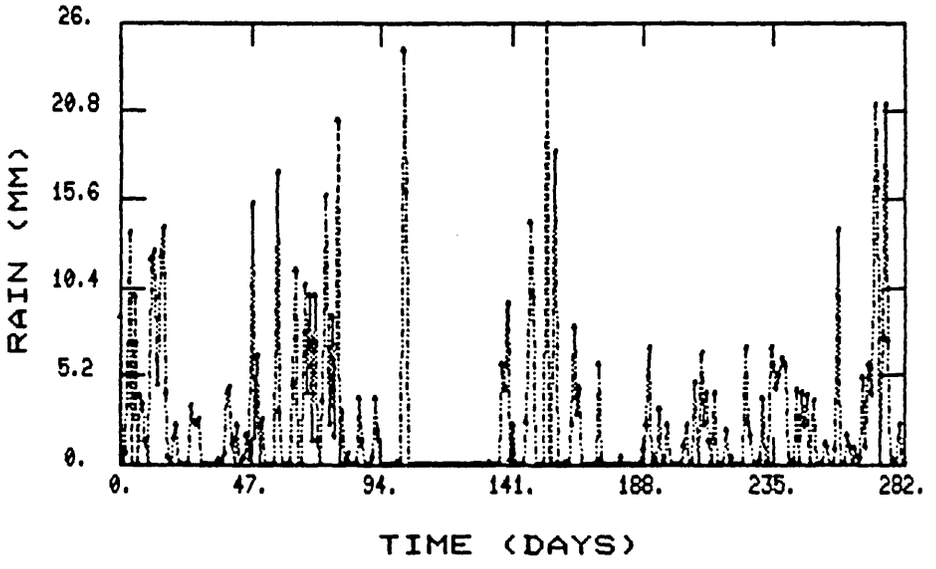


Fig. 2.10b. Rainfall at Cirencester

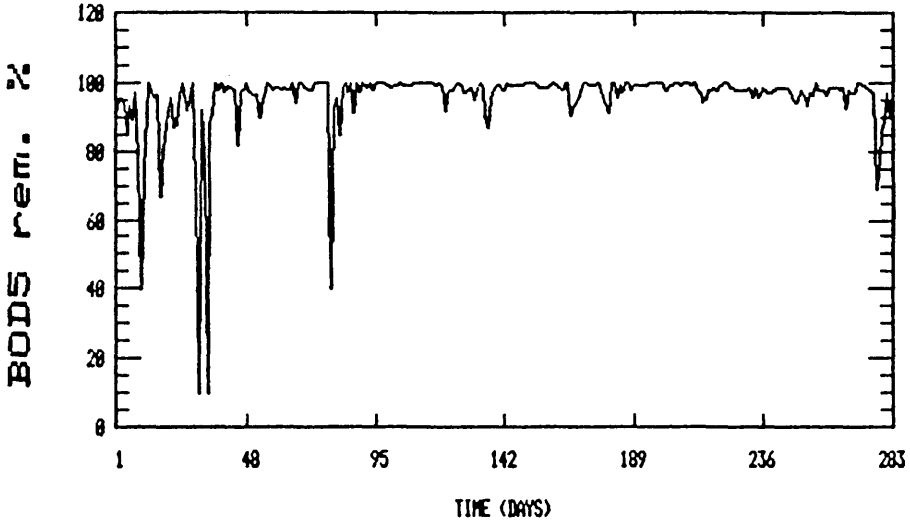


Fig. 2.11a. Percent removal of organic substrate BOD_5

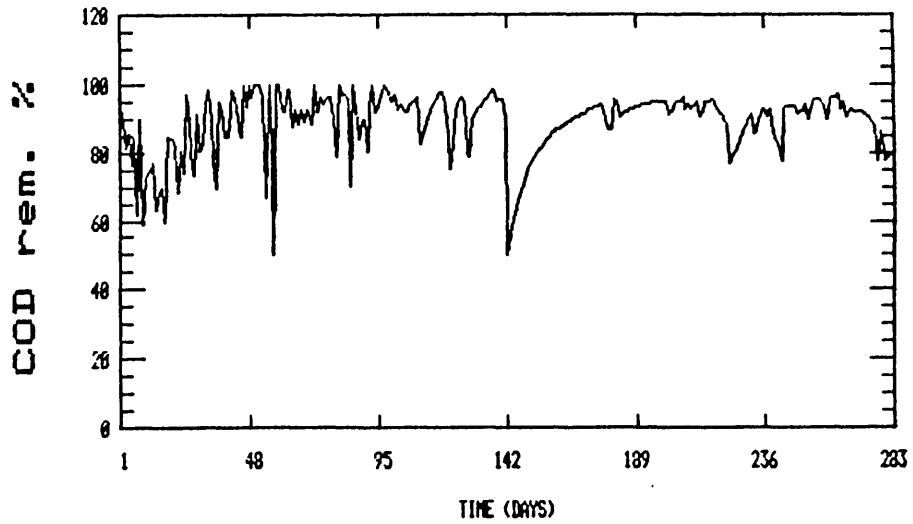


Fig. 2.11b Percent of COD removal

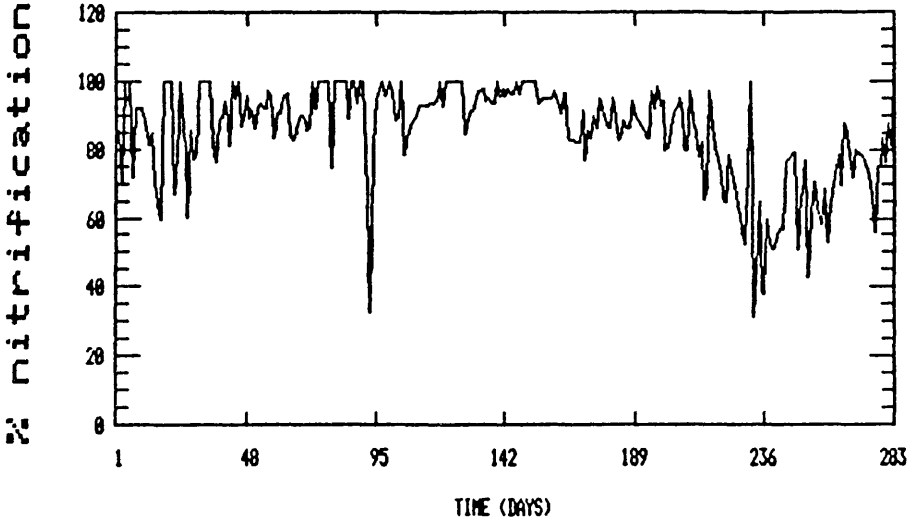


Fig. 2.11c. Percent removal of ammonia ($NHs - N$) (nitrification)

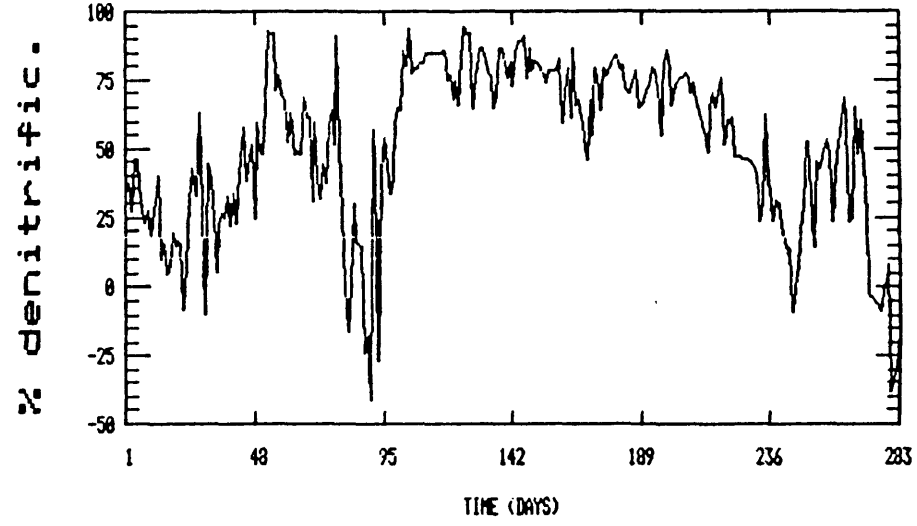


Fig. 2.11d. Percent removal of measured nitrogenous compounds (denitrification)

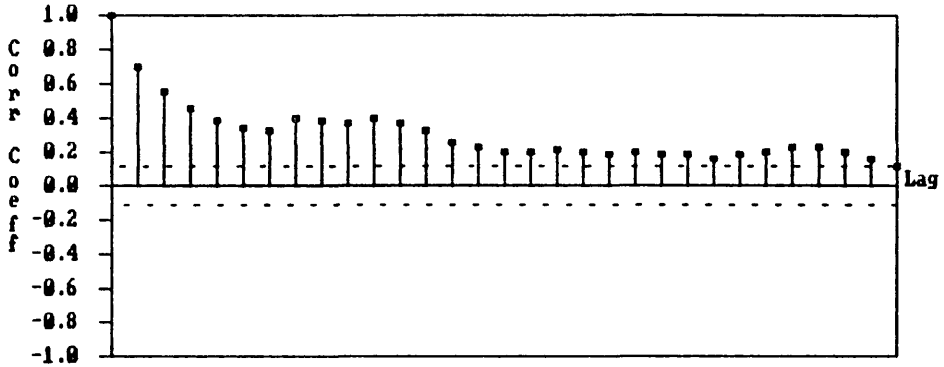


Fig. 2.12a. Autocorrelogram of input BOD_5

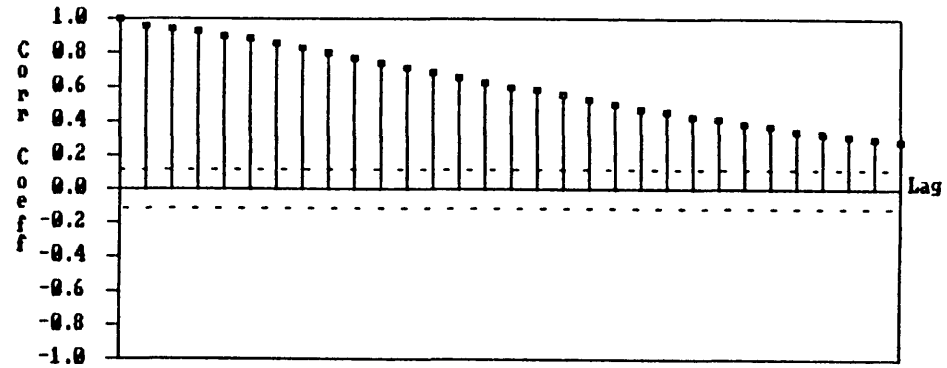


Fig. 2.12b. Autocorrelogram of input flow rate

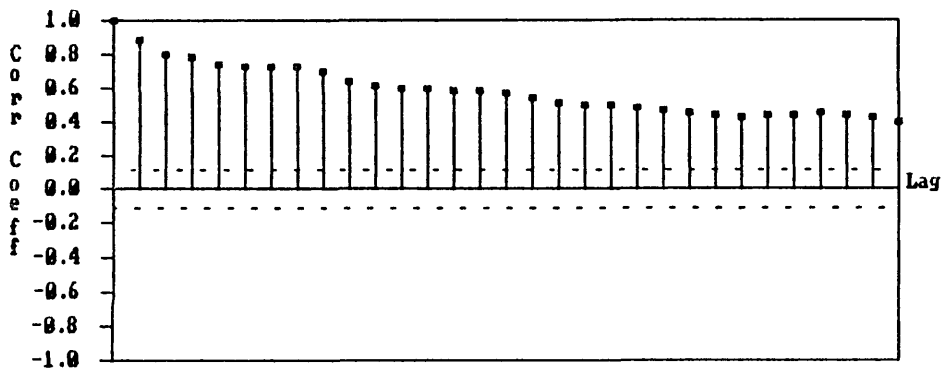


Fig. 2.12c. Autocorrelogram of input $NH_3 - N$

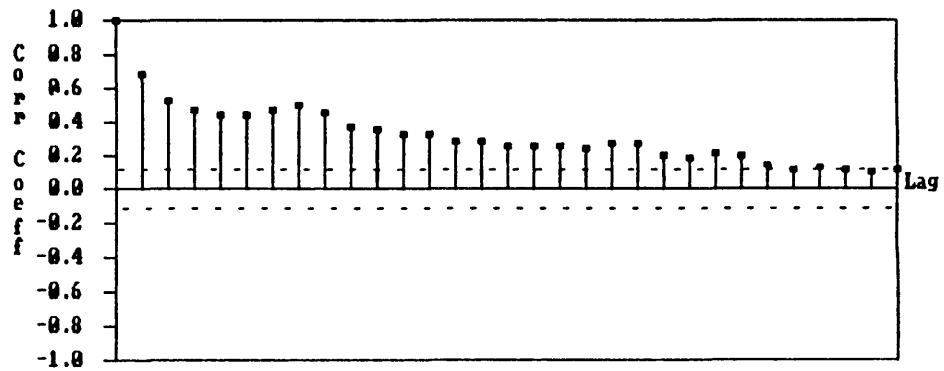


Fig. 2.12d. Autocorrelogram of input SSi

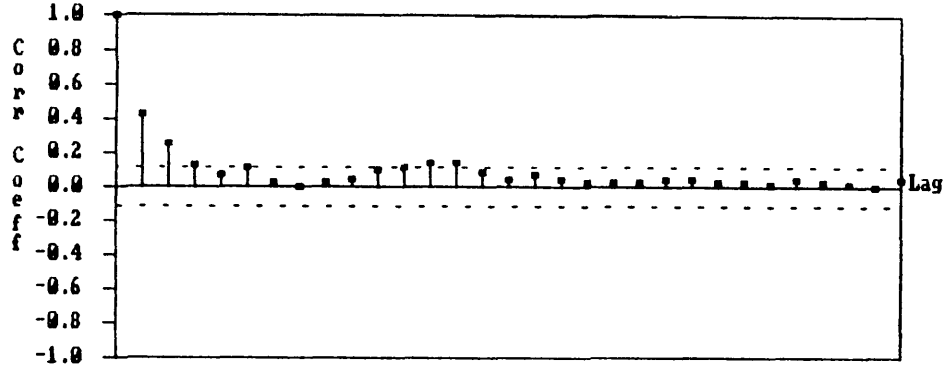


Fig. 2.13a. Autocorrelogram of output BOD_5

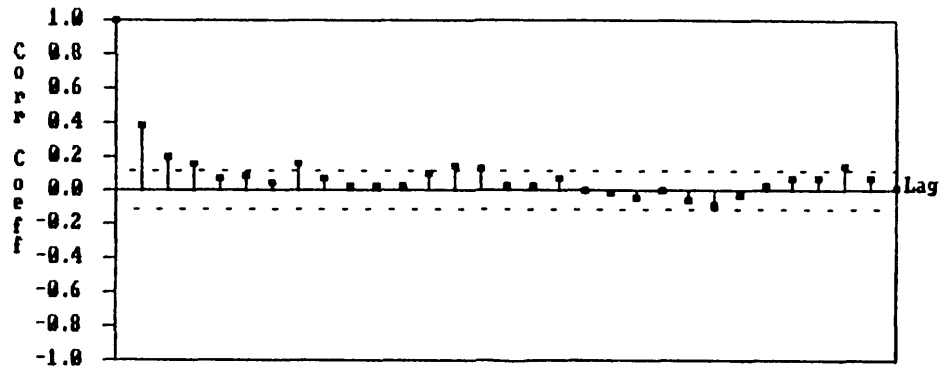


Fig. 2.13b. Autocorrelogram of output SS

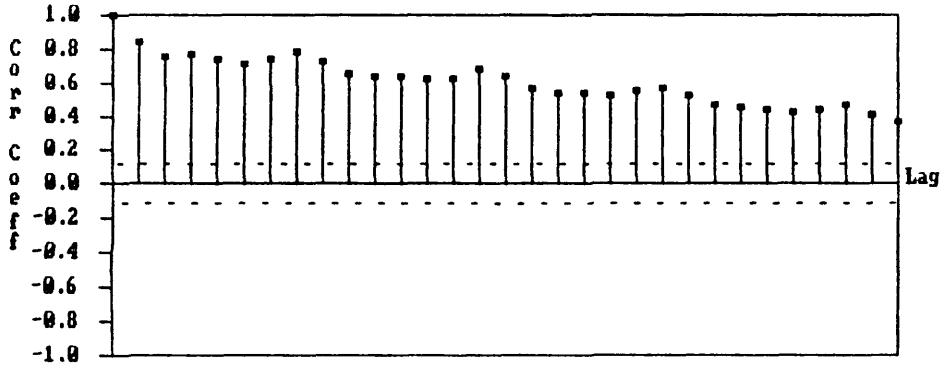


Fig. 2.13c. Autocorrelogram of output $NH_3 - N$

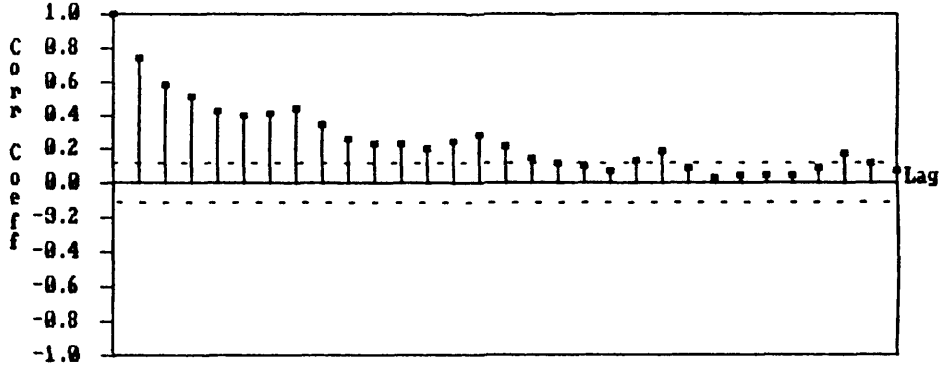


Fig. 2.13d. Autocorrelogram of output $NO_3 - N$

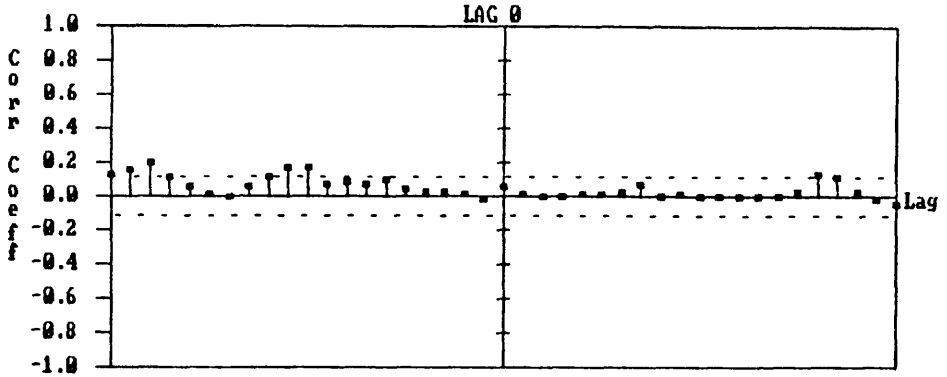


Fig. 2.14a. Cross-correlogram between input & output BOD_5

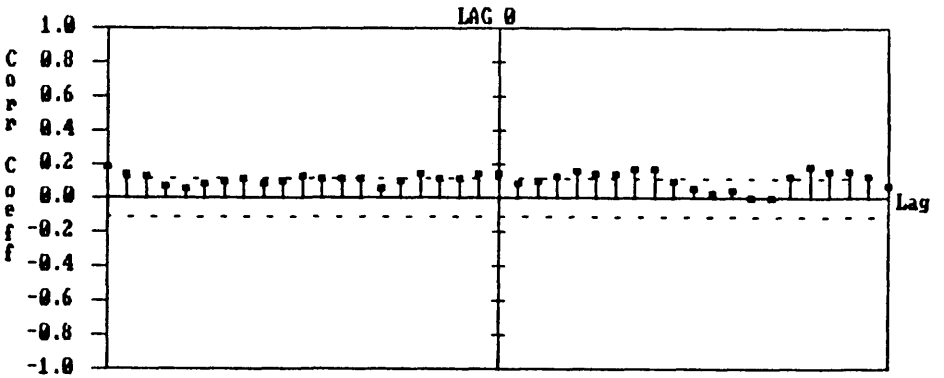


Fig. 2.14b. Cross-correlogram between input & output SS

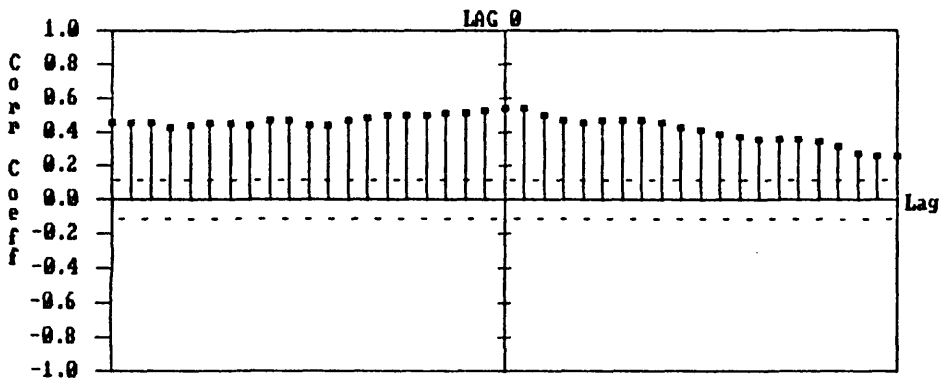


Fig. 2.14c. Cross-correlogram between input & output $NH_3 - N$

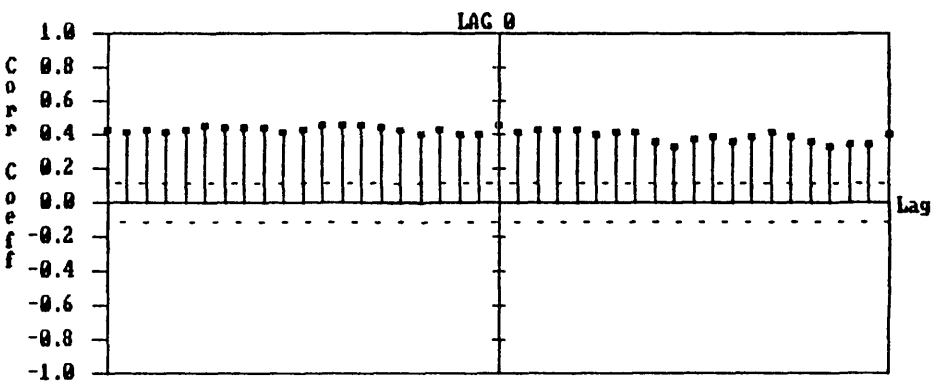


Fig. 2.14d. Cross-correlogram between input & output COD

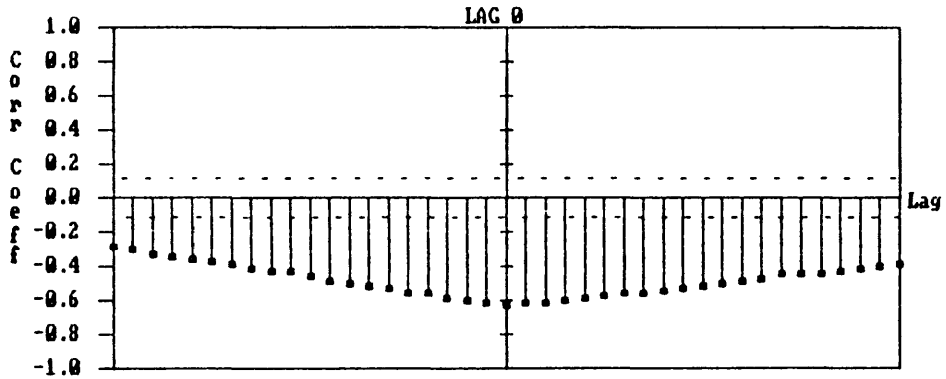


Fig. 2.15a. Cross-correlogram of $BODi$ against Qi

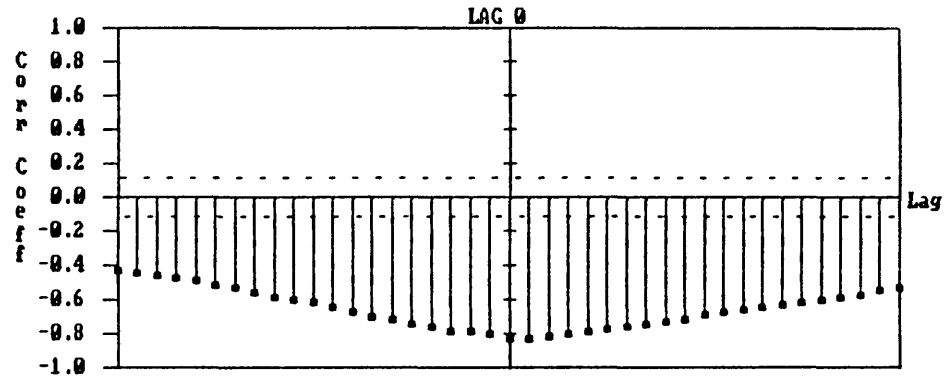


Fig. 2.15b. Cross-correlogram of NH_3i against Qi

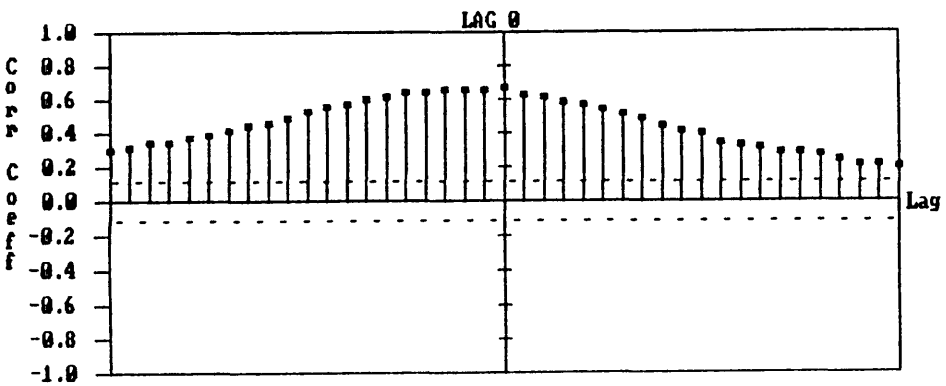


Fig. 2.15d. Cross-correlogram of NO_2i against Qi

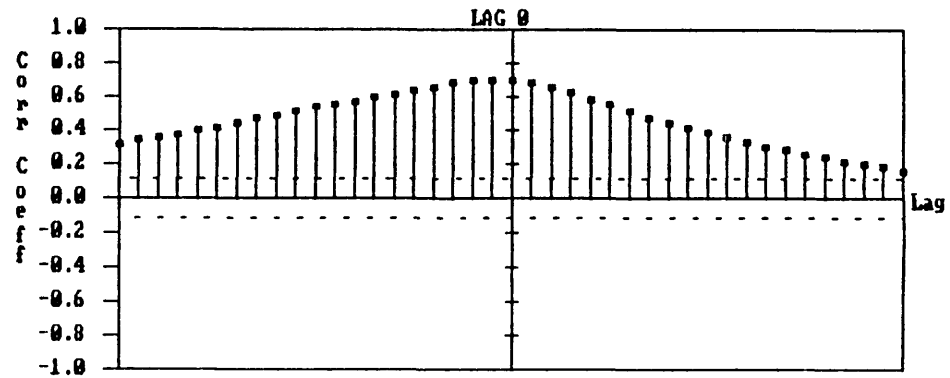


Fig. 2.15c. Cross-correlogram of NO_3i against Qi

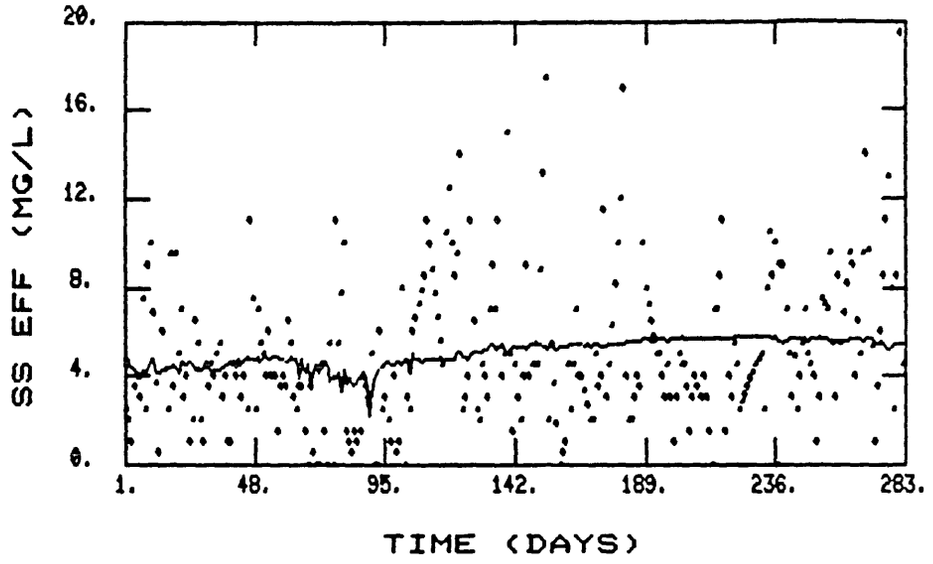


Fig. 2.16a. Steady-state model based on solids load : $SSe_t = a \cdot G_F + b$

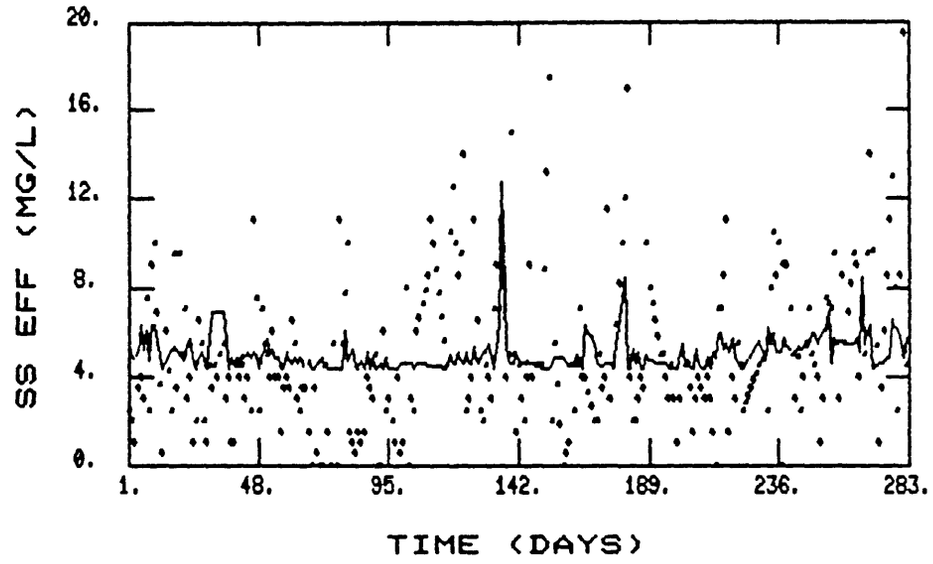


Fig. 2.16b. Steady-state model based on effluent BOD : $SSe_t = a \cdot BODe + b$

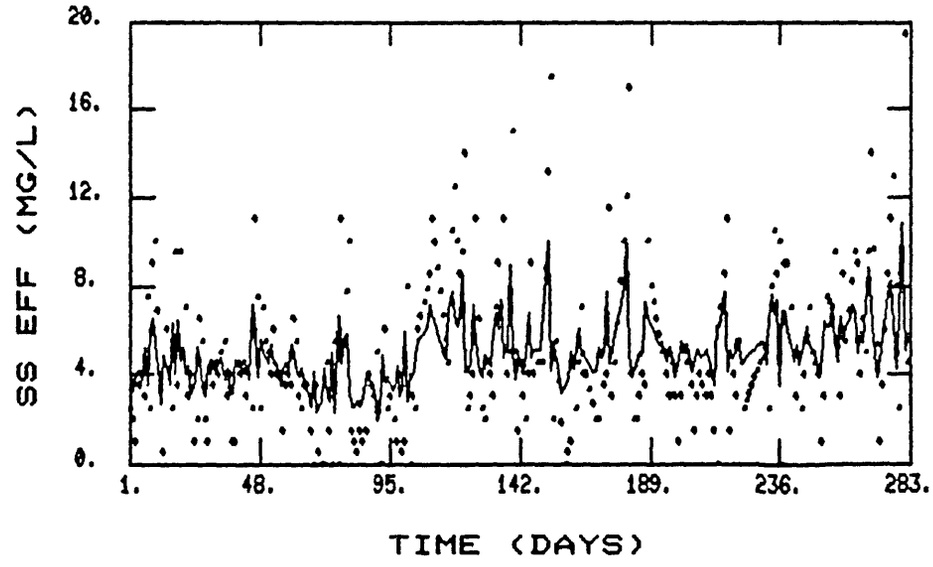


Fig. 2.16c. Autoregressive model performance: $SSe(t) = a \cdot SSe(t-1) + b \cdot G_F + c$

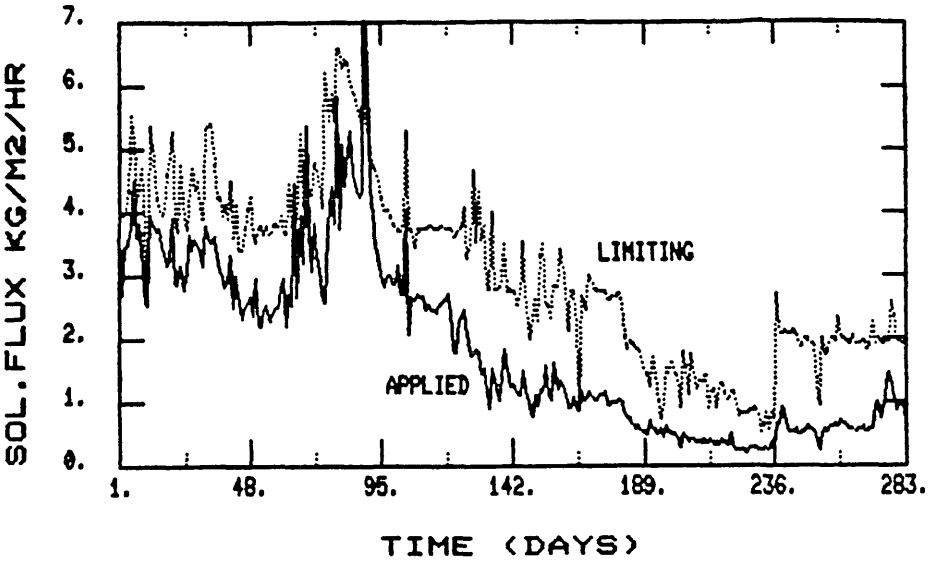


Fig. 2.17a. Applied – predicted limiting solids flux ($Vo = 5.18$, $K = 0.38$)

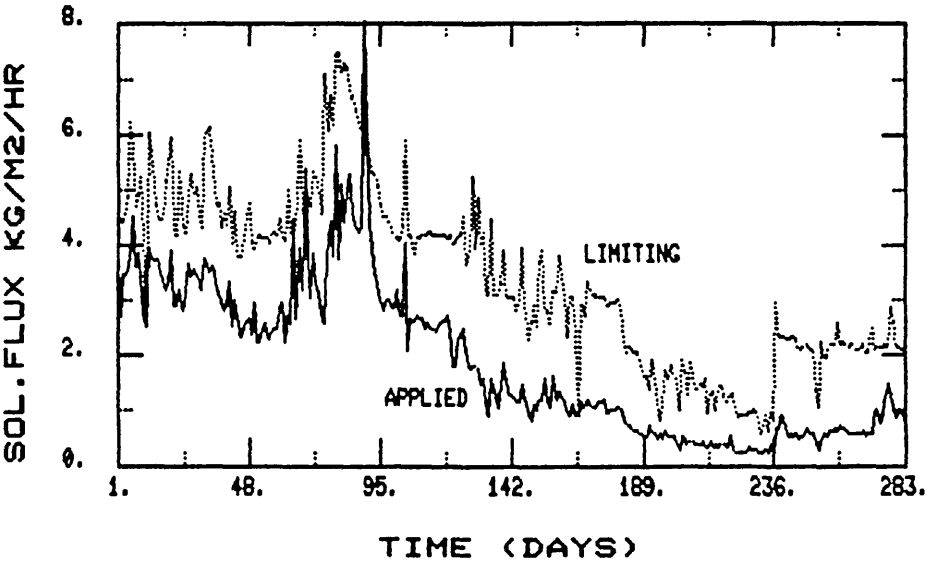


Fig. 2.17b. Applied – predicted limiting solids flux ($Vo = 6.50$, $K = 0.35$)

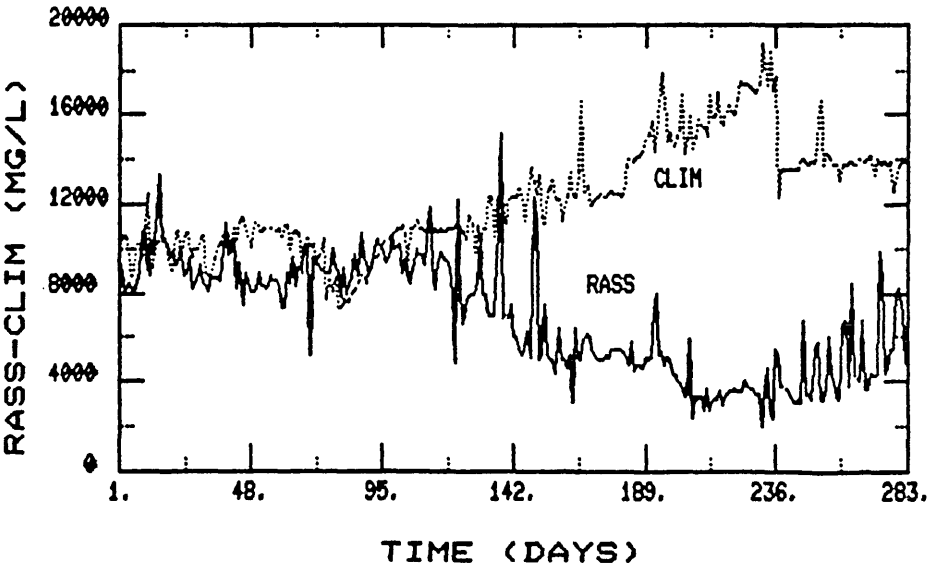


Fig. 2.17c. Observed $RASS$ – predicted limiting concentration ($Vo = 5.18$, $K = 0.38$)

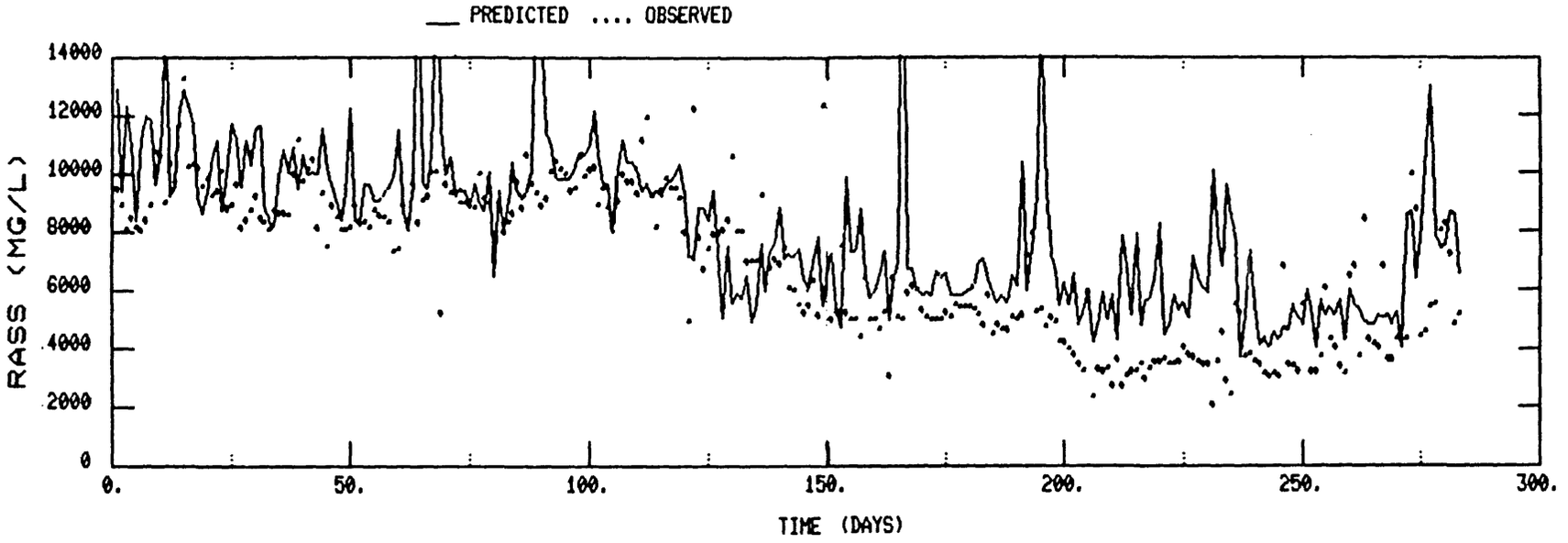


Fig. 2.18a. Predicted – observed underflow concentration from steady-state model

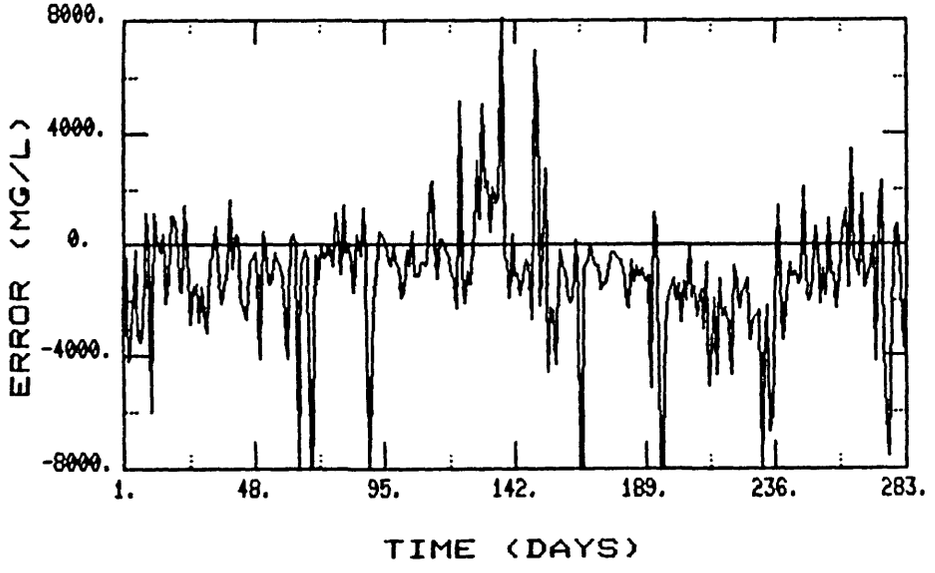


Fig. 2.18b. Prediction error in *RASS* from steady-state model

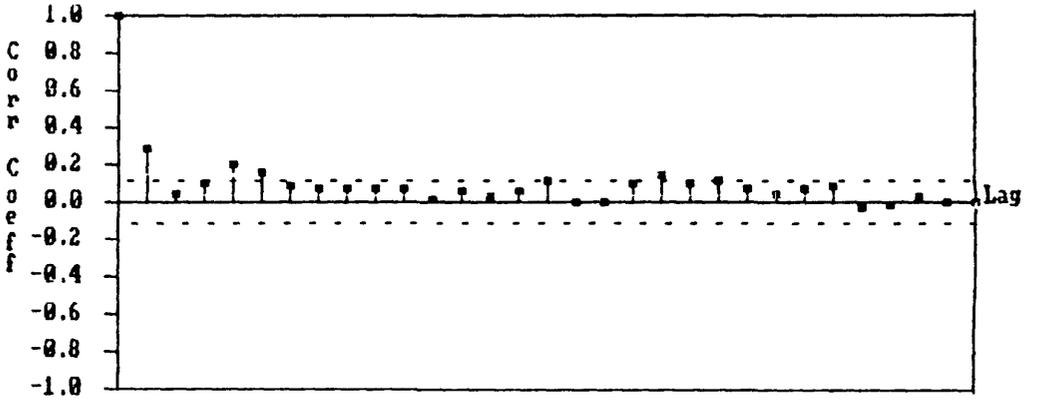


Fig. 2.18c. Autocorrelogram of error in *RASS*

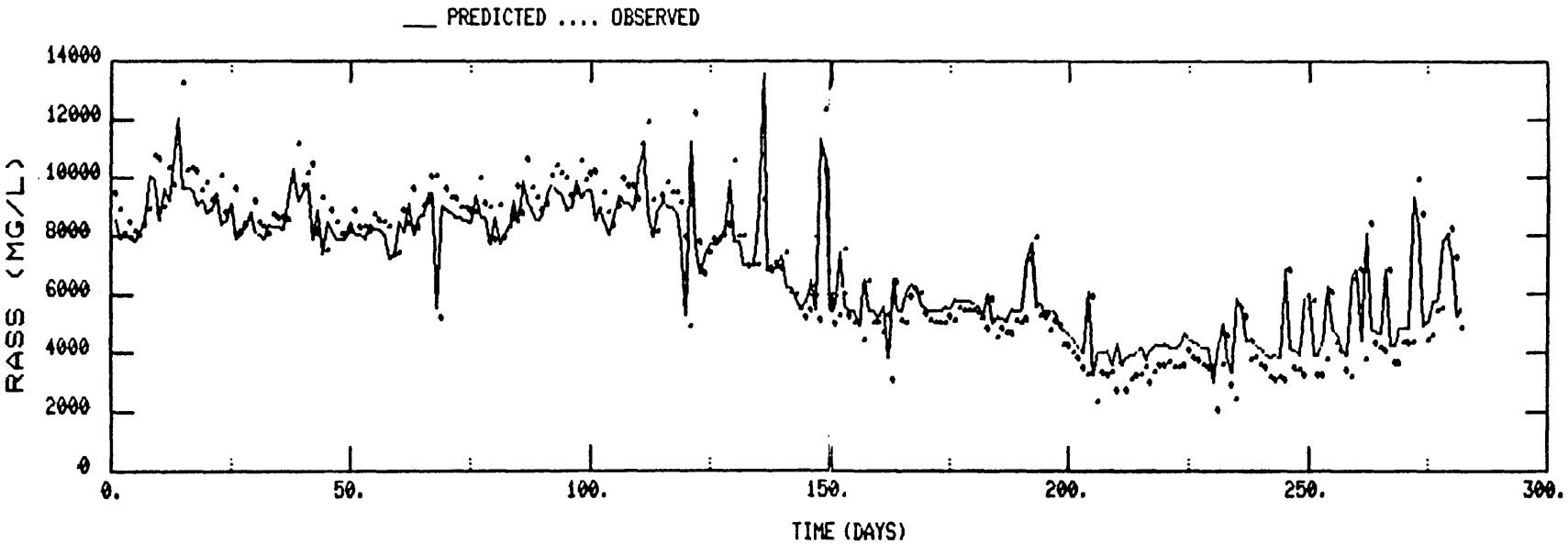
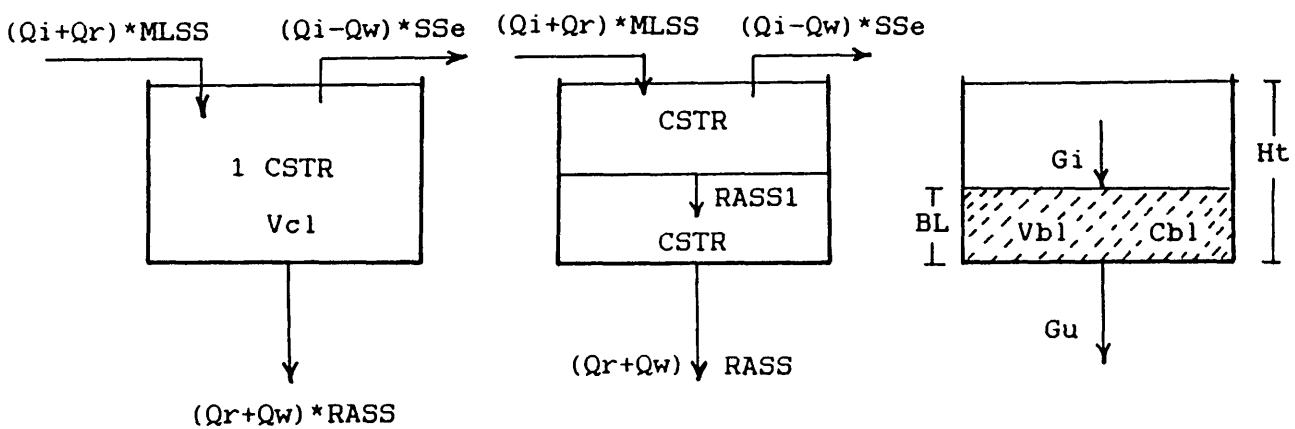


Fig. 2.19. Performance of autoregressive model : $RASS(t) = a \cdot RASS(t-1) + b$



a. single CSTR b. 2-CSTRs c. sludge blanket modelling

Fig. 2.20. Schematic representation of clarifier for modelling

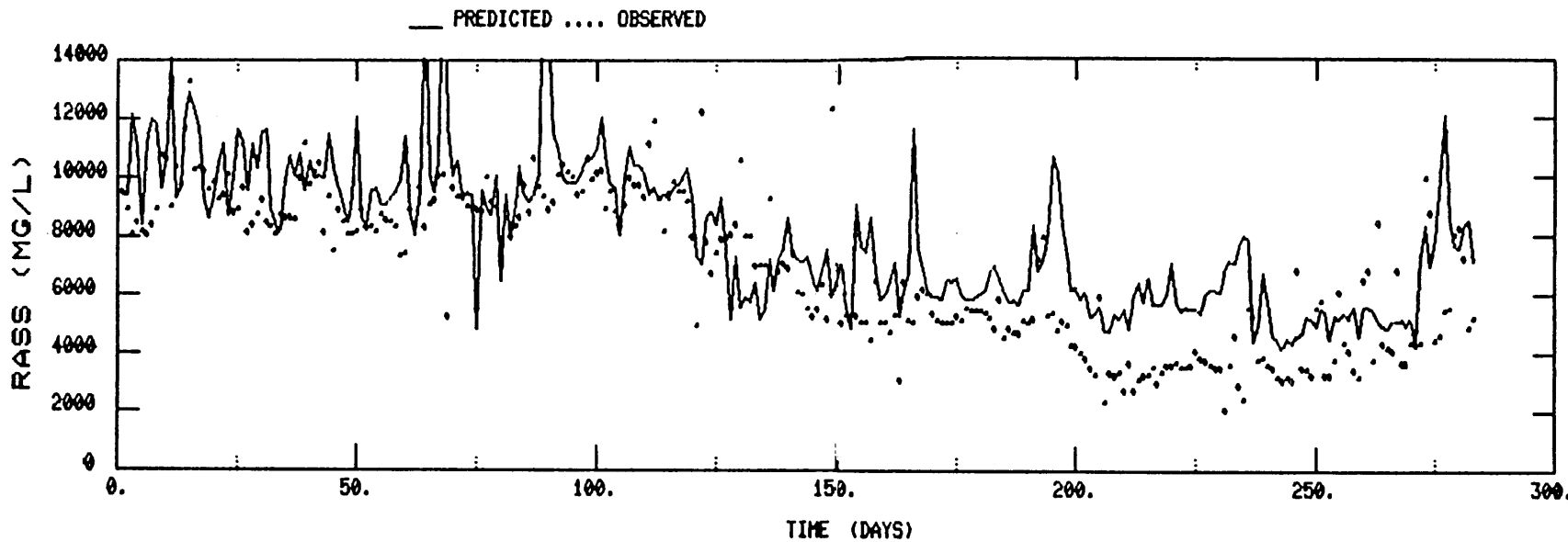


Fig. 2.21a. Predicted – observed underflow concentration from dynamic (1 CSTR) model

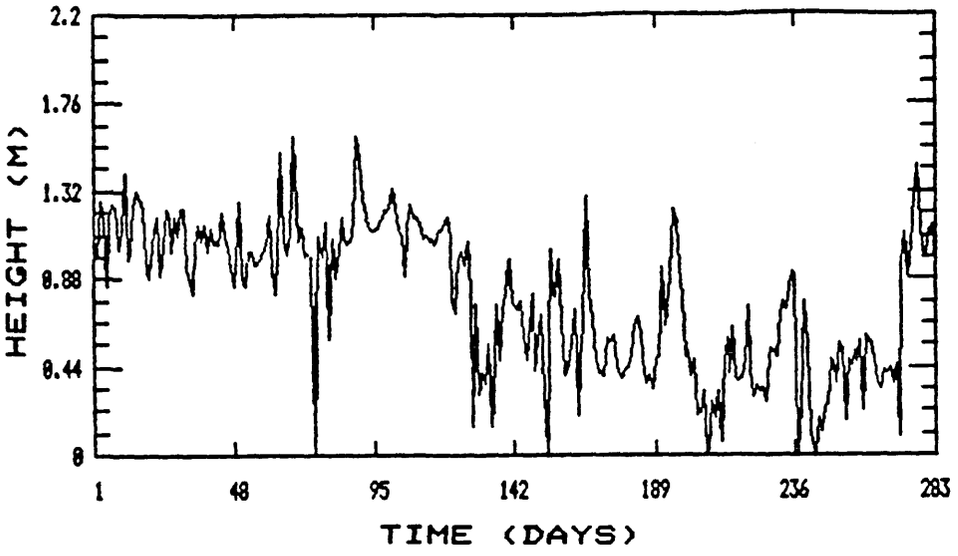


Fig. 2.21b. Predicted sludge blanket level

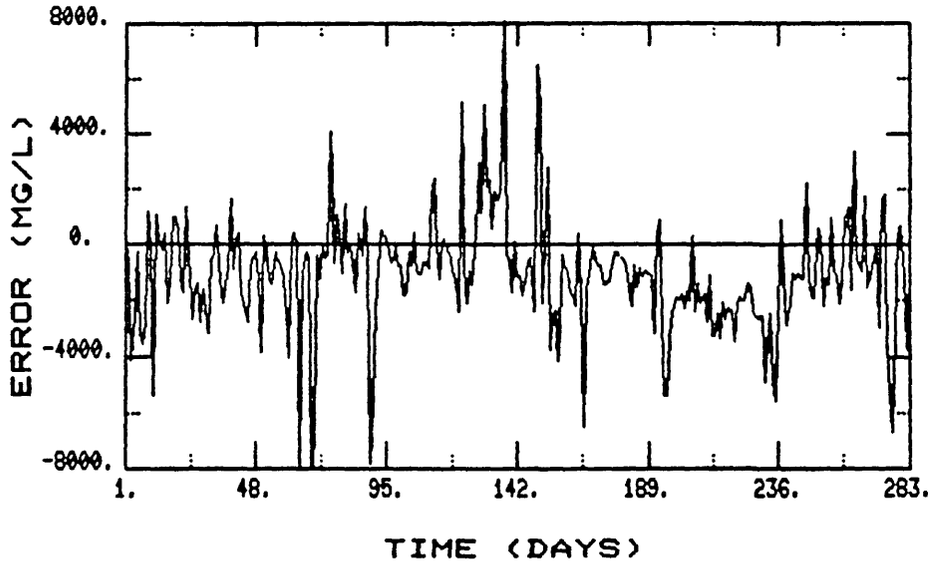


Fig. 2.21c. Prediction error in *RASS* from dynamic model

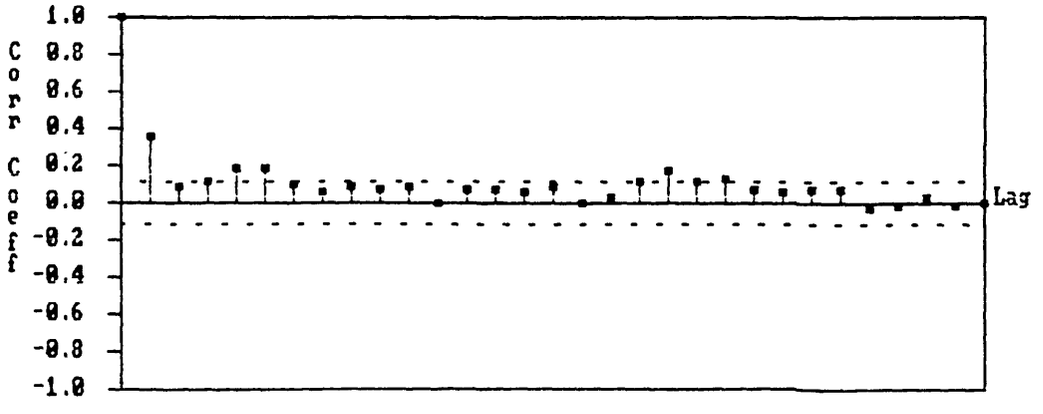


Fig. 2.21d. Autocorrelogram of error in *RASS*

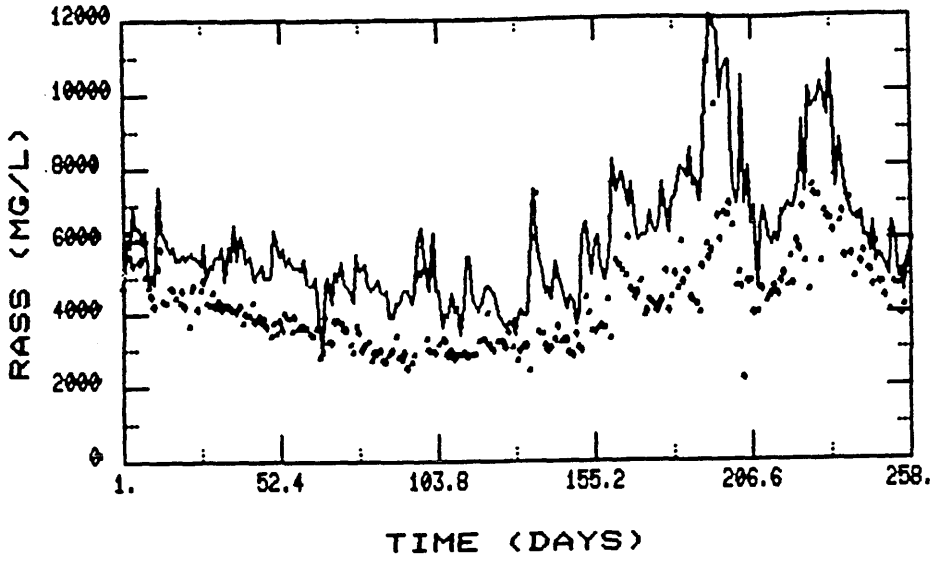


Fig. 2.22a. Predicted – observed $RASS$ from dynamic model during validation

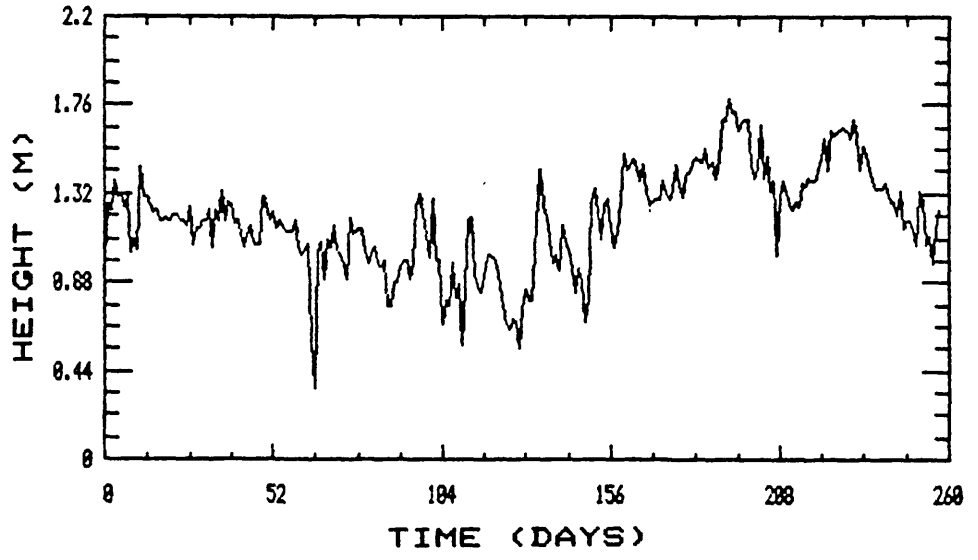


Fig. 2.22b. Predicted sludge blanket level

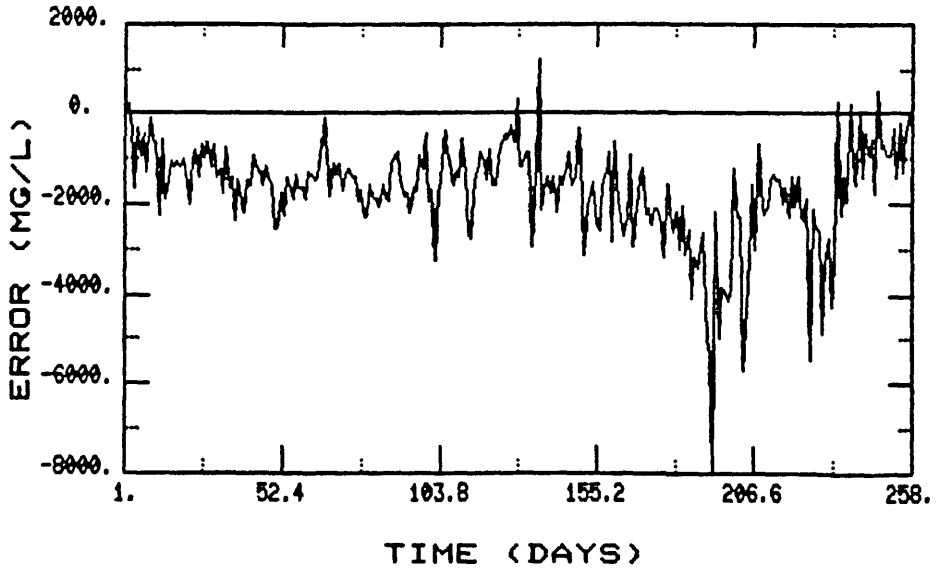


Fig. 2.22c. Prediction error in $RASS$ during validation

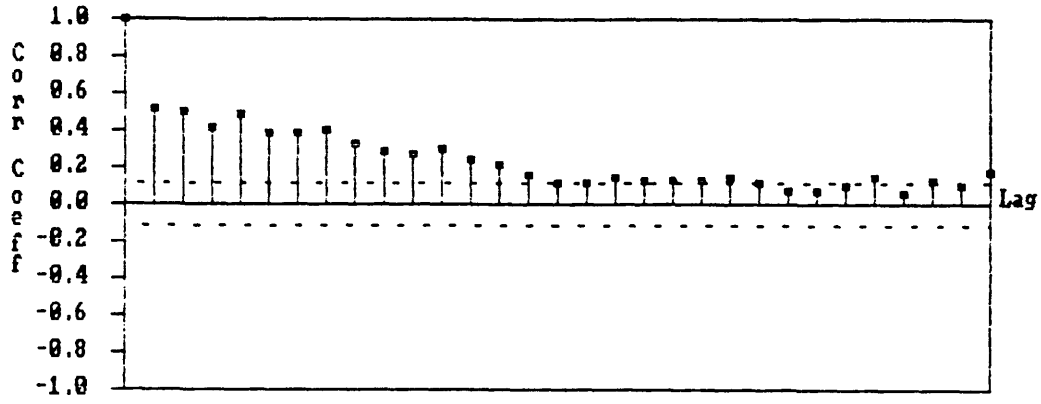


Fig. 2.22d. Autocorrelogram of error in $RASS$

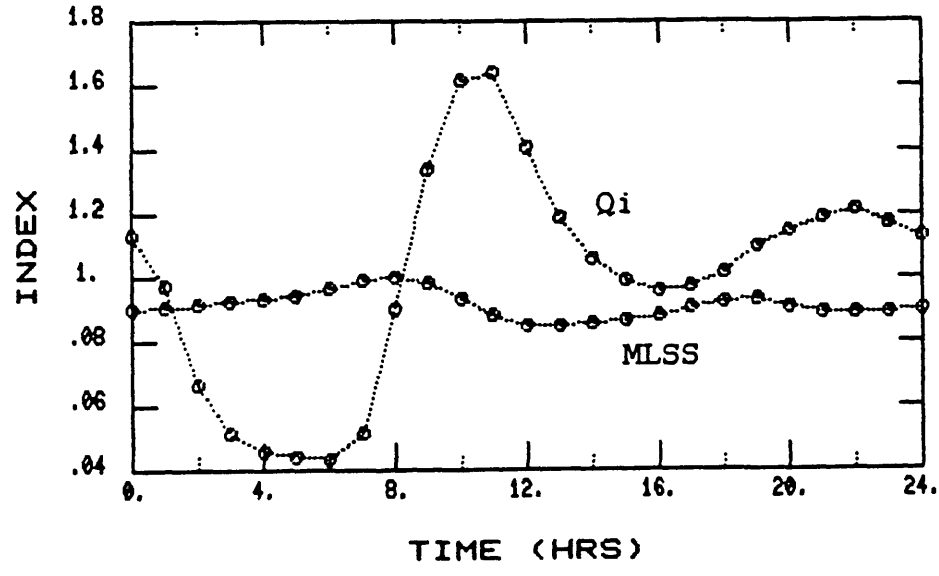


Fig. 2.23. Typical standardized diurnal variation of Qi and $MLSS$

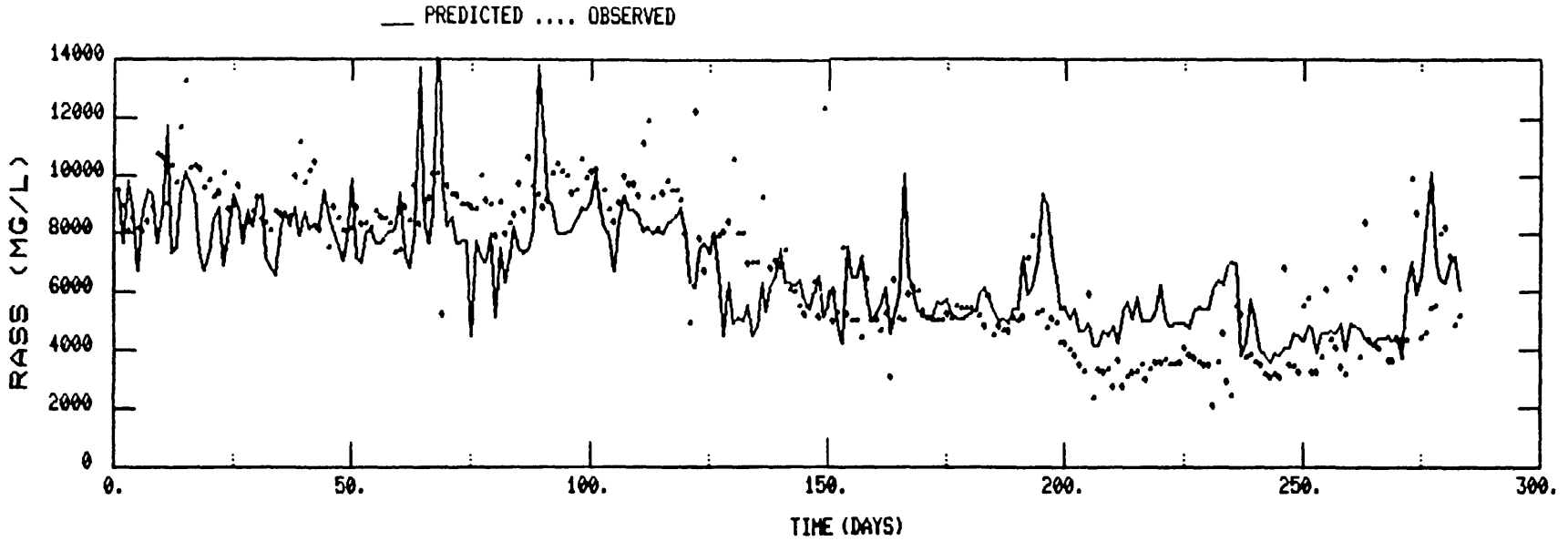


Fig. 2.24a. Performance of dynamic model with diurnally varying inputs (1979 set)

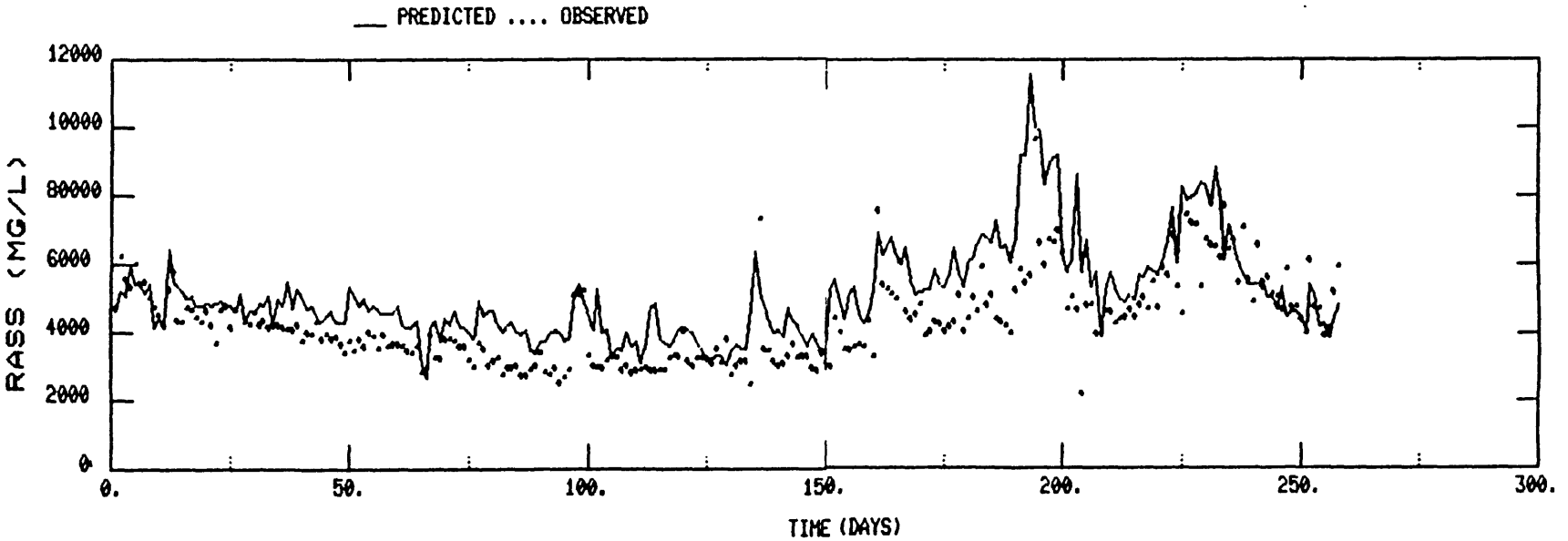


Fig. 2.24b. Performance of dynamic model with diurnally varying inputs (1980 set)

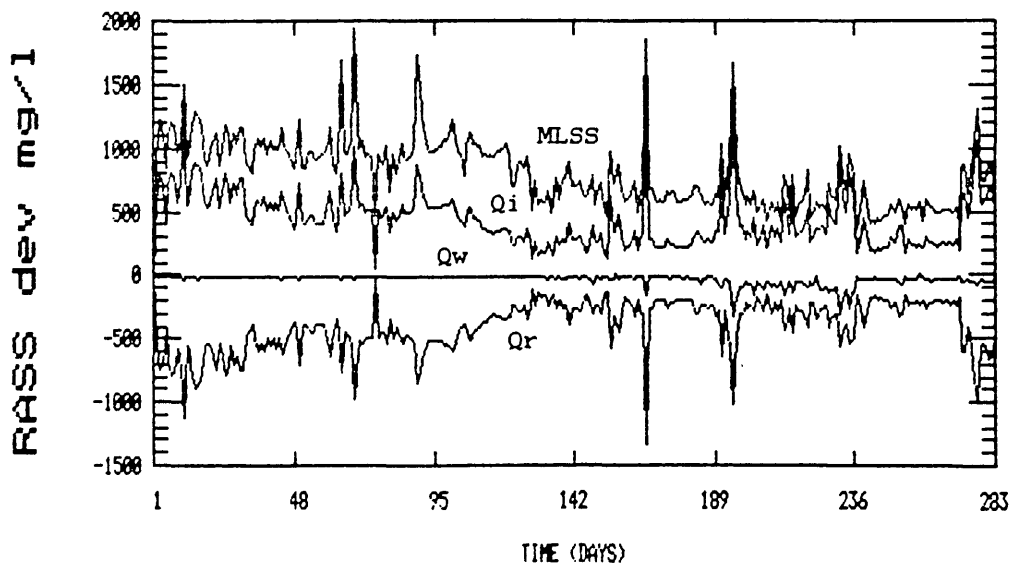


Fig. 2.25. Change in $RASS$ concentration due to 10% change in the inputs

3 Modelling the Oxidation Ditch Process

3.1 Introduction

The biochemical reactions that govern the purification of wastewater have been extensively studied for several decades by numerous researchers both from a microscopic and a macroscopic viewpoint. Since the majority of these reactions occur at the cell level, a rigorous study of their kinetics would require a detailed description of the process biochemistry. Such a study, although of interest for the biochemist, it would not be of great assistance to the engineer trying to understand and operate the sewage purification processes. Therefore, many researchers have attempted to describe the kinetics of the biochemical processes from a macroscopic viewpoint by lumping the overall effect of the microscopic reactions into a small number of main processes.

Part I of this Chapter, comprises a literature survey on the main approaches used to describe the reaction kinetics in the oxidation ditch process. These have been conveniently classified into the following four main processes, since each one of them serves a different purpose and has its own characteristics :

- Carbonaceous oxidation process.
- Nitrification process.
- Denitrification process.
- Fluid and solids mass transport.

Furthermore, mathematical models developed for the oxidation ditch but also for the activated sludge process were classified and discussed, in order to assess their applicability for modelling the oxidation ditch and for process control. Relatively few studies were found on the oxidation ditch modelling, hence the majority of the reviewed material refers to the activated sludge, which however was considered relevant due to the similarities of the two processes. In the second Part of the Chapter follows the development of an oxidation ditch model which is based on information from the literature, but also on real experimental measurements.

Part I. Review on kinetics and modelling approaches

3.2 Carbonaceous oxidation process

3.2.1 General

The consumption of organic substances in wastewater treatment is based on the theory that heterotrophic micro-organisms metabolize organic substrate in order to acquire the necessary energy and carbon for growth and maintenance. A mixed population of heterotrophic organisms are responsible for the degradation of organics in wastewater, such as fungi, protozoa, rotifers and other higher forms of life. However the bacteria are generally though to play the most important role. The growth of biomass from the metabolism of organic substrate is represented by the reactions.

oxidation

$$\text{organics} + O_2 \xrightarrow{\text{het.bacteria}} CO_2 + NH4^+ + \text{end products} + \text{Energy} \qquad (3.1)$$

synthesis

$$\text{organics} + O_2 + NH4^+ + P + \text{Energy} \xrightarrow{\text{het.bacteria}} C_5H_7NO_2 \text{ (new cells)} \qquad (3.2)$$

endogenous respiration

$$C_5H_7NO_2 + 5\ O_2 \xrightarrow{\text{het.bacteria}} 5\ CO_2 + NH4^+ + 2\ H_2O + \text{Energy} \qquad (3.3)$$

The kinetics of carbonaceous oxidation are influenced by several factors including the concentration of micro-organisms and organic substrate, the presence of inhibitory substances to biomass growth, the dissolved oxygen (DO) concentration, the ambient temperature and pH level which are discussed later in Section 3.2.7.

3.2.2 Kinetics of carbonaceous oxidation

The objective of many previous studies has been the formulation of suitable mathematical relationships to describe the biochemical reactions of organism-substrate interaction responsible for the degradation of organics in wastewater treatment. A common approach used by many workers, such as Lawrence & McCarty (1970), Jones (1978), Marais & Ekama (1976), Christoulas & Tebbutt (1976), Vandevenne & Eckenfelder (1980), and Holmberg & Ranta (1982) was to assume that the growth of organisms follows a first-order reaction with respect to their concentration in the reactor, described by the differential equation :

$$\frac{dXa}{dt} = \mu \cdot Xa \qquad (3.4)$$

where; Xa : active organism concentration $[ML^{-3}]$,
μ : active organism specific growth rate $[T^{-1}]$.

The specific growth rate was found to depend upon the species of organisms involved, and the prevailing ambient conditions, such as ambient temperature, pH, DO and presence of inhibitory or toxic substances. However, most important of all, the growth rate was found to depend upon the ambient organic substrate concentration in the reactor. The most widely accepted expression relating the organism growth rate to the substrate concentration is the so called "Monod" relationship, (Monod 1950) given by the equation :

$$\mu = \mu_{max} \cdot \frac{S}{Ks + S} \tag{3.5}$$

where; μ_{max} : maximum specific growth rate of micro-organisms $[T^{-1}]$,
Ks : half-rate substrate concentration $[ML^{-3}]$,
S : reactor's substrate concentration $[ML^{-3}]$.

The above relationship was originally developed to describe the growth of pure cultures utilizing a single and soluble substrate in batch experiments. However, in wastewater the term substrate refers to a wide range of substances many of which are in particulate form (Ekama & Marais, 1979). Jones (1978), reported that the use of Monod kinetics for mixed substrates leads to erroneous results often associated with very high saturation constants. In addition, work by Gaudy et al. (1971a) showed that the Monod expression is invalid for a period after a step change in substrate concentration, because the organisms do not respond immediately to substrate perturbations. Hence, they concluded that the Monod relationship would be valid only under steady-state operating conditions. Similarly Dold et al. (1980) suggested that under normal operating conditions with small perturbations about a steady-state the Monod relationship would be adequate.

The Monod growth relationship (eq. 3.5) combined with the first-order reaction (eq. 3.4), can adequately describe the commonly observed constant growth and declining growth phases of the micro-organisms in batch reactor kinetics. However they cannot describe the initial lag phase which is caused by natural adaptation of micro-organisms to changing ambient conditions. According to Busby & Andrews (1975) this is a deficiency of the Monod kinetics, because the lag is important in describing accurately the dynamic behaviour of the process.

The Monod relationship has occasionally been approximated by first and zero-order reactions in the two extreme cases. Under high substrate concentration ($S \gg Ks$), the constant Ks can be neglected and the specific growth rate equals to the

maximum rate ($\mu = \mu max$), but this case does not usually apply to wastewater treatment. In the case of low substrate concentration ($S \ll Ks$), then S can be neglected and the growth rate becomes first-order with respect to substrate. Hence some of the commonly used simplifications of the Monod relationship under various conditions are :

$$dX/dt = \mu \cdot S \quad \text{under low substrate or high biomass} \tag{3.6a}$$

$$dX/dt = \mu \cdot X \quad \text{under high substrate} \tag{3.6b}$$

$$dX/dt = \mu \cdot S \cdot X \quad \text{under low substrate} \tag{3.6c}$$

The rate of substrate utilization is usually considered proportional to the biomass growth, where the proportionality constant (Y), represents the yield of biomass from substrate. Combining equations 3.4 and 3.5 produces the following expression describing the removal of organic substrate :

$$\frac{dS}{dt} = -\frac{1}{Y} \cdot \frac{dXa}{dt} = -\frac{\mu max \cdot Xa \cdot S}{Y \cdot (Ks + S)} \tag{3.7}$$

The Monod relationship does not relate directly the substrate utilization rate to its influent concentration. However Grau et al. (1975), presented experimental results which show that when mixed microbial cultures are grown on multicomponent substrates, as is normally the case in the activated sludge process, the substrate utilization rate depends also on its influent concentration. Subsequently they proposed the following empirical relationship :

$$\frac{dS}{dt} = -K \cdot X \cdot \left(\frac{S}{So}\right)^n \tag{3.8}$$

where; S : effluent substrate concentration $[ML^{-3}]$,
So : influent substrate concentration $[ML^{-3}]$,
X : organism concentration $[ML^{-3}]$,
n : the reaction order,
K : substrate utilization rate constant $[T^{-1}]$.

On the basis of pilot-scale experiments, Tebbutt & Christoulas (1976) showed that the first-order reaction with retardation, as proposed by Fair et al. (1968), satisfactory described the substrate removal kinetics.

$$\frac{dS}{dt} = -K \cdot X \cdot S \cdot \left(\frac{S}{So}\right)^n \tag{3.9}$$

where the retardation factor $(S/So)^n$ depicts the decrease in sewage treatability as the reaction proceeds.

Grady & Williams (1975) also emphasized the effect of influent substrate upon its effluent concentration, which they described with the following relationship derived from a linear approximation of the Monod equation :

$$S = K \cdot So \cdot D + K' \cdot So \qquad (3.10)$$

where; K : proportionality constant $[T]$,
D : dilution rate $[T^{-1}]$,
$K' = K \cdot b$: dimensionless coefficient,
b : biomass decay rate $[T^{-1}]$.

The coefficients K and K' were fitted by linear regression using laboratory results and a high correlation coefficient was reported.

Sykes (1981) adopted an alternative theory to describe the substrate removal. He observed that for systems with high organic removal efficiency, the effluent substrate consists mostly of microbial excreta produced during cell synthesis, rather than residual substrate. Under this theory the soluble effluent substrate is nearly proportional to the influent substrate and independent of the reactor configuration (Sykes 1982).

In the above studies where the proposed relationship differs from the Monod, performance data were collected either from batch experiments in laboratory-scale units or under steady-state plant operating conditions. Further such models are mainly concerned with the removal rates of substrate which was often regarded as being independent of the kinetics of biomass. As a result the application of such models is mainly for design of treatment units or for assessing the steady-state performance of a reactor under different operating conditions. However they are considered of little use for the continuous process monitoring and control.

3.2.3 Reactor biomass structuring

In order to account more realistically for the components of the sludge and the activity of micro-organisms in the process, several workers have proposed a structure for the biomass, including Busby & Andrews (1975), Ekama & Marais (1979), Dold & Marais (1986), and Jones (1978). The most common assumption is that the biomass consists of active mass (viable organisms), stored mass and an inert fraction. The active mass is responsible for the organic substrate metabolism, the stored mass represents the organic substrate absorbed on the bioflocs, while the inert mass represents the inorganic and non-biodegradable matter in the sludge. Clifft & Andrews (1981a) proposed a structured stored mass into soluble and particulate components.

Grady & Roper (1974) in an attempt to explain the loss in bacterial viability at increasing sludge ages, structured the biomass into a viable and non-viable fractions. They suggested that the viable organisms die at a certain rate to become non-viable as a result of the substrate limiting conditions, and at the same time they also decay as a result of endogenous metabolism, lysis and predation. The non-viable organisms do not reproduce but they are lost through decay. Holmberg (1982) extending the above distinction, structured the organic biomass as active, inactive and non-biodegradable mass. She proposed that the active mass grows by consuming substrate and lower organisms, the inert mass consists of non-viable but biodegradable organisms and the non-biodegradable mass consists of non-reactive volatile solids.

Other workers, (Curds 1971, 1973) structured the biomass into specific groups of organisms commonly found in the activated sludge, such as sludge and sewage bacteria, attached and free-swimming ciliates and flagellated protozoa. Such a structure assists in studying the growth and metabolism of individual groups of organisms using predator-prey dynamics and for assessing their role in sewage purification. However it does not offers any advantage when modelling the overall kinetics of the process where the substrate metabolism is mainly performed by the active organisms.

Holmberg & Ranta (1982) structured the biomass according to its age distribution and expressed the kinetic constants in their process model as functions of the average sludge age. They reported some improvements in the performance of their age model when fitting experimental observations from a fermentation process, but no improvement when the model was applied to the activated sludge process.

3.2.4 Organic substrate structuring

Some workers have modelled the structure of organic substrate in the crude sewage according to its biodegradability and particle size in order to describe more accurately the relative availability of substrate to micro-organisms. For example Holmberg (1982) structured the reactor substrate into soluble biodegradable organics, which can be directly consumed by bacteria and colloidal organics which must be degraded to dissolved equivalents before metabolism.

Dold & Marais (1986) structured the influent COD into unbiodegradable and biodegradable fractions. The former was subdivided into particulate and soluble parts and the latter into readily and slowly degradable parts. Ekama & Marais (1977) based on experimental results with unsettled municipal sewage reported the following proportions in the influent COD :

soluble unbiodegradable $= 5\%$ of $CODi$
particulate " $= 13\%$ of $CODi$

biodegradable fraction = 82% of $CODi$.

3.2.5 Substrate storage and utilization concept

A number of investigators adopted the concept of substrate storage prior to utilization, (Busby & Andrews 1975 ; Ekama & Marais 1976 ; Tsuno & Goda 1978 ; Yeung et al. 1980; Sheffer et al. 1981). Jacquart et al. (1973) were among the first to adopt the concept of substrate storage, in order to explain the observed lag between the respiratory activity of biomass and input organic load variability. They suggested that the input particulate organic matter is entrapped onto the biofloc to build up the "reserves of undissolved origin", while the soluble input BOD is transformed into "reserves of dissolved origin". The inclusion of storage concept into the model of respiratory activity improved significantly its performance to reproduce experimental observations.

Clifft & Andrews (1981a) based on results from batch experiments, also observed a lag of 2–3 hr between the diurnal variation of oxygen utilization and the pattern of substrate removal. They suggested therefore, that the substrate was more rapidly transferred to the floc than it was metabolized which they attributed to the substrate storage phenomenon. Using a process model which accounted for the storage effects, they estimated that for a process operating at a sludge age of one day, 70–80% of the influent soluble substrate was directed through storage, while the remaining was used for direct synthesis. They also reported that the particulate substrate had an insignificant effect upon the oxygen utilization during the first 6–8 hr of aeration, however they suggested that its effect will become more important at longer sludge ages.

Dold & Marais (1986) suggested that all the influent particulate material is immediately enmeshed in the sludge, thus it is removed virtually completely from the effluent when passing through the clarification stage. This hypothesis was supported by experimental observations showing that inert particulate material did not appear in the final effluent of the plant (Dold et al., 1980). The enmeshed material was then considered to be absorbed and stored in the active heterotrophic mass. For soluble substrates, Blackwell (1971) found experimentally that their rate of transfer from the liquid to the floc phase is given by :

$$Rxs = \frac{dXs}{dt} = R_T \cdot X_V \cdot (Fs - fs) \qquad (3.11)$$

where; Rxs : rate of storage $[ML^{-3}T^{-1}]$,
R_T : substrate transfer rate $[T^{-1}]$,
X_V : total volatile suspended solids $(MLVSS)$ $[ML^{-3}]$,

Fs : maximum stored fraction in the $MLVSS$ [–],
$fs = Xs/Xa$: existing " " " [–].

Morris & Stumm (1960) using primarily suspended substrates, observed that the adsorption rate was also dependent on the substrate concentration in the liquid phase. Busby & Andrews (1975) based on the above observations proposed the following modification to equation 3.11 :

$$\frac{dXs}{dt} = R_T \cdot X_V \cdot \left(Fs \cdot \frac{S}{Ks + S} - fs\right) \tag{3.12}$$

where; Ks : sorption limiting substrate $[ML^{-3}]$,
S : substrate concentration in the liquid phase $[ML^{-3}]$.

Ekama and Marais (1977), based on simulation results reported that the above revision of the model did not improve effluent substrate predictions, however they agreed that consideration should be given to the extracellular substrate. Subsequently they proposed the following modification :

$$Rxs = Ka \cdot S_B \cdot Xa \cdot \left(Fs - \frac{Xs}{Xa}\right) \tag{3.13}$$

where; Ka : overall mass transfer coefficient $[M^{-1}L^3T^{-1}]$,
S_B : biodegradable soluble substrate concentration $[ML^{-3}]$,
Xa : active heterotrophic organism concentration $[ML^{-3}]$,
Xs : stored substrate concentration $[ML^{-3}]$.

The stored particulate substrate is hydrolysed by extracellular enzymes, in which complex molecules break down to simpler ones and it is then absorbed by the active biomass to be used for cell synthesis. Dold et al. (1980) reported that the governing rate is that of hydrolysis, which limits the rate of utilization. Next, they attempted to formulate the synthesis rate in terms of surface mediated reactions and derived the following expression.

$$\frac{dXa}{dt} = -Y \cdot \frac{dXs}{dt} = \frac{Km \cdot (Xs/Xa)^n}{Ks + (Xs/Xa)^n} \cdot Xa \tag{3.14}$$

where; Xs : stored particulate substrate $[ML^{-3}]$,
Km : maximum specific substrate utilization rate $[T^{-1}]$,
Ks : half-saturation coefficient $[ML^{-3}]$,
$(Xs/Xa)^n$: represents the stored substrate per unit area of active biomass,
$n = 1$ derived from simulations.

For the readily degradable substrates, the rate of utilization for synthesis has been considered to follow the Monod-type relationship, limited by the stored mass concentration, (Busby & Andrews, 1975 ; Ekama & Marais, 1977; Dold et al. 1980).

$$\frac{dXs}{dt} = -\frac{Km \cdot Xa \cdot Xs}{Ks + Xs} \qquad (3.15)$$

The rate of storage is reported to be faster than the rate of utilization (Marais & Ekama 1976), but under steady-state operating conditions the two rates should be equal. Subsequently, storage phenomena are no longer observed and the Monod relationship is adequate for describing the overall substrate utilization process. Furthermore, the distinction between soluble and particulate biodegradable substrates becomes less important for systems operating under long operating sludge ages, since a greater proportion of the particulate substrate is metabolized (Clifft & Andrews 1981a).

The amount of viable bacteria in the sludge has been shown by various workers to be very small. For pure cultures growing on single substrates such as glucose, acetate and stearate the bacterial content of the sludge was estimated from their activity to be in the range of 10% and from count techniques to be less than 1%. In order to explain the above discrepancy, Jones (1978) suggested that substrate utilization by bacteria is not necessarily followed by growth. He then postulated three types of biochemical activity other than growth, which utilize substrate. These are cell maintenance of viable bacteria, 'posthumous' activity of non-viable bacteria and cometabolism of substrate which is a biochemical activity of cells towards a substrate on which they do not grow. Recognition of these activities explained well the low proportion of viable bacteria in comparison to the observed biochemical activity. He also hypothesized that the posthumous activity brings inertia to the system which explains the relative insensitivity of effluent quality to abrupt changes in the operating conditions.

Daigger & Grady (1982) noticed the existence of a gap in the literature between the commonly reported growth and storage response of microbial cultures and attempted to bridge that gap by developing a unifying theory concerning the microbial growth dynamics on soluble substrates. They pointed out that physiological adaptation and microbial species selection could be used to explain transient response phenomena. They reported that in any substrate transient, the microbial growth shows two responses.

- an immediate response, known as "Available Reaction Potential", which is the ability of a microbial culture to rapidly increase its growth rate under a transient,

- a slower response, known as "Growth Rate Hysteresis", which causes the lag in growth rate from the theoretically predicted.

In addition they reported that storage and/or release of metabolic intermediates may also occur depending upon the lags in the growth response. Their unified theory integrates the above knowledge and is presented as a conceptual model with hypothesized reactions. Suitable selection of the rate constants in their model allows the description of either of the reported responses.

3.2.6 Endogenous respiration of biomass

Endogenous respiration is the biological process under which viable organisms are utilized by other organisms in order to provide energy for cell maintenance and proceeds even when excess nutrient is available (McKinney 1962). However Grady and Roper (1974) suggested that non-viable cells can also undergo endogenous metabolism. The decay of micro-organisms occurring through death, lysis, predator activity and cellular metabolism, has been widely reported to follow first-order kinetics with respect to the active biomass concentration.

$$\frac{dXa}{dt} = -Kd \cdot Xa \qquad (3.16)$$

where; Kd : decay rate coefficient $[T^{-1}]$.

The decay rate coefficient has been either assumed to be constant for a particular process or temperature dependent. However some workers (Marsili-Libelli, 1980) have assumed that the decay rate is inversely proportional to the reactor substrate concentration.

The endogenous respiration process requires an exogenous electron acceptor, such as oxygen or nitrate, in order to make the energy available, implying that it cannot take place under anoxic or anaerobic conditions. However Dold et al. (1980) observed experimentally that endogenous respiration was also taking place in anaerobic zones. In order to explain this phenomenon they proposed a death-regeneration approach to replace the endogenous respiration concept. This approach assumes that active organisms die at a certain rate; a portion of the material from death is non-degradable and forms an inert endogenous residue, while the remainder becomes available as slowly biodegradable particulate substrate and is subsequently used for new cell synthesis. The regenerated mass is less than the dead mass because of energy losses during synthesis which explains the net loss of sludge mass. Under this concept oxygen is used only during cell synthesis, while organism death with its associated lysis of biodegradable material continues even under anaerobic conditions.

Finally, the non-degradable residue from organism decay has been assumed to form an inert mass, (Busby et al. 1975; Dold 1980; Clifft et al. 1981a). Gaudy et al. (1970, 1971) based on experimental results, argued the existence of an inert fraction in the synthesized biomass, and they suggested that all cell mass can undergo lysis and subsequent metabolism by active organisms.

3.2.7 Environmental effects

The microbial growth kinetics are generally reported to be temperature dependent. Several researchers (Muck & Grady, 1974; Adams & Eckenfelder 1974; Marais & Ekama 1976), found that the effect of temperature on the growth and decay rates can be described by an Arrhenius equation :

$$R_{(t)} = R_{(T)} \cdot \theta^{(t-T)} \qquad (3.17)$$

where; $R_{(t)}, R_{(T)}$: reaction rates at temperature t and T respectively,
θ : temperature coefficient.

The carbonaceous oxidation process is also affected by the DO concentration in the reactor, which can inhibit the growth of biomass at low concentrations. The DO limitation is usually expressed by Monod-type relationship, in which the half-rate limitation constant has been reported to range between 0.25 and 1.0 mg/l (Terashima et al. 1985).

The optimum pH is reported between 6.5 and 7.5, although growth can occur over the range of 4 – 9.5. Some other conditions favourable to the growth of biomass is the presence of trace elements, such as sulphur, iron, calcium, potassium and zinc, as well as the maintenance of a $BOD : N : P$ ratio at 100 : 5 : 1. Mixing is also important for suspended growth systems, to ensure effective contact between active biomass and organic matter.

Finally the presence of toxic or other inhibitory substances can inhibit growth. For the case of competitive or allosteric inhibition, Michaelis-Menten expressions have been used to describe the organism specific growth rate (Jorgensen 1983).

$$\mu = \mu_{max} \cdot S/(Ks + S + a \cdot I) \quad \text{for competitive inhibition} \qquad (3.18a)$$

$$\mu = \mu_{max} \cdot S/[(Ks + S) \cdot (1 + a \cdot I)] \quad \text{for allosteric inhibition} \qquad (3.18b)$$

while other workers have used the Haldane equation for describing the inhibited growth rate.

$$\mu = \frac{\mu_{max} \cdot S}{Ks + S + S^2/Ki} \qquad (3.18c)$$

where; I : concentration of the inhibiting substance $[ML^{-3}]$,
S : concentration of inhibited substrate $[ML^{-3}]$,
a, Ki : inhibition constant for I.

3.3 Nitrification process

3.3.1 Reactions of nitrification

Nitrification is the biochemical process by which certain chemoautotrophic bacteria oxidize inorganic forms of nitrogen in order to derive their energy requirements for growth and cellular metabolism. The energy is stored by the organisms in the form of adenosine triphosphate (ATP), which is produced by chemical reactions involving the transfer of electrons. The free electrons are produced during the oxidation of inorganic nitrogen. In addition the necessary carbon for growth is obtained from CO_2 or bicarbonate.

The bacteria species responsible for carrying out nitrification in wastewater treatment are the genera Nitrosomonas and Nitrococcus for the oxidation of ammonia to nitrite, and the genera Nitrobacter and Nitrocystis for the oxidation of nitrite to nitrate. The conversion of ammonia, which is mainly in the form of ammonium ion (NH_4^+), to nitrates by autotrophic bacteria has been considered to proceed in two steps according to the following reactions (Painter 1970; Sharma 1977) :

oxidation

$$NH4^+ + 1.5\ O_2 \xrightarrow{\text{Nitrosomonas}} 2\ H^+ + H_2O + NO_2^- + 58 - 84\ \text{Kcal} \qquad (3.19a)$$

$$NO_2^- + 0.5\ O_2 \xrightarrow{\text{Nitrobacter}} NO_3^- + 15 - 21\ \text{Kcal} \qquad (3.19b)$$

synthesis

$$15\ CO_2 + 13\ NH4^+ \xrightarrow{\text{Nitrosomonas}} 10\ NO_2^- + 3\ C_5H_7NO_2 + 23\ H^+ + 4\ H_2O \qquad (3.20a)$$

$$5\ CO_2 + NH4^+ + 10\ NO_2^- + 2\ H_2O \xrightarrow{\text{Nitrobacter}} 10\ NO_3^- + C_5H_7NO_2 + H^+ \qquad (3.20b)$$

overall reaction of nitrification

$$NH4^+ + 1.83\ O_2 + 1.98\ HCO_3^- \longrightarrow 0.021\ C_5H_7NO_2 + 0.979\ NO_3^- + 1.041\ H_2O + 1.88\ H_2CO_3 \qquad (3.21)$$

In the nitrification process the Nitrosomonas is the slowest reacting organisms, because of the higher energy requirements for the first stage of nitrification, while

the second stage proceeds much faster. For this reason it is not common to have significant quantities of nitrites in the effluent since they are rapidly converted into nitrates (Marais & Ekama 1976). The amount of nitrifying organisms in the sludge is relatively small. Huang & Sheikholeslami (1982) reported that only 5.2% of the $MLVSS$ was composed of viable Nitrosomonas in a conventional activated sludge after 10 days of ammonia acclimation. Other workers have reported even lower levels of around 1% of the dry sludge weight (Painter 1977).

The yield of nitrifying organisms is small, estimated stoichiometrically at 0.146 grams of Nitrosomonas and 0.020 grams of Nitrobacter per gram of ammonium-nitrogen ($NH_4^+ - N$) and nitrite-nitrogen ($NO_2 - N$) oxidized respectively, while their generation times are in the range of 10 to 30 hr. As a result a rather long sludge age, of above 7 days is required to ensure an adequate population of these organisms. Finally, from the stoichiometry of the overall reaction (equation 3.21), derives that the oxidation of 1 gram of ammonium nitrogen requires 4.18 grams of oxygen and produces 0.166 grams of autotrophic biomass.

3.3.2 Kinetics of nitrification

Dold & Marais (1980) adopted the total Kjeldahl nitrogen (TKN) as a measure of the influent nitrogen into a plant, which they subdivided into four fractions, exhibiting different kinetics in the process :

(i) soluble free and saline ammonia, which is directly converted to nitrite and nitrate via nitrification,

(ii) soluble biodegradable organic nitrogen, which is converted to ammonia through ammonification by heterotrophic bacteria, prior to nitrification,

(iii) soluble unbiodegradable organic nitrogen, which is a negligible fraction of the total nitrogen (0–4% of TKN),

(iv) particulate unbiodegradable organic nitrogen, which is associated with the particulate unbiodegradable COD and the endogenous residue of the decayed biomass.

Dold et al. (1980) found that in South African municipal wastewater 65–75% of TKN was in the form of ammonia and 25–35% was in the form of organic nitrogen, while the particulate nitrogen was only 10% of TKN. Subsequently they assumed that the biodegradable organic nitrogen is principally in soluble form. On the contrary the IAWPRC task group model (Dold & Marais 1986), assumes that all the biodegradable organic nitrogen is particulate and that it is hydrolysed to soluble nitrogen at the same rate as the particulate COD. The soluble organic nitrogen

is then converted to ammonia (ammonification) by heterotrophic bacteria, and was expressed by a first-order reaction :

$$\frac{dNsd}{dt} = -Kr \cdot Nsd \cdot Xa \qquad (3.22)$$

where; Kr : ammonification rate $[M^{-1}L^3T^{-1}]$,
Nsd : soluble organic nitrogen concentration $[ML^{-3}]$,
Xa : active biomass concentration $[ML^{-3}]$.

The growth of the nitrifying bacteria is reported to follow either first-order kinetics with respect to ammonia concentration in the reactor or, more commonly, Monod kinetics when the ammonia concentration becomes a limiting factor, (Downing et al 1964; Poduska & Andrews 1975; Williamson & McCarty 1975; Gujer 1977; Dold et al 1980). Assuming Monod kinetics the specific growth rate is given by the equation :

$$\mu_N = \frac{\mu_{Nmax} \cdot N}{K_{NH3} + N} - Kd_N \qquad (3.23)$$

where; μ_N : specific growth rate of nitrifiers $[T^{-1}]$,
μ_{Nmax} : maximum growth rate $[T^{-1}]$,
N : $NH_3 - N$ concentration $[ML^{-3}]$,
K_{NH3} : half-rate $NH_3 - N$ concentration $[ML^{-3}]$,
Kd_N : endogenous respiration rate of nitrifiers $[T^{-1}]$.

In the above equation the growth rate approximates zero-order with respect to ammonia concentration, when K_{NH3} is much lower than N. However, zero-order kinetics have been reported by various authors, such as Downing et al. (1964) and Hall & Murphy (1980), even at low ammonia concentrations of 1–3 mg/l, as a result of the small value of the K_{NH3} coefficient (Terashima et al. 1975).

Further, Dold et al. (1986) suggested that ammonia also serves as the nitrogen source for heterotrophic cell synthesis, and in the case of insufficient ammonia the growth would be limited to the rate that ammonia becomes available from cell death. Finally Marais & Ekama (1976) reported that the ammonification rate is much slower than the nitrification rate and can therefore become the limiting factor in nitrification kinetics.

3.3.3 Environmental effects

The nitrification process is very sensitive to external conditions such as temperature, pH level, alkalinity, dissolved oxygen and sludge age. The optimum temperature for

the growth of nitrosomonas is about 35 ^{o}C. Downing et al. (1964) expressed the temperature dependency of the maximum growth rate by an Arrhenius equation :

$$\mu_{N\,max(T)} = \mu_{N\,max(20)} \cdot \theta^{(T-20)} \qquad (3.24)$$

where; θ : temperature dependency coefficient.

According to Fair et al. (1968), the temperature sensitivity tends to decrease with increasing sludge age. Similarly, Ekama & Marais (1979) observed experimentally that the temperature dependency of nitrification was significant at low sludge ages (3 days), but became insignificant at long sludge age (30 days). Cook (1983) based on simulation studies of an oxidation ditch process operating at long sludge ages also reported insignificant temperature dependency of nitrification.

The nitrifying organisms are obligate aerobes and Downing et al. (1964) recommended that the DO concentration should not fall below 0.5 mg/l, although other workers have suggested much higher DO levels of about 2 mg/l for uninhibited nitrification (Terashima et al. 1985). Stenstrom & Poduska (1980) reviewing the literature, concluded that for high sludge ages nitrification can be achieved at DO level of 0.5–1.0 mg/l, while at lower sludge ages higher DO concentration is needed. Huang et al. (1985) observed experimentally that some nitrification was taking place even under anoxic conditions, which they attributed to possible entrapment of oxygen onto the bioflocs. They also suggested that the optimum pH for the growth of nitrifiers was between 7.2 and 8.0, and Wild et al. (1971) reported an optimum pH at 8.4.

Terashima et al. (1985) observed experimentally that the nitrification rate decreases significantly at an alkalinity below 150 mg/l (expressed as $CaCO_3$) and they proposed a Monod-type relationship to express this inhibition. The nitrification reaction causes a reduction in alkalinity, because the produced hydrogen ions react with the bicarbonate in wastewater according to the reaction.

$$H^+ + HCO_3^- \longrightarrow H_2CO_3 \longrightarrow CO_2 + H_2O \qquad (3.25)$$

However under concurrent ammonification and denitrification reactions, as is the case in the oxidation ditch process, the majority of the alkalinity can be recovered (Dold et al. 1985). Finally, the growth of nitrifying organisms can be significantly inhibited in the presence of toxic substances such as thio-urea, phenol and free nitrous acid, and heavy metals such as copper, silver, mercury, nickel and chrome (Downing et al. 1964).

3.4 Denitrification process

Biological denitrification is a process by which a variety of facultative heterotrophic bacteria such as Pseudomonas, Achromobacter, Micrococcus and Bacillus reduce oxidized forms of nitrogen under anoxic conditions. In the absence of molecular oxygen the nitrates serve as the hydrogen acceptor for the synthesis of heterotrophic organisms, while a small part serves as the nitrogen source for growth. As a result, nitrates are reduced to nitrogen gas and other forms of nitrogen such as nitrites, ammonia and nitrous acid. For the denitrification reaction a carbon source is necessary, which is oxidized for supplying the necessary energy and carbon for cell growth. Other elements necessary for denitrification include phosphorous, sulphur and trace elements.

The reduction of nitrates to nitrites and nitrogen gas under anoxic conditions, using methanol as the carbon source is usually described by the following reactions (McCarty 1973) :

reduction

$$NO_3^- + 0.33\ CH_3OH \xrightarrow[\text{denitrifiers}]{\text{anoxic cond.}} NO_2^- + 0.33\ CO_2 + 0.67\ H_2O \qquad (3.26a)$$

$$NO_2^- + 0.5\ CH_3OH \xrightarrow[\text{denitrifiers}]{\text{anoxic cond.}} 0.5\ N_2 \uparrow + 0.5\ H_2O + OH^- + 0.5\ CO_2 \qquad (3.26b)$$

synthesis

$$3\ NO_3^- + 14\ CH_3OH + CO_2 + 3\ H^+ \xrightarrow{\text{denitrifiers}} 3\ C_5H_7NO_2 + 19\ H_2O \qquad (3.27)$$

overall reaction

$$NO_3^- + 1.08\ CH_3OH + H^+ \xrightarrow[\text{denitrifiers}]{\text{anoxiccond.}} 0.065\ C_5H_7NO_2 + 0.47\ N_2 \uparrow + 0.755\ CO_2 + 2.44\ H_2O \qquad (3.28)$$

From the stoichiometry of the overall reaction derives that 1 gram of nitrate-nitrogen (NO_3-N) reduced to nitrogen gas, produces 0.53 grams of denitrifying biomass and consumes 2.47 grams of methanol. The amount of chemically bound oxygen released during the reduction of nitrates, calculated from the stoichiometry of the overall reaction is 2.71 gO_2/g NO_3-N.

The denitrification process is sensitive to the ambient conditions. The growth rate of the group of facultative micro-organisms, which here is referred to as denitrifiers, is significantly reduced at low temperatures, pH outside the range 7–9, under low organic substrate in the reactor, or in the presence of dissolved oxygen. The energy yield from denitrification is slightly less than the yield from oxygen respiration

and this prevents denitrification to proceed when measurable amounts of oxygen are present (Christensen & Harremoes, 1977). Bauman (1975) suggested that a DO of 0.5 mg/l is the highest limit for denitrification. Sharma et al. (1977) expressed the DO inhibition by the following expression :

$$f_{(DO)} = 1 - \frac{DO}{Ko + DO}$$

where; $Ko = 0.1\ mg/l$, half-rate DO concentration $[ML^{-3}]$.

The type of carbon source has a significant influence on the denitrifier activity. Methanol is the most favourite carbon source (Bauman 1975), however raw sewage carbon or endogenous carbon can be also utilized but the reaction rate is slower.

The denitrification rate has been described as a zero-order with respect to nitrate-nitrogen concentration, however Monod kinetics can be used at very low nitrate concentrations (Christensen & Harremoes 1977). Expressing the effect of organic substrate limitation via a Monod function and the temperature dependency via an Arrhenius function, produces the following equation for the denitrification rate :

$$R_{D(T)} = R_{Dmax(20)} \cdot \frac{N}{K_{NO3} + N} \cdot \frac{S}{K_{SD} + S} \cdot \theta^{(T-20)} \qquad (3.29a)$$

and the specific growth rate of denitrifiers is given by :

$$\mu_D = R_D \cdot \frac{Y_D}{DX} - Kd_D \qquad (3.29b)$$

where; $R_{D(T)}$: denitrification rate at T $[ML^{-3}T^{-1}]$,
R_{Dmax} : maximum rate $[ML^{-3}T^{-1}]$,
N : $NO_3 - N$ concentration $[ML^{-3}]$,
K_{NO3} : half-rate NO_3-N concentration $[ML^{-3}]$,
S : organic substrate concentration $[ML^{-3}]$,
DX : denitrifier concentration $[ML^{-3}]$,
K_{SD} : half-rate organic substrate concentration $[ML^{-3}]$,
μ_D : specific growth rate of denitrifiers $[T^{-1}]$,
Y_D : yield of denitrifiers from nitrate reduction [-],
Kd_D : decay rate of denitrifiers $[T^{-1}]$,
θ : temperature coefficient [-].

3.5 Mass transport mechanism

It is widely accepted that the hydraulic regime of a reactor influences its performance and determines to some extent its behaviour under transient conditions. Hence, a

completely mixed reactor tends to attenuate the disturbance caused by a shock input load, while a plug- flow reactor tends to delay that disturbance for a period equal to the mean retention time but without reducing its amplitude. However, most reactors operate under an intermediate hydraulic regime between the complete-mixed and plug-flow conditions, which is usually simulated by representing the reactor with a number of CSTRs in series (Tomlinson & Chambers 1979).

The output response of a reactor resulting from "delta" and "step" inputs of a conservative substance is shown in Figure 3.1a, for a different number of CSTRs. For a non-conservative substance which is transformed through a biochemical reaction, the output concentration is theoretically reduced with increasing number of CSTRs. This could be explained by the reduction in axial dispersion, which allows part of the substance to escape in the effluent before it is sufficiently treated. The output response due to a step input function of a non- conservative substance transformed by a first-order reaction for different hydraulic regimes is shown in Figure 3.1b.

In order to determine the hydraulic regime of a reactor, tracer studies are usually carried out. Such studies were performed in a oxidation ditch plant at Ash Vale (Rachwal et. al, 1983), using the radioactive ^{82}Br as a tracer. The response (tracer concentration) of the reactor resulting from an input "delta" function of the tracer, was monitored with time at a specific location in the channel near the effluent weir, shown in Figure 3.1c. The dampened oscillating curve indicates that near plug-flow conditions exist for short periods of time ($1 - 2$ *hr*), since after about 4 *hr* the concentration in the reactor becomes almost uniform. Hence the oxidation ditch approximates the response of a completely mixed reactor if it is viewed over its hydraulic residence period of 10 *hr*.

The short-term plug-flow conditions are the result of the channel configuration of the reactor, which does not encourage axial dispersion of the contents. However, the feed to the oxidation ditch is continuously diluted by $50 - 300$ times with the circulating mixed liquor, which ensures complete-mixed conditions and a uniform and stable concentration in the channel.

Terashima et al. (1985) simulated the oxidation ditch by 10 CSTRs in series and studied theoretically the hydraulic regime for different dilutions of the feed. They showed that for circulation flows greater than 20 times the feed flow, the hydraulic regime is similar to complete mixing. In another simulation study they considered a 5 CSTR representation with a circulatory flow from the last to the first reactor and back flow between the reactors. Their results showed negligible spatial variation of all process variables except for the *DO*, which does not justify the adoption of the complex tank-in-series model when the *DO* profile is not simulated.

In order to simulate the mixing regime in the ditch more realistically, Cook (1983,

1984a) represented the reactor by alternating series of CSTR and plug-flow units. The CSTR configuration represented the high degree of mixing created by the aerators in the aerated zones, while the plug-flow approximated the quiescence in the non-aerated zones. Comparing the behaviour of the transfer functions of the above system with that of a single CSTR system, he reported very similar responses after an initial small time lag, during which different responses were exhibited. Therefore, in view of the simplicity offered by the single CSTR representation the configuration initially assumed was rejected.

3.6 General assessment of process models

3.6.1 Introduction

The activated sludge process and its modifications have been studied by many workers, however relatively few studies are specifically devoted to modelling the oxidation ditch process. Due to similarities in these processes, the modelling approaches used for the activated sludge can provide useful information for the subsequent modelling of the oxidation ditch. Several approaches to modelling the activated sludge have been pursued by different workers, depending on the purpose of modelling, the required complexity for describing the various processes, and the available experimental data for model calibration and validation. Modelling approaches may be broadly classified according to the following characteristics :

- according to the type of data used, such as literature-based data, laboratory data, pilot-plant data and full-scale plant operating data.
- according to type of model, such as black-box (input-output) model, descriptive steady-state or dynamic model and deterministic or stochastic model.
- according to purpose of modelling, such as for plant design, short or long term forecasts, process control and optimization.
- according to the processes considered, such as carbonaceous oxidation, nitrification, denitrification in aeration tank and/or clarification and solids thickening in the final clarifier.
- according to the complexity of the model structure such as by using lumped or spatially distributed variables, structuring the biomass and/or substrate, and describing in detail individual species and biochemical pathways.

3.6.2 General comments on models

A survey of the various models presented in the literature showed a large diversity of model types and structures developed for the activated sludge process and its main modifications depending on their potential applications. However it also revealed that most studies suffered from weaknesses such as :

- There is a general lack of model validation tests, except for few cases in which the validation was not always successful.
- The model calibration (parameter estimation) is rarely based on a formal estimation technique, while in most cases literature-based parameter values are employed or ad hoc parameter fitting is attempted.
- In most cases where a successful calibration or validation have been reported, the data used and the subsequent simulation studies covered a short operating period, which cannot guarantee the long-term validity of the proposed model.
- The thickening capability of the final clarifiers which largely affects the mixed liquor level in the aeration tank is usually neglected or poorly represented.

A brief review of the modelling approaches follows, which were classified according to the type of model used.

3.7 "Black-box" (input-output) models

"Black-box" or input-output models have been used by some workers in an attempt to develop simple relationships between influent and effluent process variables. Black-box models offer an alternative to internally descriptive models (defined in Section 1.4.4), because they require virtually no information about the process. In addition they are an alternative in a sense to deterministic models because their development is based on the statistical properties of process measurements. In the case where the input and output measurements form a time series, the methodology proposed by Box & Jenkins (1970) for Time Series analyses is usually adopted.

Berthouex et al. (1978) realizing the limited knowledge available on the internal mechanisms of the activated sludge, employed Time Series analyses techniques in an attempt to relate the effluent filtrable BOD to the influent BOD and crude sewage flow. The analysis was based on hourly data collected over a 2-week period and the Box and Jenkins methodology was employed. Their results showed that a simple first- order autoregressive model of the effluent BOD explained 73.5% of its variance, while more complex transfer function models, involving the influent BOD and flow rate improved the fit marginally. Finally they emphasized the importance of the

noise term in the model which explained most of the variance in the effluent BOD series.

Debelac et al. (1981) also employed the Box & Jenkins methodology for predicting the effluent COD from its influent concentration, using data from an industrial activated sludge plant. In order to find the best model with the minimum number of parameters they used the Akaike's information criterion (Akaike, 1974). Similarly with Berthouex, they found that single-difference models best described the individual input and output series. For the development of a transfer function model, they reported that the influent COD had an insignificant effect on its effluent concentration.

3.7.1 Discussion

The main criticism for black-box models arises from the fact that they do not exploit any available information about the process. This fact tends to reduce their forecasting ability and their applicability in situations different from those under which they were developed. Statistical and time series analyses techniques can be useful when applied for preliminary analysis of process data, because they can help in assessing their quality, and reveal potential relationships between them. However, the use of time series models for relating influent and effluent measurements in suspended growth processes, cannot adequately describe the dynamic behaviour of the process. This is caused by the insignificant correlation usually reported between inputs and outputs which may be ascribed to factors such as :

- the input load variations are highly attenuated due to the intense mixing and biochemical activity in the reactor.
- the output variables (BOD or COD), under normal operating conditions can be regarded as consisting of a smooth underlying signal with significant added noise due to various disturbances and in many cases the effluent series approximate a noise rather than a structured sequence.
- The relationship between process inputs and outputs is in general non-linear and cannot be adequately described by the general class of ARIMA models.

The above limitations have diminished the use of input-output models, as well as the use of time series techniques alone for model development.

3.8 Steady-state models

Steady-state internally descriptive process models have been used by several workers, in an attempt to relate the effluent quality to the plant input and operating conditions by simple non-dynamic equations (Goodman & Englande (1974); Muck & Grady (1974); Benefield & Randal (1975); Wang et al. (1976); Christoulas & Tebbutt 1976; Gaudy et al. (1977); Sykes (1981)). The main operating conditions employed by steady state model regarding the aeration tank performance are the biomass sludge age, the hydraulic retention time, and the sludge loading rate, and for the final clarifiers the solids loading rate, the hydraulic retention time, and the overflow rate.

The development of steady-state models is usually based on a priori knowledge of the process kinetics and the calibration is performed with data collected under normal plant operating conditions and typical input loads. Consequently such models can be very useful for design purposes, where they have been mainly applied, rather than for performance evaluation and process control.

A typical example is the model developed by Christoulas & Tebbutt (1982) for the complete-mix activated sludge using a first-order reaction kinetics for substrate utilization as proposed by Grau et al. (1975) (eq. 3.8 in Section 3.2.2). Their model falls into the category of simple steady-state relationships to be used for design purposes, and several simplifying assumptions had to be made such as :

- the biomass behaves a single species of organisms,
- the substrate is measured by means of overall parameters such as BOD or COD,
- phenomena such as substrate storage, lysis and reutilization of biomass and prey-predator interactions are negligible,
- the growth and decay rates of biomass and the yield coefficient are constant.

The model relates the mean operating sludge age with the BOD removal efficiency according to the equation :

$$\frac{1}{\theta_C} = K \cdot Y \cdot (1 - E) - b \qquad (3.30)$$

where; $E = (So - S)/So$: BOD removal efficiency [–],
θ_C : sludge age of biomass $[T]$,
K : first-order reaction rate $[T^{-1}]$,
Y : yield coefficient [–],

b : biomass decay rate $[T^{-1}]$.

They reported good performance of the simple model with data obtained from experiments with synthetic substrates, although the performance was not so satisfactory with real process data. Using average operating data from 10 wastewater treatment plants they estimated values for the model parameters by linear regression. The model can then be used for calculating key design parameters of a plant including the $MLSS$ level and the tank volume.

CIRIA in conjunction with the WRC (WRC, 1981), developed a number of models to describe a wide range of wastewater treatment processes among which is the activated sludge. The models fall into the category of steady-state and mainly intend to aid the design of unit operations. The models are based on existing knowledge of the process and are calibrated with averaged operating data from full-scale plants. It has been reported that the models can predict successfully the average performance of a plant over a period of at least one month, but they are unable to predict short-term performance resulting from abnormal changes in loads, flows or operating conditions.

3.8.1 Discussion

Steady-state models have been shown to adequately describe the behaviour of a plant under normal (steady-state) operating conditions, and predict average performance variables. However they are unable to predict the response of a plant under unsteady operation. In practice most plants operate under continuously changing conditions and steady-state operation is never established. This is a result of the time varying input loads, the dynamic behaviour of the biochemical reactions and changes applied to the operating variables.

This study focuses on simulating the dynamic behaviour of the process, hence steady-state models are considered inappropriate.

3.9 Dynamic process models

3.9.1 General

The use of dynamic models to simulate the activated sludge process has been favoured by many workers because they offer greater potential for:

- simulating the dynamic behaviour of the process,

- developing efficient control strategies and evaluating their effectiveness on process performance.

McKinney (1962) presented the first rational kinetic theory for the complete-mix activated sludge expressed with dynamic equations and established the importance of hydraulic retention time, sludge loading rate (F/M ratio) and structuring of biomass into active, endogenous and inert fractions. He also suggested that below the critical F/M ratio of 2.1, the food becomes the limiting factor. He then proposed a first-order reaction for nutrient utilization with respect to their concentration only and independent of the biomass concentration, which differs fundamentally from the Monod approach.

A subsequent important study was by Lawrence & McCarty (1970) who presented a unified approach to biodegradation kinetics based on the Monod hypothesis for substrate utilization. They clarified the connection between F/M ratio and sludge age but they did not structure the biomass.

3.9.2 Marais model

Marais and his research team developed a dynamic model in order to investigate the time-dependent behaviour of the activated sludge process. Their model was an extension of the Lawrence & McCarty (1970) model and its development was accomplished through a sequence of modifications based on comparisons between theoretical predictions and experimental observations. The initial model makes the following assumptions (Marais & Ekama, 1976; Ekama & Marais, 1977) :

- Uses the COD measure for quantifying organic substrate concentrations and the TKN measure for nitrogenous substrates,
- structures the biomass into active, endogenous residue and inert mass,
- structures the influent organic substrate into biodegradable (readily assimilable and slowly degradable), unbiodegradable soluble and unbiodegradable particulate (Sec. 3.2.4),
- assumes the soluble substrate to be stored on the biomass prior to utilization, while the particulate unbiodegradable organics to accumulate in the sludge (Sec. 3.2.5),
- describes the substrate utilization and biomass growth by the Monod relationship (Sec. 3.15),
- structures the input TKN into free & saline ammonia, soluble biodegradable organic nitrogen, and soluble & particulate unbiodegradable organic nitrogen

(Sec. 3.3.2),

- assumes that nitrification is limited by the rate of degradation of the slowly biodegradable TKN,
- relates the oxygen consumption to the growth and respiration of the active biomass, as well as, to the nitrification reaction.

The initial model was subsequently modified to include the concept of particulate substrate storage onto the biomass, the stored mass hydrolysis prior to utilization (Sec. 3.2.5), and Monod kinetics for the growth of Nitrosomonas consuming an ammonia substrate (Ekama & Marais 1979). Assuming that the majority of input biodegradable substrate is particulate (80%), the model explained well the insensitivity of reactor COD to cyclic changes of the input COD. Later they adopted a death-regeneration approach to describe the decay of active biomass (Sec. 3.2.6), which explained the continuation of cell decay and production of substrate in anaerobic zones (Dold 1980).

The experimentation was carried out in a laboratory-scale plant consisting of a single CSTR reactor and a settling tank, fed with unsettled municipal sewage under both steady-state and daily cyclic loading conditions. The model calibration was conducted by trial and error, whereby adaptive changes were made to the kinetic constants until the best correlation between model predictions and experimental results were obtained for all the experiments (Ekama & Marais 1977). Initial values for the parameters were obtained either from the literature or derived from simple experimental observations.

The final model, Dold et al. (1980), showed good performance for two different sludge ages (2.5 and 20 days) and two different temperatures (12 and 20 ^{o}C). The model was tested on both a laboratory scale and a pilot plant unit under constant and diurnally varying conditions for assessing its validity. From the above tests, Dold et al. (1980) reported satisfactory performance of the model under different operating and loading conditions without the need to change the kinetic constants.

Discussion on Marais model

The model developed by the Marais' group attempts the detailed mathematical description of the internal mechanisms of suspended-growth processes. The model was developed through a sequence of modifications incorporating as much of the existing process knowledge in order to reproduce at best the experimental observations. This led to the development of a complex model structure with a large number of parameters to be determined and several unmeasurable variables to be estimated through simulations. For the purpose of modelling the oxidation ditch process, the model describes all the main processes except denitrification. However its complex

structure would hamper the estimation of its parameters using the available operating data.

Despite the complexity of the model some potential weakness can be identified which must be considered prior to its application :

- the model was calibrated and validated with observations spanning over a period of 26 *hr* only, which does not guarantee longer-term performance, since slow process dynamics may not be adequately described.
- there is no coupling of the aeration tank model with a suitable model for the final clarifier, which is widely recognized to play an important role on the overall performance of the process.
- the model is too complex to be effectively used for other purposes such as process control and optimization.
- some of the reaction rates had to be changed for a successful application of the model to other processes, such as the contact- stabilization process or single sludge denitrification (Dold et al. 1980). This fact reduces the initially assumed robustness and generality of the model.

3.9.3 Other dynamic models

Busby & Andrews (1975) developed a similar model to that of the Marais' group for the aeration tank but without nitrification, which they coupled with a dynamic model for the final clarifier. The final clarifier model described the three main functions namely, clarification, thickening and sludge storage. The clarification function was described by an empirical relationship proposed by Pflanz (1969), while the thickening model was based on the limiting-flux theory and was discussed in Section 2.2.3.

The parameter values were selected from the literature and were suitably adjusted to produce good performance. The model validation was only based on qualitative comparisons between simulation results and averaged performance data presented in the literature. Satisfactory agreement was reported for a wide range of activated sludge modifications.

Poduska & Andrews (1975) developed a dynamic model for nitrification, which predicts effluent ammonia, nitrite and nitrate concentrations. The model considers a two-stage nitrification process and the separate growth of Nitrosomonas and Nitrobacter organisms using Monod kinetics. Here the settler was modelled with a non-dynamic relationship based on separation efficiency. The parameters were selected either from the literature or determined from experimental data. The model

was verified experimentally on a lab-scale unit, subjected to step and impulse functions of influent nitrogen concentration and flow rates and satisfactory performance was reported.

Tanthapanichacoon & Himmelblau (1981) attempted to develop a dynamic model which would be applicable for several modifications of the activated sludge process after suitable selection of some coefficients. Their model simulates the primary settler, the aeration tank using the Busby & Andrews (1975) model for carbonaceous oxidation and the Poduska & Andrews (1975) model for nitrification, while the final clarifier was modelled according to the limiting-flux theory. The final model was very complex comprising 190 ordinary differential equations to be solved simultaneously.

The dynamic models presented so far, despite their structural differences and processes considered, fall into the same category of very complex and over-parameterized models. Such models can explain certain phenomena such as the fast removal of particulate organics and the slow response of biomass growth by considering the mechanisms of storage and hydrolysis prior to utilization (Sec. 3.2.5). As a result they would be useful for a detailed study of individual biochemical pathways. However their advantage in simulating the overall dynamic behaviour is minimal since the above phenomena have a minor effect during normal plant operation. In addition from the engineering viewpoint, such complex structures are in general impossible to calibrate from operational data and use for process control and optimization. Finally, since the knowledge about the biochemical and other processes is generally weak, it would be inappropriate to formulate a complex model, when a simpler model would be able to describe adequately the major functions of the process.

3.9.4 Simple dynamic models

Several workers appreciating the problems introduced by complex model structures, attempted to formulate simpler models describing the main processes only, which would be easier to calibrate and apply for control purposes.

Marsili-Libelli (1980) in his reduced-order model makes the following simplifications :

- no structuring of biomass or organic substrate is attempted. These variables are described by the overall measures of $MLSS$ and BOD_5 respectively,
- the substrate uptake rate is proportional to the concentrations of biomass and substrate,
- micro-organisms growth rate is proportional to substrate uptake and their decay rate is a function of the substrate concentration,

- no soluble substrate is returned through the recycle flow,
- the biomass concentration in the final clarifier underflow is constant.

The model parameters were fitted employing a least square algorithm and field data, and showed similar performance with a more complex model, however data limitations were reported in the conclusions.

Holmberg (1982) starting with a comprehensive 5-state model for carbonaceous oxidation and a 2-state model for the settler with a large number of parameters, made several simplifying assumptions which she empirically verified from observations at a pilot plant. She finally obtained a simple model with three measurable states namely, the VSS in the aeration tank and recycle flow and the effluent SS having a small number of parameters. The model was implemented on a microprocessor for state and input reconstruction, as well as for process monitoring and control.

Jones & Paskins (1980) also used a simple model in which substrate is utilized by both viable and non-viable bacteria and adopted Monod kinetics. The aeration tank model included nitrification and was coupled with a model for the final clarifier based on limiting-flux theory. Their model was able to predict well the concentration of $MLSS$ and ammoniacal nitrogen resulting from shock hydraulic loading, but gave poor predictions of the underflow concentration. However the model was not tested over a sufficiently long period in order to assess the validity of the growth kinetics.

For the purpose of optimal modelling using relatively simple structures, Sheffer et al. (1984) developed a "Flexible Modelling" approach. According to this approach a set of simple hierarchical models were derived, starting from a highly complex structured model and following a sequence of mechanistic simplifications. The relative performance of intermediate models was assessed via simulations. They concluded that for predicting the dynamics of $MLVSS$ a simple model based on first-order kinetics was adequate. To facilitate the procedure of model selection they proposed two criteria :

- a "matching criterion", which quantifies the degree of similarity between the model and the data based on the least square error.
- a "comparison index", which quantifies the difference between the predictions of the models.

3.10 Stochastic-dynamic, low-order models

A number of workers realizing the general scarcity of reliable information on the process mechanisms and the stochastic nature of process disturbances attempted

to identify a suitable model structure employing 'Systems Analysis' techniques as discussed in Section 1.4. The use of such techniques which is associated with the use of stochastic models and suitable recursive estimation algorithms for parameter estimation, such as the Kalman filter and the Instrumental variables, have been reported to offer potential solutions to several problems (Beck, 1981) :

- determination of dynamic relationships between inputs, states and output variables,
- estimation of parameters in the identified model structure,
- estimation of inaccessible state variables,
- determination of current and future state values,
- investigation of the stochastic components of the process.

The implementation of such techniques requires the representation of the process as a "system" and the definition of the input, output and state variables. The uncertainty introduced by input disturbances, model inaccuracies, and observation errors, is taken into account by using dynamic-stochastic model structures.

The advantage of this approach is that even a basic a priori knowledge about the process could be sufficient as a starting point for the development of the model. In addition such a model may be more successfully applied for process monitoring and control, or even for performance and running cost optimization, because it is derived from real process observations. A drawback of this technique is the large number of operational data necessary, under a variety of operating conditions for the successful identification of the system mechanisms, which may not be always obtainable.

Cook et al. (1981) using the low-order model proposed by Marsili-Libelli (1980) employed the Extended Kalman Filter (EKF) in order to reconstruct the model states and estimate its parameters from noisy process observations. In their work they emphasized the importance of using a simple model structure and they demonstrated the applicability of the algorithm to such estimation problems.

Beck (1981) employing the EKF algorithm, examined the feasibility of applying on-line, real-time state reconstruction and performance prediction for operational control in the activated sludge process. He focused on the dynamics of nitrification, using a dynamic stochastic model with a structure based on that proposed by Poduska & Andrews (1975). He reported reasonably good performance of both the model and the estimation algorithm for the following cases :

- state estimation and reconstruction of unobservable states, such as the concentration of Nitrosomonas and Nitrobacter populations.

- on-line predictions of the short-term future plant performance.

He also criticized the unnecessary complexity of the model structure introduced by the two-stage nitrification. Finally he discussed some of the model limitations, which he attributed to the non-dynamic nature of the final clarifier model and the assumed independence of nitrification rate from the DO and $MLSS$ concentrations.

Cook (1983, 1984b), studying the nitrification dynamics in an oxidation ditch system, demonstrated the use of the EKF algorithm as a tool for the identification of poorly-defined biological systems. The development of the model hypotheses arose from a deductive approach based on a priori knowledge, while the synthesis of the model structure followed an inductive reasoning approach based on real data processing by systems analysis techniques. The criterion for the selection of an adequate model structure was the time-invariancy of the parameters. The identified model, which was ultimately used for the simulation and control of nitrification, was criticized as being too complex and not fully validated, although it was reported to perform well in pure deterministic simulations as well as in a stochastic sense.

Finally, the problem of model identifiability was addressed by Holmberg & Ranta (1982). They reported problems of convergence when attempting to estimate the parameters in Monod growth kinetics employing optimization techniques based on least square error. In an attempt to fit realistic values to the model parameters, they proposed a trial and error manual procedure. This was based on intuitive guesses and was combined with a study of the sensitivity functions in the intervals where the model fit had to be improved.

3.10.1 Discussion

The employment of systems analysis techniques for data processing, combined with the use of basic a priori knowledge of the process, seems more prominent for the development of simple and robust process models, than the exclusive use of detailed biokinetic theories. The former approach leads to the development of relatively simple model structures, while the latter produces complex and over-parameterized models, which in general have limited applicability. Some of the advantages of the former approach compared to the latter are :

- greater potential to prespecify the complexity of the model and assess its adequacy on the basis of real process observations.
- ability to estimate time-varying parameters and reconstruct unobservable state variables.
- greater potential to use the model process control.

However, limitations in the application of systems analysis techniques may hamper the development of a successful model. Some of the limitations arise from :

- lack of sufficient and suitable process measurements for successful calibration and validation of the model.
- presence of significant noise in the observations which is not always random.
- experimentation under non-ideal conditions, where the process variables may not be sufficiently excited or under substantial unmodelled disturbances.
- the use of recursive algorithms for parameter estimation with non-linear model structures pauses several limitations, discussed in Appendix 2 for the EKF algorithm.

The above limitations may introduce bias to the parameter estimates and lead to unrealistic model structures. It follows that for the development of a sensible model, well founded theory about the process should form the basis of the model structure. This may be subsequently modified in the light of process data analyses.

Part II. Modelling the oxidation ditch process

3.11 Objectives of modelling

The objective of this chapter was to develop a mathematical model describing the major processes taking place in an oxidation ditch system. The developed model was intended to be used for several purposes such as:

- Evaluation of the long-term plant performance under various operating and input conditions.
- Estimation of unmeasurable process variables.
- Investigation of the reasons for process failures.
- Assistance in the development of an operating cost model.
- Assistance in the design of rational and efficient operating policies and application for process control.

3.12 Model-type selection

The development of the model structure was based on a priori knowledge from the literature, regarding the kinetics of the main processes in suspended-growth systems and particularly in the oxidation ditch. The initial model structure was refined in the light of additional (a posteriori) information obtained from analysis of operational measurements collected from the Cirencester oxidation ditch plant.

The main mathematical model types and their definitions were presented in Section 1.4.4. From the objectives of modelling it was apparent that an internally descriptive model would be necessary for studying the internal mechanisms of the process and assessing their effect on the overall performance of the plant. An important feature of the model would be its ability to predict the dynamic behaviour of the process under time-varying input and operating conditions, rather than its steady-state performance. This requirement presupposes that the model is dynamic and its state variables are expressed as functions of time. Furthermore the states, inputs, outputs and parameters of the model were assumed for not to vary with space, which characterizes the model as lumped-parameter.

Environmental systems are, in general, poorly-defined systems because of insufficient knowledge about their internal mechanisms. Furthermore the various measurements on a process are subjected to errors, as a result of incorrect calibration and unreliability of instruments, the effect of external disturbances and even human

errors. Hence, the use of deterministic models, which do not directly account for such errors, may not be always adequate for describing the system. The alternative use of stochastic models may have to be investigated. The model should be able to predict the plant performance at any given time, thus a continuous-time model was necessary, although its calibration and validation was based on discrete-time observations. For the sake of simplicity a linear model with time-invariant parameters would be ideal. However those two features cannot be guaranteed at this stage, because the formulation of a suitable model may demand the opposite. Hence, the model type adopted was continuous, internally descriptive, dynamic and lumped-parameter.

3.13 Model development stages

A variety of process models and kinetic theories were presented in Part I, and their application area, as well as, their merits and limitations were discussed. These information form the knowledge base for modelling the oxidation ditch process. The main processes in an oxidation ditch system which were considered in the development of the model were :

- Mass-transport of fluid and solids through the reactors.
- Solid-liquid separation and sludge thickening in the final clarifiers.
- Artificial aeration mechanism.
- Carbonaceous oxidation process.
- Nitrification process.
- Denitrification process.

Each of the above processes was studied in the following sections except for the final clarifier processes, which were already modelled in Chapter 2.

3.14 Transportation mechanism

3.14.1 Model formulation

It was discussed in the review (Section 3.5) that some workers (Terashima 1985; Cook 1983), attempted to represent the hydraulic regime in an oxidation ditch as a plug flow reactor assuming a number of CSTRs in series. However from simulation results they did not observe any significant improvement in the model performance compared with the completely-mixed representation. In addition studies with tracer at the Ash-Vale oxidation ditch plant (Rachwal 1983) showed that plug-flow conditions occur over

short time periods of $1-2$ hr, while after about $3-4$ hr the concentration of any substance in the reactor becomes uniform (Figure 3.2).

In the available data the inputs and outputs of the process were monitored from daily averaged samples. It follows that any short-term transients of the process, or short period plug-flow conditions had to be neglected, because they are not easily identifiable from the available measurements. Hence the hydraulic regime of the oxidation ditch was assumed completely-mixed and the reactor was represented by a single CSTR. Furthermore, the final clarification unit was also simulated as a single CSTR (Section 2.5.5). Therefore the oxidation ditch system was represented by 2 CSTRs in series, shown schematically in Fig. 3.3.

Under the complete-mix assumption, the concentration of any substance in the reactor is uniform and equal to the output concentration. For a soluble conservative substance entering the above oxidation ditch system (Figure 3.3), its output concentration from the ditch reactor and final clarifiers at any time t, is given from the following set of simultaneous differential equations based on mass-balance :

$$\text{Accumulation} = \text{Input} + \text{Recycle} - \text{Output}$$

1. Aeration tank concentration

$$\frac{d(V \cdot C_t)}{dt} = Qi_t \cdot Ci_t + Qr_t \cdot Ce_t - (Qi_t + Qr_t) \cdot C_t \tag{3.31}$$

2. Final Clarifier concentration

$$\frac{d(Vcl \cdot Ce_t)}{dt} = (Qi_t + Qr_t) \cdot (C_t - Ce_t) \tag{3.32}$$

where; Qi_t : input flow rate at time t $[L^3T^{-1}]$,
Qr_t : recycle flow rate at t $[L^3T^{-1}]$,
Ci_t : input concentration at t $[ML^{-3}]$,
C_t : aeration tank output concentration at t $[ML^{-3}]$,
Ce_t : final clarifier effluent concentration at t $[ML^{-3}]$,
V : volume of the aeration tank $[L^3]$,
Vcl : volume of the final clarifiers $[L^3]$.

However, for a particulate conservative substance which settles out by gravity under quiescent conditions, its underflow concentration from the clarifiers is given by the following equation developed in Section 2.5.5 (eq. 2.16).

$$\frac{d(Vcl \cdot Cr_t)}{dt} = (Qi_t + Qr_t) \cdot C_t - (Qi_t - Qw_t) \cdot Ce_t - (Qr_t + Qw_t) \cdot Cr_t \tag{3.33}$$

where; Cr_t : underflow (recycle) concentration at t $[ML^{-3}]$,
Qw_t : surplus sludge flow at t $[L^3T^{-1}]$.

It is generally known that the short-term dynamic behaviour of mixed liquor solids in the units of a plant is predominantly affected by variations in the flow rates and by the prevailing hydraulic regime in the reactors; the growth kinetics of biomass have a modest short-term effect. As a result the adequacy of the oxidation ditch representation by 2 CSTR units could be assessed from the ability of the above 'hydraulic' model to reproduce the observed solids concentration in the aeration tank and clarifier underflow. For the purpose of simulating the solids behaviour alone, it was assumed that the influent solids behave as conservative substance and that no biochemical activity takes place in the reactor.

3.14.2 Results and discussion

Using the measured inputs to the plant over the study period and employing the 'hydraulic' model, described by equations 3.31 & 3.33, the behaviour of solids in the aeration tank and final clarifier underflow was simulated. The hydraulic model contained no parameters, hence it was directly used. The differential equations were solved numerically using the 4th-order Runge-Kutta integration method. The results are presented in Figure 3.4 and their basic statistics in Table 3.1. The aeration tank solids represent the mixed liquor concentration ($MLSS$), while the underflow solids represent the recycle sludge concentration ($RASS$). These were compared with the measured $MLSS$ and $RASS$ concentrations respectively. The definition of the statistical parameters are given in Appendix 1.

Parameter	$MLSS$	$RASS$
mean (mg/l)	3302.5	6717.4
std. deviat.	1357.6	2415.7
C.O.D.	0.489	0.693
R	0.855	0.840
mean error (mg/l)	573.1	185.0
RMS error	916.0	1437.0
var. error	0.5124E+6	0.2038E+7
sum sq. error	0.2375E+9	0.5844E+9

Table 3.1. Hydraulic model performance (basic statistics).

The performance of the hydraulic model in predicting the $MLSS$ and $RASS$ concentrations was satisfactory for most of the simulated period, even though the biochemical component was not included. The model reproduced sufficiently well the

observed peak in the $MLSS$ between day 100 and 130 and the subsequent decrease in both the $MLSS$ and $RASS$ concentrations after about day 170. The poorest performance was observed in the $MLSS$ series for the period between day 170 and 270, where the model predictions were substantially lower than the observations. Nevertheless the $RASS$ concentration was adequately predicted during the above period.

Examination of the operational data revealed that during the above period the recycle flow rate was dramatically reduced to levels well below the nominal design value between day 182 and 236. This was followed by an increase in the surplus sludge flow between days 196 and 212. The consequence of such operating conditions was the steady reduction of solids in the system. This reduction was predicted by the model to occur at a faster rate than it was observed, causing the underestimation of the $MLSS$. Possible reasons for the observed discrepancy were considered to be :

- Inadequate representation of the system hydraulic regime by a single CSTR for the aeration tank and final clarifiers.
- Influence of the neglected return liquor stream.
- Existence of systematic error in the flow or solids measurements during that period.
- Neglect of the endogenous respiration of biomass.

The representation of the final clarifiers by a single CSTR was found adequate when simulated as an independent system (Section 2.5.5). Here the incorporation of the aeration tank unit as a single CSTR produced a different system with two units interacting upon each other, since the outputs from one unit become the inputs to the other. This system, which represents the hydraulic configuration of the oxidation ditch plant, produced satisfactory predictions of the $RASS$ concentration over the whole study period and for the $MLSS$ during most of the period. Thus, the proposed system representation was considered adequate and other possible causes of the discrepancy were investigated.

The influence of the return liquor stream was examined by incorporating it into the model. The return liquor solids concentration was not measured, hence a constant concentration of 300 mg/l was assumed which was considered realistic for thickener supernatant and drainage liquors. The model equations were subsequently modified :

$$\frac{d(V \cdot C_t)}{dt} = Qi_t \cdot Ci_t + Qr_t \cdot Cr_t + Qrl_t \cdot Crl - (Qi_t + Qr_t + Qrl_t) \cdot C_t \qquad (3.34)$$

$$\frac{d(Vcl \cdot Cr_t)}{dt} = (Qi_t + Qr_t + Qrl_t) \cdot C_t - (Qi_t - Qw_t + Qrl_t) \cdot Ce_t - (Qr_t + Qw_t) \cdot Cr_t \qquad (3.35)$$

where; Qrl_t : return liquor flow rate $[L^3T^{-1}]$,
Crl : return liquor concentration $[ML^{-3}]$.

Parameter	$MLSS$	$RASS$
mean (mg/l)	3399.0	7016.9
std. deviat.	1399.9	2430.8
C.O.D.	0.538	0.695
R	0.855	0.840
mean error	476.6	-114.4
RMS error	871.4	1431.8
var. error	0.5341E+6	0.2044E+7
sum sq.error	0.2149E+9	0.5802E+9

Table 3.2. Hydraulic model with return liquor (basic statistics)

The simulation results are presented in Fig. 3.5 and in Table 3.2. It can be seen that the inclusion of the return liquor term reduced slightly the prediction error in $MLSS$. However it did not improve significantly the model performance, judged by the determinants R and C.O.D. Nevertheless, the marginal improvement achieved does not adequately explain the poor fit in $MLSS$ between day 170 and 270, thus the possibility of a systematic error in the flow measurements had to be examined.

This was examined by estimating the sensitivity of the predicted $MLSS$ and $RASS$ series, to a systematic deviation of the flow rates (input, recycle and surplus) from their measured values. Through simulation studies the relative change in the solids concentration was calculated, due to a 10% increase in each of the flow rates (Figure 3.6). From Figure 3.6a it can be seen that the surplus sludge flow has a more pronounced effect upon the $MLSS$ than the recycle and input flows, while the $RASS$ is also affected by the input flow (Fig. 3.6b). However the sensitivity of $MLSS$ to surplus flow is substantial throughout the simulation period. Hence from the results there is no conclusive evidence of a systematic error in the flow measurements, since such an error would have affected the model predictions throughout the study period.

At this point more information about the operation of the plant was needed, particularly regarding any operational problems encountered. In a previous study of the Cirencester plant (Cook, 1983), it was reported that between the latter half of July 1979 and December 1979 (from day 125 onwards), considerable problems were experienced with the automatic control system of the final clarifiers and as a result, manual control of the return sludge flow penstocks was necessary. Consequences of the above, was the uncontrolled or even nil return of settled sludge. Furthermore,

the surplus sludge pumps were occasionally left running for long periods resulting in significant loss of solids. These irregular operating conditions were considered partly responsible for the poor prediction of $MLSS$ after about day 170, because they were not always recorded. In the available return flow data, there were a number of missing observations in the period between day 215 and 230, where the poorest model performance was observed. The above operating conditions also affected the sludge settleability, depicted by the observed high $SSVI$ values after about day 210. This had a direct effect on the $RASS$ concentration which exhibited large variability towards the end of the study period.

Another observation from the simulation results (Table 3.1), is that although the average level of $RASS$ was adequately predicted, the $MLSS$ was relatively underestimated. Since both the $MLSS$ and $RASS$ measurements were based on spot samples collected at 8am each day, it was considered that the diurnal input flow variations would affect the model predictions, as was also shown for the final clarifier model in Section 2.5.8. As an example, it was again examined the effect of a typical input flow variation from Leatherhead oxidation ditch plant (Fig. 2.23), upon the diurnal pattern of solids concentration, simulated with the hydraulic model (Figure 3.7). It can be seen that a spot reading at 8am underestimates the $RASS$ by about 8% from its daily average level and overestimates the $MLSS$ by about 8.5%. This observation can serve as a further explanation of the generally underestimated $MLSS$ level. Unfortunately the diurnal variation of the flow rates was not recorded, so that the validity of the above explanations cannot be tested.

3.15 Artificial aeration mechanism

The oxygen required for the biochemical reactions in the Cirencester plant is provided by two vertical-shaft cone aerators located at the end of the channel. As a result of the non-uniform air distribution, the dissolved oxygen concentration varies considerably along the channel. The highest DO concentration is observed near the aerators and subsequently decreases along the channel to almost zero levels. A typical DO profile in the oxidation ditch reactor is shown in Figure 3.8.

It follows that the oxidation ditch can be theoretically divided with respect to the DO concentration into an aerobic and an anoxic reactor. In the aerobic section, where the DO concentration normally exceeds 0.5 mg/l, all the aerobic reactions take place, such as carbonaceous oxidation, nitrification and the growth of heterotrophic and autotrophic biomass. The anoxic section, where the DO concentration is generally below 0.5 mg/l, promotes anoxic reactions such as denitrification and the growth of facultative organisms, while the aerobic reactions are severely inhibited.

At the Cirencester plant the DO concentration was continuously monitored by a fixed DO probe located 32 m downstream of one of the aerators. An automatic control mechanism checked the DO concentration at specified intervals and maintained its concentration within certain limits by adjusting the immersion depth of the aerators. In the selected study period the interrogation interval was set at 15 minutes, while the low and upper DO limits were set at 0.5 and 1.5 mg/l respectively. This control mechanism maintained a relatively constant DO profile along the reactor, despite the diurnal or seasonal variations of the oxygen demand, and assisted in the formation of a relatively constant anoxic zone covering about one third of the reactor.

In order to incorporate the above features into the process model in a simple manner, the reactor was assumed to consist of fixed volume aerobic and anoxic zones (Figure 3.9). The volume of the reactor occupied by each zone was described by two parameters A and B, hence :

$$V_{aerobic} = A \cdot V \qquad (3.36a)$$

$$V_{anoxic} = B \cdot V \qquad (3.36b)$$

The two parameters were assigned the following values : $A = 0.65$ and $B = 0.35$, which correspond to an average size of the aerobic and anoxic zones.

3.16 Carbonaceous oxidation modelling

3.16.1 Main Processes

The objective of this section was to develop a model describing the removal of organic substrates and the subsequent kinetics of heterotrophic biomass in the oxidation ditch reactor. An implicit requirement was that the model had a simple structure and contained a relatively small number of parameters, which would be estimated from the available measurements. The development of the model structure was based on an a priori knowledge from the literature. A deductive approach was followed, whereby starting from a detailed description of the biochemical processes, subsequent simplifications were made until a simple model structure was obtained which adequately described the main phenomena. The adequacy of the model was judged by its ability to reproduce the observed system behaviour.

In the review (Sections 3.2.5 & 3.2.6), it was shown that the main phenomena during the biochemical oxidation of organic substrates are the following, shown schematically in Fig. 3.10.

(i) Entrapment of the influent suspended organic matter onto the bioflocs.

(ii) Absorption and storage of the enmeshed particulate material, as well as, of soluble organic material on the active biomass.

(iii) Hydrolysis of the stored particulate material by extracellular enzymes.

(iv) Utilization of the organic material for cell synthesis by active heterotrophic organisms.

(v) Endogenous respiration (decay) of active biomass.

(vi) Resolubilization of a fraction of the decayed biomass.

The rate of storage has been generally assumed to follow first-order kinetics with respect to organic substrate and active biomass concentration and to be limited by the amount of stored mass. (eq. 3.11 & 3.13). The rate of substrate hydrolysis and utilization have been predominantly described by the Monod relationship, where the reaction rate is limited by the stored mass concentration. (eq. 3.14 & 3.15). In general, the rate of storage (stages (i) and (ii)) is reported to be much faster than the rate of utilization (stages (iii) and (iv)), implying that under steady-state operating conditions the rate of storage is limited by the rate of utilization (Marais & Ekama, 1976). As a result storage phenomena are no longer observed and the removal of organic substrate could be adequately described by the process of utilization alone (stage (iv)). Finally, the decay of active biomass is widely reported to be proportional to the active mass concentration, while a fraction of the decayed mass is believed to become available as additional substrate through resolubilization (Section 3.2.6).

3.16.2 Formulation of a structured biomass model

The biomass in the reactor was initially assumed to have the following structure, which is similar to that proposed by Grady & Roper (1974) and Holmberg (1982):

- **active biomass**, consisting of viable organisms which utilize organic substrate and dead organisms for cell synthesis and maintenance and they die at a certain rate.
- **inactive biomass**, consisting of dead (non-viable) organisms in the endogenous respiration phase and is used partly for maintenance of the active organisms and partly is resolubilized serving as additional substrate.
- **inert mass**, consisting mainly of inorganic and unbiodegradable material, acting as a conservative substance during its passage from the reactor.

For the formulation of a model with the above structure of the biomass, it is necessary that the input solids is also structured in the same manner and the

concentration of each component is known. However in the available measurements the quality of the crude sewage was measured by lumped parameters such as the SS, BOD_5 and COD concentrations. These measurements had to be analysed in the light of information from the literature, in order to obtain estimates of the concentration of the individual components.

Hence, for modelling the carbonaceous oxidation process the crude sewage pollutants were assumed to have to following commonly reported structure (Ekama & Marais 1977; Dold et al. 1986), which is shown schematically in Fig. 3.11. According to this structure the crude sewage contain organic and inorganic matter. The organic matter consists of a readily degradable fraction, determined through the BOD_5 measurement, and a slowly and non-biodegradable fraction, which was assumed not to be metabolized within the process. Furthermore, the inorganic matter was structured into dissolved and suspended fractions.

The readily degradable organics (components 1 & 2) represent the input organic substrate undergoing biochemical oxidation in the reactor. For simplicity both the soluble and particulate components were assumed to exhibit the same reaction rates. The soluble non-degradable component (3) and the dissolved inorganic component (5) were unimportant for modelling since they pass almost unchanged through the process. However the suspended non-degradable (4) and suspended inorganic (6) components, although biochemically inert, were important for modelling, since they become enmeshed in the bioflocs and affect substantially the quantity of sludge production. This fraction of solids cannot be directly determined from the available measurements but for the purpose of the modelling it was estimated from the difference between the total input SS and the input biodegradable solids. The latter was assumed to be a fixed proportion of the incoming BOD, hence :

$$Xo_t = SSi_t - \frac{Sb}{100} \cdot BODi_t \qquad (3.37)$$

where ; Sb : fraction of input BOD_5 in particulate form [%],
Xo_t : slowly-degradable and inorganic fraction of input SS $[ML^{-3}]$.

The above component of input solids (Xo), was further assumed to have the same structure as the biomass, thus consisting of active, inactive and inert fractions. The proportion of each fraction was considered fixed for the whole period and for this purpose literature-based values were used in the absence of more detailed information.

For modelling the organic substrate removal the following considerations were made. The sampling interval and hence the simulation step in the modelling exercise were fixed at 1 day period. Under this time-scale any short-period dynamic phenomena or short-term transients cannot be identified while their effect upon the average

daily plant performance is relatively small. Furthermore, examination of the data showed that although the input flows and concentrations were highly variable, the effluent BOD remained relatively constant, implying 'near steady-state' operating conditions with respect to the reactor BOD.

Under these conditions the four separate mechanisms (i) to (iv) of organic substrate metabolic cycle (Section 3.16.1) could be described as a single mechanism of substrate utilization. The rate of utilization was then expressed by the widely used Monod relationship, which was reported to be adequate under normal operating conditions. Hence :

$$\frac{dS}{dt} = -\frac{R_{max} \cdot Xa \cdot S}{Ks + S} \qquad (3.38a)$$

where ; R_{max} : maximum rate of substrate utilization $[T^{-1}]$,
Xa : active biomass concentration $[ML^{-3}]$,
S : organic substrate concentration $[ML^{-3}]$,
Ks : half-rate substrate concentration $[ML^{-3}]$.

The maximum rate of substrate utilization is related to the maximum growth rate of active biomass by the following equation :

$$R_{max} = \frac{\mu_{max}}{Y} \qquad (3.38b)$$

where ; μ_{max} : maximum growth rate of active biomass $[T^{-1}]$,
Y : yield of active mass from substrate [–].

Some further assumptions were made which facilitated the model formulation :

- The DO concentration in the aerobic zones is always sufficient for uninhibited substrate oxidation and cell synthesis, while its concentration in the anoxic zones inhibits the aerobic reactions. The above assumption was based on the existence of the DO control system which maintains constant volume aerobic zones.
- There are no toxic or inhibitory substances to the biomass in the crude sewage. This is a reasonable assumption considering the domestic origin of the crude sewage, which is also depicted by the low COD : BOD ratio of 2.38 : 1 on average.
- The active biomass dies at a constant rate and becomes inactive without any loss of mass.
- The inactive biomass does not utilize organic substrate.

- The inactive biomass decays at a constant rate; a fraction of the decayed mass becomes available as additional substrate through resolubilization.
- For the effluent SS the measured concentration was used (Sec. 2.4), which was assumed to consist of all three types of biomass in the same proportion as they exist in the mixed liquor.

The equations describing the structured biomass model were also based on mass-balance and are presented below, while a schematic representation of the model is shown in Fig. 3.12.

$$\text{Accumulation} = \text{Input} + \text{Recycle} - \text{Output} + \text{Sources} - \text{Sinks}$$

1. **Active biomass in Aeration tank** (XA)

$$\frac{dXA_t}{dt} = \frac{Pa \cdot Qi_t \cdot Xo_t + Qr_t \cdot XAR_t}{V} - \frac{(Qi_t + Qr_t) \cdot XA_t}{V} + A \cdot \mu_{max} \cdot XA_t \cdot \frac{S_t}{Ks + S_t} - Ka \cdot XA_t \tag{3.39}$$

2. **Inactive biomass in A.T.** (XI)

$$\frac{dXI_t}{dt} = \frac{Pi \cdot Qi_t \cdot Xo_t + Qr_t \cdot XIR_t}{V} - \frac{(Qi_t + Qr_t) \cdot XI_t}{V} + Ka \cdot XA_t - Ki \cdot XI_t \tag{3.40}$$

3. **Inert mass in A.T.** (XN)

$$\frac{dXN_t}{dt} = \frac{Pn \cdot Qi_t \cdot Xo_t + Qr_t \cdot XNR_t}{V} - \frac{(Qi_t + Qr_t) \cdot XN_t}{V} \tag{3.41}$$

4. **Available organic substrate in A.T.** (S)

$$\frac{dS_t}{dt} = \frac{Qi_t \cdot Si_t + Qr_t \cdot SR_t}{V} - \frac{(Qi_t + Qr_t) \cdot S_t}{V} - \frac{A \cdot \mu_{max} \cdot XA_t \cdot S_t}{(Ks + S_t) \cdot Ysxa} + Ki \cdot XI_t \cdot Ysxi \tag{3.42}$$

5. **Active biomass in recycle** (XAR)

$$\frac{dXAR_t}{dt} = [(Qi_t + Qr_t) \cdot XA_t - (Qr_t + Qw_t) \cdot XAR_t - fa \cdot (Qi_t - Qw_t) \cdot SSe_t]/Vcl \tag{3.43}$$

6. **Inactive biomass in recycle** (XIR)

$$\frac{dXIR_t}{dt} = [(Qi_t + Qr_t) \cdot XI_t - (Qr_t + Qw_t) \cdot XIR_t - fi \cdot (Qi_t - Qw_t) \cdot SSe_t]/Vcl \tag{3.44}$$

7. **Inert mass in the recycle (XNR)**

$$\frac{dXNR_t}{dt} = [(Qi_t + Qr_t) \cdot XN_t - (Qr_t + Qw_t) \cdot XNR_t - fn \cdot (Qi_t - Qw_t) \cdot SSe_t]/Vcl \quad (3.45)$$

8. **Soluble organic substrate in effluent and recycle (SR)**

$$\frac{dSR_t}{dt} = (Qi_t + Qr_t) \cdot (Si_t - SR_t)/Vcl \quad (3.46)$$

9. **Net biomass growth (GR)**

$$\frac{dGR_t}{dt} = \frac{A \cdot \mu max \cdot XA_t \cdot S_t}{Ks + S_t} - Ki \cdot XI_t \quad (3.47)$$

$$MLSS_t = XA_t + XI_t + XN_t \quad (3.47a)$$

$$RASS_t = XAR_t + XIR_t + XNR_t \quad (3.47b)$$

$$fa = \frac{XA_t}{MLSS_t}, \quad fi = \frac{XI_t}{MLSS_t}, \quad fn = \frac{XN_t}{MLSS_t} \quad (3.47c)$$

where; Ka : death rate of active biomass $[T^{-1}]$,
Ki : decay/resolubilization rate of inactive biomass $[T^{-1}]$,
$Ysxa$: yield of active biomass from organic substrate [–],
$Ysxi$: yield of substrate from decayed inactive biomass [–],
Pa, Pi, Pn : fractions of active, inactive & inert mass in input n.d. solids respectively [–],
fa, fi, fn : fractions of active, inactive & inert mass in the mixed liquor and effluent SS [–].

3.16.3 Model calibration (parameter estimation)

Environmental systems are in general complex and poorly-defined systems, so that any model can only be an approximate representation of the real system. For this reason the model predictions and experimental observations are never expected to match perfectly with any parameter set. Consequently the problem of parameter estimation can be conceived as the determination of an optimum parameter set, producing the minimum prediction error with some desired statistical properties which characterize such error sequences.

Several approaches can be followed for model calibration and parameter estimation varying considerably in their complexity and area of application. Most of them involve the formal use of an estimation algorithm, whose selection depends purely on the requirements of the specific problem and there is no general rule. The most common approaches for parameter estimation are briefly discussed below :

- Parameter estimation by trial and error, whereby starting with typical parameter values obtained from the literature or previous studies, the values are subsequently modified in successive simulations. This process is repeated until the model simulates satisfactorily the experimental observations, or when no further improvement in the model predictions is observed. This is the simplest and least elaborate method and is commonly used for estimating large number of parameters in complex models. Nevertheless in view of the uncertainty regarding the experimental measurements and the developed model structures in poorly-defined systems, this method can produce satisfactory parameter values which can be further refined using more elaborate techniques. A drawback of this method is the non-uniqueness in the estimated parameter values, since several sets may produce satisfactory performance of the model. Thus, in order to obtain realistic parameter values, it is important to have some initial knowledge of their expected range of variation and their effect upon the system states.

- Parameter estimation using block (non-adaptive) estimation algorithms such as least squares, maximum likelihood and block instrumental variables, where an optimum parameter set is sought having the maximum probability of representing the reality. This is implemented by minimizing a pre-selected function of the prediction errors. In this category are also classified the various non-linear programming techniques, such as gradient and direct search optimization methods used for the calibration of nonlinear and complex model structures where linear techniques do not apply. The choice of the algorithm depends on the model type, the complexity of its structure, the quality and quantity of measurements and the expected statistical properties of the prediction error. The use of block estimation techniques implicitly assumes that the parameters are constant. Hence, their time-variation cannot be depicted which could indicate weaknesses of the model.

- Parameter estimation using recursive (adaptive) estimation algorithms, such as recursive least squares, recursive instrumental variables and the extended Kalman filter, where the parameters are estimated as time-varying quantities. In this case the parameters are updated every time a new measurement is processed. The update is based both on information received from the new measurement and on past information about the statistical behaviour of each parameter carried forward by the estimator. To start a recursive estimation scheme a subjective guess of an initial set of values is required, which is usually accompanied by an appropriately large variance. The choice of algorithm depends on the type of model used (deterministic or stochastic), as well as, on the features of the algorithm for the specific case. Their particular usefulness lies in the fact that they can assist in refining the structure of the model, by

observing the parameter variation which may reveal unmodelled features of the process.

- Parameter estimation via Monte-Carlo simulations, where a range of values is determined for each parameter, having a high probability of producing "good" performance of the simulation model. The definition of "good" and "bad" performance, although subjective, it is generally based on certain statistical criteria regarding the goodness of fit. In case were no observations exist, this is based on the expected variation of the process variables. This method requires a large number of simulations, in which the parameter values are selected randomly from a prespecified distribution. The simulation results are then classified either as "success", or "failure", while the corresponding parameter sets are classified as "good" and "bad" respectively. To start the simulations a wide range of parameter values and their distributions must be specified which is normally based on a priori knowledge. The initial range is subsequently narrowed down in successive trials by analysing statistically the simulation results.

3.16.4 Parameter estimation approach

The model for carbonaceous oxidation comprised nine non-linear ordinary differential equations which had to be solved numerically. The model also contained ten parameters whose values had to be determined either from the literature or by adopting a suitable estimation approach. Most of the model variables were unmeasured states to be estimated by the model, while the only available measurements for parameter estimation were the aggregated variables of $MLSS$, $RASS$ and effluent BOD_5.

The large number of parameters prohibited the use of optimization techniques and Monte-Carlo simulations for their estimation. The main reason was the enormous computing power requirements to perform large number of simulations necessary for converging to the optimum parameter set, while it is not guaranteed that a global optimum solution would be obtained with an optimization scheme. In addition a suitable objective function, which significantly affects the optimization results, cannot be formally determined in view of the uncertainty regarding the model structure and the unknown quality of the experimental observations. Another drawback of such technique is that constrained optimization would be necessary in order to obtain sensible parameter values, requiring the specification of suitable upper and lower bounds for the parameters.

The application of recursive estimation techniques for estimating the time variation of parameters, was also not justifiable for this model due to the large number of parameters compared to the small number of measured states. Therefore in this case the parameters were assumed time-invariant and the estimation proceeded by trial

and error through successive simulations and parameter adjustments. The updating of parameters was performed after studying the results from each simulation and aimed at improving the correlation between model predictions and observations and reducing the prediction error. The main statistics chosen to characterize the model performance were the mean, variance, RMS and sum square of prediction error, and in addition the correlation C.O.D. coefficients between the observed and predicted states.

In order to facilitate the comparison between predicted and observed variables, the sum of active, inactive and inert mass in the aeration tank was assumed to represent the total $MLSS$ concentration (eq. 3.47a), and their respective sum in the recycle stream to represent the $RASS$ concentration (eq. 3.47b). Finally, the estimated soluble organic substrate in the effluent was compared with the effluent BOD_5 measurements.

3.16.5 Model results and discussion

In the proposed model there are two main components which determine the dynamic behaviour of the state variables :

- the hydraulic component.
- the biochemical component.

The first component determines the mass-transport of soluble and particulate matter through the process units and was already studied in Section 3.14. This study demonstrated the importance of the input and operating flow rates (Qi, Qr, Qw) in determining the daily solids variation in the aeration tank and underflow stream. This can be attributed to the short time constants of the solids dynamics in the hydraulic model. These are approximately $V/(Qi + Qr)$ and $Vcl/(Qr + Qw)$ for $MLSS$ and $RASS$ respectively and are generally less than 1 day. On the contrary, the biochemical component is a much slower process with time-constants in the range of several days, thus its effect on the process variables can only be observed over longer term periods.

Due to this slow response, the biochemical component cannot be easily identified from the noisy daily observations. As a result it may be misrepresented in the model even if the overall performance is satisfactory. For this purpose the net growth of biomass was chosen as an additional checking variable, because it is directly related to the biochemical kinetics of carbonaceous oxidation. Direct measurements of the biomass net growth did not exist. For this purpose the net growth was assumed equal to the excess sludge production after subtracting the non-biodegradable solids

entering the plant. Hence:

$$GR_t = [Qw_t \cdot RASS_t + (Qi_t - Qw_t) \cdot SSe_t - Qi_t \cdot Xo_t]/V \qquad (3.48)$$

where; GR_t : net sludge production $[ML^{-3}T^{-1}]$.

The above equation is based on a number of simplifying assumptions such as :

- the equation is non-dynamic and uses daily average values,
- the load of non-biodegradable solids entering the plant is estimated by eq. 3.37,
- the accumulation of solids in the process (aeration tank and clarifiers) was neglected.

To minimize the effect of daily changes in the accumulated solids mass, the cumulative net growth was used rather than its daily variation. The above assumptions tend to reduce the effectiveness of the proposed variable, nevertheless it was considered useful in assessing whether the biochemical component was adequately simulated.

The model equations were solved numerically using the 4th-order, variable-step Runge-Kutta integration technique. Starting with an initial parameter set which gave good steady-state performance under average input conditions, the parameter values were subsequently updated until no further improvement in the fit was obtained. The parameters that were mainly adjusted, were the kinetic rates (μmax, Ka and Ki) and the yield of biomass from substrate $Ysxa$, which mostly affect the model states. The proportions of active, inactive and inert mass in the crude sewage were assigned constant values, while the suspended fraction of the input BOD_5 was taken to be 60%. Typical parameter values are shown in Table 3.3 which were mainly derived for the conventional activated sludge process.

The initial and final parameter values are shown in Table 3.4 and the simulation results with the final parameter set are presented in Figure 3.13 and Table 3.5.

Param.	Units	Metcalf & Eddy (1979)		Ekama (1977)	Terashima (1985)	Olsson (1975)	Sincic (1978)
μmax	d^{-1}	2.0-10.0	(5.0)	3.0	4.8	4.8	4.8
Kd	d^{-1}	0.04-0.075	(0.06)	0.24	0.048	0.18	0.012
Ks	mg/l	25-100	(60)	100.0	100	150	200
Ysx	—	0.4-0.8	(0.6)	0.49	0.7	0.5	0.5
θ	—	1.0-1.02	(1.02)	1.029	—	—	—

Table 3.3. Typical parameter values for heterotrophic biomass kinetics

The structured biomass model adequately predicted both the solids concentrations and the net growth of biomass as shown in Fig. 3.13a, b & e. The performance for both the $MLSS$ and $RASS$ series has improved compared to the hydraulic model, evident from the lower prediction error and the higher C.O.D. However the improvement was not substantial. The poor fit for the $MLSS$ between days 170 and 270 remained and this was reflected upon the estimated biomass growth, which became less than the observed growth during the above period.

Parameter	Units	Init.value	Final value
μmax	d^{-1}	4.80	5.52
Ka	d^{-1}	0.084	0.0672
Ki	d^{-1}	0.08	0.0552
Ks	mg/l	20.0	20.0
$Ysxa$	—	0.90	0.95
$Ysxi$	—	0.67	0.67
Sb	%	60.0	60.0
Pa	%	15.0	15.0
Pi	%	40.0	40.0
Pn	%	45.0	45.0
$XA_{(0)}$	mg/l	1800	1800
$XI_{(0)}$	mg/l	1804	1604
$XN_{(0)}$	mg/l	1000	1200
$RASS_{(0)}$	mg/l	9472	9472
$BODe_{(0)}$	mg/l	3.6	3.6

Table 3.4. Parameter & initial values for structured biomass model.

Parameter	$MLSS$	$RASS$	$BODe_{(sol)}$	$GR_{(cum)}$
mean (mg/l)	3444.8	7021.4	0.711	—
std. deviat.	1341.8	2362.6	0.346	—
C.O.D.	0.5878	0.702	-0.306	—
R	0.858	0.841	0.076	—
mean error	430.8	-118.9	1.63	1832
RMS error	823.0	1415.6	3.32	2791.5
var. error	0.4936E+6	0.1997E+7	8.97	—
sum sq.error	0.1917E+9	0.5671E+9	3129	0.2205E+10

Table 3.5. Structured biomass model performance.

The model predicted fairly well the average level of the effluent BOD_5 concentration. However it did not reproduce the observed high peaks and its daily variation. This was attributed to the following factors:

- the predicted effluent BOD represents only the soluble organic matter, while the measured BOD also includes suspended organic matter.
- the high peaks in the observations can be attributed to the presence of suspended organic matter in the effluent, whose concentration is influenced by the clarification performance of the final tanks.

Incorporating the effect of effluent SS through a linear expression ($BODe = BOD_{(sol)} + b \cdot SSe$ with $b = 0.28$), the fit was improved (Fig. 3.13d), achieving lower prediction error ($Em = 0.219 + 2.82$) and higher correlation ($R = 0.249$).

Finally the variation of the active, inactive and inert mass in the reactor is shown in Fig. 3.13c. An important observation to be made is that all three components of the biomass exhibit similar pattern of variation. This can be attributed to the small effect of growth and decay functions upon the active and inactive biomass dynamics compared to the large effect of the hydraulic component. An additional reason can be the assumption of fixed proportion for the active, inactive and inert components of the crude sewage solids, which was made in the absence of more detailed information.

3.17 Simple carbonaceous model

3.17.1 Model formulation

In the light of the previous results some further simplifications to the developed model were justifiable in order to reduce the number of state variables and parameters. Since the three components of the biomass did not exhibit significantly different behaviour (Sec. 3.16.5), it was considered reasonable to lump them into a single variable describing the overall behaviour of the three previous variables, which was defined as heterotrophic biomass. Another justification is that the active, inactive and inert components of the biomass were unmeasurable variables, which introduces uncertainty in the idenitification and validation of the structured biomass model even if the aggregated variables ($MLSS$ and $RASS$) are adequately predicted.

Following the above simplification, the growth and decay rates of the heterotrophic biomass were described by aggregated parameters. These are expected to have lower values than before, since they refer to the total solids in the reactor. Furthermore the structuring of the input non-degradable solids was not necessary. Thus, the following simple carbonaceous model evolved, shown schematically in Fig. 3.14 and described by the equations :

1. **Heterotrophic biomass in A.T.** (X)

$$\frac{dX_t}{dt} = \frac{Qi_t \cdot Xo_t + Qr_t \cdot XR_t - (Qi_t + Qr_t) \cdot X_t}{V} + A \cdot \mu_{max} \cdot X_t \cdot \frac{S_t}{Ks + S_t} - Kd \cdot X_t \tag{3.49}$$

2. **Soluble organic substrate in A.T.** (S)

$$\frac{dS_t}{dt} = \frac{Qi_t \cdot Si_t + Qr_t \cdot SR_t - (Qi_t + Qr_t) \cdot S_t}{V} - A \cdot \mu_{max} \cdot X_t \cdot \frac{S_t}{Ysx \cdot (Ks + S_t)} + Yxs \cdot Kd \cdot X_t \tag{3.50}$$

3. **Recycle heterotrophic biomass** (XR)

$$\frac{dXR_t}{dt} = \frac{(Qi_t + Qr_t) \cdot X_t - (Qr_t + Qw_t) \cdot XR_t - (Qi_t - Qw_t) \cdot SSe_t}{Vcl} \tag{3.51}$$

4. **Recycle-effluent soluble organic substrate** (SR)

$$\frac{dSR_t}{dt} = \frac{(Qi_t + Qr_t) \cdot (Si_t - SR_t)}{Vcl} \tag{3.52}$$

5. **Net biomass growth** (GR)

$$\frac{dGR_t}{dt} = A \cdot \mu_{max} \cdot X_t \cdot \frac{S_t}{Ks + S_t} - Kd \cdot X_t \tag{3.53}$$

where; Kd : decay rate of heterotrophic biomass $[T^{-1}]$,
Ysx : yield of heterotrophic biomass from substrate [–],
Yxs : yield of substrate from decayed biomass [–].

3.17.2 Parameter estimation — discussion

The parameter estimation proceeded initially by trial and error in order to obtain parameter values producing reasonable performance of the model. The initial and final parameter sets are shown in Table 3.6. It can be noted that the yield of biomass from substrate is significantly higher than reported values in the literature (Table 3.3). This could be explained by the fact that the 5-day BOD represents approximately 60–70% of the total biodegradable organic substrate entering the process. However, due to the extended aeration of mixed liquor in the oxidation ditch, a larger proportion of the ultimate BOD is metabolized than measured by the BOD_5 value. Accordingly the true yield coefficient ($gVSS/gBOD$ oxidized) would be significantly lower.

The remaining kinetic rates are within reported values but towards the lower end of the reported range, indicating that the biochemical activity is relatively low. This can be attributed to the large proportions of inactive and inert mass and the low sludge loading rate in the oxidation ditch process compared to the conventional activated sludge, for which most of the kinetic rates were derived.

Parameter	Units	Init.value	Final value
μmax	d^{-1}	3.80	1.92
Kd	d^{-1}	0.06	0.0288
Ks	mg/l	35.0	20.0
Ysx	—	0.85	1.10
Yxs	—	0.75	0.67
Sb	%	60.0	60.0
$X_{(0)}$	mg/l	4604	4604
$XR_{(0)}$	mg/l	9472	9472
$BODe_{(0)}$	mg/l	3.6	3.6

Table 3.6. Parameter & initial values for carbonaceous oxidation model.

Parameter	$MLSS$	$RASS$	$BODe_{(sol)}$	$BODe_{(tot)}$	$GR_{(cum)}$
mean (mg/l)	3623.1	7373.9	1.019	2.43	—
std. deviat.	1395.4	2392.3	0.48	1.08	—
C.O.D.	0.641	0.667		0.054	0.964
R	0.857	0.841		0.261	0.986
mean error	252.5	-470.0		0.087	37.7
RMS error	767.0	1493.3		2.82	1457.5
var. error	0.5264E+6	0.2015E+7		7.996	0.2130E+7
sum sq.error	0.1665E+9	0.6311E+9		2257	0.6012E+9

Table 3.7. Carbonaceous oxidation performance.

The simulation results with the final parameter set are presented in Figure 3.15 and Table 3.7. The results show some improvement in predicting the $MLSS$ trajectory compared to the structured biomass model (Table 3.5), but this was obtained at the expense of a poorer fit for the $RASS$ series. Overall the performance of the model in reproducing the observed variation of the $MLSS$ and $RASS$ series was reasonable, depicted by a C.O.D. value of 0.641 and 0.667 respectively. In addition the cumulative net growth reproduced well the observed growth variation (Fig. 3.15d) with a C.O.D. of 0.964, suggesting that the current parameter set could be accepted as the final one.

As a concluding remark it can be said that the overall performance of the structured biomass and simple carbonaceous models was similar, which further justifies the rejection of the former complex model for simplicity reasons. The latter model has a relatively simple structure, contains fewer parameters and showed satisfactory performance. Hence it was considered adequate according to the objectives of modelling.

The above model does not account for the effects of temperature variations upon

the biochemical reaction kinetics, discussed in Section 3.2.7. This was subsequently investigated by assuming temperature dependency of the growth and decay rates using an Arrhenius function :

$$R_{(T)} = R_{(10)} \cdot \theta^{(T-10)} \tag{3.54}$$

where; $R_{(T)}, R_{(10)}$: kinetic rate at T and 10 ^oC respectively $[T^{-1}]$,
T : mixed liquor temperature in ^oC,
θ : temperature dependency coefficient [-].

Using the previous parameter values and assigning a typical value for the temperature coefficient ($\theta = 1.03$), the following simulation results were obtained summarized in Table 3.8.

Parameter	$MLSS$	$RASS$	$BODe_{(sol)}$	$GR_{(cum)}$
mean (mg/l)	3593.7	7320.8	0.985	—
std. deviat.	1390.6	2416.9	0.47	—
C.O.D.	0.638	0.676	-0.202	0.953
R	0.859	0.842	0.131	0.984
mean error	281.9	-418.3	1.35	282.0
RMS error	769.5	1473.4	3.18	1664.4
var. error	0.5144E+6	0.2003E+7	8.32	0.2691E+7
sum sq. error	0.1676E+9	0.6144E+9	0.2870E+4	0.7814E+9

Table 3.8. Carbonaceous oxidation model with temperature effect.

From the results it is apparent that the incorporation of the temperature coefficient did not produce any improvement to the predictive performance of the model, judged by the determinands R, C.O.D. and the prediction error statistics. Therefore it was concluded that the temperature dependency was insignificant. In contrast with the widely reported temperature effect on the reaction kinetics (Sec. 3.2.7), a temperature factor was not included in the carbonaceous model. However it can be suggested that the high organic removal efficiency under a wide range of temperatures and the noisy structure of the data hampered the accurate identification of temperature dependency of the kinetic rates.

3.17.3 Model verification

For the verification of the model the statistical properties of the residual error sequences were examined. Although the residual errors did not behave as pure noise, they approximated quite well the properties of a noise sequence. The mean of the

error sequences was generally small compared to the mean of the corresponding variables, while their correlation with the model states and system inputs was small. The autocorrelograms of the residuals are shown in Figure 3.16. The correlogram of the $MLSS$ residuals contained several significant values at low lags indicating some autoregressive structure, but the remaining correlograms exhibited insignificant serial structure at 5% level, suggesting that the model is adequately verified.

3.17.4 Adaptive estimation

In order to improve the performance of the simulation model and study the variation of key parameters with time, recursive (or adaptive) estimation of parameters was attempted. The current model contains fewer parameters and the use of adaptive estimation techniques can be justified. Among the various techniques, the Extended Kalman Filter (E.K.F.) was selected in this study for the following reasons :

- It provides filtering of the estimated parameters and reconstructs state variables, taking into account the existence of errors in both the model equations and process measurements.
- It is possible to estimate time-varying parameters even when their dynamics are unknown.
- It provides some means of model structure identification by examining the estimated parameter trajectories.

The Kalman filter can be used for state estimation, parameter estimation or both. In the case of combined state-parameter estimation the parameters are considered as additional states and a new augmented state vector is formed. The algorithm employs a "prediction-correction" scheme of updating the augmented state vector:

- The **prediction stage**, in which the states are predicted for the next time step, using the system model and the current set of state and input values.
- The **correction stage**, in which the difference between predicted and observed states is transformed into a set of corrections to be applied to the existing state vector.

The Kalman filter equations are presented in Appendix 2 and some of the algorithm limitations when applied to non-linear systems are discussed. Taking into account the various limitations, the E.K.F. was employed for a combined state and parameter estimation using the previously developed carbonaceous oxidation model. The augmented state vector consisted of eight states among which were three model parameters, namely μ_{max}, Kd and Ysx and the 5 state variables of the carbonaceous

model. The above parameters were chosen as being the most important ones likely to vary with time, because they depict the effects of unmodelled environmental factors and operating conditions upon the process kinetics. The remaining parameters were assumed time-invariant and were assigned constant values taken from the block estimation.

The E.K.F. algorithm takes into account the effect of stochastic errors in both the observations and model equations. For this purpose the deterministic model was transformed into a stochastic one by including a random noise term in each equation, which represents unmodelled disturbances. Employing the notation used in the Appendix 2 the system was written as :

$$\frac{d\underline{X}}{dt} = f(\underline{X}(t), \underline{u}(t), t) + \underline{\xi}(t) \qquad (3.55)$$

where; $f(*)$: general non-linear system functions,
$\underline{\xi}(t)$: vector of unmodelled system disturbances,
$\underline{X}(t)$: augmented state vector,
$\underline{u}(t)$: input vector.

The various components of the augmented state vector vary significantly in magnitude ie. the $MLSS$ is in the range of 10^3, while some kinetic constants are in the 10^{-3} range. Thus, in order to avoid ill-conditioned matrices during the application of the algorithm, the variables were suitably rescaled (Cook et al. 1981). Hence, the following assignments were made to the state vector:

$X_1(t) \equiv MLSS \times 10^{-3}$ (mg/l)
$X_2(t) \equiv BOD$ in A.T. (mg/l)
$X_3(t) \equiv RASS \times 10^{-3}$ (mg/l)
$X_4(t) \equiv BOD$ in F.E. (mg/l)
$X_5(t) \equiv GR \times 10^{-1}$ $(mg/l/d)$
$X_6(t) \equiv \mu max \times 10^3$ (hr^{-1})
$X_7(t) \equiv Kd \times 10^3$ (hr^{-1})
$X_8(t) \equiv Ysx \times 10$ $(-)$

The process observations used for updating the augmented state vector were also considered to contain random measurement error. Hence :

$$\underline{y}(t_k) = h(\underline{X}(t_k), \underline{u}(t_k), t_k) + \underline{\varsigma}(t_k) \qquad (3.56)$$

where; $h(t_k)$: measurement matrix,
$\underline{\varsigma}(t_k)$: random measurement error vector,
$\underline{y}(t_k)$: observation vector.

The following assignments were made to the observation vector :

$y_1(t_k) \equiv BODe(t_k)$ observed
$y_2(t_k) \equiv MLSS(t_k)$ "
$y_3(t_k) \equiv RASS(t_k)$ "
$y_4(t_k) \equiv GR(t_k)$ (daily) "

Finally, the measurement matrix had the following form :

$$h = \begin{vmatrix} 0 & 0 & 0 & 1 & 0 & 0 & 0 & 0 \\ 1 & 0 & 0 & 0 & 0 & 0 & 0 & 0 \\ 0 & 0 & 1 & 0 & 0 & 0 & 0 & 0 \\ 0 & 0 & 0 & 0 & 1 & 0 & 0 & 0 \end{vmatrix}$$

3.17.5 Results and discussion

Initially the parameters were estimated as non-dynamic states $[\underline{a}(t_{k+1}) = \underline{a}(t_k)]$. The error vectors $\underline{\xi}(t)$ and $\underline{\zeta}(t_k)$ were assumed stationary, Gaussian, white noise processes. The covariance matrix of these processes Q and R respectively were assigned the following values.

$$Q = \begin{vmatrix} 0.02 & & & & & & & \\ & 0.2 & & & & & & \\ & & 0.05 & & & & & \\ & & & 0.2 & & & & \\ & & & & 0.5 & & & \\ & & & & & 0 & & \\ & & & & & & 0 & \\ & & & & & & & 0 \end{vmatrix} \qquad R = \begin{vmatrix} 3.0 & & & \\ & 0.5 & & \\ & & 1.0 & \\ & & & 5.0 \end{vmatrix}$$

The initial state error covariance matrix was :

$$P_{(0)} = \begin{vmatrix} 0.1 & & & & & & & \\ & 0.2 & & & & & & \\ & & 0.3 & & & & & \\ & & & 0.2 & & & & \\ & & & & 1.0 & & & \\ & & & & & 0.01 & & \\ & & & & & & 0.03 & \\ & & & & & & & 0.2 \end{vmatrix}$$

The estimated parameter trajectories are presented in Figure 3.17 and their basic statistics in Table 3.9. The parameter values were perturbed slightly from their initial

values, but after about 30 days they showed relative convergence. The maximum growth rate showed significant reduction during the first 35 days, and thereafter exhibited a slightly upward trend. The decay rate and yield coefficient increased during the first 30 days but then showed general convergence.

Parameter	μ_{max} (hr^{-1})	Kd (hr^{-1})	Ysx (-)	
mean	0.050	0.00138	1.151	
std. deviat.	0.00699	0.0000485	0.027	
Parameter	$MLSS$ (mg/l)	$RASS$ (mg/l)	$BODe_{(sol)}$ (mg/l)	$GR_{(daily)}$ $(mg/l/d)$
mean	3672.1	7413.8	1.766	88.4
std. deviat.	1312.0	2178.2	0.917	101.0
C.O.D.	0.667	0.693	0.044	0.995
R	0.850	0.856	0.284	0.998
mean error	203.5	-511.3	0.575	-0.67
RMS error	738.8	1434.2	2.84	7.15
var. error	0.5062E+6	0.1802E+7	7.75	51.3
sum sq.error	0.1545E+9	0.5821E+9	0.2280E+4	0.1459E+5

Table 3.9. Recursive estimation with non-dynamic parameters.

In another estimation the parameters were assumed to contain random additive noise $[\underline{a}(t_{k+1}) = \underline{a}(t_k) + \underline{\zeta}(t_{k+1})]$. The new system covariance matrix was:

$$Q = \begin{vmatrix} 0.02 & & & & & & & \\ & 0.0 & & & & & & \\ & & 0.05 & & & & & \\ & & & 0.0 & & & & \\ & & & & 0.0 & & & \\ & & & & & 0.002 & & \\ & & & & & & 0.006 & \\ & & & & & & & 0.04 \end{vmatrix}$$

The parameter trajectories are shown in Figure 3.18. Their scatter from the initial values was increased considerably and no convergence was observed. Furthermore the improvement in the predictions of $MLSS$ and $RASS$ was small compared to the non-adaptive simulation, indicating that the solids concentration is not significantly affected by variations in the kinetic rates of biomass. The period of particular interest was between day 175 and 260, in which the trajectories of μ_{max} and Kd exhibited dramatic drops, and the yield coefficient showed a significant rise. This irregular behaviour could not be explained from the kinetics of the biomass or the effect of adverse external conditions, since the effluent BOD_5 was marginally affected.

However, during that period in which several operating problems were encountered (Sec. 3.14.2), the previous non-adaptive simulation results showed a systematic error in the $MLSS$ predictions (Fig. 3.15a). Such an error was capable of introducing considerable bias to the parameter estimates during adaptive estimation.

Parameter	μ_{max} (hr^{-1})	Kd (hr^{-1})	Ysx (-)	
mean	0.0482	0.001168	1.186	
std. deviat.	0.0172	0.000499	0.108	
Parameter	$MLSS$ (mg/l)	$RASS$ (mg/l)	$BODe_{(sol)}$ (mg/l)	$GR_{(daily)}$ $(mg/l/d)$
mean	3626.1	7303.2	2.021	88.1
std. deviat.	1332.1	2246.6	1.765	101.2
C.O.D.	0.645	0.704	0.254	0.996
R	0.849	0.854	0.523	0.999
mean error	249.5	-400.7	0.32	-0.31
RMS error	762.2	1407.2	2.51	5.99
var. error	0.5206E+6	0.1826E+7	6.21	36.1
sum sq. error	0.1644E+9	0.5604E+9	0.1780E+4	0.1027E+5

Table 3.10. Recursive estimation with additive noise in the parameters.

3.17.6 Conclusions

The structured biomass model developed initially did not simulate the dynamics of the process better than the simple model, thus it was subsequently discarded for the sake of simplicity. The latter model, described by equations 3.49 to 3.53, was considered adequate according to the modelling objectives (Sec. 3.16.1), since it describes the main processes of organic substrate removal and kinetics of biomass based on generally accepted theory and in addition retains a relatively simple structure.

The significant noise and potential measurement errors in both the input and output observations hampered the complete identification of the biochemical kinetics, such as the temperature dependency, and the accurate estimation of the kinetic rates. The adaptive parameter estimation showed that marginal improvements in simulating the solids behaviour could be obtained even under substantial variation in the kinetic rates. This was explained by the substantial effect of the hydraulic component upon the solids behaviour as discussed in Section 3.16.5. The performance of the hydraulic model was examined initially, and a number of potential causes were suggested to explain the occasional poor model performance (Sec. 3.14.2). However the available information on the process were not sufficient for testing the validity of the explanations presented.

Under these conditions the carbonaceous oxidation model performance was considered satisfactory for the purpose of this study and the model was also verified on the basis of the prediction error statistical properties. The simulation results depict some of the characteristics of extended aeration systems, such as the relatively low growth kinetics of biomass and the high removal of organic substrates under a variety of operating conditions. Finally, the temperature dependency of the kinetic rates was found to be unimportant on the basis of simulation results for the particular oxidation ditch system.

3.18 Nitrification-denitrification modelling

3.18.1 Introduction

The nitrification process is of vital importance in wastewater treatment for the removal of ammonia. Ammonia is undesirable in final effluents discharged into natural watercourses for several reasons :

- Free ammonia is toxic to fish and other aquatic life even in very low concentrations such as 0.2 mg/l.
- It exerts a high oxygen demand which may cause oxygen depletion in streams with low oxygenation capacity.
- Water containing ammonia has a high chlorine demand upon disinfenction and it may become unsuitable for water supply or other usage if the free ammonia content exceeds certain limits.

The denitrification process in wastewater treatment is also desirable especially in cases where a high degree of nitrification is achieved. The main reasons are :

- Through denitrification a significant proportion of the oxygen used for nitrification (up to 40%) can be reclaimed, resulting in considerable savings in energy and running cost of the plant.
- It reduces the nitrate and nitrite content of the final effluent, thus minimizing the adverse effects of these substances to public health and eutrophication problems in streams or lakes.
- Denitrification recovers part of the alkalinity which is lost during nitrification, hence there is no need for additional pH control in the reactor.
- Eliminates the problem of rising sludge in the final clarifiers.

The oxidation ditch process is particularly capable of achieving both nitrification and denitrification if operated well. The long operating sludge age promotes the growth of the slow-growing autotrophic organisms while the long hydraulic retention time ensures high degree of ammonia oxidation. In addition the non-uniform air distribution in the reactor assists in the formation of anoxic zones (Section 3.15), which promote the reduction of nitrates and nitrites.

The nitrification and denitrification processes involve different type of micro-organisms and substrates from the carbonaceous oxidation and for this purpose were studied separately. The only common term with the carbonaceous oxidation is the organic substrate which is utilized for both the growth of heterotrophic biomass and denitrification, implying that the two models should be solved simultaneously. However the amount of substrate used for denitrification is much less than for heterotrophic biomass growth. This suggests that the two models may be decoupled and solved separately with the introduction of relatively small error, which can be accepted considering the uncertainty in the determination of the organic substrate.

The objective of this section was to develop a model which adequately describes the oxidation of ammonia by autotrophic organisms and the reduction of nitrates by certain microbial species under anoxic conditions. Hence the model should be able to predict the effluent ammonia and nitrate concentrations, under a given set of input and operating conditions of the plant. The development of model structure was also based on information from the literature and was calibrated in the light of operational data.

3.18.2 Model development

It was shown in the review (Sections 3.3.2 & 3.4) that the main phenomena describing the biochemical transformations of nitrogenous compounds in wastewater treatment are the following, shown schematically in Fig. 3.19:

a. Hydrolysis of particulate organic nitrogen to soluble nitrogen.

b. Ammonification of soluble organic nitrogen.

c. Assimilation of ammonia for cell synthesis.

d. Oxidation of ammonia to nitrites.

e. Oxidation of nitrites to nitrates.

f. Growth of nitrifying organisms.

g. Decay of nitrifying organisms.

h. Reduction of nitrates to nitrites.

i. Reduction of nitrites to nitrogen gas.

j. Growth of denitrifying organisms.

k. Decay of denitrifying organisms.

In the above list the hydrolysis, ammonification and assimilation processes are carried out by heterotrophic organisms. The first two processes increase the ammonia load, while the assimilation process results in a loss of ammonia from the system. The processes (d) to (g) describe the main kinetics in nitrification and reactions (h) to (k) refer to the denitrification process.

In domestic sewage the majority of nitrogenous compounds are in the form of free and saline ammonia (Dold et al. 1980). Their organic nitrogen content is reported to be generally low, because it is partly hydrolyzed to ammonia inside the sewerage system before reaching the treatment plant. Furthermore, the loss of ammonia due to assimilation is relatively small compared to the removal through nitrification, due to the domestic origin of the crude sewage with high proportion of ammonia relative to organic substrate. The processes of hydrolysis-ammonification and the assimilation process, whose effect upon the ammonia load is almost counter-balanced, were subsequently neglected in the absence of organic nitrogen measurements. The above assumption offered substantial simplicity to the model without introducing significant error.

The nitrification reactions have been modelled either as a single-stage or a two-stage process (Sections 3.9 & 3.10). It is widely accepted that nitrification proceeds in two stages with different organisms and reactions involved in each stage (equat. 3.19 & 3.20), suggesting that a two-stage representation would be necessary to simulate the process. However the two-stage representation would result in a rather complex and over-parameterized model structure (Poduska & Andrews 1975; Beck 1981), which in addition would be very difficult to calibrate. It is reported in the literature (Sec. 3.3) that the oxidation of ammonia to nitrites is a much slower reaction than the oxidation of nitrites to nitrates. Subsequently the concentration of the intermediate product of nitrites is generally low, since they are rapidly oxidized to nitrates as soon as they are produced. This was also confirmed from the operational data.

According to the above remarks, nitrification can be adequately modelled as a single-stage process involving the oxidation of ammonia to nitrates by a group of nitrifying organisms. These organisms were considered to describe the aggregated behaviour of Nitrosomonas, Nitrobacter and other autotrophic species responsible for nitrification. The growth rate of nitrifiers was described by Monod kinetics limited by the ambient ammonia concentration, and their decay was considered to proceed

at a constant rate (eq. 3.23).

Similarly the reduction of nitrates to nitrogen gas also proceeds in two stages (eq. 3.26), with the intermediate production of nitrites. However, for the same reasons as before, the two stages were simply described as a single stage, whereby nitrates are reduced to nitrogen gas by certain species of facultative bacteria, which were referred to as denitrifiers. The growth of denitrifiers was assumed to follow Monod kinetics limited by both the nitrate and soluble substrate concentrations in the reactor.

Some further assumptions made for the development of the model were :

- The dissolved oxygen in the aerobic zones is always adequate for uninhibited nitrification while its concentration in the anoxic zones is sufficiently low for uninhibited denitrification. Hence no oxygen limitation term was included in the model. The assumption was justified in view of the existing automatic DO control mechanism, the advantages of which were discussed in Sec. 3.15.
- The nitrifying and denitrifying biomass in the crude sewage and final effluent is negligible.
- The nitrogen assimilated for cell synthesis is negligible.
- The influent and effluent nitrite concentration is negligible.
- The decay of both nitrifiers and denitrifiers takes place in both aerobic and anoxic regions.

Finallythe model for the nitrification - denitrification process was expressed by the following set of equations and is schematically represented in Fig. 3.20.

1. **Ammonia-nitrogen in A.T.** (NH_3)

$$\frac{dNH_{3_t}}{dt} = \frac{Qi_t \cdot NH_3i_t + Qr_t \cdot NH_3R_t - (Qi_t + Qr_t) \cdot NH_{3_t}}{V} - \frac{A \cdot \mu_N}{Y_N} \quad (3.57)$$

2. **Nitrifying biomass in A.T.** (BX)

$$\frac{dBX_t}{dt} = \frac{Qr_t \cdot BR_t - (Qi_t + Qr_t) \cdot BX_t}{V} + A \cdot \mu_N - Kd_N \cdot BX_t \cdot T_N \quad (3.58)$$

3. **Nitrate-nitrogen in A.T.** (NO_3)

$$\frac{dNO_{3_t}}{dt} = \frac{Qi_t \cdot NO_3i_t + Qr_t \cdot NO_3R_t - (Qi_t + Qr_t) \cdot NO_{3_t}}{V} + \frac{A \cdot \mu_N}{Y_N} - \frac{B \cdot \mu_D}{Y_D} \quad (3.59)$$

4. **Denitrifying biomass in A.T.** (DX)

$$\frac{dDX_t}{dt} = \frac{Qr_t \cdot DR_t - (Qi_t + Qr_t) \cdot DX_t}{V} + B \cdot \mu_D - Kd_D \cdot DX_t \cdot T_D \quad (3.60)$$

5. **Ammonia-nitrogen in recycle and final effluent (NH_3R)**

$$\frac{dNH_3R_t}{dt} = \frac{(Qi_t + Qr_t) \cdot (NH_{3t} - NH_3R_t)}{Vcl} \tag{3.61}$$

6. **Nitrifying biomass in the recycle (BR)**

$$\frac{dBR_t}{dt} = \frac{(Qi_t + Qr_t) \cdot BX_t}{Vcl} - \frac{(Qr_t + Qw_t) \cdot BR_t}{Vcl} \tag{3.62}$$

7. **Nitrate-nitrogen in recycle and final effluent (NO_3R)**

$$\frac{dNO_3R_t}{dt} = \frac{(Qi_t + Qr_t) \cdot (NO_{3t} - NO_3R_t)}{Vcl} \tag{3.63}$$

8. **Denitrifying biomass in the recycle (DR)**

$$\frac{dDR_t}{dt} = \frac{(Qi_t + Qr_t) \cdot DX_t}{Vcl} - \frac{(Qr_t + Qw_t) \cdot DR_t}{Vcl} \tag{3.64}$$

where; $\mu_N = \mu_{Nmax} \cdot BX \cdot NH_3/(K_{NH3} + NH_3) \cdot T_N$ (3.65a)

$\mu_D = \mu_{Dmax} \cdot DX \cdot NO_3/(K_{NO3} + NO_3) \cdot S/(K_{SD} + S) \cdot T_D$ (3.65b)

$T_{N(T)} = T_{N(10)} \cdot \theta_N^{(T-10)}$ (3.66a)

$T_{D(T)} = T_{D(10)} \cdot \theta_D^{(T-10}$ (3.66b)

μ_N : specific growth rate of nitrifiers $[T^{-1}]$,

μ_{Nmax} : maximum growth rate of nitrifiers $[T^{-1}]$,

K_{NH3} : half-rate NH3-N concentration $[ML^{-3}]$,

Y_N : yield of nitrifiers from ammonia oxidation [–],

μ_D : specific growth rate of denitrifiers $[T^{-1}]$,

μ_{Dmax} : maximum growth rate of denitrifiers $[T^{-1}]$,

K_{NO3} : half-rate NO3-N concentration $[ML^{-3}]$,

S : soluble organic substrate concentration $[ML^{-3}]$,

K_{SD} : half-rate organic substrate concentration $[ML^{-3}]$,

Y_D : yield of denitrifiers from nitrate reduction [–],

θ_N : temperature coefficient for nitrification [–],

θ_D : temperature coefficient for denitrification [–],

and the temperature dependent parameters are considered at 10 ^oC.

3.18.3 Parameter estimation

Typical values for the kinetic rates of nitrification and denitrification are shown in Table 3.11. The proposed values show significant diversity and can only serve as guidelines to give a rough estimate of their expected range for parameter estimation. The model was solved numerically because its complex structure prohibited its analytical solution.

Parameter units	Metcalf-Eddy (1979)		Marais (1976)	Cook (1983)	Downing (1964)	Terashima (1985)	Busby (1975)
μ_{Nmax} (d^{-1})	0.3-3.0	1.0	0.2-0.65	0.285	0.33	0.72	1.08
KdN (d^{-1})	0.03-0.06	0.05	0.04	0.151	—	—	0.12
K_{NH3} (mg/l)	0.2-5.0	1.4	1.0	1.50	1.0	0.5	0.063
Y_N (-)	0.1-0.3	0.2	0.10-0.15	0.047	0.05	0.17	0.05
μ_{Dmax} (d^{-1})	0.3-0.9	0.3				0.48	
KdD (d^{-1})	0.04-0.08	0.04					
K_{NO3} (mg/l)	0.06-0.2	0.1				0.1	
K_{SD} (mg/l)							
Y_D (-)	0.4-0.9	0.8					
θ_N (-)		1.10	1.03-1.12				
θ_D (-)		1.10					

Table 3.11. Typical parameter values for nitrification–denitrification kinetics.

From the formulation of the model equations it is apparent that the soluble organic substrate term is common with the previously described carbonaceous oxidation model, as discussed in 3.18.1. The soluble substrate term was considered as a known variable for simulation purposes. The values obtained from the non-adaptive simulation of the carbonaceous model without temperature dependency were subsequently employed.

From the stoichiometry of the reaction 3.21 (Sec. 3.3), it was shown that 1 gram of ammonia (NH_3-N) oxidized to nitrate yields 0.166 grams of nitrifiers, which is within the reported values of cell yield. Similarly from reaction 3.28 (Sec. 3.4), it was shown that 1 gram of nitrate (NO_3-N) reduced to nitrogen gas yields 0.53 grams of denitrifiers.

The current model contains several unmeasurable variables, such as the concentrations of nitrifier and denitrifier organisms in the process units. Furthermore the large number of parameters does not justify the use of block estimation techniques. For this purpose the parameters were initially selected by trial and error on the basis that the steady-state model performance under average input conditions would predict the average effluent ammonia and nitrate concentrations. The initial parameter set was subsequently modified in the light of simulation results with the measured inputs over the study period. The procedure was repeated until no further improvement was obtained in matching the observed effluent performance (Table 3.12). The final parameter values lie within the reported range except for the temperature dependency coefficients. From simulation results the temperature dependency was found to be insignificant for nitrification and relatively small for denitrification. The final

simulation results are presented in Fig. 3.21 and Table 3.13.

Parameter	Units	Init. values	Final values
μ_{Nmax}	d^{-1}	0.30	0.24
Kd_N	d^{-1}	0.048	0.048
K_{NH3}	mg/l	1.0	0.6
Y_N	—	0.166	0.166
μ_{Dmax}	d^{-1}	0.569	0.614
Kd_D	d^{-1}	0.042	0.042
K_{NO3}	mg/l	0.15	0.15
K_{SD}	mg/l	1.0	1.0
Y_D	—	0.53	0.53
θ_N	—	1.03	1.00
θ_D	—	1.05	1.03
$BX_{(0)}$	mg/l	36.0	33.0
$DX_{(0)}$	mg/l	100.0	75.0
$NH3_{(0)}$	mg/l	1.5	1.5
$NO3_{(0)}$	mg/l	9.7	9.7

Table 3.12 Parameter and initial state values

Parameter	$NH3e$	$NO3e$	Nitrifiers	Denitrif.
mean (mg/l)	2.92	6.13	22.67	52.84
std. deviat.	2.96	3.30	7.56	17.31
C.O.D.	0.576	0.007		
R	0.762	0.400		
mean error	0.064	-0.22		
var. error	5.49	17.5		
sum sq. error	1549	4622		
RMS error	2.34	4.18		

Table 3.13. Performance of nitrification-denitrification model.

3.18.4 Discussion of results

From Figure 3.21a it is apparent that the model can satisfactorily reproduce the observed effluent ammonia concentration under varying operating conditions of both low and high nitrification performance. The C.O.D. value of 0.576 was considered adequate in view of the noisy structure of the measurements which were not filtered in any way. The residual error had almost zero mean and relatively small correlation with the system states and inputs. However it showed significant autocorrelation at low lags (Figure 3.22a).

The adequacy of the model to describe the denitrification process was judged by its ability to predict the measured effluent nitrate concentration. From Figure 3.21b it can be seen that the model performance is poorer than for ammonia although the average level of effluent nitrate was adequately predicted. The residual error had a small mean and insignificant correlation with the system inputs and states. However its autocorrelogram (Figure 3.22b) exhibited significant serial structure at 5% level, suggesting that further improvements to the model might be possible.

In view of the simplifying assumptions made during its development such as, single stage denitrification, neglect of the intermediate nitrite product and fixed volume anoxic zones, and considering the stochastic nature of external environmental disturbances upon the process kinetics, the model predictions were considered satisfactory. The current model was already complex and any improvement would increase further its complexity and the number of parameters. This would create further difficulties in the identification of parameters and perhaps render the model unsuitable for the purpose of investigating and controlling the process. On the basis of the above hypotheses the model was accepted as adequate, although not fully verifiable particularly regarding the denitrification process.

Using the model an attempt was made to explain the observed poor nitrification performance of the plant during part of the study period. The deterioration in nitrification performance started at around day 165 and was exacerbated between day 214 and 268, where the effluent ammonia exceeded its design value of 5.0 mg/l. The model predicted the deterioration in effluent ammonia sufficiently well, although the observed effluent ammonia peak around day 260 was not well reproduced. The model also reconstructed the unobservable nitrifier concentration in the mixed liquor (Fig. 3.21c) and predicted that their concentration reached a peak of 40.0 mg/l on day 118. On subsequent days their concentration was predicted to fall steadily reaching a minimum of 7.4 mg/l on day 236. This major drop in the nitrifier population was primarily caused by the high rate of sludge surplussing and the low recycle ratio after day 170, resulting in substantial washout of nitrifiers from the system. The period of low nitrifier concentration which coincided with relatively high input ammonia, can be regarded as the main cause of the poor nitrification performance associated with high effluent ammonia concentrations.

Finally the model reconstructed the unmeasurable denitrifier concentration (Figure 3.21d). Their dynamic behaviour was similar to the nitrifiers, with a peak of 81.8 mg/l on day 119 and a lowest value of 17.8 mg/l on day 236. The relatively high effluent nitrates during the first 30 days can be explained by the rather high influent nitrate concentration and the low mixed liquor temperature inhibiting the denitrification reaction. Furthermore the increased effluent nitrate after day 220 can be attributed to the low denitrifier population in the system, also caused by the high

sludge surplussing rate.

3.18.5 Adaptive parameter estimation

Adaptive parameter estimation would reveal the time variation of the kinetic rates and possibly assist in identifying deficiencies in the model structure by examining the parameter trajectories. The E.K.F. algorithm was again employed as was described in Sec. 3.17.4 and Appendix 2.

The nitrification-denitrification model contains nine parameters and their simultaneous estimation is likely to produce biased estimates, considering the limitations of the algorithm when applied to non-linear systems and the fact that only two measured variables were available. Among the model parameters the two yield coefficients (Y_N, Y_D) were sufficiently well estimated stoichiometrically and were not expected to vary with time. In addition the half-rate limitation constants (K_{NH3}, K_{NO3}, & K_{SD}) can be also considered time-invariant, since a change in these constants would result from serious changes in the characteristics of substrates or organism behaviour. This was unlikely to happen under normal operating conditions of the plant. The remaining four kinetic rates were more likely to vary, because they depict the effect of unmodelled environmental factors and operating conditions upon the micro-organism activity. Therefore these four parameters were selected for adaptive estimation.

Accordingly the augmented state vector contained the following state variables and parameters which were suitably rescaled for the application of the algorithm :

$X_1(t) \equiv NH3$ in A.T. (mg/l)
$X_2(t) \equiv BX \times 10^{-1}$ (mg/l)
$X_3(t) \equiv NO3$ in A.T. (mg/l)
$X_4(t) \equiv DX \times 10^{-1}$ (mg/l)
$X_5(t) \equiv NH3$ in F.E. (mg/l)
$X_6(t) \equiv BR \times 10^{-1}$ (mg/l)
$X_7(t) \equiv NO3$ in F.E. (mg/l)
$X_8(t) \equiv DR \times 10^{-1}$ (mg/l)
$X_9(t) \equiv \mu_{Nmax} \times 10^2$ (hr^{-1})
$X_{10}(t) \equiv KdN \times 10^3$ (hr^{-1})
$X_{11}(t) \equiv \mu_{Dmax} \times 10^2$ (hr^{-1})
$X_{12}(t) \equiv KdD \times 10^3$ (hr^{-1})

The process observations which the algorithm used for updating the states were the effluent ammonia (NH_3-N) and effluent nitrate (NO_3-N) concentrations. Hence, the observation vector ($\underline{y}$) and measurement matrix (h) were as follows :

$y_1(t_k) \equiv NH3e$ measured (mg/l)
$y_2(t_k) \equiv NO3e$ " (mg/l)

$$h = \begin{vmatrix} 0 & 0 & 0 & 0 & 1 & 0 & 0 & 0 & 0 & 0 & 0 & 0 \\ 0 & 0 & 0 & 0 & 0 & 0 & 1 & 0 & 0 & 0 & 0 & 0 \end{vmatrix}$$

The remaining states of the augmented vector, were reconstructed by the algorithm using the model equations, while the time-invariant parameters were assigned the values from the block estimation. The four kinetic rates were estimated as non-dynamic states, with the following values assigned to the system (Q), measurement (R) and initial (P) error covariance matrices :

$$Q(i,i) = 0.01 \quad for \quad i = 1,8 \text{ (states)}$$
$$Q(i,i) = 0 \quad for \quad i = 9,12 \text{ (parameters)}$$

$$P_{(0)} = \begin{vmatrix} 0.05 & & & & & & & & & & & \\ & 0.3 & & & & & & & & & & \\ & & 0.4 & & & & & & & & & \\ & & & 0.5 & & & & & & & & \\ & & & & 0.1 & & & & & & & \\ & & & & & 0.6 & & & & & & \\ & & & & & & 0.4 & & & & & \\ & & & & & & & 0.8 & & & & \\ & & & & & & & & 0.05 & & & \\ & & & & & & & & & 0.05 & & \\ & & & & & & & & & & 0.2 & \\ & & & & & & & & & & & 0.05 \end{vmatrix}$$

$$R = \begin{vmatrix} 0.8 & \\ & 1.50 \end{vmatrix}$$

The estimated parameter trajectories are shown in Figure 3.23 and the basic statistics summarized in Table 3.13. It can be seen that the corrected state vector reproduced well the observations without the need to significantly change the parameters. Compared to the non- adaptive estimation, the performance of the model was substantially improved, as indicated by the higher C.O.D. coefficients and lower prediction errors. Both the growth and decay rates of nitrifiers were slightly reduced towards the middle of the simulation period, while the nitrifier concentration was predicted to be higher than before. The maximum growth rate of denitrifiers dropped slightly from its initial value during the first few days but then showed good convergence, while the decay rate exhibited small perturbations throughout the period. The estimated denitrifier concentration was also higher than in pure simulation.

The estimated parameter trajectories did not exhibit any distinct pattern of variation, suggesting that no important processes were neglected by the model. The observed parameter variation mainly reflects the effect of unmodelled system disturbances and unknown environmental factors upon the nitrification and denitrification kinetics.

Parameter	μ_{Nmax}	KdN	μ_{Dmax}	KdD
mean (hr^{-1})	0.931E-1	0.1748E-2	0.207E-1	0.1662E-2
std.deviat.	0.981E-2	0.147E-3	0.61E-2	0.146E-3
Parameter	$NH3e$	$NO3e$	BX	DX
mean (mg/l)	2.74	6.05	28.6	62.2
std. deviat.	3.51	3.36	10.6	21.4
C.O.D.	0.702	0.713		
R	0.851	0.847		
mean error	0.247	-0.138		
RMS error	1.96	2.24		
var. error	3.79	5.04		
sum sq.error	1087.6	1427.9		

Table 3.14. Recursive estimation with non-dynamic parameters.

3.18.6 Conclusions

The non-adaptive simulation results indicated that the developed model could be further improved particularly regarding the denitrification process, by considering perhaps a two-stage nitrification and denitrification or variable volume aerobic and anoxic zones based on the DO profile in the reactor. However in the light of the adaptive estimation results it was shown that the developed model was adequate, since a relatively small variation in the parameters improved substantially the model performance. Furthermore, the model was critisized as being already complex for the complete identification of the process dynamics and adaptive estimation of all the parameters. Further improvements were not justifiable in view of the stochastic nature of the processes described and according to the initial objective of seeking a relatively simple model structure. Consequently the present model was accepted as sufficient for the purpose of this study.

3.19 Integrated process model

Combining the carbonaceous oxidation model with the nitrification - denitrification model produced an integrated model for the oxidation ditch process. The only mod-

ification to be made, concerns the dynamics of soluble substrate in the mixed liquor, in which a term had to be incorporated, describing its utilization for denitrification. Thus equat. 3.50 became :

$$\frac{dS_t}{dt} = \frac{Qi_t \cdot Si_t + Qr_t \cdot SR_t - (Qi_t + Qr_t) \cdot S_t}{V} - \frac{A \cdot \mu_H}{Ysx} - \frac{B \cdot \mu_D \cdot Y_{SD}}{Y_D} + \frac{}{Yxs \cdot Kd \cdot X_t} \tag{3.67}$$

where; $Y_{SD} = 2.47$, utilization of substrate for denitrification (McCarty et al. 1969).

The performance of the integrated model using the previously estimated parameters values from Tables 3.6 and 3.12 was slightly lower than in the individual models. This was attributed to the modification in the above equation, which subsequently affected slightly the other model states. However this effect did not justify the re-estimation of model parameters.

3.20 Sensitivity analysis

Even after the parameter estimation and model verification stages have been completed the parameter values are not known exactly. The existing error in their values, which also causes difference between model predictions and observations, will propagate whenever the model is used for forecasting. Thus the parameter sensitivity of the states offers useful information about the identified model. According to Meissinger (1960) the parameter sensitivity can be used for several applications such as :

- Prediction of solutions in the neighbourhood of known solutions by linear extrapolation.
- Determination of parameter tolerances and detection of critical parameters.
- Application to statistical studies of the effect of random influences of initial values.
- Determination of system stability boundaries.
- Optimization of system parameters.

The approach to calculate the parameter sensitivity coefficients depends on the expected variation of the parameters. In case of large variations a large number of simulations must be performed with different parameter values. However if the expected variations are small then the sensitivity coefficients can be determined from the first derivative of the states with respect to the parameters around a nominal value (Rinaldi et al. 1979).

Here the expected variation of the parameters was small as indicated by the adaptive estimation. Thus the sensitivity coefficients were calculated by the so called "sensitivity theory" which is described in Appendix 3.

Param.	X	BX	DX	BOD	NH_3	NO_3	XR	GR
μ_{max}	46.90	0.0	-5.36	-0.101	0.0	0.685	92.67	376.1
	(7)	(5)	(4)	(1)	(5)	(5)	(7)	(7)
Kd	-79.15	0.0	3.97	0.659E-1	0.0	-0.504	-153.9	-720.0
	(5)	(6)	(9)	(5)	—	(10)	(5)	(3)
μ_{Nmax}	6.143	0.769	-0.75	0.136E-2	-0.611	-0.626	11.95	54.17
	(12)	(2)	(12)	(12)	(1)	(8)	(12)	(12)
KdN	-16.64	-1.266	2.07	-0.418E-2	0.227	1.718	-33.07	-136.7
	(11)	(1)	(11)	(11)	(3)	(1)	(11)	(11)
μ_{Dmax}	-85.65	0.0	10.4	-0.211E-1	0.0	-1.337	-169.3	-671.0
	(3)	—	(1)	(7)	—	(2)	(3)	(4)
KdD	29.84	0.0	-4.78	0.768E-2	0.0	0.498	59.11	213.8
	(10)	—	(8)	(10)	—	(11)	(10)	(10)
Ks	-45.39	0.0	5.18	0.991E-1	0.0	-0.66	-89.66	-364.1
	(8)	—	(7)	(4)	—	(7)	(8)	(8)
K_{NH3}	-2.305	-0.223	0.283	-0.278E-3	0.138	0.200	-4.487	-19.98
	(14)	(4)	(14)	(14)	(4)	(12)	(14)	(13)
K_{NO3}	2.424	0.0	-0.295	0.577E-3	0.0	0.037	4.762	18.86
	(13)	—	(13)	(13)	(10)	(14)	(13)	(14)
K_{SD}	43.98	0.0	-5.21	0.105E-1	0.0	0.666	84.86	337.3
	(9)	—	(6)	(9)	—	(6)	(9)	(9)
Ysx	508.7	0.0	5.35	0.101	0.0	-0.686	986.2	5102.
	(1)	—	(5)	(2)	—	(4)	(1)	(1)
Yxs	365.6	0.0	3.97	0.657E-1	0.0	-0.505	702.0	3696.
	(2)	—	(10)	(6)	—	(9)	(2)	(2)
A	53.00	0.766	-6.11	-0.999E-1	-0.611	0.064	104.5	429.8
	(6)	(3)	(3)	(3)	(2)	(13)	(6)	(6)
B	-85.64	0.0	10.4	-0.211E-1	0.0	-1.337	-169.3	-671.0
	(4)	—	(2)	(8)	—	(3)	(4)	(5)

Table 3.15. Sensitivity coefficients (mean) and sensitivity ranking of parameters (in parenthesis).

The sensitivity of the model states is presented in Fig. 3.25 which depict the effect of a 10% variation in a parameter from its nominal value upon a state variable with time. Table 3.15 shows the mean of the sensitivity coefficients for the whole period and a sensitivity ranking of parameters for each state variable based on the

absolute mean values of the sensitivity coefficients.

3.20.1 Discussion

From Fig. 3.25 it can be observed that the sensitivity coefficients vary significantly throughout the period, which is attributed to the non-linear relationships between model states and parameters. In addition from Table 3.15 it can be seen that the parameters sensitivity ranking can be quite different among the states, while the sensitivity coefficients for a given state may vary within a wide range of values.

In this respect, the two yield coefficients Ysx and Yxs affect mainly the heterotrophic biomass and overall biomass growth, while the growth and decay rates play secondary role and the half-rate constants play almost insignificant role. For the nitrification and denitrification processes the kinetic rates are the most significant parameters, since their respective yields were not included, while the half-rate constants play a minor role. Another interesting observation is the importance of changing the aerobic and anoxic volumes upon the activity of biomass and the effluent quality of the plant.

3.21 Model validation

Following the calibration and verification stage a model should be validated. The validity of a model is usually assessed on the basis of its performance with a different data set or under different conditions. However, there are cases where it is not possible to confirm the validity of a model on the basis of its performance alone with a particular data set. In such cases the validity may be assessed on the basis of the underlying theory in the model, the quality and quantity of observations and the objectives of the modelling exercise.

For the model validation, operational data from a different period of the Cirencester plant were used. The data covered the period between 9/5/80 and 21/1/81, comprising 258 days of operation, as was also used in Sec. 2.5.7.

Using the previous parameter values from the calibration phase, the model performance was relatively poor. Subsequently some of the parameters were modified, shown in Table 3.16. The temperature dependency of both nitrification and denitrification appeared to be more pronounced, while the other modified parameters were related to the kinetic rates of the various types of organisms in the model. Nevertheless, the modification in the parameters did not improve significantly the model performance, shown in Figures 3.26 & 3.27 and Table 3.17.

Parameter	Calibration	Validation
μ_{max} (d^{-1})	1.92	2.04
μ_{Nmax} (d^{-1})	0.24	0.252
μ_{Dmax} (d^{-1})	0.614	0.63
Ysx	1.10	1.05
K_{SD} (mg/l)	1.0	0.8
θ_N	1.00	1.05
θ_D	1.03	1.06

Table 3.16. Modifications in model parameters during validation.

Parameter	$MLSS$	$RASS$	$NHse$	$NOse$	$GR_{(daily)}$
mean	2140.3	4596.3	2.74	5.01	59.92
std. deviat	. 608.0	670.3	2.42	2.07	42.38
R	0.405	0.153	0.296	0.199	-0.10
mean error	488.0	-315.0	-0.42	1.40	-9.47
RMS error	775.8	1336.0	2.77	4.68	98.7
var. error	0.3629E+6	0.1685E+7	7.55	20.0	9690
sum sq.error	0.1547E+9	0.4587E+9	1988	5652	0.2513E+7

Table 3.17. Model performance during validation.

The prediction of the solids concentration in the process was particularly poor. (Figures 3.26a & b). The $MLSS$ concentration was significantly underestimated after day 150, and the $RASS$ concentration was overestimated between day 50 and 150. During the validation of the final clarifier model similar discrepancies were experienced with the $RASS$ concentration (Sec. 2.5.7). Among the potential causes investigated, were the diurnal variation of input flow and $MLSS$ concentration and in addition the effect of spot measurements for the solids concentration (Sec. 2.5.8), which were shown to explain partially the poor model performance. Furthermore a general underestimation of the $MLSS$ and overestimation of the $RASS$ was observed, as to some extent with the previous data set used for calibration (Sec.3.14.2). This was also attributed to the effects of diurnal variation of solids concentration. Finally for the above operating period there are no information regarding any operational problems or malfunctioning of the measuring instruments which might also affect the model performance.

The effluent ammonia concentration was fairly well predicted during most of the period except for the last 40 days, where two out of the three observed peaks were not reproduced by the model. Similarly for the effluent nitrate concentration, although the average level was adequately predicted the observed peak between day 110 and 160 was not reproduced.

3.21.1 Discussion

The validation of the model was not completely successful, since the solids behaviour and the observed peaks in the effluent concentrations were not adequately reproduced. The residual error sequences exhibited significant autoregressive structure at low lags indicating that further improvements to the model could be possible. The diurnal variation in the inputs was considered among the potential causes of the poor performance, however no information were available for assessing their effect on the model predictions. The developed model was based on well accepted theory regarding the internal biochemical reactions and was already quite complex. Any further modifications would introduce undesirable complexity to its structure. This fact combined with the insufficient information about any operating problems and the random disturbances to the process, did not justify further improvements to the model and consequently the current model was accepted as valid.

3.22 Summary

In this chapter the biochemical kinetics in the oxidation ditch process were reviewed and the approaches to model suspended-growth processes were classified and discussed. Next, a dynamic model was developed to simulate the main processes in an oxidation ditch system. Its development was based on a priori knowledge from the literature and a deductive approach of subsequent simplifications was adopted, whereby a relatively simple structure was developed producing satisfactory performance. The model was calibrated and partially validated using real process observations.

The quality of the process measurements was questioned, particularly regarding the various flow rates, while missing observation existed in both the input and output data. The model parameters were estimated both by trial and error and recursively by the E.K.F. The time-variation of parameters during adaptive estimation did not indicate that important processes were neglected, but rather reflected the effect of external disturbances upon the process kinetics. The validation stage was not very successful. Among the possible causes identified were the effect of diurnal input variations upon the solids behaviour and unmodelled external factors upon the kinetic rates.

Limitations for the complete identification of biochemical kinetics and the accurate parameter estimation were encountered due to the large number of parameters and unmeasured states and the noisy structure of the observations. These were collected under various operating regimes including periods of unpredictable plant failures. Finally, the application of the E.K.F. algorithm offered assistance during the model calibration stage. However limitations in its use were also experienced due to the non-linear structure of the model and the small number of measured process variables.

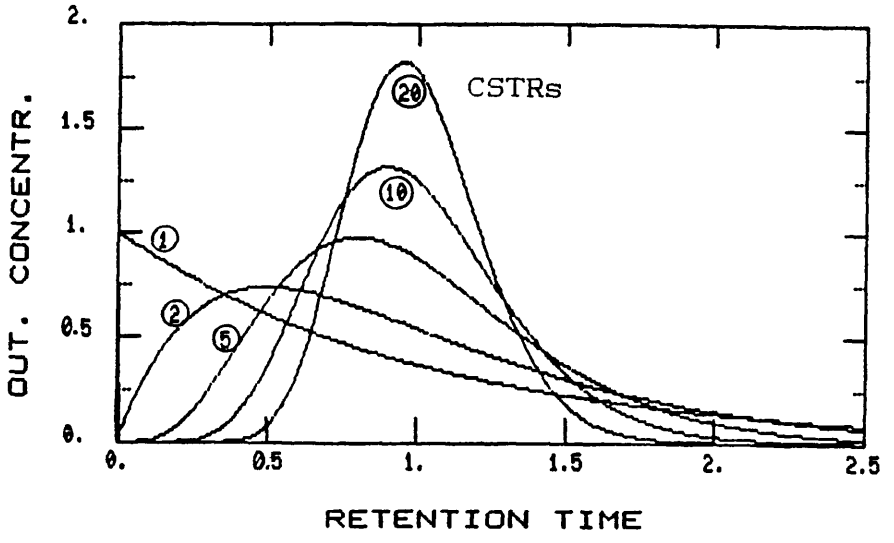


Fig. 3.1a. Output response due to a "delta" input of a conservative substance

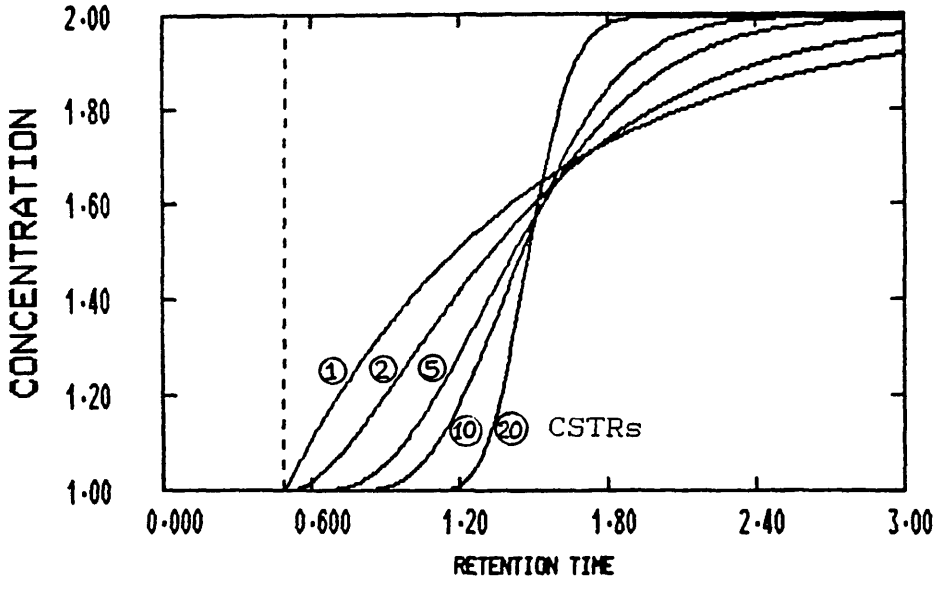


Fig. 3.1b. Output response due to a " step " input of a conservative substance

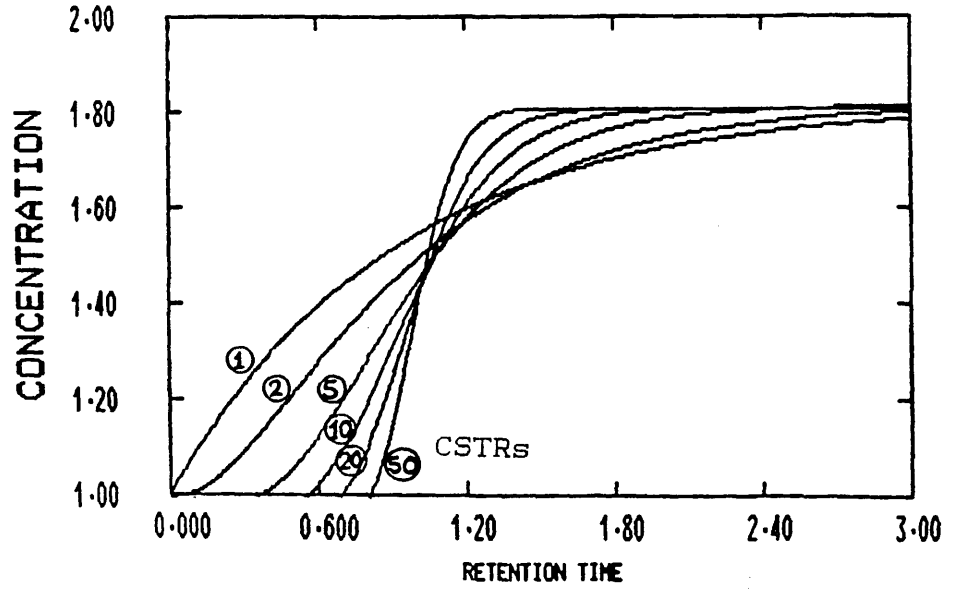


Fig. 3.1c. Output response due to a " step " input of a non-conservative substance

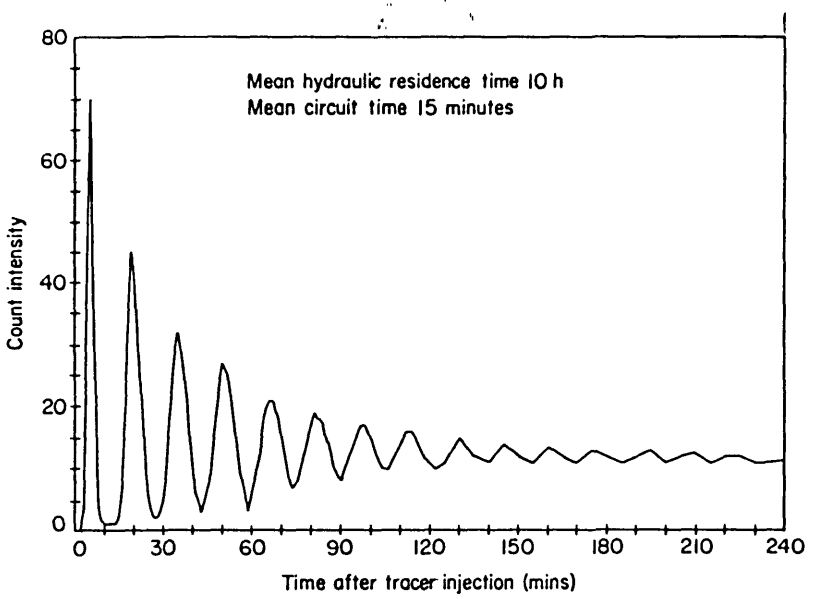


Fig. 3.2. Radioactive tracer output from an oxidation ditch plant

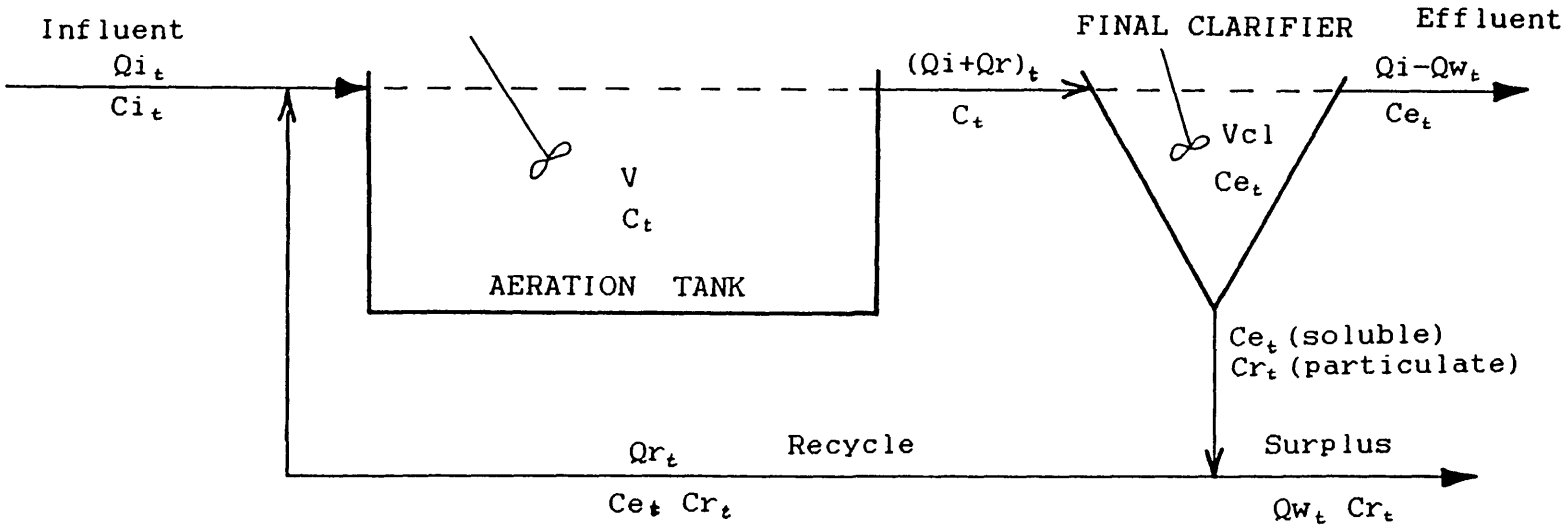


Fig. 3.3. Schematic representation of the oxidation ditch plant

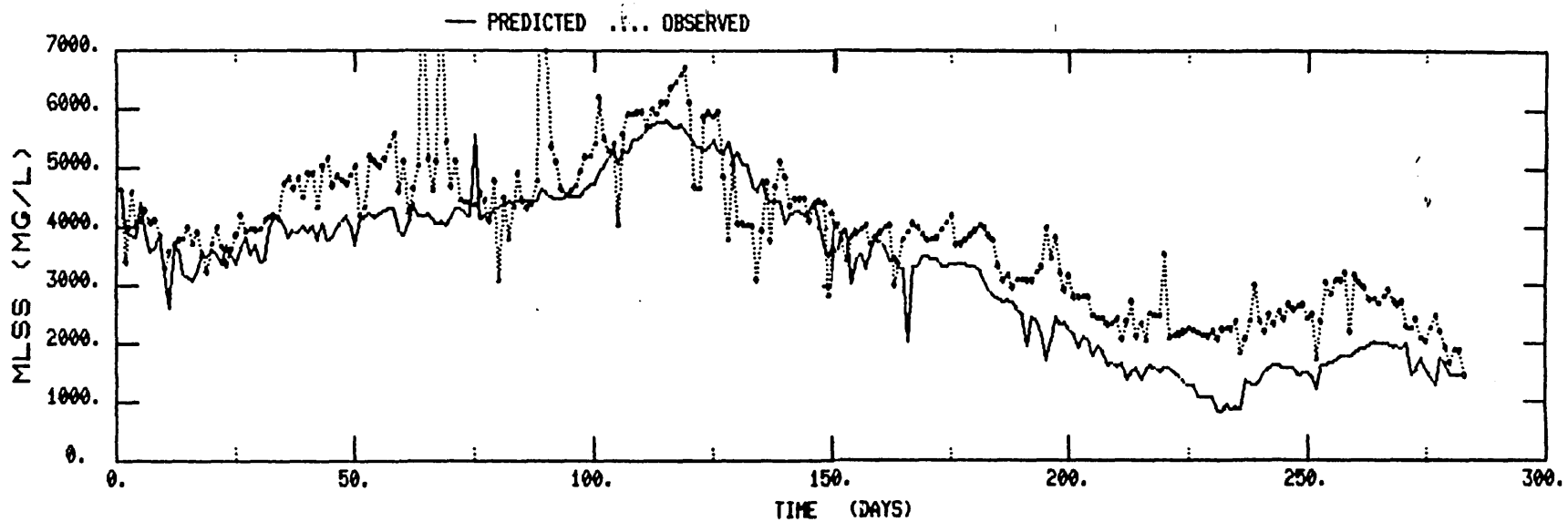


Fig. 3.4a. Predicted – observed $MLSS$ from hydraulic model

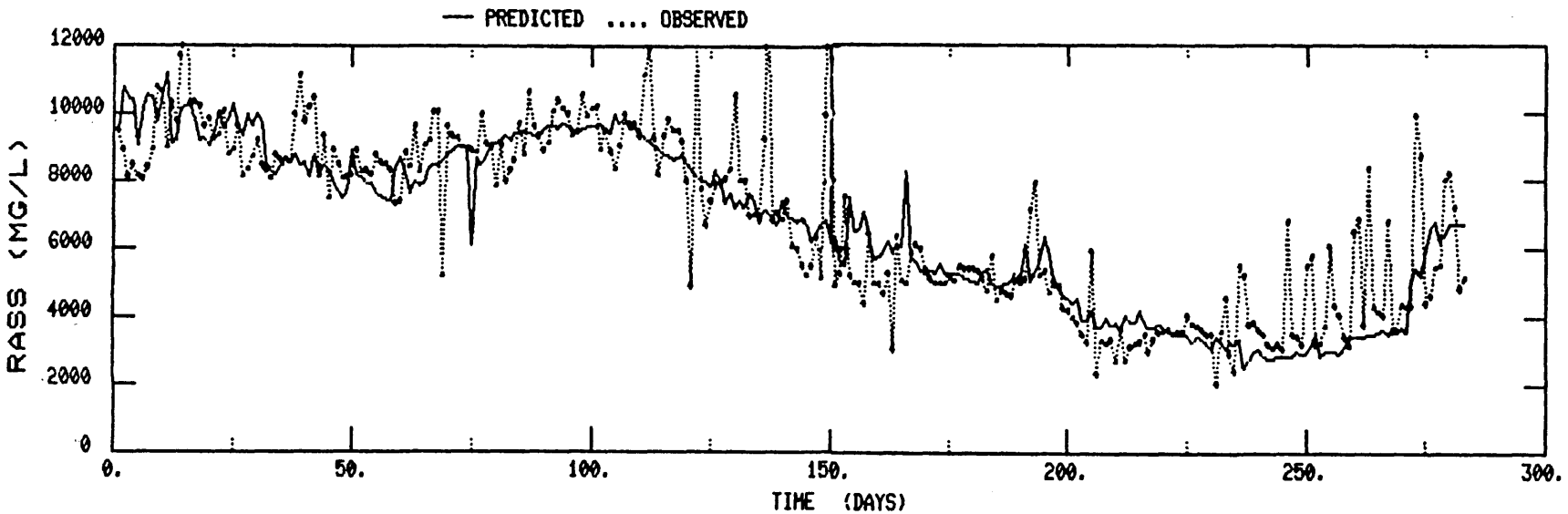


Fig. 3.4b. Predicted – observed $RASS$ from hydraulic model

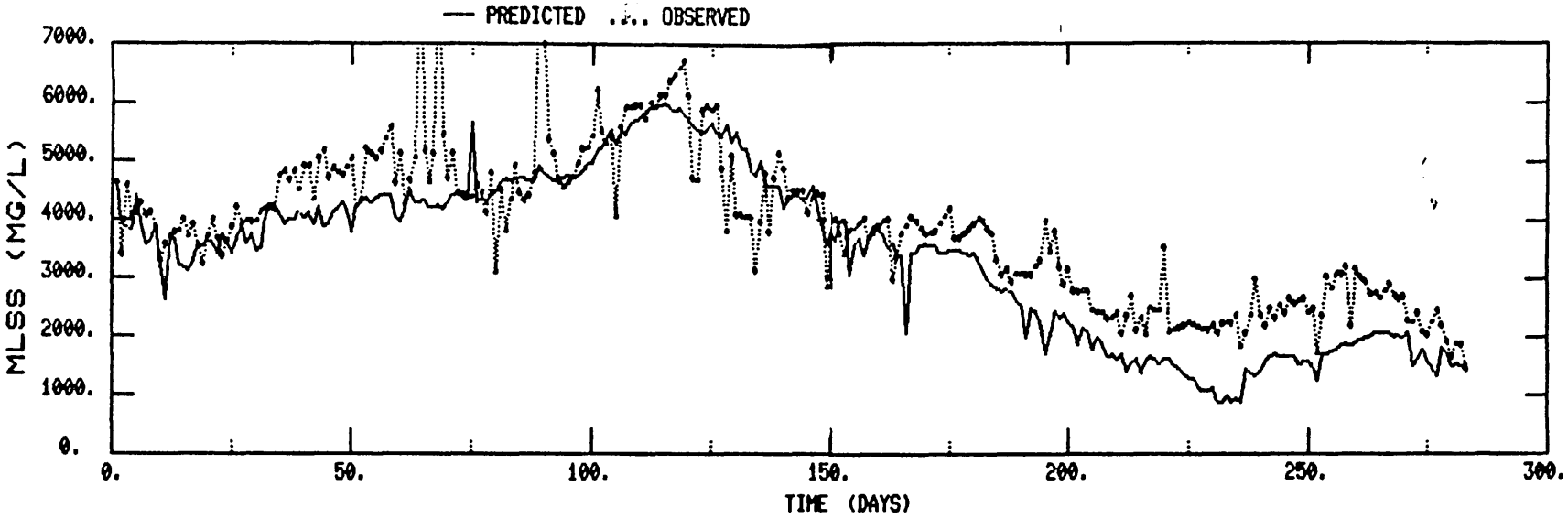


Fig. 3.5a. Predicted – observed $MLSS$ incorporating return liquor stream

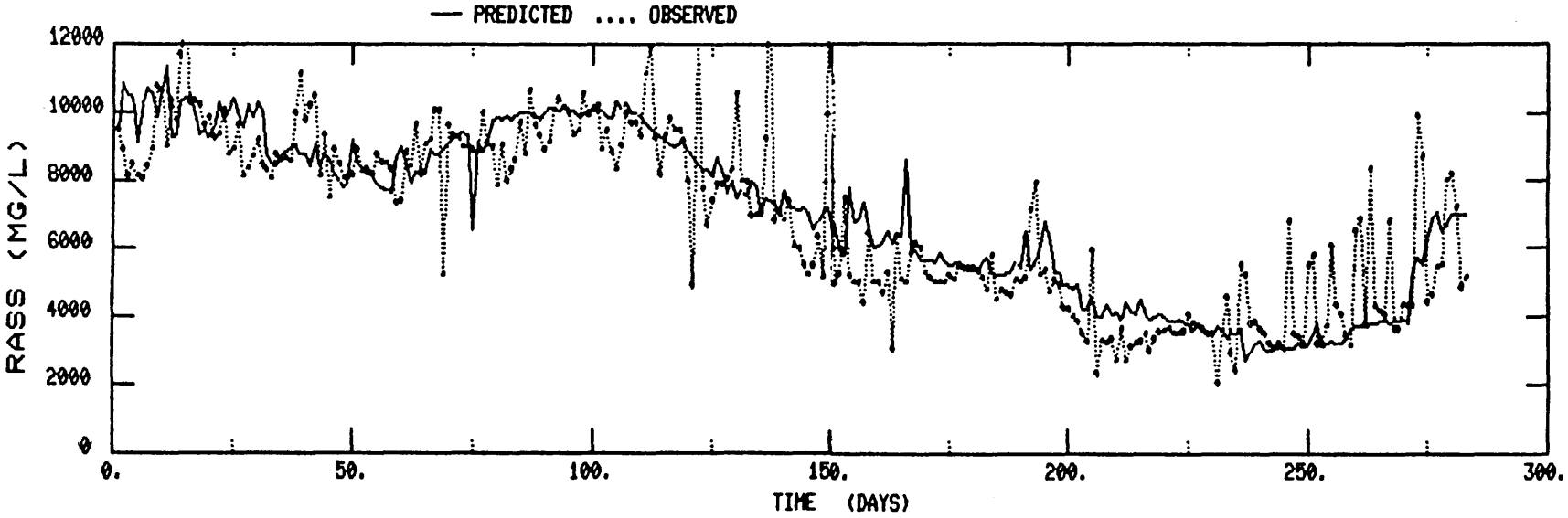


Fig. 3.5b. Predicted – observed $RASS$ incorporating return liquor stream

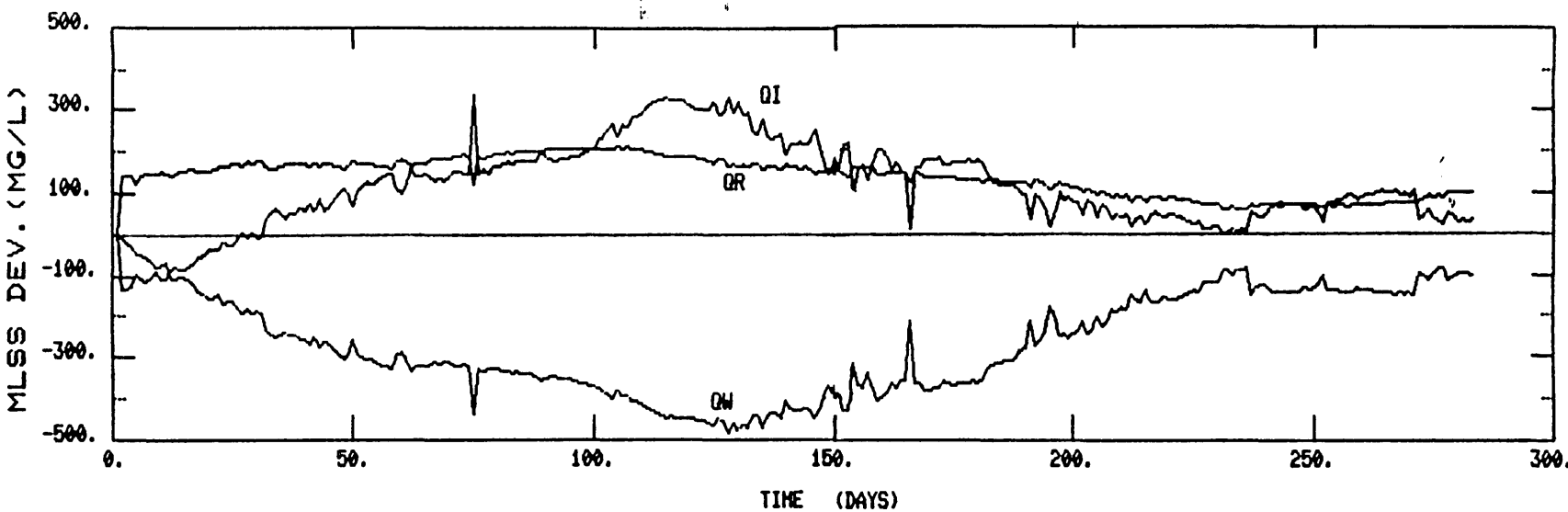


Fig. 3.6a. Sensitivity of $MLSS$ due to 10% increase in flow rates

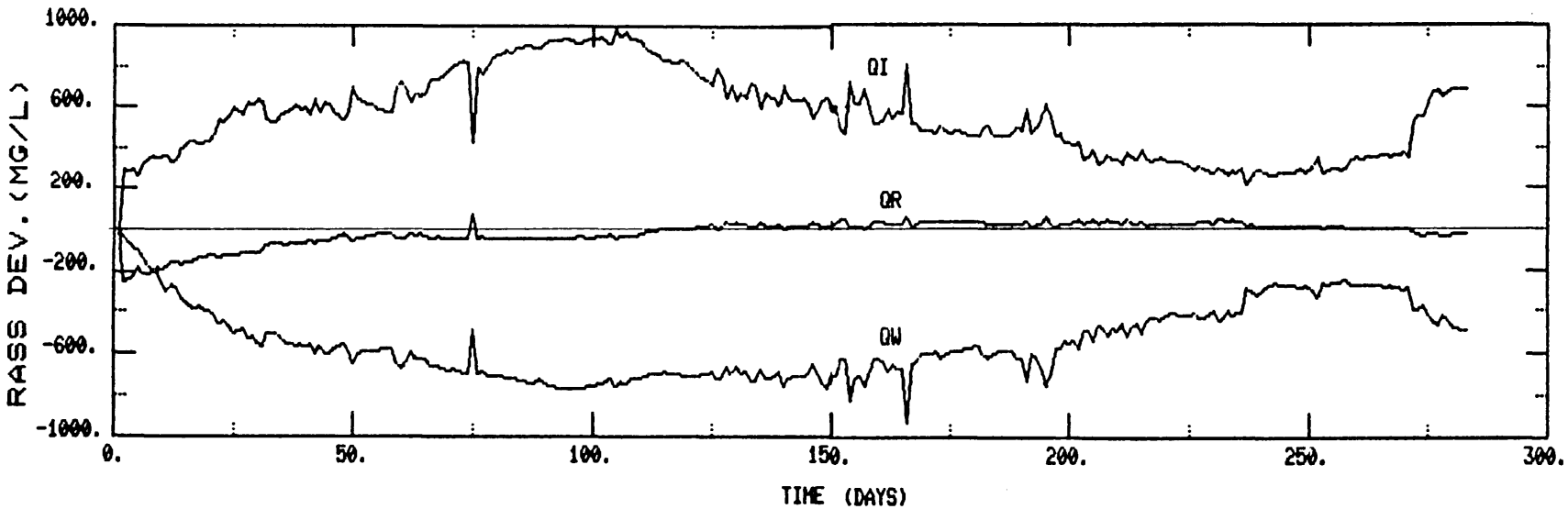


Fig. 3.6b. Sensitivity of $RASS$ due to 10% increase in flow rates

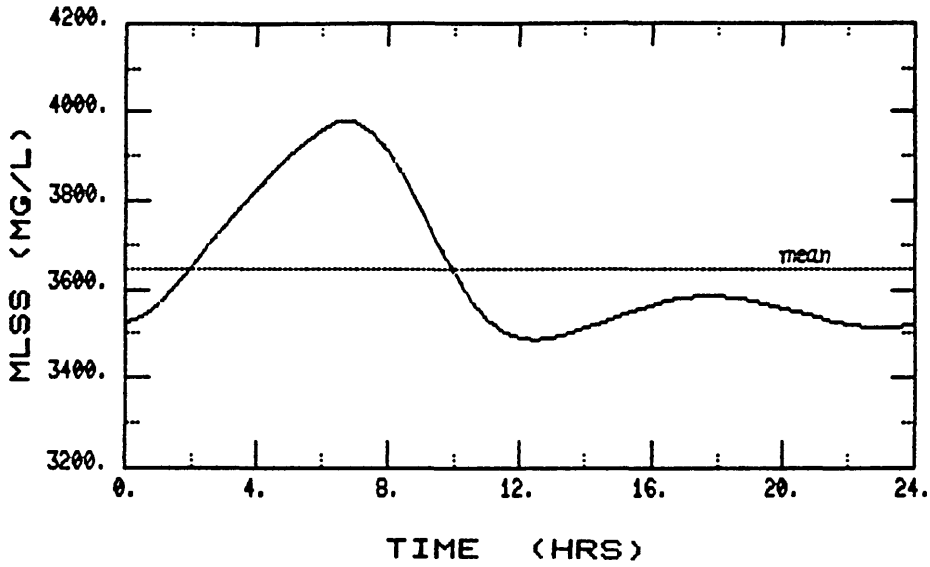


Fig. 3.7a. Simulated diurnal variation of $MLSS$

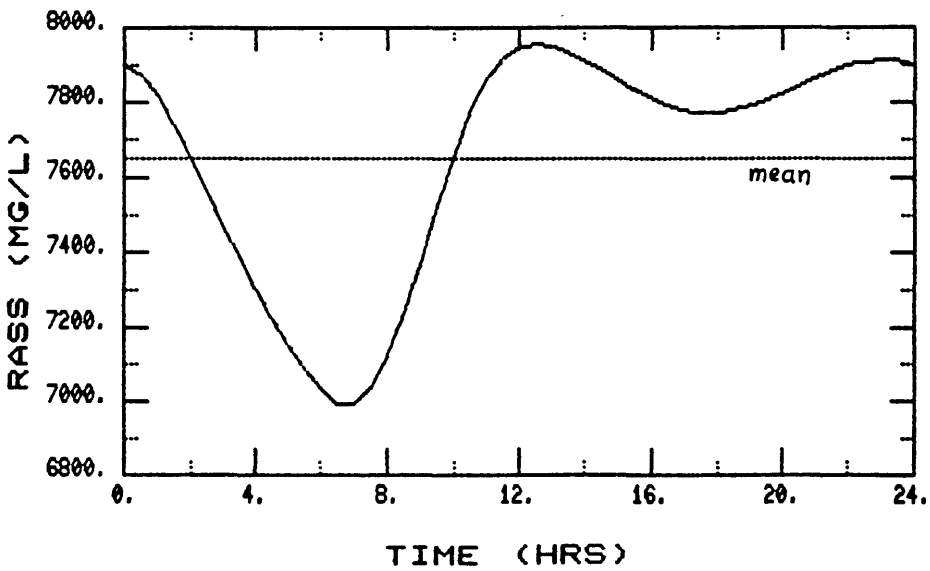


Fig. 3.7b. Simulated diurnal variation of $RASS$

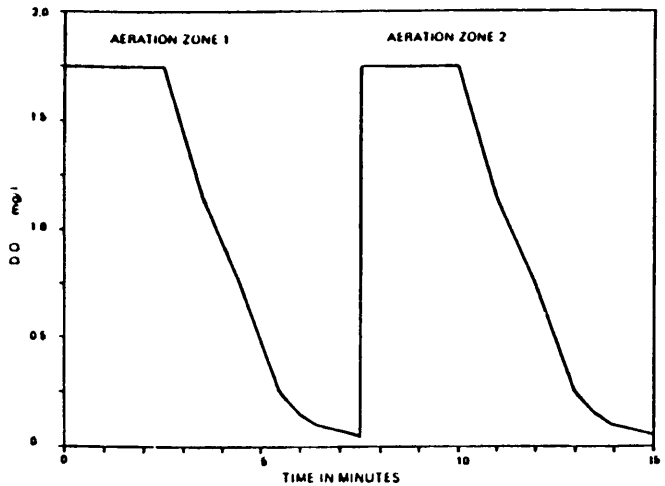


Fig. 3.8. Typical *DO* profile in an oxidation ditch reactor

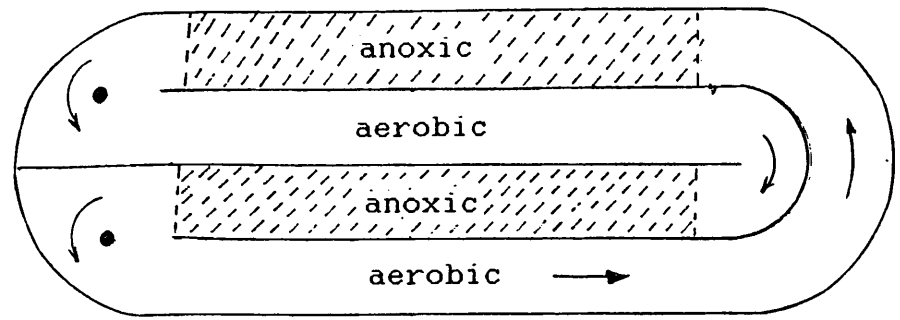


Fig. 3.9. Representation of the aerobic-anoxic zones in the oxidation ditch

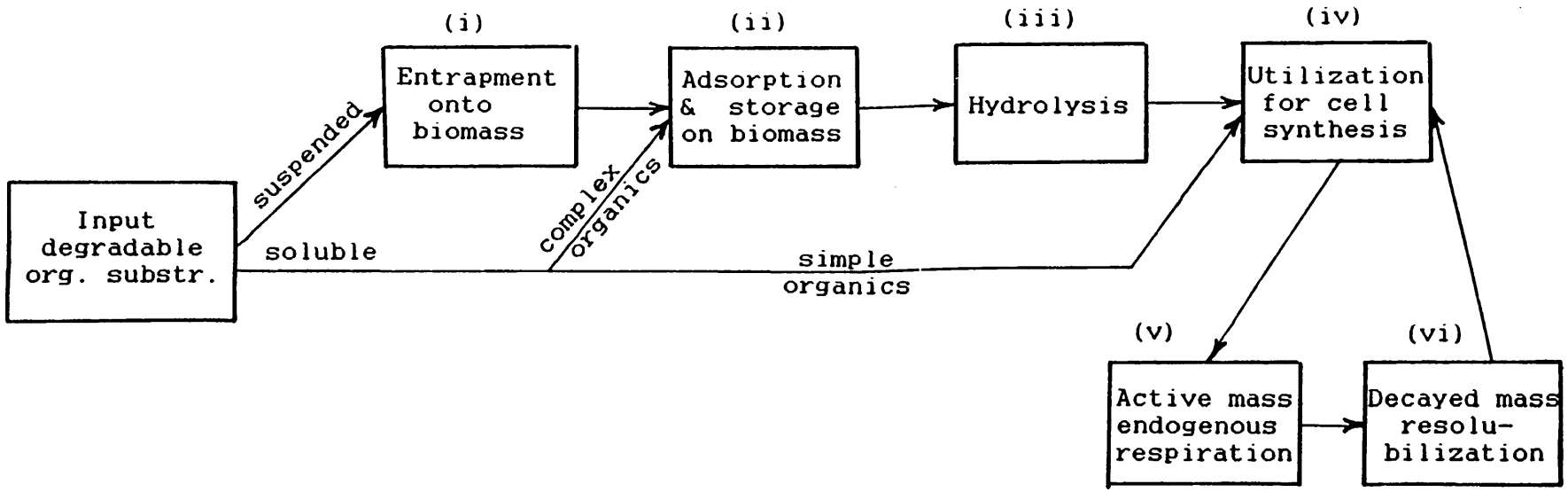


Fig. 3.10. Main processes for the removal of organic substrates

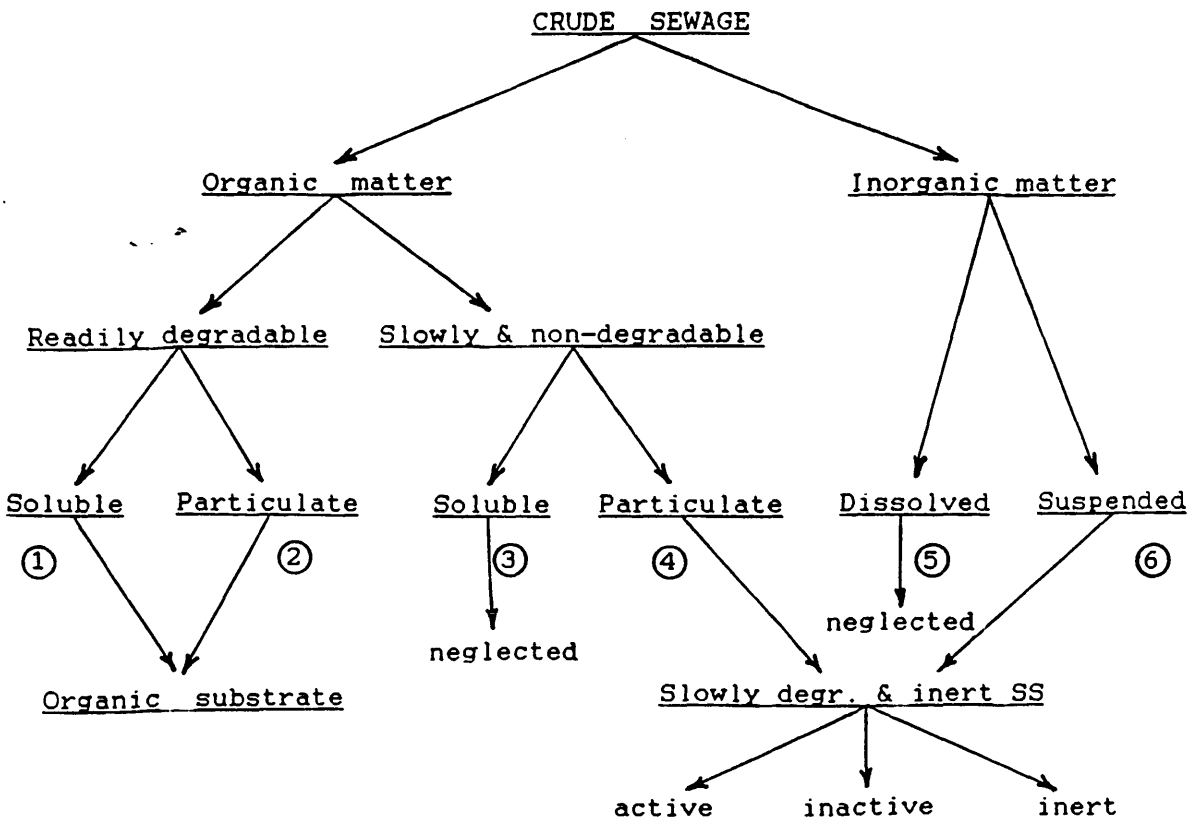


Fig. 3.11. Assumed structure of crude sewage for carbonaceous oxidation modelling

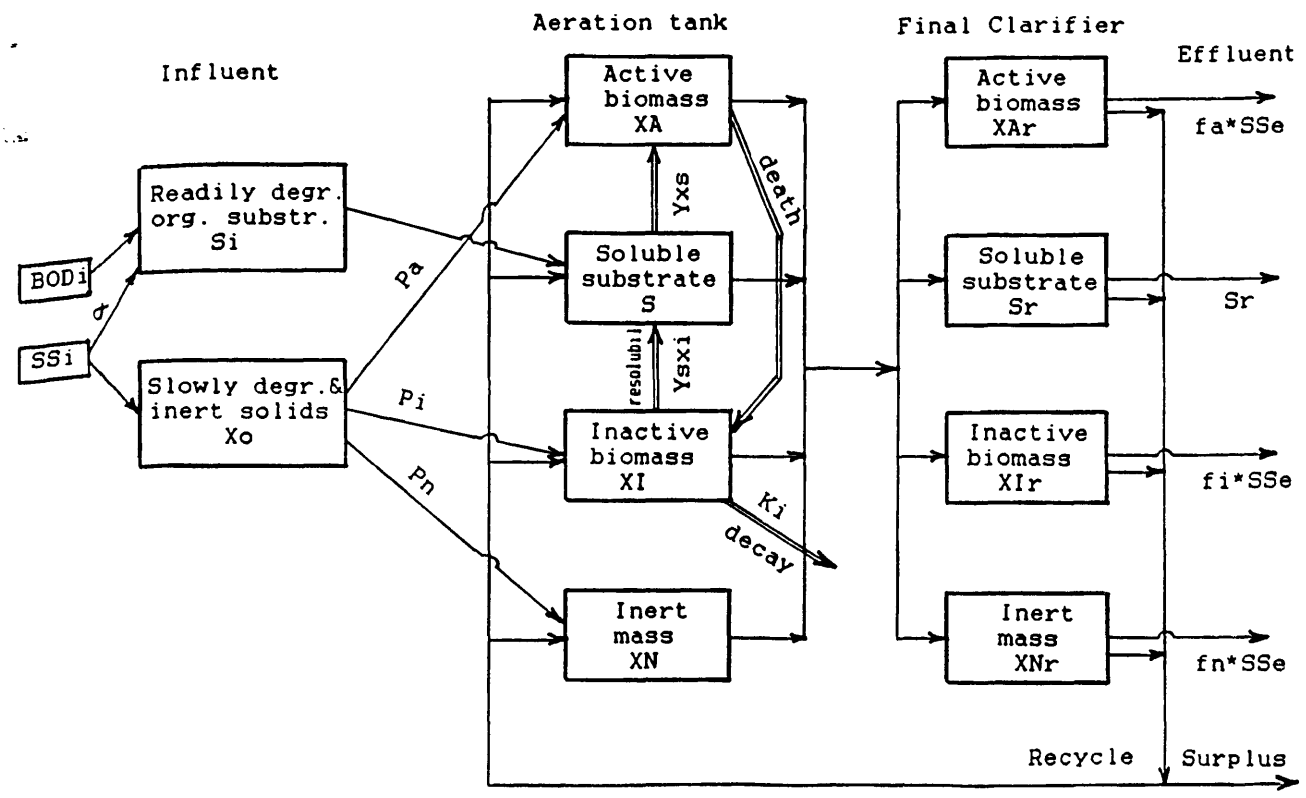


Fig. 3.12. Schematic representation of structured biomass model for carbonaceous oxidation

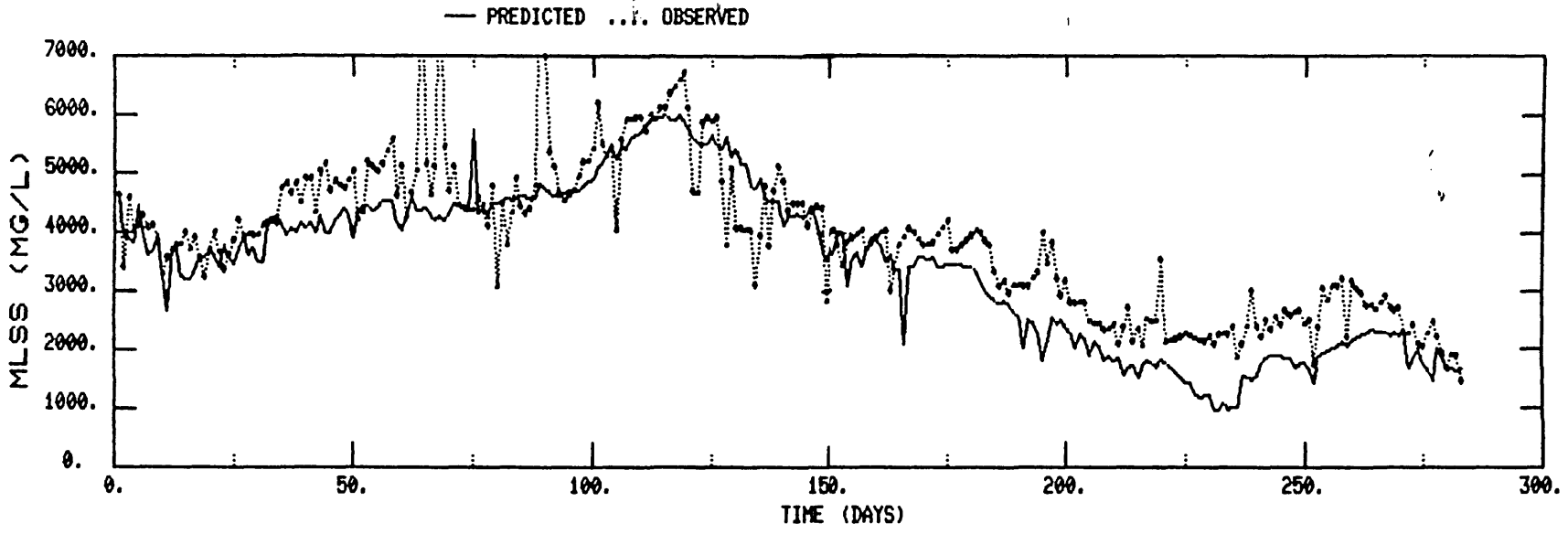


Fig. 3.13a. Predicted – observed $MLSS$ from structured biomass model

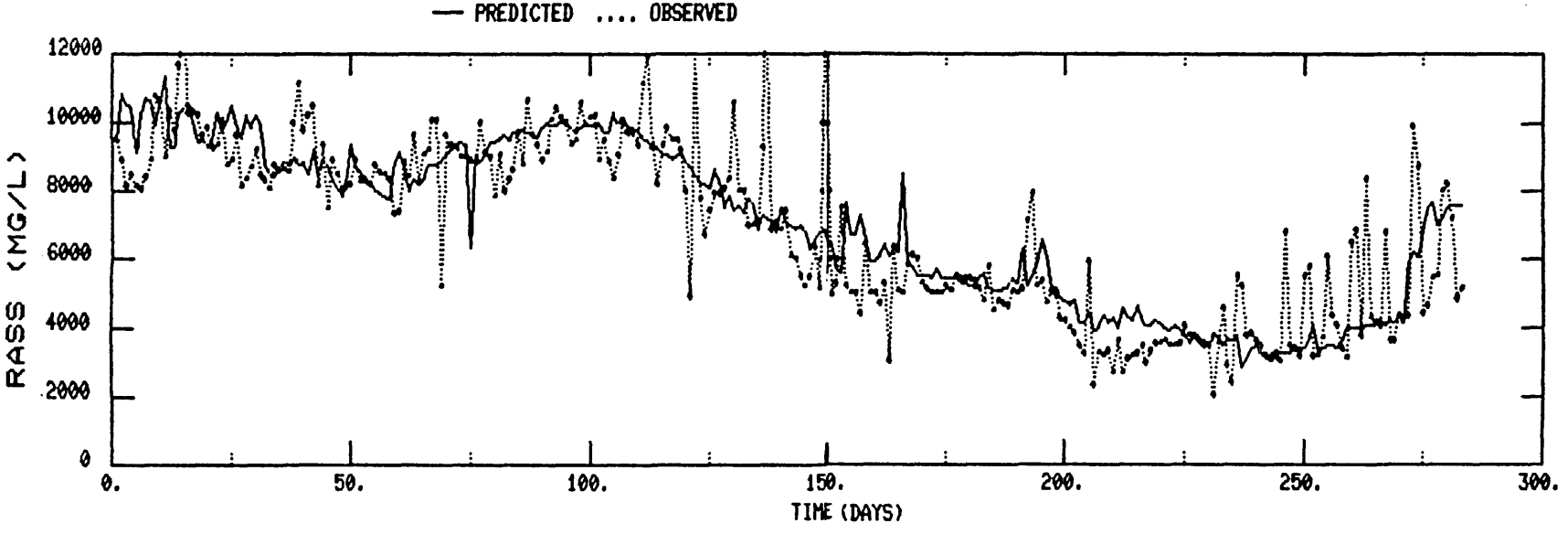


Fig. 3.13b. Predicted – observed $RASS$ from structured biomass model

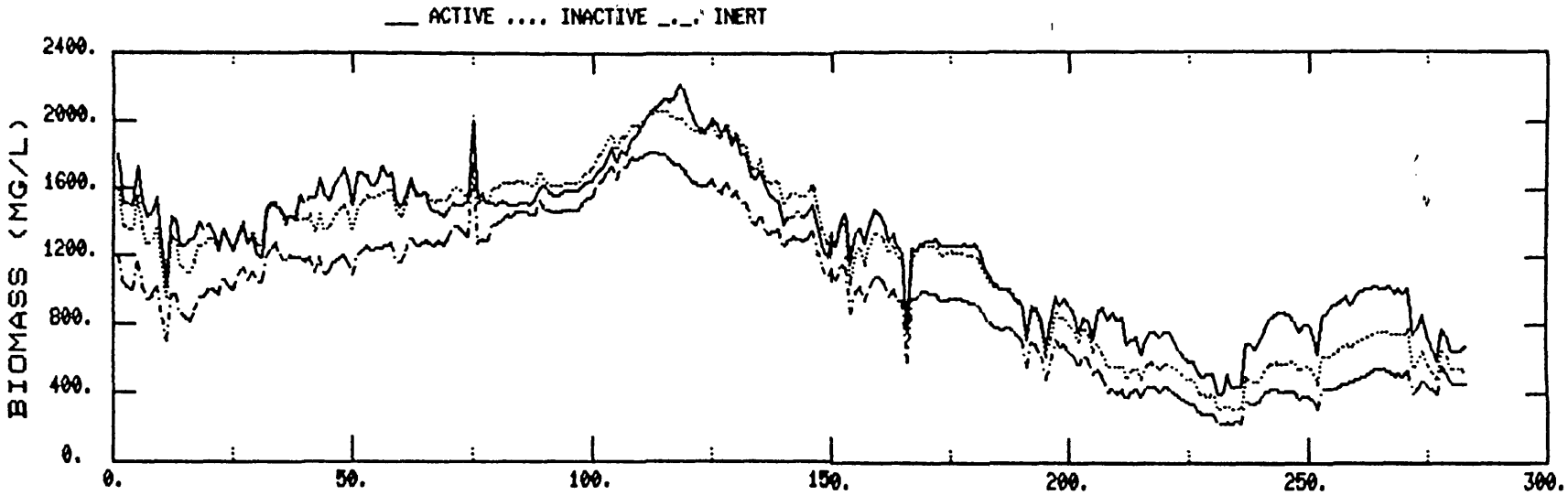


Fig. 3.13c. Predicted active, inactive and inert mass from structured biomass model

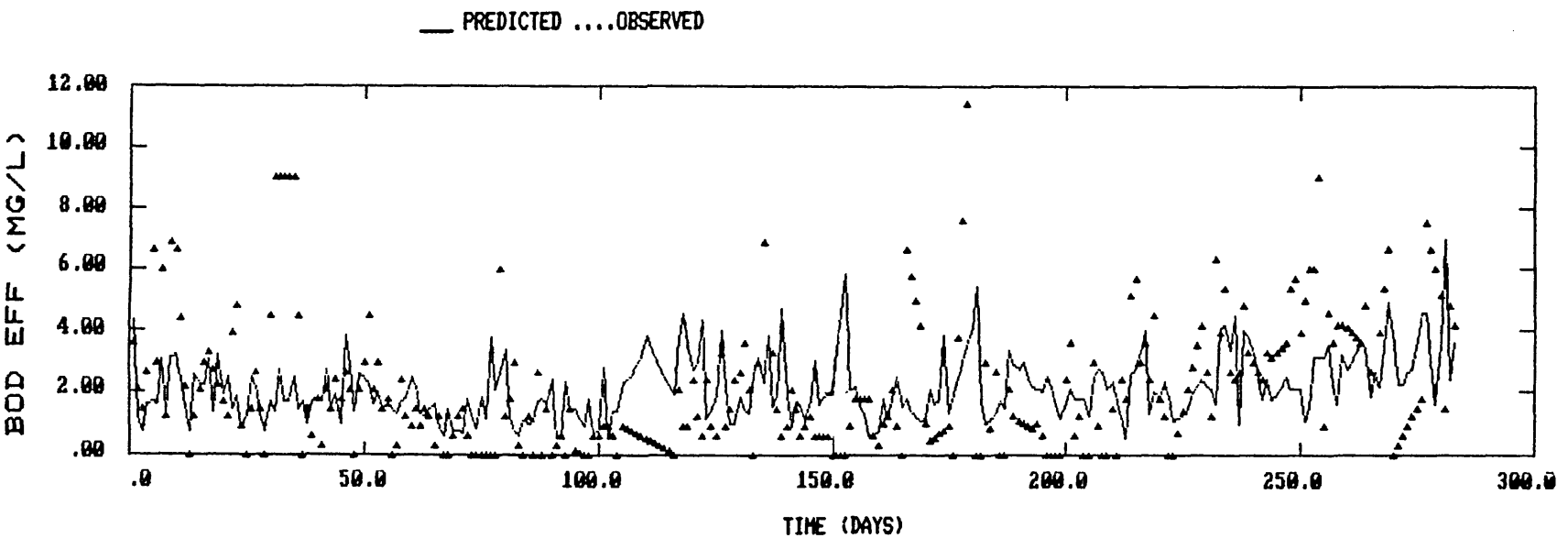


Fig. 3.13d. Predicted – observed effluent soluble organic substrate

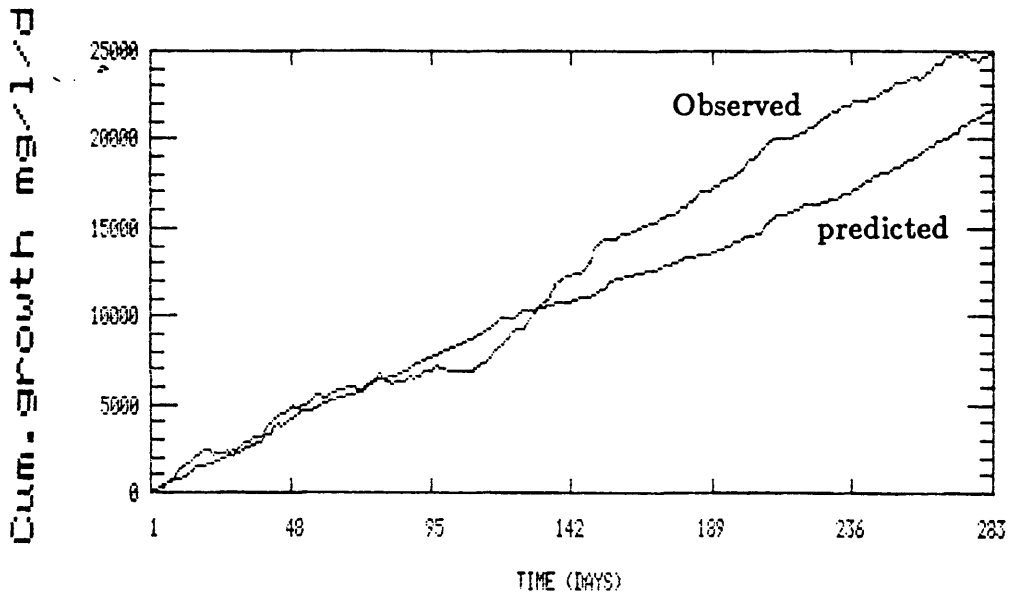


Fig. 3.13e. Predicted – observed cumulative net biomass growth

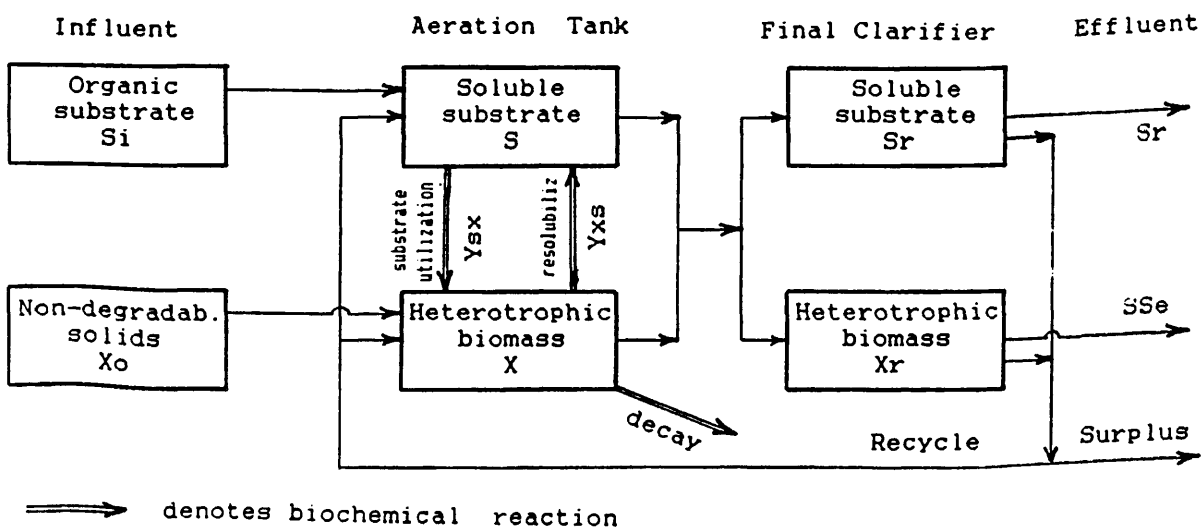


Fig. 3.14. Schematic representation of simple carbonaceous model

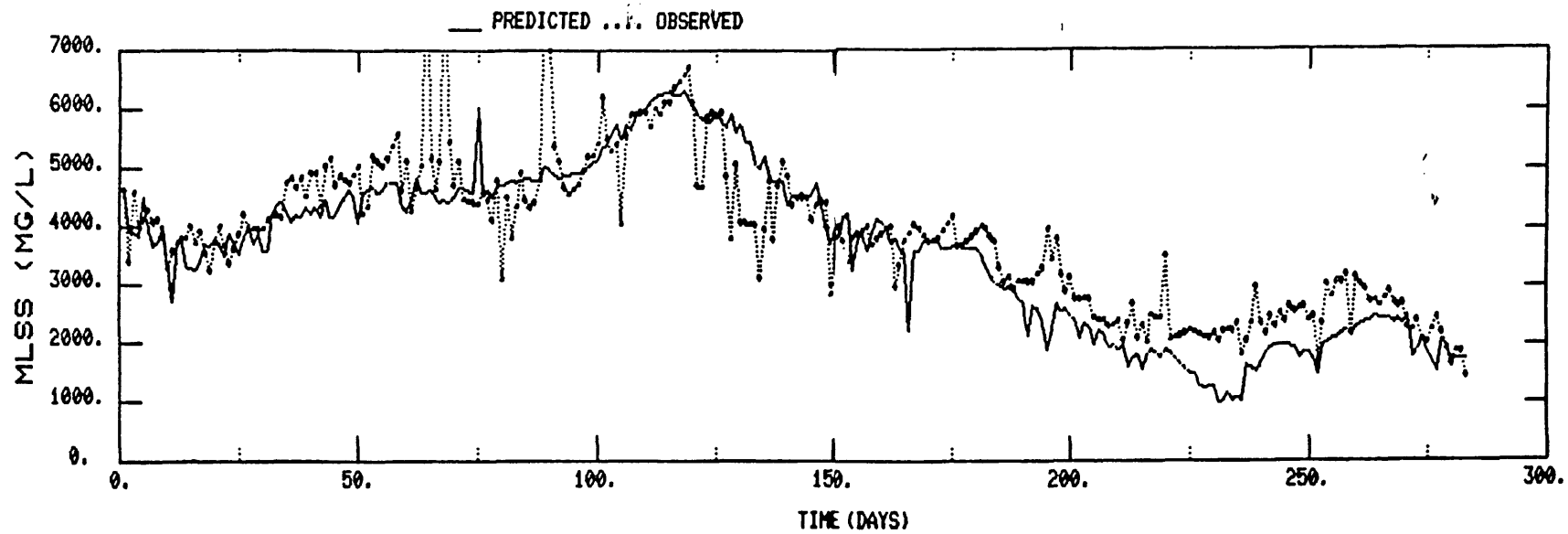


Fig. 3.15a. Predicted – observed heterotrophic biomass ($MLSS$) from carbonaceous model

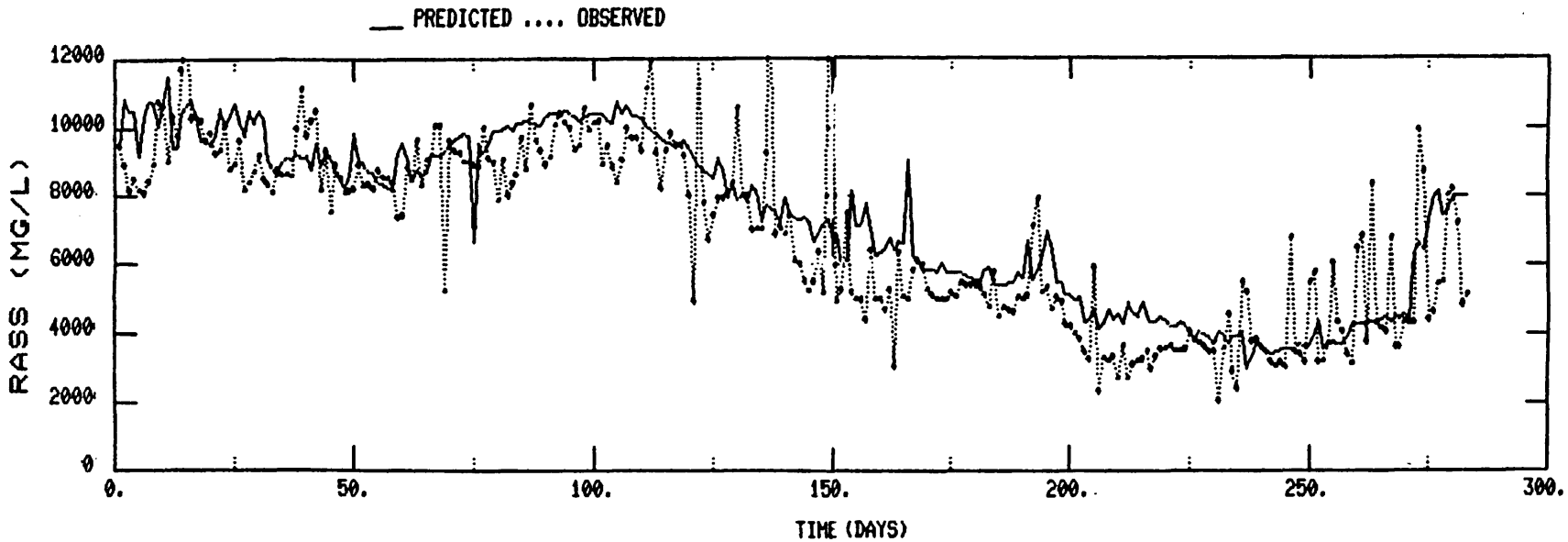


Fig. 3.15b. Predicted – observed recycle heterotrophic biomass ($RASS$) from carbonaceous model

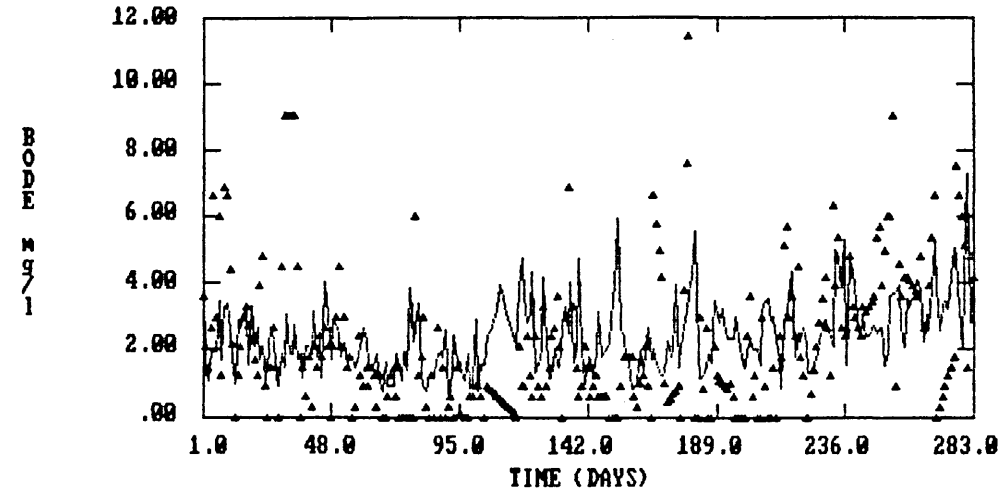


Fig. 15c. Predicted–observed effluent BOD_5

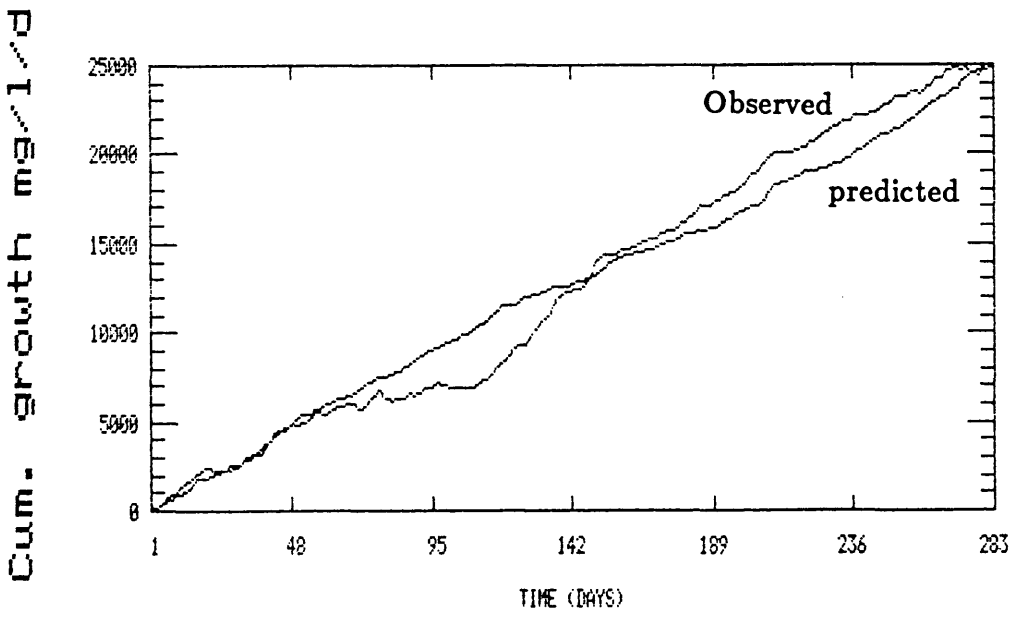


Fig. 3.15d. Predicted – observed cumulative net biomass growth

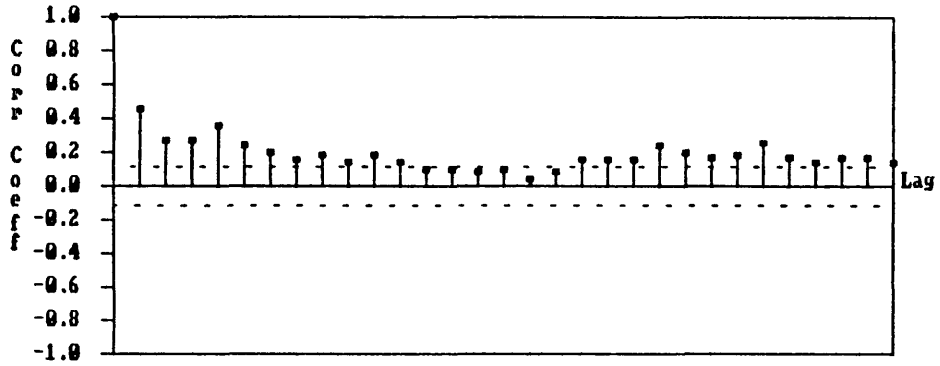


Fig. 3.16a. Autocorrelogram of error in *MLSS*

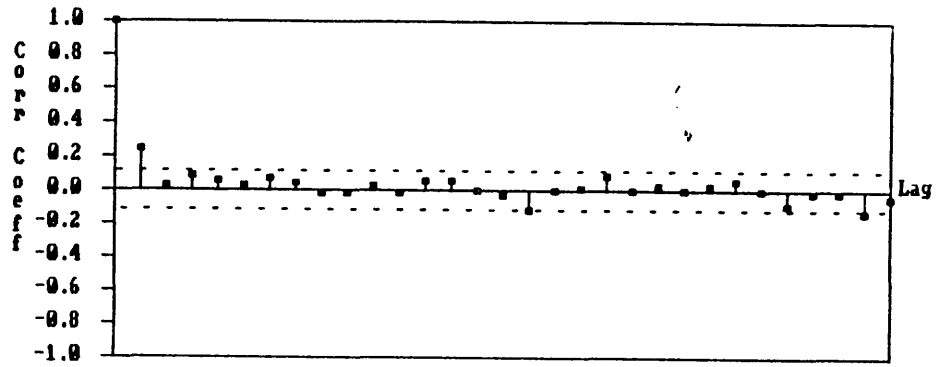


Fig. 3.16b. Autocorrelogram of error in *RASS*

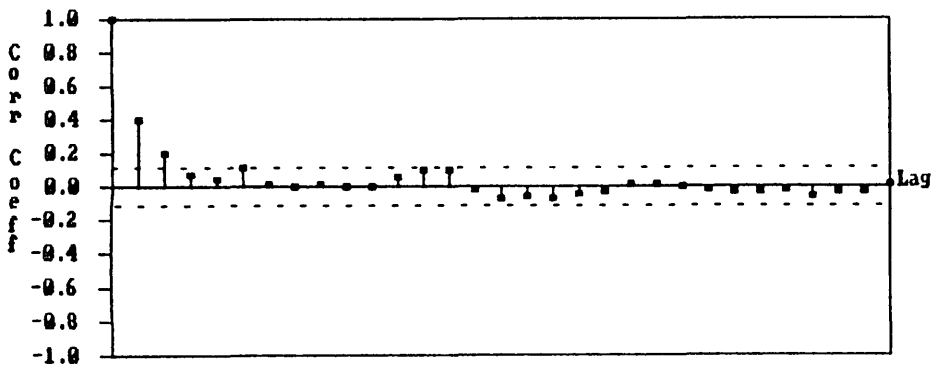


Fig. 3.16c. Autocorrelogram of error in *BODe*

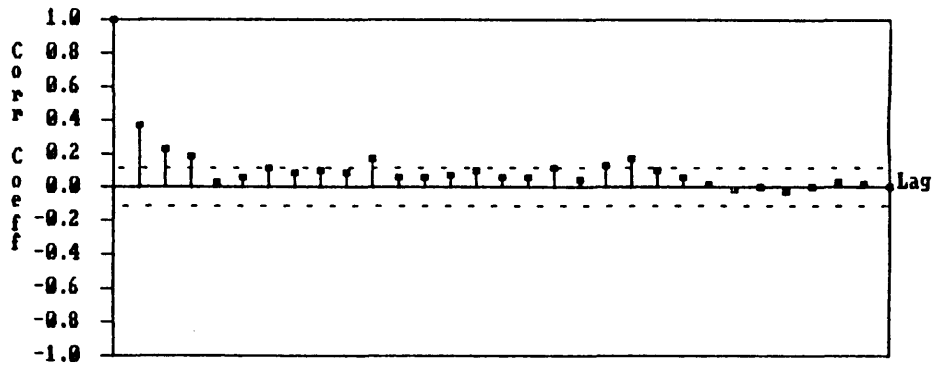


Fig. 3.16d. Autocorrelogram of error in daily net growth

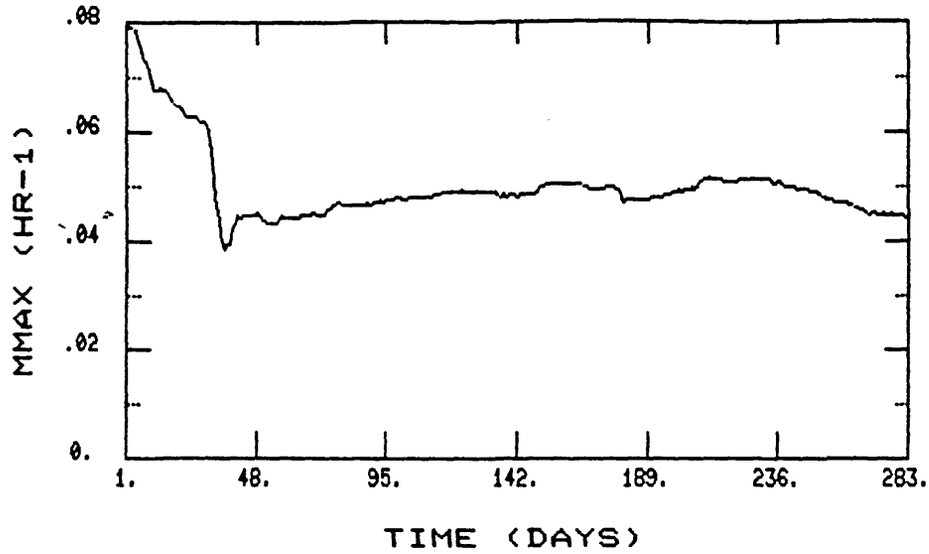


Fig. 3.17a. Estimated trajectory of μ_{max} (as non-dynamic state)

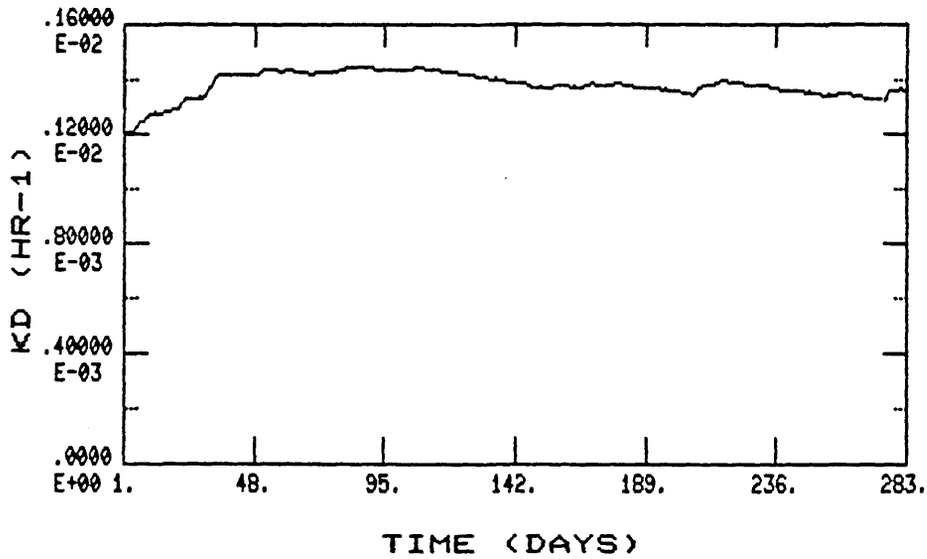


Fig. 3.17b. Estimated trajectory of Kd (as non-dynamic state)

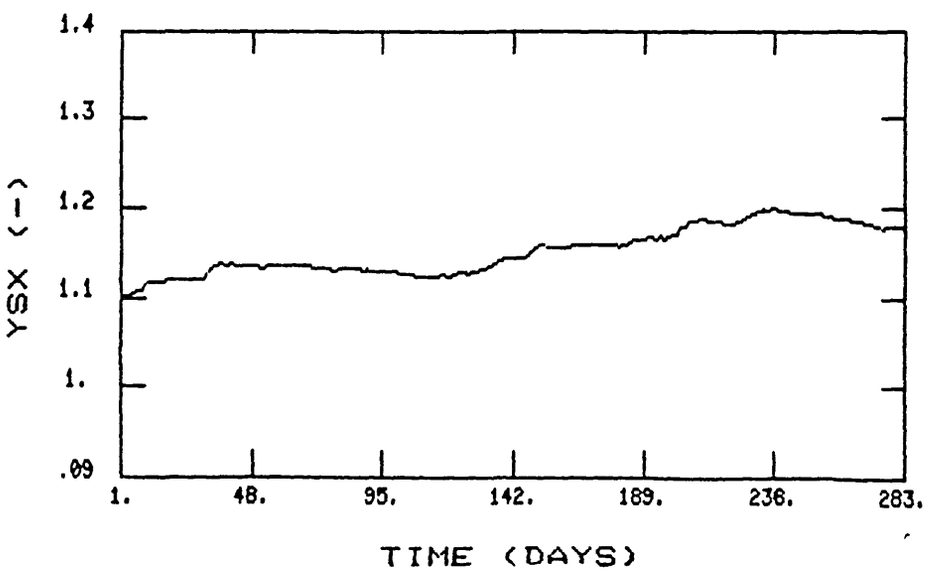


Fig. 3.17c. Estimated trajectory of Ysx (as non-dynamic state)

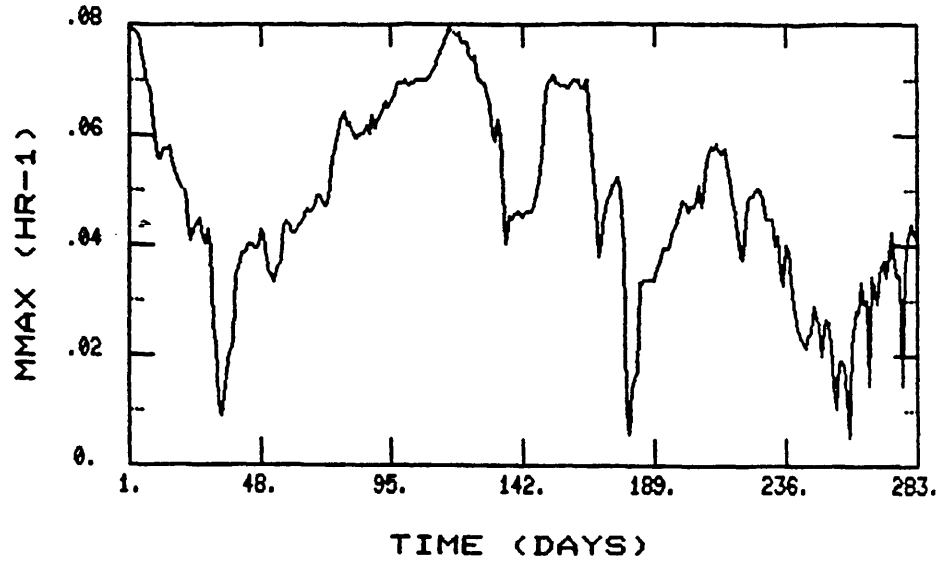


Fig. 3.18a. Estimated trajectory of μ_{max} (with additive noise)

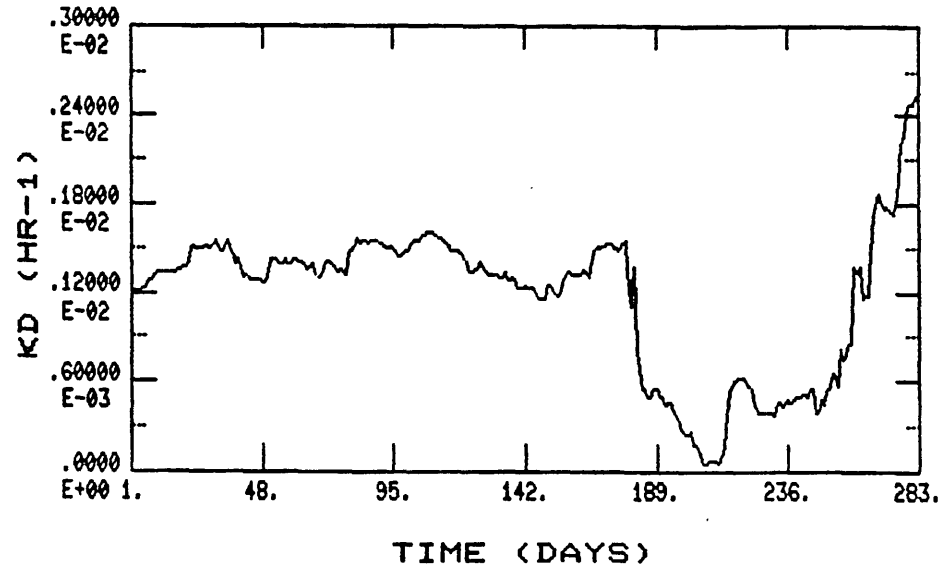


Fig. 3.18b. Estimated trajectory of Kd (with additive noise)

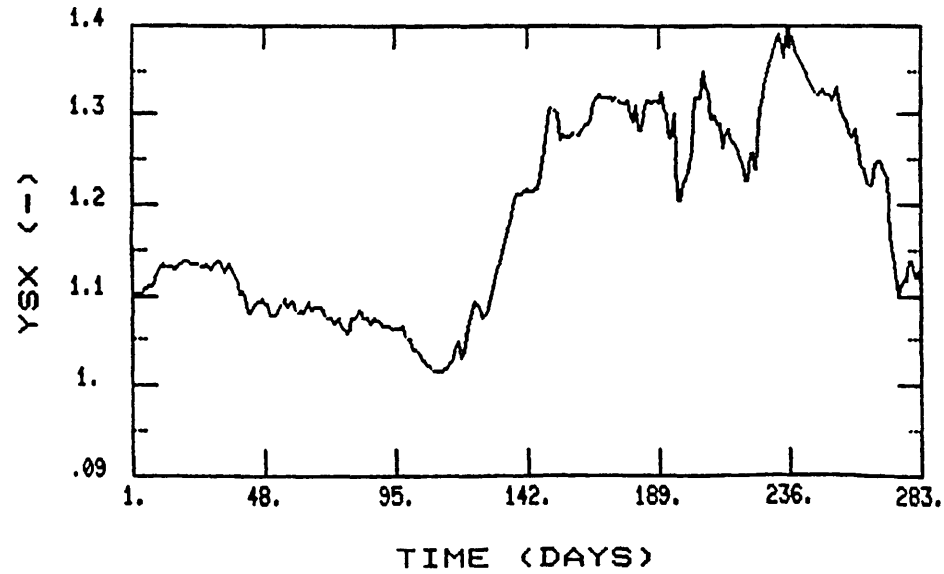


Fig. 3.18c. Estimated trajectory of Ysx (with additive noise)

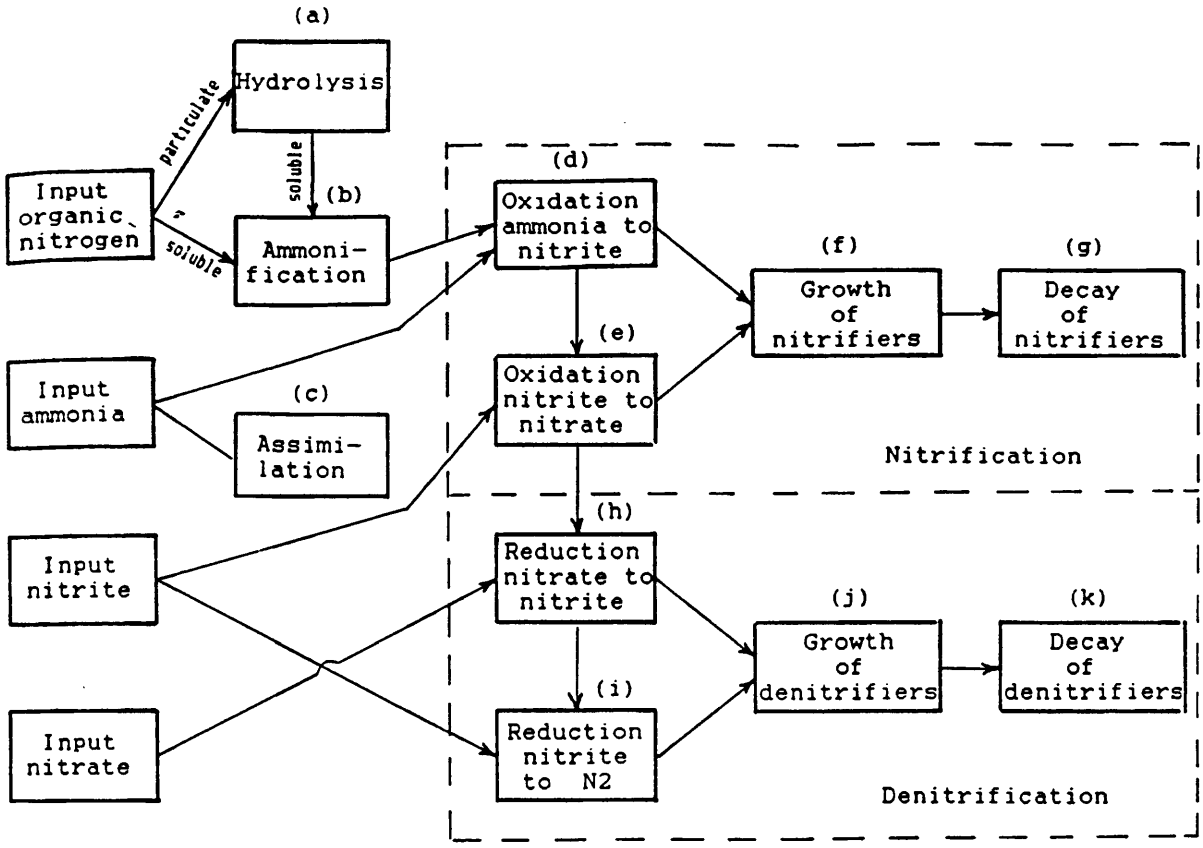


Fig. 3.19. Main processes in the biochemical transformation of nitrogenous compounds

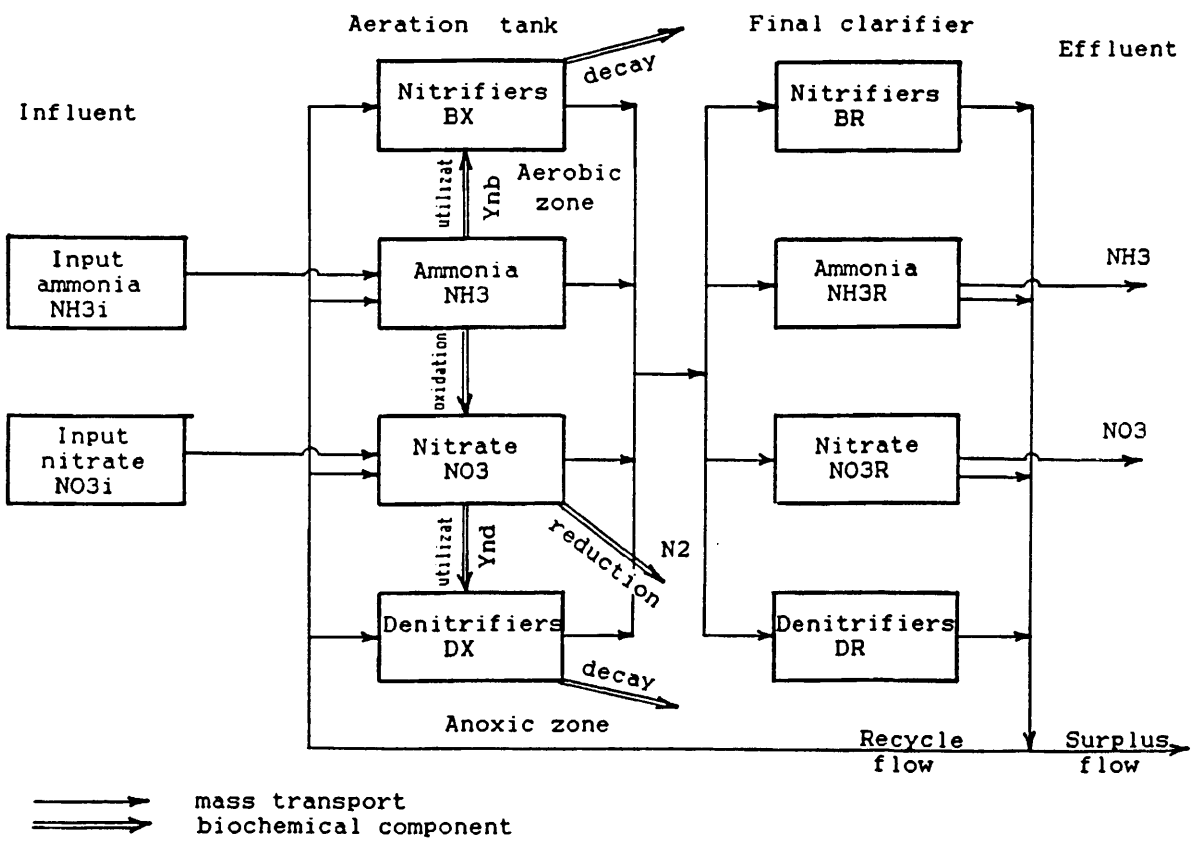


Fig. 3.20. Schematic representation of nitrification-denitrification model

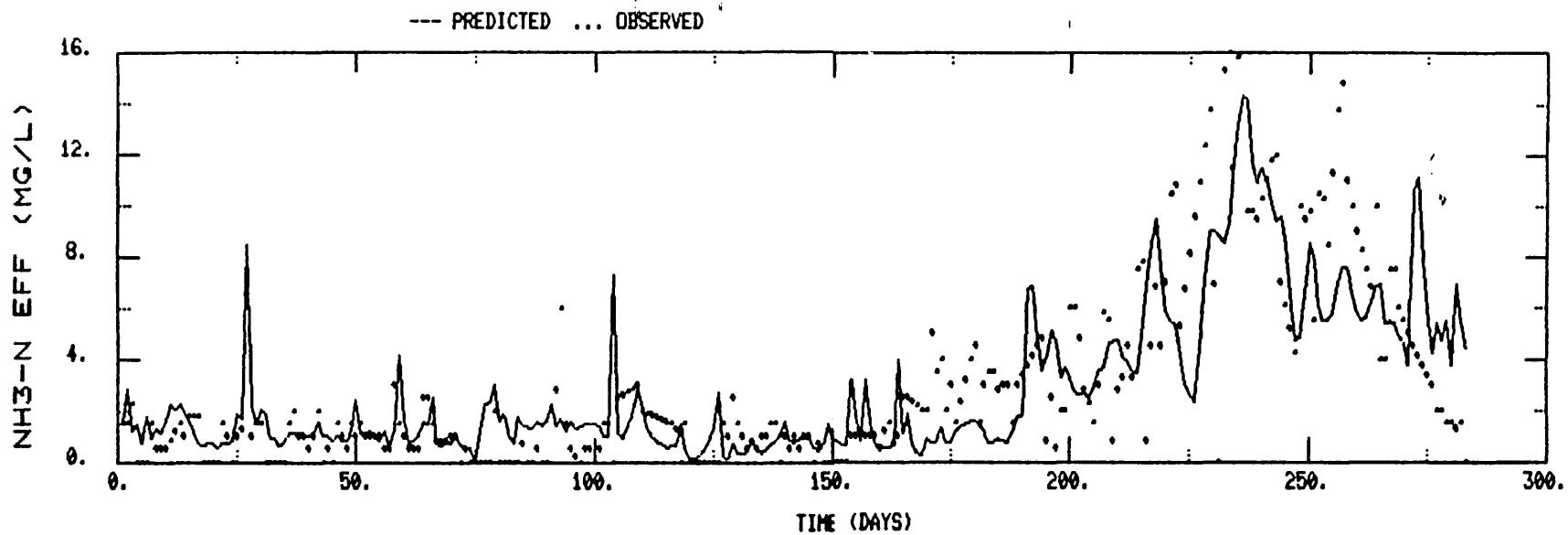


Fig. 3.21a. Predicted – observed effluent ammonia concentration

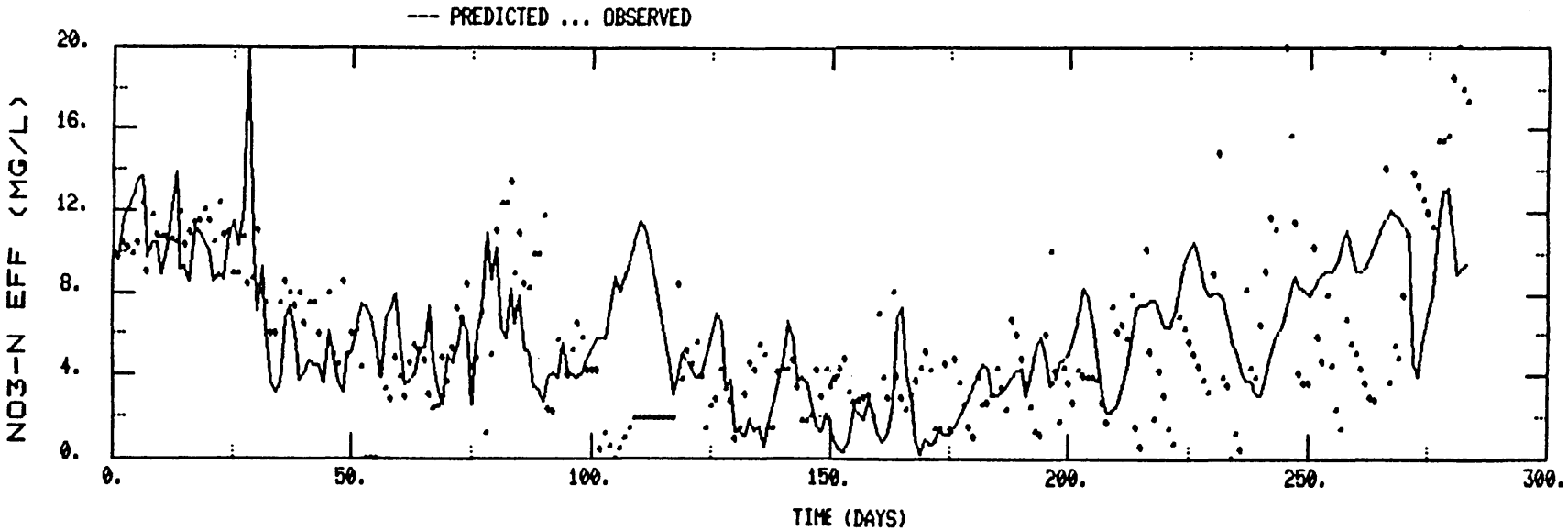


Fig. 3.21b. Predicted – observed effluent nitrate concentration

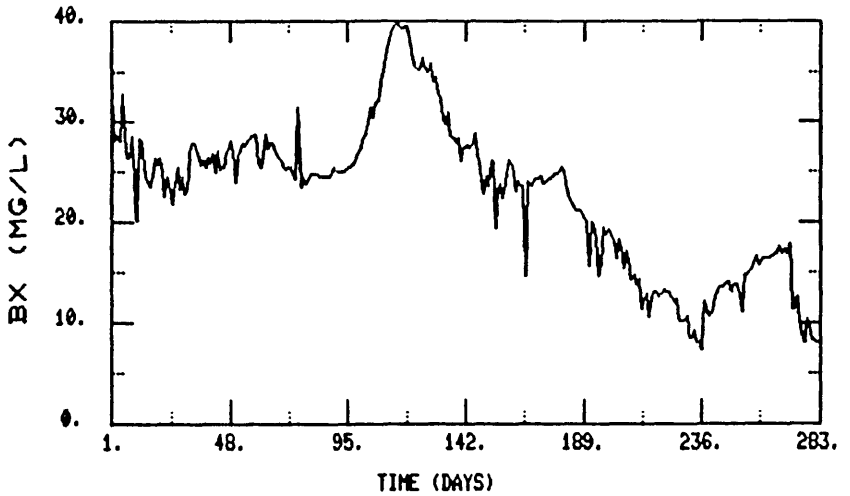


Fig. 3.21c. Predicted nitrifier concentration in M.L.

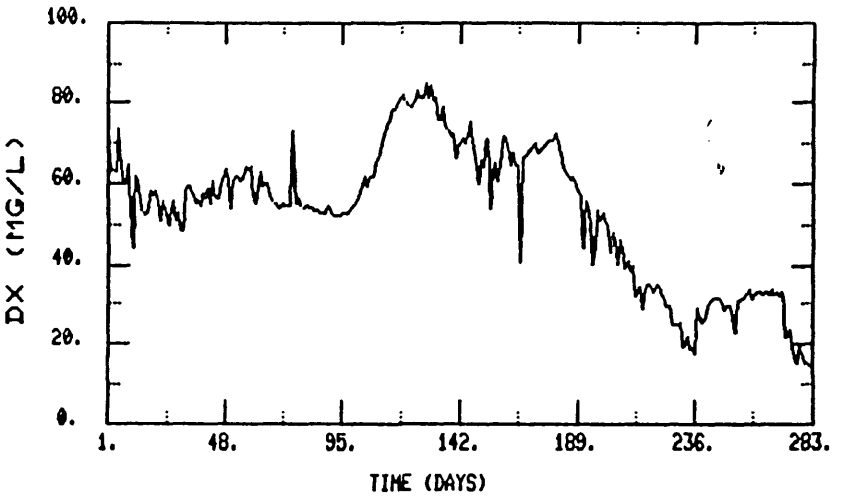


Fig. 3.21d. Predicted denitrifier concentration in M.L.

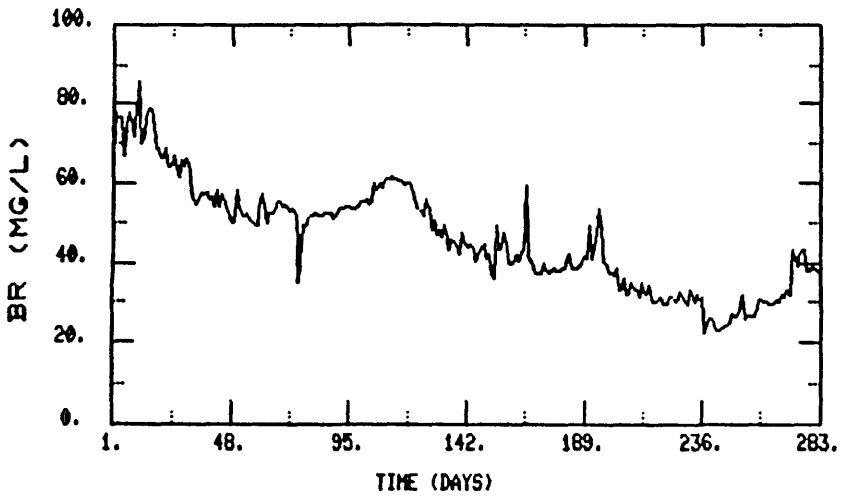


Fig. 3.21e. Predicted nitrifier concentration in recycle

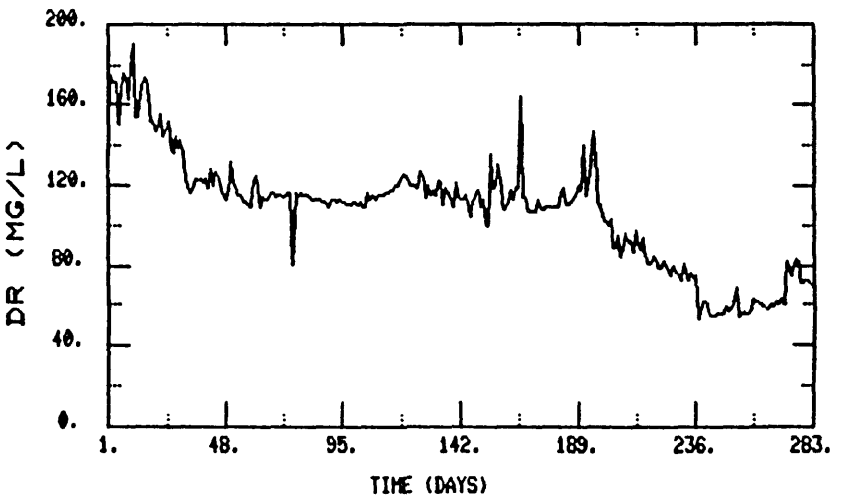


Fig. 3.21f. Predicted denitrifier concentration in recycle

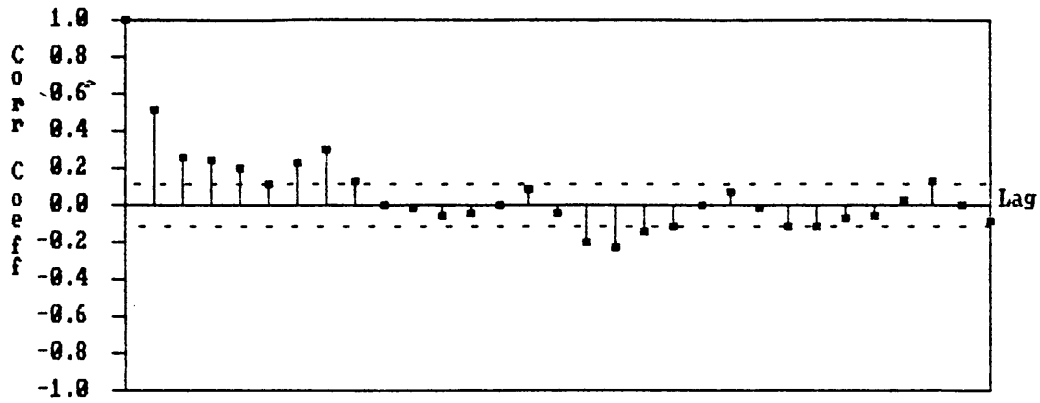


Fig. 3.22a. Autocorrelogram of error in $NH3e$

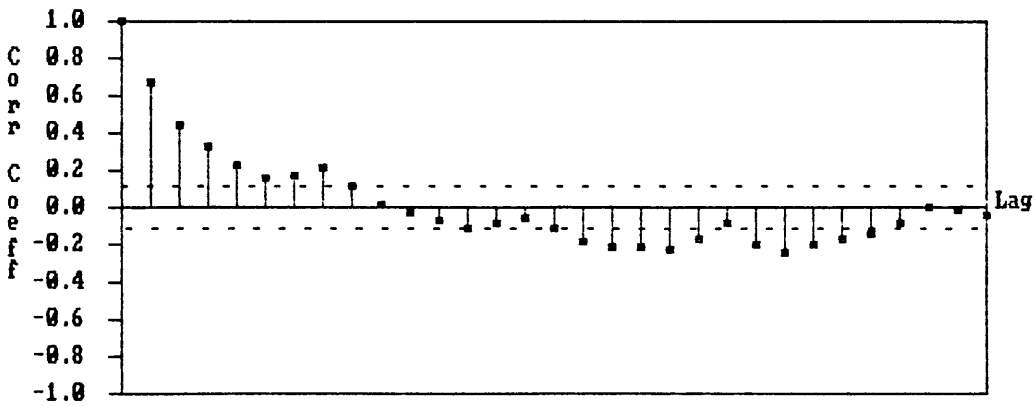


Fig. 3.22b. Autocorrelogram of error in $NO3e$

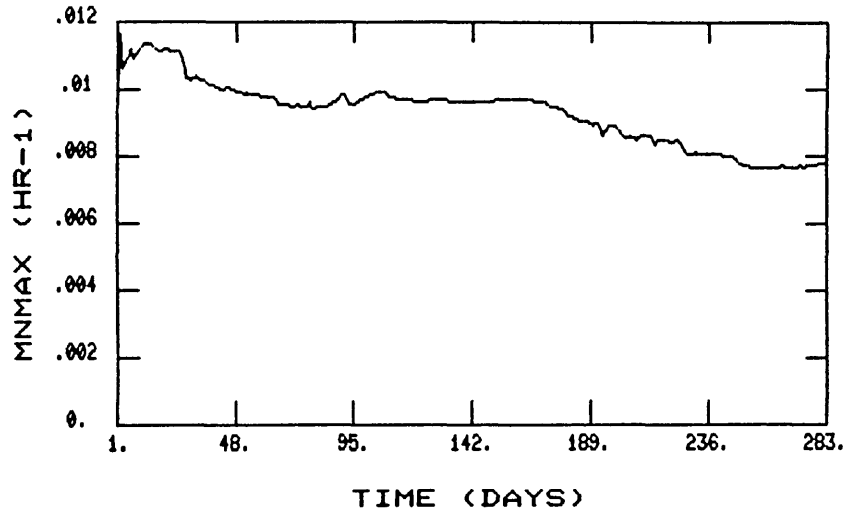


Fig. 3.23a. Estimated trajectory of μ_{Nmax}

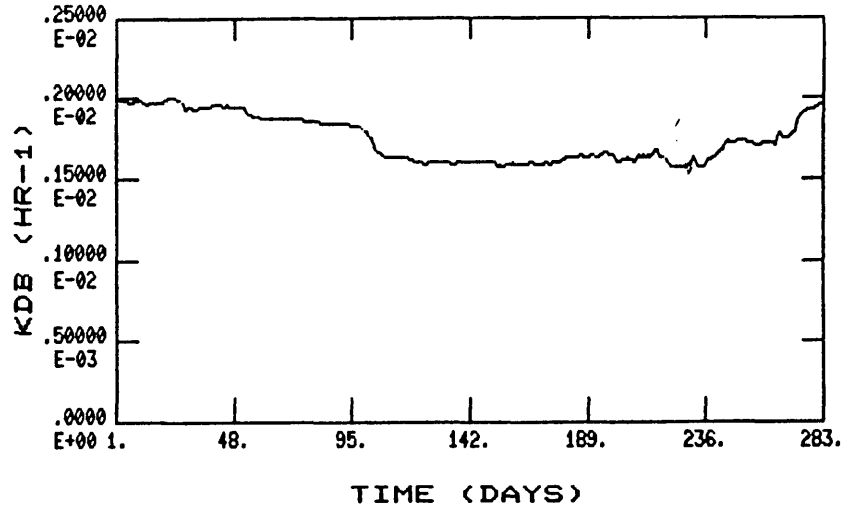


Fig. 3.23b. Estimated trajectory of Kdb

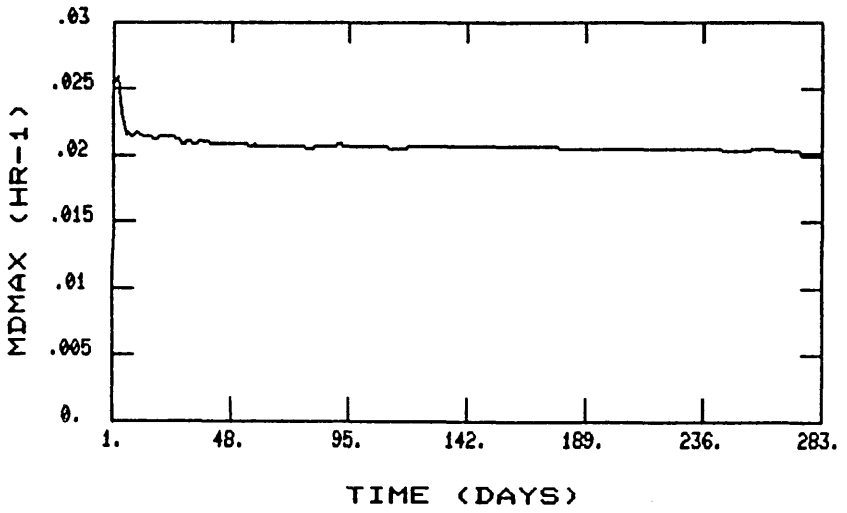


Fig. 3.23c. Estimated trajectory of μ_{Dmax}

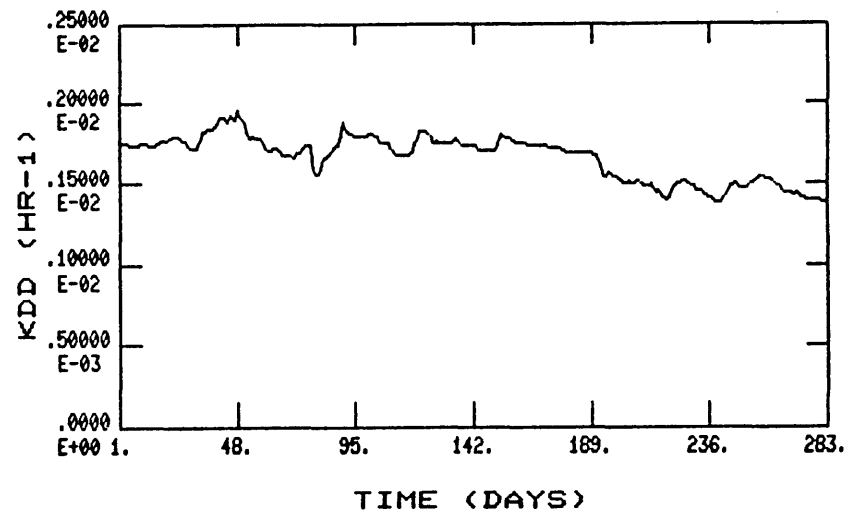


Fig. 3.23d. Estimated trajectory of Kdb

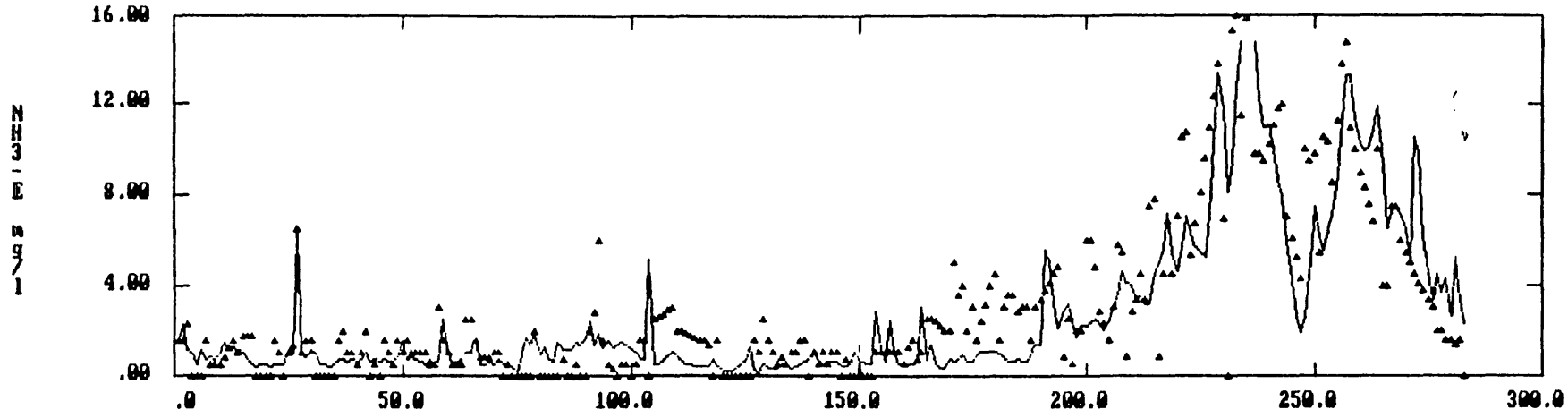


Fig. 3.24a. Predicted effluent ammonia from adaptive simulation

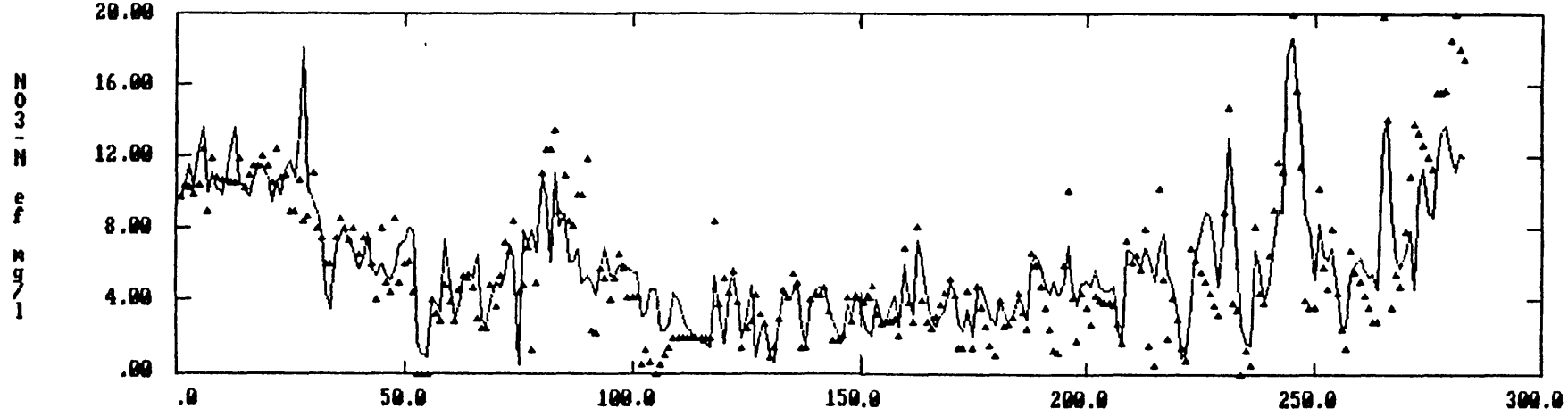


Fig. 3.24b. Predicted effluent nitrate

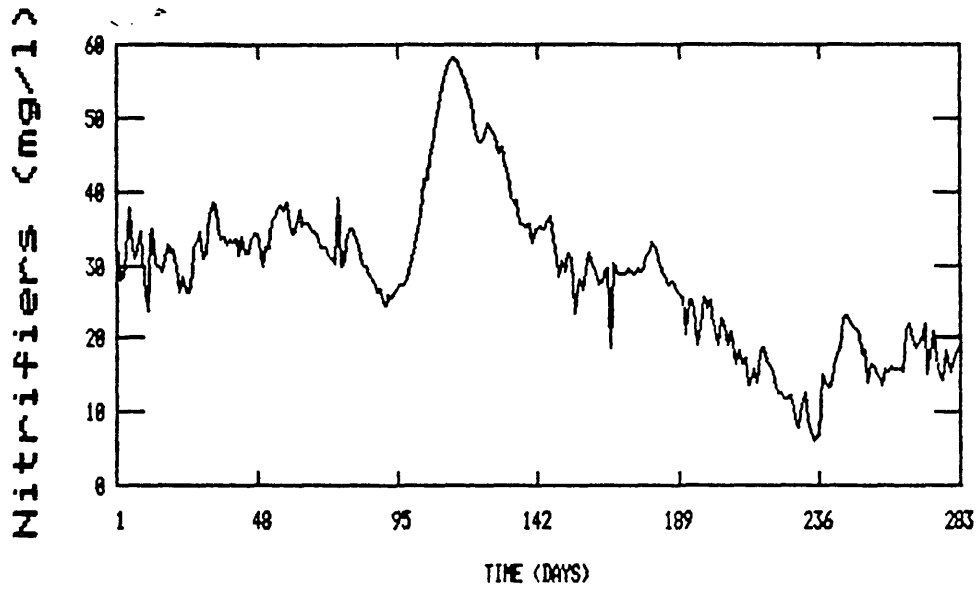


Fig. 3.24c. Predicted nitrifier concentration in A.T.

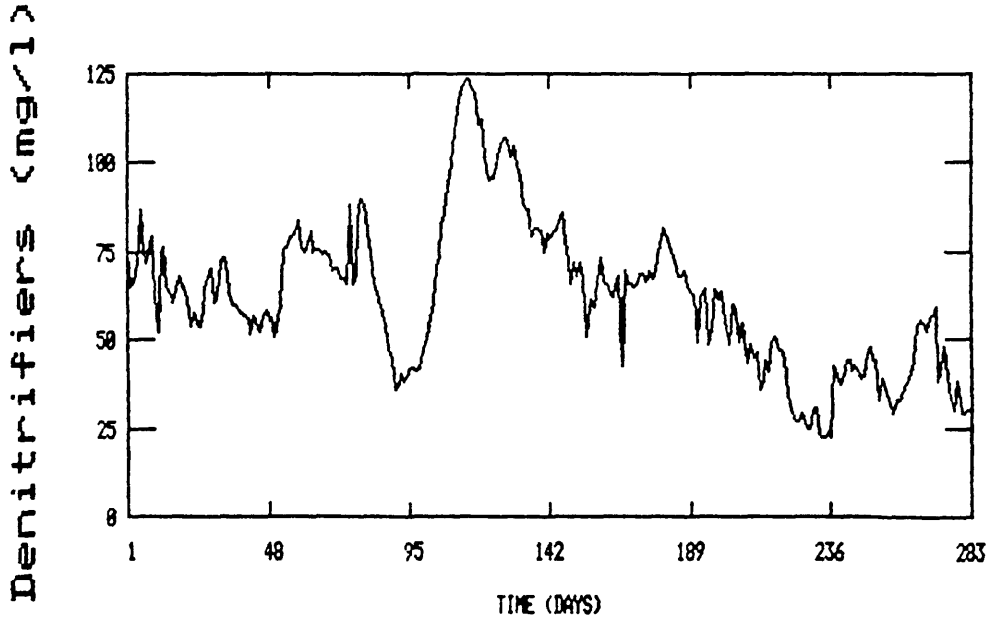
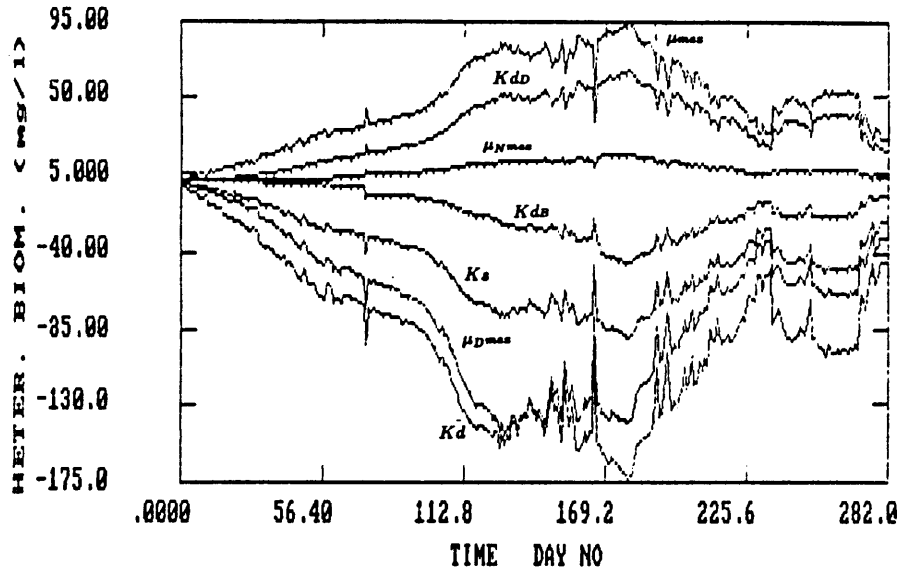
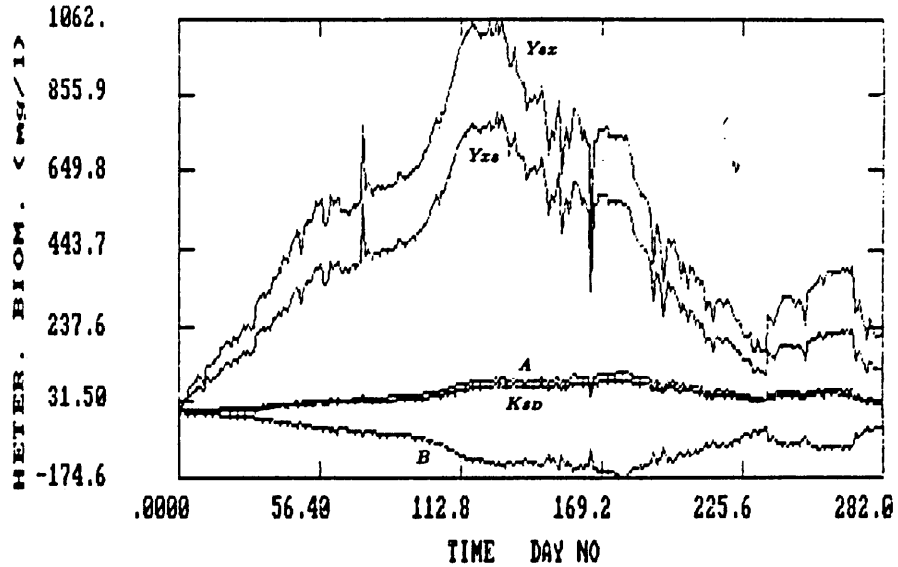


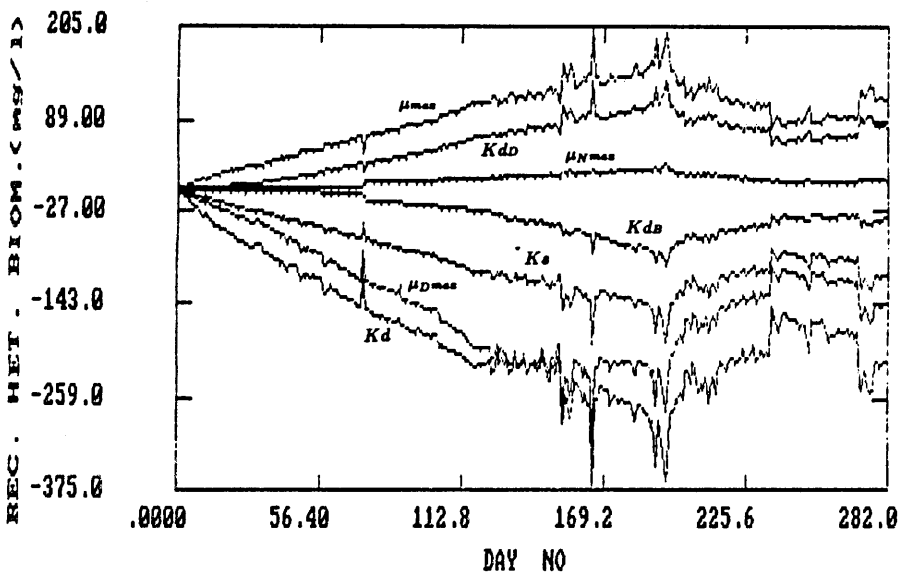
Fig. 3.24d. Predicted denitrifier concentration in A.T.



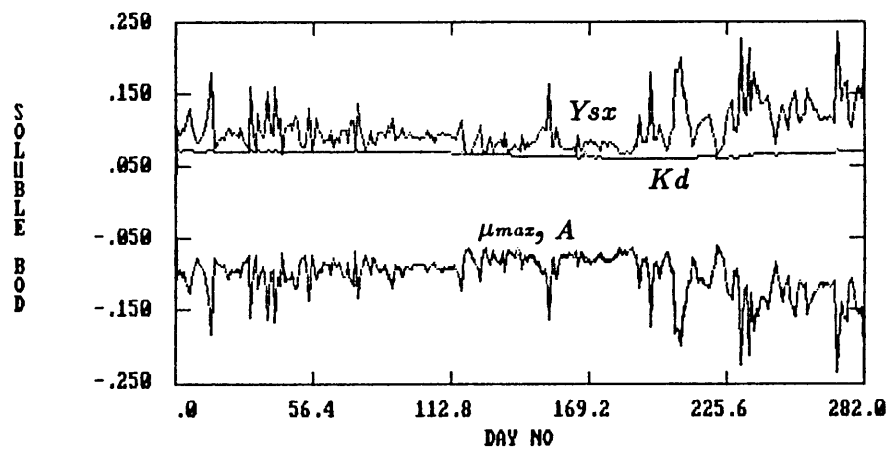
a. Sensitivity of heterotrophic biomass



b. Sensitivity of heterotrophic biomass

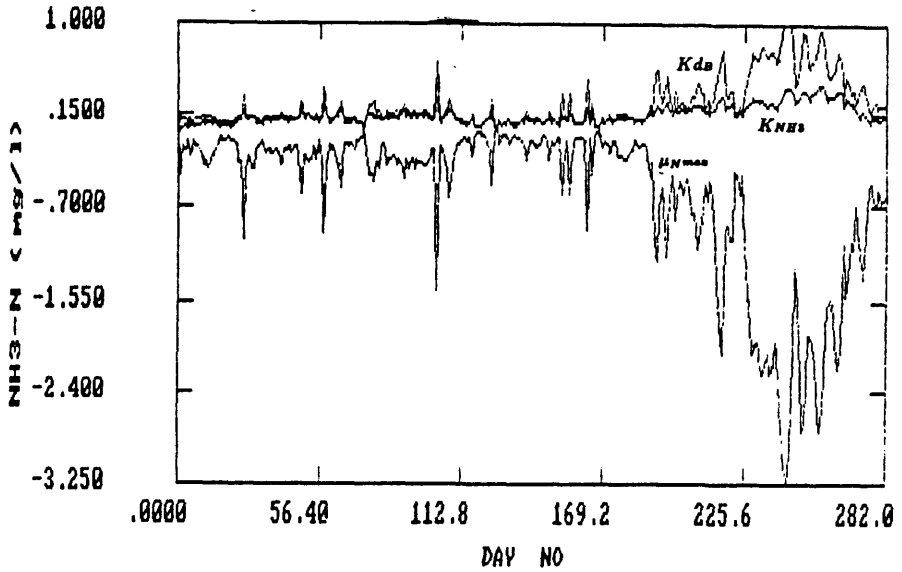


c. Sensitivity of recycle heterotrophic biomass

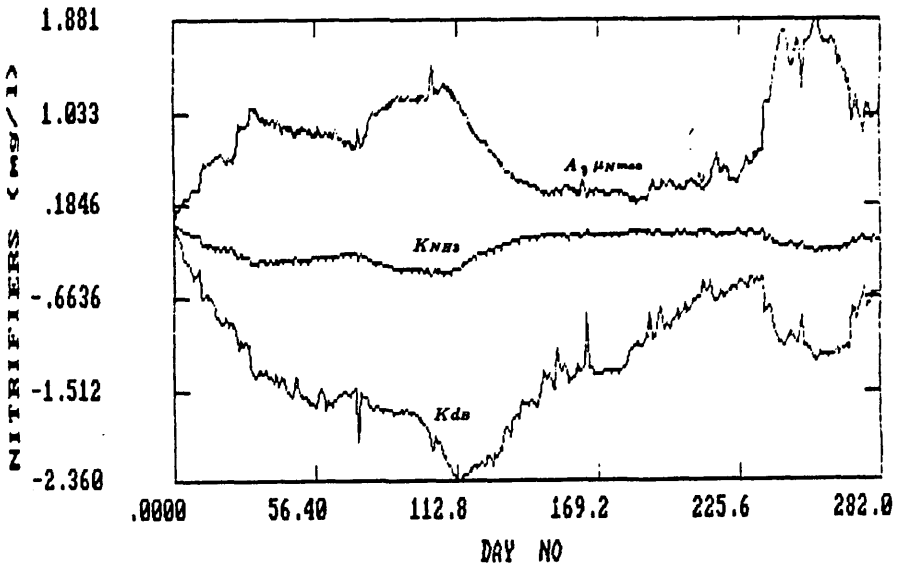


d. Sensitivity of soluble *BOD* in A.T.

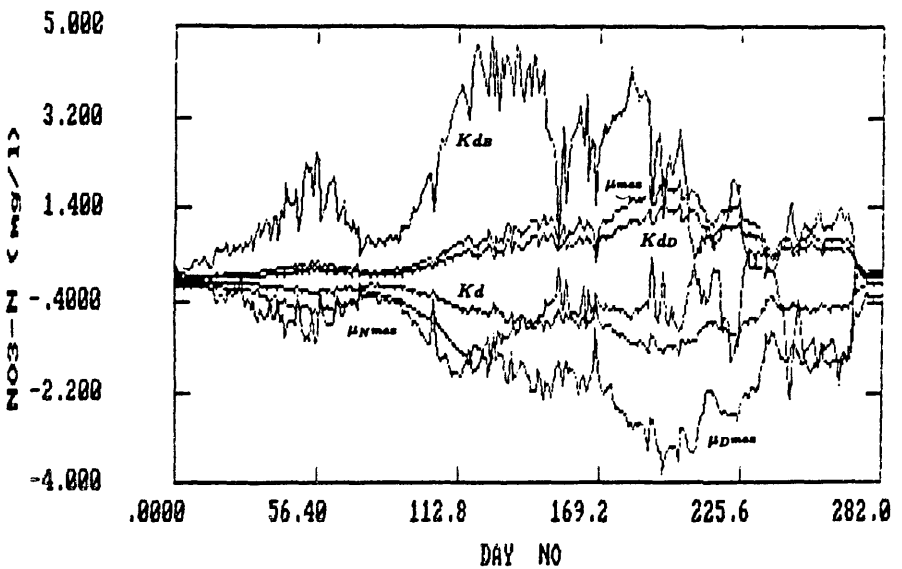
Fig. 3.25. Parameter sensitivity results



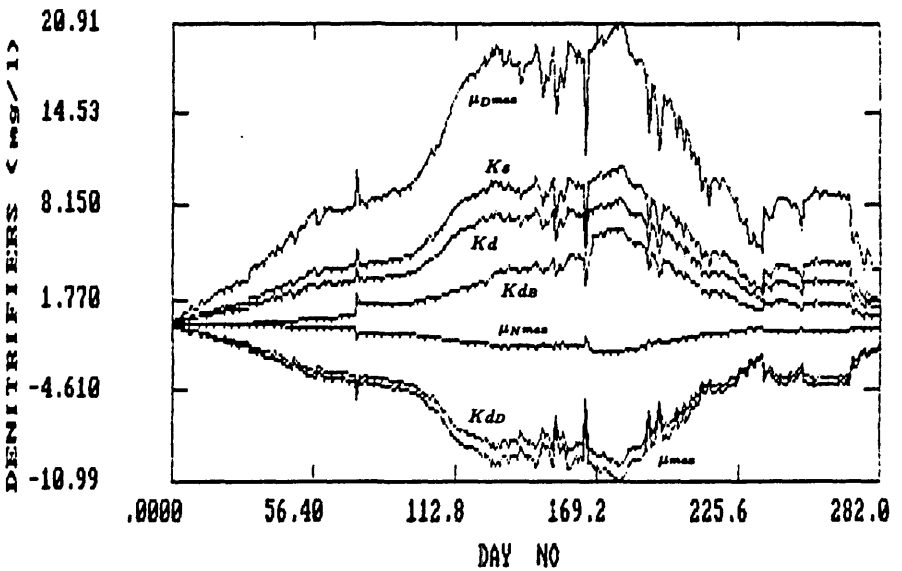
e. Sensitivity of ammonia (NH_3) *in A.T.*



f. Sensitivity of nitrifiers



g. Sensitivity of nitrate (NO_3) in A.T.



h. Sensitivity of denitrifiers

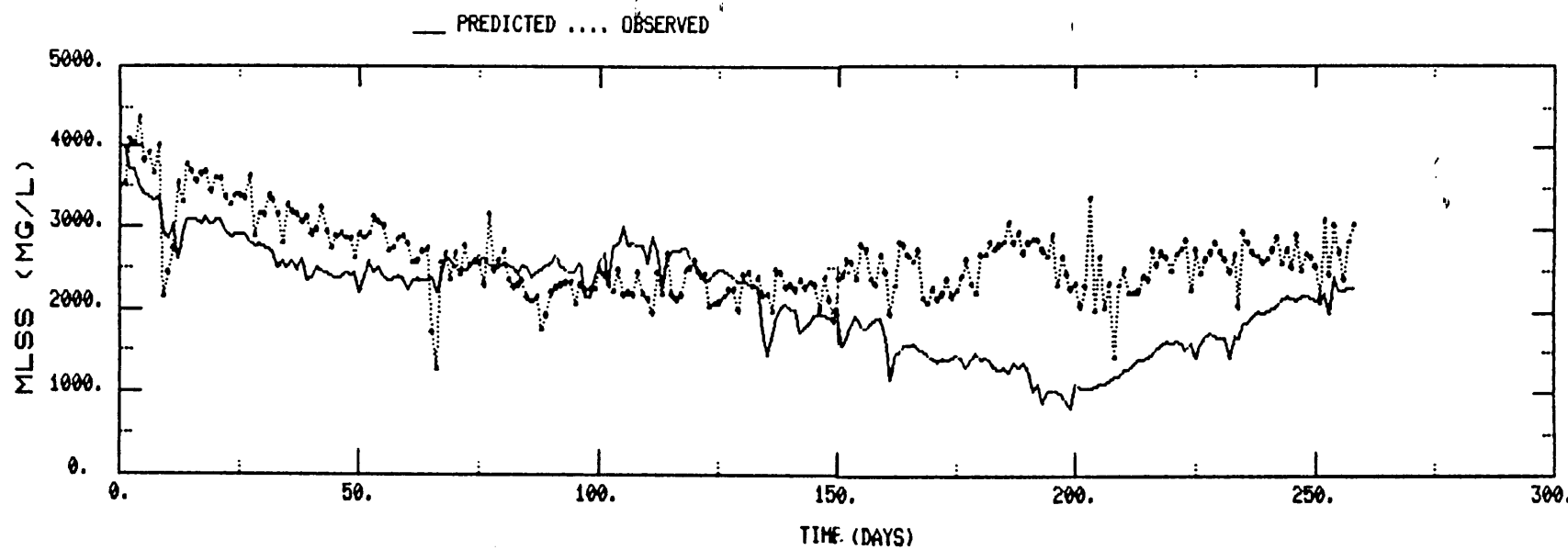


Fig. 3.26a. Predicted – observed $MLSS$ concentration during validation

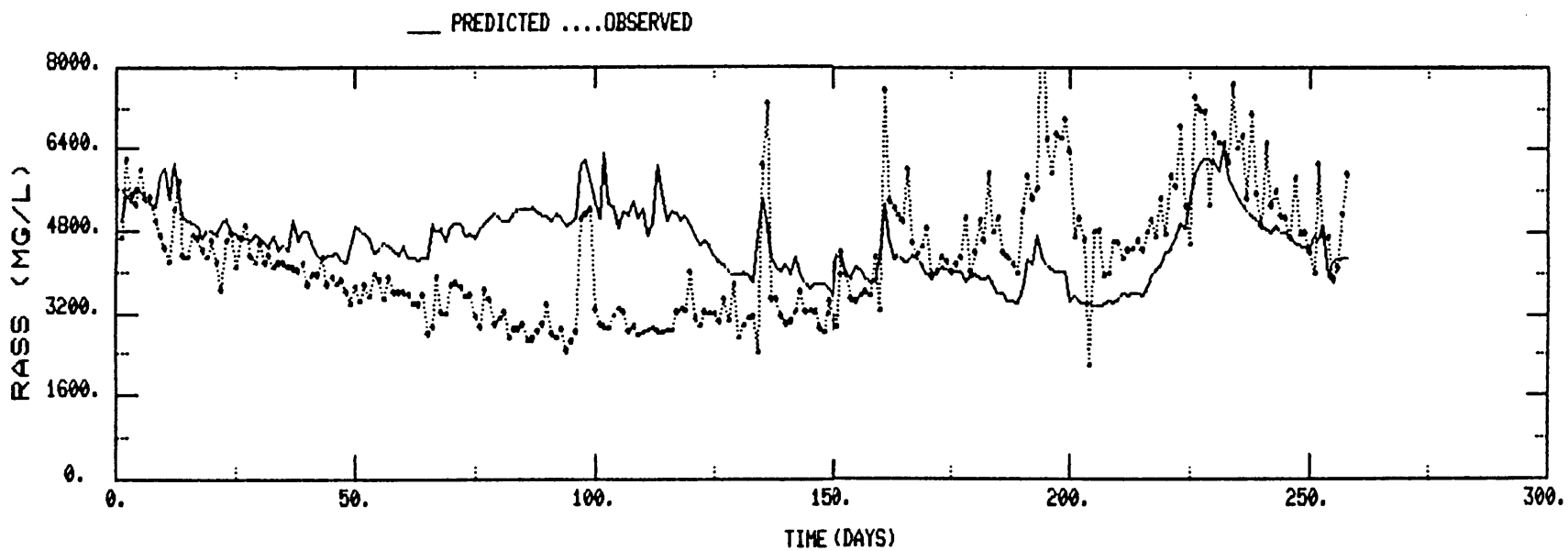


Fig. 3.26b. Predicted – observed $RASS$ concentration during validation

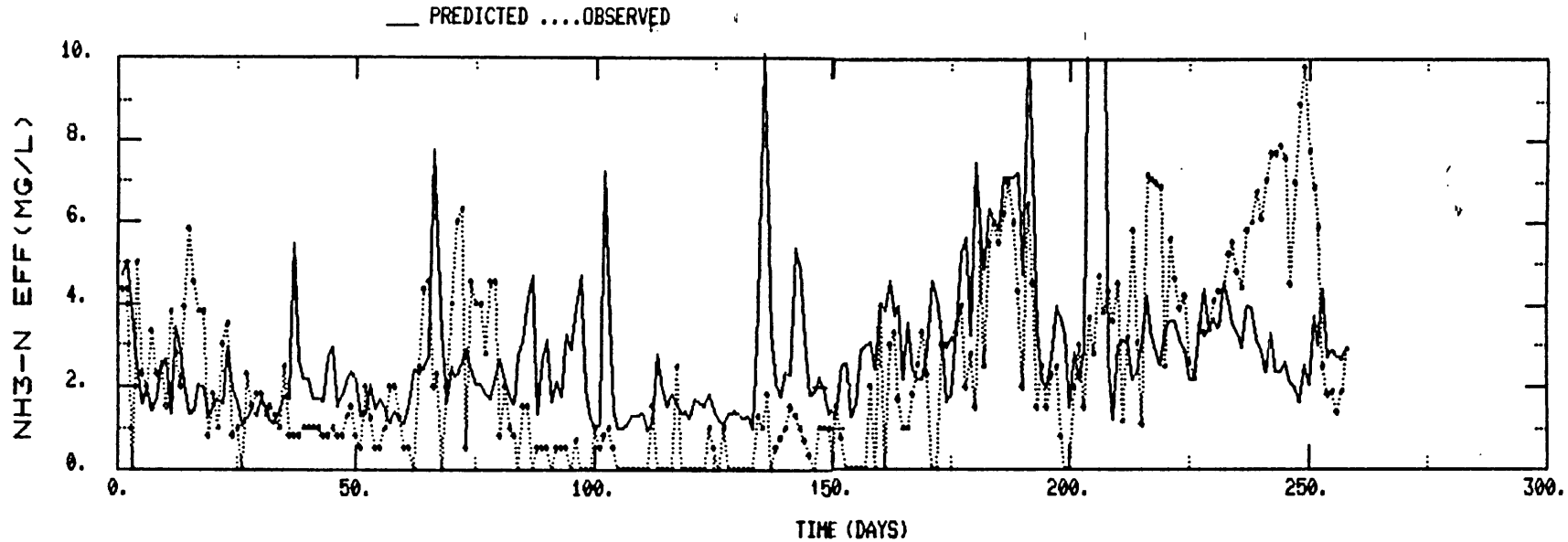


Fig. 3.27b. Predicted – observed effluent NH_3 concentration during validation

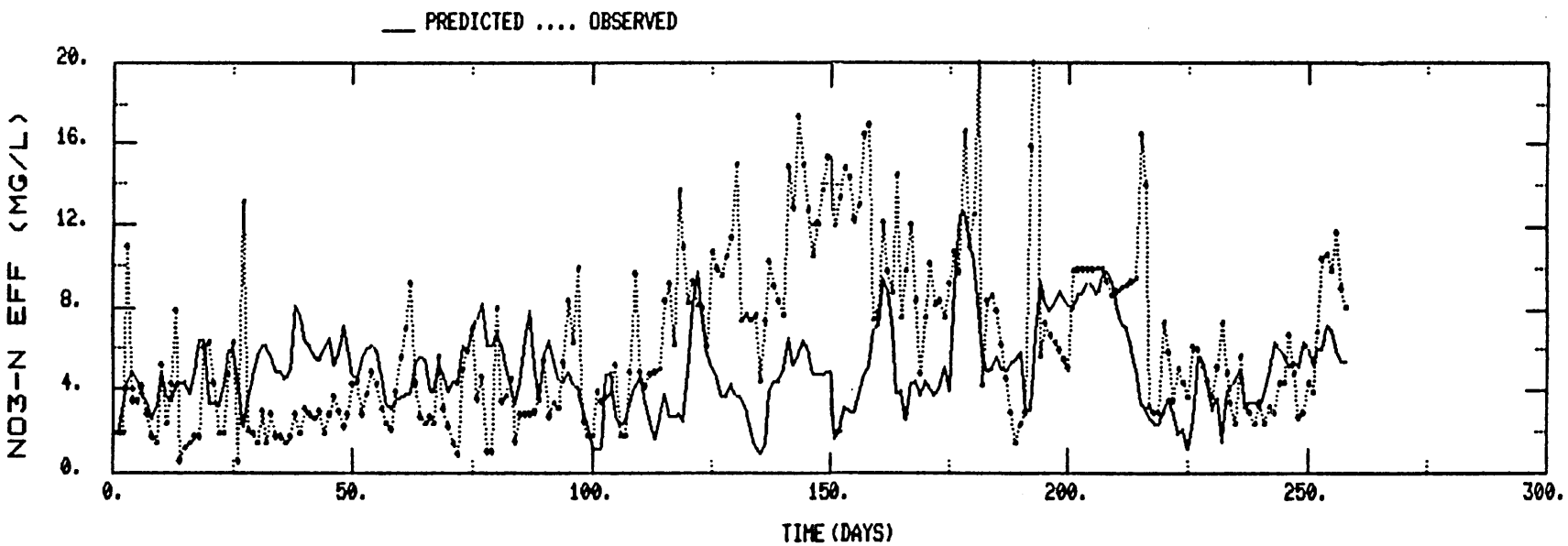


Fig. 3.27c. Predicted – observed effluent NO_3 concentration during validation

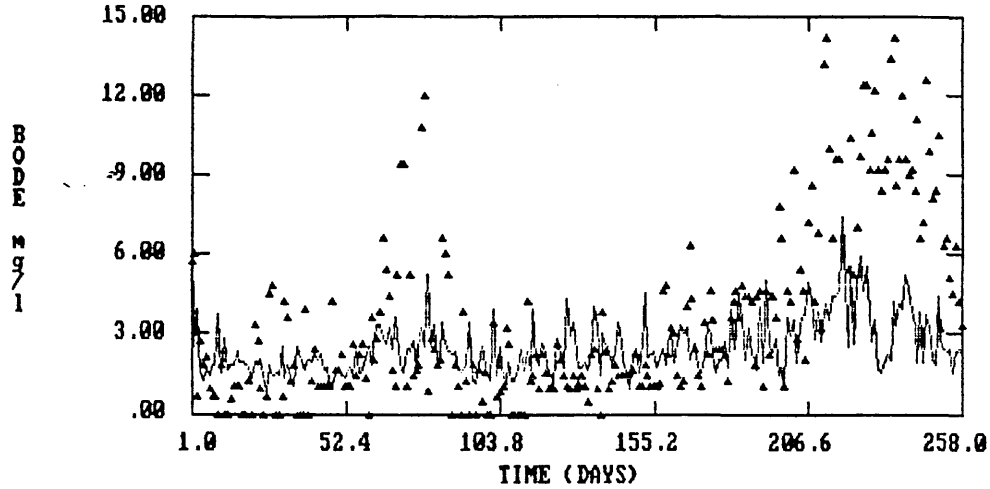


Fig. 3.27a. Predicted effluent *BOD* in validation

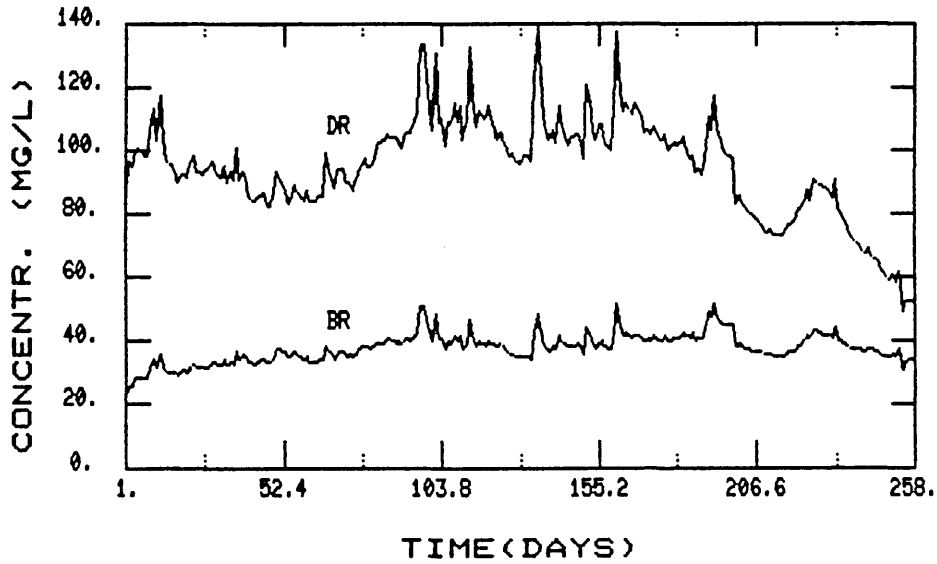


Fig. 3.27d. Predicted nitrifier-denitrifier concentration in the mixed liquor

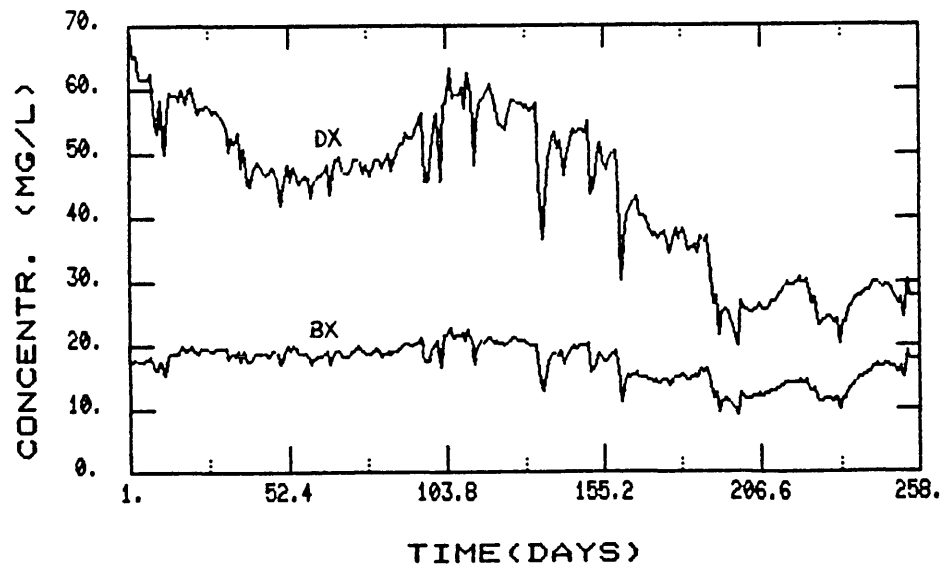


Fig. 3.27e. Predicted recycle nitrifier-denitrifier concentration

4 Modelling and Real-Time Estimation of Oxygen Demand

4.1 Monitoring of wastewater treatment plants

4.1.1 Current practices of monitoring

Monitoring of wastewater treatment works aims primarily at assessing their compliance with the existing discharge standards. In addition monitoring is necessary for evaluating the performance and efficiency of the process and to assess the current operating state which is prerequisite for the implementation of any kind of process control.

Current practices of process monitoring are mainly based on manual collection and analysis of samples for the purpose of monitoring the performance and for operational use. The most common sampling locations are the influent crude sewage stream, the final effluent stream, the recycle stream and the biological reactor. The frequency of sampling, the number of monitored parameters, as well as, the techniques used for sample collection and analysis vary considerably. These mainly depend on the size of the works, the availability of personnel and instrumentation for sample collection and the existing laboratory facilities for sample analyses.

Large works are usually sampled once per day, using in most cases automatic samplers for the collection of 24-hour composite samples, although spot samples from certain locations may also be collected. In medium and small-size works sampling is carried out less frequently ranging from once to three times per week depending on the location of the works, the importance of the receiving river quality and the availability in personnel and laboratory facilities for the analyses. Finally, the number of quality parameters monitored on a regular basis depends on the size of the works, the type of the wastewater treated (domestic, industrial), the receiving water body (inland river, tidal estuary etc.) and the available instrumentation for the analyses. The most commonly measured parameters are the BOD_5, COD, suspended solids (SS), ammoniacal nitrogen ($NH_3 - N$) and the various flow rates in the plant. Among the less commonly measured parameters are the nitrates ($NO_3 - N$), nitrites ($NO_2 - N$), phosphates ($PO_4 - P$), pH, chlorides, alkalinity or specific heavy metals and toxic substances depending on their importance in the crude sewage and final effluent.

The current practices of monitoring are in most cases sufficient for assessing the overall performance of a plant and its compliance with the discharge standards. However, they offer little potential assistance in any attempt to improve performance and efficiency of a plant through application of process control, using the information

obtained through monitoring. Some of their limitations are listed below :

- Sampling is usually restricted to working days only.
- The frequency of sampling depends on the availability of personnel and instrumentation for sample collection.
- The quality of samples largely depends on the methods of collection and analysis used, the reliability of sampling equipment and the representativeness of any spot samples taken.
- The time required to carry out the analyses can be substantial as in the case of BOD_5 measurement, while additional delays may be attached to the possible need for transportation and storage of samples prior to their analysis.

In addition the current monitoring practices are in general too costly involving a large number of skilled and unskilled personnel which generates a tendency to reduce sampling to the minimum acceptable level. However, this is also a consequence of the limited use of the information obtained through monitoring for improving the performance and efficiency of the plant. This does not instigate more effort and funding into sampling under the financial constraints faced by the water industry.

4.1.2 Advantages of "on-line" monitoring

In the past two decades the advances in sensor technology and microelectronics have provided the potential facilities for "on-line" monitoring of wastewater treatment plants. Implementation of on-line monitoring requires the installation of sensors at various locations in the process. Their signal is either recorded by local dial gauges and chart recorders, or collected and processed by a central monitoring system. The application of on-line monitoring compared to the previously discussed "off-line" monitoring, which is based on analysis of samples, offers distinct advantages and potential for improving process performance and efficiency, as discussed below :

- Frequent measurements of process variables can be obtained automatically in real-time, which can then prompt the operator to take an early action.
- On-line measurements can be used in conjunction with process models for real-time estimation of unmeasurable variables and time-varying process parameters.
- On-line measurements provide information on the current state of the process, so they can be used for manual or automatic process control for improving its performance and reliability.

- On-line instrumentation can be combined with automation of certain functions, which will reduce manpower requirements and the level of supervision.

However until now relatively few process variables can be reliably monitored by on-line sensors. In addition, due to the relatively high cost of installing on-line instrumentation, only a small number of plants have been adequately equipped. Among the currently available sensors, the dissolved oxygen monitor is one of the most reliable and least expensive sensors, and has received wide application in activated sludge plants, mainly for the purpose of DO control in the aeration unit. However, automatic on-line DO measurements can also be used for the estimation of oxygen utilization rate in real-time, which is an important process indicator as discussed below.

4.2 The oxygen utilization rate as a process indicator

Among the various measurements taken from a wastewater treatment process, the majority are of little importance for assessing the biological activity in the reactor or for the application of real-time control. While the BOD measurement depicts the biodegradability of organic matter, it cannot be used for automatic control due to the long time lag associated with its determination. Other measurements, such as COD, TOD and TOC require shorter times, but do not give indication of the biodegradability, while measurements of the biomass concentration such as the $MLSS$ and VSS, do not give any indication of biomass activity (Olsson & Andrews, 1978). For this purpose several workers proposed the oxygen utilization rate (OUR), as a suitable indicator of the biomass activity which can be also estimated in real-time (Stenstrom & Andrews 1979; Holmberg 1981; Yust 1981; Young 1981).

The OUR reflects the influent variation of organic load to the process (Yust 1981 ; Goto & Andrews 1985) and provides information on the activity and growth rate of the sludge (Stenstrom & Andrews 1979 ; Holmberg 1982). Furthermore it is reported to be related to the effluent quality and settling properties of the sludge (Goto & Andrews 1985). Schroeder & Irvine (1979) recommended the use of OUR as a control parameter due to its high sensitivity to changes in the available organic material in the reactor. Some workers have used the specific OUR ($SCOUR$), as a process indicator, which is defined as the OUR per unit mass of solids. According to Young (1981), changes in $SCOUR$ represent shifts in population dynamics caused by changes in waste load and its characteristics, while a sudden drop in $SCOUR$ indicates the presence of toxic substances (Holmberg 1982). Yust et al. (1981, 1984) suggested that a constant low value of $SCOUR$ would indicate complete removal of influent organics and low activity of biomass, while a high value indicates that

substrate removal is far from completion. Finally, Novak et al. (1984), recommended the *SCOUR* as a good indicator for assessing the stability of biological sludges from aerobic processes.

In addition to the above information on the process, the *OUR* represents the instantaneous oxygen demand of the mixed liquor for carrying out the biochemical reactions, and therefore determines the energy requirements for aeration. Oxidation ditch systems have, in general, higher energy requirements per unit organic substrate removed compared to the conventional activated sludge, due to greater degree of oxidation. As a result a reduction in aeration energy requirements is of paramount importance in any study aiming at improving efficiency and reducing operating costs of the process. Such a study would be facilitated if the observed oxygen demand was directly related to the various oxygen consuming processes involved, so that a more rational judgement could be made in any attempt to contain the oxygen demand.

In the following the various components of the oxygen demand were analyzed, after a study on the oxygen transfer mechanisms in wastewater treatment. Next, a procedure was presented for real-time estimation of the *OUR* from on-line *DO* measurements in an operational activated sludge plant, and its potential applications for improved process monitoring and control were discussed.

4.3 Oxygen transfer in wastewater treatment

4.3.1 Oxygen transfer mechanisms

The oxygen transfer from the air to the liquid phase is an important process for the aerobic purification of wastewater. However the exact mechanisms by which oxygen is transferred are not known and several pathways have been proposed by different researchers.

Lewis & Whitman (1924), proposed the two-film theory, according to which boundary films are formed at the gas-liquid interface. The rate of gas diffusion through the films depends on the area of interface and the concentration gradient within the component films. Hence, the rate of oxygen transfer into the liquid phase, dM/dt, was expressed by the equation:

$$\frac{dM}{dt} = V \cdot \frac{dC}{dt} = K_L \cdot Ai \cdot (Ci - C_L) \qquad (4.1)$$

where; K_L : mass transfer coefficient $[LT^{-1}]$,
Ai : interfacial area $[L^2]$,
Ci : interfacial oxygen concentration $[ML^{-3}]$,
C_L : bulk liquid oxygen concentration $[ML^{-3}]$.

Marais (1975), proposed a similar pathway in which oxygen molecules are transferred to the liquid interface establishing a thin saturated layer. The transfer of molecules into the bulk of the liquid is then achieved through molecular diffusion and convection which is assisted by the intensity of mixing in the reactor.

Under turbulent flow conditions, Higbie (1935) suggested that oxygen transfer is effected by elements of the liquid in the oxygen rich interface being replaced by elements from the liquid bulk. According to this theory the average mass-flux is given by:

$$\frac{dM}{dt} = 2 \cdot \sqrt{\frac{D_e}{t_e \cdot \pi}} \cdot Ai \cdot (Ci - C_L) \qquad (4.2)$$

where; D_e : diffusivity of oxygen through water $[L^2T^{-1}]$,
t_e : exposure time $[T]$.

Hoyland (1979) related the oxygen transfer rate to the mass transfer resistance at the air/liquid interface and in the liquid bulk through the equation :

$$\frac{dC}{dt} = \frac{C_{SAT} - \overline{C}_L}{\overline{R}} \qquad (4.3)$$

where; $\overline{C}_L$: mean oxygen concentration in the liquid $[ML^{-3}]$,
$\overline{R}$: average mass transfer resistance $[T]$.

From experimental results he observed that the mass transfer resistance was changing with time. This led him to suggest that the resistance is initially exerted by the interface and then is caused by the incomplete mixing of DO in the liquid bulk.

In the above equations, it can be seen that the oxygen transfer rate is always expressed as the product of a driving force and a suitable transfer coefficient. The driving force represents the DO concentration difference between the saturated interface and the liquid bulk, while the coefficient depicts the physical and hydrodynamic characteristics of the bulk liquid. Hence the rate of oxygen transfer into water can be simply expressed by the equation :

$$V \cdot \frac{dC}{dt} = K_{LA} \cdot (C_{SAT} - C_L) \qquad (4.4)$$

where; K_{LA} : overall oxygen transfer coefficient $[T^{-1}]$,
C_{SAT} : saturation DO concentration in water $[ML^{-3}]$.

The oxygen transfer rate can be increased by increasing either the saturation concentration C_{SAT}, or the transfer coefficient K_{LA}. The solubility of oxygen into

water which determines its saturation concentration, is known to be influenced by the liquid temperature, atmospheric pressure and presence of solutes. Attempts have been made to derive the temperature dependency from thermodynamic considerations. However they did not produce absolute values of solubility and for this reason most relationships were derived from experimental observations. The most common relationships for pure water and atmospheric pressure of 760 $mmHg$ are :

$$C_{SAT(T)} = 14.16 - 0.3943 \cdot T + 0.007714 \cdot T^2 - 0.0000646 \cdot T^3 \pm 0.05 \ g/m^3$$
Truesdale et al. (1955) (4.5a)

$$C_{SAT(T)} = \frac{468}{31.6 + T} \pm 0.04 \ g/m^3$$ Montgomery et al. (1964) (4.5b)

$$C_{SAT(T)} = C_{SAT(20)} \cdot 1.024^{(20-T)}$$ common simplification (4.5c)

where; T : temperature in ^oC.

For pressures different than the standard atmosheric pressure, the saturation concentration must be corrected to allow for the different partial pressure of oxygen according to Henry's law:

$$C_{SAT}(\text{at } Pa) = C_{SAT}(\text{at } 760mmHg) \cdot \frac{Pa - Pv}{760 - Pv} \quad (4.6)$$

where; Pa : current air pressure ($mmHg$),
Pv : vapour pressure of water.

Finally, the solubility of oxygen is reduced in the presence of solutes such as chlorides and surfactants (Winkler 1981). The overall effect of solutes upon C_{SAT} is usually expressed by a factor β, which represents the ratio of oxygen solubility in an aqueous solution and in pure water. For domestic sewage this factor has been found to be close to unity.

The oxygen transfer coefficient K_{LA}, is affected by the physical and hydrodynamic properties of the gas-liquid system, as well as, by external environmental factors. The type of aeration system and the reactor configuration determine the value of K_{LA} that can be achieved. The oxygen transfer coefficient is usually expressed as a function of either the operating power of the aeration system or the air-flow rate supplied to the tank. Among the environmental factors that affect K_{LA} are liquid temperature, presence of solutes and suspended solids. The effect of temperature is commonly described by the following Arrhenius equation :

$$K_{LA(T)} = K_{LA(20)} \cdot \theta^{(T-20)} \quad (4.7)$$

where; $\theta = 1.02$ Eckenfelder (1966),
$\theta = 1.024$ Abberley et al. (1974), Metcalf & Eddy (1979),
$\theta = 1.0248$ Winkler & Thomas (1978).

The presence of solutes, such as electrolytes, dissolved salts and surfactants has been found to increase K_{LA} in surface aeration systems because they improve the stability of small droplets, thus increasing the interfacial area. However they reduce K_{LA} in diffused-air systems by retarding molecular diffusion (Winkler 1981). This effect can only be studied experimentally and is usually expressed through factor a, defined as:

$$a = \frac{K_{LA}\ \text{(wastewater)}}{K_{LA}\ \text{(cleanwater)}}$$

Boon (1978) found experimentally that factor a in plug-flow activated sludge plants equipped with surface aeration systems varied between 1.0 and 1.2, while for a bubble diffuser system varied between 0.3 and 0.8.

Finally, the overall effect of environmental factors upon the oxygen transfer rate is more difficult to establish, because they were shown to have both advantageous and adverse effects upon its two main components. For example, temperature does not affect significantly the oxygen transfer, because the temperature effects upon K_{LA} have been found to be opposite and of similar magnitude to those upon C_{SAT} (Marais, 1975). Furthermore, the effect of solutes can only be determined experimentally by comparing the oxygen transfer into the mixed liquor and clean water.

4.3.2 Determination of oxygen supply at Cirencester plant

The oxygen supply to the Cirencester ditch is provided by two vertical shaft Simcar surface aerators powered by a 37 KW motor, located at the rounded end of the channel. The aerators are fitted with a rise-and-fall gearbox allowing the submergence to be varied up to 400 mm, permitting the control of oxygen supply according to the DO concentration in the mixed liquor.

The performance of the aeration system was evaluated prior to commissioning the plant, from experimental trials carried out by Thames Water Authority (Carmichael & Johnstone, 1982 ; Rachwal et al., 1983). The experiments involved non steady-state aeration trials in clean water at five immersion depths aiming to relate the oxygenation capacity, efficiency and power consumption to the aerator's submergence in the mixed liquor. The results are presented in Fig. 4.1 and demonstrate the importance of immersion depth on the aeration system performance. The oxygenation capacity increased with submergence, but reached a plateau level at immersions above 300 mm. As a result the oxygenation efficiency, defined as $kgO2$ supplied per KWh consumed, showed a maximum value of 2.6 kgO_2/KWh at 170 mm immersion, but it was substantially reduced at depths above 250 mm or below 100 mm.

From the experimental results the following empirical relationships were derived

by regression analysis, between the main performance parameters and depth of immersion (Johnstone & Carmichael, 1982):

$$P = 10.47 + 0.074 \cdot D \quad (4.8)$$

$$OC = 28.58 + 0.67 \cdot D - 0.00096 \cdot D^2 \quad (4.9)$$

where; P : operating power per aerator (KW),
OC : oxygenation capacity under test conditions (10 $^{\circ}C$, zero ambient DO concentration, clean water)(kgO_2/hr),
D : depth of immersion (mm).

Using the eq. 4.8 and the available measurements of aeration energy consumption, the average daily operating power over the study period was estimated, as well as, the average daily immersion depth. The results (Fig. 4.2 & 4.3) show that for the period between day 95 and 126 the aerators were frequently operated at their maximum power.

Using the estimated daily submergence, the daily oxygenation capacity of the aeration system was calculated under standard conditions from equation 4.9. The standard oxygenation capacity had to be corrected for the actual operating conditions, in order to account for the effect of temperature variations, wastewater characteristics and the existence of ambient DO. The temperature dependency for C_{SAT} and K_{LA} was described by equations 4.5c and 4.7 (with $\theta = 1.024$) respectively. Factor a was found to be close to unity (Johnstone et al., 1982). Finally, the DO concentration in the mixed liquor close to the aerators was reported to be about 2 mg/l throughout most of the day (Johnstone et al., 1982). Thus, the oxygenation capacity and efficiency were calculated from the following equations and are presented in Fig. 4.4 & 4.5 :

$$OC_t = OCST_t \cdot \frac{C_{SAT(T)} - 2.0}{C_{SAT(T)}} \quad (4.10)$$

$$EF_t = \frac{OC_t}{EN_t} \quad (4.11)$$

where; OC_t : oxygenation capacity (kgO_2/d),
EF_t : oxygenation efficiency (kgO_2/KWh),
EN_t : energy consumption for aeration (KWh/d).

The oxygenation capacity represents the mass of oxygen supplied to the mixed liquor by the aeration system assuming that the oxygen transferred through natural aeration is negligible. At this stage the main assumptions made for the estimation of the daily oxygenation capacity must be recognized, because they contain potential sources of error. The aerator's submergence varies throughout the day in order to

maintain a constant DO concentration, so the assumption of constant immersion will introduce error to the estimates of standard OC due to their nonlinear relationship. Furthermore, in the absence of information on the DO variation, a constant DO concentration was assumed, which may have affected the estimates of oxygenation capacity and efficiency.

4.4 Modelling the oxygen demand in the oxidation ditch process

4.4.1 Components of oxygen demand

It is known that most of the biochemical reactions in the aerobic treatment of wastewater consume oxygen. However some reactions consume large amounts of oxygen, while others consume very small amounts. Among the oxygen consuming reactions, is the organic substrate metabolism and concurrent cell synthesis, the oxidation of ammonia, and the endogenous respiration of biomass. Other processes which form part of the substrate metabolic cycle, such as hydrolysis and glycolysis, as well as physical processes, such as adsorption and storage, have negligible or no oxygen requirements (Tsuno & Goda 1978; Clifft & Andrews 1981a). Finally, the reduction of nitrates releases significant quantities of chemically bound oxygen for the oxygen consuming reactions.

Accordingly, the oxygen requirements of the oxidation ditch process can be related to the growth of biomass or organic substrate metabolism, the biomass respiration, the nitrification and the denitrification process :

$$\begin{aligned} \text{Total } O_2 \text{ demand} = \quad & O_2 \text{ for growth/substrate metabolism} \\ + \quad & O_2 \text{ for biomass endogenous respiration} \\ + \quad & O_2 \text{ for nitrification} \\ - \quad & O_2 \text{ released from denitrification} \end{aligned}$$

The oxygen demand for substrate metabolism is usually considered proportional to the mass of organic substrate removed (Tsuno & Goda 1978 ; Johnstone et al. 1982), while according to other workers it is proportional to the biomass growth (Holmberg,1982 ; Marsili-Libelli 1980). Clifft & Andrews (1981a) suggested that the oxygen consumed during active mass synthesis is proportional to both the stored and extracellular substrate removed, after subtracting the substrate mass assimilated into the new cells. They also observed experimentally, that oxygen utilization usually lags substrate removal by about 2–3 hr.

Gujer & Jenkins (1975) determined the total oxygen demand from a mass-balance of the oxygen equivalent (OE) of substances in the process. The OE of a substance was defined as the mass of oxygen consumed or liberated to oxidize or reduce the substance to a well defined Redox reference level, such as CO_2 for carbon, H_2O for hydrogen and NH_3 for nitrogen. Applying the oxygen balance to the activated sludge process, where insignificant losses of volatile gas occurs, produced the following relationship for the oxygen demand :

$$\text{OE (substrate removed)} = \text{OE (biomass formed)} + \text{OE (satisfied by } O_2\text{)}$$

They reported that 95% of substrate removed could be accounted for by sludge production and oxygen uptake. According to that balance, low sludge production is associated with high oxygen demand, which is the case for extended aeration systems.

The oxygen required for endogenous respiration is usually considered to be proportional to the amount of biomass in the reactor, representing the energy requirements for cell maintenance (Johnstone et al. 1982 ; Holmberg, 1981 ; Schlegel & Lochmann 1981). Other workers have assumed that the oxygen demand is proportional to the decay rate of biomass (Marsili-Libelli 1981 ; Tsuno & Goda, 1978). This process is usually depicted by the following reaction using a typical synthesis of the biomass.

$$C_5H_7NO_2 + 5\ O_2 \xrightarrow{\text{oxidation}} 5\ CO_2 + 2\ H_2O + NH_3 \qquad (4.12)$$

From the stoichiometry of the reaction, the complete oxidation of 1 gram of biomass requires 1.42 grams of oxygen.

The oxygen utilized for nitrification is proportional to the amount of ammonia oxidized. Assuming that all ammonia is oxidized to nitrates, the stoichiometric oxygen requirements can be calculated from the reaction in equation 3.19. Finally the denitrification process, involving the reduction of nitrates to nitrites and nitrogen gas, liberates oxygen which is proportional to the mass of nitrates reduced. However since nitrates are simultaneously produced via nitrification, the degree of denitrification is better calculated from the mass of inorganic nitrogen removed from the crude sewage. The amount of oxygen liberated can be calculated from the stoichiometry of reaction in eq. 3.28. Hence the daily oxygen demand in an oxidation ditch system can be estimated from the following equation :

$$OD_t = a \cdot L_t + b \cdot M_t + c \cdot N_t - d \cdot D_t \qquad (4.13)$$

where; L_t : daily mass of organic substrate removed $[MT^{-1}]$,

M_t : biomass in the aeration tank $[M]$,

N_t : daily mass of ammonia-nitrogen removed $[MT^{-1}]$,
D_t : daily mass of inorganic nitrogen removed $[MT^{-1}]$,
a : empirical coefficient denoting the oxygen consumption per mass of substrate removed $[kgO_2/kgL]$,
b : coefficient denoting the mass of oxygen consumed per mass of solids in the reactor per day $[kgO_2/kgSS \cdot d]$,
c : coefficient denoting the mass of oxygen used per mass of ammonia-nitrogen oxidized to nitrates $[kgO_2/kgN]$,
d : coefficient denoting the mass of oxygen liberated per mass of nitrate-nitrogen reduced to nitrogen gas $[kgO_2/kgD]$.

The four empirical coefficients in the above equation should ideally be determined from the stoichiometry of the biochemical reactions involved. However only coefficients c and d can be sufficiently well estimated from stoichiometric calculations, because the reactions of nitrification and denitrification are fairly well defined since they involve single substrates. On the contrary, the metabolism of multicomponent organic substrates cannot be adequately described by a single reaction, since the various organic components exhibit different reaction rates and oxygen requirements. As a result coefficient a represents the aggregated oxygen requirements and is affected by the composition of organic substrates and the operating process conditions. Similarly, coefficient b which is related to the biomass endogenous respiration, is affected by the type and activity of organisms found in the sludge and various external environmental factors.

Vosloo (1973) reported that both coefficients can vary between wide limits, depending mainly on the operating sludge loading rate and to some extent on the amount of non-degradable material contained in the raw sewage. He reported that the value of a increases at low loading rates, because a greater proportion of the absorbed particulate substrate is oxidized, due to the longer sludge retention time in the system. He also reported that the value of b decreases at low loading rates, because the activity of the sludge is reduced and because it contains a greater proportion of inert material. Consequently, Vosloo argued that there is no justification in estimating the oxygen requirement as two separate components. Instead he related the oxygen consumption per unit mass BOD removed to the sludge loading rate of the process, from which it is apparent that oxygen demand is higher at low loading rates.

The above relation is useful for the purpose of designing aeration systems. However it does not show how the individual components influence the oxygen demand, thus offers little potential in an attempt to reduce the apparently high oxygen demand in extended aeration systems. Johnstone (1984) also demonstrated that car-

bonaceous oxygen demand increases considerably at low sludge loading rates, due to the increased endogenous respiration. However he reported that a large proportion of the "excess" oxygen in extended aeration processes, is used to stabilize the sludge and reduce net sludge production. However, Gujer & Jenkins (1975), observed experimentally that the contribution of endogenous respiration to the total respiration decreases with decreasing substrate removal rates.

Kordes (1985), cited work of previous authors who expressed coefficient b as a function of the organic substrate and biomass concentration in the reactor, the process loading rate and temperature. Other workers, such as Holmberg & Ranta (1982), suggested that coefficient b is age dependent and increases at higher sludge ages, because old cells consume more oxygen for maintenance and auto- oxidation than younger cells.

Some of the reported values for the two coefficients are shown in Table 4.1, from which the wide diversity of values can be observed. Consequently these coefficients should be determined ideally from experimental observations for the particular case study.

Reference		a [-]	b $[hr^{-1}] \cdot 10^{-3}$	Experimental conditions
Johnstone et al.	1982	1.00	2.00	Oxidation ditch, $10°C$, s.age 25d.
Holmberg et al.	1982	1.50	12.0	Pilot activated sludge plant
Tsuno et al.	1978	0.19	4.80	Lab. act. sl., F/M=0.3, syn.sub.
Boon	1983	0.75	2.00	Conv. act. sludge, settled sewage
Vosloo	1973	1.60	—	Activ. sludge plant, F/M=0.1
Suidan et al.	1983	0.52	5.80	Typical for conv. activ. sludge

Table 4.1. Proposed values for oxygen yield coefficients.

4.4.2 Estimation of oxygen yield coefficients

Under *DO* controlled conditions in the oxidation ditch reactor, the mass of oxygen supplied is equivalent to the oxygen utilized for the biochemical reactions. Consequently the oxygenation coefficients a and b in equation 4.13 can be estimated by matching the oxygen demand with the oxygen supplied to the reactor, using the 283-day operational data from the plant. The coefficients c and d were assigned the stoichiometric values, $c = 4.18$ and $d = 2.71$, (Sections 3.3 & 3.4). Dividing the oxygen demand and supply by the observed oxygenation efficiency of the aeration system, these can be expressed in terms of energy demand and energy consumption for aeration. Thus eq. 4.13 can be written in the following form, where the left hand

is a measured variable :

$$\widehat{EN}_t = \frac{a \cdot L_t + b \cdot M_t + 4.18 \cdot N_t - 2.71 \cdot D_t}{EF_t} \qquad (4.14)$$

The model is non-dynamic and uses daily measurements for the various loads to predict the daily energy demand. The model has a simple linear structure, but despite its simplicity depicts the contribution of individual processes upon the total oxygen demand. For the development and application of the model for parameter estimation some further assumptions were made :

- The reported lag between substrate removal and oxygen demand was considered negligible when estimating the daily energy demand.
- All the ammonia-nitrogen removed from the system is oxidized to nitrates.
- The inorganic nitrogen, in the form of ammonia and nitrates, removed from the system is converted to nitrogen gas through denitrification.
- The nitrites in influent and effluent of the reactor are negligible, which can be justified by their low concentration compared to that of ammonia or nitrates.
- the mass-transport of dissolved oxygen in the reactor is negligible compared to the mass of oxygen supplied and utilized.

The above assumptions, as well as those made for the determination of oxygenation capacity, tend to reduce the adequacy of the model and the accuracy of parameter estimation results. However, for the purpose of assessing the importance of individual processes upon the oxygen and energy demand, the simple model structure was considered adequate.

Neglecting initially the temperature dependency of the respiration rate the following values for the oxygenation coefficients were obtained through least squares regression, shown in Table 4.2.1. The fit between the observed and predicted energy consumption (Fig. 4.6), was rather poor judged by the low coefficient of determination, while the predicted aeration energy was quite variable compared with the observed series. This was partly attributed to the noisy structure of the input data (organic and ammonia loads removed) and the relatively small variation in the observed energy consumption. In addition the use of daily values for the components of oxygen demand and the assumptions made for the model development were additional causes of the poor performance. However, it is important to note that for the current parameter estimates, the proportion of energy used for direct substrate oxidation was 16.8%, for nitrification-denitrification was 8.7%, while the largest proportion was used for biomass respiration (74.5%). Similar observations were made

by Johnstone (1982) who found that the oxygen demand in oxidation ditch systems was dominated by the endogenous respiration of the biomass.

Assuming a temperature dependency of the biomass respiration rate, as suggested by some workers (Johnstone et al. 1982, Gujer & Jenkins, 1975), coefficient b was replaced by the following expression:

$$b_{(T)} = b_{(10)} \cdot \theta^{(T-10)} \tag{4.15}$$

where; θ is a temperature dependency coefficient to be estimated.

Subsequently equation 4.13 became non-linear in the parameters b and θ and their estimation could only be performed via optimization. For this purpose the multi-variable, direct search, Rosenbrock's constrained optimization technique was employed (Rosenbrock, 1960), which automatically includes penalty functions for the constraints. The objective function was defined as the sum of square error between the observed and predicted values of aeration energy, hence the optimization problem can be stated as :

$$\min_{a,b,\theta} \quad J = \sum_{i=1}^{N} (EN(i) - \widehat{EN}(i))^2$$

Case	Eff.	a [-]	$b_{(10)}$ $hr^{-1} \cdot 10^{-3}$	θ [-]	Emean kWh/d	RMS error	R	C.O.D.
1.	Var.	0.6070	3.045	1.0000	98.3	339.0	0.656	-3.067
2.	Var.	0.6372	2.861	1.0189	100.6	335.5	0.706	-2.983
3.	Ct.	0.6055	2.783	1.0452	80.2	304.7	0.670	-2.286

Table 4.2. Block estimation of oxygen yield coefficients.

Using the same input data the following values were obtained through optimization shown in Table 4.2(2). The model performance showed only a marginal improvement over the previous case, while the estimated temperature coefficient was substantially lower than values reported by Johnstone (1982).

Finally the effect of the variable oxygenation efficiency upon the estimation results was examined, by assuming constant efficiency of the aerators. The average efficiency under standard conditions was estimated at 2.35 kgO_2/KWh and the average mixed liquor temperature was 12.3 ^oC. Assuming a DO concentration near the aerators of 2 mg/l the average actual efficiency was:

$$EF = EF_{ST} \cdot \frac{C_{SAT(12.3)} - 2}{C_{SAT(12.3)}} = 1.90 \; kgO_2/kWh \tag{4.16}$$

Using the average efficiency for the whole the period the estimated parameter values were found to be close to the previous estimates under variable efficiency,

with the exception that the temperature dependency of respiration rate was more pronounced (Table 4.2(3). The model performance was slightly improved as a result of the smaller variability of the predicted series.

4.4.3 Discussion of results

From Fig. 4.6 showing the fit between predicted and observed energy, four periods can be identified regarding the performance of the model. In the first period covering the first 94 days of operation, the predictions reproduce the observations well, while in the second period spanning between day 95 and 126 the predictions are substantially higher than the observations. In the third period between day 127 and 155 the fit is again satisfactory, while in the fourth period after day 155 the predictions are persistently lower than the observations.

The first period corresponds to average levels of biomass concentration and organic loading in the reactor and both the predicted oxygen demand and aeration energy closely follow the estimated oxygen supply and observed energy consumption. During this period the aerators were operated at a relatively high efficiency estimated at 1.973 kgO_2/kWh on average and below their maximum power, so that oxygen limitation is not expected to have occurred.

The second period with high predicted oxygen demand, corresponds to high biomass concentration of 5,625 mg/l on average and a higher than average organic loading of the reactor. During this period the aerators were operated under high power, which occasionally reached their maximum capacity throughout the day (Fig. 4.2). Hence it can be suggested that the aerators occasionally failed to meet the high oxygen demand and subsequently oxygen limiting conditions may have occurred in the ditch. Under these conditions the ditch was expected to operate with smaller aerobic zones and larger anoxic regions which would promote denitrification and inhibit the aerobic reactions.

Examination of the effluent quality measurements (Fig. 2.6a,c,d,e), showed that between day 95 and 126 the effluent BOD was unaffected, the effluent SS and ammonia were slightly deteriorated, while the effluent nitrate concentration was reduced. Hence the effect upon the aerobic processes appears to be minimal and can be attributed to the high capacity of the oxidation ditch process in coping with extreme events, as well as, to the short period of the expected oxygen limitation. On the contrary, the settleability of the sludge during that period was deteriorated which is evident from the high $SSVI$ values observed during high $MLSS$ concentrations and is an additional indication of oxygen limiting conditions. Similar observations were made by Johnstone (Johnstone et al., 1982), during another operating period of the

Cirencester plant, where high $MLSS$ caused very high oxygen demand, resulting in a low DO throughout the ditch impairing nitrification and sludge settleability.

The oxygenation efficiency of the aerators during the above period was significantly reduced due to the high operating power and immersion depth (Fig. 4.5), which produced only a minimal increase in their oxygenation capacity (Fig. 4.4). The above observations indicate that conditions of high oxygen demand may cause oxygen limitation problems and in addition lead to inefficient operation of the aeration system which is associated with high energy consumption.

The third period is somewhat similar to the first one, since the predictions match the observations reasonably well, while the operating plant conditions are at normal levels. In the fourth period however, the predicted aeration energy is persistently lower than the observed, and corresponds to low biomass concentration and a relatively low organic and ammonia load to the reactor. The crude sewage flow is also low for most of the period due to the absence of surface water infiltration, and the hydraulic retention time, is approximately 40% above the average for the study period. It is expected that during this period the size of the aerobic zones would be generally larger, particularly during the early morning hours. During that time the oxygen demand is at its lowest level and the DO at the monitoring location usually reaches its upper limit of 1.5 mg/l, which can be seen from the results of a 48-hr survey at Cirencester plant conducted by TWA (Rachwal et al., 1983) (Fig. 4.7). As a result the DO concentration near the aerators is expected to be higher than 2 mg/l used for the calculation of oxygenation capacity (Section 4.3.2, eq. 4.10), implying that a lower oxygen mass would be supplied, which is closer to the estimated oxygen demand.

In the light of the above discussion, the second period in which oxygen limitation was predicted, is likely to introduce bias to the estimation results, since the oxygenation coefficients would be affected by these conditions. Excluding the period between day 95 and 126, the coefficients were re-estimated under both variable and constant oxygenation efficiency and the results are summarized in Table 4.3.

Case	Eff.	a [–]	$b_{(10)}$ $[hr^{-1} \cdot 10^{-3}]$	θ	Emean	RMSe	R	C.O.D.
					(for the whole data set)			
1.	Var.	0.6804	3.200	1.0000	24.92	347.7	0.655	-3.28
2.	Var.	0.7621	2.808	1.0448	9.31	357.0	0.753	-3.51
3.	Ct.	0.6778	2.771	1.0617	16.99	315.3	0.704	-2.52

Table 4.3. Block estimation of oxygen coefficients (period d.95-126 excluded).

It can be seen that the estimated values of coefficient a were higher in all cases by 11%, 20% and 12% respectively. Coefficient b was affected by less than 5%, but

showed a significantly higher temperature dependency. A probable explanation was that the proportion of organic substrate undergoing complete oxidation is drastically reduced under oxygen limiting conditions, which was depicted by a lower value for a, while the effect on the biomass respiration was less severe. The model performance in case 2 (Fig. 4.8), is still relatively poor, suggesting that the oxygen coefficients may vary with time in response to changes in the operating and environmental conditions. An important observation to be made is that using the estimated parameters for case 2, the oxygen demand is dominated by the endogenous respiration of biomass, which accounts for 72% of the total oxygen requirements. The proportion of oxygen demand for direct substrate oxidation is 20%, and for nitrification-denitrification is only 8.0% , since almost half (45%) of the oxygen used in nitrification is released through denitrification.

4.4.4 Recursive parameter estimation

Adaptive estimation of the oxygenation coefficients can provide information about their respective variability with time throughout the period and reveal potential weaknesses of the model. Already several limitations in reproducing the observed aeration energy were discussed and possible causes suggested including the simple structure of the model, inadequacy of assumptions, data inaccuracies and unmodelled disturbances affecting the oxygen coefficients.

The adaptive estimation was expected to depict the likely variation of the coefficients in response to variations in the operating conditions and other external factors which were not accounted by the current model. The Kalman Filter algorithm was employed with the system and measurement equations given by eq. 4.14. The oxygen coefficients were considered as additional states of the augmented state vector with unknown dynamics. The aeration energy was the only measured state against which the augmented state vector was to be updated. In order to reduce the number of states to be estimated, the aeration energy was considered as a deterministic variable. Hence the augmented state vector was :

$$X_1(t) \equiv a \quad [kgO_2/kg\ BOD \text{ rem.}]$$
$$X_2(t) \equiv b \quad [gO_2/kgSS \cdot h]$$

The observation vector y contained a single measurement, namely the aeration energy, while the measurement matrix (h) was given by the first derivative of eq. 4.14 with respect to a and b. Hence :

$$y(t_k) \equiv EN\ [KWh/d] \text{ observed}$$
$$h^T = \left| \frac{d(EN)}{d\,a} \quad \frac{d(EN)}{d\,b} \right|$$

The difference between the predicted and observed aeration energy was used for updating the two coefficients, which were estimated both as non-dynamic and random walk states. The temperature coefficient was not expected to vary with time, so it was assigned constant value taken from the block estimation. As initial values for the parameters were used the values from the block estimation, with the following initial covariance matrix :

$$P_{(0)} = \begin{vmatrix} 10^{-3} & 0 \\ 0 & 10^{-2} \end{vmatrix}$$

Case	1	2	3	4
Q_{11}, Q_{22}	0 0	0 0	10^{-5} 10^{-4}	10^{-5} 10^{-4}
R	$2 \cdot 10^3$	$5 \cdot 10^3$	$2 \cdot 10^3$	$5 \cdot 10^3$
EN (pred.)	1218.0	1216.2	1295.4	1278.4
Error (mean)	129.4	131.1	51.9	68.9
RMS error	337.1	337.8	190.1	216.3
Corr. coef.	0.689	0.687	0.700	0.681
C.O.D.	-3.022	-3.040	-0.279	-0.656
a (mean)	0.4928	0.5640	0.3217	0.4397
a (std. dev.)	0.1147	0.0901	0.1763	0.1487
$b_{(10)}$ (mean)	2.746	2.673	3.406	3.196
$b_{(10)}$ (std.dev)	0.266	0.222	0.881	0.743
θ	1.045	1.045	1.0450	1.0450

Table 4.4. Recursive estimation of coefficients by Kalman filter.

The results of four estimations with different values for the error matrices Q and R, are shown in Table 4.4 and in Fig. 4.9 & 4.10. The results show that the parameters exhibit substantial variation with time, particularly parameter a. Furthermore the parameter variation is largely determined by the selected values for Q and R. However, the determination of these matrices cannot be based on a formal approach, thus they were selected by a trial and error procedure. The values for $P_{(0)}$ and Q matrices were chosen to be relatively small and R rather high, in order to avoid excessive variation of the parameter trajectories, due to the noisy structure of the input data and deficiencies in the assumptions made. Improvement in model performance was only evident in cases 3 & 4, and was associated with a substantial variation in the parameters.

The estimated parameter trajectories showed considerable differences in their mean and standard deviation, but exhibited similar trends. Parameter a decreased steadily during the first 63 days and subsequently increased to a medium level until day 110. During the period of expected oxygen limitation, parameter a showed a rapid fall and remained at a low level until about day 190, while it increased progressively

until the end of the study period.

Parameter b exhibited variation which was related, to some extent, to the variation in a. After an initial increase during the first 30 days, parameter b remained at a high level for about 30 days and subsequently fell progressively to a low level until day 120, which corresponded to the steady rise in $MLSS$ concentration. In the second half of the period coefficient b showed steady increase which was particularly obvious when the parameters were estimated as "random walk" states (cases 3 and 4).

It is expected that the noisy structure of the system measurement matrix (h) would interfere with the simultaneous parameter estimation and introduce bias to their estimated trajectories. Nevertheless, the apparent variability in the parameters indicates deficiencies in the model structure, particularly regarding the effect of operating conditions and external environmental factors upon the oxygen coefficients. From the parameter trajectories it was observed that in the period of high oxygen demand, the endogenous respiration coefficient was suppressed and coefficient a exhibited a decreasing trend, while during periods of lower oxygen demand both coefficients were high. Furthermore, coefficient b was found to be negatively correlated with the operating sludge age and positively correlated with the process sludge loading rate, which would indicate that at high sludge age and low loading rates the oxygen requirements of the biomass are reduced. However, the variation in both the sludge age and loading rate over the study period were not of sufficient magnitude to confirm the existence of a strong relation between coefficient b and the operating conditions.

4.4.5 Conclusions

From the previous analyses it can be concluded that, although the oxygen demand model (eq. 4.14) showed limitations in reproducing the observed aeration energy, its simple structure positively assisted in evaluating the relative importance of the various processes upon the oxygen demand. It was shown that the largest proportion of the oxygen demand was related to endogenous respiration of the biomass, while that of direct substrate oxidation was relatively small. In addition the combined effect of nitrification-denitrification was also small, since 45% of the oxygen used in nitrification is released upon denitrification.

The main weaknesses of the model were attributed to the variation of the oxygen coefficients resulting from changes in the operating conditions and other unmeasurable external factors. Furthermore the assumptions made for the calculation of the oxygenation capacity and efficiency, in the absence of information on

the diurnal variation of aerator submergence and DO in the reactor, were identified as potential sources of error. The derived values for the coefficients from the block estimation, excluding the period of suspected oxygen limitation, were : $a = 0.75$, $b_{(10)} = 2.8\ gO_2/kgSS \cdot h$, $c = 1.045$, which are within the range of reported literature values.

4.5 Methods for the estimation of K_{LA} and OUR coefficients

4.5.1 Models for the dissolved oxygen dynamics

The rate of oxygen transfer into the bulk of a liquid is described by equation 4.4 in Section 4.3.1. In the previous study (Sec. 4.4) the dissolved oxygen was controlled to a relatively constant level. However under uncontrolled conditions its concentration would vary with time. The dynamic behaviour of DO concentration in the aeration tank can be described by the following differential equation based on oxygen mass-balance over the reactor, assuming complete-mixed conditions :

$$\text{Accumulation} = \text{Transfer} - \text{Utilization} + \text{Transport}$$

$$\frac{dC_t}{dt} = K_{LA_t} \cdot (C_{SAT} - C_t) - OUR_t + \frac{Qi_t + Qr_t}{V} \cdot (Ci_t - C_t) \qquad (4.17)$$

where; K_{LA_t} : overall oxygen transfer coefficient $[T^{-1}]$,
OUR_t : oxygen utilization rate $[ML^{-3}T^{-1}]$,
C_t : DO concentration in the reactor $[ML^{-3}]$,
Ci_t : incoming DO concentration $[ML^{-3}]$,
C_{SAT} : saturation DO concentration $[ML^{-3}]$.

The oxygen transport component is usually small compared to the oxygen transfer and utilization components, especially when there is small concentration difference between influent and effluent. Thus its omission from the equation would not introduce a large error. The following simplified equation is then derived for the DO dynamics :

$$\frac{dC_t}{dt} = K_{LA_t} \cdot (C_{SAT} - C_t) - OUR_t \qquad (4.18)$$

In the above equation the K_{LA} coefficient represents a characteristic parameter of the aeration system performance. For systems with variable aeration capacity, the K_{LA} coefficient can be expressed as a function of either the operating power or the air-flow rate supplied to the reactor. Knowledge of the K_{LA} coefficient under different operating conditions of the aeration system is necessary for the subsequent estimation

of the OUR from DO measurements employing either of the equations 4.17 and 4.18. The DO concentration can be monitored on-line through the installation of DO probes in the reactor. The saturation level (C_{SAT}) can be adequately calculated for the particular mixed liquor characteristics from existing relationships (Sec. 4.3.1). Subsequently the OUR can be estimated in real-time.

Several methodologies have been proposed for the estimation of K_{LA} coefficient from experimental aeration trials conducted either in clean water or in wastewater with varying degrees of success. In clean water tests, where no oxygen utilization occurs, the oxygen transfer coefficient can be more easily estimated from the dynamic response of DO during "unsteady-state" experiments. During these tests the reactor is deoxygenated initially by the addition of chemicals and the subsequent rise of the DO level is monitored with time. However, when the plant is in operation, the determination of K_{LA} becomes more complex due to the simultaneous oxygen utilization. This is usually an unknown and time-varying quantity, although for simplicity it has been often assumed to remain constant over short periods of time.

Simultaneous estimation of the oxygen transfer and utilization rates is therefore necessary. For the successful estimation of these parameters, it is important that the system dynamics be sufficiently excited, so that the DO concentration exhibits transient behaviour. Step changes of the air-flow rate produce transients in the DO concentration, which can then be used for parameter estimation. The DO dynamic equation can be employed either by discretizing it at small time intervals, or by taking its analytical solution. The two solutions resulting from differential equation 4.18 are given below assuming that the K_{LA} and OUR coefficients remain constant over the integration period :

Discretized solution

$$C_{t+\Delta t} = (1 - K_{LA} \cdot \Delta t) \cdot C_t + (K_{LA} \cdot C_{SAT} - OUR) \cdot \Delta t \qquad (4.19)$$

where; Δt : discretization step.

Analytical solution

$$C_{t+\Delta t} = e^{-K_{LA} \cdot \Delta t} \cdot C(t) + \left(C_{SAT} - \frac{OUR}{K_{LA}}\right) \cdot (1 - e^{-K_{LA} \cdot \Delta t}) \qquad (4.20)$$

The discretized solution is simpler and linear in the parameters K_{LA} and OUR. However the analytical solution is often preferred, because it offers greater accuracy, which is independent of the discretization step. Equation 4.20 is non-linear in the parameters and ideally non-linear programming techniques should be applied. Although the two solutions have different structure, they can be expressed by the same simple linear relationship between the variables $\underline{C}(t + \Delta t)$ and $\underline{C}(t)$:

$$C(t+\Delta t) = a \cdot C(t) + b \tag{4.21}$$

where; $a = (1 - K_{LA} \cdot \Delta t)$ based on eq. 4.19 (4.21a)

$b = (K_{LA} \cdot C_{SAT} - OUR) \cdot \Delta t$ (4.21b)

$a = e^{-K_{LA} \cdot \Delta t}$ based on eq. 4.20 (4.21c)

$b = (C_{SAT} - OUR/K_{LA}) \cdot (1 - a)$ (4.21d)

4.5.2 Non-adaptive estimation techniques

In the previous relationship (eq 4.21), the parameters a and b can be estimated by regressing $C(t + \Delta t)$ upon $C(t)$, which are consecutive DO measurements with a lag of Δt. The oxygen transfer and utilization coefficients can then be estimated by rearranging eq. 4.21a-d, depending on the selected equation. In the case of the analytical solution the coefficients are given by :

$$\widehat{K_{LA}} = -\frac{ln(\hat{a})}{\Delta t} \tag{4.22a}$$

$$\widehat{OUR} = (C_{SAT} - \hat{b}/(1 - \hat{a})) \cdot \widehat{K_{LA}} \tag{4.22b}$$

From equation 4.22a can be noted that when a small lag in the DO measurements is used, then a small error in the parameter $\hat{a}$ can cause a significant error in $\widehat{K_{LA}}$. Also under a small time lag, the measurement errors contained in the regressors may be significantly correlated resulting in biased parameter estimates. Howell et al. (1984), selected a lag period of at least 70 seconds between successive DO measurements in order to minimize the correlation of measurement errors. In addition they recommended that the lag should be chosen so as parameter a is below 0.95 for greater accuracy in the results, implying that the time-constants of the DO dynamics also influence the choice of lag.

For the application of linear regression, a necessary condition is that the dependent variable is error free. However, in equation 4.21 this condition is not fulfilled, since both variables are subject to measurement error. In that case Howell suggested that the "Error-in- Variables Model" (EVM) should be used, where the parameters are determined as a probability distribution, from which values with the maximum probability can be derived. Alternatively, Cook (1984c), recommended the "Orthogonal least squares" method as an equivalent to the EVM approach, in which the prediction error is measured normal to the "best fit" line rather than in the y-direction. In this method the error to be minimized and the parameter estimates are given by:

$$\min_{\hat{a},\hat{b}} \sum_{i=1}^{N} e_i^2 \tag{4.23}$$

where; $e_i = (C(t_i + \Delta t) - \hat{a} \cdot C(t_i) - \hat{b})/\sqrt{1 - \hat{a}^2}$ (4.23a)

$\hat{a} = Z \pm \sqrt{Z^2 + 4 \cdot cov(\underline{C}(t + \Delta t), \underline{C}(t))^2}/(2 \cdot cov(\underline{C}(t + \Delta t), \underline{C}(t))$ (4.23b)

$\hat{b} = \overline{C}(t + \Delta t) - \hat{a} \cdot \overline{C}(t)$ (4.23c)

$Z = var(\underline{C}(t + \Delta t)) - var(\underline{C}(t))$

Cook also suggested the use of the "Instrumental Variables" method (IV), in order to overcome the bias problem created in autoregressive model structures, such as eq. 4.21, when the process observations are corrupted by noise. In the IV method a set of variables are sought which are correlated with the "true" process states but not with the noise. These variables can be found by using an auxiliary model having the same structure as the process model, which propagates IVs rather than process observations. The non-recursive form of the estimator is given by (Cook 1984) :

$$V(t + \Delta t) = \hat{a} \cdot V(t) + \hat{b} \quad (4.24)$$

$$\hat{a} = \frac{cov[\underline{C}(t + \Delta t), \underline{V}(t)]}{var[\underline{V}(t)]} \quad (4.24a)$$

$$\hat{b} = \overline{C}(t + \Delta t) - \hat{a} \cdot \overline{C}(t) \quad (4.24b)$$

where; $\underline{V}(t)$ is the instrumental variable vector.

The use of non-linear programming techniques for estimating the parameters in eq. 4.20, has been also suggested by several workers as the most accurate approach. Boyle et al (1974) and Stenstrom et al. (1981), recommended the application of search techniques for the estimation of K_LA from clean water aeration trials using the integrated form of the DO dynamics. Alternatively they proposed linearisation of the model by first-order Taylor expansion and subsequent use of linear regression.

Among of the quoted advantages of non-linear programming techniques, is that no transformation of the data is necessary, so that the actual error in the DO values is minimized, the residuals are more uniform and that they lead to greater precision in the estimated parameters. However some of the reported pitfalls are the possible lack of convergence under certain initial conditions, and the possibility of obtaining local optima which lead to erroneous parameter estimates (Stenstrom et al, 1981). For this purpose they recommended the examination of the residual distribution before assessing the validity of the estimation results.

For the application of non-adaptive estimation techniques, the oxygen transfer and utilization rates have to be assumed constant during each set of experimental observations. The K_LA coefficient can be maintained constant under constant operation of the aeration system, however the OUR generally varies in response to changes in the loading conditions of the reactor. For detecting changes in the OUR, Howell et al. (1984), recommended the examination of the correlation between $\underline{C}(t + \Delta t)$ and $\underline{C}(t)$, and standard deviation of the best fit residuals.

The success of simultaneous parameter estimation largely depends on the accuracy of the DO measurements. In general it is not possible to assess the accuracy of the estimated parameters, unless one of them has been determined independently. Cook (1984c) faced several difficulties during the simultaneous parameter estimation from noisy DO measurements, which caused an oscillating pattern of the OUR in successive experiments, and produced a weak dependence of K_LA upon the air-flow rate. For this purpose he recommended the estimation of OUR by independent means.

4.5.3 Adaptive estimation techniques

Adaptive parameter estimation has been used by several authors (Holmberg 1981, 1982 ; Marsili-Libelli 1982 ; Ko et al. 1982), in order to depict the time variation of the oxygen transfer and utilization rates. Adaptive techniques are particularly suitable for real-time estimation of the respiration rate from on-line DO measurements. Furthermore, recursive estimation algorithms allow the use of stochastic process models which account for random measurement errors and the effect of unmodelled disturbances, thus reducing their effect upon the estimated parameters.

Holmberg (1981), and Ko et al. (1982) attempted simultaneous estimation of K_LA and OUR from step response experiments employing the discretized DO dynamics (eq. 4.17) and the recursive least squares algorithm. Holmberg reported good convergence of the estimation algorithm during periods of sufficient DO dynamic changes, while Ko et al. reported poor convergence in the case of coloured noise in the measurements.

Marsili-Libelli (1982) developed a state observer of the DO dynamic system which adequately reconstructed the OUR trajectory. This was subsequently coupled with an adaptive scheme for estimating the oxygen transfer coefficient, but the combined scheme exhibited slower convergence and a slight bias in the results. Consequently he recommended that the robustness of the algorithm and its noise sensitivity must be assessed before it is used for simultaneous $K_LA - OUR$ estimation. Finally, Cook (1984c) successfully applied the Extended Kalman Filter and recursive Instrumental Variables for estimating the long-term OUR behaviour from DO measurements, when the K_LA coefficient was determined as a function of the air-flow rate.

4.6 Estimation of K_{LA} coefficient from on-line DO measurements

4.6.1 Experimental programme

The experimental programme for demonstrating the procedure of estimating the oxygen transfer coefficient and utilization rate in an operational plant, was carried out at the Hogsmill Valley Sewage treatment works. This is a conventional diffused-air activated sludge plant receiving mainly domestic wastewater and surface runoff from Epsom, Ewell, Kingston and Malden. The works comprise preliminary treatment (grit chambers and comminutors), primary sedimentation, the aeration unit, secondary sedimentation and sludge digestion. The aeration unit consists of two rectangular tanks, each one divided into ten parallel channels offering a total volume of 16,430 m^3. One of the channels was equipped with four Kent I.M. Ltd. dissolved oxygen probes, placed at distances of 11, 26, 41 and 56 m from the inlet of the reactor. The channels are 60 m long and 4.65 m wide, and their configuration promote plug-flow conditions, although some degree of axial dispersion is also introduced by the diffused-air aeration system.

The DO concentration at the first probe was always very low and for this reason it was not recorded, while the remaining three probes were connected to a multi-pen continuous-feed chart recorder. For the purpose of recording the measurements in digital form, a microcomputer was located on-site and connected to the DO monitoring system. The electric current transmitted from the probes is a function of the dissolved oxygen concentration. The current was measured by the microcomputer from the voltage drop across a fixed 1000 Ohm resistance and was then passed through a preamplifier and an A/D converter to give a digital output. Specially prepared software by supplied by Dr S.C. Cook was used for collecting and storing the voltage readings from the three probes onto floppy disks at prespecified time-intervals.

The experimental programme involved continuous monitoring of the DO concentration with the three on-line probes, under step changes of the air-flow rate. The air supply generated by three fixed-speed blowers, is transported into the aeration unit by two downpipes and is then distributed from a large number of diffuser domes. The air-flow rate supplied from each downpipe to the monitoring channel, was determined from the air pressure in the pipe using a manometer. The pressure was subsequently converted to the air-flow rate supplied to the channel, using a standard nomograph for the works.

Step changes in the air-flow rates were produced by regulating a valve on each downpipe (Fig. 4.11). Successive rises and falls of the DO concentration were subsequently generated, which are referred to as deoxygenation and reoxygenation trials

respectively (Fig. 4.12). Four deoxygenation and three reoxygenation trials were conducted and the experimental conditions are summarized in Table 4.5. The duration of each experiment was long enough to allow the system to reach a steady-state DO concentration, while the monitoring interval was chosen to be 15 seconds. At the same time the respiration rate was monitored separately from the deoxygenation curve in the absence of aeration, in an isolated volume of mixed liquor collected from the location of the on-line probes. These experiments intended to provide an independent estimate of OUR for comparison with estimates obtained using the on-line DO measurements.

No	Exper. type	Temp. ^oC	C_{SAT} mg/l	Qa (1) l/s	Qa (2) l/s	Qi l/s	Qr l/s	Qw l/s
1	Deox.	14.5	10.2	10.6	2.3	852	215	10.4
2	Reox.	14.6	10.2	57.5	62.2	867	222	10.5
3	Deox.	14.8	10.1	34.9	40.0	762	202	10.5
4	Reox.	15.0	10.1	57.5	60.3	790	232	10.5
5	Deox.	15.0	10.1	27.8	22.1	868	260	10.6
6	Reox.	15.0	10.1	54.2	59.4	868	260	10.6
7	Deox.	15.0	10.1	48.3	51.8	790	221	10.5

Table 4.5. Experimental conditions during the "on-line" aeration trials.

4.6.2 Estimation of K_{LA} and OUR coefficients

The signal from the on-line probes contained significant noise and for this reason the measurements were smoothed for removing the high frequency variations. The following Kalman filter algorithm was used for data filtering :

$$
\begin{aligned}
&\text{initial state} && : X(t_k) = Y(t_k) \\
&\text{" variance} && : Pt_k = Pin. \\
&\text{predicted value} && : \hat{X}(t_{k+1}) = X(t_k) \\
&\text{gain} && : Gt_{k+1} = Pt_k/(Pt_k + R) \\
&\text{new covariance} && : Pt_{k+1} = (1 - Gt_{k+1}) \cdot (Pt_k + Q) \\
&\text{corrected value} && : X(t_{k+1}) = \hat{X}(t_{k+1}) + Gt_{k+1} \cdot [Y(t_{k+1}) - \hat{X}(t_{k+1})]
\end{aligned}
\tag{4.25}
$$

where; $k = 1, .., N$ the number of measurements,

$Y(t_k)$: original data series,

$X(t_k)$: filtered data series.

The algorithm passes twice through the measurements (forward and backward pass) in order to minimize the bias in the filtered series, while the degree of smoothing is determined by the selected values for the error variance parameters Pin, Q and R.

For the conversion of the voltage readings into DO concentrations a calibration exercise was undertaken. This involved simultaneous collection of DO measurements via a portable probe and voltage readings from each on-line probe at different DO concentrations. The experiments were conducted in an isolated volume of mixed liquor in order to minimize any disturbance due to oxygen mass transport. The DO concentration was varied in steps by regulating the air-flow into the liquid volume and after it was stabilized to a particular level, several readings were taken which were averaged together. Next, a quadratic equation was fitted through the data points by least squares regression, relating the voltage to the corresponding DO concentration. The following calibration equations were derived for the three on-line probes and the results are also presented in Fig. 4.13.

$$\begin{array}{lllll} \textbf{Probe 2} & C = -2.356 + 13.854 \cdot V - 0.363 \cdot V^2 & R = 0.99987 & \text{RMSe} = 0.0527 \\ \textbf{Probe 3} & C = -2.370 + 14.06 \cdot V - 1.13 \cdot V^2 & R = 0.99989 & \text{RMSe} = 0.0463 \\ \textbf{Probe 4} & C = -2.03 + 11.773 \cdot V - 1.12 \cdot V^2 & R = 0.99943 & \text{RMSe} = 0.1127 \end{array} \qquad (4.26)$$

Following the calibration an attempt was made to estimate simultaneously the oxygen transfer coefficient and utilization rate using some of the techniques described in Section 4.5.2. Examination of the DO measurements at the three monitoring locations, showed distinct differences in its dynamic behaviour as a result of the near plug-flow hydraulic regime in the reactor. The DO gradient between the monitoring locations was significant during the experimental trials, so the effect of the oxygen mass transport was considered to be of some importance. For this reason the oxygen transport component was included in the DO model. Modelling the mass transport was facilitated by representing the reactor with four units in series and assuming that the DO gradient in each unit was constant. These units were assumed to extend between the fixed probes, where the DO concentration was measured, and the physical boundaries of the reactor, shown schematically in Fig. 4.14. The following differential equations were derived for the first three compartments describing the DO dynamics at the three monitoring locations :

$$\frac{dC_i}{dt} \doteq K_{LAi} \cdot (C_{SAT} - C_i) - OUR_i + \frac{Q_i + Q_r}{V_{i-1}} \cdot (C_{i-1} - C_i) \qquad (4.27)$$

where; subscript $i = 2, 3, 4$ refers to the conditions at probe 2,3,4 respectively,

$C_1 = 0.1\ mg/l$ assumed inlet DO concentration to the reactor,

V_i volume of each compartment $[L^3]$.

The analytical solution of the above differential equation is given by :

$$C_i(t+\Delta t) = a_i \cdot C_i(t) + b_i \tag{4.28}$$

where; $a_i = exp[(-K_{LAi} - \frac{Qi+Qr}{V_{i-1}}) \cdot \Delta t]$ (4.28a)

$$b_i = [V_{i-1} \cdot (K_{LAi} \cdot C_{SAT} - OUR_i) + (Qi+Qr) \cdot \overline{C}_{i-1}] \cdot \frac{(1-a_i)}{V_{i-1} \cdot K_{LAi} + Qi + Qr} \tag{4.28b}$$

$\overline{C}_{i-1} = 1/N \ \sum_{k=1}^{N} C_{i-1}(t_k)$ mean input DO concentration over the integration period.

The monitoring interval was 15 seconds, however the lag time (Δt) between the regressors in eq. 4.28 was chosen to be 60 seconds. This intended to reduce the effect of serially correlated measurement errors and increase the accuracy in the estimates as suggested by Howell et al. (1984). The non-adaptive estimation of parameters a and b was conducted by five different methods for comparison of the results. The first three methods involved linear regression techniques using the simple and orthogonal least squares, as well as, the Instrumental Variables method, discussed in Section 4.5.2. The desired coefficients were then derived by rearranging eq. 4.28a & b.

$$\widehat{K_{LAi}} = -\frac{ln(\hat{a}_i)}{\Delta t} - \frac{Qi+Qr}{V_{i-1}} \tag{4.29a}$$

$$\widehat{OUR_i} = \left(C_{SAT} - \frac{\hat{b}_i}{1-\hat{a}_i}\right) \cdot \widehat{K_{LAi}} + \frac{Qi+Qr}{V_{i-1}} \cdot \left(-\frac{\hat{b}_i}{1-\hat{a}_i}\right) + \overline{C}_{i-1} \tag{4.29b}$$

The other two methods were based on non-linear programming via direct search optimization, employing the Rosenbrock's algorithm. The objective functions in the optimizations were the sum square error and absolute error in the predicted DO series. Hence, the optimization problems can be stated as :

$$\min_{\widehat{KLAi},\widehat{OURi}} J_1 = \sum_{k=1}^{N} (C_i(t_k) - \widehat{C}_i(t_k))^2 \tag{4.30a}$$

$$\min_{\widehat{KLAi},\widehat{OUR}} J_2 = \sum_{k=1}^{N} \left| C_i(t_k) - \widehat{C}_i(t_k) \right| \tag{4.30b}$$

where; $\widehat{C}_i(t_k)$ is given by solving equation 4.28.

The measurements from the first five experiments were used for parameter estimation. The last two experiments contained only a small number of observations, due to the low DO concentration throughout the reactor even at maximum aeration capacity. The measurements for each experiment were suitably truncated so that linearity between the lagged DO measurements was obtained, which serves as an indication of a constant OUR.

No	Probe	Time mean	Simple LSQ	Orthog. LSQ	I.V.	Optimization	
						Sq. error	Abs. err.
a.	Estimation of K_{LA} (min^{-1})						
	2	11:53	0.0400	0.0334	0.0213	0.0371	0.0375
1	3	11:55	0.0294	0.0283	0.0292	0.0427	0.0389
	4	12:05	-0.0043	-0.0046	-0.0042	0.0000	0.0000
	2	12:45	0.1374	0.1362	0.1363	0.1360	0.1388
2	3	12:46	0.0810	0.0801	0.0808	0.0757	0.0832
	4	12:50	0.0724	0.0721	0.0723	0.0811	0.0725
	2	13:30	0.0731	0.0722	0.0719	0.0723	0.0708
3	3	13:31	0.0419	0.0400	0.0380	0.0445	0.0420
	4	13:36	0.0453	0.0444	0.0453	0.0440	0.0542
	2	14:46	0.1387	0.1374	0.1376	0.1299	0.1298
4	3	14:51	0.0794	0.0769	0.0797	0.0812	0.0762
	4	14:58	0.0783	0.0765	0.0785	0.0808	0.0767
	2	15:22	0.0658	0.0585	0.0554	0.0614	0.0611
5	3	15:23	0.0623	0.0553	0.0619	0.0603	0.0603
	4	15:24	0.0673	0.0659	0.0664	0.0680	0.0684
b.	Estimation of OUR $(mg/l/min)$						
	2	11:53	0.7945	0.7353	0.6283	0.7699	0.7730
1	3	11:55	0.5857	0.5759	0.5841	0.6980	0.6639
	4	12:05	0.1103	0.1080	0.1110	0.1343	0.1368
	2	12:45	1.1696	1.1581	1.1596	1.1590	1.1820
2	3	12:46	0.6428	0.6345	0.6412	0.5968	0.6650
	4	12:50	0.4898	0.4871	0.4886	0.5611	0.4903
	2	13:30	0.8008	0.7920	0.7900	0.7958	0.7824
3	3	13:31	0.5752	0.5576	0.5399	0.5970	0.5744
	4	13:36	0.5099	0.5020	0.5099	0.4980	0.5839
	2	14:46	1.1857	1.1740	1.1749	1.1048	1.1046
4	3	14:51	0.6501	0.6281	0.6534	0.6663	0.6217
	4	14:58	0.6095	0.5940	0.6113	0.6329	0.5985
	2	15:22	0.8989	0.8311	0.8018	0.8639	0.8687
5	3	15:23	0.8136	0.7490	0.8095	0.8129	0.8129
	4	15:24	0.7991	0.7873	0.7916	0.8045	0.8072

Table 4.6. Simultaneous block estimation of K_{LA} and OUR.

The estimation results are presented in Table 4.6 and the following comments can be made :

- The various methods produced different estimates for K_{LA} and OUR as a result of the different assumptions made by each method. However this discrepancy can be also attributed to: possible occurrence of local optima in the optimization results; high sensitivity of parameter estimates to measurement errors and other unmodelled system disturbances. The short length of the DO transient curves would also affect the accuracy of linear regression techniques.
- The estimates of OUR showed a general upward trend with time, which was expected due to the declining DO concentration in successive experiments under maximum aeration capacity.
- The $\widehat{OUR}$ also exhibited some oscillations between successive deoxygenation and reoxygenation trials, particularly at the location of probe 2, for which there is no apparent explanation.

The DO concentration during the experimental trials exhibited significant variations as a result of the air-flow rate step changes. During high air supply the DO concentration was generally high in all monitoring locations for uninhibited biochemical activity. However during reduced aeration the DO concentration fell to very low levels throughout the reactor and oxygen limiting conditions were established. Under these conditions it was expected that the activity of aerobic organisms would be affected in the short-term, which would have a direct effect on their oxygen utilization rate.

For this reason the OUR was also determined independently in an isolated volume of mixed liquor in which any disturbance from oxygen transport and DO limitation were minimized. Furthermore, the mixed liquor was artificially aerated to a high initial DO concentration (80–90% saturation) and the subsequent fall in its concentration was monitored manually every 15 seconds. The DO dynamics in the absence of external aeration are given by :

$$dC/dt = -OUR \qquad (4.31a) \quad \text{or}$$
$$C(t) = C(0) - OUR \cdot t \qquad (4.31b)$$

Using linear regression the OUR and $C(0)$ were estimated from the slope and interception of the best fit line to the DO measurements and the results are summarized in Table 4.7 and in Fig. 4.15. The measurements were taken with a portable pHoX DO probe and contained insignificant measurement noise. Consequently the estimates of the OUR were consistent with small standard error. The linearity in the DO measurements, depicted by the high correlation coefficient, indicates that the OUR remained constant during each experiment. Comparing the OUR estimates with those obtained from the simultaneous estimation, they were generally lower in

value, particularly for probe 2. These OUR estimates were subsequently used for the estimation of K_{LA} coefficient alone, using the on-line DO measurements.

No	Probe	Time mean	C_{SAT} mg/l	OUR $mg/l/min$	Std. error mg/l	R ($C(t)$ vs t)
1	4	11:54	10.2	0.1566	1.080E-3	0.99816
2	2	12:45	10.2	0.6036	2.086E-3	0.99975
3	3	13:19	10.1	0.5691	1.443E-3	0.99987
4	4	13:45	10.1	0.3160	1.476E-3	0.99974
5	2	14:54	10.1	0.6326	1.948E-3	0.99983
6	3	15:21	10.1	0.5910	1.288E-3	0.99989
7	4	15:52	10.1	0.5282	1.691E-3	0.99980
8	2	16:18	10.1	0.6640	2.899E-3	0.99967

Table 4.7. Independent estimation of OUR by simple least squares

No	Exper.	Probe	Time mean	OUR $mg/l/min$	K_{LA} (1) min^{-1}	K_{LA} (2) min^{-1}
		2	11:53	0.5918	0.01720	0.01706
1	Deox.	3	11:55	0.5554	0.02570	0.02581
		4	11:55	0.1566	0.00308	0.00277
		2	12:45	0.6036	0.07675	0.07689
2	Reox.	3	12:46	0.5690	0.07272	0.07273
		4	12:50	0.2360	0.04183	0.04160
		2	13:30	0.6137	0.05244	0.05238
3	Deox.	3	13:31	0.5720	0.04167	0.04182
		4	13:45	0.3160	0.02244	0.02238
		2	14:54	0.6326	0.07810	0.07810
4	Reox.	3	14:51	0.5858	0.07220	0.07209
		4	14:58	0.4380	0.05795	0.05784
		2	15:22	0.6429	0.03752	0.03680
5	Deox.	3	15:23	0.5920	0.03682	0.03636
		4	15:24	0.4811	0.03133	0.03120
		2	15:49	0.6532	0.07523	0.07470
6	Reox.	3	15:49	0.5959	0.07131	0.07125
		4	15:49	0.5230	0.06686	0.06679
		2	16:09	0.6606	0.06142	0.06106
7	Deox.	3	16:09	0.5993	0.04806	0.04932
		4	16:09	0.5562	0.04491	0.04439

Table 4.8. Estimation of K_{LA} for a fixed OUR by optimization.

The OUR value for the particular time of each experimental trial was calculated by linear interpolation or extrapolation from the existing estimates. Subsequently the K_{LA} coefficient was estimated alone via direct search optimization using the same model as before (eq. 4.28 & 4.30) and the results are presented in Table 4.8.

4.6.3 Relation between K_{LA} and air-flow rate

The estimates of K_{LA} for each monitoring location were then related to the corresponding air-flow rates. Since the air was supplied by two main downpipes and distributed by a large number of diffuser domes, it was not possible to determine the exact amount of air supplied to each monitoring location. It was assumed therefore that the first downpipe supplied the front half of the channel while the second supplied the rear half. Accordingly, the estimated K_{LA} at probe 2 was related to the air-flow of the first downpipe, and the K_{LA} at the other two probes was related to the flow of the second downpipe.

Linear relationships between K_{LA} and air-flow rate (Qa) have been used by several workers such as Holmberg (1981), Cook (1984c), Yust et al. (1981), Olsson et al. (1985) and Goto et al. (1985), although some authors have used a power function (Chen et al. 1980 ; Fujimoto et al. 1981). Here, due to the small number of observations and the relatively high degree of linearity between the two variables, a simple linear equation was fitted having the form :

$$K_{LA} = k_1 \cdot Qa + k_2 \qquad (4.32)$$

Method	Determinant	Probe 2	Probe 3	Probe 4
	Air flow	Qa_1	Qa_2	Qa_2
	Corr. coef.	0.99335	0.92495	0.86737
Simple	k_1	0.1281E-2	0.7863E-3	0.8221E-3
LSQ	k_2	0.3714E-2	0.1915E-1	0.3334E-2
	C.O.D.	0.98674	0.85552	0.75233
	Std. err.	2.4508E-3	6.8171E-3	9.9505E-3
Orthog.	k_1	0.1262E-2	0.7648E-3	0.7966E-3
LSQ	k_2	0.4536E-2	0.2007E-1	0.4420E-2
	C.O.D.	0.98651	0.85488	0.75161
	Std. err.	2.4724E-3	6.8323E-3	9.9651E-3
Instrum.	k_1	0.1284E-2	0.6750E-3	0.8738E-3
Variable	k_2	0.3578E-2	0.2389E-1	0.1131E-2
	C.O.D.	0.98673	0.83837	0.74935
	Std. err.	2.4514E-3	7.2104E-3	10.010E-3

Table 4.9. Relationship between K_{LA} and air-flow rate.

The parameters k_1 and k_2 were estimated by three different methods, namely the simple and orthogonal least squares and the Instrumental Variables and the results are presented in Table 4.9 and Fig. 4.16. Differences in the parameter estimates can be observed, particularly for probes 3 and 4 for which poorer linear correlation was obtained. Among the three methods the orthogonal least squares was considered as the most appropriate, since measurement error was expected in both regressors.

4.7 Estimation and importance of real-time *OUR*

4.7.1 Real-time *OUR* estimation

After the oxygen transfer coefficient had been determined as a function of the air-flow rate, it was possible to estimate the oxygen utilization rate from measurements of the *DO* concentration. For this purpose the *DO* concentration was monitored every 5 minutes over a 3-day period, under maximum capacity of the aeration system. The *DO* profile showed a distinct diurnal variation, (Fig. 4.17), falling below 1 mg/l in all locations during the afternoon and evening hours and increasing to high levels during early morning hours until about midday.

The *DO* dynamic equation 4.27 can be employed again to estimate the *OUR*, when both the K_{LA} coefficient and the flow rate through the reactor are known. During normal process operation the *DO* concentration at any point in the reactor changes rather slowly with time, so that the differential term dC/dt, is small compared with the oxygen transfer and utilization terms. Neglecting the differential term, the following non-dynamic equation was derived for the *OUR*:

$$\widehat{OUR}i(t) = \widehat{K_{LA}}i(Qa) \cdot (C_{SAT} - C_i(t)) + \frac{(Qi + Qr)_t}{V_{i-1}} \cdot (C_{i-1}(t) - C_i(t)) \quad (4.33)$$

In case that the oxygen transport component is small compared to the other components in the above equation, or in the absence of continuous flow measurements, the *OUR* can be estimated from continuous *DO* and air-flow measurements only from the equation:

$$\widehat{OUR}i(t) = \widehat{KLa}i(Qa) \cdot (C_{SAT} - C_i(t)) \quad (4.33a)$$

Comparison of the *OUR* estimates obtained from eq. 4.33 and 4.33a, using typical average values for the flows ($Qi = 800\ l/s$, $Qr = 220\ l/s$), showed insignificant differences for periods of low *DO*, while the difference was more pronounced during *DO* transient periods (Fig. 4.18a) However, the overall effect of mass-transport upon the diurnal variation of *OUR* was considered to be minimal for most practical purposes of using the *OUR* estimates.

The above methods for estimating OUR do not account for the effect of random noise in the DO measurements or for unmodelled system disturbances. The effect of noise can be reduced by smoothing the DO measurements with the Kalman Filter algorithm described by equation 4.25. Alternatively, the OUR can be estimated from a stochastic DO model as a time-varying parameter by applying adaptive estimation algorithms, which account for both measurement error and unmodelled disturbances. The simplest DO model can be derived by neglecting the oxygen transport and the differential term (dC/dt), and the OUR can be estimated as a random walk variable. Hence:

$$C_i(t) = C_{SAT} - \frac{\widehat{OUR_i}(t)}{\widehat{K_{LA_i}}(Qa)} + \xi(t) \qquad (4.34)$$

$$OUR_i(t) = OUR_i(t - \Delta t) + \varsigma(t) \qquad (4.34a)$$

where; $\xi(t), \varsigma(t)$ are random noise terms.

Comparing the OUR estimates from the above model (eq. 4.34) with those obtained from eq. 4.33a, showed negligible differences, indicating that the effect of noise upon the estimates was insignificant, when using the above non-dynamic model. Application of the dynamic DO model (eq. 4.27,4.28) with the E.K.F. algorithm produced small difference in the OUR estimates compared to the non- dynamic estimates, which was evident only during DO transient periods (Fig. 4.18b). It is interesting to note that the inclusion of the dynamic term, considerably increased the effect of noise on the estimates. However application of the dynamic model in the linear form, given by eq. 4.28, reduced substantially the effect of noise in the results (Fig. 4.18c). This happened because the analytical solution of the dynamic model is non-linear with respect to OUR. As a result linearisation errors are encountered during the application of the E.K.F. which are exacerbated in the presence of measurement noise.

Finally, the OUR trajectories were estimated from the simplest model (eq. 4.33a), during the 3-day monitoring period and the results are shown in Fig. 4.19. In the absence of continuous flow readings the above model was shown to produce satisfactory results compared with more complex models, which are adequate for most practical purposes, considering the existence of noise in the DO measurements and the uncertainty in the $K_{LA} - Qa$ relationship.

4.7.2 Importance of OUR for process monitoring

The estimated trajectory of OUR at three locations along an activated sludge reactor can reveal important information about the inputs and operating conditions of the plant as discussed in Section 4.2. The daily variation of OUR reflects the variability

of both the hydraulic and organic input loading, while its profile indicates the degree of completion of biochemical reactions along the tank (Olsson & Andrews 1978). Low OUR towards the end of the reactor indicates an almost complete biodegradation associated with low organic substrate concentration and a higher than average degree of nitrification. On the contrary, a high and uniform OUR profile would indicate the presence of organic matter throughout the reactor which will eventually escape in the effluent.

From the OUR estimates (Fig. 4.19) it can be seen that the DO variation is directly reflected upon the daily OUR variation ; this was low during high DO levels and remained rather high at low DO concentrations. However during low DO, some inhibition of the aerobic reactions can be expected. In such cases the estimated OUR does not reflect the potential activity of the biomass under the particular loading and operating conditions, but the true biochemical activity under oxygen limiting conditions. Hence the OUR profile along a plug-flow reactor can serve as an additional indicator of biomass activity and degree of completion.

The OUR profile of a typical day is shown in Fig. 4.20 every 4 hours, and the substantial spatial variation of OUR during the day can be noticed. The readings at 4:00, 8:00 and 12:00 *hr* showed a rapid decline of OUR towards the end of the reactor, indicating completion of reactions, since the observed oxygen demand at the outlet is mainly due to biomass respiration. However the readings at 16:00, 20:00 and 24:00 *hrs* showed a high OUR throughout the reactor, due to the low DO concentration, indicating incomplete biodegradation. Hence, the OUR profile can be used in conjunction with the DO profile, suggested by Olsson & Andrews (1978), for continuous monitoring and even for control of the process.

Some workers have used the OUR for the reconstruction of unmeasurable process or input variables using simple process models, although the validity of such techniques has yet to be assessed. For example, Holmberg and Ranta (1982) attempted to estimate the biomass growth rate and reconstruct the input organic load for an activated sludge process without nitrification and reported satisfactory prediction of the input organic load variation. Marsili-Libelli (1984) reconstructed the reactor substrate and biomass concentration from OUR estimates using a low-order dynamic state observer. The observer performed well when the model parameters were known, but was rather sensitive to changes in some of the parameters.

However in the presence of significant nitrification, as in some activated sludge plants, or under simultaneous nitrification- denitrification, as in oxidation ditch plants, the previous estimations become more complex, due to the additional effect of those reactions upon the OUR. In order to isolate the effect of nitrification and denitrification, additional measurements of input ammonia would be necessary.

Furthermore, the effluent ammonia and nitrate concentration should be either measured or estimated using a process model. The development of estimation algorithms which account for nitrification and denitrification requires further research and will not be discussed in this study. The wider availability of reliable, on-line sensors in the future will assist the development of algorithms for real-time estimation of unmeasurable process inputs such as the organic load.

4.8 Summary

The limitations of the current monitoring practices, based on individual sample analysis, for monitoring the process performance and for operational control were discussed and compared with the potential advantages of "on-line" continuous monitoring techniques. The oxygen utilisation rate was shown to be an important process indicator which in addition can be determined in real time.

A simple model was developed to relate the daily oxygen demand and aeration energy with the processes of organic substrate metabolism, endogenous respiration, nitrification and denitrification in the oxidation ditch. The oxygen coefficients for the latter two processes were calculated stoichiometrically. For the former two processes the coefficients were estimated by linear regression and also adaptively by the E.K.F. Significant variation in the oxygen parameters was observed and was attributed to deficiencies in the model assumptions, the effect of unmodelled external factors and changes in the operating conditions. Nevertheless the simple model structure was considered adequate because it clearly showed the contribution of each process to the total oxygen demand, indicating that the largest part is used for endogenous respiration.

Next a procedure was presented for estimating the oxygen transfer coefficient and OUR from on-line DO measurements in an operating activated sludge plant. A number of block estimation methods were employed and their applicability discussed. Limitations were experienced during the simultaneous estimation of the two parameters leading to biased estimates and for this reason the parameters were estimated independently. The K_{LA} coefficient was linearly related to the air-flow rate and the relationship was then used for "real-time" estimation of the OUR from continuous DO and air-flow measurements. Finally the potential use of OUR and its profile in the reactor for improved process monitoring was discussed.

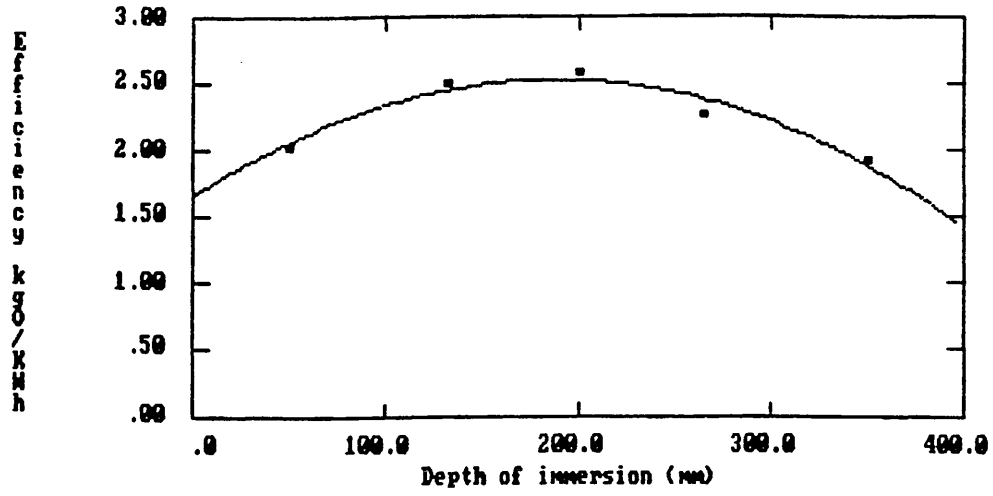


Fig. 4.1a. Aeration efficiency against aerator submergence (from Rachwal et al. 1983)

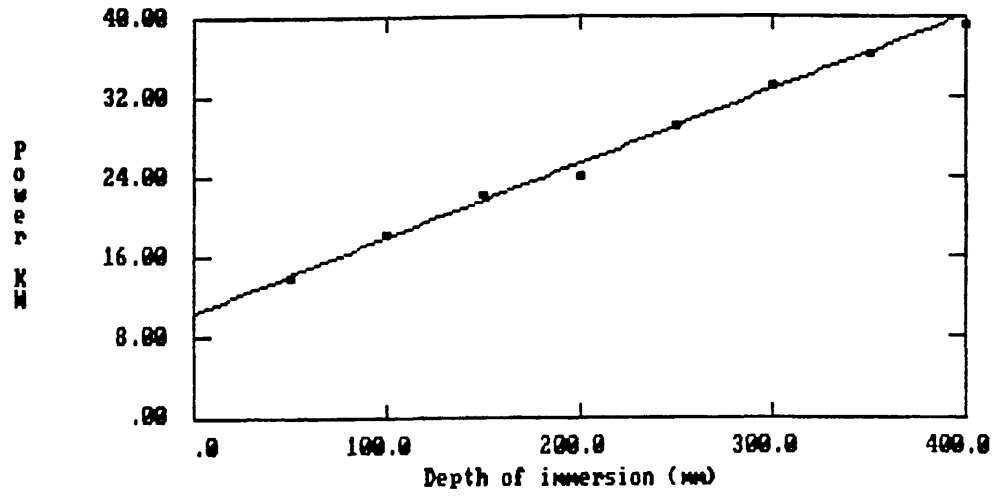


Fig. 4.1b. Power drawn against aerator submergence (from Rachwal et al., 1983)

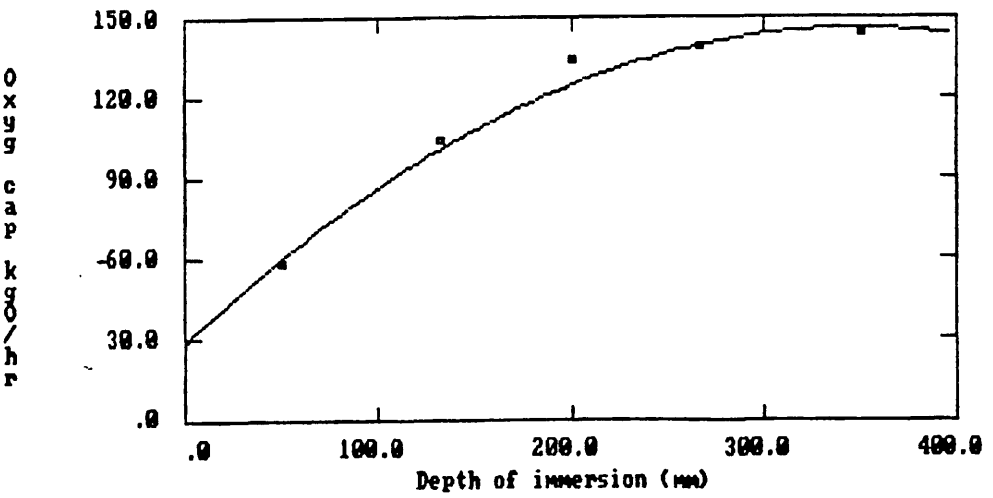


Fig. 4.1c. Oxygenation capacity against aerator submergence (from Rachwal et al., 1983)

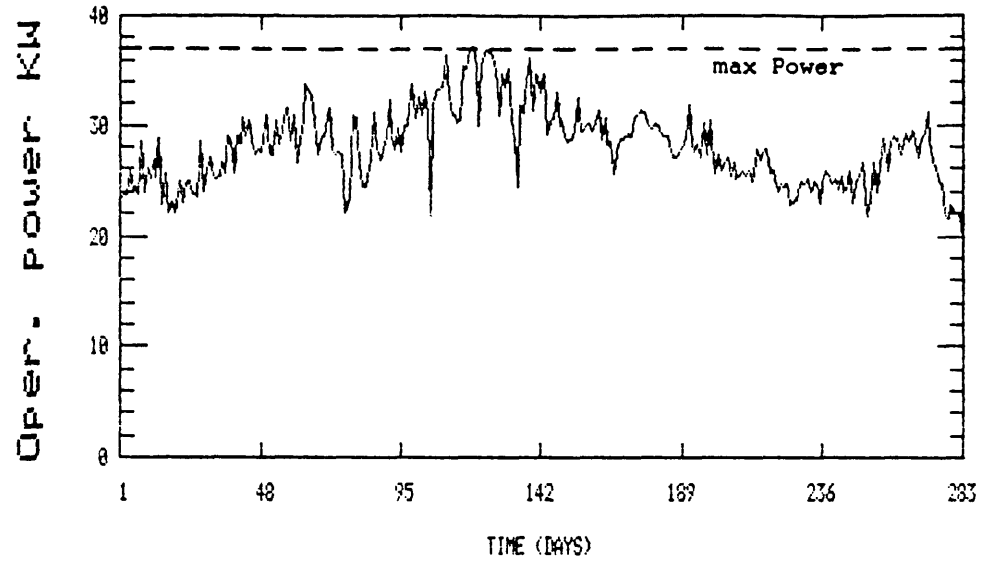


Fig. 4.2. Average daily power drawn per aerator during selected operating period

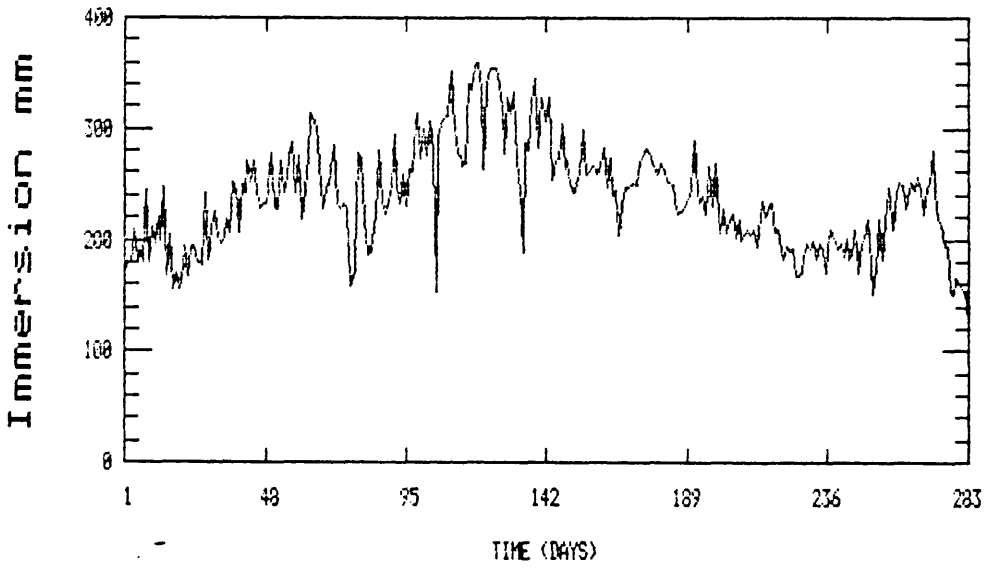


Fig. 4.3. Average daily immersion depth of aerators during selected operating period

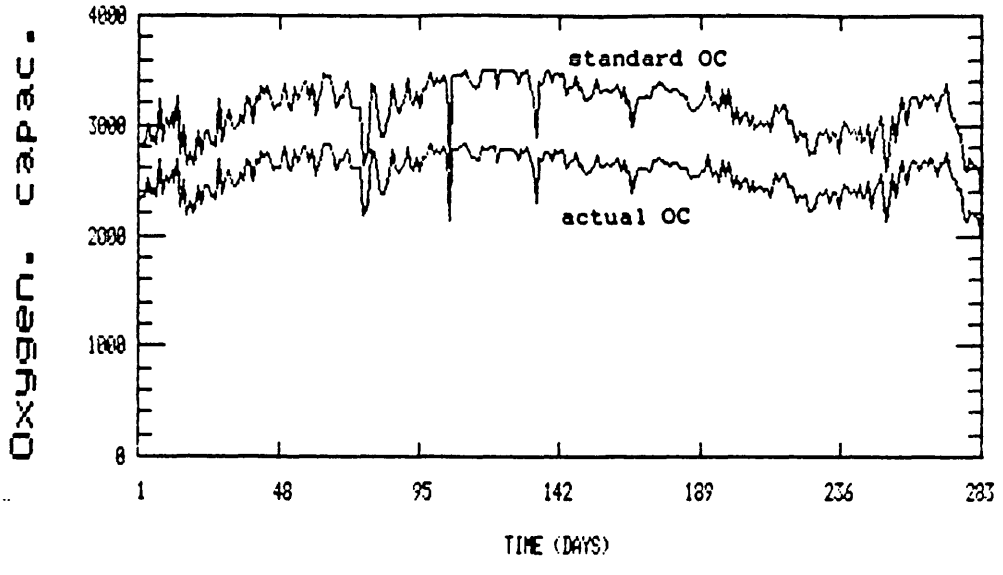


Fig. 4.4. Standard & actual oxygenation capacity

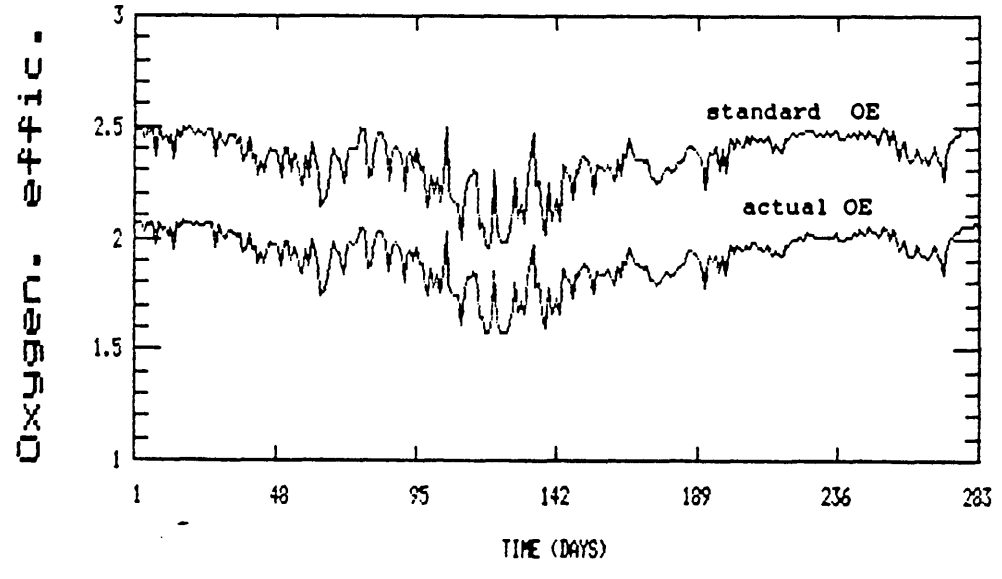


Fig. 4.5. Standard & actual oxygenation efficiency

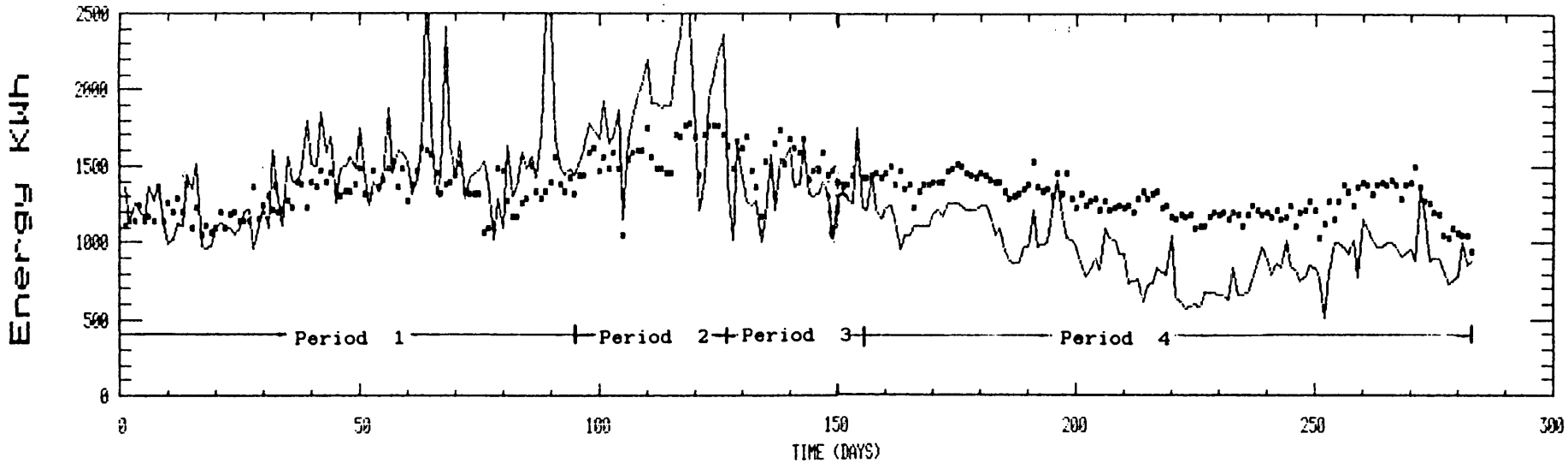


Fig. 4.6. Observed and predicted energy consumption (Case 1)

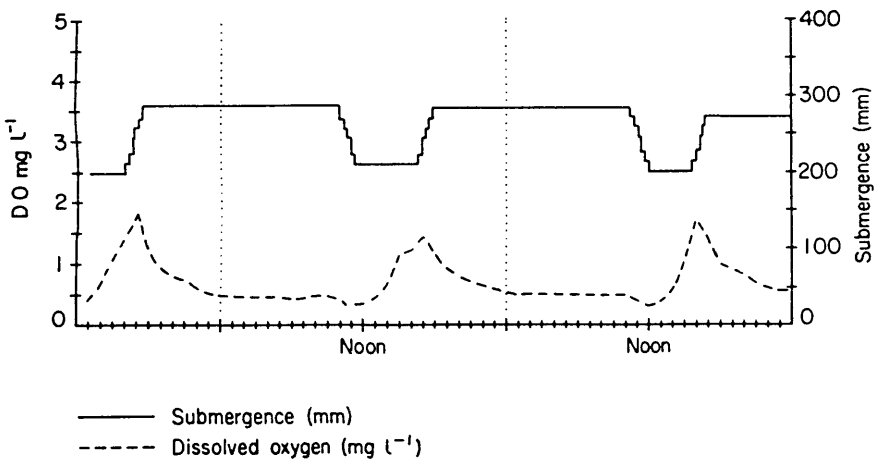


Fig. 4.7. Typical diurnal variation of aerator submergence, and *DO* (from Rachwal et al., 1983)

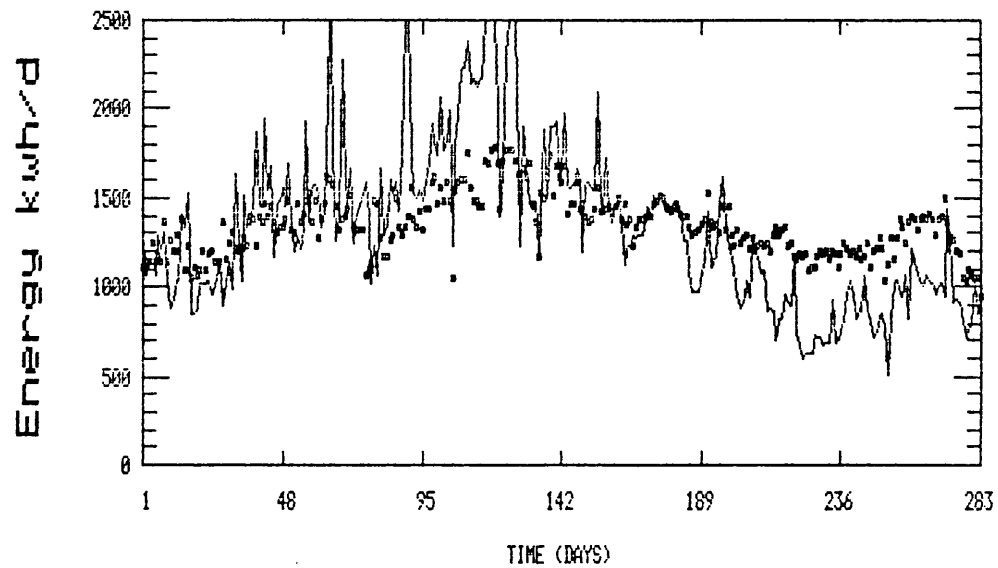


Fig. 4.8. Observed and predicted aeration energy (Case 2)

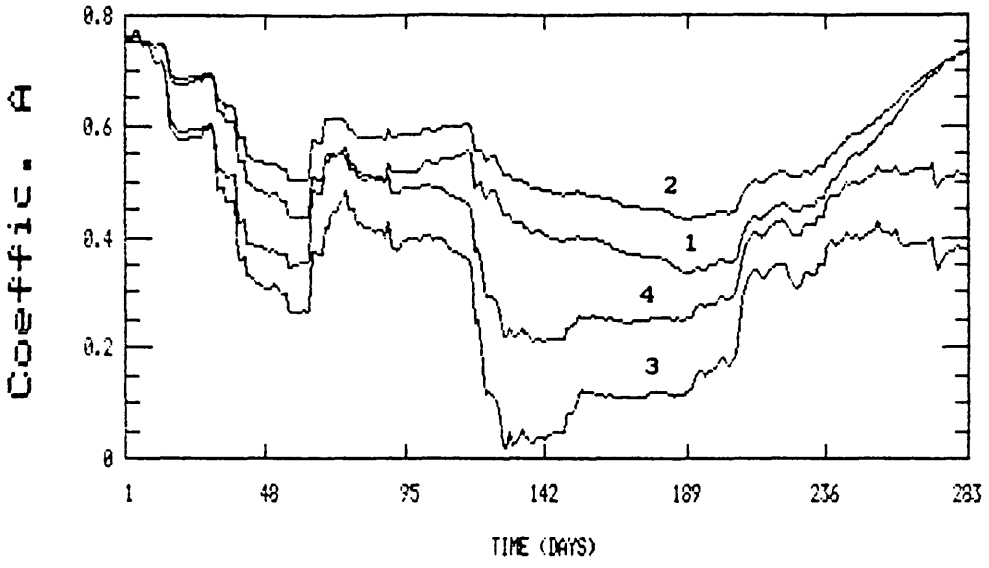


Fig. 4.9. Adaptive estimation of oxygenation coefficient *'a'*

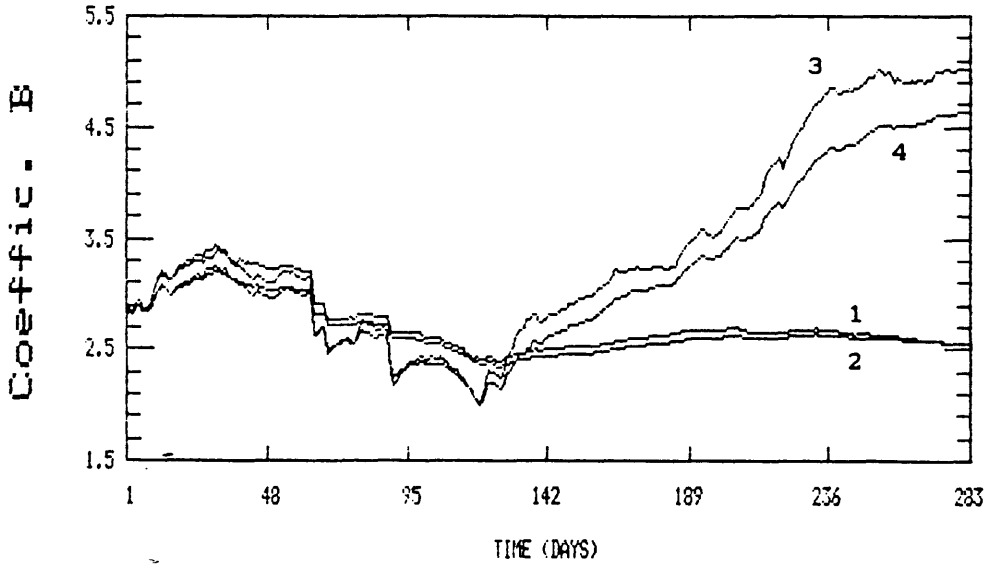


Fig. 4.10. Adaptive estimation of oxygenation coefficent *'b'*

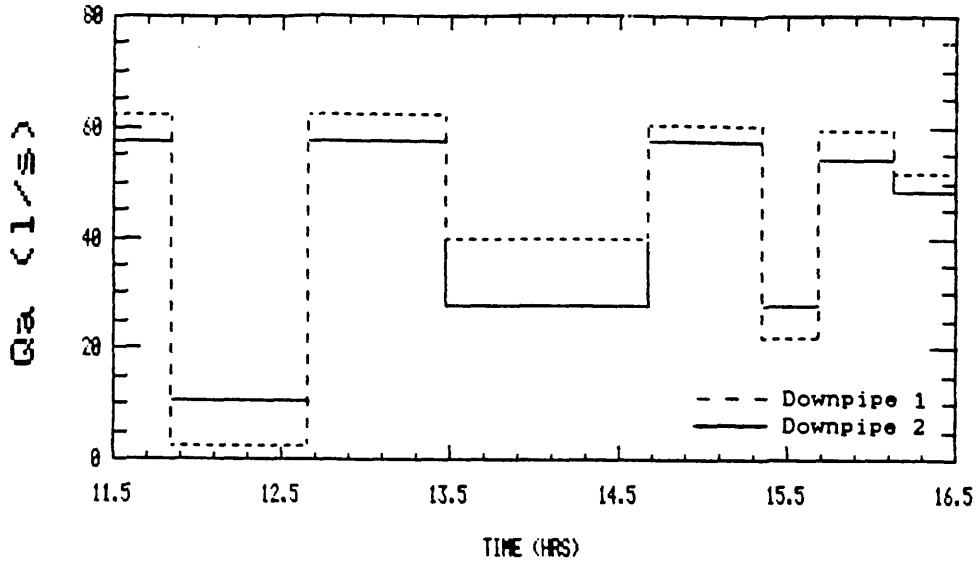


Fig. 4.11. Air-flow rate profile during the experiments

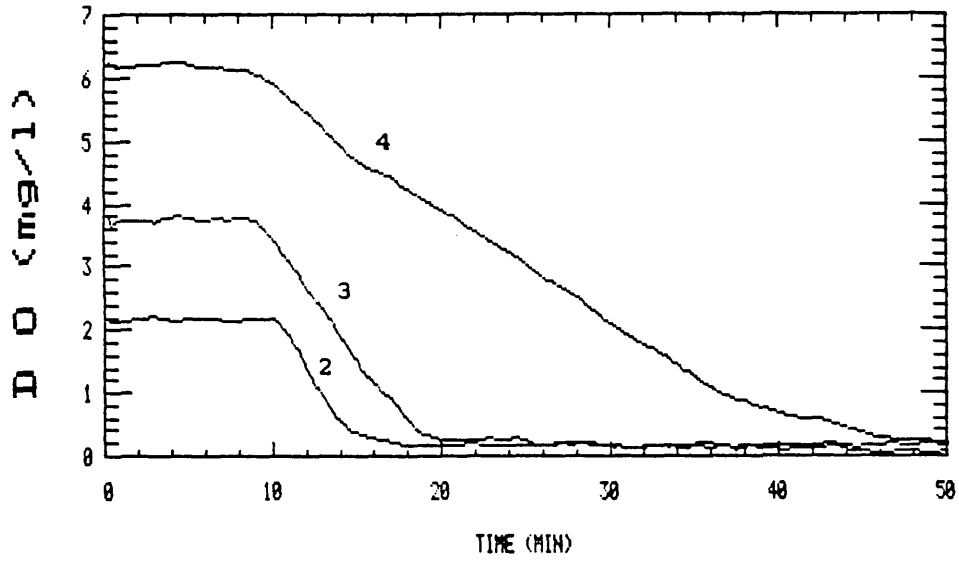


Fig. 4.12a. First deoxygenation trial (Exp. 1)

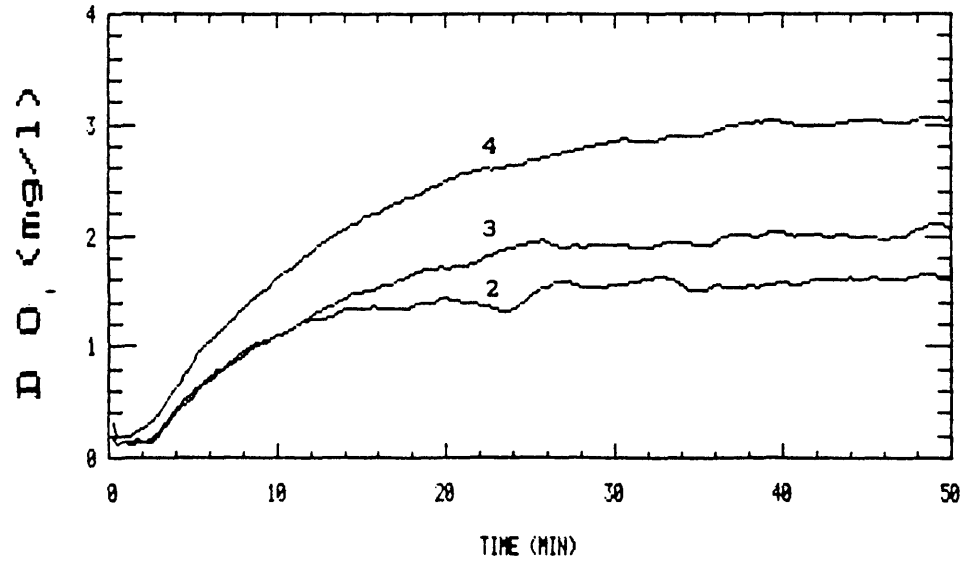


Fig. 4.12b. First reoxygenation trial (Exp. 2)

Fig. 4.12. On-line measurements of *DO* concentration (smoothed) for three locations

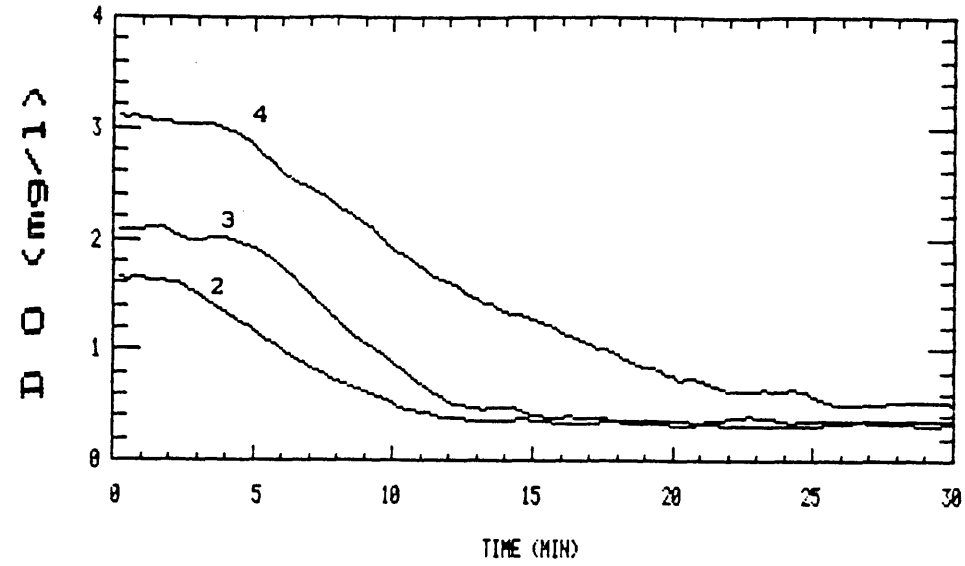


Fig. 4.12c. Second deoxygenation trial (Exp. 3)

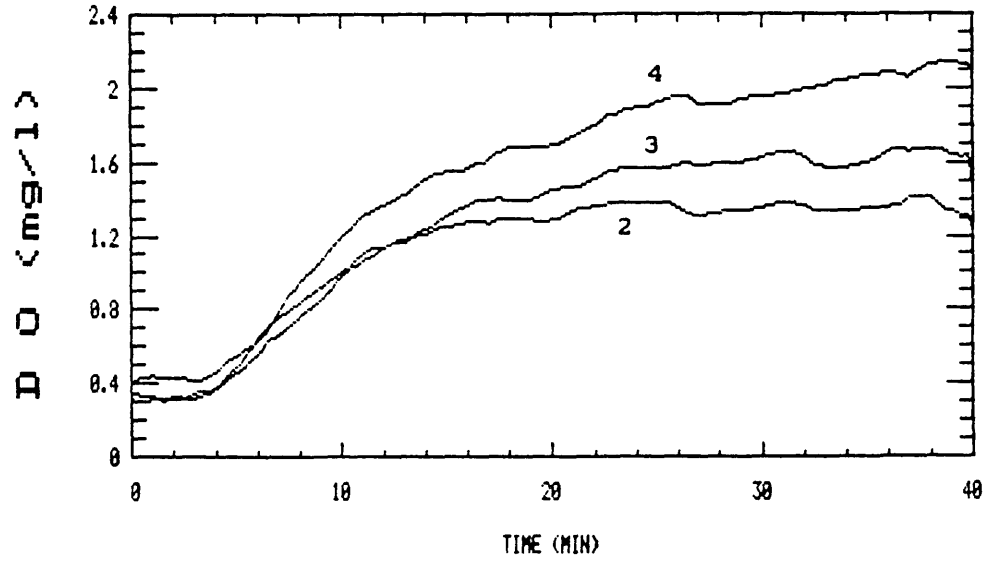


Fig. 4.12d. Second reoxygenation trial (Exp. 4)

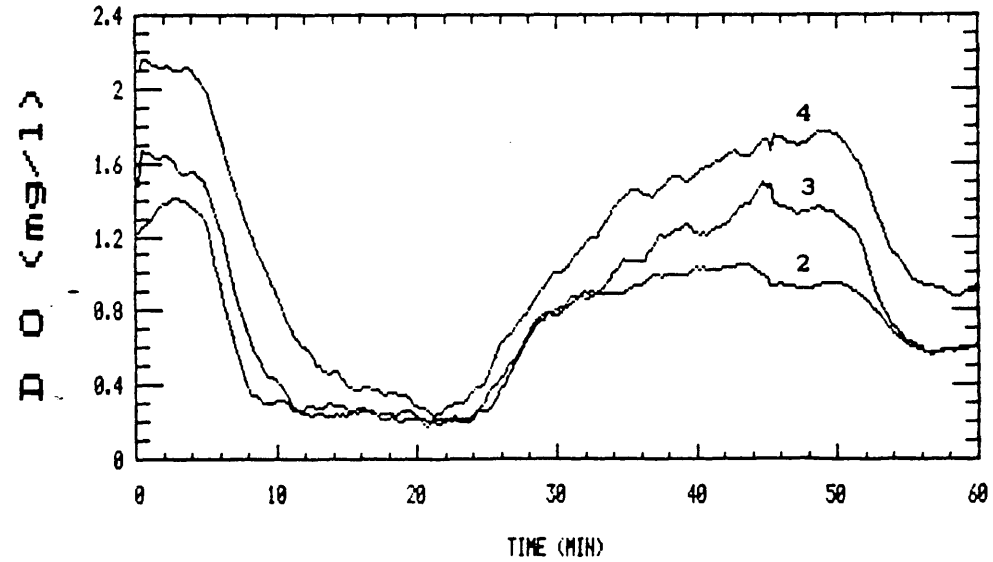


Fig. 4.12e. Experiments 5 to 7

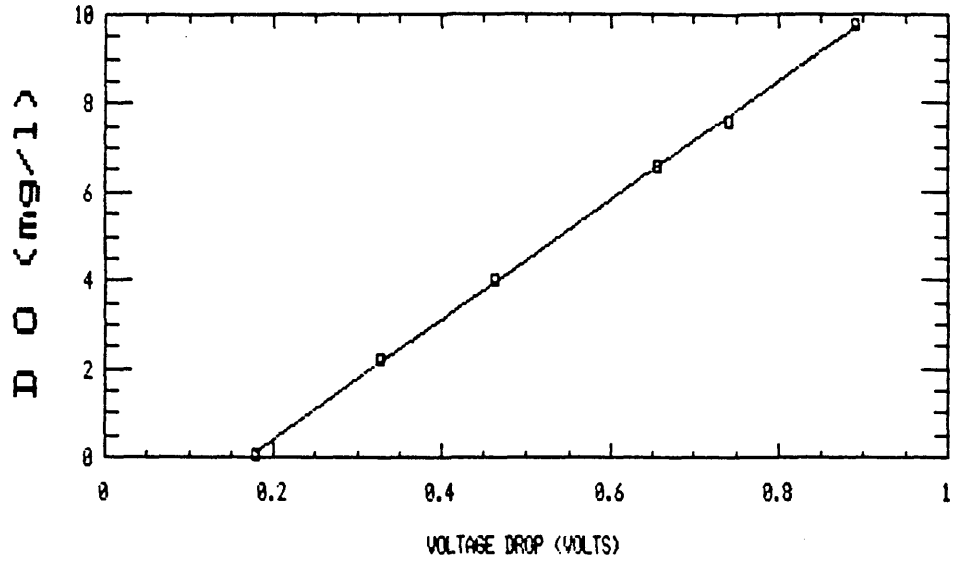


Fig. 4.13a. Calibration curve for Probe 2

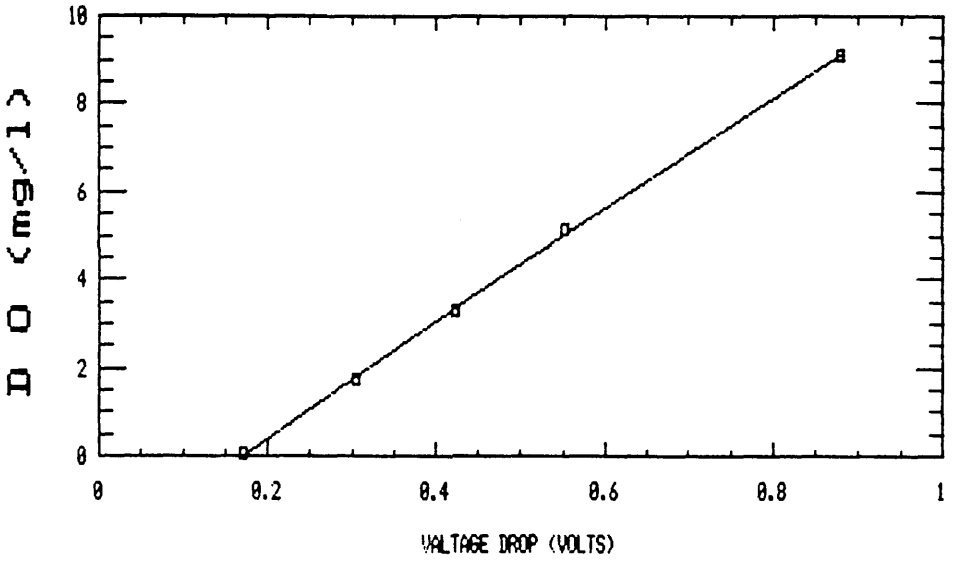


Fig. 4.13b. Calibration curve for Probe 3

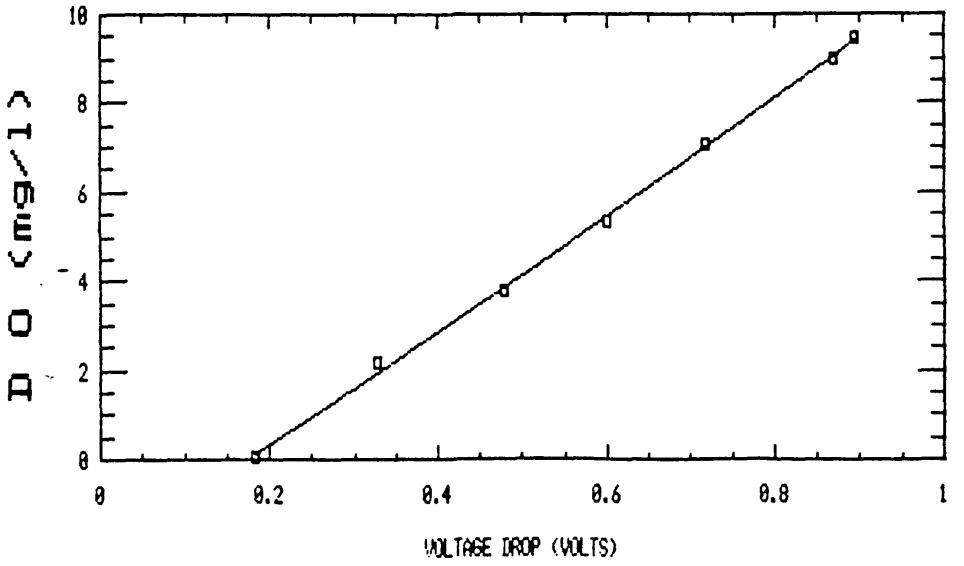


Fig. 4.13c. Calibration curve for Probe 4

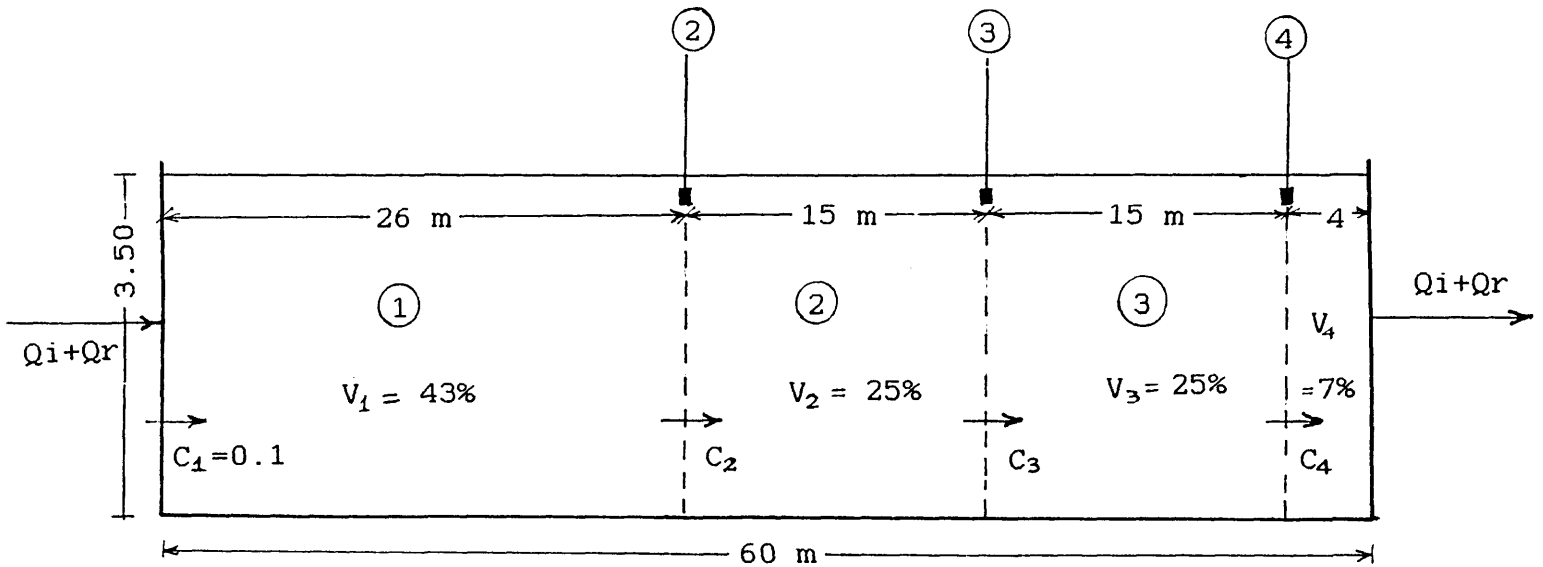
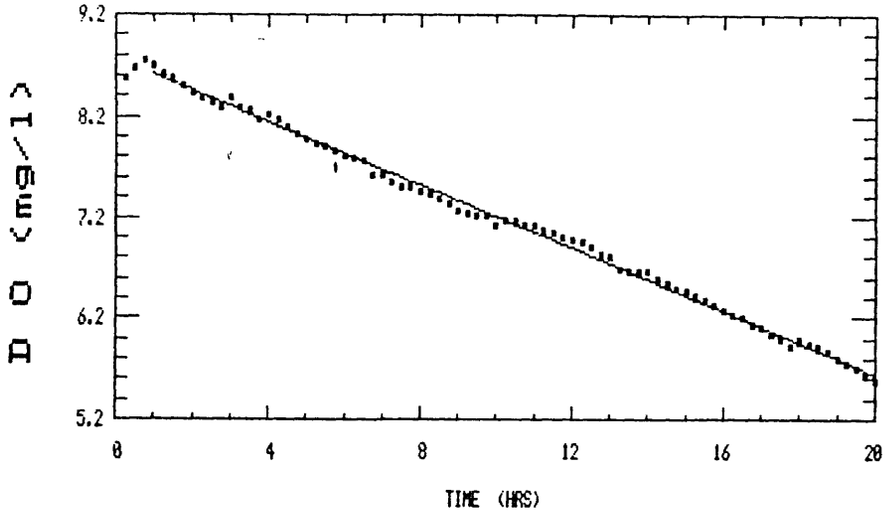
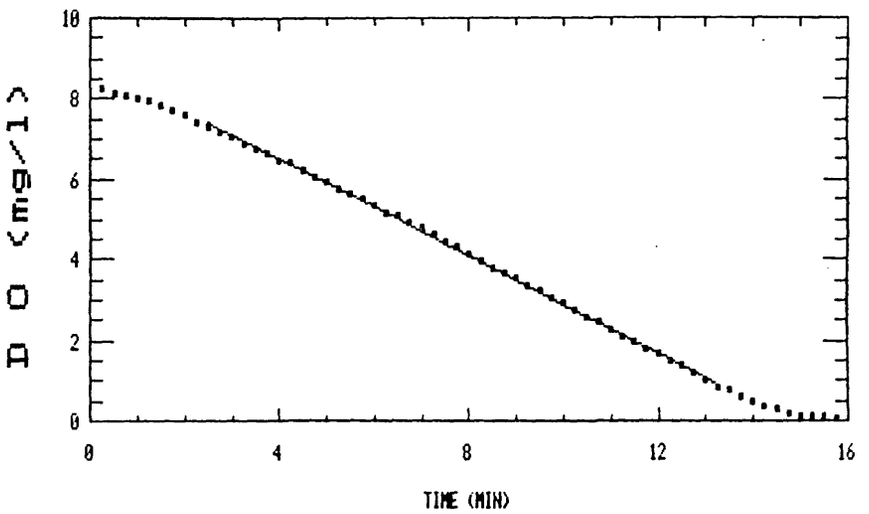


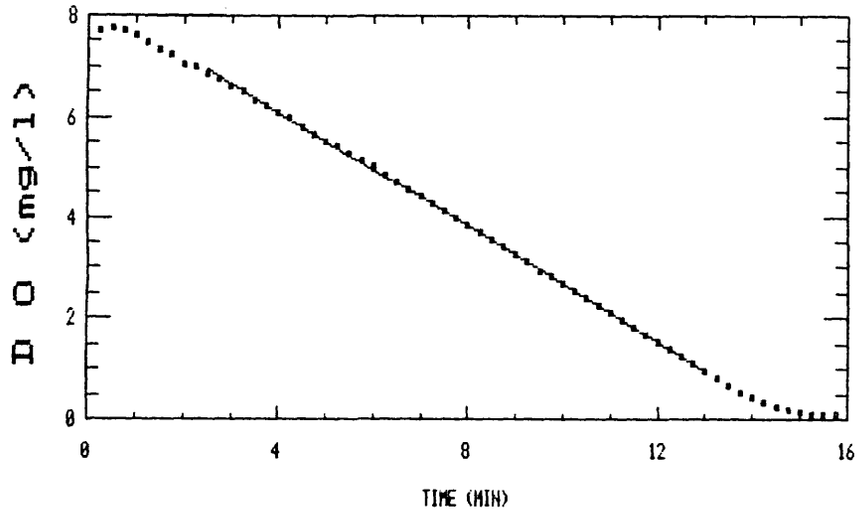
Fig. 4.14. Schematic representation of the activated sludge reactor



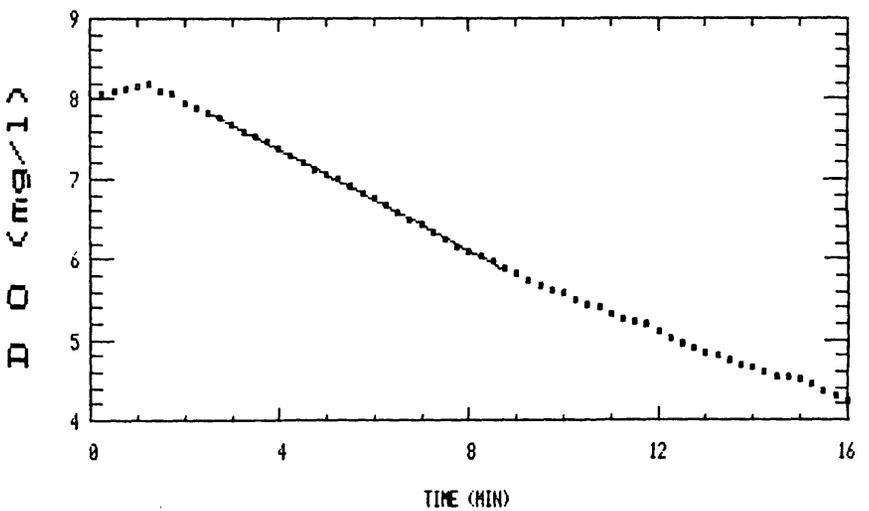
a. Experiment 1



b. Experiment 2

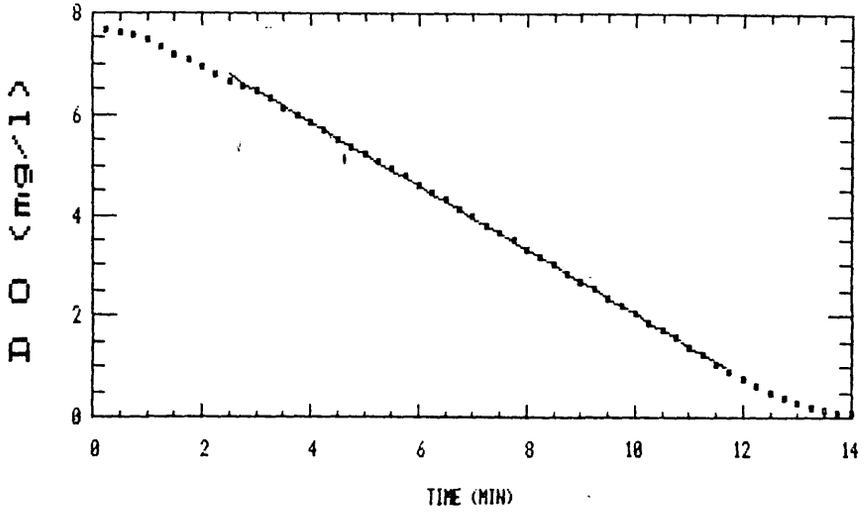


c. Experiment 3

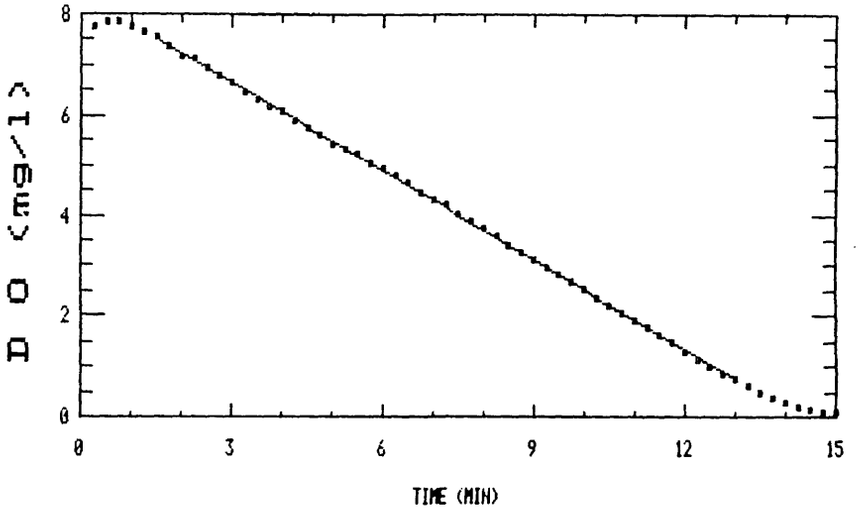


d. Experiment 4

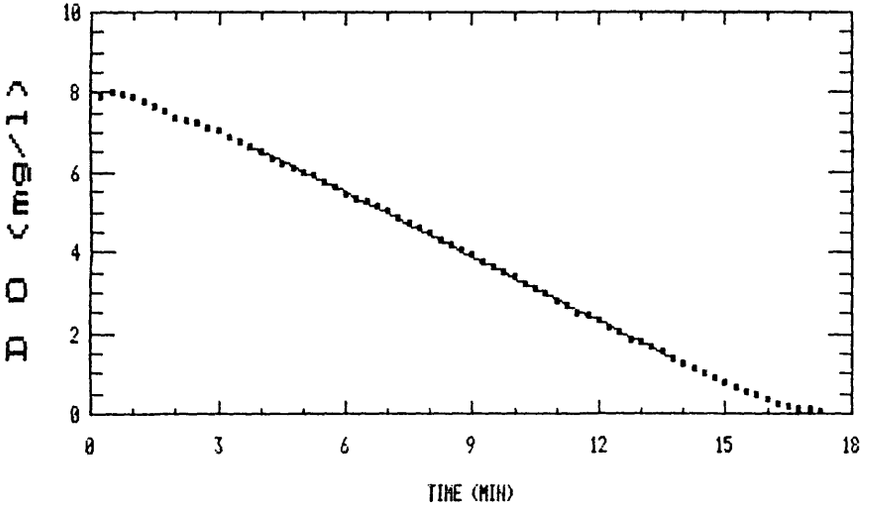
Fig. 4.15. Off-line DO monitoring for OUR determination



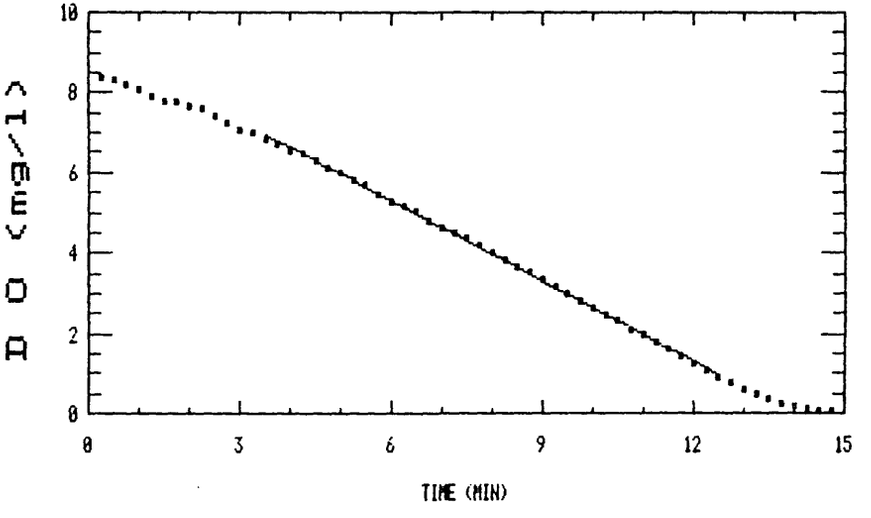
e. Experiment 5



f. Experiment 6

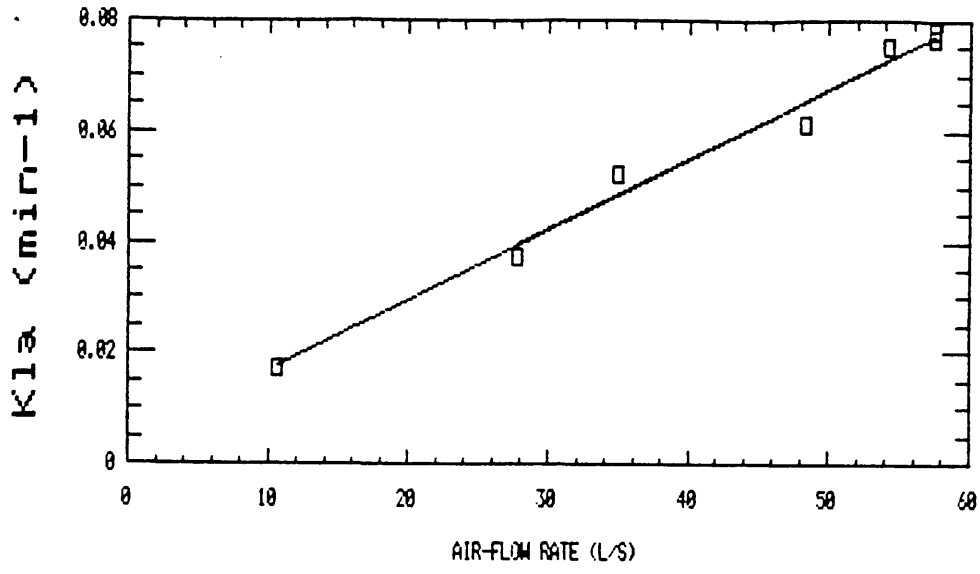


g. Experiment 7

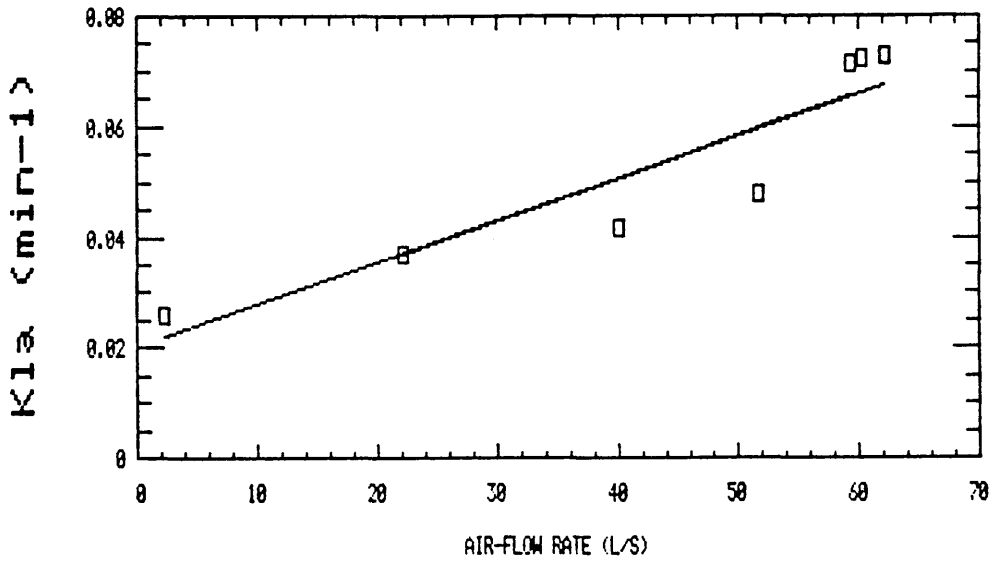


h. Experiment 8

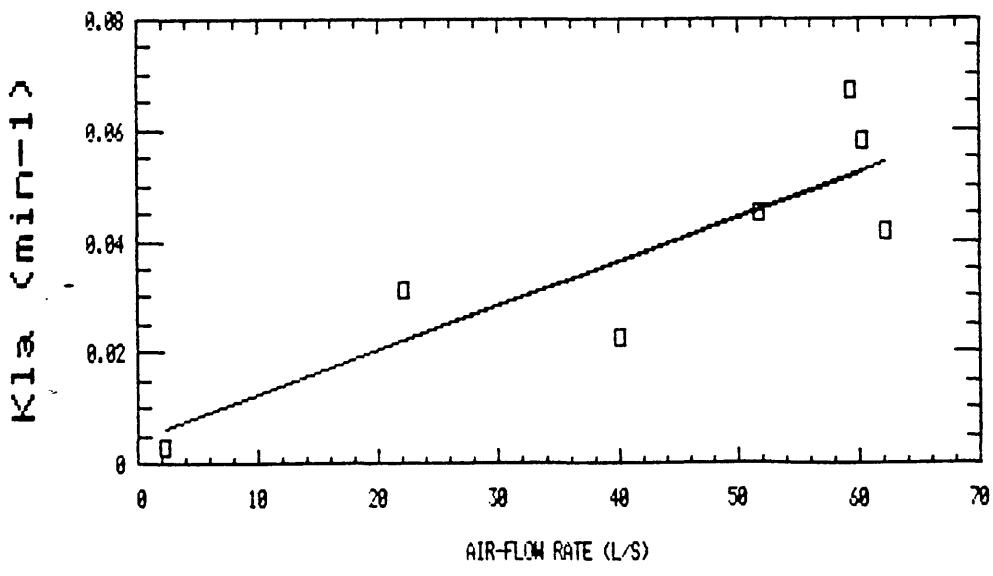
4.15. Off-line *DO* monitoring for *OUR* determination



a. For probe 2



b. For probe 3



c. For probe 4

Fig. 4.16. Relationship between K_{LA} and air-flow rate

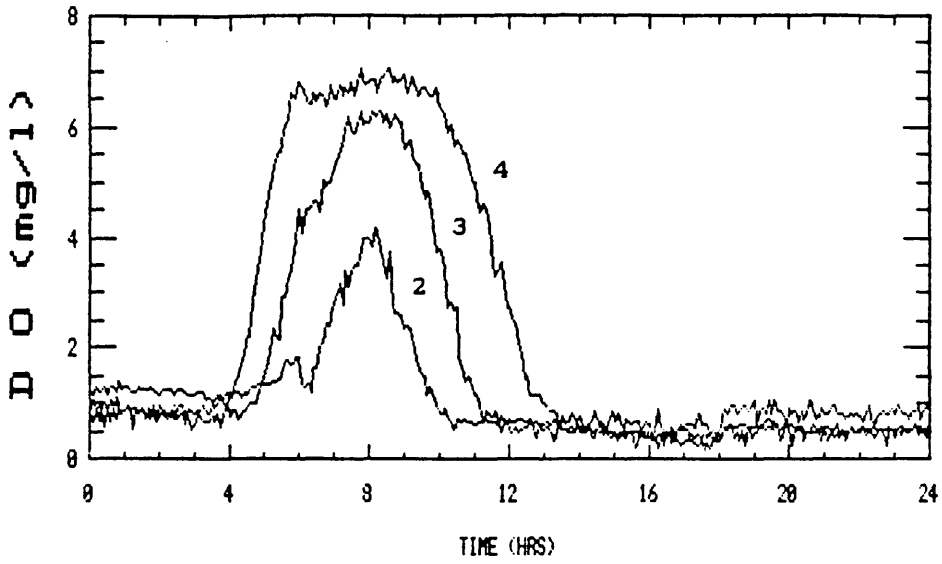


Fig. 4.17a. *DO* profile during 25/5/85

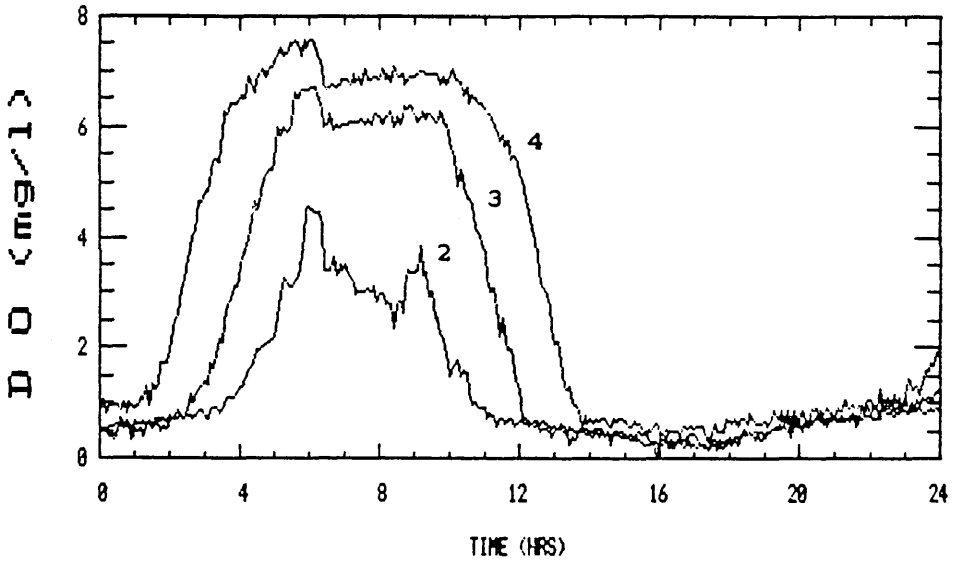


Fig. 4.17b. *DO* profile during 26/5/85

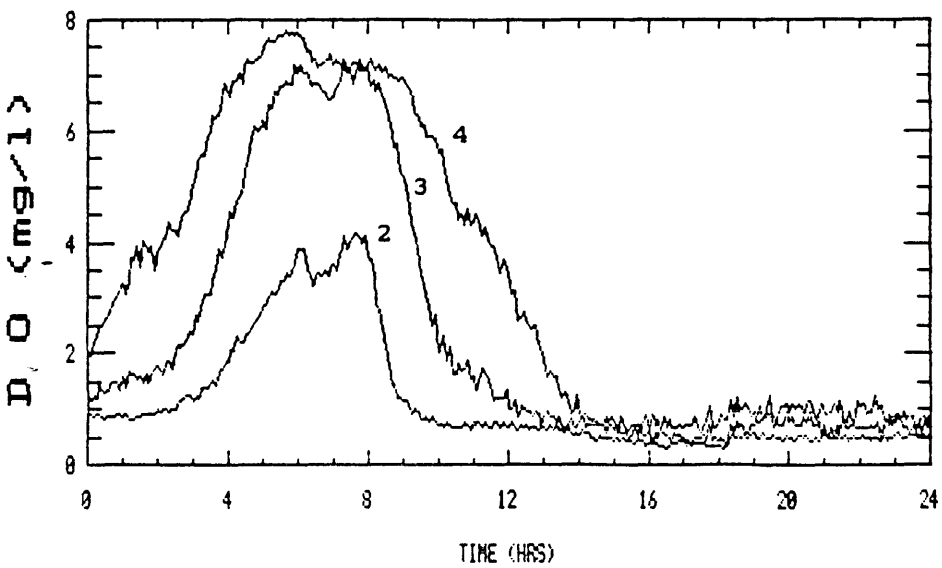


Fig. 4.17c. *DO* profile during 27/5/85

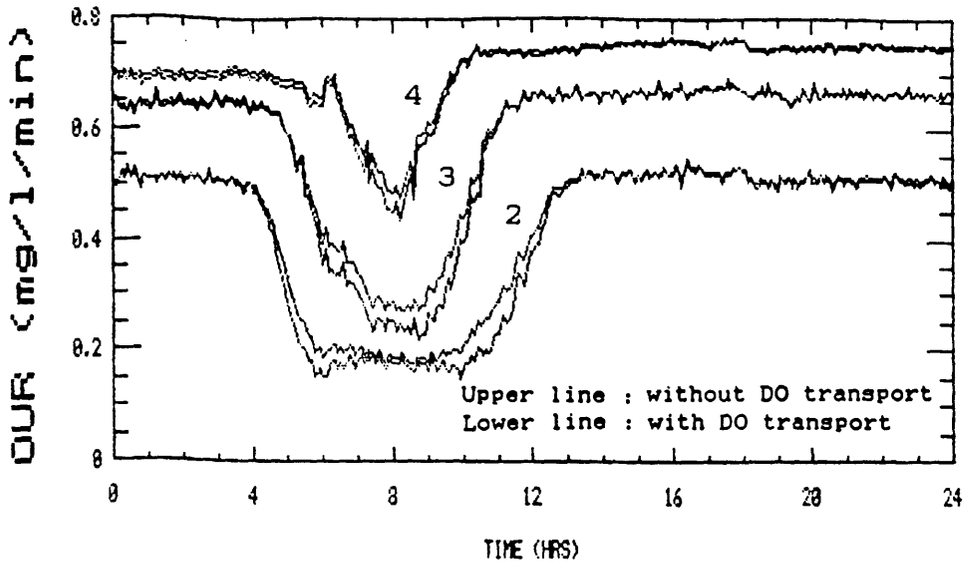


Fig. 4.18a. Effect of oxygen mass-transport upon the OUR estimates

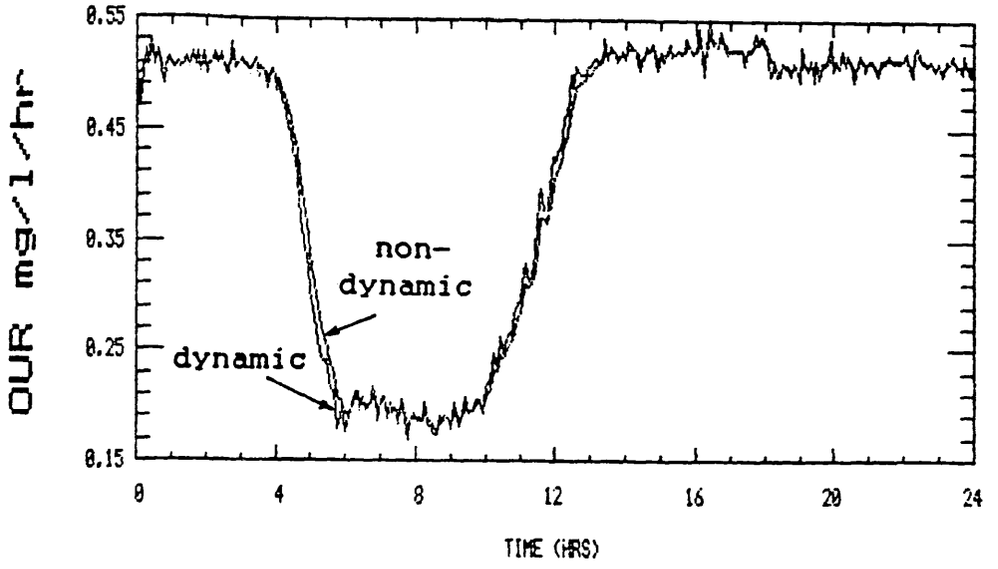


Fig. 4.18b. OUR estimates from a dynamic and non-dynamic DO model

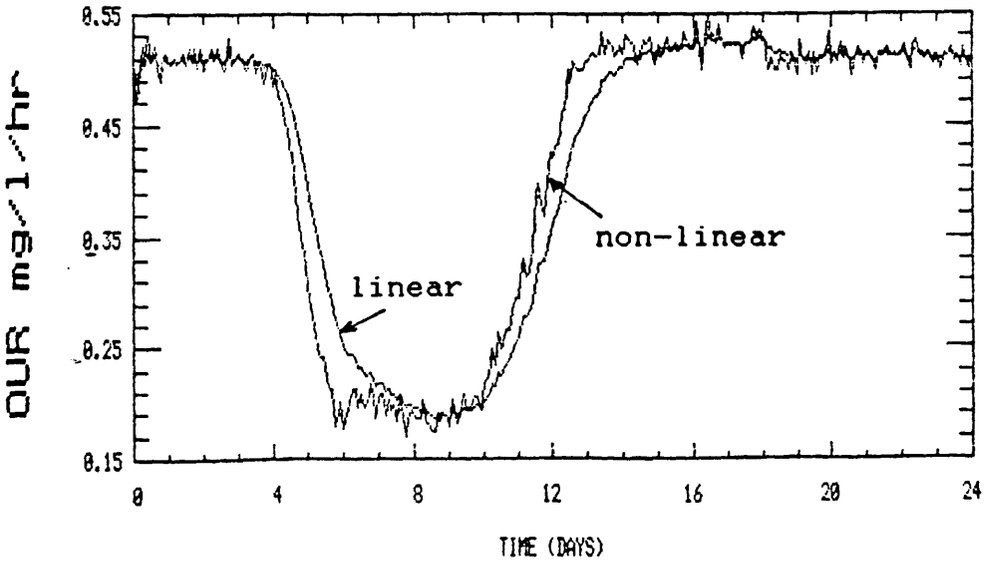


Fig. 4.18c. OUR estimates from the linear and non-linear dynamic DO model

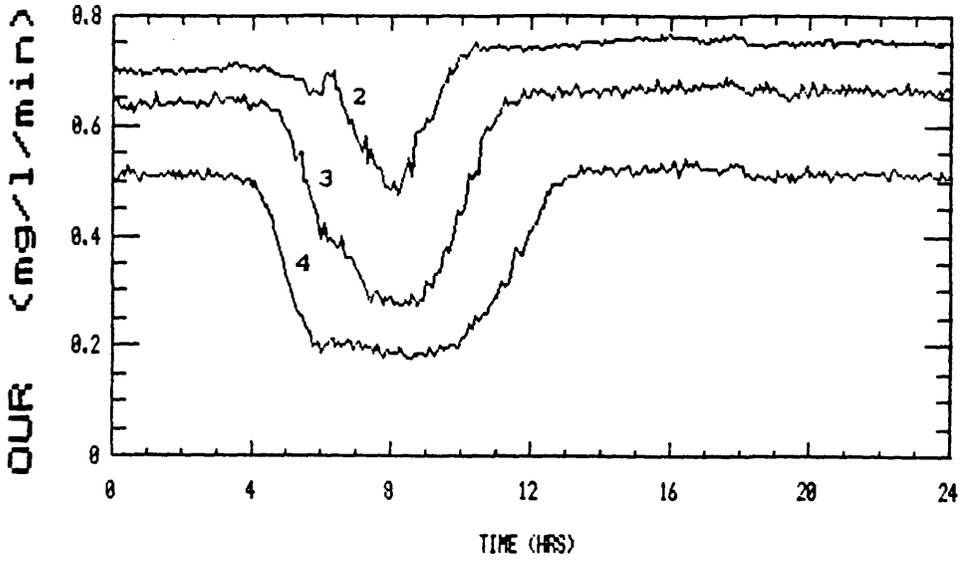


Fig. 4.19a. Estimated OUR profile during 25/5/85

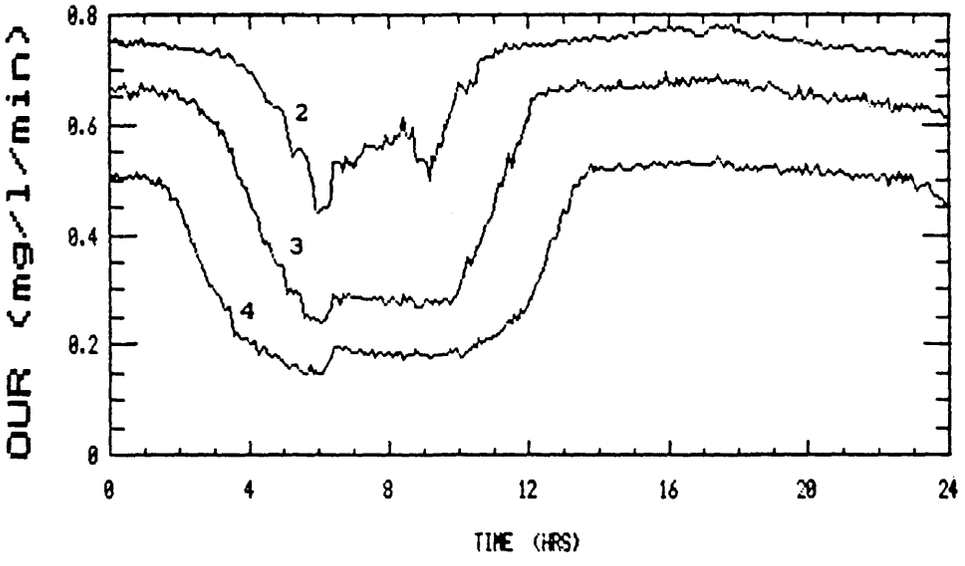


Fig. 4.19b. Estimated OUR profile during 26/5/85

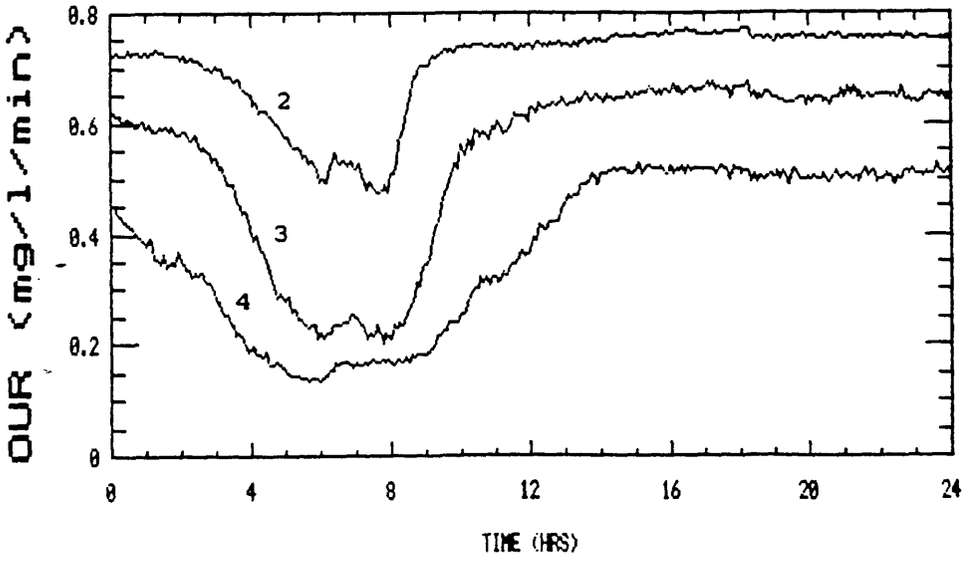


Fig. 4.19c. Estimated OUR profile during 27/5/85

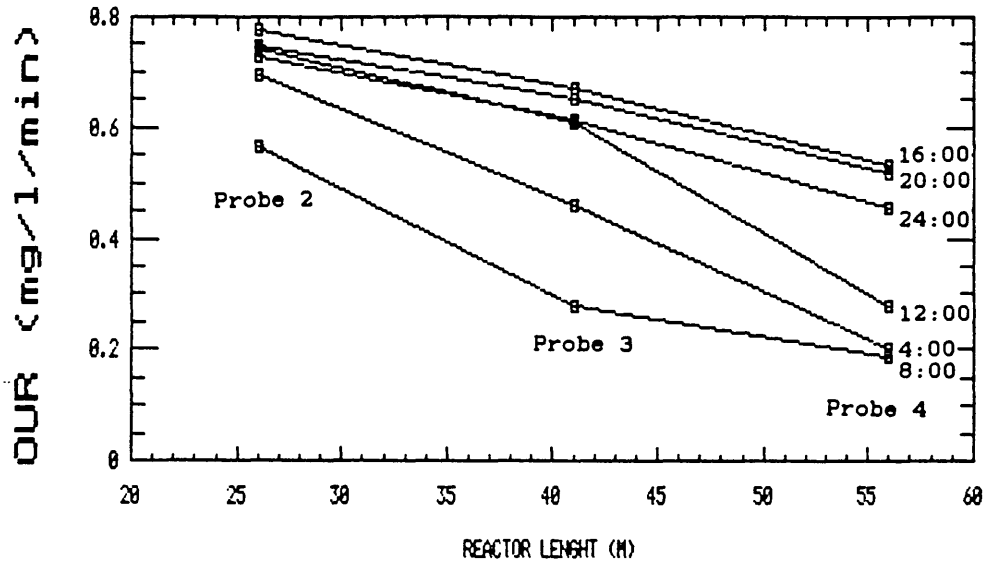


Fig. 4.20. *OUR* profile in the reactor during 26/5/85

5 Cost-Related Operational Control Strategies for the Oxidation Ditch Process

5.1 Introduction

The formulation of sensible operational control strategies for reducing running cost and improving performance in the oxidation ditch process was the ultimate objective of this study. So far, the study had focused on the development of a suitable model for the process, which could then be used both as a substitute to experimentation, for simulating process behaviour under various conditions, and as a rational basis for designing an efficient control system.

The incentive for applying operational control to wastewater treatment systems, arises from the desire to improve their effluent quality discharged into the rivers, and the growing need to minimize their operating cost as discussed in the Introduction (Sec. 1.1). These broad objectives however, form the overall framework, within which more specific operating targets may be defined, according to the particular requirements of each case and can be benefited from the application of process control and automation (Sidwick & Bonnick 1981 ; White 1981) such as:

- Produce an effluent quality complying with the imposed discharge standards; expressed by the BOD_5, SS or NH_3-N parameters.
- Minimize effect of serious process failures, such as sludge blanket spillage, loss of nitrification and bulking sludge.
- Reduce effluent quality variability ; caused by input load variations.
- Minimize energy consumption.
- Reduce manpower requirements, as well as, the number of unpleasant or dangerous tasks by introducing more instrumentation and automation to the works.
- Defer future extensions by increasing the overall efficiency of the process.

However the design and implementation of efficient control strategies faces many potential difficulties reducing their effectiveness. Such difficulties have hindered, to some extent, the wider application of automatic control in wastewater treatment systems (Lumbers, 1982) :

- The various inputs to the process are of a dynamic/stochastic nature. In addition unknown disturbances superimpose variations onto process dynamics together with measurement noise.

- The response to control actions varies significantly for different process variables, both in time and magnitude.
- There is a general scarcity of information, mainly due to lack of reliable on-line sensors, upon which to base the control system.
- The use of models in developing control algorithms also possesses some problems such as :
  - Although complex models may simulate the process satisfactorily, they cannot be used easily in the development of control algorithms.
  - Simplified models are more appropriate for control purposes, however the resulting control strategy may not be always successful.
- Not all of the required process variables can be measured directly and further the reliability of measured variables is not always known.
- The control action upon the manipulated process variables is usually bounded due to physical constraints.

As a result, the application of a closed-loop automatic control system was not pursued here and the intervening role of the operator was considered of primary importance. The objective was therefore, to provide sufficient information to the operator regarding an efficient means of operation and the expected future plant performance so that he can make better judgement of the likely actions to be taken.

5.2 Review of control strategies for the activated sludge process

5.2.1 Introduction

The many types of controllers commonly used in industrial processes have also been applied to the wastewater treatment processes, either through theoretical studies or on full-scale plants, with varying degrees of success. The main difference between controlling an industrial process and a wastewater treatment plant, lies in the different nature of inputs in the two processes. The inputs to the former process are either deterministic or exhibit small deviations from their reference value and are usually directly controllable. However in the latter process they are stochastic in nature and generally uncontrollable. This feature combined with the limited knowledge of the biochemical reactions in wastewater treatment, may reduce the efficiency of control schemes and has to some extent become an obstacle in the widespread application of manual or automatic control in process operation.

Although several studies have been undertaken on operational control of the activated sludge process in the past two decades, the control of the oxidation ditch process has not been sufficiently studied. Despite the operating differences between the two processes, a review of the current studies on activated sludge control could reveal the advantages and limitations of the proposed control tactics and identify strategies with potential to satisfy the operating objectives in the oxidation ditch process.

5.2.2 Design characteristics of control systems

Prior to designing a control system the potential 'control' and 'manipulated' variables of the process must be identified. Control variables are considered those that directly influence process performance, while their level cannot be directly controlled by the operator. Manipulated variables, or alternatively referred to as control inputs, are those that can be directly regulated by the operator for controlling the behaviour of the former variables. In the activated sludge process and more specifically in the oxidation ditch process, the main control variables are :

- Mixed liquor concentration in the aeration tank.
- Dissolved oxygen concentration and its spatial distributed in the aeration tank.
- Sludge blanket level in the final clarifier.

The control variables determine the operating conditions of the plant, such as the sludge retention time, the sludge loading rate (F/M ratio), the clarifier solids loading and indirectly affect the effluent quality. Since there is no direct means for controlling effluent quality, this must be achieved indirectly by suitable selection of the control variables. This can be implemented by regulating the manipulated variables of the process which are :

- Recycle sludge flow rate.
- Surplus sludge flow rate.
- Air-flow rate.
- Input flow-rate and its feed distribution.

In the activated sludge process regulation of the recycle and surplus flow rates is accomplished by adjusting the recycle and surplus flow valves or pumps located in the return sludge pumping station. The air-supply is regulated either through the number of air-compressors in operation for diffused-air systems, or by the submergence of aerators in surface aeration systems. Regulation of the input flow requires

the existence of additional tanks for temporary storage of excess flow, while its feed distribution can only be controlled in the step-feed activated sludge modification. Normally, in an oxidation ditch plant the input flow rate is uncontrollable. In the case of the Cirencester plant the DO concentration in the reactor was also controlled by an automatic system, (Section 3.15) and for this purpose DO control was not considered in the following.

The control of a process state through a manipulated variable represents a control loop and requires the existence of a control function. Control systems may be consisted of one, two or several control loops and often each manipulated variable is used to control more than one state variables. According to the configuration of the loops, control systems are broadly classified into the following types :

- Feedback or closed-loop control (FB).
- Feedforward or open-loop control (FF).
- Combined feedback and feedforward control (FB/FF).

The main advantage of FB control is that it requires little knowledge about the process for its design. However a corrective action is initiated only after an error is detected in the state variable to be controlled. Subsequently, for a process with large time constants, considerable time may elapse until the operation is restored. On the contrary, feedforward control requires substantial knowledge of the process for developing the control algorithm, but a control action is taken early enough, in response to the input variability, before performance deterioration takes place. Combined control systems enjoy the advantages of both types and in general perform better, however as their complexity increases through additional control loops, other problems may arise such as instability. This can be caused by interactions between the process units, such as between the aeration tank and the final clarifiers and in addition by the small number of manipulated variables usually available.

All the above types of control systems have been applied to the activated sludge process. Another important distinction to be made is between adaptive and non-adaptive control. In the former case the control function is updated at each time step according to the current inputs and operating conditions, while in the latter case the control function remains unchanged. Furthermore hierarchical control of the activated sludge process has been also attempted in order to distinguish between the decision-making stage and the actual control implementation.

Holmberg (1982), suggested a two-level hierarchical control for the activated sludge process. The upper level determines the criteria for satisfactory process operation, ie. by defining set-point values for the process variables. This level also involves

investigation of process performance, identification and analysis of the reasons for any operational failure and finally suggestions for operational changes that will improve performance and achieve the set-points. The lower level aims to maintain the process at the set-point, by applying more conventional control strategies, involving the control of operating variables such as the *DO* level, sludge age, sludge loading rate and sludge blanket level.

Hiraoka et al. (1985), proposed a three-level hierarchical control system. They defined that the lower level aims to stabilize the effluent quality from diurnal input variations, while the second level aims at optimizing the longer-term plant performance, by employing process models to determine optimum modes of operation. Finally, the third level attempts to maintain flexibility against long-range variations in the environment, by selecting control strategies and by regulating the lower level control subsystems.

The complexity to process control introduced by the stochastic nature of the inputs, was simplified by Sincic and Bailey (1978) who distinguished between the base case operating policy and the associated regulating control strategy. They suggested that the base case is a predetermined operating objective, for achieving a set of desired process outputs under typical input conditions of the plant. Then, the regulating control strategy is required to maintain the process outputs as close as possible to the base case values under varying feed conditions. However, such a distinction cannot be successfully applied in cases where the input conditions exhibit large and unpredictable variations from the base case, which usually happens for plants receiving large quantities of surface runoff.

In the following some of the proposed operational control systems are presented and discussed.

5.2.3 Control systems for effluent variability

In many treatment plants the effluent quality varies significantly from its average level, mainly as a result of input load fluctuations. Andrews in two papers (Andrews 1974 ; Andrews et al., 1976) reviewed some of the classical control algorithms applied to the activated sludge process for reducing the variability of effluent quality. Among them are the two-position 'on-off' control, the commonly used Proportional-Integral-Derivative (PID) feedback control and the simplified modes of proportional and PI control. In these algorithms the control action is a function of the difference between measured and desired value of the particular variable. Other control algorithms reviewed include the 'ratio' Feedforward control, in which the manipulated variable is maintained at a pre set-ratio of an input variable and the 'cascade' control, which

is a combined FB/FF system involving a 'master' and a 'slave' controller.

Westberg (1969), was the first to attempt feedforward control of the activated sludge process, for maintaining constant effluent substrate under diurnal input load variations, by manipulating the recycle sludge flow. The derivation of the control strategy was based on a process model which described the dynamics of limiting substrate, living and dead organisms in the aerator and assumed constant growth kinetics and a non-dynamic model for the final clarifier. However the derived control function was based on the simplifying assumption that the clarifier underflow was maintained at a pre-set ratio of the input flow. Brett et al. (1973), applied standard methods for designing FF controllers using a linearization of Westberg's model. They found that proportional control of the recycle according to input flow variations together with derivative control according to input substrate changes, was an adequate control policy for reducing effluent substrate variability given sufficient sludge storage facilities.

Davies et al. (1973), solved analytically the linearized model equations to derive a control function for the general case. They showed that the best recycle flow policy was proportional-derivative control to input flow changes and derivative control to substrate changes, and that the control gains were independent of the growth kinetics assumed in the model. It should be noted however, that the three previous control strategies were reported to perform poorly in the absence of external sludge storage facilities. This can be attributed to the assumption of a fixed underflow ratio, as well as, to failure to consider the potential storage capabilities of the final tanks. Another weakness of these control strategies arises from the fact that the process model does not consider for the dynamic behaviour of the clarifiers and their thickening limitations as described by hindered settling theory.

Von Jeszenszky & Dunn (1976) studied the implications of linear ($\mu = \mu_o \cdot S$) and Monod ($\mu = \mu_{max} \cdot S/(Ks+S)$) growth kinetics, with and without time lag, upon recycle flow control. They reported that proportional recycle FB control with a large gain was best for the linear kinetics, while FF control gave best results for Monod kinetics. Finally, inclusion of a time-lag in the kinetics gave poorer performance for most types of controllers, due to the slower response of biomass to changes in substrate concentration. Lech et al. (1978b), investigated the efficacy of different controllers for reducing effluent variability under diurnal input variations. Among the various schemes examined, the multiple-loop FF controller gave the best performance, judged by three performance indices being the effluent SS, the effluent soluble and total BOD. They also pointed out that in a multiple-loop FB system, designed for simultaneous control of effluent substrate and SS, strong interactions existed in the process which could lead to instability problems.

Several workers attempted to determine an optimal recycle control strategy for reducing effluent variability, exploiting the commonly observed periodicity in the input load variations. Sincic and Bailey (1978), developed such a recycle control strategy which approximated a 'bang-bang' form. The recycle flow rate was set either at its minimum or maximum value, and achieved an effluent BOD reduction of 38%. However the process model used contained a gross simplification, namely that the underflow concentration ($RASS$) remained constant under any flow conditions. Normally, the $RASS$ concentration is influenced by the underflow rate, and this can lead to a different optimal recycle trajectory. Stehfest (1985), extended the work of Sincic & Bailey, but in his study he related the underflow concentration to the recycle flow rate by an empirical relationship derived from experimental observations. From simulation results he reported that an optimal periodic control policy can produce lower effluent substrate, compared to a control system based on constant sludge loading rate.

Work by Yeung, Sincic & Bailey (1980), explored the performance of recycle control strategies using structured sludge kinetics, employing the model proposed by Busby & Andrews (1975). Through simulations they observed that proportional recycle control produced poorer effluent quality than with a constant recycle which they attributed to the effect of transient lags exhibited by the structured kinetics. Even with an optimal periodic control policy, determined through minimization of the flow-averaged effluent BOD, the reduction in its average concentration was marginal, however its variability was more substantially reduced. Finally they reported that changing the sludge kinetics from Monod to a structured form, altered substantially the optimal recycle control policy.

Brune (1985) employing the analytical solution of a simple dynamic process model, determined an optimal recycle control policy minimizing the effluent TOC, which also had a 'bang-bang' form. Based on simulation studies he concluded that the introduction of process control allows operation at substantially lower biomass concentrations in the reactor and only during peak loads a short-term increase would be necessary. However no quantitative results of the likely reduction in $MLSS$ level were presented.

The control strategies presented so far, offer some improvements to process operation regarding its effluent quality. However most of them suffer from potential weaknesses limiting their efficiency and practical applicability. Some of these weaknesses are :

- In many cases the proposed control strategy approximates a 'bang-bang' recycle control, which is neither practical for implementation on a daily basis, nor desirable since it may introduce large disturbances to the hydraulics of the

plant with adverse effects on clarifier performance.

- The dynamics of the final clarifier are not well represented and its thickening limitations are ignored.
- The sludge blanket level is not simulated, so the effect of the proposed strategies upon the blanket level cannot be assessed, while in many cases an override sludge blanket control is assumed to exist.
- The potential storage capabilities of the final tanks are not sufficiently exploited, which generally underestimates the effectiveness of the developed control schemes.
- The control strategies presented so far, are only judged by their ability to improve effluent quality, while their effect upon the main operating variables, such as *MLSS* concentration, sludge loading and running cost of the process are rarely considered.
- In most cases recycle flow control is designed independently from surplus sludge control, despite the fact that a more effective control policy might derive from simultaneous control of the two variables.

5.2.4 Control systems for solids management

The important role of the reactor biomass upon the effluent quality has been recognized by many workers including Busby and Andrews (1975), Cook et al (1981), and Tanuma et al (1981). This has prompted the design of control systems to regulate either the total sludge contained in the system or the *MLSS* concentration in the aeration tank. Control of solids to a desired level requires substantial knowledge of the process dynamics. For the implementation of solids control several approaches have been proposed differing in their complexity. Some of the simplest methods commonly practised in real process operation are based on a specific policy for the surplus sludge flow, while more efficient strategies also exploit the recycle control.

For maintaining constant sludge mass in the system, Andrews (1974) suggested that the surplus sludge should be maintained equal to the net growth of biomass. Walker (1971) however recommended operation under a constant sludge age, achieved by surplussing (100/SRT) percent of the total solids each day. Application of the latter strategy by Busby & Andrews (1975), showed that it can also achieve a constant sludge loading rate.Another surplussing policy suggested by Busby & Andrews (1975) involves control of solids through the sludge blanket level, whereby the wastage rate is increased according to a proportional-error FB system, whenever the sludge blanket exceeds a critical level.

Tanuma et al. (1981), showed that a total sludge quantity control is more effective for changing or stabilizing the in-process sludge than sludge age control. The desired sludge quantity can be calculated from mass-balance equations according to a specific control objective, such as a desired $MLSS$ concentration. Then the surplus flow rate can be determined from a PI Feedback function. Miura (1981), used real process data to simulate a similar strategy based on SRT control. The proposed strategy adequately controlled the reactor $MLSS$ to a constant level except during periods of storm, where significant variation was observed due to the slow response of the surplus sludge controller. Takase & Miura (1985), improved the performance of the above strategy by considering an additional FB control loop involving recycle flow control.

Cook and Marsili-Libelli (1981), employed a PID feedback control of the recycle flow for achieving a constant $MLSS$ set-point, in which the control gains were specified by optimizing two different performance indices. They reported satisfactory performance of the controlled system, when both the $MLSS$ set-point error and effluent substrate variations were included in the objective function.

Angelbeck and Shah Alam (1975), used variational calculus to derive optimal control policies for both the recycle and surplus sludge flow, in an attempt to minimize variations in effluent substrate and aerator volatile solids. The optimization was based on minimization of both the set-point deviation of the above states and the expenditure for control energy. The process model assumed exponential-type kinetics $[\mu = \mu_{max} \cdot (1 - e^{-k \cdot S})]$ and was calibrated using measurements from a laboratory-scale plant. The derived optimal Feedforward control policy was applied to the plant offering reductions in the effluent substrate and $MLVSS$ variability ranging between 13 and 66%, depending on the loading conditions and physical limitations of the plant (Shah Alam and Angelbeck, 1976).

For the control of total sludge in the process, Masui et al. (1981) proposed a short-term sludge management system for determining the daily flows of recycle and surplus sludge based on a simple dynamic model and predictions of the influent load. The necessary control action would then be implemented by an on-line FF control system, which also performed on-line corrections to compensate for the deviation between predicted and actual input loads. Through simulation studies with real process data, they reported that the proposed system was able to maintain the $MLSS$ within 5% of the desired level.

Lochmann & Schlegel (1981) argued that recycle control cannot achieve perfect set-point $MLSS$ control, due to the limited sludge storage capabilities of the final tanks. Based on experimental results they concluded that adoption of a proportional recycle policy, does not control the $MLSS$ significantly better than a constant recycle

policy. Furthermore, Nogita et al. (1981), suggested the use of additional sludge storage for effective $MLSS$ control. Subsequently they introduced the "Dynamic Sludge Reserving" process, in which the sludge is stored in the front end of the reactor during low flow periods and released into the aeration tank at high flows. From experiments at a pilot-plant they observed lower effluent COD and better sludge settleability compared with the conventional activated sludge process without storage.

Cheruy et al. (1982), argued that classical control methods based on deterministic, linearized models are not suitable for the activated sludge, because of process non-linearities, unreliability of measurements and the time-variation of process parameters. As an alternative they proposed a control strategy, in which modelling and measurement errors are taken into account by stochastic models and system non-linearities by a multi-model adaptive approach. However application of the control system to the activated sludge process did not produce satisfactory results, which they attributed to the adverse effect of surplus sludge flow upon effluent SS, although the effluent BOD showed on average 15% improvement.

The above control strategies related to solids management, offer a more rational approach to improve effluent performance and reliability by controlling the operating state of the process. However most of them also have the following deficiencies.

- The selection of the desired operating $MLSS$ or total sludge mass in the system, is either made arbitrarily or based on experience from previous plant performance and is rarely related to the running cost of the process.
- In most cases the control objective is to maintain a constant operating $MLSS$ in the reactor, while there is no attempt to relate the solids level to the input conditions and the desired effluent performance of the plant.
- The control of solids has been studied over short-term periods and emphasis given to the diurnal variability, while a longer- term operating strategy to account perhaps for the effect of seasonal input variations has not received so much attention.

5.2.5 Control systems for the nitrification-denitrification processes

In many cases, the control of ammonia and other oxidized forms of nitrogen, in natural watercourses is of primary importance. This can be achieved to some extent through control of nitrification and denitrification within a wastewater treatment system. These reactions however are very sensitivity to the operating conditions of a plant, which led several workers to design specific systems for their control. Fujimoto

and Sekine (1981), recognized the importance of nitrification rate for supervising the plant performance, because it is mostly affected by the operating conditions and also because it affects the energy cost of the process. In another study, (Sekine et al., 1985), they showed both experimentally and via simulations the importance of DO concentration upon nitrification rate in a plug-flow activated sludge reactor. Subsequently they proposed that constant nitrification rate control can be implemented through a variable DO set-point control in conjunction with sludge age control of the biomass.

Kayser and Ermel (1984), implemented control of simultaneous nitrification-denitrification in an oxidation ditch reactor, by regulating the aeration rate. Their control policy was to increase the rate of aeration during low nitrate concentrations in the reactor and reduce it when the nitrates reached a certain high level. The control system was applied to several activated sludge and oxidation ditch plants and they reported large reductions in effluent nitrates, followed by elimination of scum in the clarifiers and considerable energy savings.

Bahre (1987), proposed a similar nitrate control system which would guarantee the optimal recovery of aeration energy used for nitrification. The control was implemented through intermittent aeration of the plant aiming to achieve a 'saw tooth' variation of nitrates in the reactor. He reported that adequate control of nitrification was also achieved and suggested that during long anoxic periods the accumulated ammonia in the system could be absorbed by most micro-organisms for their anabolism.

Cook (1983a), examined various control tactics for controlling effluent ammonia concentration from an oxidation ditch plant according to a preselected seasonal policy, by regulating the recycle and surplus sludge flows. The control system design was based on a suitable nitrification model for the particular plant. The model stability was examined for various nitrification conditions and instability was observed for ratios of effluent to influent ammonia concentration above 1:4. Among several control tactics examined, including proportional FB, adaptive P-I and prediction error FB controllers, the latter gave the best performance in terms of effluent ammonia concentration. The control gains were estimated adaptively by minimizing the predicted set-point error and the variability in the control inputs using the sensitivity matrix of the process model.

5.2.6 Control systems based on oxygen uptake rate

In an attempt to develop a control strategy that can be applied in real-time, several workers selected the oxygen uptake rate (OUR), or more commonly the specific

OUR (*SCOUR*) as their control variable. The information contained in these two process indicators are numerous, as discussed in Section 4.2. In addition they have the advantage that they can be determined in real-time, either from respirometry measurements or through estimation from on-line *DO* measurements (Section 4.7). Workers such as, Benefield et al. (1975), Andrews et al. (1976), Schroeder & Irvine (1979), Haas (1979), Young (1981) and Yust et al. (1981) recommend the use of *OUR* or *SCOUR* for process control, because of their extreme sensitivity to changes in the inputs and biological growth kinetics. However some workers, such as Edwards & Sherrard (1982), argue that *OUR* will be of little use for effluent quality control, due to the relative insensitivity of effluent quality to *OUR* variations.

Benefield et al. (1975), based the surplus sludge policy upon measurements of *SCOUR*, in an attempt to maintain a constant specific growth rate and observed higher performance of this strategy compared to sludge age control. Andrews et al. (1976), proposed a set-point *SCOUR* control for real-time application, in order to improve effluent quality and reduce growth variability under input load fluctuations. Stenstrom & Andrews, (1979) improved the simulated performance of this strategy by incorporating into the algorithm predictions of the input flow rate. This reduced the diurnal *SCOUR* variability by 86% under the best FB/FF control strategy. Finally, they stressed the benefits of *SCOUR* control for fast detection of shock loads compared to conventional methods based on sludge load or sludge age control.

Yust et al. (1981, 1984), proposed a similar strategy to maintain a constant *SCOUR* by adjusting the *MLSS* concentration. They tested the performance of the controller at a pilot-plant and reported effective *SCOUR* control for a step-feed activated sludge process, but poor performance for a single-tank process. They also reported that in the step-feed process, the introduction of *SCOUR* control reduced the effluent variability of filtrable organic carbon, but increased the effluent SS during high loading periods.

The main advantage of control strategies based on *OUR* or *SCOUR* is their greater potential for real-time application. Hence more effective process control can be achieved as a result of the higher frequency of applying corrective actions. The main obstacle for applying well-proven conventional control strategies in real-time, is the lack of reliable sensors for on-line monitoring of key variables such as the influent and effluent quality parameters. Since both influent variations and sludge activity are reflected by the oxygen uptake rate, fewer process variables need to be measured, such as the *DO*, the *MLSS* and the various flow rates. Furthermore these variables may be easily measured on-line. Such control schemes however, require more intensive data processing for the estimation of unmeasurable states and even process inputs, such as the *OUR* and the input *BOD* discussed in Section 4.7. This would increase the uncertainty in the control action compared to conventional schemes based on

real measurements of the input and output quality variables. However, this is largely offset by the real-time application of the strategy and the adaptive nature of the controllers.

The above control strategies were designed mainly for the control of organic substrate removal in conventional activated sludge process, where the control of nitrification is not of major importance. However in oxidation ditch plants, both nitrification and denitrification are important processes and their control is not necessarily achieved via a set-point *SCOUR* control policy, due to the different reaction kinetics involved from that of carbonaceous oxidation. Furthermore, the *OUR* in an oxidation ditch reactor was shown to be dominated by the endogenous respiration of biomass (Section 4.4.2). As a result, the value of *SCOUR* would be significantly affected by variations in the oxygenation coefficient for the biomass, making the selection of a set-point *SCOUR* level more difficult.

5.2.7 Applicability of control systems to the oxidation ditch process

In the oxidation ditch process, consideration of the operating cost in the design of a control system is of greater importance than in the conventional activated sludge, due to the substantially higher aeration cost per unit volume of wastewater treated. Furthermore, the operating objectives for the oxidation ditch can be quite different from the conventional activated sludge, because of differences in their operating conditions and effluent performance as discussed below.

The effluent organic concentration from a well-operated oxidation ditch plant is generally low, even under large input load fluctuations. Therefore there is usually no strong incentive for its control. However, the attention usually focuses on the control of nitrification and denitrification processes which are very sensitive to the operating and input conditions of the plant. Efficient control of solids and *DO* distribution in the reactor are of great importance for controlling those processes and for achieving potential reductions in aeration cost and sludge production. In addition, solids control can positively assist in reducing or even eliminate cases of process failure, resulting from sludge blanket overflow, oxygen depletion and biomass washout. Finally, the application of real-time control based on the *OUR* or *SCOUR*, is more complex for the oxidation ditch process, as was discussed in Sec. 5.2.6, and needs further investigation before it can be successfully applied.

5.3 Development of an operational cost model

The objective for developing an operational cost model of the process is to study the effect of different operating conditions upon the total running cost and identify those conditions leading to minimum cost operation. The running cost of a wastewater treatment plant involves costs which are both directly and indirectly related to the operating conditions. The first category involves the aeration, pumping and sludge disposal costs, while the second category involves such expenditures for personnel wages, materials, services and rates.

Only the costs which are directly related to the operating conditions were included in the cost model, because the effect of different control strategies upon cost can be easily quantified. Application of operation control may also lead to reductions in manpower, especially if automation is introduced. However such additional benefits were not considered here, since they were not in the objectives of this study. Simple cost functions were developed relating the cost for aeration, pumping and sludge disposal to the input and operating conditions of the plant. The developed process model was employed for supplying the necessary relationships for oxygen demand and sludge production. The structure of the cost model was chosen to be simple and non-dynamic which was considered adequate for predicting the daily cost.

5.3.1 Formulation of the operating cost relationships

I. Energy cost for aeration

The energy consumption for aeration at the Cirencester plant was shown to be a function of the aerator's submergence. The submergence was regulated by a *DO* control mechanism in order to maintain the *DO* concentration within a specified range. As a result, the aeration energy is directly related to the oxygen demand exerted by the mixed liquor in the reactor. The oxygen demand was expressed as a function of the biomass respiration, organic substrate removal, nitrification and denitrification processes through equation 4.13 in Section 4.4.1. Consequently the oxygen demand can be used to estimate the aeration energy necessary for supplying the equivalent amount of oxygen to the reactor, by rearranging equations 4.8 to 4.11 (Sect. 4.3.2)

II. Energy cost for pumping

The energy requirements for crude sewage and recycle sludge pumping are directly related to the pumped liquid flow rate and its concentration. The daily measurements of pumping energy consumption and the corresponding pumped liquid flow from the

study period were related by a simple expression derived through linear regression. Among the various forms examined, the simplest linear model gave the most satisfactory performance shown in Table 5.1 and Figures 5.1 & 5.2. Thus the use of more complex relationships was not justified. The linear model has the following form :

$$\hat{E}(t) = a \cdot Q(t) + b \qquad (5.1a)$$

where; $\hat{E}(t)$: energy consumption for pumping on day (t) (KWh/d),
$Q(t)$: pumped liquid flow on day (t) (m^3/d),
a, b : model parameters to be determined.

The high degree of linearity between flow rates and energy consumption can be attributed to the small effects of friction losses and solids concentration, as well as, to a constant pump efficiency over their normal operating capacity.

The daily pumping cost in pounds is given from the following equation based on a simplification of the tariff system :

$$C_{pump}(t) = \hat{E}(t) \cdot EL \qquad (5.1b)$$

where; EL the average electricity unit cost $(£/KWh)$.

The electricity tariff system for industrial users is relatively complex, providing the option for different unit cost prices between day- and night-time consumption and even for weekend consumption. Furthermore it includes standing costs and maximum demand charges. However for the purpose of comparing the energy cost under different operating conditions rather than deriving exact cost figures, the assumption of an average unit price was considered a reasonable simplification.

Parameter	Crude sewage	Return sludge
Flow variable	*Qworks*	$(Qr + Qw)$
Energy variable	*Esp*	*Erp*
R	0.9606	0.9312
C.O.D.	0.9228	0.8671
RMS error	25.86	16.6
var. error	671.0	276.6
a (KWh/m^3)	(11.96±0.21)E-3	(9.51±0.22)E-3
b (KWh/d)	64.5±2.4	65.5±2.0

Table 5.1. Linear model performance for pumping energy requirements.

III. Sludge disposal cost

The excess sludge from the Cirencester plant is tankered on to farmland after thickening. The cost of sludge disposal is specified by a fixed price per cubic meter of wet

sludge. Hence the disposal cost depends on the amount of excess sludge produced, and its moisture content expressed by the solids concentration. The thickened sludge concentration may vary depending on the operating conditions of the thickeners and physical properties of the sludge, however at this stage it was assumed to remain constant. The production of excess sludge is a result of the net growth of biomass and the incoming non-degradable and inert solids in the crude sewage. The latter can be a substantial proportion of the total sludge in the absence of primary sedimentation facilities.

Assuming that the net growth of nitrifiers and denitrifiers is negligible compared to the growth of heterotrophs, the carbonaceous model (eq. 3.49–3.53 in Section 3.17) was used to derive the following non-dynamic relationship for the daily net biomass growth:

$$\widehat{GR_{net}}(t) = Ysx \cdot [Qi_t \cdot (Si_t - Se_t) + Yxs \cdot Kd \cdot X_t] - Kd \cdot X_t \qquad (5.2a)$$

where; Si_t, Se_t : influent and effluent substrate concentrations (BOD_5) (mg/l).

The effluent substrate term, Se_t was shown to be generally low from process observations and simulation results, hence its removal from the above equation would not introduce significant error. Hence the excess sludge production and sludge disposal cost can be derived from the equations :

$$\widehat{SP}(t) = Qi_t \cdot Xo_t + Ysx \cdot (Qi_t \cdot Si_t + Yxs \cdot Kd \cdot X_t) - Kd \cdot X_t \qquad (5.2b)$$

$$C_{disp}(t) = \frac{\widehat{SP}(t)}{SL_{conc}} \cdot SL \qquad (5.2c)$$

where; $\widehat{SP}(t)$: daily sludge production ($kg\ SS/d$),
Xo_t : non-degradable input SS given from eq. 3.37 (mg/l),
$C_{disp}(t)$: daily sludge disposal cost ($£/d$),
SL_{conc} : thickened sludge concentration (kg/m^3),
SL : unit sludge disposal cost ($£/m^3$).

5.3.2 Operating cost at Cirencester plant

The operating cost of Cirencester plant for the fiscal year between April 1978 and March 1979 reached the sum of £54,600 (Carmichael & Johnstone, 1982).The most important expenditure was for electricity which accounted for 33.5% of the cost. The other principal expenditures were for wages (26.4%), rates (21%) and transportation of sludge (10%). From the annual cost figures it was possible to estimate the average

electricity and sludge disposal unit costs for that period, as shown below :

$$EL = \frac{\text{Total cost for electricity } (£)}{\text{Total electricity consumption } (KWh)} = \frac{18,300}{797,867} = 0.023\, £/KWh \qquad (5.3a)$$

$$SL = \frac{\text{Total cost for sludge disposal } (£)}{\text{Total volume of tankered sludge } (m^3)} = \frac{5,400}{312,000} = 0.56\, £/m^3 \qquad (5.3b)$$

Although the above unit cost prices may be quite different from the present time, they were considered adequate for illustrating the effect of different operating policies upon the running cost. Subsequently as time basis for cost results was adopted the period 1978-79, which also coincides with the period of data collection.

5.3.3 Sensitivity analysis of the cost model

A sensitivity analysis of the cost model was performed in order to study the cost variation with $MLSS$ concentration under different input conditions and parameter values. The $MLSS$ concentration is the key variable determining the running cost of the process, because it affects directly the energy consumption and indirectly the sludge production. The effect of $MLSS$ on the components of total cost was initially examined, assuming typical values for the inputs and constant values for the parameters, derived during the model calibration. These values are shown in Table 5.2 and the sensitivity results are presented in Figures 5.3 & 5.4.

Parameter	Units	Value
Input flow Qi	m^3/d	8700
Recycle flow Qr	m^3/d	7500
SSi (non-degr.)	mg/l	90
Organic load rem.	kg(BOD_5)/d	650
Ammonia load rem.	$kg(NH_3-N)/d$	95
Denitrified mass	kg/d	70
Oxyg. par. a	—	0.75
Oxyg. par. b	day^{-1}	0.0672
Yield (Ysx)	—	1.10
Decay rate (Kd)	day^{-1}	0.0288
Thick. sludge conc.	kg/m^3	36
Electricity cost	$£/KWh$	0.023
Disposal cost	$£/m^3$	0.56

Table 5.2. Typical values of inputs/parameters for sensitivity analysis.

From Figure 5.3 it can be seen that the energy cost increases with $MLSS$ concentration in a non-linear manner. This is explained by the increased oxygen demand for biomass respiration at high $MLSS$ levels, while the non-linearity is a consequence

of the variable efficiency of the aeration system. The sludge disposal cost however, decreases gradually with $MLSS$ concentration as a result of the higher biomass decay reducing the sludge production. It is important to note that the energy cost is substantially higher than the sludge disposal cost for the selected unit cost prices and that their difference increases at high $MLSS$ concentrations. The combined effect of these two components, is that the total running cost of the process increases with $MLSS$ concentration. Finally, from Figure 5.4 showing the componentsof energy cost, it can be observed that the aeration cost is much larger than the pumping cost for this particular works.

The sensitivity of the total cost to the inputs and parameter values was examined by allowing one component to vary at a time within a range of values, while the remaining components were kept constant (Table 5.2). The sensitivity results are presented in Figures 5.5 to 5.7, from which the following conclusions can be drawn.

- The total cost increases with increasing $MLSS$ under a wide range of input and parameter values, with no minimum point occurring in the $MLSS$ range considered.
- The parameters found to affect mostly the total running cost were the unit cost prices, the input flow rate, the input SS, the organic load, the yield coefficient, oxygenation parameter 'b' and the thickened sludge concentration.
- Under low electricity tariffs, the total cost increases slowly with $MLSS$ concentration, however the increase becomes more important under higher tariffs (Fig. 5.7a).
- At low sludge disposal unit cost, the total cost increases significantly with $MLSS$, while at higher disposal costs the increase becomes less pronounced (Fig. 5.8b).

Similar results on the effect of unit cost prices upon the operating cost were reported by Stenstrom & Andrews (1980), derived from simulation studies on the conventional activated sludge process under different mean cell residence times.

5.3.4 Effect of variable thickened sludge concentration

So far, it was assumed that the thickened sludge concentration was constant for the particular thickener and independent of its operating conditions. However, examination of the available measurements (Fig. 2.9a) showed that the thickened sludge concentration was quite variable having a mean of 36.0 kg/m^3 and a standard deviation of 8.0 kg/m^3. Consequently it was considered appropriate to examine the effect of operating conditions upon the thickened sludge concentration. Through linear re-

gression a number of models were examined, involving those process variables that were most likely to affect the thickener performance, such as the $RASS$ concentration, the surplus sludge flow (Qw) and the $SSVI$, and are summarized in Table 5.3. In order to employ a relatively simple relationship, Equation 5.4.4 was selected because it contained both the solids concentration and flow rate entering the thickener and showed comparatively good performance (Figure 5.8.). Although equations 5.4.2 and 5.4.5 produced a lower RMS error, they were discarded because they contained large constant terms, while their predictions showed much lower variability than the observed series. Equation 5.4.6 was also discarded, since the addition of the $SSVI$ term did not produce any significant improvement.

Model Structure $C, RASS(mg/l), Qw(m^3/d)$		Parameter estimates	R	RMS error mg/l	Predicted C mean-std.dev $\times 10^3 mg/l$
$C = a \cdot RASS$	(5.4.1)	a=4.74	0.429	11410	32.74±12.28
$C = a \cdot RASS + b$	(5.4.2)	a=1.33 b=26860	0.429	7242	36.05±3.44
$C = a \cdot Qw \cdot RASS$	(5.4.3)	a=2.51E-5	0.294	12252	32.54±11.93
$C = a \cdot RASS + b \cdot Qw$	(5.4.4)	a=3.09 b=69.5	0.379	8314	35.33±6.80
$C = a \cdot RASS + b \cdot Qw$ $+c$	(5.4.5)	a=1.45 b=8.72 c=24226	0.434	7224	36.05±3.49
$C = a \cdot RASS + b \cdot Qw$ $+c \cdot SSVI$	(5.4.6)	a=2.83 b=57.6 c=60.0	0.355	8184	35.48±6.14

Table 5.3. Models for the thickened sludge concentration.

Equation 5.4.4 relates the thickened sludge concentration to the operating conditions of the plant and particularly to the final clarifier performance. According to this relationship the production of more concentrated underflow ($RASS$), results in thicker sludge from the thickeners (Fig. 5.9), which has then a marked effect upon the sludge disposal cost (Fig. 5.10). Inclusion of equation 5.4.4 into the cost model alters the relationship between sludge disposal cost and $MLSS$ (Figure 5.11). The disposal cost increases up to a $MLSS$ concentration of about 2,500 mg/l and then progressively decreases. The total cost again increases with $MLSS$ throughout the range, but shows different behaviour from the previous case.

5.3.5 Evaluation of running cost under different operating conditions

The developed cost model was then used to evaluate the average operating cost for different $MLSS$ concentrations, under natural input conditions experienced at the Cirencester plant. The measured inputs over the study period were employed for

this purpose and the average daily values of the operating cost components, oxygen demand, thickened sludge concentration and sludge production were calculated, presented in Table 5.4a.

MLSS	*RASS*	*Qr*	*Qw*	O.D.	SL_{conc}	Slud. prod.	Total cost	Aer. cost	Disp cost	R.P. cost
mg/l	*mg/l*	m^3/d	m^3/d	*kg/d*	kg/m^3	*kg/d*	£/*d*	£/*d*	£/*d*	£/*d*
a. Under different *MLSS* concentrations										
6000	11000	9485	114	3475	42.1	1250	61.95	38.5	15.9	3.59
5500	10500	8918	121	3243	41.0	1274	61.71	37.7	16.6	3.47
5000	10000	8273	130	3010	40.1	1298	61.03	36.5	17.3	3.33
4500	9500	7526	139	2778	39.2	1321	59.21	34.2	18.0	3.17
4000	9000	6681	149	2545	38.4	1345	56.23	30.7	18.7	2.99
3500	8000	6454	171	2312	36.8	1368	53.83	27.2	19.8	2.94
3000	7500	5502	185	2080	36.2	1392	51.21	24.2	20.4	2.74
2500	6500	5125	217	1847	35.3	1415	49.41	21.7	21.2	2.66
2000	5500	4670	257	1615	35.0	1439	47.65	19.5	21.8	2.57
b. Under different *RASS* concentrations										
3500	5000	13362	266	2312	34.1	1368	56.69	27.2	21.1	4.47
3500	6000	10258	226	"	34.4	"	55.84	"	20.9	3.78
3500	7000	8155	195	"	35.4	"	54.90	"	20.5	3.32
3500	8000	6453	171	"	36.8	"	53.83	"	19.8	2.94
3500	9000	5306	152	"	38.5	"	52.76	"	18.9	2.69
3500	10000	4571	137	"	40.6	"	51.73	"	18.1	2.52
3500	12000	3706	114	"	45.2	"	49.83	"	16.4	2.33
Crude sewage pumping : 3.87 £/*d*										

Table 5.4. Average daily cost & main process variables at different operating conditions.

Both the *MLSS* and the *RASS* concentrations were assumed constant throughout the period, while the operating recycle and surplus sludge flow rates were estimated from the following pseudo steady-state equations:

$$\widehat{Qw}_t = SP_t/RASS \qquad (5.5a)$$

$$\widehat{Qr}_t = (Qi_t \cdot MLSS - SP_t)/(RASS - MLSS) \qquad (5.5b)$$

Comparing the daily cost results (Fig. 5.12) with those obtained under constant input values (Fig. 5.11), there are many similarities regarding the trend of the cost functions with *MLSS* concentration, however there are also some differences to be reported. The total cost under variable process inputs increased at a higher rate up to a *MLSS* of about 4,500 *mg/l* while for concentrations above 5,500 *mg/l* the

cost reached a plateau. This was explained by the small increase in energy cost, because the aeration system reached its maximum capacity for a large number of days. Hence it can be concluded that operation of the plant at $MLSS$ concentrations above 5,000 mg/l is undesirable because frequent oxygen depletion problems are expected to occur. Comparing the costs for two cases operating at an average $MLSS$ of 3,000 and 5,000 mg/l respectively, it can be seen that the total cost is 19% higher in the latter case. This is due to a 51% increase in aeration cost and 21% in recycle pumping cost, associated with only a 15% reduction in sludge disposal cost.

Finally, the effect of the underflow concentration upon the running cost was examined by selecting different $RASS$ levels with the same operating $MLSS$. The simulation results show that the total cost decreased with increasing $RASS$ concentrations due to the higher thickened sludge concentration and indicates an alternative means of reducing operating cost (Table 5.4b, Fig. 5.13). The $RASS$ concentration is known to be a function of the clarifier operating conditions and the settling properties of the sludge. However in this study there were limited information on the sludge characteristics, hence their effect upon the $RASS$ concentration could not be examined.

In conclusion it was shown that for the particular work's data considered, the running cost of the oxidation ditch process can be reduced by operating at lower $MLSS$ and higher $RASS$ concentrations. However the selection of the operating $MLSS$ should not be based on cost criteria alone and should also be related to the effluent performance required from the plant.

5.4 Transient response of the oxidation ditch system

5.4.1 Introduction

Before attempting to control a particular system, the controllability and stability of the system must be examined. This can be achieved by analyzing its transient response behaviour to synthetic input functions. It has been stated that a system is controllable when controls exist, which in a finite time can transfer the dynamic system states between any two arbitrarily chosen points in the state-space (Jacobs, 1974). The controllability is formally determined by the rank of the system controllability matrix, but could be also assessed by evaluating the response of the states to changes in the system control inputs.

Furthermore, a system is asymptotically stable in a region when after excitation settles to some steady value without exhibiting continuous or growing oscillations. Stability can be assessed formally by examining the roots of the system characteristic

equation. For complex systems stability can be more simply assessed by observing its transient response to synthetic input functions. However in this case the results will only be valid for the particular conditions examined. In a stable system, a step-input function produces a new steady-state, while the introduction of a pulse function should not affect the original steady-state of the system.

The transient response of the oxidation ditch system was evaluated from the response of the developed model for that system, when subjected to a pulse function in the control inputs. The selected initial steady-state operation of the system was characterized by poor nitrification performance associated with a low population of nitrifiers and $MLSS$ concentration in the aeration tank. Subsequently a pulse in the recycle and surplus sludge flow was introduced and the transient response of the operating and effluent variables studied. The initial control inputs were characterized by a low recycle ratio (50% of the input flow) and a relatively high surplussing rate (7.33% of Qr). The input conditions, which remained constant throughout the simulation period were : Qi = 6,000 m^3/d, $BOD5i$ = 180 mg/l, $NH3i$ = 25 mg/l, and $NO3i$ = 2.5 mg/l.

5.4.2 Response to a pulse in the recycle flow

The process model was used to simulate the effect of a change in the recycle flow rate from 3,000 m^3/d to 5,000 m^3/d on day 20 (Fig. 5.14a). In response, the $MLSS$ in the aeration tank increased together with the nitrifying population producing a significant reduction to the effluent ammonia. However, both the $RASS$ concentration and the sludge blanket level were reduced, since a larger amount of solids was returned from the clarifiers to the aeration tank. On day 100 the recycle ratio was reduced to its original level and in response to this action the process variables exhibited an opposite transient behaviour towards their original steady-state values.

From the transient response illustrated in Figures 5.15–5.22, the following remarks can be made :

- the transient response of the state variables consists of two components:

  an **immediate response**, producing a significant variation to the states over a short period of time, in the order of 1 day. This response results from changes in the internal hydraulic pattern of the plant, causing a differential distribution of solids between the aeration tank and final clarifiers.

  a **slow response**, producing additional variation to the states over a longer period of time, in the order of several days. This response is attributed to the biological component and results from changes in the growth and decay rates of the biomass under the new operating conditions.

- The system is controllable with respect to the $MLSS$ concentration, effluent ammonia and nitrates, since a change in the recycle flow produced a significant change to these variables. However, the system showed relative insensitivity regarding the effluent BOD_5, which remained low under all conditions.

5.4.3 Response to a pulse in the surplus sludge flow

Starting with the same initial conditions as before, the effect of changing the sludge surplussing rate was then examined. On day 20 the surplus flow was reduced from 220 m^3/d to 150 m^3/d (Fig. 5.14b), while the recycle rate was kept constant. As a result the state variables exhibited an exponential-type response shown in Figure 5.15–5.22. The $MLSS$ and nitrifier levels were subsequently increased producing a significant reduction in the effluent ammonia concentration. Furthermore, a large increase in both the $RASS$ and sludge blanket level took place, due to a net accumulation of solids in the system. It is important to note that the transient response of the states was effected more gradually than before, over a period of several days. Finally on day 100 the surplussing rate was returned to its original level and the state exhibited an opposite response towards their original steady-state values.

5.4.4 Comparison of the transient responses

From the previous study it can be concluded that the oxidation ditch system is controllable through the recycle and surplus sludge flows. Comparing the responses generated from a pulse in these two controls there are certain similarities, as well as differences to be reported. A step change in the control inputs produces qualitatively similar response of the $MLSS$ concentration and effluent quality variables, but opposite response of the underflow concentration and sludge blanket level.

The response from a step change in surplus flow was smoother approximating a first-order curve and also slower regarding its effect on the effluent variables. The immediate response generated by a step change in recycle flow, is an important characteristic of the system to be exploited in the design of an efficient control system, because it can produce substantial variation to the states over a short period of time. Finally, the system showed asymptotic stability for the selected inputs and operating conditions, although this cannot be guaranteed for any set of conditions.

5.5 Analysis of operational control problem for the oxidation ditch process

5.5.1 Definition of control objectives

The objective for introducing operational control to the oxidation ditch process is twofold.

1. Improve the process performance and reliability, so that the effluent quality complies with the desired discharge standards.
2. Reduce the operating cost to the lowest level possible.

The variables chosen to characterize process performance and reliability are the effluent BOD_5, SS, ammonia (NH_3-N) and nitrate (NO_3-N) concentrations. In addition to these variables, the performance of the oxidation ditch may be also assessed by the stability of the produced sludge and settleability of the mixed liquor, however these determinands were not considered in this study. Hence, the operational control problem can be defined as :

Operate the process under minimum cost,

subject to effluent quality constraints.

Among the operating conditions affecting the performance of the aeration tank, are the *DO* concentration, the sludge loading rate and the hydraulic and sludge retention times. Moreover the final clarifier performance is affected by the settleability of the sludge, the solids loading and underflow rates. Most of the above operating conditions are either directly or indirectly influenced by the *MLSS* concentration in the reactor. Besides, the *MLSS* concentration was found to be the key variable determining the operating cost (Section 5.3.3). The above suggest that the *MLSS* can be selected as the principal variable for operational control. Furthermore, the operating state of the clarifiers is reflected by the sludge blanket level in the tanks, which suggests that this variable is also important for process control. Both variables can be directly controlled through the manipulated variables, as it was shown from the transient response analysis.

The operational control of the oxidation ditch process was considered as a two-level hierarchical problem, similar to that proposed by Holmberg (1982) (Section 5.2.2). At the higher or 'planning' level of the control hierarchy, an optimum operating *MLSS* concentration can be determined based on both performance and cost criteria. For this purpose process performance should be expressed as a function of the inputs and operating conditions of the plant. A number of rational operating

policies may be designed at this stage for achieving the operating objectives, whose performance must be evaluated either through simulation studies or ideally from real process implementation. The reliability of the process can be assessed from the long-term compliance with the effluent consent conditions. The planning level might also involve a study of the inter-relation between operating cost and process performance, which may lead to a reassessment of the operating objectives, however such a study was not undertaken here. Hence, the objectives at the planning level can be stated as :

Define an optimum operating $MLSS$ level,

to produce the desired process performance at the lowest cost.

The lower or 'process' level of the control hierarchy aims to regulate the $MLSS$ concentration in the reactor to the desired level, by employing conventional control methods to the manipulated variables. In addition the sludge blanket should be controlled to a relatively constant level, for which the final clarifiers have shown good long- term performance with respect to their effluent solids concentration. In practice the control action imposed to the manipulated variables is usually bounded due to physical limitations of the pumping system and other operational constraints. Subsequently, the control objectives at the process level can be defined as:

achieve a desired $MLSS$ conc. and a constant Sludge Blanket level,

by regulating the recycle (Qr) and/or surplus (Qw) flow rates,

subject to : $Qr_{\min} < Qr < Qr_{\max}$ and $Qw_{\min} < Qw < Qw_{\max}$.

5.5.2 Frequency of control application

Following the formulation of control objectives, the time period for achieving the desired operating conditions must be specified. This period is defined as the time that may elapse after a control action has been taken, until the states reach their set-point value. The selection of this period, which influences the dynamic characteristics of the control system, depends on the frequency of monitoring, the time constants of the process and the intended frequency and purpose of control application.

The monitoring interval at Cirencester plant was one day, which cannot depict the diurnal pattern of process performance (Section 2.3.3) and hence does not allow for the control of diurnal variability. Consequently, the control system was designed to optimize the average daily plant performance, rather than its diurnal variability. Furthermore, the control system envisaged would be for manual implementation by the operator and for this purpose low frequency control actions would be preferable.

Finally the time constants of the process states depend on the operating flow rates and the kinetic rates as was discussed in Section 5.4.2.

Under these circumstances the frequency of control application was chosen to be once per day, which coincides with the monitoring frequency. From the practical viewpoint, such frequency is considered reasonable for manual implementation, although higher or lower frequencies have also been employed in plant operation. For retaining simplicity in the control system design, the one-day interval between successive control actions was also considered adequate for achieving the desired operating conditions.

5.5.3 Determination of the desired operating *MLSS*

The objective of the 'planning level' was to define an optimum operating *MLSS* producing the desired plant performance at the lowest possible cost. From simulations using the developed running cost model, it was shown that the total cost decreases at lower *MLSS* concentrations. However process performance may also deteriorate at low *MLSS* levels, as it was observed during the last 80 days of the study period (Section 3.18.4).

The effluent standards specified for the Cirencester Works are quite stringent, due to the sensitive location of the plant near the headwaters of the River Thames, (Section 2.3). Compliance with the discharge standards imposes certain constraints to the operating conditions of the plant. These can be achieved to a great extent by confining the operating *MLSS* variation within a suitable range, for which the process is expected to produce the desired effluent quality under a given set of inputs. An optimum *MLSS* concentration can then be selected from that range on the basis of minimum operating cost. For the specification of the above operating range the developed process model was employed. This represents the only alternative source of information, since further experimentation on the full-scale plant was not feasible.

5.5.4 Determination of the maximum operating *MLSS*

The purpose for specifying a maximum *MLSS* concentration was to avoid exceeding the physical limitations of certain process units, such as the oxygenation capacity of the aeration system and the thickening capability of the final clarifiers. The first event would lead to dissolved oxygen depletion in the reactor followed by a reduction in the size of aerobic zones. This could have adverse effects on the activity of aerobic organisms and lead to deterioration of nitrification and even carbonaceous oxidation under prolonged conditions. The second event would cause a sudden rise in the sludge blanket level followed by excessive turbulence in the clarification zone and

upward movement of suspended solids. The result would be an increased effluent SS concentration associated with an increased effluent BOD, since the solids also contribute to the effluent BOD.

The developed process model did not simulate the DO concentration or its profile in the reactor. However by maintaining the oxygen demand of the mixed liquor below the maximum oxygenation capacity of the aeration system would ensure that the DO pattern in the reactor does not inhibit the aerobic processes.

During the study period the final clarifiers were operated at a solids loading substantially lower than the estimated maximum capacity and the observed effluent SS for that period was consistently low. Under these circumstances it was not possible to identify a successful relationship between the main process variables and the effluent SS, (Section 2.4). However it can be suggested that the effluent SS would be low, as long as the clarifiers are operated below their limiting-flux capacity and the sludge blanket level is below a certain depth, so that sufficient volume is provided for clarification.

The effluent BOD, consisting of a soluble and a particulate component, is also expected to be low under the above conditions. This is based on the fact that the soluble component was predicted to be low through simulations under a wide range of $MLSS$ concentrations, which can be explained by the low organic loading and long retention times prevailing in oxidation ditch systems. Consequently, if the particulate BOD is also low, through control of the effluent SS, the total effluent BOD is expected to satisfy the discharge limit of 10 mg/l.

In conclusion, the maximum limit for the operating $MLSS$ was defined as the concentration which satisfies simultaneously the following conditions :

1. The daily oxygen demand is below the maximum oxygenation capacity of the aeration system.
2. The solids loading of the final clarifiers does not exceed their limiting-flux capacity.

5.5.5 Determination of a minimum operating $MLSS$

The purpose for determining a minimum operating $MLSS$ was to prevent deterioration of the plant's effluent quality below the desired limits. According to the previous discussion, both the effluent SS and BOD_5 are expected to be low, as long as the process is operated below some maximum $MLSS$ concentration. Hence, the critical state variable to be controlled is the effluent ammonia concentration which depends on the degree of nitrification achieved. The nitrification process is reported

to be sensitive to process operating conditions (Section 5.2.5), due to the slow growth rate of nitrifying organisms and their sensitivity to external environmental factors (Section 3.3.3). During the study period high effluent ammonia concentrations were experienced from the plant which was shown to be the result of inefficient operation associated with certain operating problems leading to a substantial reduction in $MLSS$ level. The $MLSS$ indirectly affects the effluent ammonia, by influencing the concentration of the contained nitrifying population. Hence, the minimum operating $MLSS$ should not result in the effluent ammonia exceeding the desired limit.

The effluent nitrates are not restricted by a discharge limit, however a low effluent concentration benefits both the receiving waterbody and the plant operation (Section 3.19). Hence, the denitrification process may also be considered in the control problem and certain conditions can be specified related to either the effluent nitrate concentration or the percent of denitrification achieved. These conditions however, may be treated as 'soft' constraints in contrast to the constraints imposed to the other effluent variables, since their value may be modified to suit the particular plant operation.

The control of nitrification is often based on simple common practice approaches. A common remedial action to improve nitrification is to increase the operating sludge age by reducing the surplussing rate, which leads eventually to an increased $MLSS$ concentration. Such a control policy intends to promote the growth of the autotrophic organisms. However if their concentration in the system has fallen to very low levels, a significant time may elapse until nitrification is restored. Consequently the efficacy of such control policy depends largely on the skills and experience of the operator to act promptly, and for this reason frequent and prolonged exceedances of the ammonia limit are more likely to occur. A more formal approach to control nitrification would be based on a study of the process dynamics. For this purpose the developed process model was employed for relating the effluent ammonia concentration with the corresponding input and operating conditions of the plant.

The process model for nitrification-denitrification (Section 3.18.2) is a rather complex one, consisting of a set of non-linear differential equations which cannot be solved analytically. A simplification of the model would be necessary for deriving relatively simple relationships to be used for nitrification and denitrification control. The criterion for simplifying the model was the relative importance of each term in the equations, in determining the dynamic behaviour of the corresponding state over the one-day control interval. Consequently for the determination of nitrifier and denitrifier concentrations, the growth and decay functions were expressed by constant terms, due to their small short-term effect compared to the hydraulic components. For the determination of the effluent variables, their respective concentrations in the aeration tank and final clarifier were assumed equal. The following simplified model

was derived for the nitrification and denitrification processes.

I. Simplified model for nitrification

Nitrifiers

$$\frac{dBX}{dt} = \frac{Qr}{V} \cdot BR - \frac{Qi+Qr}{V} \cdot BX + GR_{BX} \qquad (5.6a)$$

$$\frac{dBR}{dt} = \frac{Qi+Qr}{Vcl} \cdot BX - \frac{Qr+Qw}{Vcl} \cdot BR \qquad (5.6b)$$

Effluent ammonia

$$\frac{dNH3e}{dt} = \frac{Qi}{V} \cdot NH3i - \frac{Qi}{V} \cdot NH3e - A \cdot f_N \cdot \mu_N \cdot BX \cdot 6.02 \qquad (5.7)$$

where ; $f_N = NH3e/(K_{NH_3} + NH3e)$.

The rate of change of nitrifiers due to a change in the flow rates is proportional to the total $MLSS$. The difference in their rate results from the different net growth rates and the effect of incoming non- degradable solids. However over a short time-period these effects are small compared to the hydraulic terms. Hence the nitrifiers were assumed to change proportionally to the $MLSS$.

The main reason for developing the above simplified model was to specify the necessary nitrifier concentration producing a given effluent ammonia concentration. Equation 5.7 is a first-order differential equation having the following analytical solution :

$$NH3e(\Delta t) = NH3e(0) \cdot e^{-Qi/V \cdot \Delta t} + NH3e(ss) \cdot (1 - e^{-Qi/V \cdot \Delta t}) \qquad (5.8a)$$

where; $NH3e(ss) = [Qi \cdot NH3i - A \cdot V \cdot f_N \cdot \mu_N \cdot BX \cdot 6.02]/Qi$, steady-state term (5.8b)

$NH3e(0)$: initial value,

$e^{-Qi/V \cdot \Delta t}$: transient term.

The importance of the transient term in determining the effluent ammonia concentration depends on the input flow rate and the time horizon of predictions (Δt). Table 5.5 shows the percentage contribution of the steady-state and initial-value terms to the final value, for two prediction periods and several input flows. It can be seen that the steady-state term affects the final value more than the initial term for a prediction period of one day, and even more for a period of 2 days. Hence, the use of the steady-state equation 5.8b for predicting effluent ammonia would not introduce significant error. This equation forms a simplified relationship describing the effect of inputs and operating conditions upon the effluent ammonia concentration.

Input flow	I.V.	S.V.	I.V.	S.V.
(m^3/d)	$\Delta t = 1$ day		$\Delta t = 2$ days	
4000	52.4 %	47.6 %	27.5 %	72.5 %
6000	38.0 %	62.0 %	14.4 %	85.6 %
8000	27.5 %	72.5 %	7.6 %	92.4 %
12000	14.4 %	85.6 %	2.0 %	98.0 %
16000	7.6 %	92.4 %	0.6 %	99.4 %

Table 5.5. Percent contribution of initial value (I.V.) and steady- state value (S.V.) for a range of flow rates.

Equation 5.8b can be solved directly to determine the desired operating conditions that produce a given effluent ammonia as shown below :

$$BX(des)_t = \frac{Qi_t \cdot [NHsi_t - NHse(sp)]}{A \cdot V \cdot f_N \cdot \mu_N \cdot 6.02} \tag{5.9a}$$

or

$$(A \cdot BX)des_t = \frac{Qi_t \cdot [NHsi_t - NHse(sp)]}{V \cdot f_N \cdot \mu_N \cdot 6.02} \tag{5.9b}$$

where; $NHse(sp)$: set-point effluent ammonia concentration,
$f_N = NHse(sp)/(K_{NH_3} + NHse(\text{sp}))$.

From eq. (5.9a & b) it can be seen that the operating conditions which can be used to control effluent ammonia are the population of nitrifiers (BX) and the volume of the aerobic zone (A). These variables can be controlled through the $MLSS$ concentration and the DO distribution respectively. Under a known proportion of nitrifiers in the biomass, the corresponding $MLSS$ concentration can be specified for a given size of the aerobic zone.

The developed process model does not take into account the commonly observed lag in the activity of nitrifying organisms under unsteady operating conditions resulting from the growth hysteresis phenomenon. Neglecting the lag does not produce significant error under normal operating conditions where the nitrifier concentration changes slowly. However under operational control, their concentration may be forced to change dramatically, ie. through increased transfer of biomass from the clarifiers into the ditch. In such case the model predictions regarding nitrification may not be realistic, since for example, a sudden increase in nitrifiers will not result in an immediate increase of nitrification rate. Therefore in cases where large fluctuations in the nitrifiers is necessary, their concentration should not be allowed to fall to very low levels, as may be dictated by equation 5.9.

II. Simplified model for denitrification

Denitrifiers

$$\frac{dDX}{dt} = \frac{Qr \cdot DR}{V} - \frac{(Qi + Qr) \cdot DX}{V} + GR_{DX} \tag{5.10a}$$

$$\frac{dDR}{dt} = \frac{(Qi + Qr) \cdot DX}{Vcl} - \frac{(Qr + Qw) \cdot DR}{Vcl} \tag{5.10b}$$

Effluent Nitrates

$$\frac{dNO3e}{dt} = \frac{Qi \cdot NO3i}{V} - \frac{Qi \cdot NO3e}{V} + A \cdot f_N \cdot \mu_N \cdot BX \cdot 6.02 - B \cdot f_D \cdot \mu_D \cdot DX \cdot 1.89 \cdot \theta_3^{(T-10)} \tag{5.11}$$

where; $f_D = \frac{BODe}{K_{SD} + BODe} \cdot \frac{NO3e}{K_{NO_3} + NO3e}$

The rate of change of denitrifiers can be considered proportional to that of $MLSS$, as was assumed for the nitrifiers. The model for effluent nitrates (eq. 5.11), can be used in a similar manner for deriving a simple relationship between inputs, operating conditions and the denitrification performance. The time constant in eq. 5.11 is the same as in eq. 5.8a, and it was shown (Table 5.5) that the steady-state term can adequately predict the effluent concentration. The steady-state term of eq. 5.11 is given by:

$$NO3e(ss) = [Qi \cdot NO3i + A \cdot V \cdot f_N \cdot \mu_N \cdot BX \cdot 6.02 - B \cdot V \cdot f_D \cdot \mu_D \cdot DX \cdot 1.89 \cdot \theta_3^{(T-10)}]/Qi \tag{5.12}$$

Hence the operating conditions to control denitrification are the concentration of denitrifiers and volume of anoxic zones. The above equation can be used for estimating the desired denitrifier concentration to satisfy a number of criteria regarding the denitrification performance, such as :

- achieve a given set-point effluent nitrate concentration NO3e(sp).

$$DX(des)_t = \frac{Qi_t \cdot (NH3i_t + NO3i_t - NH3e(sp) - NO3e(sp))}{B \cdot V \cdot f_D \cdot \mu_D \cdot 1.89 \cdot \theta_3^{(T-10)}}$$

since: $A \cdot V \cdot f_N \cdot \mu_N \cdot BX_t \cdot 6.02 = Qi_t \cdot (NH3i_t - NH3e(sp))$, (5.13a)

which is valid under the assumption that effluent ammonia is also controlled to a set-point value.

- achieve a given percentage of denitrification ($a\%$).

$$DX(des)_t = \frac{\frac{a}{100} \cdot Qi_t \cdot (NH3i_t + NO3i_t)}{B \cdot V \cdot f_D \cdot \mu_D \cdot 1.89 \cdot \theta_3^{(T-10)}} \tag{5.13b}$$

5.5.6 Discussion

From the previous analysis it was shown that nitrification and denitrification are very sensitive reactions and can seriously affect the effluent performance of an oxidation ditch plant. It was also shown that control of effluent ammonia can be achieved either by regulating the nitrifier concentration and/or altering the volume of the aerobic zones. Similarly, control of effluent nitrate can be achieved by regulating the denitrifier concentration and/or the volume of the anoxic zones.

In practice the volume of aerobic and anoxic zones is usually fixed, maintained via an automatic *DO* control system as in the case of the Cirencester plant. The respective volumes are normally selected by trial and error, so that the reactor attains simultaneous nitrification and denitrification, but it is also constrained by the oxygenation capacity of the aeration system. Changing the *DO* distribution in the reactor, alters the volume of aerobic and anoxic zones, and can be referred to as *DO* profile control. This can be implemented by adjusting the *DO* set-point level at the monitoring location. However such method is not practised as a short-term control tactic, but it may serve as an additional longer-term control measure. For example, in the case of persistently poor denitrification and high nitrification, the anoxic zone could be increased at the expense of the aerobic zone by lowering the *DO* set-point.

In conclusion it was shown that for the operational control of the oxidation ditch, the nitrifiers and denitrifiers constitute the main variables of concern regarding effluent quality, in addition to the sludge blanket variation. However the former two variables are unmeasurable quantities, and their control can only be implemented indirectly through the *MLSS* concentration. The desired concentration of nitrifiers and denitrifiers can be specified according to a selected operating policy for controlling effluent ammonia and nitrates, which can then be used to determine the operating *MLSS*. Furthermore, the *MLSS* should be bounded by a maximum level, in order to prevent exceeding the capacity of certain process units.

5.6 Design of control systems for the oxidation ditch process

5.6.1 Main control methods

So far the operational control problem of the oxidation ditch process was analyzed and a methodology presented for determining an optimum operating *MLSS* concentration. Next, a control system was designed for achieving the desired operating conditions. This stage forms the lower level in the control hierarchy in which classical control methods were applied. Initially the advantages and weaknesses of classical control methods were examined regarding their applicability to the oxidation ditch

process.

The simplest type of control would be a proportional error feedback with constant gains having the general form :

$$\Delta \underline{u}(t) = F \cdot [\underline{X}_{des}(t) - \underline{X}(t)] \qquad (5.14)$$

where; $\Delta \underline{u}(t)$: applied change to the control inputs at time t,
F : matrix of proportionality coefficients (FB gain matrix),
$\underline{X}(t)$: state vector at time t,
$\underline{X}_{des}(t)$: set-point values of the state vector at time t.

The advantage of this control system, shown schematically in Fig. 5.23a, is that its application requires little knowledge of the process dynamics. However its performance largely depends upon the selection of the feedback gains. In the simplest case the gains are constant usually estimated by a trial and error procedure which does not require any knowledge of the process. This type of control can produce satisfactory performance for linear non-dynamic systems, but can deteriorate dramatically in complex dynamic systems. The efficiency of the above controller can be substantially improved if applied in adaptive mode, where the gains are updated at each step in response to changes in the inputs and current state of the process. However such a control system would require a suitable model of the process dynamics.

Proportional error FB control has an inherent disadvantage of producing steady-state error under step-input functions, meaning that the control system cannot accurately achieve the desired operating conditions. The addition of an integral control function eliminates the steady-state error during constant set-point control. The proportional-integral FB control function has the following form :

$$\Delta \underline{u}(t) = F \cdot \underline{E}(t) + Fi \cdot \int_0^t \underline{E}(\tau) \cdot d\tau \qquad (5.15)$$

where; $\underline{E}(t) = \underline{X}_{des}(t) - \underline{X}(t)$: set-point error vector at time t,
Fi : integral gain matrix.

However under variable set-point control, which is the case here with *MLSS* control, the above controller does not eliminate the set-point error. Furthermore, in the application of adaptive feedback control to an oxidation ditch system at discrete time intervals, several other more important sources of error can arise due to the following factors :

1. The variability in the inputs, affecting the process states during the control interval.

2. Simplifications and assumptions made in the derivation of the process model.
3. Difference between the final values of the control inputs and their initial values used in the adaptive estimation of gain matrix.

A prediction-error FB control algorithm accounts for the effect of variable future inputs over the forthcoming control interval. However its application requires the existence of an adequate process model, to predict the system states at the end of the control interval and in addition a forecasting model to predict the future process inputs. The algorithm uses the predicted set-point error, at the end of the control interval, instead of the current error. The control law is identical to the simple FB (equation 5.14), but the control system representation is more complex as shown in Fig. 5.23b. This algorithm is particularly efficient under application of discrete control in cases where the inputs are likely to vary considerably during the control interval, as for the particular oxidation ditch process. However its performance depends largely on the ability to accurately forecast the inputs. The efficiency of the algorithm also depends on the performance of the process model, the frequency of control application and the time constants of the process. Another disadvantage of the algorithm is the relatively high computing power requirements for both input and state predictions.

The determination of gains in feedback control systems can be conducted by two different approaches depending on the nature of the control system and the existing knowledge of the process.

- The first approach is to specify the constant gains through a trial and error procedure, where the existence of a process model is optional. In this approach the gains are adjusted until the control system exhibits satisfactory long- term performance. A similar approach is commonly employed by process operators, who exert control actions based on intuition and past experience on how the process responds to changes in the controls. This approach can be formalized by adopting a proportional error constant-gain FB system, in which the gains can be determined by minimizing some function of the predicted set-point error over the simulated period.
- The second approach involves the adaptive estimation of the gain matrix at each time step in response to changes in the inputs and operating conditions. This approach requires a process model and leads to the formulation of adaptive control. The gains are estimated on the basis of certain criteria such as, elimination of the set-point error at a given time instant and minimization of the corrective action upon the control inputs. This approach is more complex and is rarely implemented on-site, since it requires the availability of computing

facilities, as well as, specifically prepared control algorithms. However, there is better prospect of applying adaptive control in the future because it provides more efficient and reliable means of operational control, which is related to the current input and operating state of the process and independent of the operator's experience.

Both adaptive and constant-gain FB control systems were investigated and the merits and disadvantages of each assessed via simulations.

Finally the application of Feedforward control requires measurements of the inputs and the existence of a process model. The control law is expressed as a function of the inputs, rather than of the set-point error. As a result feedforward control may be simpler for on-site application compared to feedback control ; however its design can be much more complicated if the process is complex or under variable set-point control. Nevertheless, application of FF control alone cannot eliminate the set-point error in the control variables, due to inherent weaknesses of the process model, potential errors in the input measurements and random process disturbances. Hence it is usually combined with a simple FB controller. The resulting combined FB-FF control system can have a rather complex structure, as shown schematically in Fig. 5.23c, while its performance may not be higher than some of the previously described FB controllers. For this purpose FF control was not considered in this study. Real-time application of FF control at short time-intervals, can achieve higher performance, however the inputs must be monitored continuously requiring the installation of on-line instrumentation.

The design and selection of a suitable system for the oxidation ditch process was influenced by factors such as :

- The ability of the system to achieve the desired operating conditions.
- The dynamic behaviour of the process and nature of the inputs.
- The available measurements of input, output and process variables and frequency of monitoring.
- The stability of the controlled system.
- The desired complexity of the control algorithm.
- The available knowledge of the internal process mechanisms.

5.6.2 Available measurements for process control

The available measurements for the design and application of the control system, concern the following variables shown below by their notation :

Process inputs : Qi, $BODi$, $NHsi$, $NO3i$, $Temp.$
Process states : $MLSS$, BL, $(RASS)$.
Process outputs : $BODe$, $NH3e$, $NO3e$, (SSe).
Control inputs : Qr, Qw.

Measurements of the input variables serve as the forcing functions of the control system and simulation model. The process states are necessary for comparison with the desired set-point values and determination of set-point error in FB control systems. The output variables serve for assessing the process performance and its compliance with the discharge standards. The process states and output variables can be either measured or estimated via the simulation model. Finally the control inputs are necessary for setting them to the desired level dictated by the control system.

In this study the measured input values were employed. It was assumed that the current inputs were available before calculating the control action for the following time-step. This assumption is not realistic for the BOD measurement due to the long time required for its determination. However the BOD value was only used for simulation purposes rather than for control, so that in the absence of the current BOD measurement, an estimated value could be used without affecting the performance of the control system.

5.6.3 Simplified process model for solids control

In most control problems linear control theory is applied because of its simplicity. This implies that the model should be linearized with respect to the manipulated variables around a steady-state operating conditions. Highly non-linear process models tend to give very complex linearized forms showing poor performance outside the steady-state level due to the large effect of the 2nd- and higher- order terms. Furthermore in case that the controller gains are determined on the basis of some optimization procedure, a complex model would substantially increase the computational load, while its use may not be always justified in view of the stochastic disturbances of the process and the uncertainty in the process model. Therefore, a less accurate but simple model is generally preferable for the design of a control system. For the operational control of $MLSS$ concentration and sludge blanket level a

simplified process model was used, in which the bacterial growth and decay functions were expressed collectively by a non- dynamic term and the effluent solids mass was neglected. Due to the application of the model under a wide range of operating conditions, the thickening limitations of the clarifiers had to be considered, as discussed in Section 2.5.5. The simplified model equations are shown below :

$$\frac{d(MLSS_t)}{dt} = \frac{Qi_t \cdot Xo_t}{V} + \frac{Qr_t \cdot RASS_t}{V} - \frac{(Qi_t + Qr_t) \cdot MLSS_t}{V} + GR_{net} \qquad (5.16)$$

$$\frac{d(RASS_t)}{dt} = \frac{G_{A_t} \cdot Acl}{Vcl} - \frac{(Qr_t + Qw_t) \cdot RASS_t}{Vcl} \qquad (5.17)$$

For $RASS_t < C_L$: $C_t = RASS_t$ and

$$\frac{d(BL_t)}{dt} = [(Qi_t + Qr_t) \cdot MLSS_t - (Qr_t + Qw_t) \cdot RASS_t] \cdot \frac{(H_T - BL_t)}{C_t \cdot Vcl} \qquad (5.18a)$$

For $RASS_t \geq C_L$: $C_t = C_L$ and

$$\frac{d(BL_t)}{dt} = [(Qi_t + Qr_t) \cdot MLSS_t - (Qr_t + Qw_t) \cdot RASS_t] \cdot \frac{H_T}{C_t \cdot Vcl} - \frac{\Delta(BL)}{\Delta t} \cdot V_{BL} \qquad (5.18b)$$

where; GR_{net_t} given by equation 5.2b.

$$G_{A_t} \cdot Acl = (Qi_t + Qr_t) \cdot MLSS_t \leq G_L(Qr_t, Qw_t, t)$$

$$C_L = f(Qr_t, Qw_t, t)$$

An approximate analytical solution of the above system of differential equations was found by solving equation 5.17 independently, assuming that the $MLSS$ and the input variables remain constant over the one-day integration period. The solution was then substituted into eq. 5.16, which becomes a first-order differential equation. Finally eq. 5.18 was solved using the modified Euler's method and substituting the state values from the previous equations. This equation was further simplified under the assumption that the blanket level does not deviate significantly from the set-point level. The procedure is illustrated below :

$$\widehat{RASS}(t_{k+1}) = RASS(t_k) \cdot e^{-a \cdot \Delta t} + \frac{(Qi + Qr) \cdot MLSS(t_k)}{Qr + Qw} \cdot (1 - e^{-a \cdot \Delta t}) \qquad (5.19)$$

$$\frac{dMLSS_t}{dt} = \frac{Qi \cdot Xo}{V} + \frac{Qr \cdot RASS(t_k)}{V} \cdot e^{-a \cdot \Delta t} + [\frac{(Qi + Qr) \cdot Qr}{(Qr + Qw) \cdot V} \cdot (1 - e^{-a \cdot \Delta t}) - \frac{Qi + Qr}{V}] \cdot MLSS_t + GR_{net} \qquad (5.20)$$

$$\widehat{MLSS}(t_{k+1}) = MLSS(t_k) \cdot e^{-b \cdot \Delta t} + \frac{Qi \cdot Xo + Qr \cdot RASS(t_k) \cdot e^{-a \cdot \Delta t} + V \cdot GR_{net}}{V \cdot b} \cdot (1 - e^{-b \cdot \Delta t}) \qquad (5.21)$$

$$\widehat{BL}(t_{k+1}) = BL(t_k) + 0.5 \cdot \Delta t \cdot [(Qi + Qr) \cdot (MLSS(t_k) + \widehat{MLSS}(t_{k+1})) - (Qr + Qw) \cdot (RASS(t_k) + \widehat{RASS}(t_{k+1}))] \cdot \frac{H_T - BL_{sp}}{C \cdot Vcl} \qquad (5.22)$$

where; $a = (Qr + Qw)/Vcl$

$b = (Qi + Qr)/V - (Qi + Qr) \cdot Qr/(Qr + Qw) \cdot V \cdot (1 - e^{-a \cdot \Delta t})$

$\Delta t = t_{k+1} - t_k$ the one-day integration interval.

For the variables Qi, Qr, Qw, Xo, and GR_{net} their predicted value at t_{k+1} is assumed in the above equations.

5.6.4 Constant-gain proportional feedback control systems

The objective at the lower level of the control hierarchy was to control primarily the $MLSS$ in the aeration tank and secondarily the sludge blanket level in the final clarifiers (Section 5.5.1). The simplest type of $MLSS$ control would be a proportional-error, single-loop FB controller by regulating the recycle and surplus sludge flow rates. The control law derived from the general form (eq. 5.14), for the case of discrete control is given by :

$$\underline{u}(t_{k+1}) = \underline{u}(t_k) + F \cdot [MLSS_{sp}(t_k) - MLSS(t_k)] \tag{5.23}$$

where; $\underline{u}(t_k) = \begin{vmatrix} Qr(t_k) \\ Qw(t_k) \end{vmatrix}$: vector of manipulated variables,

$F = \begin{vmatrix} F_1 \\ F_2 \end{vmatrix}$: the Feedback gain matrix,

$MLSS_{sp}(t_k)$: desired $MLSS$ concentration at time t_k,

$MLSS(t_k)$: observed " " " t_k.

The gain matrix in the simplest algorithm is constant and can be calculated through a trial and error procedure (Section 5.6.1). For this purpose the Rosenbrock's constrained optimization technique was employed for estimating the gains by minimizing the square deviation of $MLSS$ from its desired value. Hence, the optimization problem was :

$$\min_F J = \sum_{k=1}^{N} [MLSS_{sp}(t_k) - MLSS(t_k)]^2$$

subject to : $Qr_{min} < Qr(t_k) < Qr_{max}$

and $Qw_{min} < Qw(t_k) < Qw_{max}$.

where; J is the objective function,

N number of observations.

The simplified process model (eq. 5.19-5.22) was employed for simulating the $MLSS$ concentration. As inputs to the model were used the measurements from the

283-day study period, while the initial conditions for the $RASS$ and the manipulated variables were specified externally. The optimum gain values were estimated for a number of $MLSS$ set-point levels, ranging from 2,000 to 5,000 mg/l, in order to assess their sensitivity with the operating $MLSS$. The operating boundaries for the control inputs were specified as :
$Qr_{\min} = 1{,}500$, $Qr_{\max} = 20{,}000$, $Qw_{\min} = 0$ and $Qw_{\max} = 500\ m^3/d$.

$MLSS$	Initial			Average			Optimum		Minimum
(sp)	$RASS$	Qr	Qw	$RASS$	Qr	Qw	F_1	F_2	$\sum(E_{ML})^2$
2000	5000	5000	300	5356	4366	336.9	7.7027	-0.2357	3.076E+6
2500	6000	5000	300	6158	5123	301.1	7.8500	-0.2603	4.060E+6
3000	7000	5500	280	7010	5696	275.0	7.1246	-0.2389	4.695E+6
3500	7500	6500	260	7623	6494	260.2	7.3366	-0.2440	4.922E+6
3500	8000	6000	250	7975	6031	251.0	6.8858	-0.2112	5.225E+6
3500	7000	7000	270	7373	7037	270.6	7.9643	-0.2316	4.757E+6
4000	8000	7000	250	8383	7155	246.6	7.3198	-0.2411	5.374E+6
4500	9000	7500	230	9137	7556	230.5	7.4595	-0.1927	5.487E+6
5000	9500	9000	200	9672	8248	220.4	7.7080	-0.1939	5.715E+6

Table 5.6. Determination of gains in the single-loop FB controller.

The results are summarized in Table 5.6 and in Figure 5.24 for a $MLSS$ set-point of 3,500 mg/l. It can be seen that the gains are slightly affected by the set-point $MLSS$ concentration, while the initial conditions can have a more marked effect. This is because the initial conditions determine, to some extent, the average operating conditions of the plant. The performance of the controller slightly deteriorates at higher $MLSS$ levels, judged by the increased set-point error. The gain for the recycle (F_1) is several times greater than the corresponding gain for the surplus flow (F_2), due to the different magnitude of the two flows. In general, this simple FB scheme showed satisfactory performance in controlling the $MLSS$ to a constant set-point level. However its application requires the existence of a separate override controller for maintaining a constant sludge blanket level, which was observed to vary significantly in the previous simulations.

Control of the sludge blanket can also be achieved via a separate FB loop involving the regulation of the underflow rate. Since the underflow represents the sum of recycle and surplus flows, the control law for the sludge blanket can be also expressed with a function similar to equation 5.23. The resulting two-loop FB controller has

the following form :

$$\begin{vmatrix} Qr(t_{k+1}) \\ Qw(t_{k+1}) \end{vmatrix} = \begin{vmatrix} Qr(t_k) \\ Qw(t_k) \end{vmatrix} + \begin{vmatrix} F_{11} & F_{12} \\ F_{21} & F_{22} \end{vmatrix} \cdot \begin{vmatrix} MLSS_{sp}(t_k) - MLSS(t_k) \\ BL_{sp}(t_k) - BL(t_k) \end{vmatrix} \tag{5.24}$$

hence,

$$\begin{aligned} Qr(t_{k+1}) &= Qr(t_k) + F_{11} \cdot [MLSS_{sp}(t_k) - MLSS(t_k)] + F_{12} \cdot [BL_{sp}(t_k) - BL(t_k)] \\ Qw(t_{k+1}) &= Qw(t_k) + F_{21} \cdot [MLSS_{sp}(t_k) - MLSS(t_k)] + F_{22} \cdot [BL_{sp}(t_k) - BL(t_k)] \end{aligned} \tag{5.25}$$

The gain matrix can be calculated via optimization as before. In this case the objective function contained the square deviation of both states from their set-points, multiplied by suitable weighting factors. Hence the optimization problem was :

$$\min_F J = \sum_{k=1}^{N} \{w_1 \cdot [MLSS_{sp}(t_k) - MLSS(t_k)]^2 + w_2 \cdot [BL_{sp}(t_k) - BL(t_k)]^2\}$$

where; $w_1 = 1$ and $w_2 = 100$, the values assigned to the weights.

Initial simulation results with two different set-points for $MLSS$, produced very high recycle and surplus sludge flows frequently reaching their upper limits (Table 5.7, cases 1 & 2 and Figure 5.25). However such operating conditions lead to the production of a dilute $RASS$ concentration, which is undesirable, since it was shown to reduce the thickened sludge concentration and hence increase the sludge disposal cost (Section 5.3.5). Furthermore, high recycle flow rate leads to higher cost for pumping. For this purpose the objective function was modified in order to maximize the $RASS$ concentration, in addition to minimizing the square set-point error.

$$\begin{aligned} \min_F J = \sum_{k=1}^{N} \{ & w_1 \cdot [MLSS_{sp}(t_k) - MLSS(t_k)]^2 + w_2 \cdot [BL_{sp}(t_k) - BL(t_k)]^2 \\ & - w_3 \cdot (RASS(t_k))^2\} \end{aligned}$$

Results with different values for weight w_3 and $MLSS$ set-point, showed an increase in the operating $RASS$ concentration associated with a reduction in the flow rates (Table 5.7, cases 3-6) and Fig. 5.26. However the set-point error also increased indicating poorer performance of the controlled system. It is important to note that both gains for sludge blanket control were positive, implying that a positive error in sludge blanket would produce an increase in the underflow rate. However from the transient response analysis (Fig. 5.22, Section 5.4) it can be seen that such an action would further increase the set-point error, suggesting that the two- loop controller may cause instability. This phenomenon can be attributed to the strong interaction between the two control loops, because they employ the same control inputs. The results also show that the surplus sludge gains F_{21} and F_{22} are much lower compared

to the single-loop case, implying that the two-loop system approximates to a recycle control system, where the surplus flow plays a minor role in process control. Finally, it must be recognized that the gain matrix would be also affected by the changes in the settling characteristics of the sludge, which were assumed constant in the previous simulations.

The constant-gain, proportional-error FB controller is simple and can be easily implemented by the process operator because it requires minimal computing facilities. However, from the previous analysis it was shown that such controller cannot be efficiently applied to the oxidation ditch, due to the complex and dynamic nature of the process. Some of the observed weaknesses of such a control system are summarized below :

Param.	Case 1	Case 2	Case 3	Case 4	Case 5	Case 6
$MLSS_{sp}$	4000	3000	4000	4000	3500	3000
$Qr(in)$	7000	5500	7000	7000	6500	5500
$Qw(in)$	250	280	250	250	260	280
$RASS_{in}$	8000	7000	8000	8000	7500	7000
w_3	—	—	0.2	0.4	0.4	0.4
$\widehat{MLSS}$	4008±120	3006±114	3989±164	3998±144	3498±147	2999±143
$\widehat{RASS}$	5917±1443	4756±946	8349±1861	8406±2104	8264±2254	7657±2150
$\widehat{BL}$	1.07±0.04	1.06±0.7	1.04±0.14	1.04±0.14	1.03±0.17	1.03±0.18
Qr	17251±2484	12962±5164	7196±4213	6962±3179	5537±2502	4799±2280
Qw	349±157	401.7±118	237.9±3.0	237±16.2	233.2±27	242.3±34
F_{11}	10.048	8.54141	5.8790	6.70048	6.59361	7.05963
F_{12}	-29.994	-34.4359	3.2632	0.83968	3.00432	3.16809
F_{21}	-2.771	-1.33587	-0.001823	-0.037478	-.089515	-0.127964
F_{22}	-6.056	-7.14652	0.006864	0.000597	0.0002988	-0.00221
$\sum E_{ML^2}$	6.089E+6	6.015E+6	13.866E+6	12.252E+6	14.57E+6	15.131E+6

Table 5.7. Estimation of gains in the two-loop Feedback controller.

- Although single-loop $MLSS$ control showed satisfactory performance, it must be used in conjunction with an override sludge blanket controller.
- The two-loop system for combined $MLSS$ and sludge blanket control became less efficient due to strong interactions between the control loops, which could also lead to instability problems.
- The introduction of a maximum $RASS$ function resulted in very small gains for the surplus flow suggesting that the controller was mainly based on recycle control, and the function of the surplus flow was not adequately exploited.

- Under a variable thickening capacity of the clarifiers the constant-gain control is very inefficient, and causes either overloading or underloading of the final tanks followed by a dramatic variability of the sludge blanket level.
- The gain matrix was shown to be affected by both the set-point level and initial state values.

5.6.5 Adaptive, prediction-error feedback control systems

Application of adaptive FB control was expected to overcome some of the previous deficiencies arising from the complex dynamic behaviour of the process. The adaptive proportional-error controller was not examined, because the control action is based on the current set-point error and no consideration is given to the effect of future inputs, upon the control variables (Section 5.6.1). Consequently the prediction-error controller was studied, but its application requires knowledge of the future process inputs over the forthcoming control interval. Time-series and linear regression analysis techniques were employed in an attempt to forecast the input variables by exploiting their autoregressive structure and the correlation between them. The input flow was found to exhibit significant serial correlation (Fig. 2.12e) and to a lower degree the input BOD_5 and ammonia concentrations (Fig. 2.12a,d), as discussed in Section 2.3.5. However the corresponding loads showed insignificant autocorrelation (Fig. 5.27). The above indicate that although the input concentrations have a strong serial structure, the corresponding loads vary stochastically and hence they cannot be accurately forecasted in deterministic terms.

Nevertheless, several non-dynamic model structures were examined for predicting the main process inputs which are summarized in Table 5.8 in order of performance. It can be seen that the ability of the models to forecast the inputs is poor, except for the input flow. In addition the improvement in their performance increases marginally with the complexity of the models, ranging between 6-18% in terms of reduction in the RMS error between the first and last model examined. Therefore, in view of the stochastic nature of the inputs and the generally poor model performance, there was no justification of employing a complex model structure for their prediction. For this purpose the simplest model was employed, which assumes that the current inputs are the best estimates of the future inputs. Next, two adaptive prediction-error FB schemes, based on a different approach for calculating the control action, were designed and compared. These were referred to as "iterative" and "adaptive-gain" FB control systems.

Model structure	Correl.	C.O.D.	RMSer
Input flow prediction: $\hat{Qi}(t_{k+1})$ =			
$Qi(t_k)$	0.969	0.937	1592
$a \cdot Qi(t_k)$	0.969	0.938	1580
$a \cdot Qi(t_k) + b$	0.969	0.938	1575
$a \cdot Qi(t_k) + b \cdot Rain(t_k) + c$	0.969	0.939	1568
$a \cdot Qi(t_k) + b \cdot Temp(t_k) + c$	0.969	0.939	1563
$a \cdot Qi(t_k) + b \cdot Qi(t_{k-1}) + c$	0.971	0.943	1508
$a \cdot Qi(t_k) + b \cdot Qi(t_{k-1}) + c \cdot Qi(t_{k-2}) + d$	0.972	0.944	1491
Input organic concentration prediction: $\widehat{BODi}(t_{k+1})$ =			
$BODi(t_k)$	0.710	0.420	58.4
$a \cdot BODi(t_k) + b$	0.710	0.504	53.9
$a \cdot BODi(t_k) + b \cdot BODi(t_{k-1}) + c$	0.714	0.510	53.6
$a \cdot BODi(t_k) + b \cdot Temp(t_k) + c$	0.724	0.524	52.8
$a \cdot BODi(t_k) + b \cdot Qi(t_k) + c$	0.746	0.556	51.0
Input organic load prediction : $\widehat{BODLD}(t_{k+1})$ =			
$BODLD(t_k)$	0.350	-0.295	390
$a \cdot BODLD(t_k)$	0.350	-0.143	367
$a \cdot BODLD(t_k) + b$	0.350	0.123	321
$a \cdot BODLD(t_k) + b \cdot BODLD(t_{k-1}) + c$	0.350	0.123	322
$a \cdot BODLD(t_k) + b \cdot Qi(t_k) + c$	0.363	0.132	320
$a \cdot BODLD(t_k) + b \cdot Qi(t_k) + c \cdot Temp(t_k) + d$	0.367	0.135	319
Input ammonia concentration prediction : $\widehat{NH3i}\ (t_{k+1})$ =			
$NH3i(t_k)$	0.892	0.785	4.24
$a \cdot NH3i(t_k) + b$	0.892	0.796	4.12
$a \cdot NH3i(t_k) + b \cdot NH3i(t_{k-1}) + c$	0.894	0.799	4.09
$a \cdot NH3i(t_k) + b \cdot Temp(t_k) + c$	0.896	0.803	4.05
$a \cdot NH3i(t_k) + b \cdot Qi(t_k) + c$	0.907	0,823	3.83
Input ammonia load prediction : $\widehat{NH3LD}(t_{k+1})$ =			
$NH3LD(t_k)$	0.486	-0.032	33.9
$a \cdot NH3LD(t_k) + b$	0.486	0.236	29.2
$a \cdot NH3LD(t_k) + b \cdot NH3LD(t_{k-1}) + c$	0.492	0.242	28.8
$a \cdot NH3LD(t_k) + b \cdot Temp(t_k) + c$	0.514	0.264	28.6
$a \cdot NH3LD(t_k) + b \cdot Qi(t_k) + c$	0.519	0.270	28.5
$a \cdot NH3LD(t_k) + b \cdot Temp(t_k) + c \cdot Qi(t_k) + d$	0.523	0.273	28.5
Input suspended solids prediction : $\widehat{SSi}(t_{k+1})$ =			
$SSi(t_k)$	0.689	0.379	72.6
$a \cdot SSi(t_k) + b$	0.689	0.475	66.6
$a \cdot SSi(t_k) + b \cdot SSi(t_{k-1}) + c$	0.694	0.481	66.2
$a \cdot SSi(t_k) + b \cdot Temp(t_k) + c$	0.710	0.505	64.7
$a \cdot SSi(t_k) + b \cdot Qi(t_k) + c$	0.738	0.544	62.0

Table 5.8. Comparison of performance of models for process input forecasting.

5.6.6 Iterative feedback control system

This is an adaptive control system where the control action for achieving the desired condition for $MLSS$ and sludge blanket level is calculated for each step by an iterative procedure. The aim of this system is to determine optimum values for the control inputs minimizing the predicted set-point error at the end of the current control interval. This is equivalent to an optimization problem in which the objective function contains the deviation of the control variables from their set-point value, as shown below :

$$J_1 = w_1 \cdot \left| MLSS_{sp}(t_{k+1}) - \widehat{MLSS}(t_{k+1}) \right| + w_2 \cdot \left| BL_{sp}(t_{k+1}) - \widehat{BL}(t_{k+1}) \right| \qquad (5.26)$$

where; w_1, w_2 : weighting factors to be determined,
t_{k+1} : time at the end of current control interval,
$\widehat{MLSS}(t_{k+1})$: predicted $MLSS$ at the end of the control interval (t_{k+1}),
$MLSS_{sp}(t_{k+1})$: set-point $MLSS$ at t_{k+1},
$\widehat{BL}(t_{k+1})$: predicted sludge blanket level at t_{k+1},
$BL_{sp}(t_{k+1})$: set-point sludge blanket at t_{k+1}.

The optimization problem can then be stated as :

$$\min_{Qr(t_{k+1}),Qw(t_{k+1})} J_1 = f(Qr(t_{k+1}), Qw(t_{k+1}))$$

$$\text{subject to : } Qr_{\min} \leq Qr(t_{k+1}) \leq Qr_{\max} \quad \text{and}$$
$$Qw_{\min} \leq Qw(t_{k+1}) \leq Qw_{\max}.$$

The Rosenbrock's constrained optimization technique was employed for determining the optimum flow rates at t_{k+1} . The states were predicted at the end of the control interval using the simplified process model (eq. 5.19-5.22). As inputs to the model were used their current values at t_k, which were assumed to serve as best estimates of the future inputs during the period $t_k - t_{k+1}$. The desired $MLSS$ level at t_{k+1} was to be determined according to a selected operating policy at the higher level of the control hierarchy (Section 5.5.6). Regarding a desired level for the sludge blanket, this is usually specified in practice by an acceptable range of variation, for which the clarifiers have shown good long-term performance. Accordingly, sludge blanket control is effected only when the predicted level lies outside the specified range. Incorporating this feature into objective function J_1 gives :

$$J_2 = w_1 \cdot \left| MLSS_{sp}(t_{k+1}) - \widehat{MLSS}(t_{k+1}) \right| + w_2 \cdot [\mathrm{H}\ (\widehat{BL}(t_{k+1}) - BL_{max}) - \mathrm{H}\ (BL_{min} - \widehat{BL}(t_{k+1}))] \qquad (5.27)$$

where; H : Heaviside operator,

$$\mathrm{H}\,(a-b) = \begin{cases} 1 & \text{if } a \geq b \\ 0 & \text{if } a < b \end{cases}$$

BL_{min}, BL_{max} : lower and upper limit in sludge blanket variation.

The iterative FB system based on objective function J_2 can eliminate ideally the set-point error in both states at the end of the control interval (t_{k+1}), unless :

- One or both of the control inputs reach their operating boundaries.
- The desired conditions for the two controlled states cannot be satisfied simultaneously, (ie. to increase simultaneously the $MLSS$ and sludge blanket levels).

Nevertheless, some set-point error in the states is expected to occur, even if zero error is predicted by the control algorithm. Such error would be the result of inaccuracies in predicting the future inputs and weaknesses in the assumptions for deriving the simplified process model.

The magnitude of the corrective action depends on the current process inputs and state variables, as well as, on the magnitude of the set-point error. In general, large set-point errors require large changes to the control inputs which may then cause disturbances to the process and particularly to the clarification performance. Hence, it is preferable to avoid excessive control actions even at the risk of not achieving the desired operating conditions. This suggestion is further justified under the existence of other potential sources of error discussed already. Subsequently objective function J_2 was modified, in order to minimize the square variation in the controls between successive steps :

$$\begin{aligned} J_3 \;=\; & \{w_1 \cdot |MLSS_{sp}(t_{k+1}) - \widehat{MLSS}(t_{k+1})| + \\ & w_2 \cdot [\mathrm{H}\,(\widehat{BL}(t_{k+1}) - BL_{max}) - \mathrm{H}\,(BL_{min} - \widehat{BL}(t_{k+1}))] + \\ & w_3 \cdot [\widehat{Qr}(t_{k+1}) - Qr(t_k)]^2 + w_4 \cdot [\hat{Q}w(t_{k+1}) - Qw(t_k)]^2\} \end{aligned} \qquad (5.28)$$

Every term in the objective function is multiplied by a suitable weighting factor, which accounts for the different magnitude of each component and in addition determines their relative importance in the control problem. Large weighting factors for the $MLSS$ and sludge blanket terms (w_1 & w_2), would indicate that emphasis is given to eliminate set-point errors irrespective of the variability in the control inputs. However the reverse would produce relatively small changes to the control inputs, leading to a more stable process operation. The weights w_3 and w_4 can be related to the respective changes in the recycle and surplus flow under different control situations. A ratio in w_3/w_4 of about 1:1000 was found to spread reasonably well the

control action between the two flow rates.

These weights can be simply selected by trial and error, until a reasonable performance of the controlled system is observed. The weight w_1, associated with the predicted *MLSS* set-point error, can be also calculated formally by exploiting the process dynamics. This procedure requires the use of a process model and some criterion, such as zero prediction error at t_{k+1}, for adaptive estimation of the weight in each step. However by this approach the derived control action can be very large particularly when large set-point errors are predicted, so that the objective of reducing the control input variability cannot be fulfilled. Alternatively, by specifying a constant value for w_1, large changes to the controls can be mitigated by allowing some set- point error to occur.

Finally, the weight for the sludge blanket variation (w_2), was assigned a suitably high value so that a corrective action is always initiated in response to a predicted deviation outside the specified range. As a result the system approximates to an override sludge blanket control. This in addition mitigates the interaction between the two control loops, discussed in Section 5.6.4, by giving higher priority to the sludge blanket loop.

5.6.7 Adaptive-gain feedback control system

Another adaptive control system can be based on the sensitivity coefficients of the process states with respect to the control inputs for the estimation of the gain matrix. The sensitivity matrix $S(t)$ of the system is :

$$S(t) = \frac{d\underline{X}(t)}{d\underline{u}} = \begin{vmatrix} d\,MLSS_t/d\,Qr & d\,MLSS_t/d\,Qw \\ d\,BL_t/d\,Qr & d\,BL_t/d\,Qw \end{vmatrix} = \begin{vmatrix} S_{11} & S_{12} \\ S_{12} & S_{22} \end{vmatrix} \tag{5.29}$$

In finite-difference terms the above equation becomes :

$$H \cdot S(t) \cdot \Delta\underline{u}(t) = H \cdot \Delta\underline{X}(t) \tag{5.30}$$

where; H : the measurement matrix,
$\Delta\underline{u}, \Delta\underline{X}$: small differences in $\underline{u}$ and $\underline{X}$.

Thus, when an error $\underline{e}(t) = H \cdot \Delta\underline{X}(t)$ occurs, the corrective action would be :

$$\hat{\underline{e}}(t) = H \cdot S(t) \cdot \Delta\underline{u}(t) \tag{5.31}$$

The above system can be solved for $\Delta\underline{u}$. Thus :

$$\Delta\underline{u}(t) = [H \cdot S(t)]^{-1} \cdot \hat{\underline{e}}(t) \tag{5.32}$$
or $\quad \Delta\underline{u}(t) = G(t) \cdot \hat{\underline{e}}(t)$

where; $G(t) = \begin{vmatrix} G_{11} & G_{12} \\ G_{21} & G_{22} \end{vmatrix}$ the time-varying feedback gain matrix.

After the calculations, the corrective action at t_k in response to a predicted set-point error, $\hat{e}(t_{k+1})$, is given by :

$$\begin{vmatrix} \Delta Qr(t_k) \\ \Delta Qw(t_k) \end{vmatrix} = \begin{vmatrix} G_{11}(t_{k+1}) \cdot \hat{e}_{ML}(t_{k+1}) + G_{12}(t_{k+1}) \cdot \hat{e}_{BL}(t_{k+1}) \\ G_{21}(t_{k+1}) \cdot \hat{e}_{ML}(t_{k+1}) + G_{22}(t_{k+1}) \cdot \hat{e}_{BL}(t_{k+1}) \end{vmatrix} \tag{5.33}$$

where; $G_{11}(t_{k+1}) = \left(1 + \dfrac{\hat{S}_{21}(t_{k+1}) \cdot \hat{S}_{12}(t_{k+1})}{det(St_{k+1})}\right) / \hat{S}_{11}(t_{k+1})$

$G_{12}(t_{k+1}) = -\hat{S}_{12}(t_{k+1})/det(St_{k+1})$

$G_{21}(t_{k+1}) = -\hat{S}_{21}(t_{k+1})/det(St_{k+1})$

$G_{22}(t_{k+1}) = \hat{S}_{11}(t_{k+1})/det(St_{k+1})$

$det(St_{k+1}) = \hat{S}_{11}(t_{k+1}) \cdot \hat{S}_{22}(t_{k+1}) - \hat{S}_{12}(t_{k+1}) \cdot \hat{S}_{21}(t_{k+1})$

$\hat{e}_{ML}(t_{k+1}) = MLSS_{sp}(t_{k+1}) - \widehat{MLS}S(t_{k+1})$

$\hat{e}_{BL}(t_{k+1}) = BL_{sp}(t_{k+1}) - \widehat{BL}(t_{k+1})$ or

$= [\mathrm{H}\ (\widehat{BL}(t_{k+1}) - BL_{max}) - \mathrm{H}\ (BL_{min} - \widehat{BL}(t_{k+1}))]$

Hence the new control inputs for the interval between t_k and t_{k+1} would be :

$$Qr(t_{k+1}) = Qr(t_k) + \Delta Qr(t_k) \tag{5.34a}$$

$$Qw(t_{k+1}) = Qw(t_k) + \Delta Qw(t_k) \tag{5.34b}$$

The control inputs are usually bounded by operational limits as discussed in Section 5.5.1. When a control input lies outside the boundaries, it is automatically set at the nearest boundary. Subsequently the other control input must be re-calculated from system 5.30, which then comprises two equations but only one unknown variable. Two possible solutions can be found from which their mean was chosen as the most practicable. The procedure is illustrated below for the case where control input $u_2(t_k)$ is set at the boundary u_{2b} :

$$\begin{aligned} \Delta u_2(t_k) &= u_{2b} - u_2(t_k) \\ \Delta u_1(1) &= [\hat{e}_{ML}(t_{k+1}) - \hat{S}_{12}(t_{k+1}) \cdot \Delta u_2(t_k)]/\hat{S}_{11}(t_{k+1}) \\ \Delta u_1(2) &= [\hat{e}_{BL}(t_{k+1}) - \hat{S}_{22}(t_{k+1}) \cdot \Delta u_2(t_k)]/\hat{S}_{21}(t_{k+1}) \\ \Delta u_1(t_k) &= [\Delta u_1(1) + \Delta u_1(2)]/2 \end{aligned} \tag{5.35}$$

In case where both control inputs lie outside the boundaries, then both are set automatically to the nearest boundary. Under such conditions the elimination of set-point error cannot be achieved, since : $\hat{e}(t) \neq H \cdot S(t) \cdot \Delta \underline{u}(t)$.

The predicted sensitivity matrix of the simplified process model at t_{k+1} can be determined by integrating the following system of differential equations between t_k and t_{k+1} :

$$\frac{dS_{ij}(t)}{dt} = \left[\frac{\partial f_i(\underline{X}(t), \underline{u}(t), t)}{\partial \underline{X}}\right]_x \cdot S_{ij}(t) + \left[\frac{\partial f_i(\underline{X}(t), \underline{u}(t), t)}{\partial \underline{u}}\right]_x \qquad (5.36)$$

where; $i = 1, 3$ and $j = 1, 2$.

$[*]_x$: denotes the reference state vector,

$\underline{X} = [MLSS \quad RASS \quad BL]^T$

$\underline{u} = [Qr \quad Qw]^T$

Hence,

$$\hat{S}_{ij}(t_{k+1}) = \int_{t_k}^{t_{k+1}} \frac{dS_{ij}(t)}{dt}$$

with initial condition at t_k :

$$S_{ij}(t_k) = [\frac{\partial \underline{X}(t)}{\partial \underline{u}}]_{(t=t_k)} = 0.$$

5.6.8 Comparison of adaptive feedback control systems /

The constant-gain proportional error FB system was not considered further because of its limitations in coping with complex and time-varying systems (discussed in Section 5.6.4). Subsequently the two adaptive FB systems were compared regarding their ability to control the *MLSS* concentration and sludge blanket level to their desired levels. The performance of the controlled systems was examined under two different operating conditions :

- Under a pulse in the *MLSS* set-point and constant process inputs.
- Under constant *MLSS* set-point, but naturally varying input conditions.

The controller performance was assessed on the basis of the observed stability in the controlled system states, the variability in the control inputs and the time lag for achieving the desired conditions.

In the first test the system performance was studied under a step- increase and step-reduction in the *MLSS* set-point between 3,000 and 5,000 mg/l on days 10 and 25 respectively. The process inputs for the simulation period were assigned constant values,thesebeing typical of those measured during the study period. The simulated response of both systems is presented graphically in Fig. 5.28 & 5.29 and similarities as well as differences in their behaviour can be observed. In both systems a step

increase in the set-point level caused a sudden increase in the recycle flow and a reduction in the surplus sludge flow, while the opposite response was observed under a step reduction of the set-point. However the increase in the recycle trajectory was gradual for the iterative system producing an almost linear rise of the *MLSS* level, while for the adaptive-gain system the increase was immediate producing an exponential rise of *MLSS*. The estimated trajectory of surplus flow was similar in both systems, exhibiting large variability often reaching the boundary values.

The stability of the controlled system was directly affected by the controller characteristics and the selected sludge blanket settings. For the iterative system employing objective function J_2, instability in the control inputs and process states, was observed for a ratio in the weights w_1/w_2 of 1 : 2.5. However, stability was substantially improved for a lower ratio of 1 : 12.5, due to the smaller interaction between the *MLSS* and sludge blanket loops. In case where the sludge blanket settings were specified by a single value (objective function J_1), the system stability was further improved. It can be suggested that in the latter case the control action is defined better, because sludge blanket control is continuously applied, resulting in a smoother objective function. On the contrary, the adaptive-gain system became less stable under a fixed sludge blanket setting. This can be attributed to the influence of linearization errors in the sensitivity coefficients, causing instability during the simultaneous control of *MLSS* and sludge blanket.

Overall, the two systems showed comparable performance under step changes in *MLSS* set-point, regarding the time lag for achieving the new set-points and their dynamic behaviour under transient conditions. It is important to note that although a reduction in *MLSS* level can be realized immediately in both systems, an increase in its level is a much slower process. This can be explained by the fact that a large set-point increase must be accompanied by a net increase of solids mass contained in the system through growth of biomass and accumulation of incoming solids. However both of these processes are generally slow.

The slow increase in *MLSS* level does not produce an overshoot, unless the controlled system becomes unstable. However an abrupt reduction in its level is associated with a substantial overshoot, as a result of linearization and other errors affecting the accuracy of the estimated control action. The observed overshoot for the adaptive-gain system was around 24% of the set-point reduction. For the iterative system this was much lower (around 5%) due to smaller errors involved arising from the simplified structure of the process model used.

In the second test the behaviour of the controlled system was studied under naturally varying input conditions, where the current inputs were taken as best estimates of future inputs. The observed inputs from the first 100 days of the study

period were selected for this purpose, because they represent an operating period with particularly large fluctuations. The $MLSS$ set-point was assumed constant at 4,000 mg/l, while the sludge blanket was controlled either to a fixed level or within a specified range. The performance of both systems is summarized in Table 5.9 (cases 1 & 3) and also presented graphically in Figures 5.30 & 5.31 for cases 1 & 4.

Param.	Adaptive-gain control		Iterative control		
Weights	—	—	w_1/w_2=1/12.5 w_3=w_4=0	w_1=20 w_3=0.0002	w_2=1000 w_4=0.2
Case No.	(1)	(2)	(3)	(4)	(5)
BL_{sp}	0.9–1.1	1.00	0.90–1.10	0.90–1.10	1.00
$\widehat{MLSS}$	3960±205	3898±212	3948±210	3990±200	3829±501
$\widehat{ERR}_{ML}$	40±205	102±212	52±210	10±200	171±501
$MLSS_{pr}$	3965±124	3907±207	3952±134	3994±128	3832±498
Qr	10247±3248	9541±3211	10156±2997	10353±3242	9730±2527
Qw	154±121	148±166	157±114	155±63	161±90
$\widehat{BL}$	0.964±0.096	0.965±0.104	1.003±0.107	0.993±0.112	0.999±0.108
$\widehat{RASS}$	9841±449	10157±547	9833±470	9860±503	9686±488
$R_{(Qr-Qi)}$	0.895	0.896	0.901	0.905	0.605

Table 5.9. Summary statistics of adaptive control systems performance under variable input conditions.

For sludge blanket settings between 0.90 and 1.10 m, the overall performance of the two systems was similar. The adaptive-gain system (case 1), showed marginally lower set-point error and variation in the $\widehat{MLSS}$, while for the iterative system (case 3), the control inputs exhibited slightly lower variability. The performance of the iterative system however, can be improved by minimizing the daily variation of the control inputs, employing objective function J_3 (case 4). Both the mean set-point error and its standard deviation were reduced in addition to the variability of surplus sludge flow, with no observed deterioration in the sludge blanket behaviour. The simulated trajectory of recycle flow was quite similar to the input flow variation for all cases examined, with a correlation coefficient of around 0.9, indicating an approximate ratio control. The trajectory of surplus flow however, exhibited a more random variation which was not correlated to the inputs, serving as an auxiliary to recycle flow control by adjusting the mass of solids in the system.

The control of sludge blanket to a fixed level caused substantially poorer performance for both systems under variable input conditions which is in contrast to observations with constant inputs (Table 5.9, cases 2 & 5). This can be attributed to strong interactions between the control loops in the presence of errors in the predicted

states, due to the unpredictable nature of the process inputs. Hence, it can be concluded that under highly variable and unpredictable input conditions, the stability and performance of the control system can be improved by restricting the variability of the control inputs and by allowing some flexibility into the system, such as, by specifying an acceptable range for sludge blanket variation instead of a fixed set-point level.

Regarding the design of the two controllers, the iterative system is simpler and more flexible than the adaptive-gain system, since additional features for restricting the control input variability can be easily incorporated into the objective function. However in the latter system, the control algorithm must be re-designed every time an additional feature is to be included. Comparing their performance under varying input conditions, which is normally the case in the oxidation ditch control, the iterative system performed slightly better when objective function J_3 was employed. Furthermore, the iterative system did not suffer significantly from the effect of linearization errors during step changes in the set-point. Consequently, the iterative FB control system was selected for process control of the oxidation ditch.

5.7 Design and comparison of alternative operational control policies

In the planning level of the control hierarchy (Section 5.5.6), it was shown that the nitrifiers and denitrifiers constitute the main process variables requiring tight control, to be implemented indirectly via $MLSS$ control. It was suggested therefore, that the $MLSS$ set-point should be specified according to the necessary operating conditions for achieving the desired nitrification and denitrification performance.

Next, a number of operational control policies were designed for controlling these processes. Their performance was evaluated via simulation studies employing the process model developed in Chapter 3, since implementation on the full-scale plant was not feasible. In all subsequent simulations the observed inputs at the Cirencester plant during the study period were employed. At the lower level of the control hierarchy, the control actions upon the recycle and surplus sludge flows were calculated using the iterative system described in Section 5.6.6, employing objective function J_3. Finally comparison of the control policies and evaluation of their performance was based on the following factors :

- Compliance of effluent quality (particularly effluent ammonia) with the discharge limits.
- Ability of the control system to maintain the specified set- points for $MLSS$

concentration and sludge blanket level.

- Reduction in the total running cost of the process.

The development and evaluation of alternative operating policies is presented below. Their development followed a sequential procedure, whereby the results from the application of each policy were analyzed and considered in the design of the subsequent policy.

5.7.1 Policy 1

In the first policy the simplified nitrification model (eq. 5.9a) was employed for calculating the desired nitrifier concentration that would produce the set-point effluent ammonia concentration. Consequently the control action at time t_{k+1}, was based on the desired concentration of nitrifiers at the end of the control interval t_{k+1}, which was calculated from the equation:

$$\widehat{BX}_{des}(t_{k+1}) = \hat{Q}i(t_{k+1}) \cdot \frac{\widehat{NHsi}(t_{k+1}) - NHse(sp)}{A \cdot V \cdot f_N \cdot \mu_N \cdot 6.02} \tag{5.37}$$

where; $f_N = NHse(sp)/(NHse(sp) + K_{NHs})$

The proportion of nitrifiers in the biomass was determined from the current simulation results at t_k. Assuming that this proportion does not change over the control interval, as discussed in Section 5.5.5, the desired $MLSS$ concentration at t_{k+1} was given from :

$$\widehat{MLSS}_{des}(t_{k+1}) = \frac{\widehat{BX}_{des}(t_{k+1})}{P_{BX}(t_k)} \tag{5.38}$$

where; $P_{BX}(t_k) = \frac{BX(t_k)}{MLSS(t_k)}$ the proportion of nitrifiers at t_k.

Similarly, for the control of effluent nitrates, the simplified denitrification model was employed to estimate the denitrifier concentration for achieving either a given set-point effluent nitrates (eq. 5.13a), or a percentage of nitrogen removal (eq. 5.13b). The corresponding $MLSS$ concentration was calculated from :

$$\widehat{MLSS}_{des}(t_{k+1}) = \frac{\widehat{DX}_{des}(t_{k+1}) \cdot MLSS(t_k)}{DX(t_k)} \tag{5.39}$$

For satisfying both the nitrification and denitrification conditions, the maximum $MLSS$ value from equations 5.38 and 5.39 had to be selected. The $MLSS$ level is also bounded from above by a maximum value for satisfying the physical limitations of

the aeration system and the thickening capacity of the final clarifiers (Section 5.5.4). Furthermore it was shown in Section 5.6.8 that an increase in $MLSS$ concentration is a slow process. Hence the $MLSS$ concentration should be also bounded by some minimum operating level, even if all other performance conditions are satisfied, in order to avoid large disturbances to the process operation resulting from a sudden reduction in the biomass level. The minimum operating $MLSS$ cannot be specified on a formal basis, however in practice process operators often have a feel for a sensible lower level of $MLSS$ based on experience. Here, the minimum level was chosen arbitrarily for the particular plant as 2,000 mg/l.

Therefore, Policy 1 adopted the aforementionted procedure for calculating the desired $MLSS$ concentration on a daily basis satisfying the following conditions :

i. $NH3e(sp) = 5\ mg/l$,
ii. $NO3e(sp) = 15\ mg/l$ or 70% of denitrification,
iii. minimum $MLSS = 2{,}000\ mg/l$,
iv. Sludge blanket range : 0.90–1.10 m.

From initial simulation results it was observed that the $MLSS$ set- point trajectory was highly variable and the control system was unable to follow closely its variation, due to the time-lag associated with any large increase of the set-point (Section 5.6.8). Subsequently the $MLSS$ set-point trajectory was smoothed by a 10-day Moving Average filter, which substantially reduced its variability and the simulated set-point error. Nevertheless the performance of Policy 1, which is summarized in Table 5.10 (case 1), and Fig. 5.32, was not considered satisfactory, since frequent exceedances of the effluent ammonia limit were encountered, due to the low nitrifier concentration at peak load periods. This happens because the nitrifier population is reduced during periods of low input ammonia load, but when the load suddenly increases their concentration requires considerable time to increase.

Some of the advantages from the application of process control can be also realized, by comparing the simulated system performance with the observed performance under natural operating conditions (Table 5.10, case 0). The simulated $MLSS$ trajectory was quite different from the observed and showed a 23% reduction in its average level, leading to lower energy consumption and running cost of the process. It is also noticeable that prolonged periods of low $MLSS$, which could impair process performance, did not exist. Furthermore, the average recycle and surplus flow rates were substantially reduced which is partly attributed to the higher underflow concentration ($RASS$) achieved, and partly to the lower operating $MLSS$ level. The recycle flow trajectory after an initial transition period, followed to some extent the input flow variation, while the surplus flow showed a more variable and random behaviour. Finally, the sludge blanket level was sufficiently well controlled within its

desired limits.

Paramet.	Case 0	Case 1	Case 2	Case 3	Case 4
	Natural	Policy 1	Policy 2	Policy 3	Policy 4
$\widehat{MLSS}$	3876±1280	2992±786	3221±529	3295±568	3022±582
$\widehat{ER}$	—	-75±298	33.7±235	20.5±234	-105±281
$MLSS_{pr}$	—	2994±782	3224±502	3298±543	3025±563
$MLSS_{sp}$	—	2917±792	3188±486	3275±529	2917±573
$\widehat{BL}$	—	0.995±0.133	1.003±0.125	1.003±.126	.997±.123
$\widehat{RASS}$	6902±2589	9096±572	9146±544	9147±546	9105±531
$\widehat{NH_{3e}}$	2.99±3.59	3.62±2.93	2.23±1.85	2.29±1.87	2.90±2.14
$NH_{3e}(95\%)$	10.94	9.53	5.26	5.37	6.70
Exceed.%	19.78	29.32	5.65	6.36	13.78
$\widehat{NO_{3e}}$	5.91±4.19	12.68±5.89	11.58±4.00	6.49±4.03	7.47±3.82
$NO_{3e}(95\%)$	13.37	21.21	17.26	13.3	13.62
Qr	7472±4496	3592±2381	4271±2930	4364±2869	3834±2626
Qw	202±70.8	147±110	142±95	137±96.5	140±90.5
Ener. cost	33.6±9.5	31.3±6.1	32.5±5.4	32.0±6.0	30.4±5.6
Disp. cost	19.5±9.3	19.4±9.4	18.8±9.1	18.1±9.4	18.5±9.1
Tot. cost	15054	14358	14505	14184	13819
$R_{(Qi-Qr)}$	0.761	0.694	0.834	0.826	0.786

Table 5.10. Performance comparison of alternative operational control policies.

5.7.2 Policy 2

In the previous operating policy it was observed that effluent ammonia exceedances occurred as a result of the slow growth of nitrifiers and the inability to forecast the inputs over several days ahead. This observation suggests that examination of the input behaviour over a long operating period, might provide an alternative basis for designing a more reliable control policy. Subsequently the daily measured inputs were analyzed as independent events, in an attempt to gain more information about their behaviour in statistical terms.

The crude sewage flow entering the Cirencester plant varies considerably over the year due to the extensive ground water infiltration into the sewerage system, and affects substantially the input pollutant concentrations. However, when a relatively constant effluent concentration is desired from the plant, the substrate load which must be removed in the process would be also variable and related to the input flow variation. In the case of nitrification, the excess ammonia load (L) which must be oxidized for achieving the desired effluent conditions is given by the equation :

$$L(t_k) = Qi(t_k) \cdot [NH3i(t_k) - NH3e(sp)] \qquad (5.40)$$

where; $NH3e(sp) = 5.0 mg/l$

Plotting the excess ammonia load versus input flow (Fig. 5.33), shows that the load is reduced at high input flows, especially for flows above 10,000 m^3/d. The statistics of the series are :

$L = 76.3 \pm 23.7$, skewness $= 0.587$, coef. var. $= 0.3098$ for $Qi < 10{,}000\ m^3/d$
$L = 44.7 \pm 40.5$, " $= 1.961$, " $= 0.9068$ for $Qi > 10{,}000\ m^3/d$

The first series (for Qi <10,000) approximates the normal distribution (Fig. 5.34a) with the upper 95 percentile of the excess load being approximately 115 $kg(NH3 - N)/d$. However the second series (for $Qi > 10{,}000$), deviates from the normal distribution exhibiting large spread and substantial positive skewness (Fig. 5.34b), which may be attributed to the occurrence of extreme events. Assuming that the upper 95 percentile of excess ammonia load is 120 and 80 kg/d under 'low' and 'high' input flow conditions, the desired nitrifier concentration from eq. 5.37 is 23 and 15 mg/l respectively, for an aerobic zone covering 65% of the reactor.

Hence, in Policy 2 the control of effluent ammonia was based on the long-term statistical behaviour of the inputs. These were classified into two groups according to the input flow rate and a minimum operating level for the nitrifiers was determined in each case. The input flow trajectory was smoothed by a 10-day Moving Average filter in order to avoid high frequency variation of the operating conditions. The conditions for denitrification, minimum $MLSS$ and sludge blanket level were the same as in Policy 1. Hence, Policy 2 for nitrification was :

Maintain $BX \geq 23\ mg/l$ when $\hat{Q}i_{sm}(t_{k+1}) < 10{,}000\ m^3/d$
" $BX \geq 15\ mg/l$ " $\hat{Q}i_{sm}(t_{k+1}) > 10{,}000\ m^3/d$

The performance of this policy summarized in Table 5.10 (case 2) and Fig. 5.35 was significantly better than Policy 1, with effluent ammonia exceedances close to the 5% acceptable level. The nitrifier concentration was maintained close to the desired level, which prevented high ammonia concentrations escaping in the effluent. The total operating cost was slightly increased compared to Policy 1, due to an increase in the average $MLSS$ level. However the effluent nitrate concentration was only marginally reduced from the previous case.

5.7.3 Policy 3

In the results of the previous policy it can be observed that during 'dry' weather, where the input flow is close to the design DWF, the level of effluent ammonia was persistenlty low (Fig. 5.35e), while the effluent nitrate was relatively high (Fig. 5.35g). Under these conditions an improvement in the denitrification process was considered feasible, by altering the volume of aerobic and anoxic zones through the *DO* profile, as discussed in Section 5.5.6. The anoxic volume was assumed to increase during the 'dry' period from the 35% to 40% at the expense of the aerobic zone. Examination of the input flow data showed that the 'dry' period can be considered for input flows below 5,500 m^3/d. The minimum level of nitrifiers was again calculated (eq. 5.37) for the new conditions. Hence operating Policy 3 becomes :

Maintain $BX_{des} \geq 15\ mg/l$ with A=65% & B=35% for $\hat{Q}i_{sm}(t_{k+1}) > 10{,}000\ m^3/d$
" $BX_{des} \geq 23\ mg/l$ " " for $5500 < \hat{Q}i_{sm}(t_{k+1}) < 10000$
" $BX_{des} \geq 25\ mg/l$ with A=60% & B=40% for $\hat{Q}i_{sm}(t_{k+1}) < 5{,}500\ m^3/d$

The simulation results with this policy are summarized in Table 5.10 (case 3) and in Figures 5.36. The nitrification performance was similar to Policy 2, but the denitrification process was dramatically improved with the 95 percentile of effluent nitrate falling from 17.3 to 13.3 mg/l. This was mainly attributed to the increasing concentration of denitrifiers throughout the 'dry' period as a result of the larger anoxic zones. Furthermore, the total cost was slightly reduced due to the smaller aerobic zone between day 120 and 273, leading to lower aeration cost and sludge production.

5.7.4 Policy 4

In this policy an attempt was made to reduce the minimum operating level of nitrifiers in the system, by relating it also to the daily load of excess ammonia. Hence, this policy is a combination of Policy 1 and 3 and aims to further reduce the operating *MLSS* level and running cost of the process. Here, the desired nitrifier concentration was calculated on a daily basis from equation 5.37, but a minimum level was also specified depending on the input flow conditions. The minimum level was calculated as in Policy 3, but using lower values for the excess ammonia load, of 100 and 60 kg/d for the 'dry' and 'wet' period respectively. Hence, Policy 4 can be stated as :

$$\widehat{BX}_{des}(t_{k+1}) = f\{\hat{Q}i(t_{k+1}), \widehat{NH}_{3i}(t_{k+1})\}$$

subject to :

$$\widehat{BX}_{des}(t_{k+1}) \geq 12mg/l, \quad A = 65\% \ \& \ B = 35\% \quad \text{for } \hat{Q}i_{sm}(t_{k+1}) > 10{,}000\ m^3/d$$

$$\widehat{BX}_{des}(t_{k+1}) \geq 19mg/l, \quad " \quad " \quad \text{for } 5,500 < \hat{Q}i_{sm}(t_{k+1}) < 10,000\ m^3/d$$
$$\widehat{BX}_{des}(t_{k+1}) \geq 21mg/l, \quad A = 60\% \ \& \ B = 40\% \ \text{for } \hat{Q}i_{sm}(t_{k+1}) < 5,500\ m^3/d$$

The performance of this policy is summarized in Table 5.10 (case 4) and shown in Fig. 5.37. The average $MLSS$ concentration was reduced by 8.3% compared to Policy 3 and the operating cost by 2.5% due to lower energy consumption. However both effluent ammonia and nitrates were slightly increased and the frequency of exceeding the ammonia limit was above the desired level.

5.7.5 Conclusions

From the previous comparison of alternative operational control policies, it can be seen that Policy 3 produces the best overall performance. The unpredictable, high frequency variations of input loads together with the slow growth kinetics of the nitrifier population, produced rather poor performance in Policies 1 and 4. In these policies the desired nitrifier concentration was determined from daily measurements of input ammonia load, while in Policy 3 this was related to the long-term statistical behaviour of the inputs. Furthermore, Policy 3 exploits the potential of regulating the DO distribution in the reactor, as an additional low frequency control measure for improving denitrification performance during periods of high nitrification. This feature improved its overall performance compared to Policy 2.

Application of operational control Policy 3 at the planning level, with the iterative prediction-error FB control system at the process level, was shown to offer certain benefits to the operation of the oxidation ditch summarized below :

- Improved process reliability, particularly regarding nitrification and denitrification performance.
- Reduction in the operating $MLSS$ level leading to lower aeration energy and total running cost.
- Elimination of cases of process failure resulting from biomass washout, sludge blanket spillage and oxygen depletion.

Furthermore, the process performance and operation is not dependent upon the skills and experience of the operator. However the operator will need to play a supervisory role on the control system performance and he would select the performance targets to be achieved according to the overall management of the plant and receiving waterbody. Also, in the absence of automation in the plant, the operator would implement the necessary operating changes dictated by the control system.

At this point, it must be recognized that the simulated process performance under various control policies can be affected by limitations in the process model used. The main limitations arising from the assumptions made during its development, discussed in Chapters 2 & 3 are summarized below according to their importance :

- The settling characteristics of the sludge determining the maximum handling capacity of the clarifiers, were assigned fixed literature-based values. In fact these are time-varying quantities and should be measured ideally from specifically designed experiments on full-scale clarifiers.
- The *DO* distribution in the reactor has been represented simply by fixed-volume aerobic and anoxic zones. This was made under the assumption that the existing *DO* control mechanism can adequately eliminate the effects of time-varying process inputs and control actions upon the *DO* profile.
- The kinetic rates of the biochemical reactions were assumed constant throughout the period, although in reality they exhibit slow variation with time in response to changing operating conditions and crude sewage characteristics. From adaptive estimation of parameters it was shown that significant parameter variation can be also attributed to unmodelled processes and random disturbances. Hence a low frequency, adaptive estimation scheme could be incorporated into the model for updating the parameters, according to the difference between simulated and observed system behaviour.
- The effect of diurnally varying process inputs upon the effluent quality and the derived daily control action was not considered.

5.8 Topics for future research

The previous application of operational control was directed towards optimization of the average daily plant performance and operating cost. As a result daily measurements of the process inputs were used, which were assumed to remain constant over the 24-hr period. However both the crude sewage flow and input pollutant concentrations vary considerably throughout the day and a typical daily variation of the input flow and *MLSS* in an oxidation ditch plant was presented in Fig. 2.23. Such conditions produce a diurnal variation of the operating and effluent quality variables. The implications of diurnal variability to process performance may be that violation of the discharge limits can occur, even when compliance is predicted on average conditions. Furthermore, sub-optimal operation may result in terms of cost, by maintaining constant recycle and surplus sludge flows over the 24-hr period.

Higher frequency of control would be necessary for regulating the diurnal vari-

ability, to be applied at intervals in the order of hours. This would require high frequency of monitoring, which would be practical using on-line instrumentation. Sensors for on-line monitoring of SS and ammonia have reached a good stage of their development. However the organic load has yet to be determined from laboratory analyses or estimated from other process variables, such as the OUR, discussed in Section 4.7.2.

Under high frequency control, estimation of the oxygen demand using Equation 4.13 in Section 4.4.1 is not recommended, because the observed lag between the removed load and oxygen utilization would affect the results, and in addition requires a large amount of measurements for its application. A better method would be to estimate the OUR from the DO measurements as was shown in Section 4.6 and 4.7. The estimates of OUR can then be used in conjunction with measurements of $MLSS$ for the determination of $SCOUR$. This process variable has been used by several workers for controlling the biomass growth and effluent variability in activated sludge plants through a set-point $SCOUR$ control policy. However the application of such policy to the oxidation ditch process may not be adequate for the control of nitrification and denitrification performance, as discussed in Section 5.2.6. Consequently, real-time control of the oxidation ditch via OUR or $SCOUR$ requires further research before it can be successfully applied.

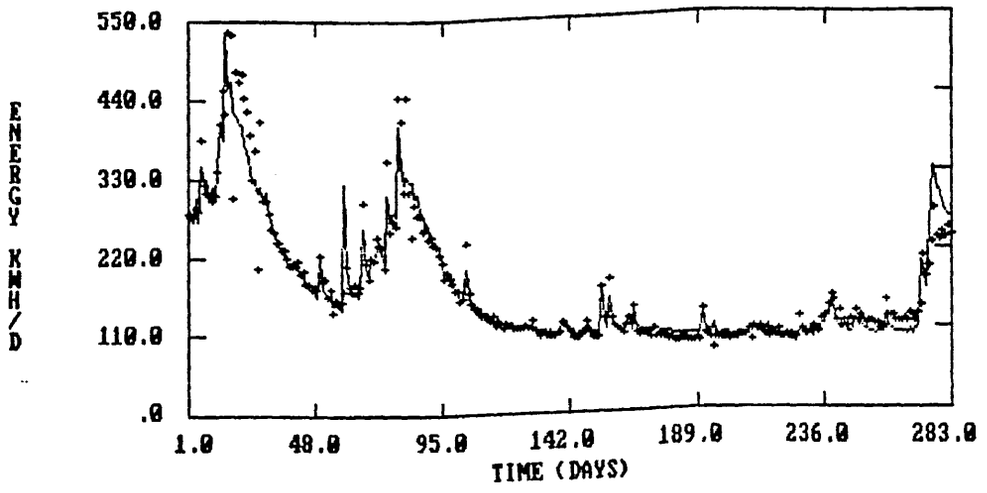


Fig. 5.1. Observed and predicted energy for crude sewage pumping

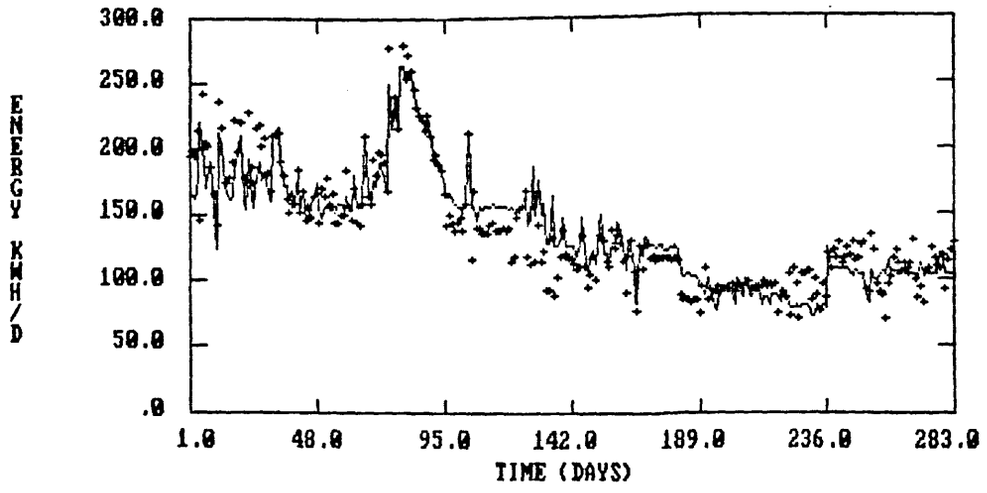


Fig. 5.2. Observed and predicted energy for return sludge pumping

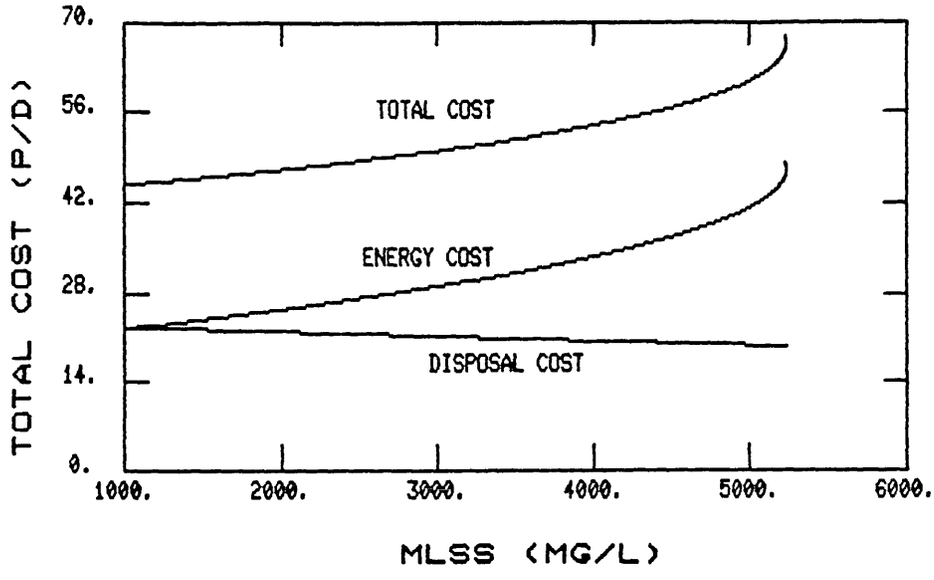


Fig. 5.3. Effect of $MLSS$ level on total operating cost

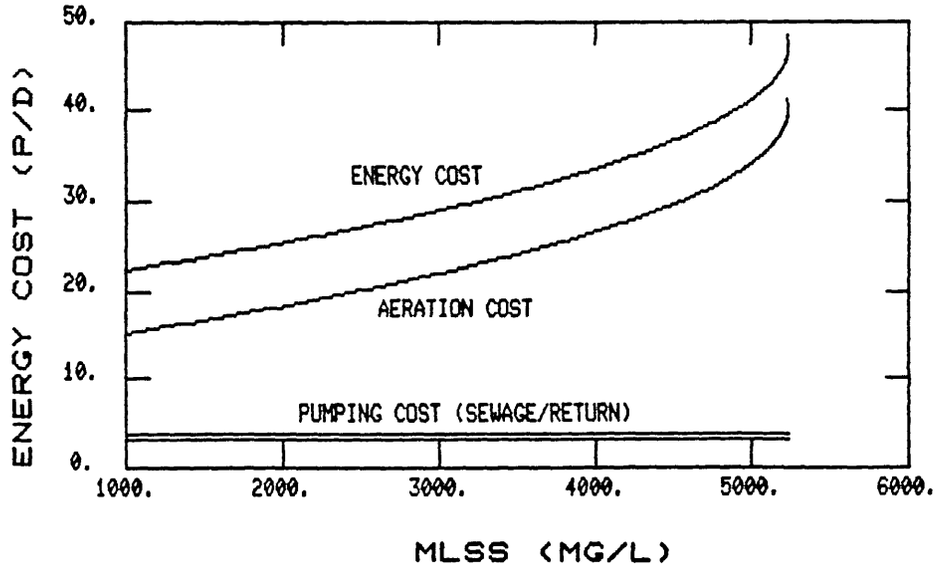
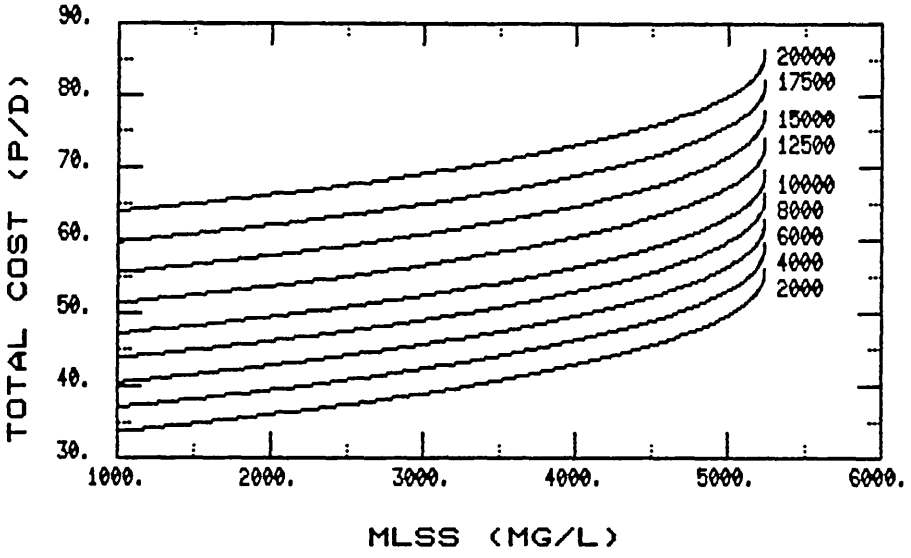
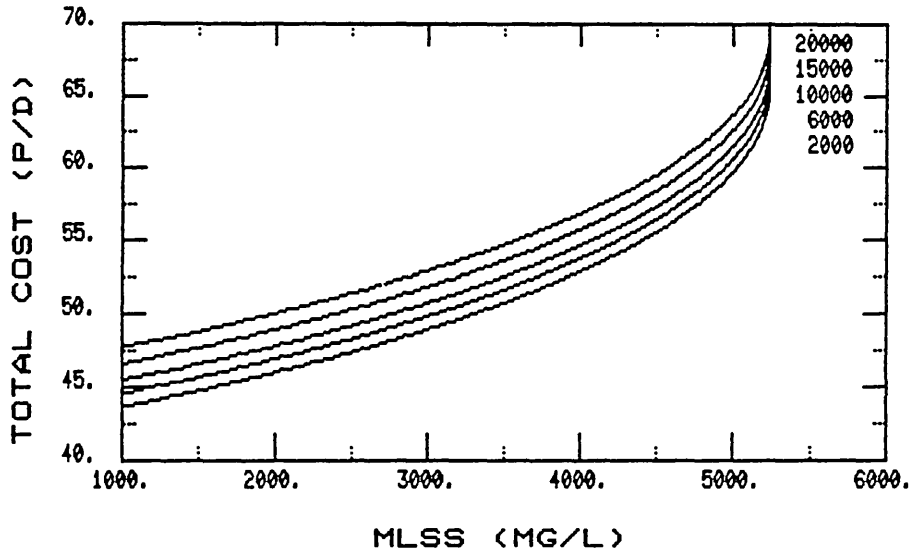


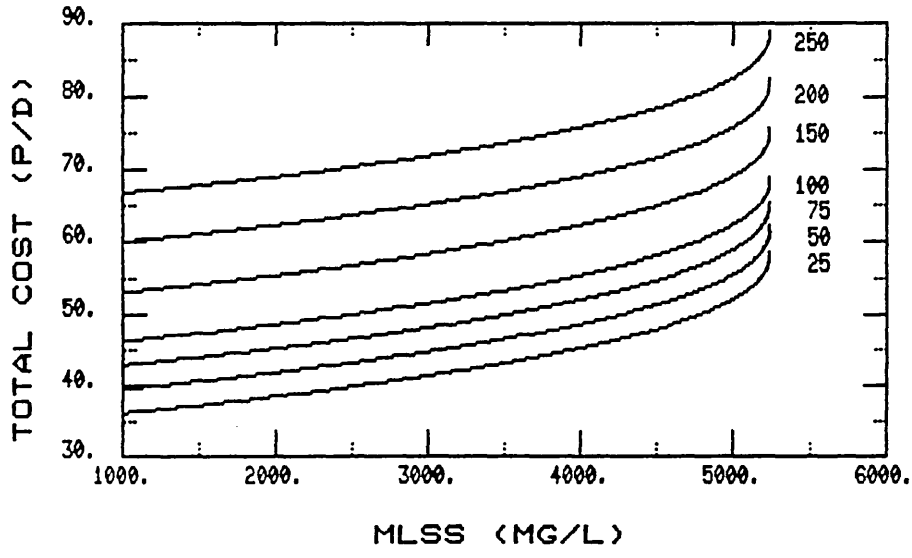
Fig. 5.4. Effect of $MLSS$ level on Energy cost



a. Input flow Qi (m^3/d)

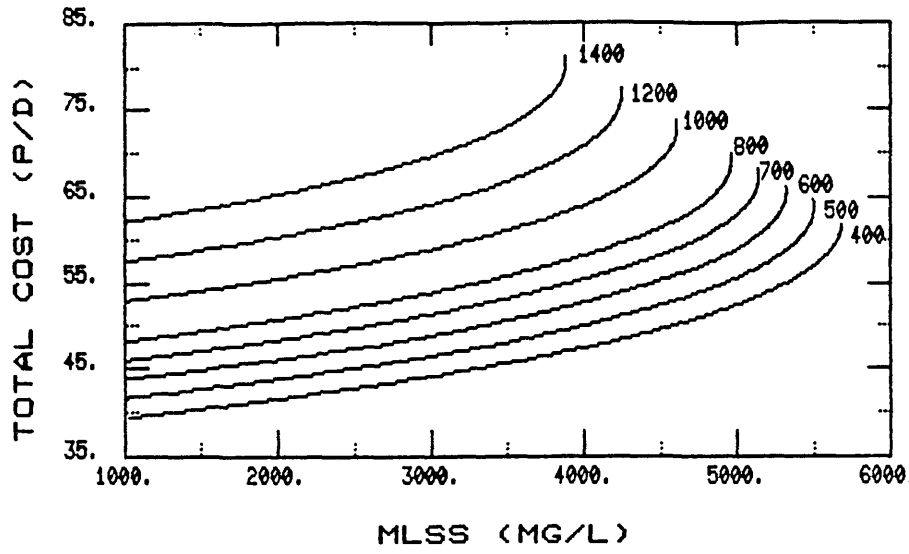


b. Recycle flow Qr (m^3/d)

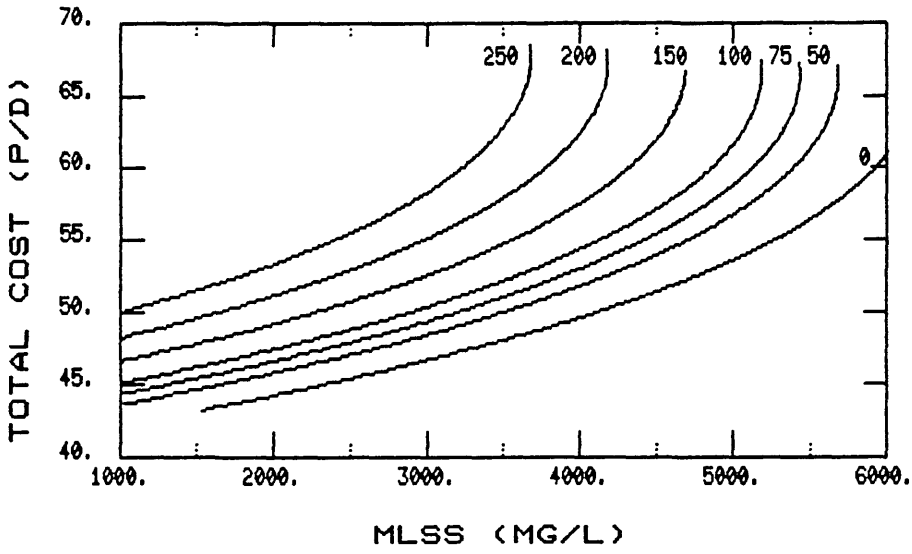


c. Input SSi (mg/l)

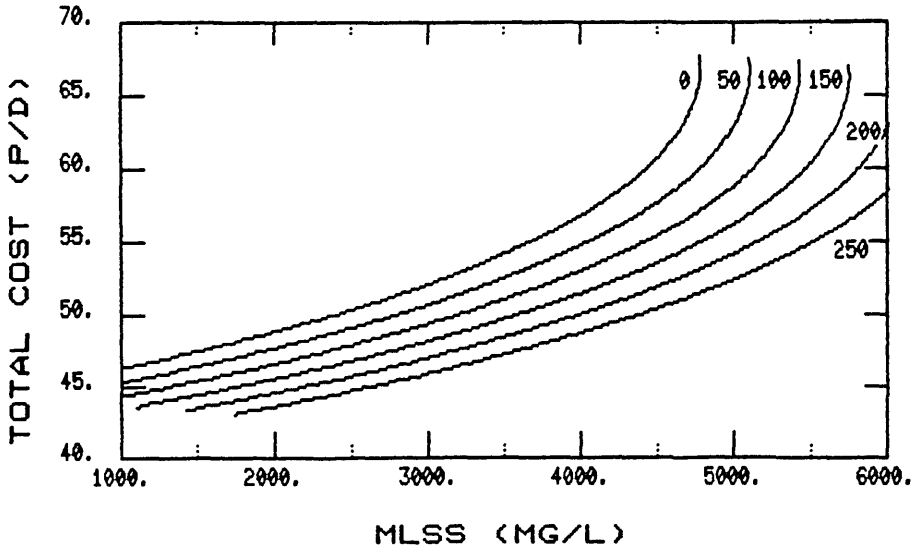
Fig. 5.5. Sensitivity of total cost to process inputs



d. Organic load $(kgBOD/d)$

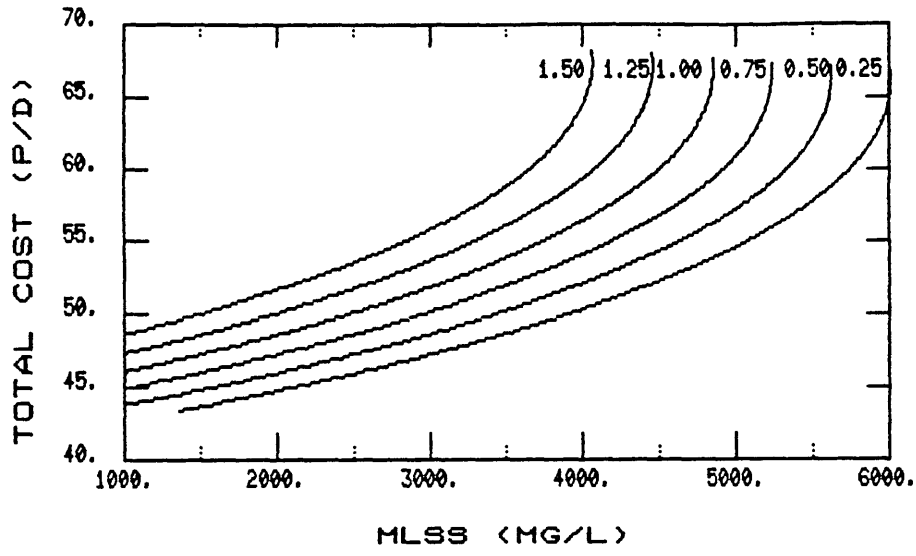


e. Ammonia load $(kg\ NH_3 - N/d)$

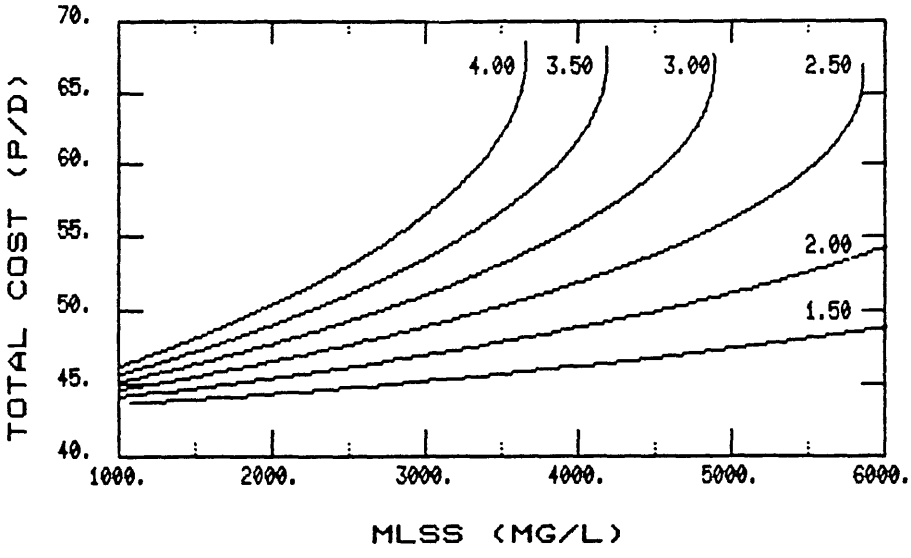


f. Denitrified mass $(kgNitrogen/d)$

Fig. 5.5. Sensitivity of total cost to process inputs

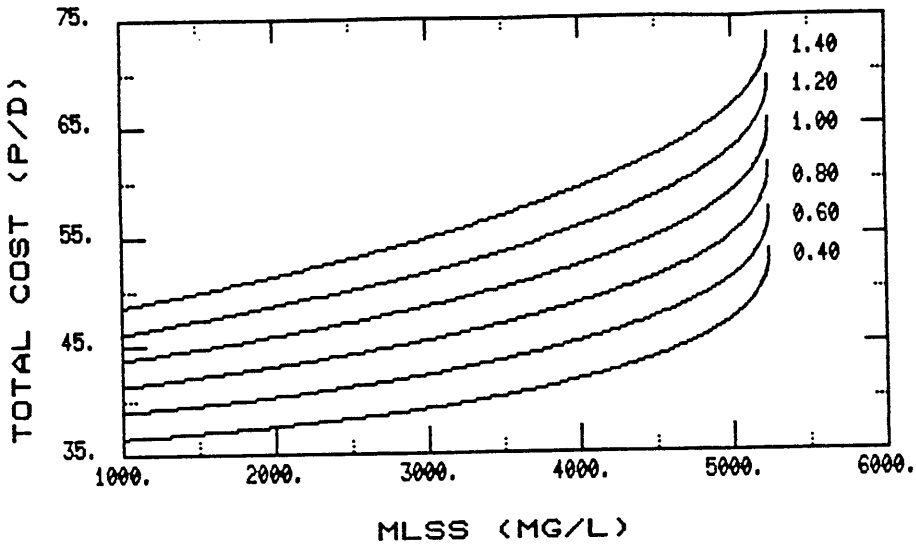


a. Oxygenation parameter a $(kgO_2/kgBOD)$

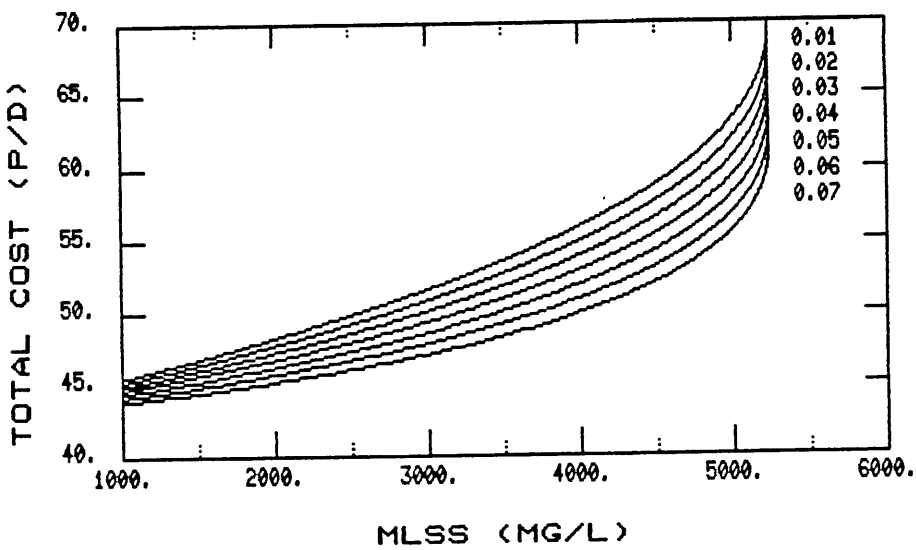


b. Oxygenation parameter b $(gO_2/kgSS \cdot hr)$

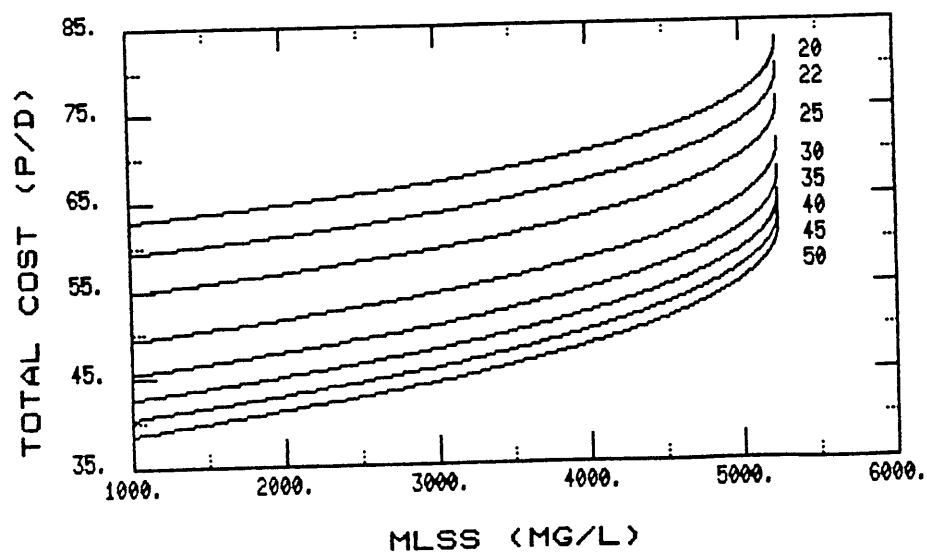
Fig. 5.6. Sensitivity of total cost to model parameters



c. Biomass yield

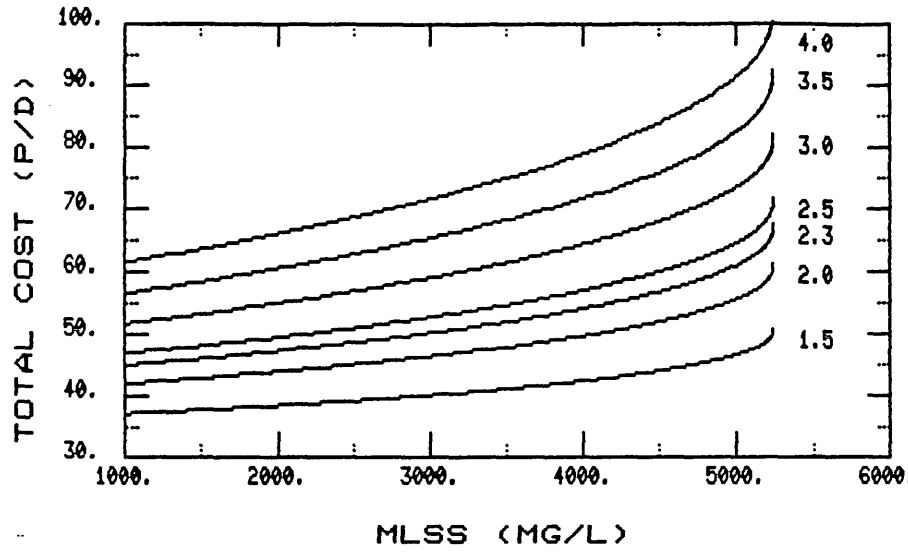


d. Biomass decay rate (d^{-1})

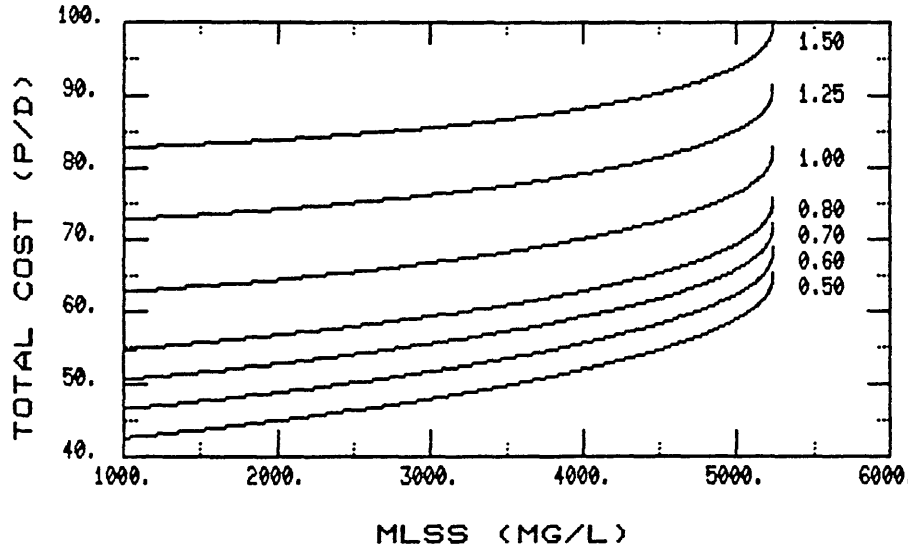


e. Thickened sludge concentration (kg/m^3)

Fig. 5.6. Sensitivity of total cost to model parameters



a. Electricity cost (pence/kWh)



b. Sludge disposal cost ($£/m^3$ sludge)

Fig. 5.7. Sensitivity of total cost to unit cost prices

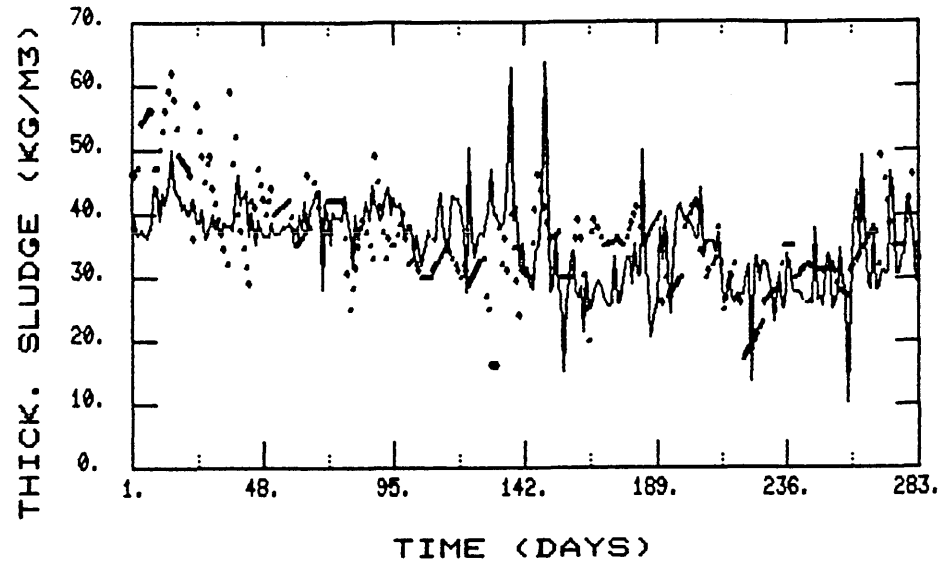


Fig. 5.8. Observed and predicted thickened sludge concentration

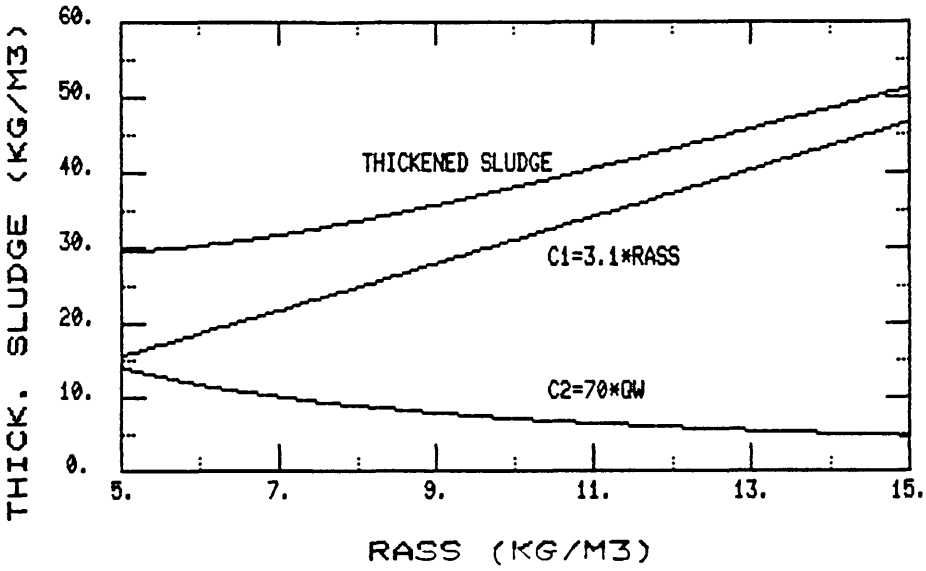


Fig. 5.9. Relationship between operating conditions $(RASS, Qw)$ and thickened sludge

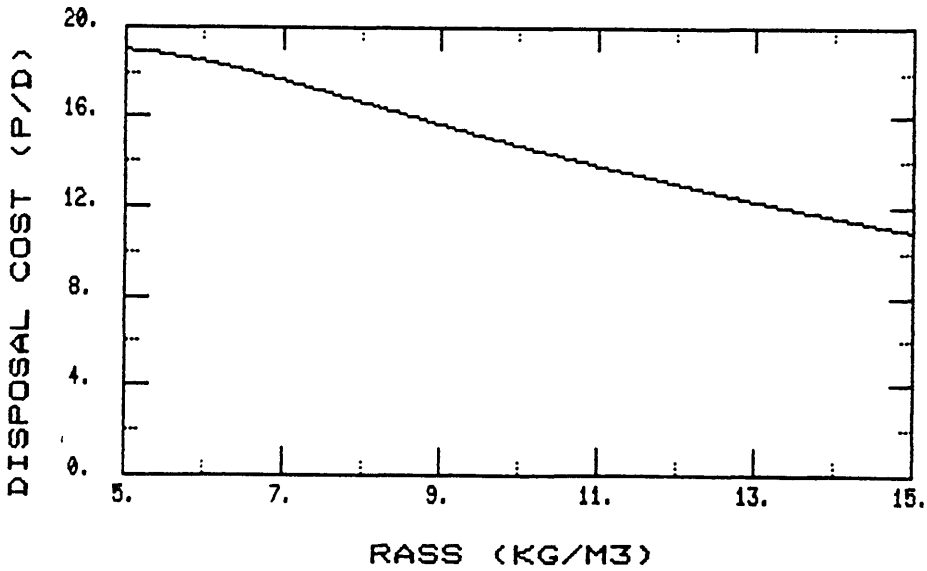


Fig. 5.10. Relationship between disposal cost and $RASS$

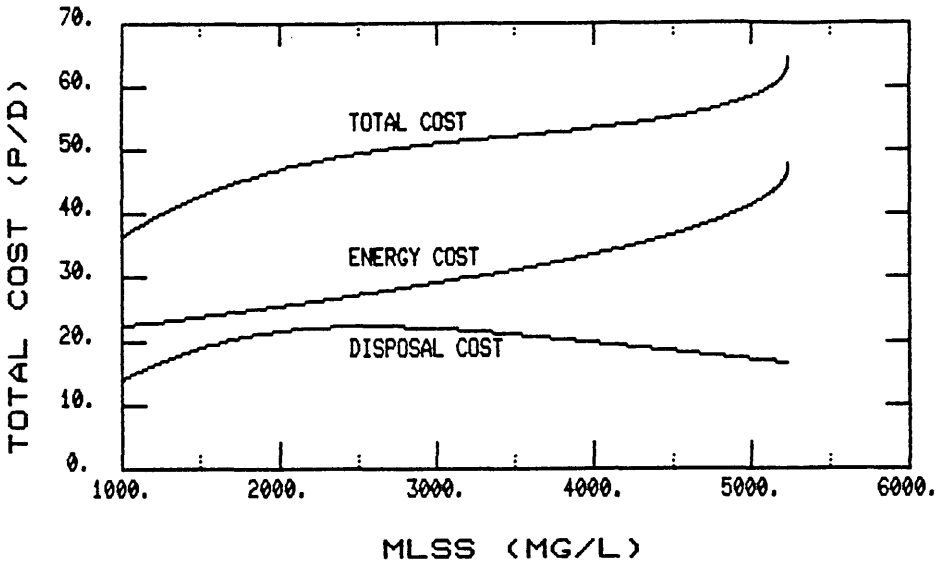


Fig. 5.11. Effect of variable thickened sludge on Total cost

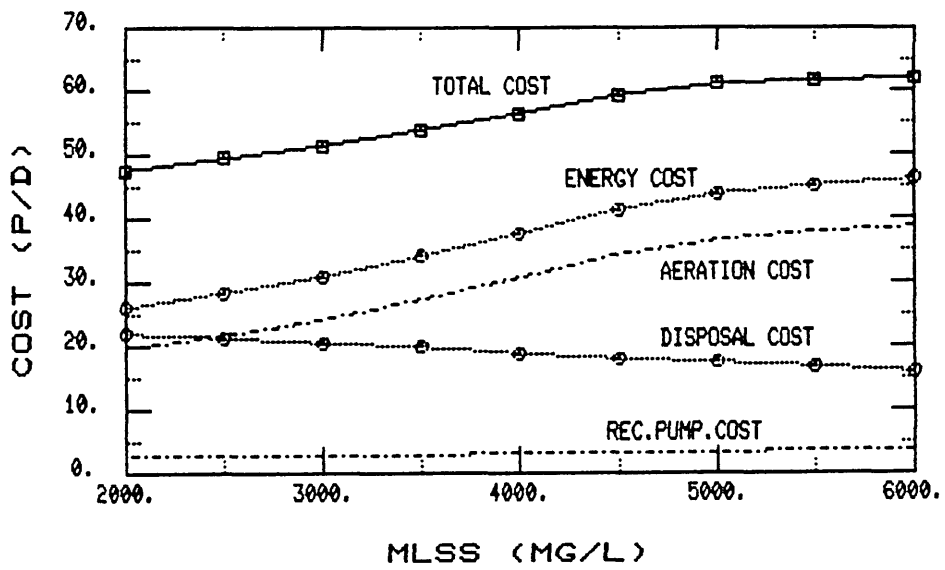


Fig. 5.12. Effect of operating $MLSS$ on average daily cost under real input conditions

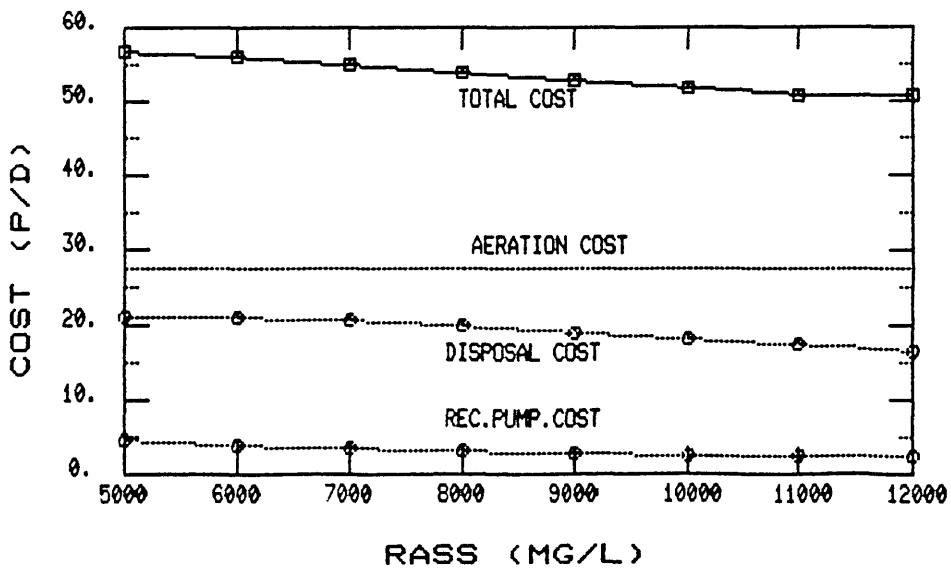


Fig. 5.13. Effect of operating $RASS$ on average daily cost

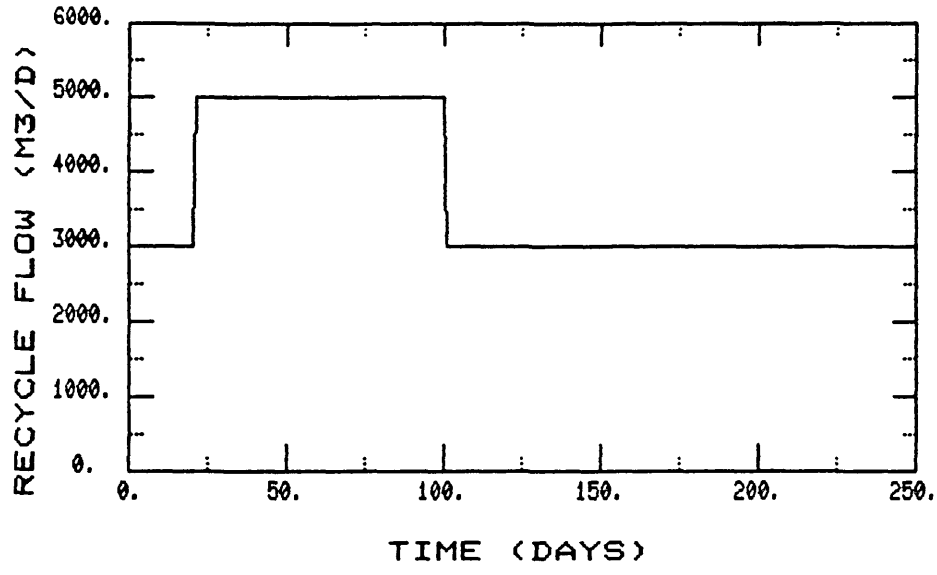


Fig. 5.14a. Generated pulse in the recycle flow

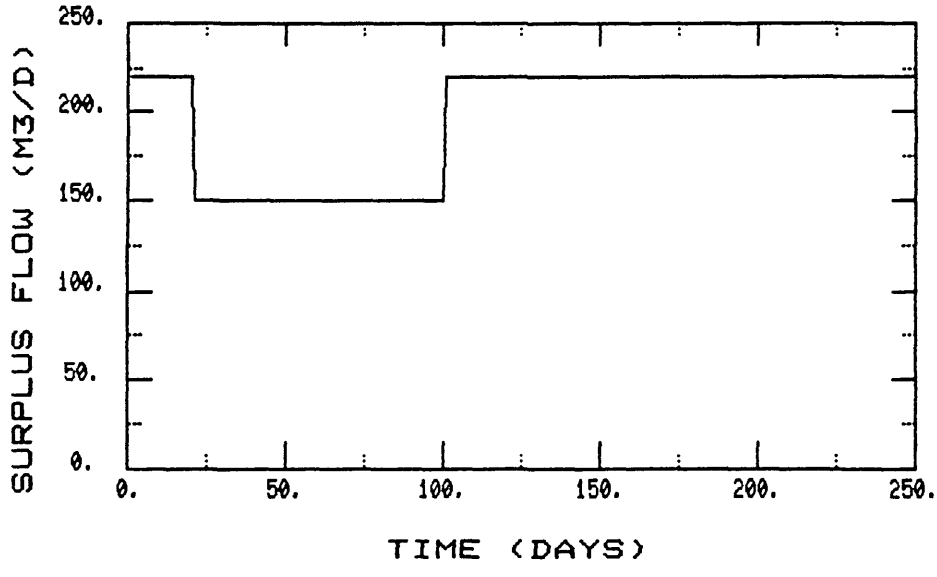


Fig. 5.14b. Generated pulse in the surplus sludge flow

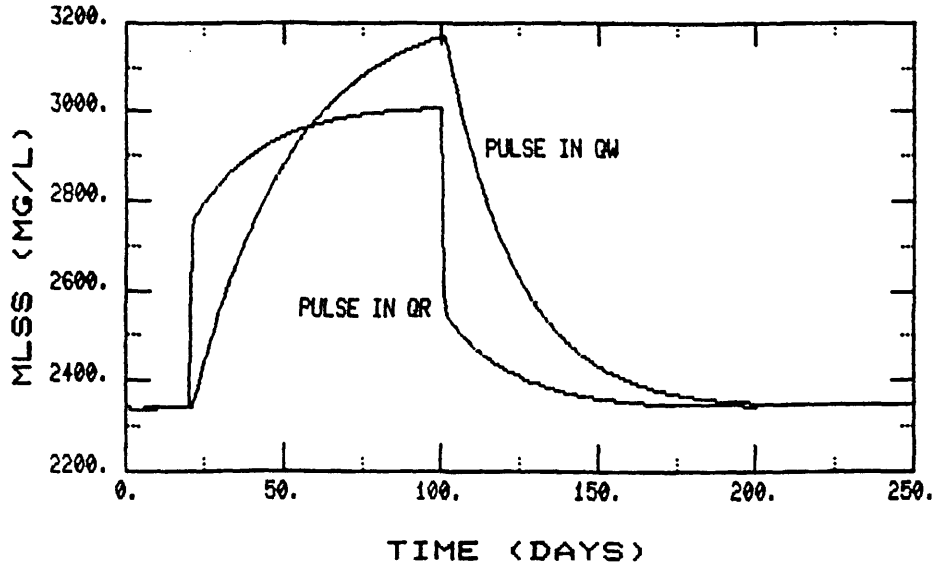


Fig. 5.15. Transient response of $MLSS$ to a pulse in control inputs

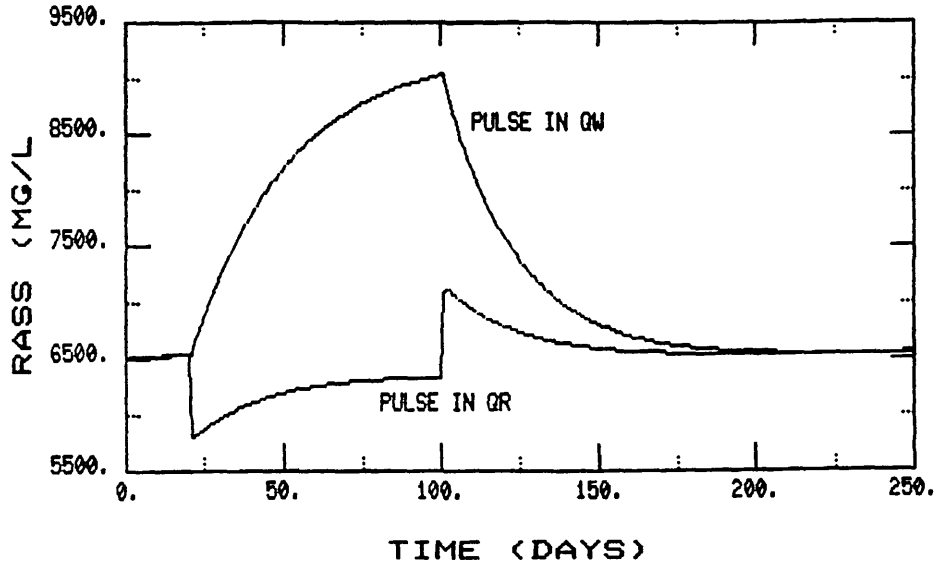


Fig. 5.16. Transient response of $RASS$ to a pulse in control inputs

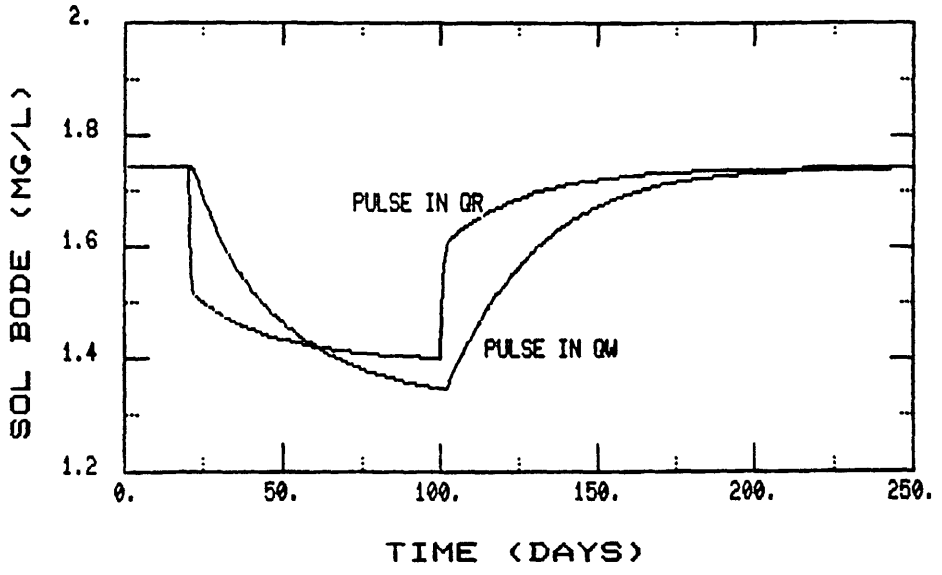


Fig. 5.17. Transient response of soluble effluent BOD_5 to a pulse in control inputs

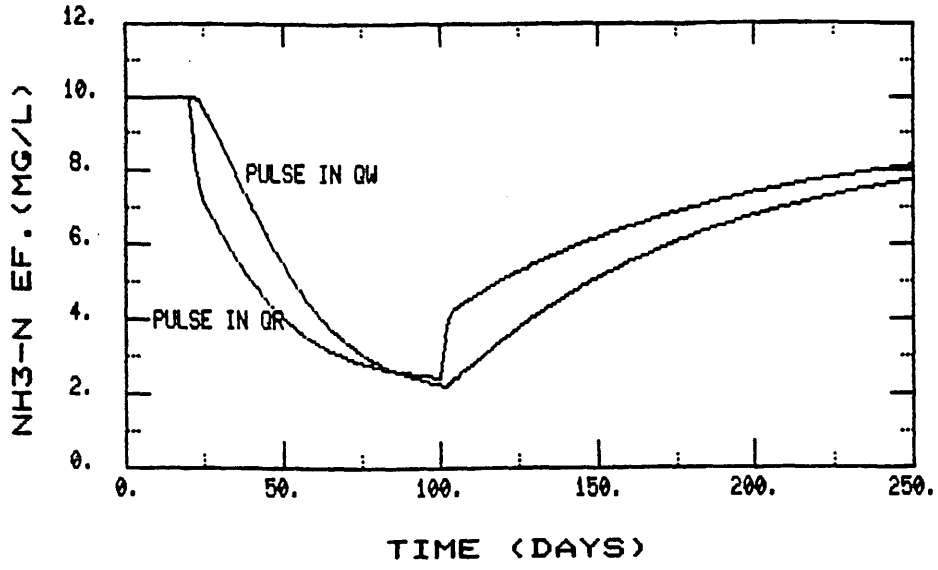


Fig. 5.18. Transient response of effluent $NH_3 - N$ to a pulse in control inputs

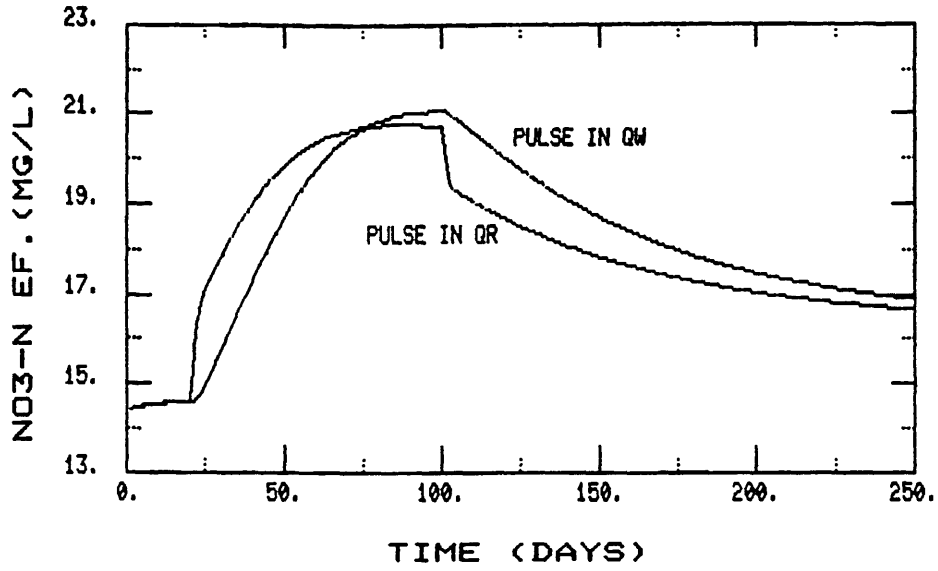


Fig. 5.19. Transient response of effluent $NO_3 - N$ to a pulse in control inputs

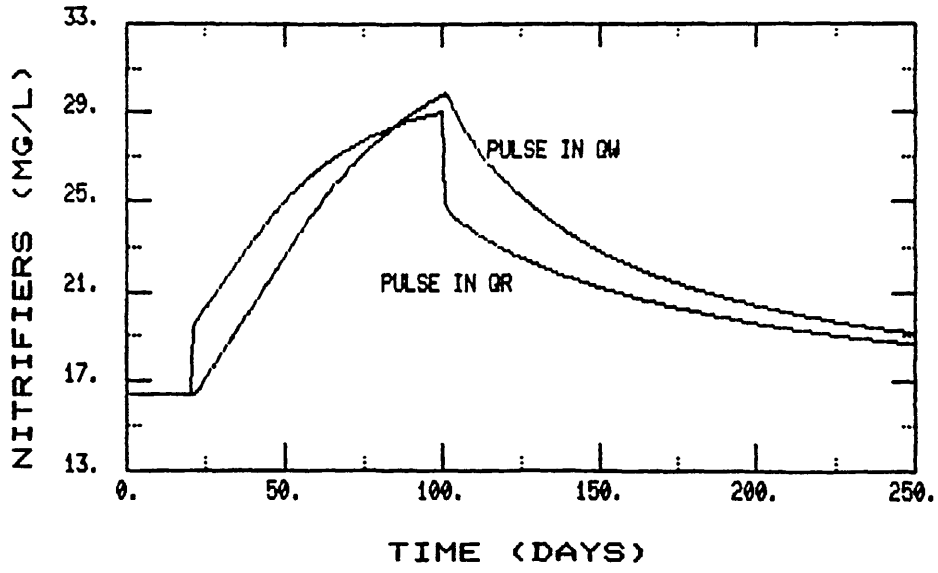


Fig. 5.20. Transient response of nitrifiers to a pulse in control inputs

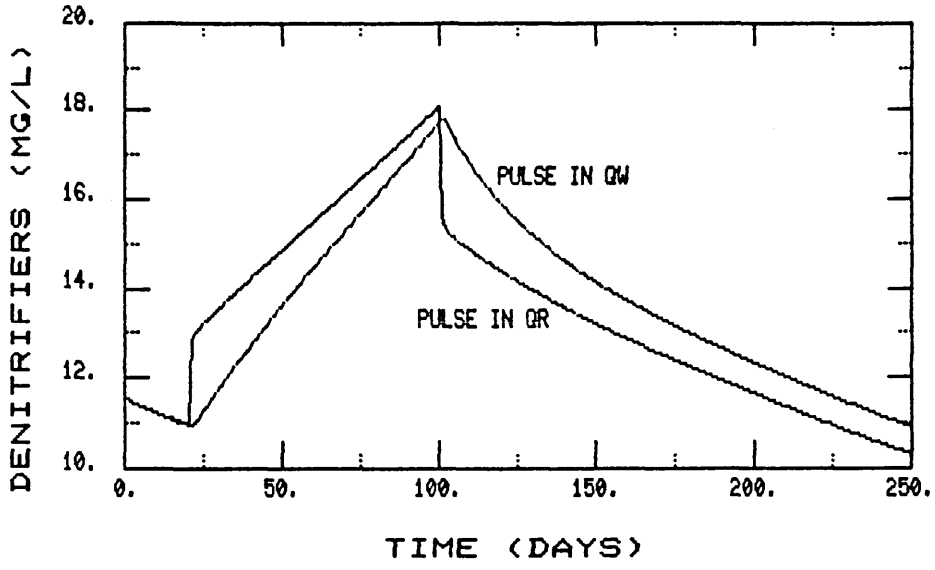


Fig. 5.21. Transient response of denitrifiers to a pulse in control inputs

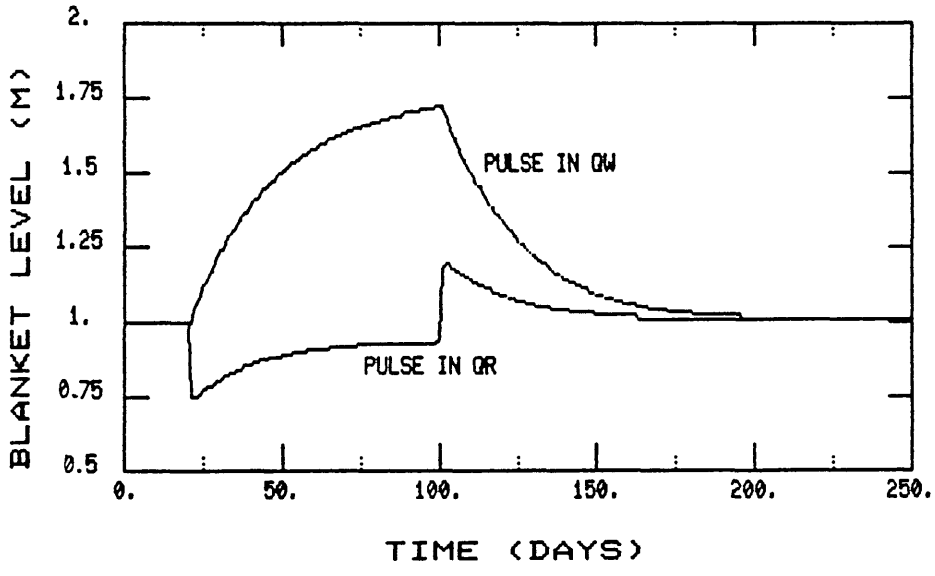


Fig. 5.22. Transient response of sludge blanket level to a pulse in control inputs

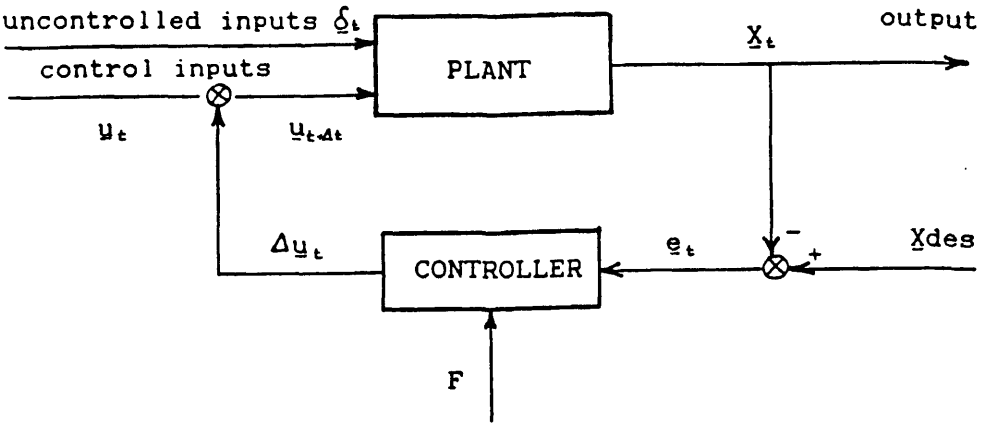


Fig. 5.23a. Schematic representation of a proportional-error FB control system

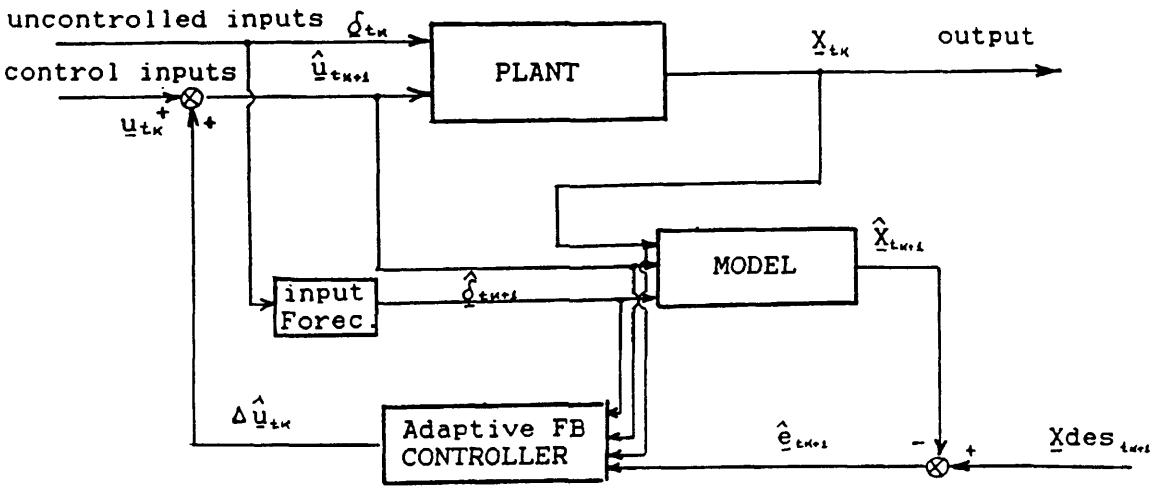


Fig. 5.23b. Schematic representation of an adaptive prediction error FB control system

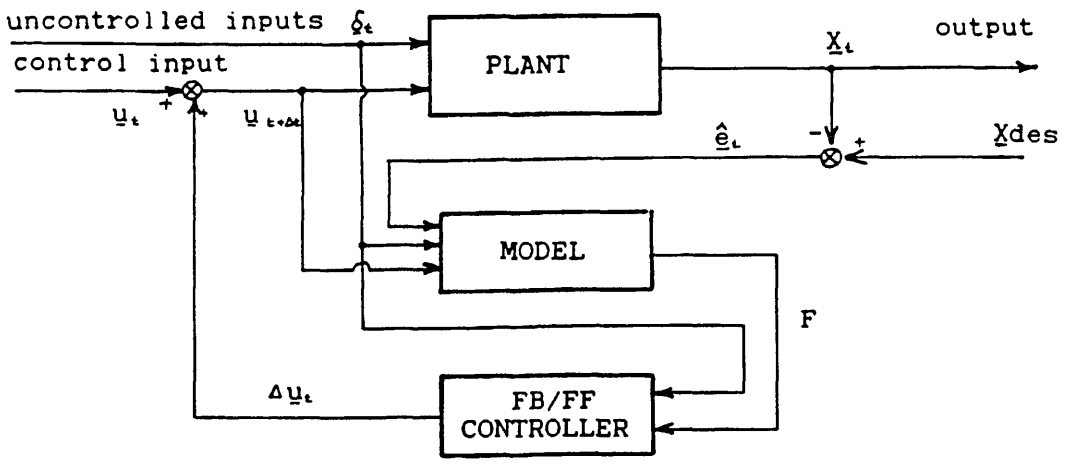
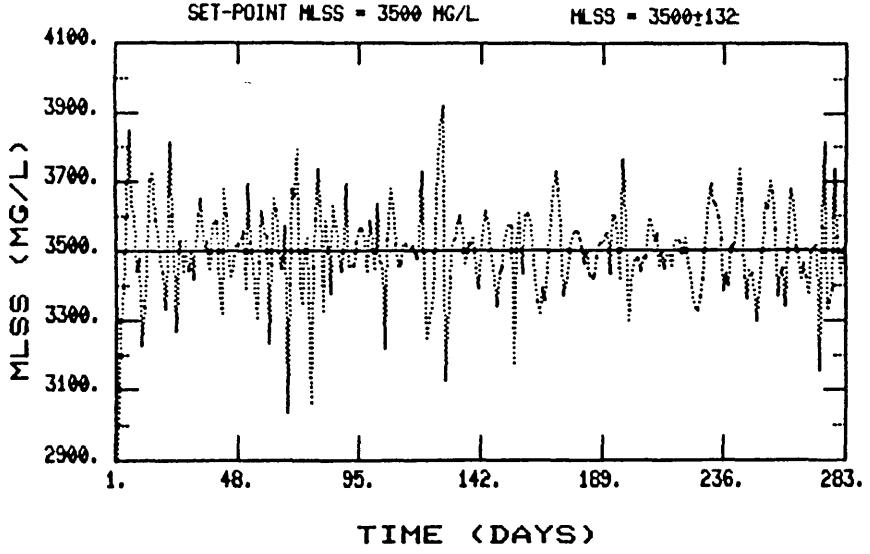
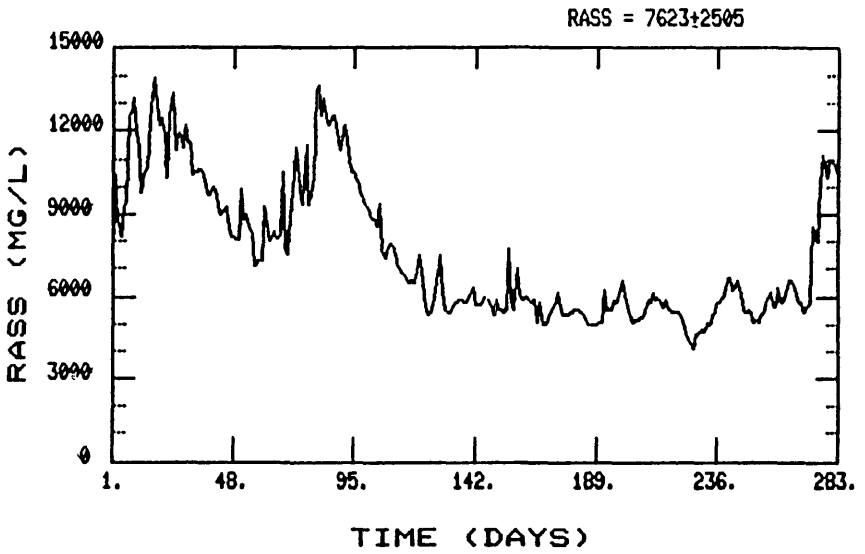


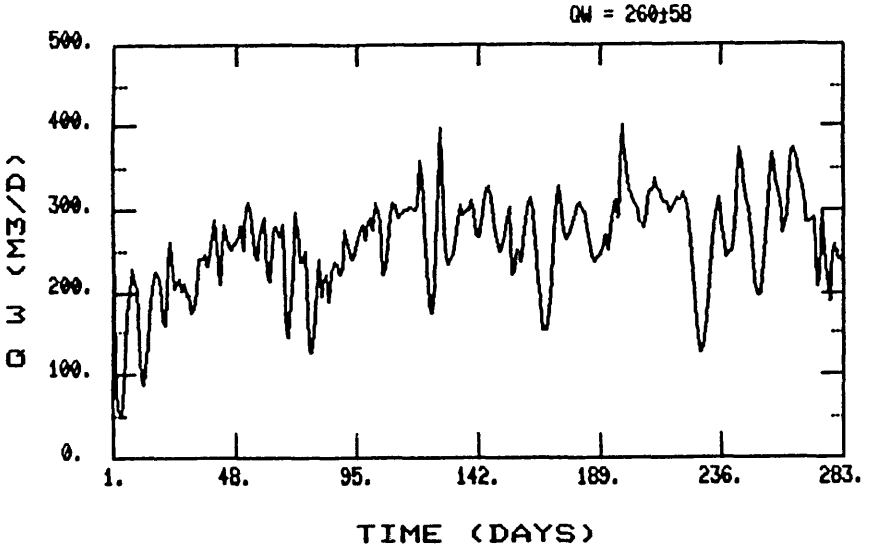
Fig. 5.23c. Schematic representation of a combined FB/FF control system



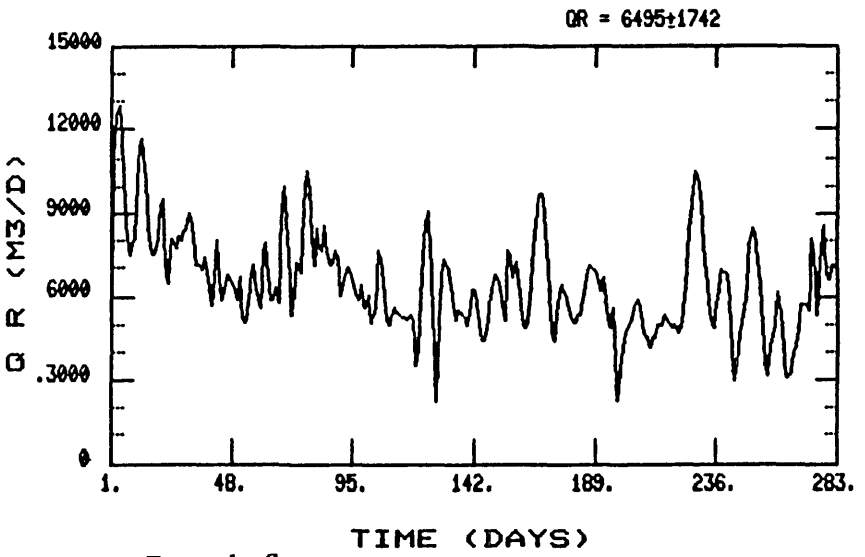
a. *MLSS* concentration



b. *RASS* concentration

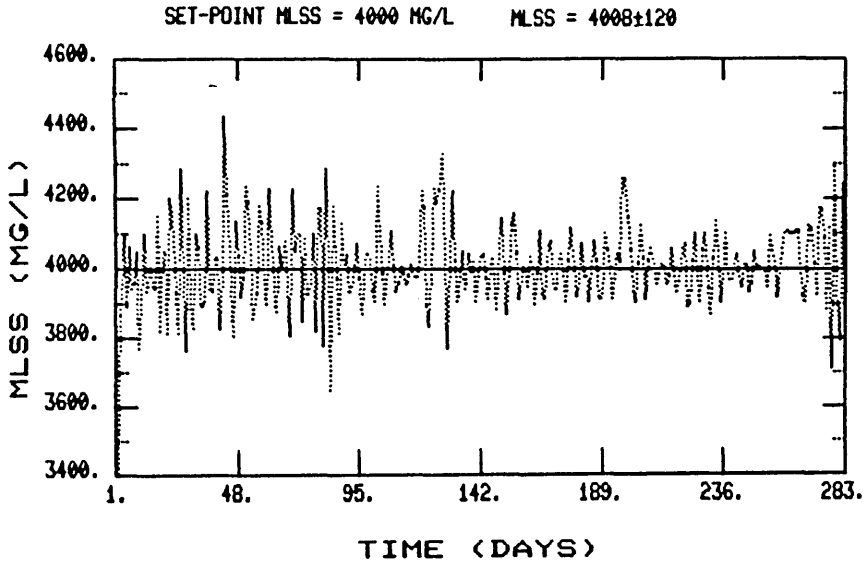


d. Surplus sludge flow

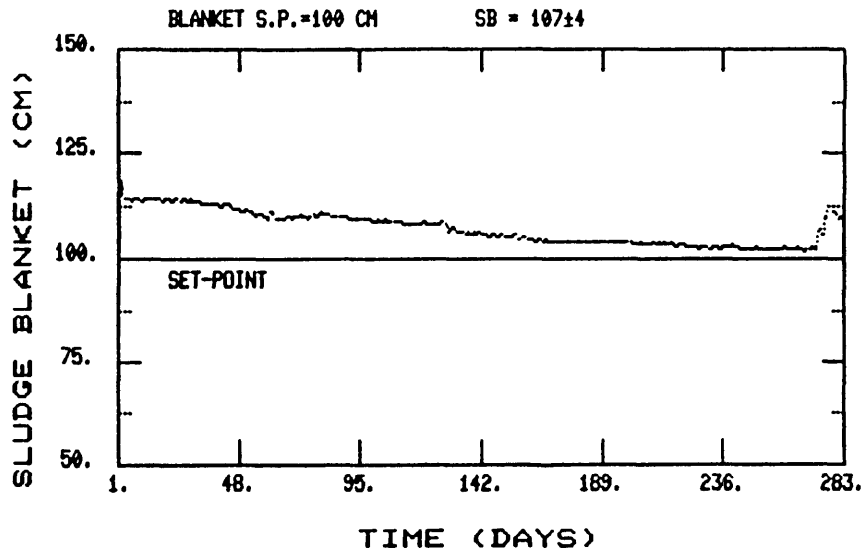


c. Recycle flow

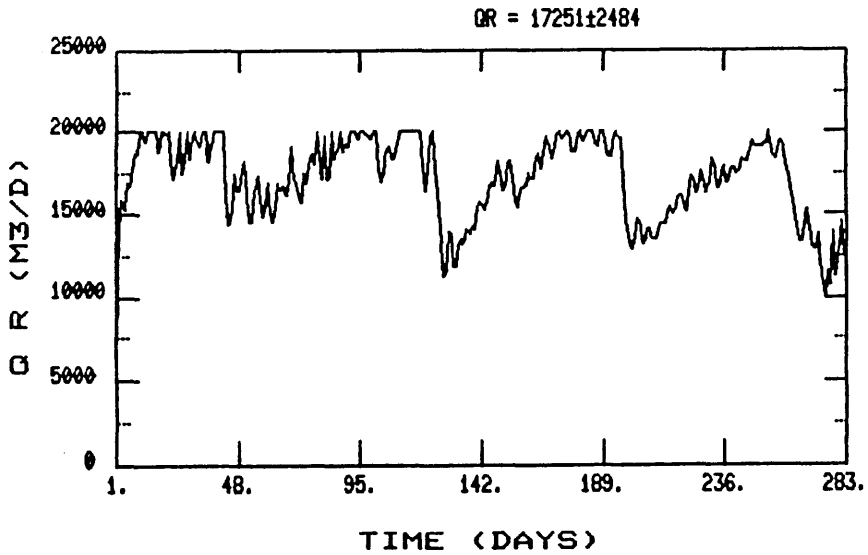
Fig. 5.24. Performance of a single-loop FB control with constant gain



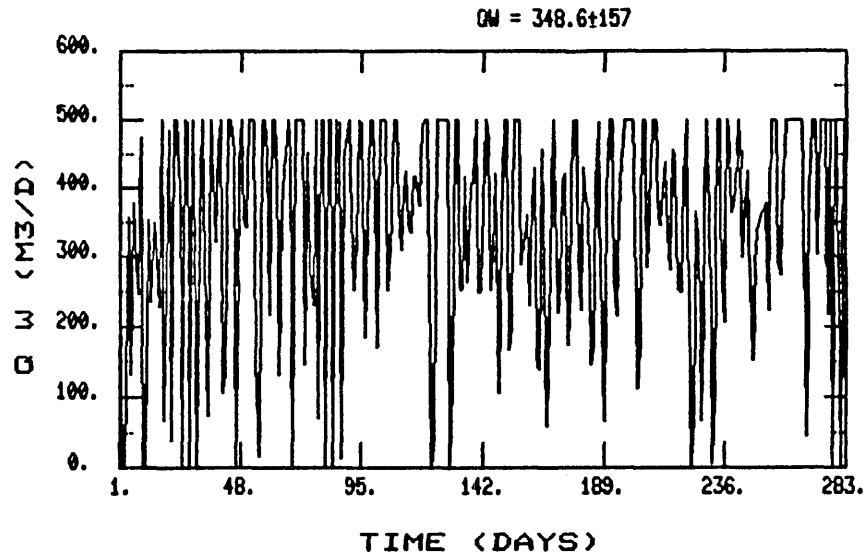
a. *MLSS* concentration



b. *RASS* concentration

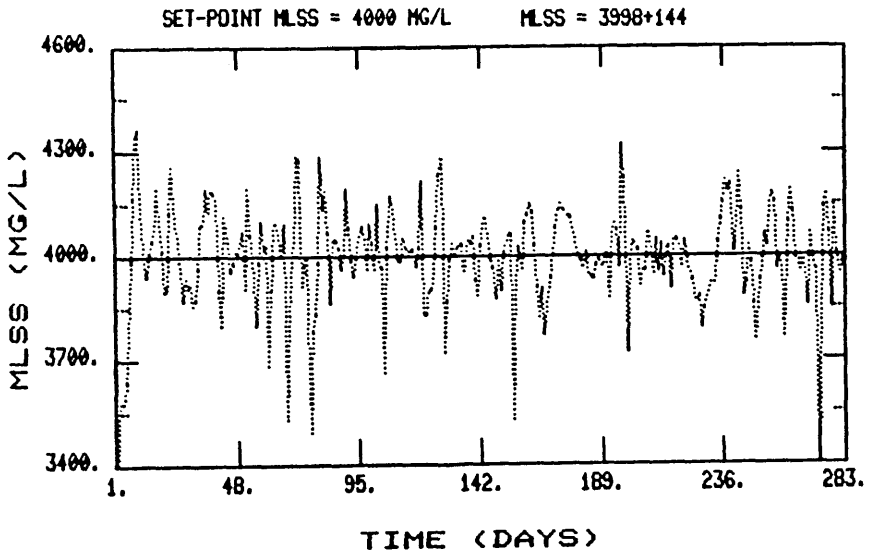


c. Recycle flow

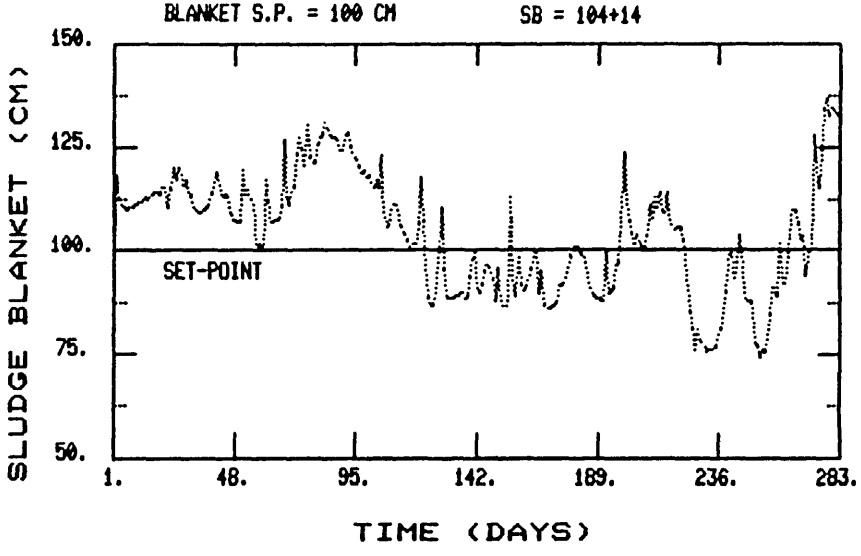


d. Surplus sludge flow

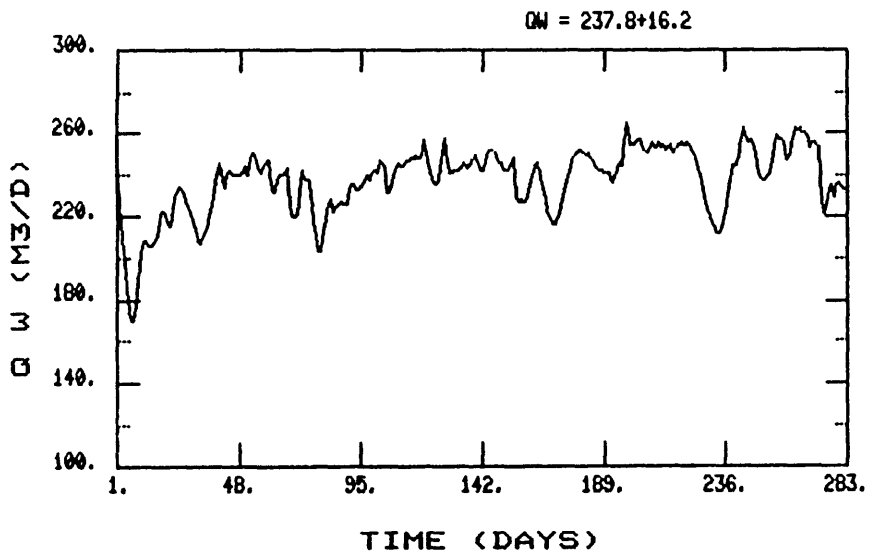
Fig. 5.25. Performance of a two-loop FB control with constant gains (Case 1)



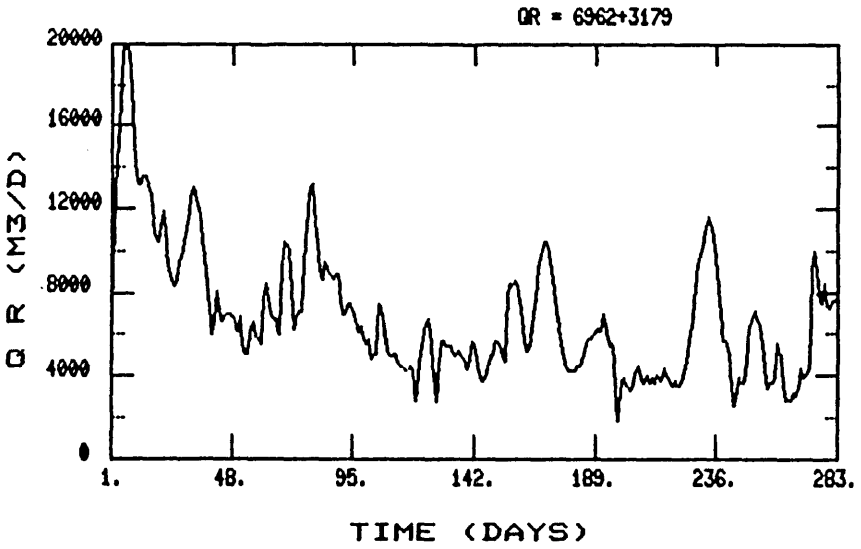
a. *MLSS* concentration



b. *RASS* concentration



c. Recycle flow



d. Surplus sludge flow

Fig. 5.26. Performance of a two-loop FB control with constant gains with modified objective function (Case 4)

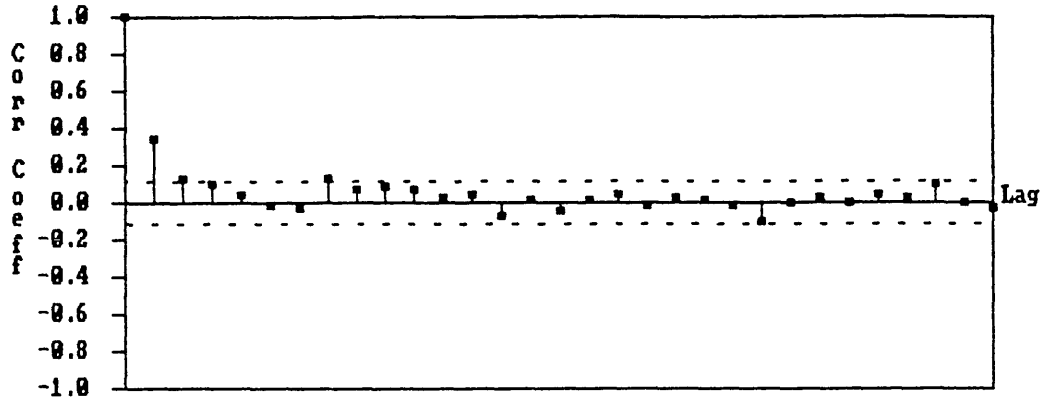


Fig. 5.27a. Autocorrelogram of input *BOD* load

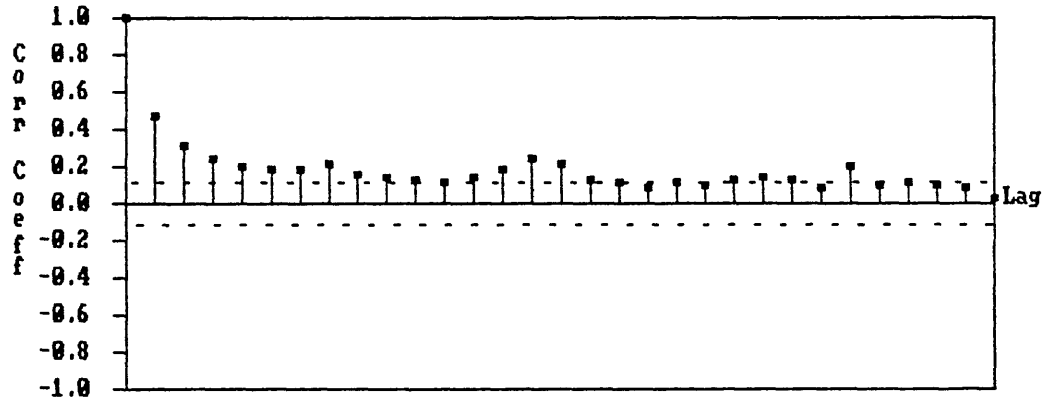
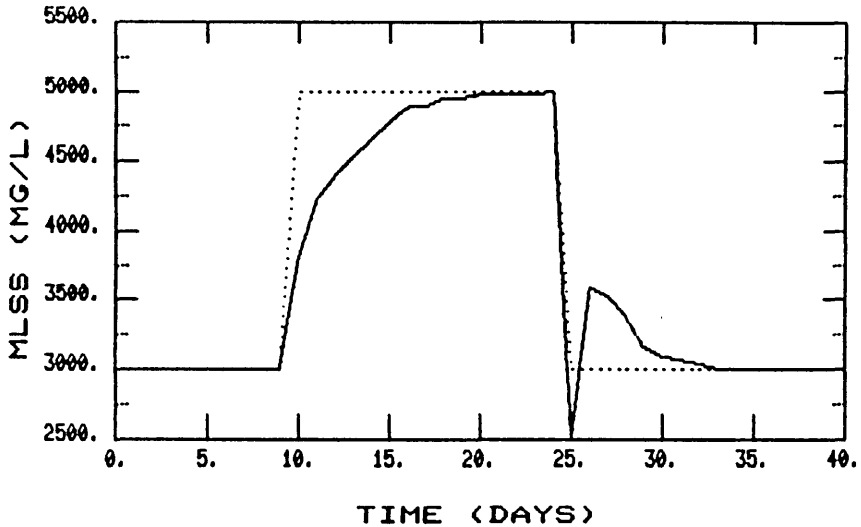
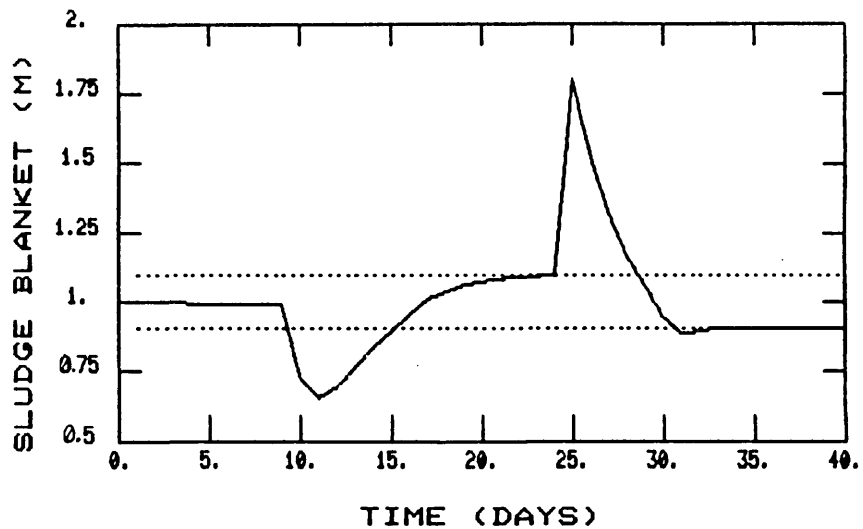


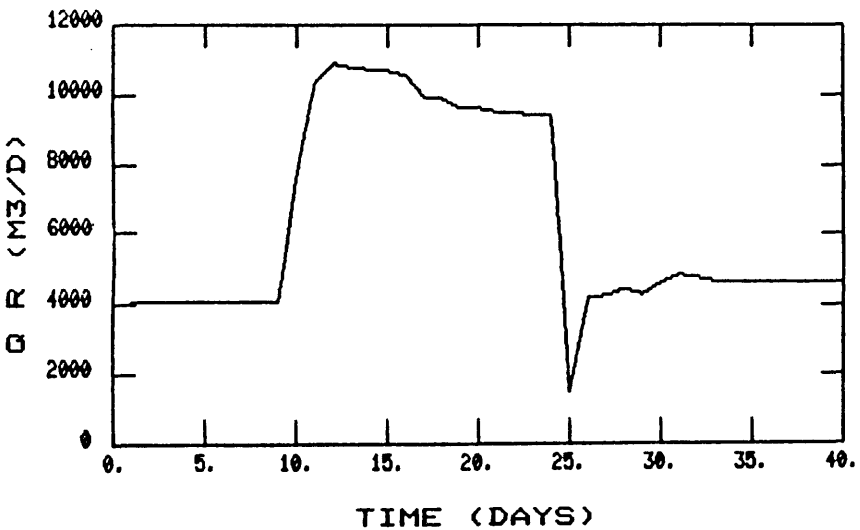
Fig. 5.27b. Autocorrelogram of input ammonia load



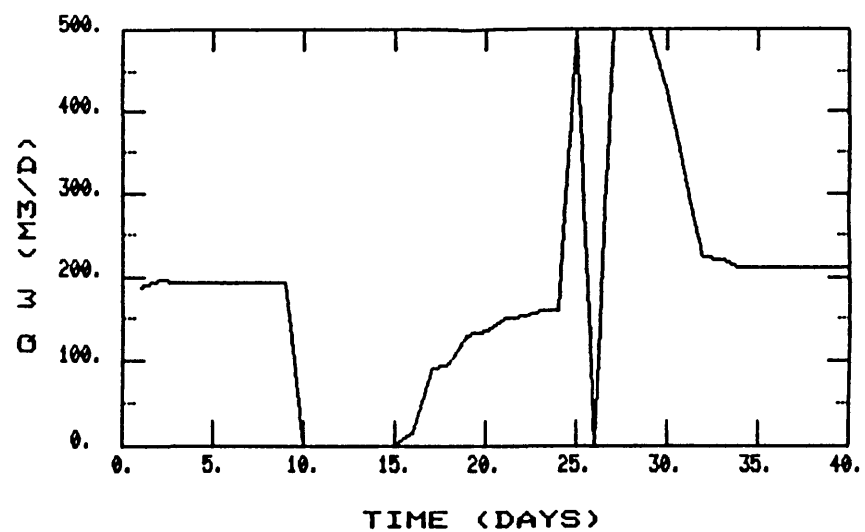
a. $MLSS$ concentration



b. Sludge blanket level

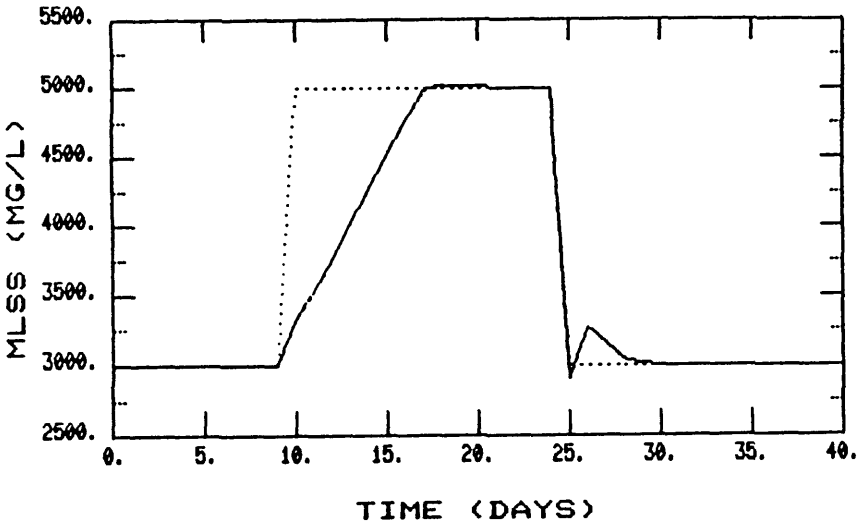


c. Recycle flow

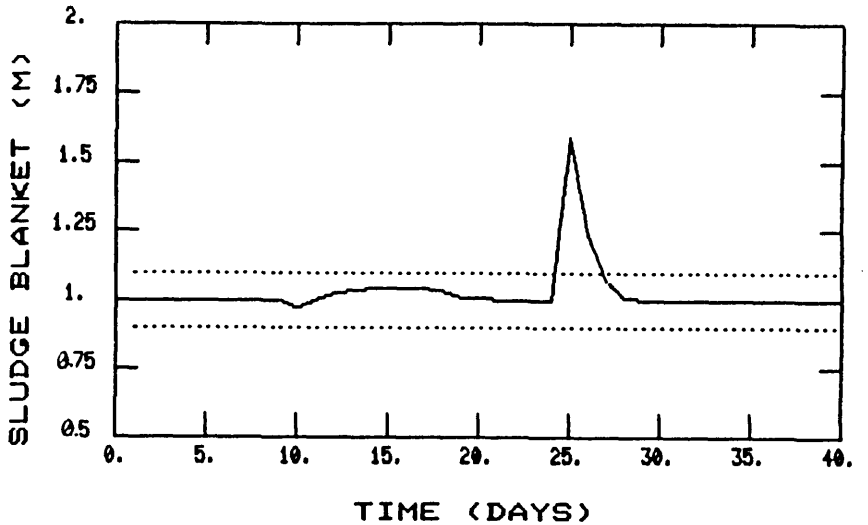


d. Surplus sludge flow

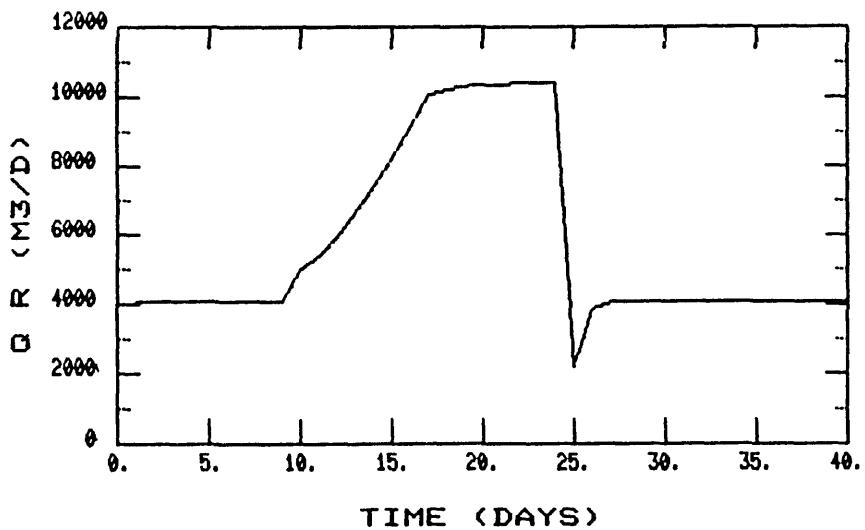
Fig. 5.28. Performance of the 'adaptive-gain' Feedback system to a pulse in the $MLSS$ set- point (with $BL = 0.90 - 1.10$)



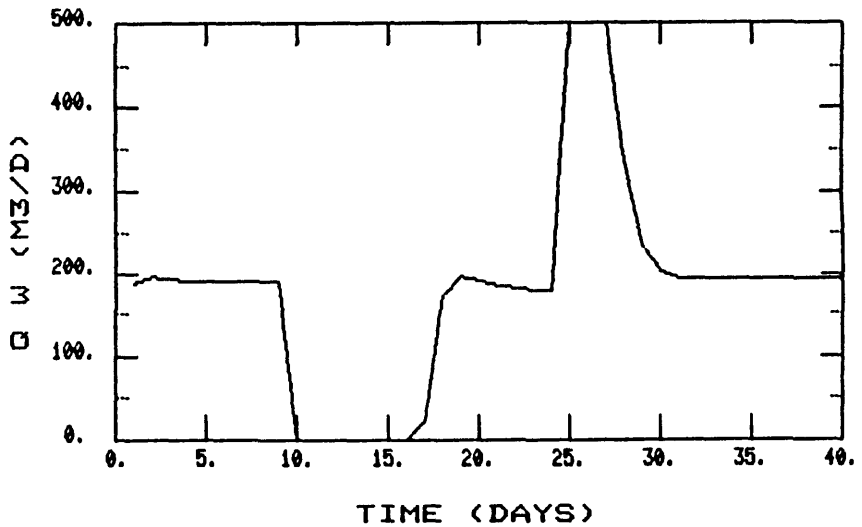
a. $MLSS$ concentration



b. Sludge blanket level

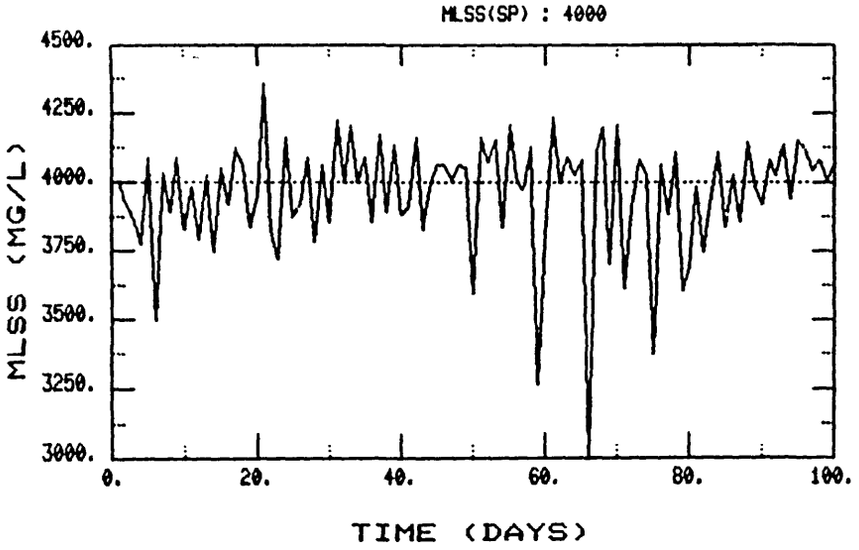


c. Recycle flow

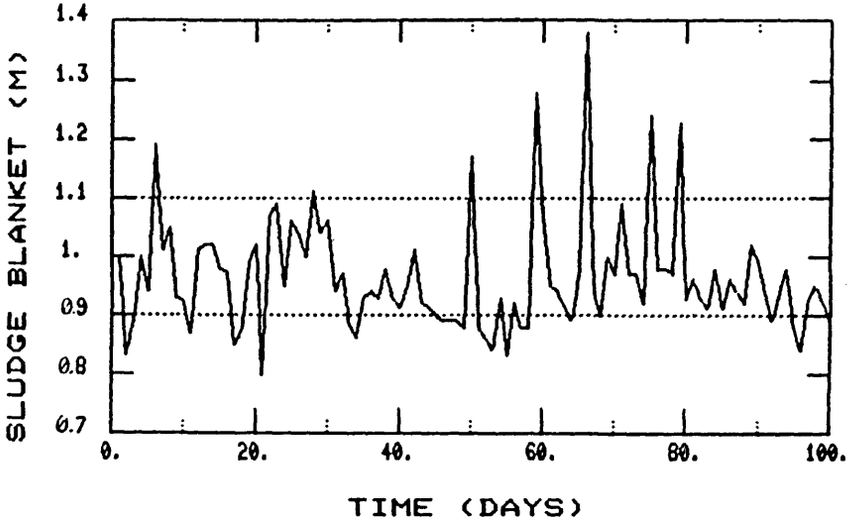


d. Surplus sludge flow

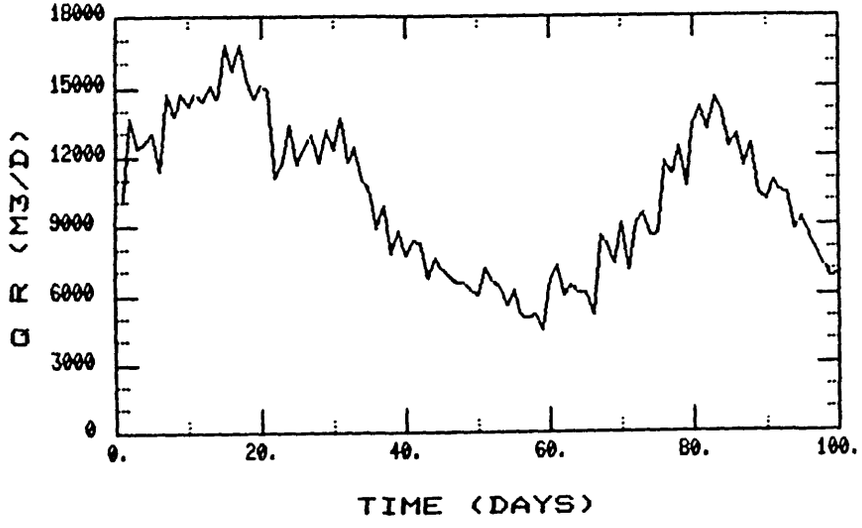
Fig. 5.29. Performance of the 'iterative' Feedback system to a pulse in the $MLSS$ set-point (with $w_1/w_2 = 1/12.5$ & $BL = 0.9 - 1.10$)



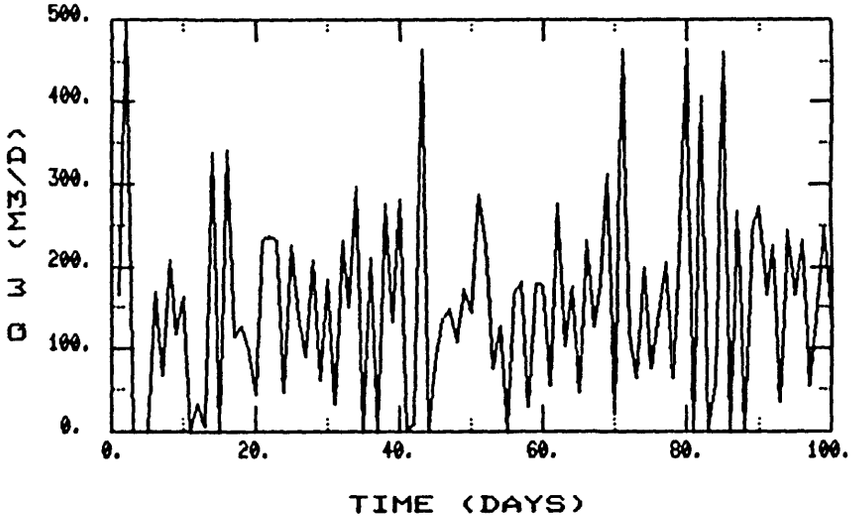
a. $MLSS$ concentration



b. Sludge blanket level

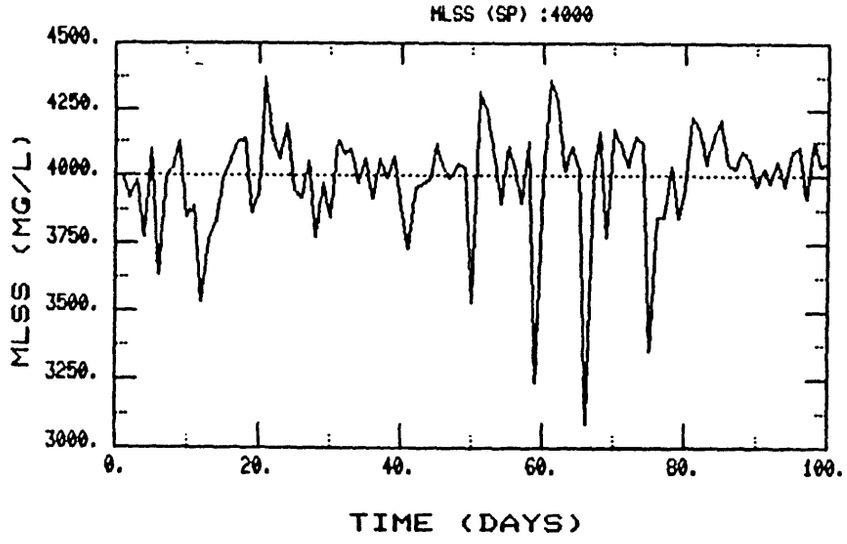


c. Recycle flow

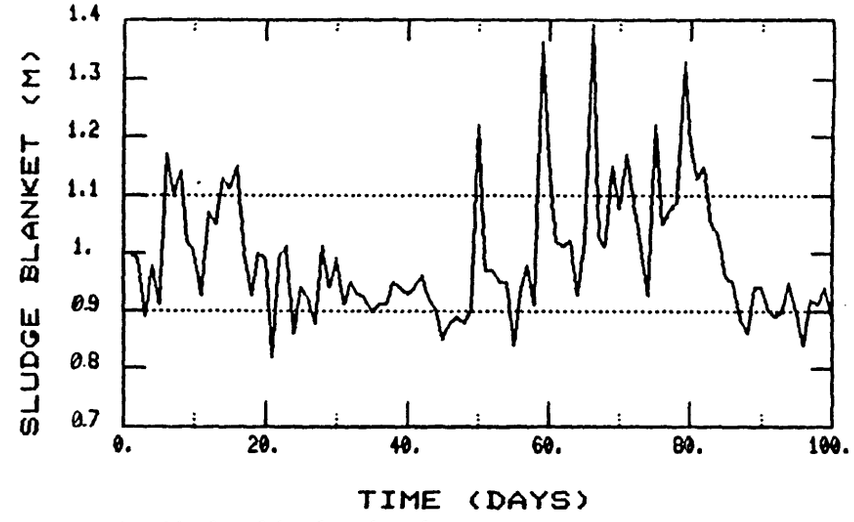


d. Surplus sludge flow

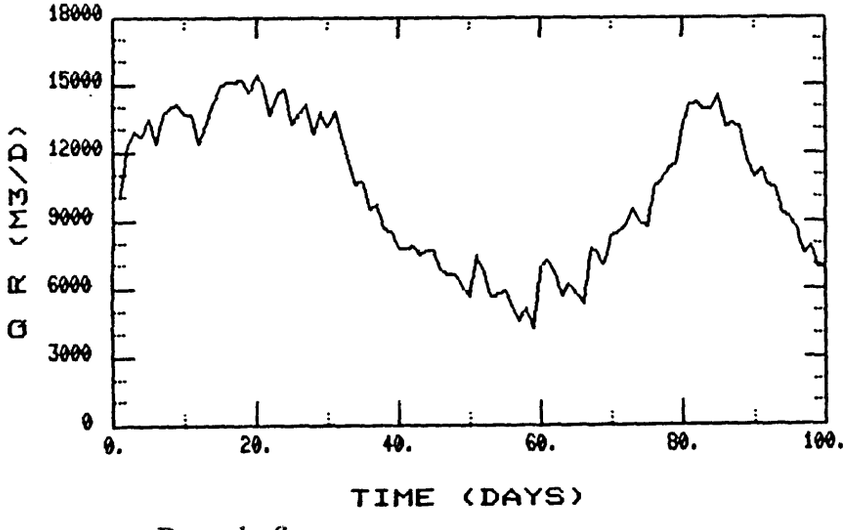
Fig. 5.30. Performance of the 'adaptive-gain' Feedback system under variable input conditions (with $BL = 0.90 - 1.10$)



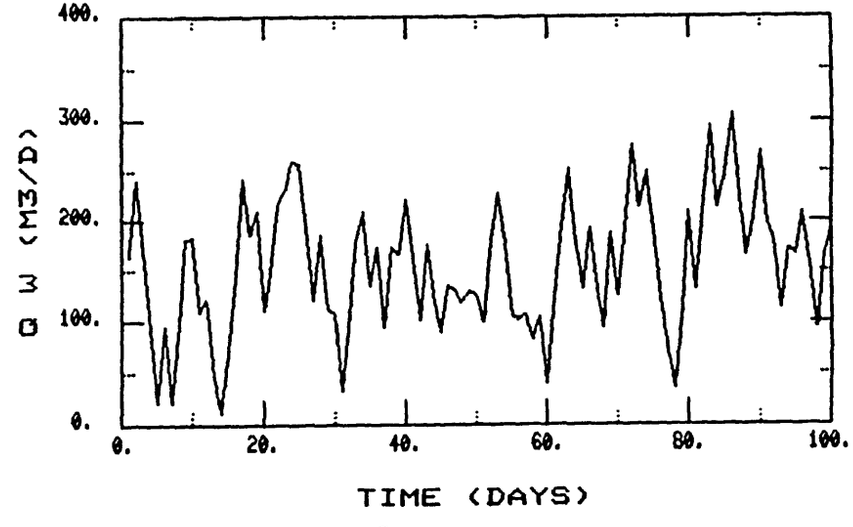
a. $MLSS$ concentration



b. Sludge blanket level

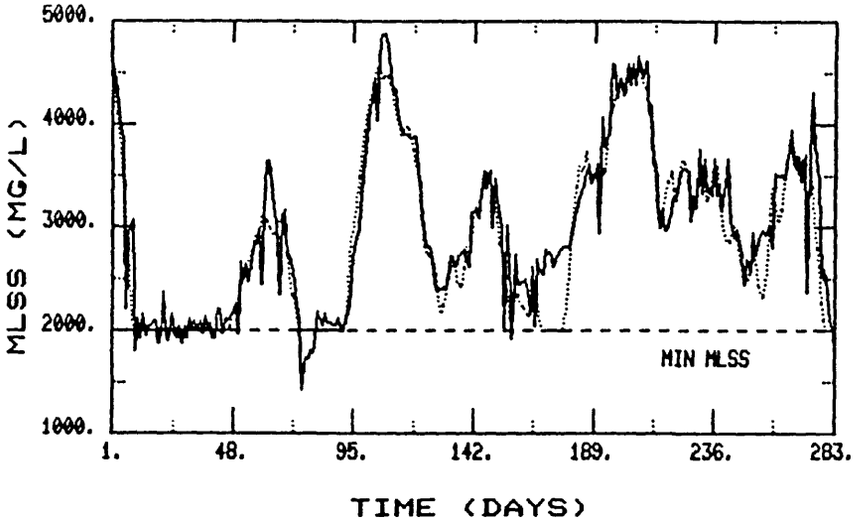


c. Recycle flow

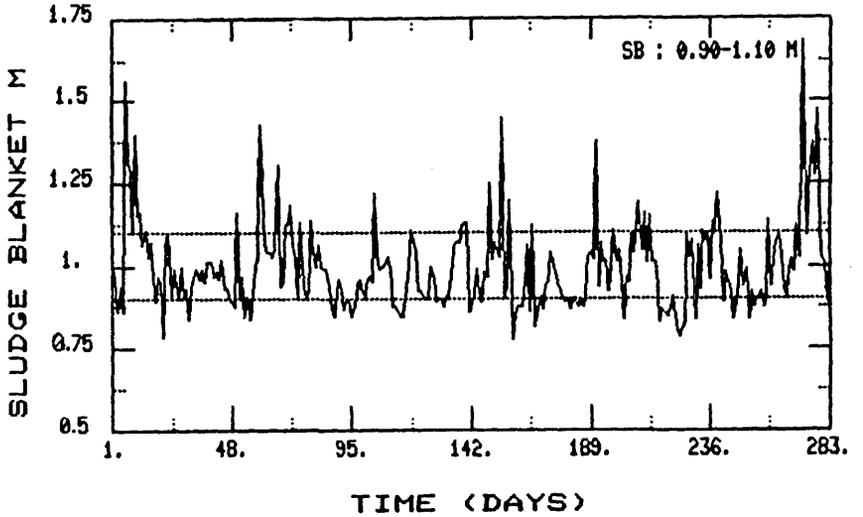


d. Surplus sludge flow

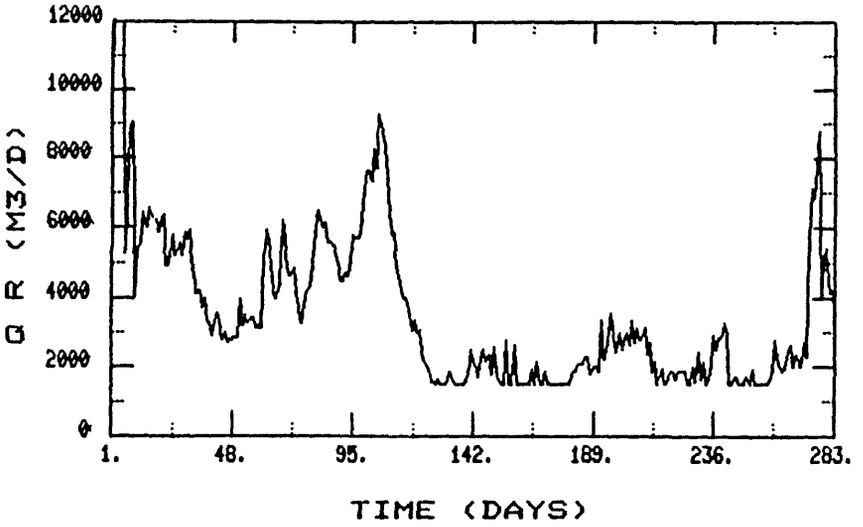
Fig. 5.31. Performance of the iterative Feedback system under variable inputs
(with $BL = 0.90 - 1.10$ $w_1 = 20, w_2 = 1000, w_3 = 0.002$ & $w_4 = 0.2$)



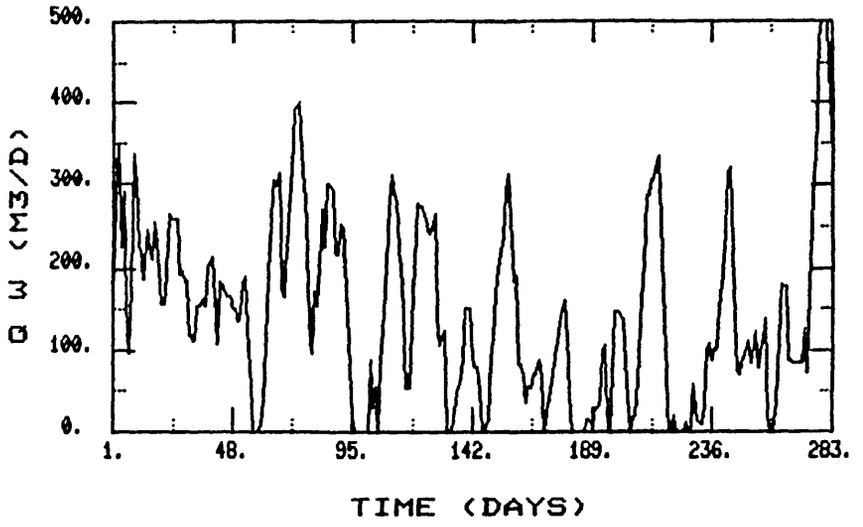
a. *MLSS* concentration



b. Sludge blanket level

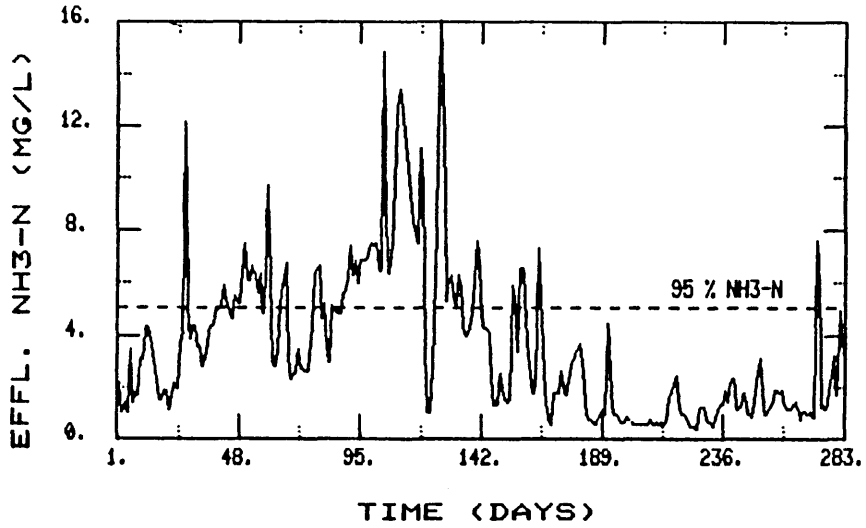


c. Recycle flow

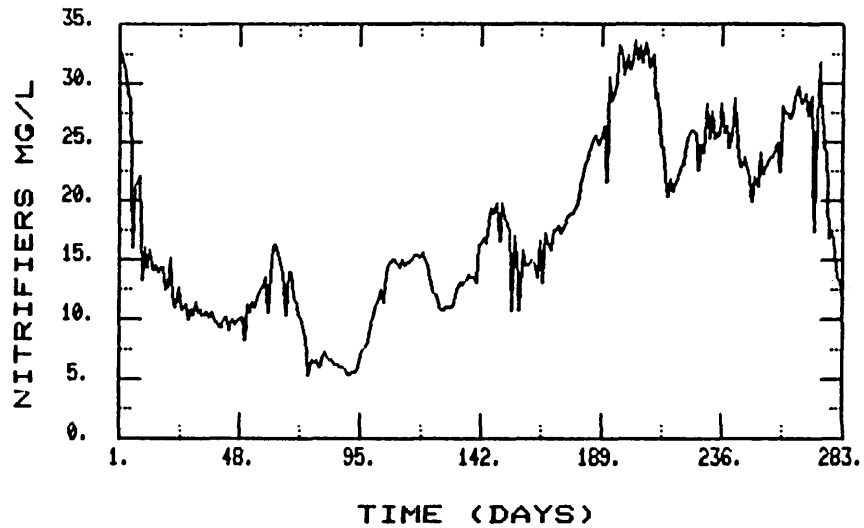


d. Surplus sludge flow

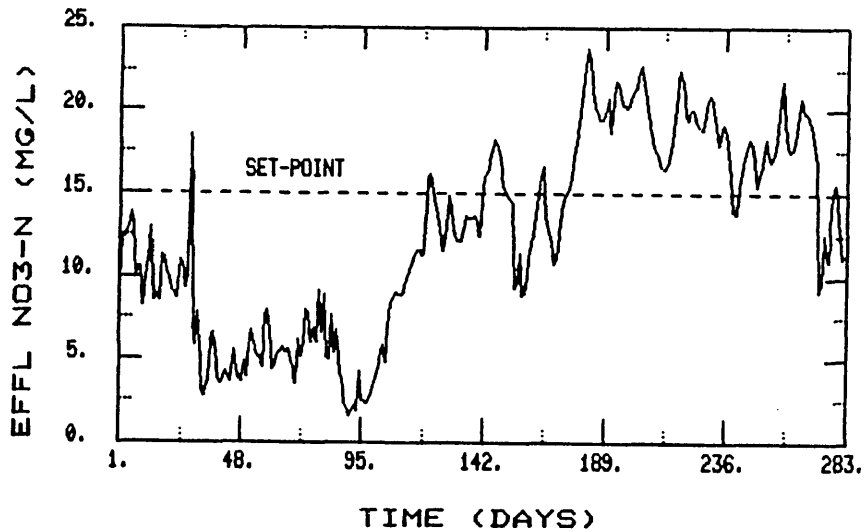
Fig. 5.32. Performance of controlled system under Policy 1



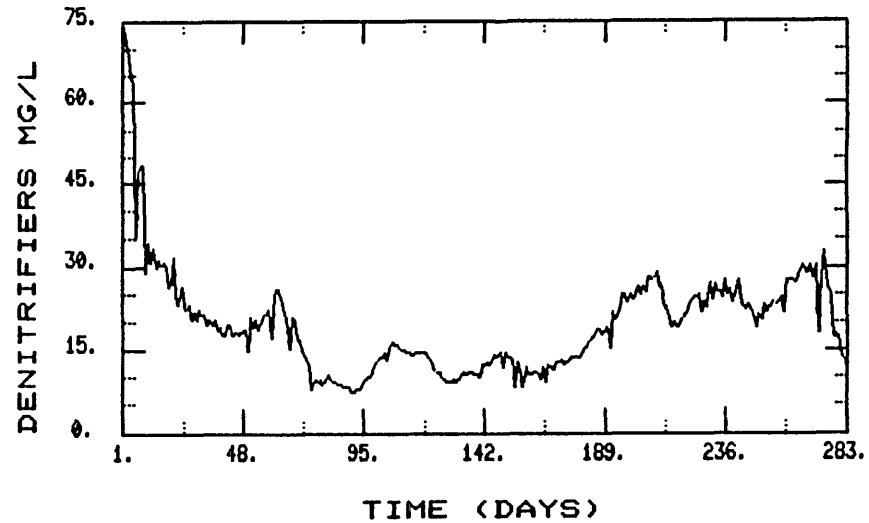
e. Effluent ammonia



f. Nitrifier concentration



g. Effluent nitrate



h. Denitrifier concentration

Fig. 5.32. Performance of controlled system under Policy 1

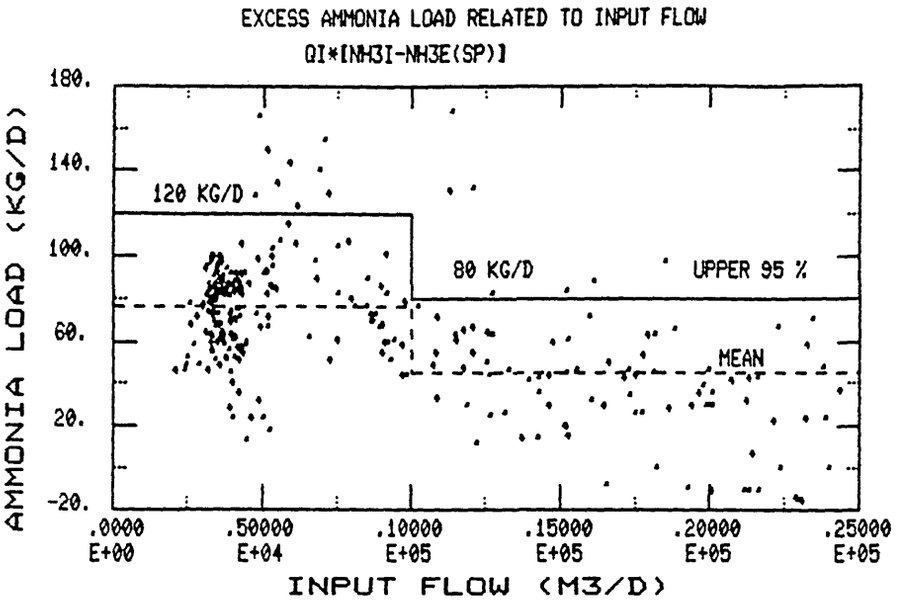
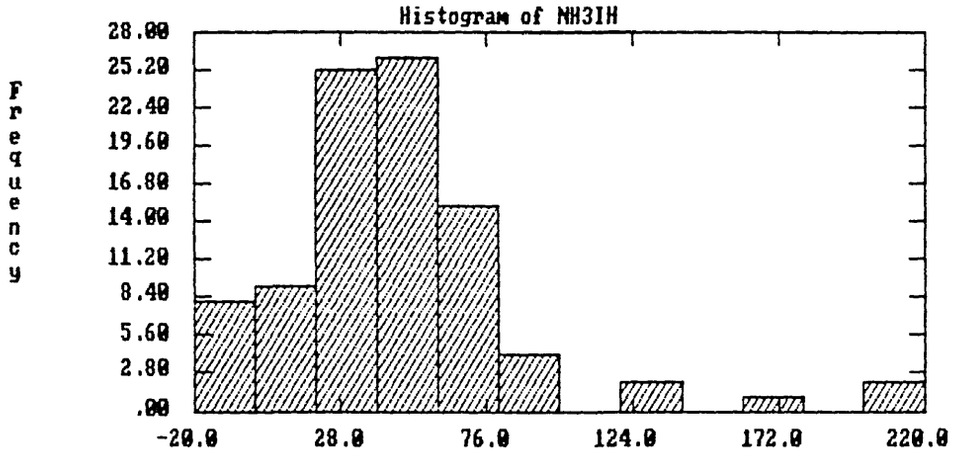
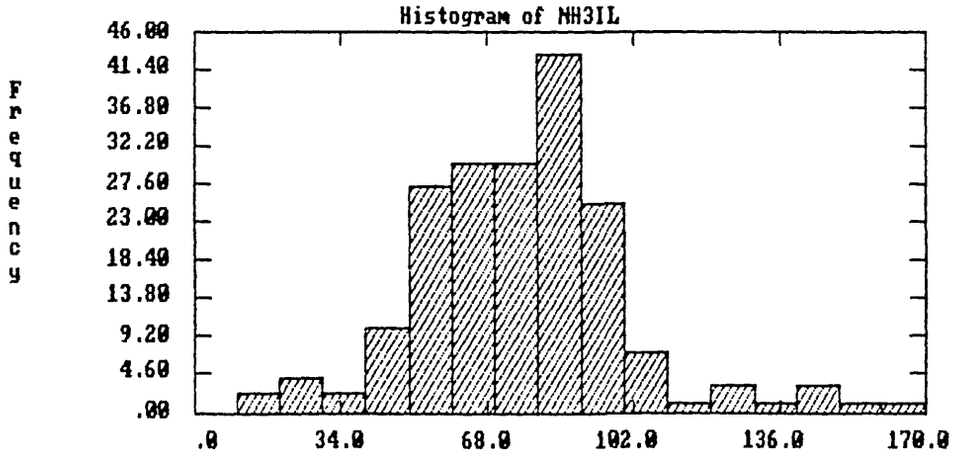


Fig. 5.33. Excess ammonia load versus input flow rate

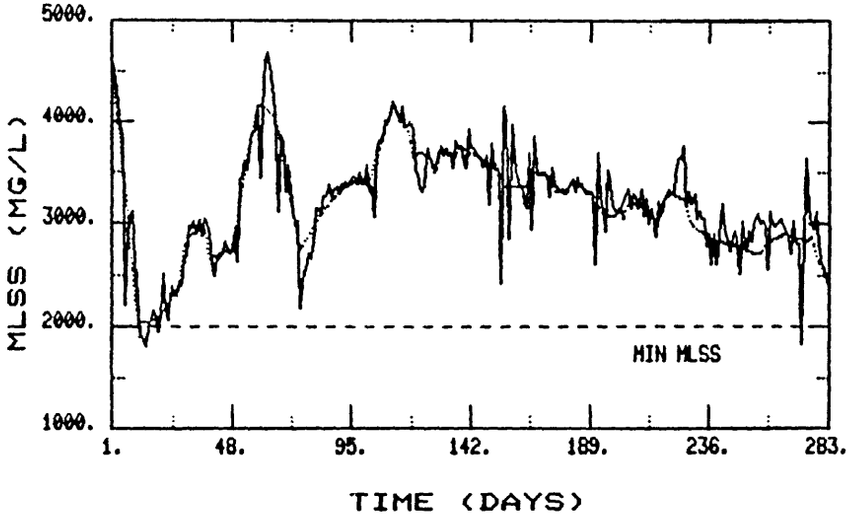


a. For Qi above 10,000 m^3/d

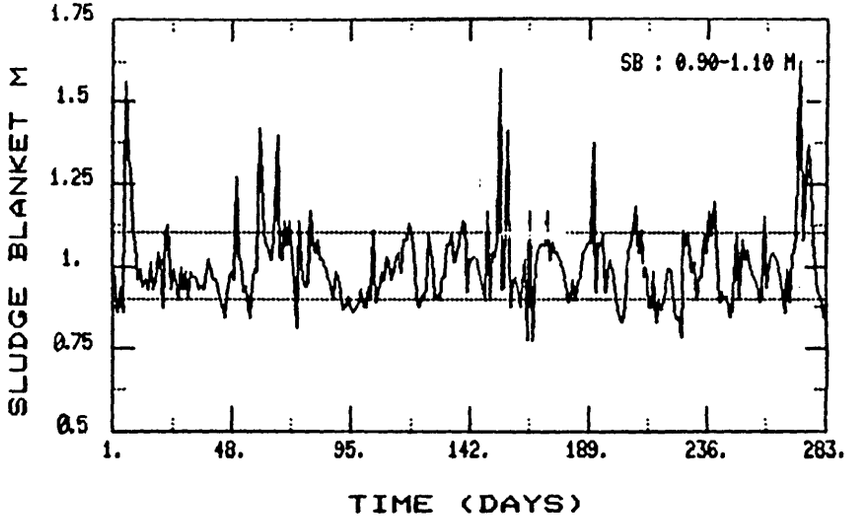


b. For Qi below 10,000 m^3/d

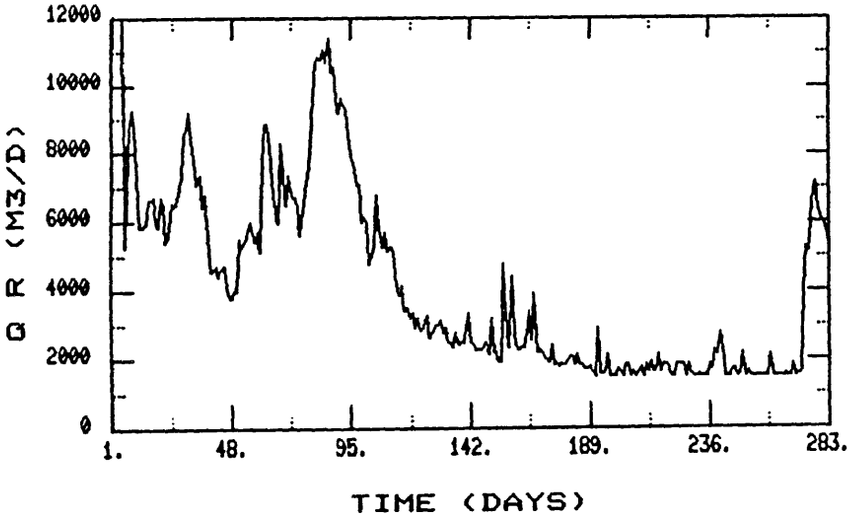
Fig. 5.34. Frequency distribution of excess ammonia load



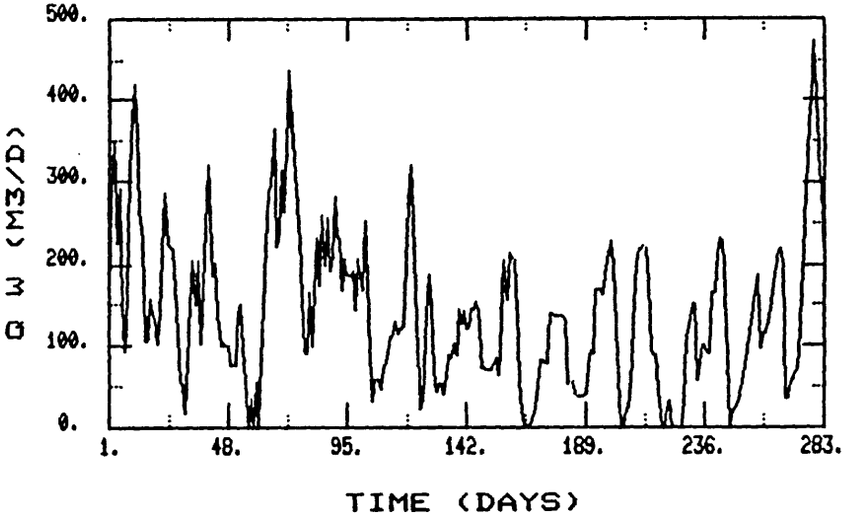
a. *MLSS* concentration



b. Sludge blanket level

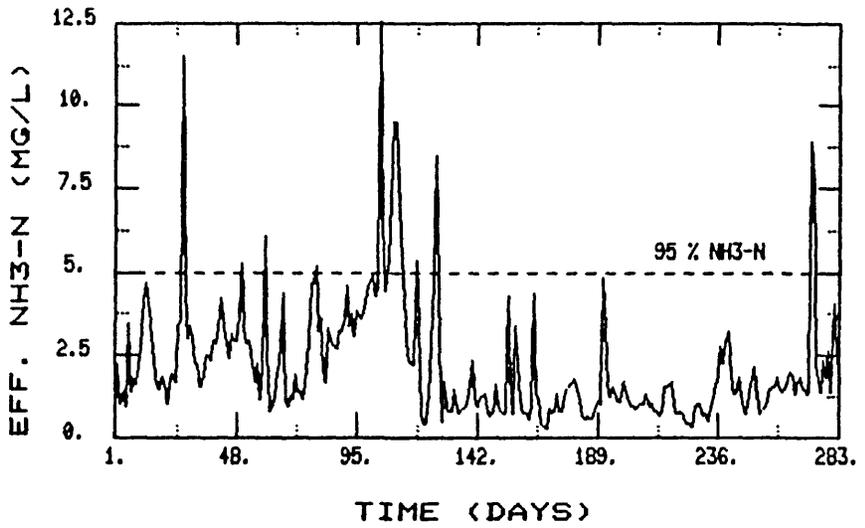


c. Recycle flow

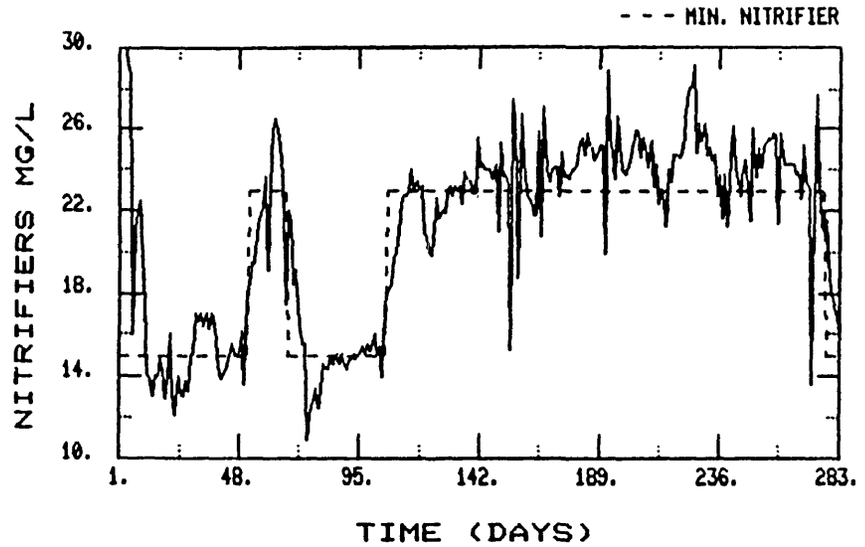


d. Surplus sludge flow

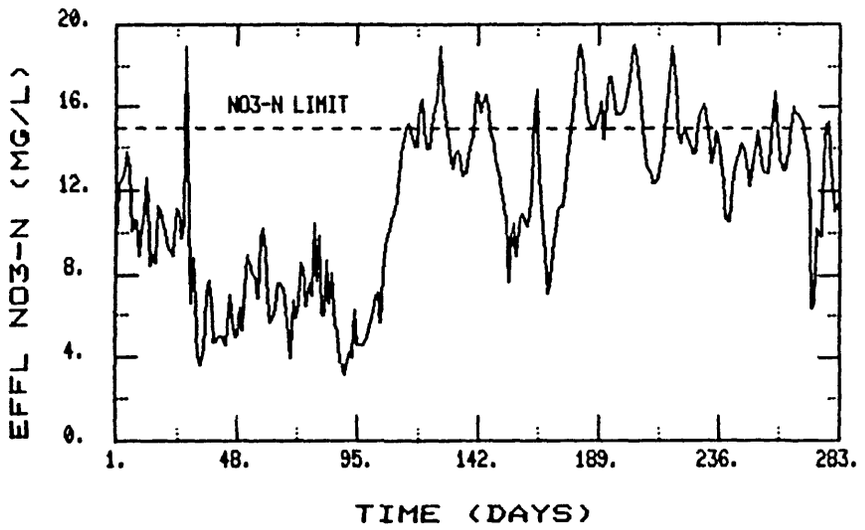
Fig. 5.35. Performance of controlled system under Policy 2



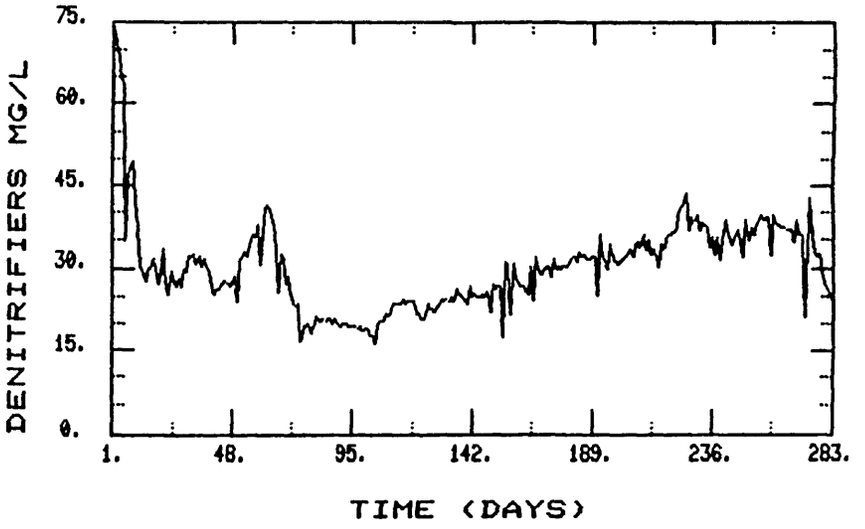
e. Effluent ammonia



f. Nitrifier concentration

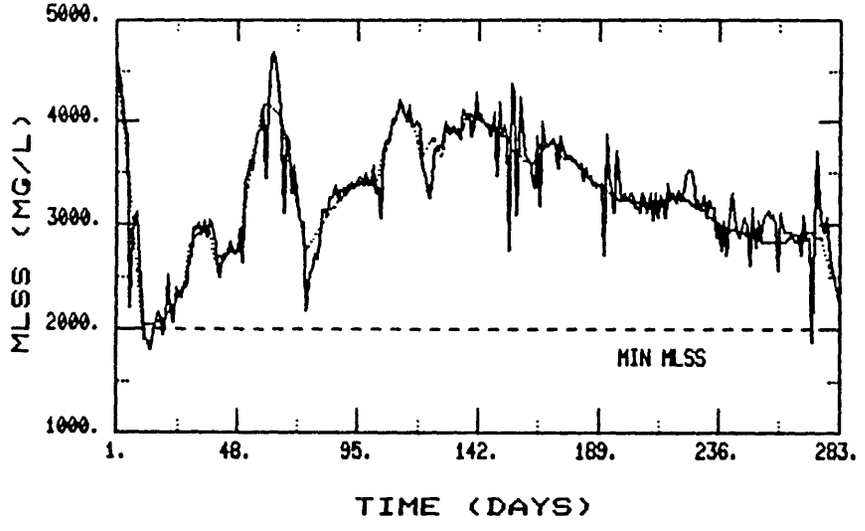


g. Effluent nitrate

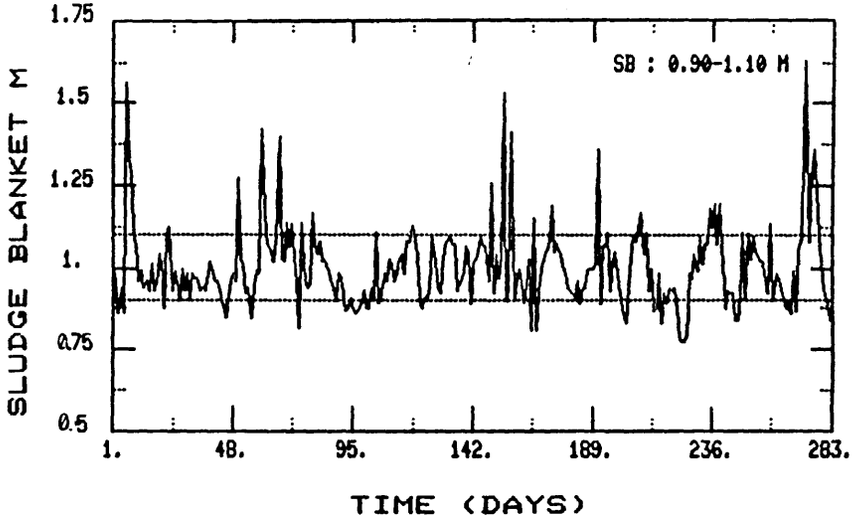


h. Denitrifier concentration

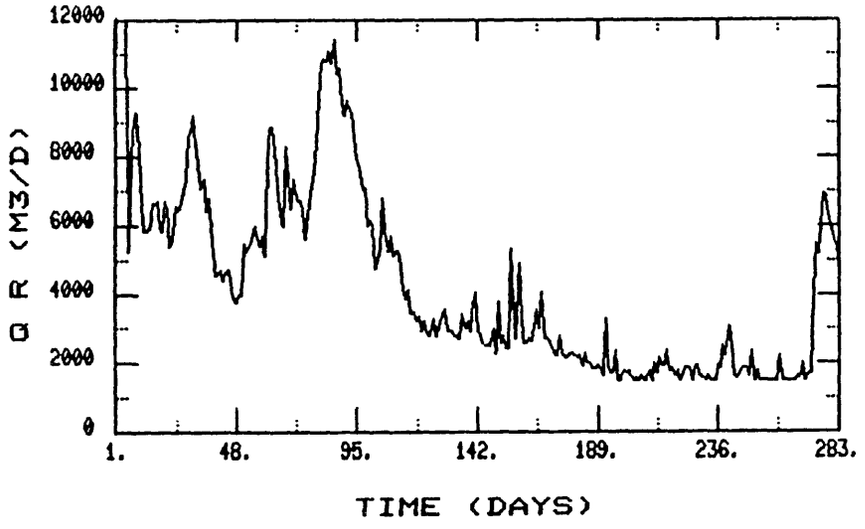
Fig. 5.35. Performance of controlled system under Policy 2



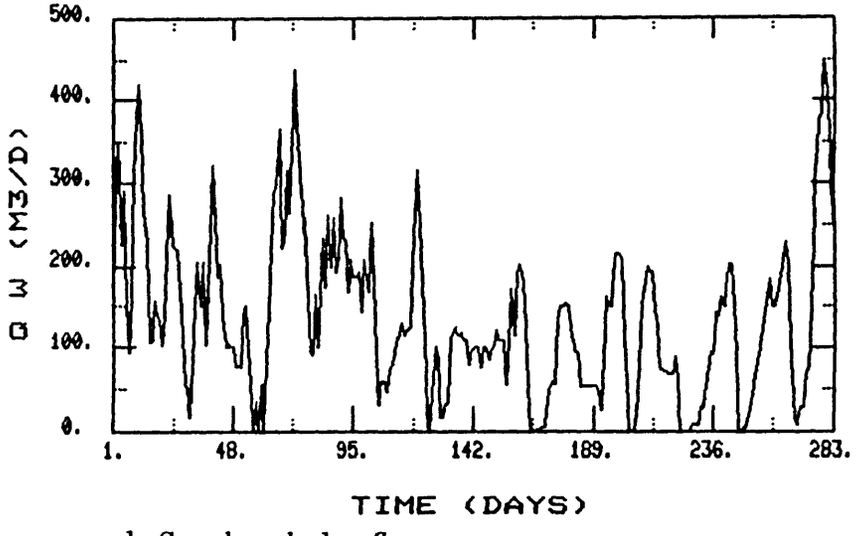
a. *MLSS* concentration



b. Sludge blanket level

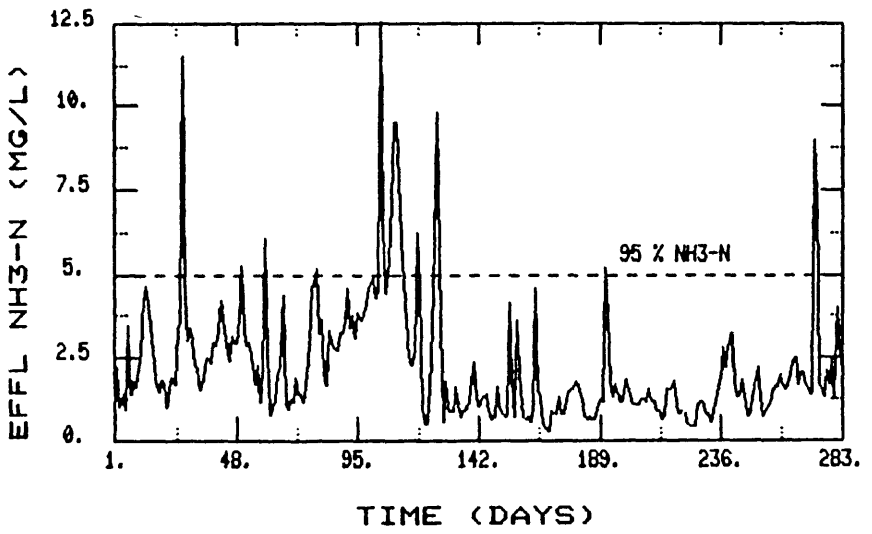


c. Recycle flow

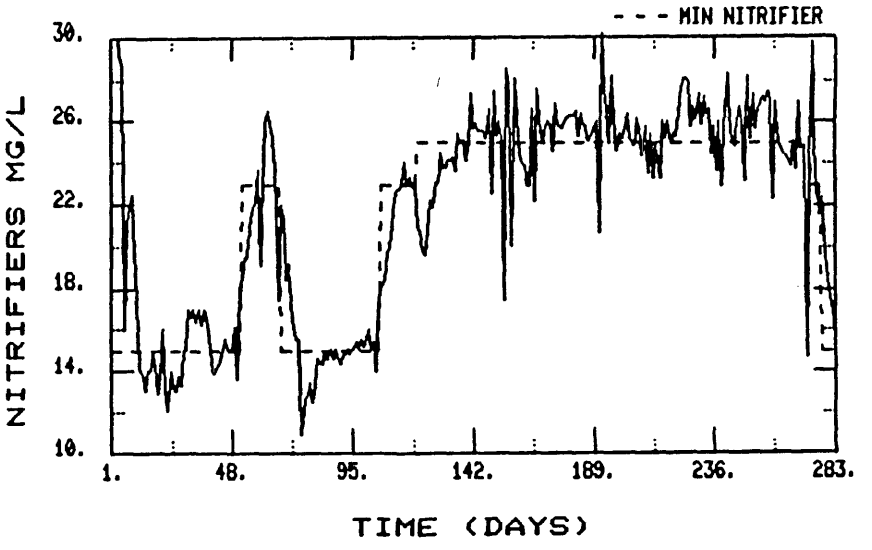


d. Surplus sludge flow

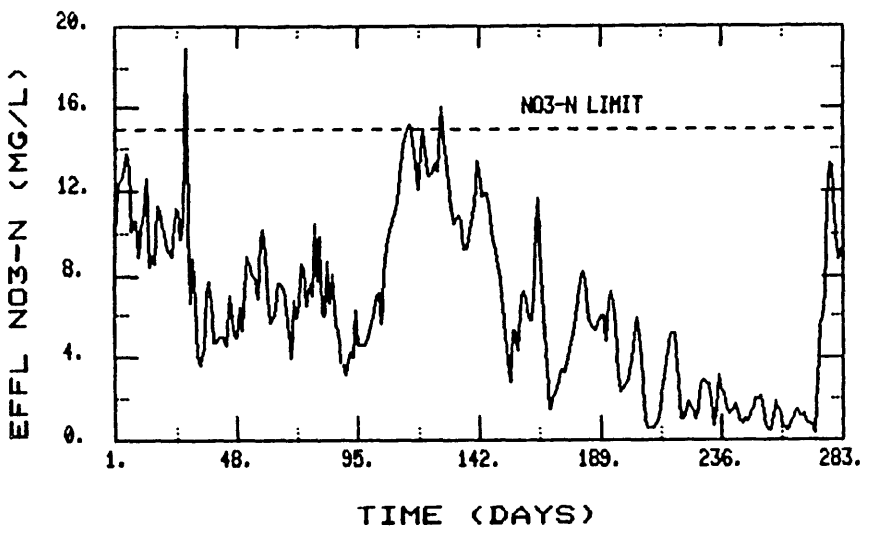
Fig. 5.36. Performance of controlled system under Policy 3



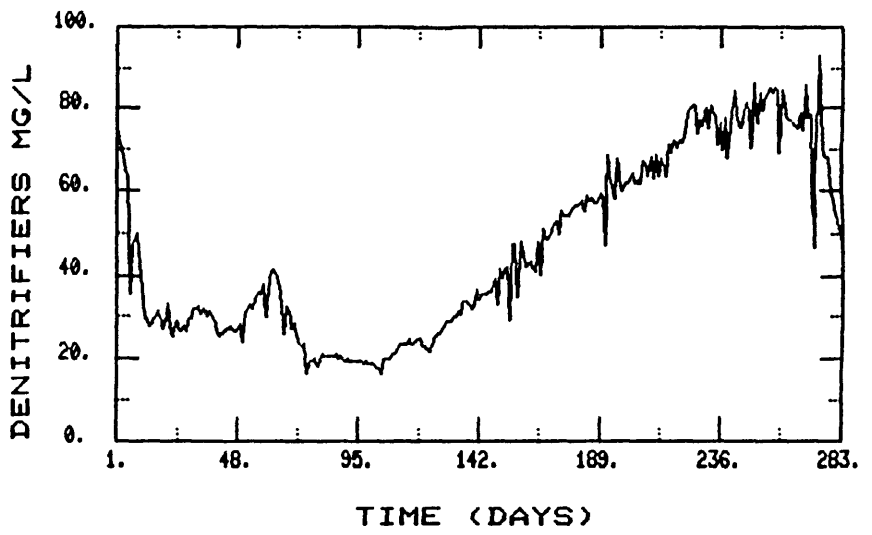
e. Effluent ammonia



f. Nitrifier concentration

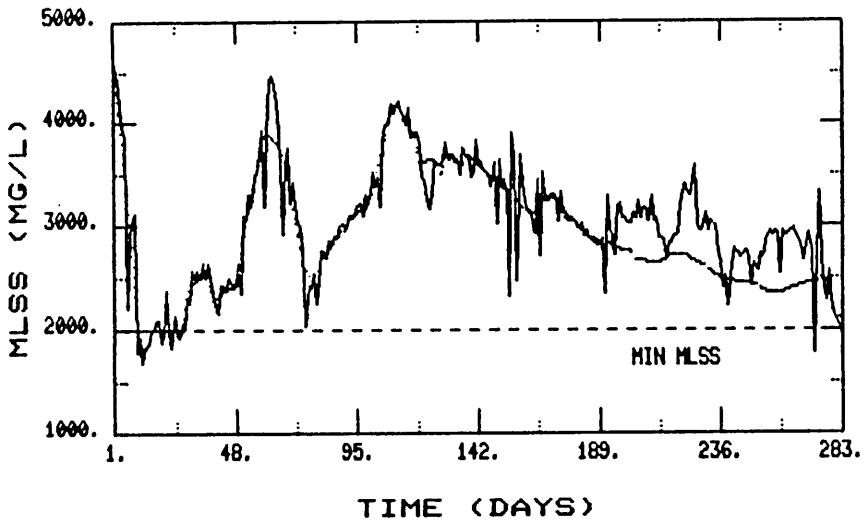


g. Effluent nitrate

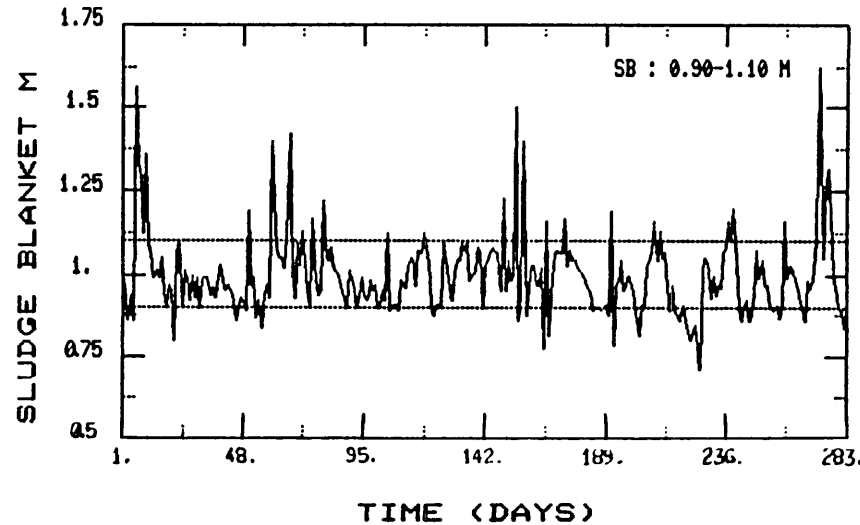


h. Denitrifier concentration

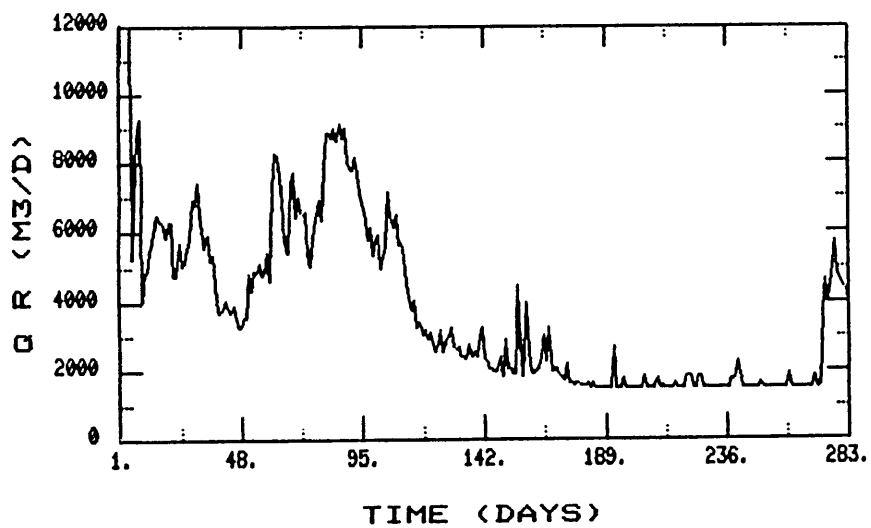
Fig. 5.36. Performance of controlled system under Policy 3



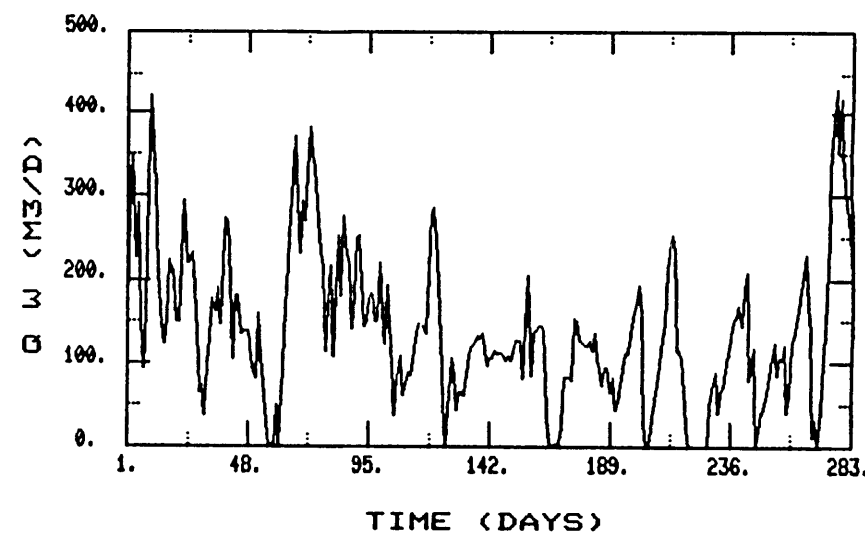
a. $MLSS$ concentration



b. Sludge blanket level

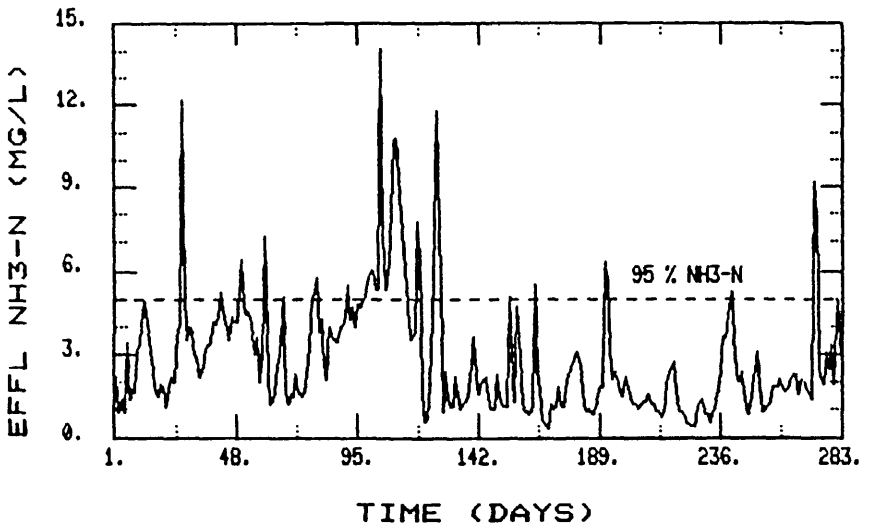


c. Recycle flow

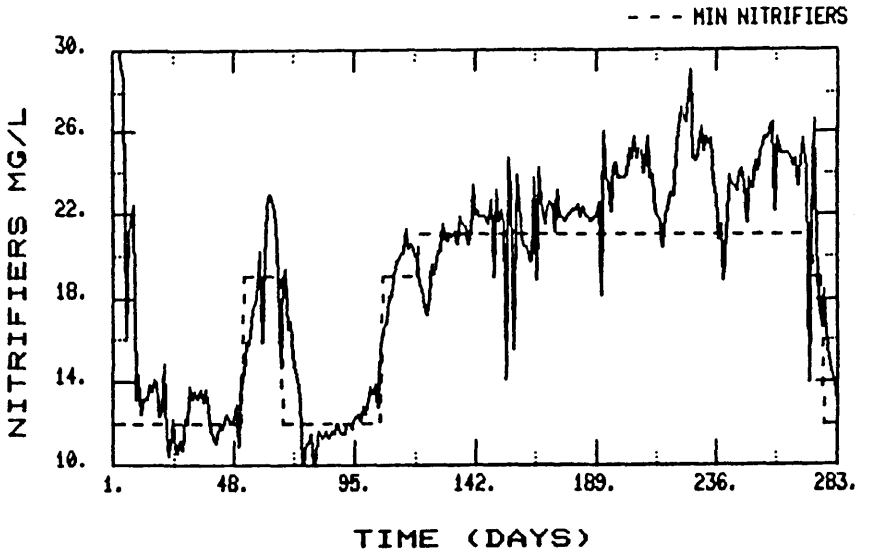


d. Surplus sludge flow

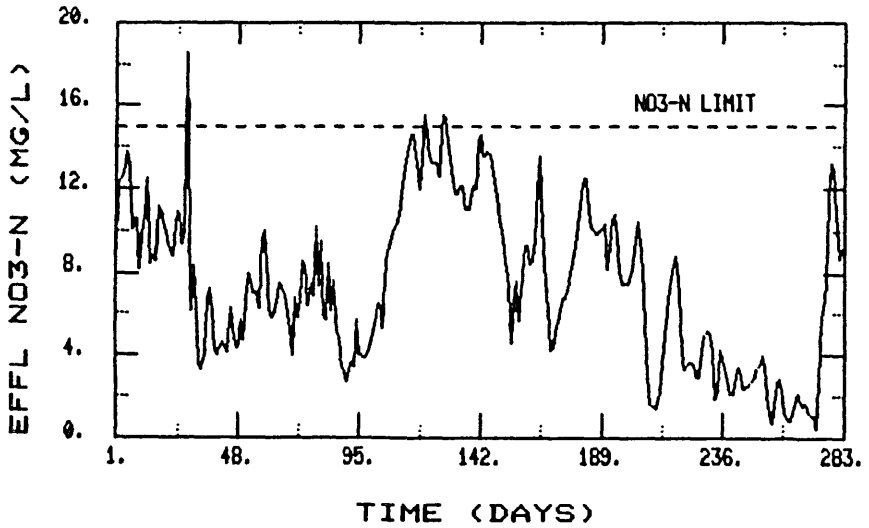
Fig. 5.37. Performance of controlled system under Policy 4



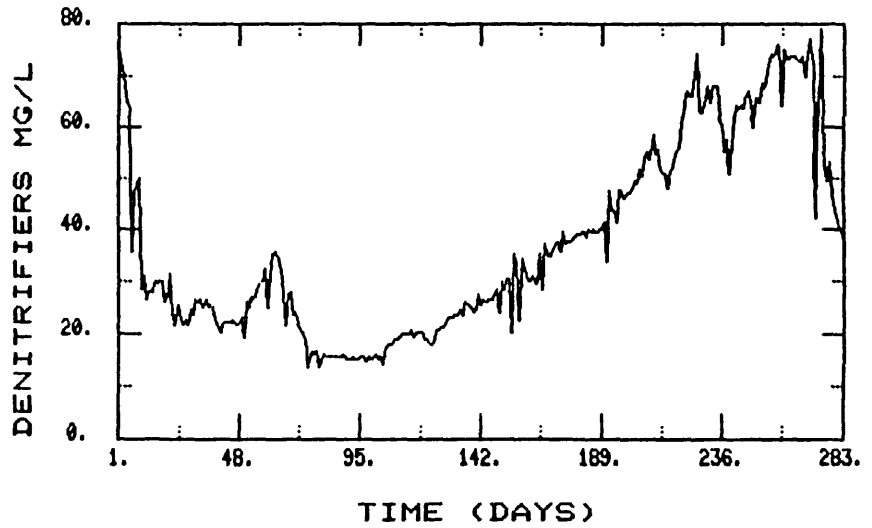
e. Effluent ammonia



f. Nitrifier concentration



g. Effluent nitrate



h. Denitrifier concentration

Fig. 5.37. Performance of controlled system under Policy 4

6 Conclusions

The study on the oxidation ditch process focused on three main areas, namely the development of process models, the real-time estimation of oxygen demand and finally the design and application of operational control. From these topics the following conclusions were drawn :

6.1 Process modelling

6.1.1 Final clarifier modelling

From the analysis of the thickening and clarification functions in the final tanks the following conclusions were reached :

- During periods when the final clarifiers were underloaded, the limiting flux theory was unable to predict the existence of a dilute sludge blanket in the tank.
- A simple dynamic model of the clarifiers based on a solids mass- balance, representing the tanks by a single CSTR was found to be adequate for simulating the underflow concentration. However for wider applicability of the model the constraints dictated by the solids flux theory need to be considered.
- Validation of the model with data from a different operating period produced a systematic deviation in the predictions. However, simulation under an assumed typical diurnal variation of the inputs was shown to improve substantially the ability of the model to predict the daily clarifier performance.
- The low and near constant effluent solids concentration throughout the study period prohibited the identification of a suitable model to describe the clarification function.

6.1.2 Oxidation ditch modelling

Modelling of the biochemical kinetics in the aeration tank showed that :

- For carbonaceous oxidation modelling the structuring of biomass into active, inactive and inert mass did not produce better results compared to a simpler model considering the aggregated kinetics of the total biomass.

- The nitrification and denitrification processes can be adequately modelled as single stage reactions. This simplification is justified in view of the sensitivity of these processes to changes in operating and environmental conditions.
- The dynamic behaviour of solids in the process units is mainly affected by the hydraulic flow rates through and within the plant, while the biochemical component has a modest effect in the short-term.

The main conclusions from process modelling were :

- The oxidation ditch model developed was based on generally accepted theory but found too complex for the complete estimation of the parameters included.
- The performance of the model was not always satisfactory. Among the possible causes were weaknesses in the model assumptions, the effect of unmodelled environmental factors upon the biochemical kinetics and the neglected influence of diurnal input variations.
- Adaptive estimation of the main parameters indicated that further improvements to the model structure were possible.
- Some limitations were experienced with the operational data, as a result of missing values, their noisy structure and lack of measurements regarding the diurnal input variations.
- Validation of the model with data from a different operating period was of limited success. However, the model was considered adequate for simulating the process behaviour given the simplifying assumptions made for its development and the effect of unmeasurable disturbances on the process.
- The model adequately explained the poor nitrification performance observed during part of the study period. This was attributed to the low nitrifier population in the reactor resulting from a combination of a high sludge wastage rate and a low recycle ratio.

6.2 Real-time OUR estimation

The oxygen utilization rate (OUR) was considered as a suitable process indicator for on-line monitoring with potential application for process control. By relating the OUR to the main process kinetics it was shown that the total oxygen demand in the oxidation ditch was dominated by the respiration of biomass due to the extensive oxidation of sludge. From the study and implementation of continuous OUR estimation in an activated sludge reactor it was found that :

- Real-time estimation of OUR is possible when the oxygenation coefficient K_{LA} is known as a function of the aeration system capacity (eg. air-flow rate or depth of immersion).
- Estimation of K_{LA} can be accomplished during deoxygenation- reoxygenation trials involving step changes of the aeration capacity to generate transients in the DO concentration of at least 2–3 mg/l. This procedure also requires simultaneous estimation of the OUR.
- The results from the simultaneous $K_{LA}-OUR$ estimation were affected by noise in the DO measurements, the mass-transport of oxygen in the reactor and the probable effects of DO changes upon the organism respiration. Independent (off-line) estimation of the OUR was shown to alleviate the above difficulties.
- Under a known K_{LA}, the OUR can be adequately estimated for most practical purposes from on-line DO measurements alone, employing a simple non-dynamic DO model, for which measurement noise and system disturbances have insignificant effect.

6.3 Operational control

The operational control of the oxidation ditch process was considered as a hierarchical two-level problem. From the study on the operational control problem and the design of a suitable control system the following conclusions were drawn :

- The most critical variables to process performance were the concentration of nitrifying and denitrifying organisms.
- The capacity of the aeration system and the thickening limitations of the clarifiers were important for preventing conditions of oxygen depletion and high effluent solids respectively.
- In general the running cost of the process, including energy and sludge disposal costs, can be reduced by operating at lower $MLSS$ concentrations.
- The operating $MLSS$ was identified as the key variable for process control, since it could satisfy the above operating conditions and, in addition, it is directly related to the running cost.
- Adaptive feedback control based on one-step-ahead predictions was necessary to account for the dynamic nature of the process under discrete control application.
- From simulation studies under different operating policies it was concluded that for a plant operating under highly variable input loads, effective control of

nitrification and/or denitrification can be achieved by maintaining an adequate nitrifier and/or denitrifier population in the reactor based on the long-term statistical behaviour of the inputs rather than on their daily variation.

- The exploitation of the DO distribution in the reactor which regulates the size of anoxic and aerobic zones was shown to offer potential for improving the simultaneous nitrification and denitrification performance.

Finally the application of operational control through process simulations, was shown to offer the following benefits related to the oxidation ditch operation :

- Improved process reliability, ie the effluent quality violates the desired conditions less frequently.
- Reductions in running cost which were realized by operating at a generally lower $MLSS$ concentration.
- Elimination of process failures associated with biomass washout, sludge blanket spillage and oxygen depletion.

REFERENCES

1. ABBERLEY, R.C., RATTRAY, G.B., DOUGAS, P.P., (1974).
'Air diffusion unit.'
J. Water Pollut. Control Fed. 46 No 5 pp 895-910.

2. ADAMS, C.E., ECKENFELDER, W.W., (1974).
'Process design techniques for industrial waste treatment.'
Enviro Press, Nashville, Tenessy.

3. AKAIKE, H., (1974).
'A new look at the statistical model identification.'
IEEE Trans. Autom. Control 19 pp 716-723.

4. ANDREWS, J.F., (1974).
'Dynamic models and control strategies for wastewater treatment processes.'
Water Res., 8 pp 261-289.

5. ANDREWS, J.F., STENSTROM, M.K., BURH, H.O., (1976).
'Control systems for the reduction of effluent variability from the activated sludge process.'
Prog. Water Technol., 8 No. 1 pp 41-68.

6. ANGELBECK, D.I., SHAH ALAM, A.B., (1975).
'Simulation of optimal control strategies in a dynamic continuous flow activated sludge system.'
Proc. 30th Ind. Waste Conf., Purdue Univ., pp 159-170.

7. BAHRE, G., (1987).
'Computer aided control of nitrogen removal in small activated sludge wastewater treatment plants.'
Water Sci. Technol. 19 No. 3/4, pp 657-667.

8. BAUMAN, R.E., (1975).
'Process design manual for nitrogen control.'
U.S. E.P.A.

9. BECK, M.B., (1979).
'System identification,estimation and forecasting of water quality Part 1: Theory.'
Working paper WP-79-31. International institute for applied systems analysis, Laxenburg, Austria.

10. BECK, M.B., (1980).
'Model structure identification from experimental data.'
Intern. Inst. for Applied Systems Analysis, RR-80-4, Laxenburg, Austria.

11. BECK, M.B., (1981).
'Operational estimation and prediction of nitrification dynamics in the activated sludge process.'
Water Res. 15 pp 1313-1330.

12. BECK, M.B., (1983a).
'A procedure for modelling.'
'In Mathematical Modelling of Water Quality: Streams, Lakes and Reservoirs'.
Ed. G.T. Orlob, John Wiley & Sons, Chichester,pp 11-41.

13. BECK, M.B., (1983b).
'Sensitivity analysis, calibration and validation.'
In 'Mathematical Modelling of Water Quality: Streams, Lakes and Reservoirs'.
Ed. G.T. Orlob, John Wiley & Sons, Chichester,pp 425-467.

14. BENEFIELD, L.D., RANDALL, C.W., KING, P.H., (1975).
'Process control by oxygen uptake and solids analysis.'
J. Water Pollut. Control Fed., 47 No. 10 pp 2498-2503.

15. BERTHOUEX, P.M., HUNTER, W.G., PALLESEN, L., (1978).
'Dynamic behaviour of an activated sludge plant.'
Water Res. 12 pp 957-972.

16. BISOGNI, J.J., LAWRENCE, A.W., (1971).
'Relationships between biological solids retention time and settling characteristics of activated sludge.'
Water Res. 5 pp 753

17. BLACKWELL, L.G., (1971).
'A theoretical and experimental evaluation of the transient response of the activated sludge process.'
PhD thesis, Clemson Univ., Clemson, S.C.

18. BONNICK, A.S., SIDWICK, J.M., (1981).
'Instrumentation,control and automation - The choices.'
Water Sci. Technol. 13 No 8 pp 35-40.

19. BOON, A.G. (1978).
'Oxygen transfer in the activated sludge process.'
In 'New processes of waste-water treatment and recovery', (ed.) Mattock G. SCI and Ellis Horwood, pp 17-33.

20. BOON, A.G., (1983).
'Aeration methods.'
In 'Oxidation ditches in wastewater treatment', Pitman, London, pp 173- 187

21. BOX, G.E.P., & JENKINS, G.M., (1970).
'Time-series Analysis, Forecasting and Control.'
Holden-Day, San Francisco CA.

22. BOYLE, W.C., BERTHOUEX, P.M., ROONEY, T.C., (1974).
'Pitfalls in parameter estimation for oxygen transfer data.'
J. Envir. Eng. Div. ASCE, Vol. 100, pp 391-408.

23. BRETT, R.W.J., KERMODE, R.I., BURRUS B.G., (1973).
'Feed-forward control of an activated sludge process.'
Water Res., 7 pp 525-535.

24. BRUNE, D., (1985).
'Optimal control of the complete-mix activated sludge process.'
Environ. Technol. Letters 6 pp 467-476.

25. BRYANT, J.O., WILCOX, L.C., (1972).
'Real-time simulation of the conventional activated sludge process.'
Proc. on the Joint Automatic Control Conf. of the American Automatic Control Counsil.

26. BUSBY, J.B., ANDREWS, J.F., (1975).
'Dynamic modelling and control strategies for the activated sludge process.'
J. Water Pollut. Control Fed., 47 No. 5 pp 1055-1080.

27. CARMICHAEL, W.F., JOHNSTONE, D.W.M., (1982).
'Initial operating experiences at Cirencester carrousel plant.'
Water Pollut. Control 81 No. 5 pp 573

28. CHAPMAN, D.T., (1983).
'The influence of process variables on secondary clarification.'
J. Water Pollut. Control Fed., 55 No. 12 pp 1425-1434.

29. CHAPMAN, D.T., (1985).
'Final settler performance during transient loading.'
J. Water Pollut. Control Fed. 57 pp 227-234.

30. CHEN, C.Y., ROTH, J.A., ECKENFELDER, W.W., (1980).
'Response of dissolved oxygen to changes in influent organic loading to activated sludge systems.'
Water Res., 14 pp 1449-1457.

31. CHERUY, A., PANZARELLA, L., DENAT, J.P., (1982).
'Multimodel simulation and adaptive stochastic control of an activated sludge process.'
Proc. of 1st IFAC workshop on 'Modelling and Control of Biotechnical Processes', Helsinki, Finland, August 17-19, 1982 pp 127-133.

32. CHRISTENSEN, M.H., HARREMOES, P., (1977).
'Biological denitrification of sewage: a literature review.'
Prog. Water Technol. 8 No 4/5, pp 509-555.

33. CHRISTOULAS, D.G., TEBBUTT, T.H.Y., (1976).
'Mathematical model of a completely mix activated sludge plant.'
Water Res., 10 pp 797-804.

34. CHRISTOULAS, D.G., TEBBUTT, T.H.Y., (1982).
'A simple model of the complete-mix activated sludge process.'
Environ. Technol. Letters 3 pp 89-96.

35. CLIFFT, R.C., ANDREWS, J.F., (1981a).
'Predicting the dynamics of oxygen utilization in the activated sludge process.'
J. Water Pollut. Control Fed., 53 No. 7 pp 1219-1232.

36. COOK, S.C., MARSILI-LIBELLI, S., (1981).
'Estimation and control problems in activated sludge processes.'
Water Sci. Technol., 13 pp 737-742.

37. COOK, S.C., (1983).
'Systems identification and control of wastewater treatment processes in river basin management.'
Ph.D. Thesis, Imperial College, University of London, June 1983 London.

38. COOK, S.C., JOWITT, P.W., (1984a).
'Estimation in non-linear continuous/discrete water quality systems.'

Proceedings of an international workshop at the institute of hydrology, Wallingford, July 1984 Report No 88

39. COOK, S.C., (1984b).
'Nitrification dynamics in the oxidation ditch wastewater treatment process.'
Water Sci. Technol. 16 No 5-7, pp 595-611.

40. COOK, S.C., (1984c).
SERC Interim report IR 2.7.84, Imperial College

41. CURDS, C.R., (1971).
'Computer simulations of microbial dynamics in the activated sludge process.'
Water Res., 5 pp 1049-1066.

42. CURDS, C.R., (1973).
'A theoretical study of factors influencing the microbial population dynamics of the activated sludge process.'
Water Res. 7 pp 1269-1284.

43. DAIGGER, G.T., GRADY, C.P.L., (1982).
'The dynamics of microbial growth on soluble substrates, a unifying theory.'
Water Res., 16 pp 365-382.

44. DAVIS, J.J., KERMODE, R.I., BRETT, R.W., (1973).
'Generic feed forward control of activated sludge.'
J. Environ. Eng. Div. ASCE, 99 No. EE3, pp 301-313.

45. DEBELAC, K.A., SIMS, C.A., (1981).
'Stochastic modelling of an industrial activated sludge process.'
Water Res. 15 pp 1173-1183.

46. DICK, R.I., (1970).
'Role of activated sludge final settling tanks.'
J. Sanit. Eng. Div. ASCE, 96 SA 2 pp 423-436.

47. DICK, R.I., EWING, B.B., (1967).
'Evaluation of activated sludge thickening theories.'
J. Environ. Eng. Div. ASCE, 93 No 4 pp 9-29.

48. DICK, R.I., YOUNG, K.W., (1972).
'Analysis of thickening performance of final settling tanks.'

Proc. 27th Ind. Waste Conf., Purdue Univ. pp 33-54.

49. DICK, R.I., JAVAHERI, A.R., (1972).
'WRC Research Report No 45 University of Illinois, Urbana, USA.

50. DoE, NWC (1981).
'Final Report of the Working Party on Control Systems for the Water Industry, Standing Technical Committee Report no. 27 National Water Counsil, London.

51. DOLD, P.L., EKAMA, G.A., MARAIS,G.vR., (1980).
'A general model for the activated sludge process.'
Prog. Water Technol. 12 pp 47-77.

52. DOLD, P.L., EKAMA, G.A., MARAIS, G.vR., (1985).
'pH control and cost savings in aerobic digestion.'
In 'Instrumentation and Control of Water and Wastewater Treatment and Transport Systems', Proc. 4th IAWPRC Workshop, Houston & Denver, pp 375-381.

53. DOLD, P.L., MARAIS, G.vR., (1986).
'Evaluation of the general activated sludge model proposed by the IAWPRC task group.'
Water Sci. Technol. 18 No 6 pp 63-89.

54. DOWNING, A.L., PAINTER, H.A., KNOWLES, G., (1964).
'Nitrification in the activated sludge process.'
J. Proc. Inst. Sew. Purif. 64 No 2 pp 130

55. ECKENFELDER, W.W., (1966).
'Industrial Water Pollution Control.'
McGraw-Hill, New York.

56. EDWARDS, G.L., SHERRARD, J.H., (1982).
'Measurement and validity of oxygen uptake as an activated sludge process control parameter.'
J. Water Pollut. Control Fed., 54 No. 12 pp 1546-1552.

57. EKAMA, G.A., MARAIS, G.vR., (1977).
'The activated sludge process. Part II.-Dynamic behaviour.'
Water S.A., 3 No.1, pp 18-50.

58. EKAMA, G.A., MARAIS, G.vR., (1979).
'Dynamic behaviour of the activated sludge process.'
J. Water Pollut. Control Fed., 51 No. 3 pp 534-556.

59. EVES, E.G., (1981).
'Hogsmill valley works: Twenty years on.'
Water Pollut. Control, 80 pp 452-462.

60. EYKHOFF, P., (1974).
'Systems Identification,Parameter and State Estimation.'
A Wiley-Interscience Publication, London.

61. FAIR, G.M., GEYER, J.C., OKUN, D.A., (1968).
'Water purification and wastewater treatment and disposal.'
Wiley & Sons, New York.

62. FORSTER, C.F., (1983).
'Continuously operated ditches.'
In 'Oxidation Ditches in Wastewater Treatment', Pitman, London, pp 75- 131.

63. FOSTER, D.M., (1985).
'The dynamic modelling of the secondary settlement of activated sludge.'
MSc. Report, Imperial College, Univ. of London.

64. FUJIMOTO, E., SEKINE, T., (1981).
'Study on necessary factors for adaptive control of activated sludge system.'
Water Sci. Technol., 13 pp 445-449.

65. FUJIMOTO, E., IWAHORI, K., SATO, N., (1981).
'Automatic measurement device of the respiration rate and experimental investigation on the constant DO control by using the device for the activated sludge process.'
Water Sci. Technol., 13 pp 193-198.

66. GAUDY A.F., RAMANATHAN, M., YANG, P.Y., & DeGEARE T.V., (1970).
'Studies on the operational stability of the extended aeration process.'
J. Water Pollut. Control Fed., 42 pp 165-179.

67. GAUDY, A.F., OBAYASHI, O., GAUDY, E.T., (1971).
'Control of growth rate by initial substrate concentration at values below maximum rate.'

Appl. Microbiol. 22, pp 1041-1047.

68. GAUDY, A.F., YANG, P.Y., OBAYASHI, A.W., (1971).
'Studies on the total oxidation of activated sludge with and without hydrolytic pre-treatment.'
J. Water Pollut. Control Fed., 43 pp 312-332.

69. GAUDY, A.F., SRINIVASARAGHAVAN,R., SALEH, M., (1977).
'Conceptual model for activated sludge process.'
J. Environ. Eng. Div. ASCE, 103 No. EE1, pp 71-85.

70. GEORGE, D.B., KEINATH, T.M., (1978).
'Dynamics of continuous thickening.'
J. Water Pollut. Control Fed. 50 pp 2560-2572.

71. GHOBRIAL, F.H., (1978).
'Importance of the clarification phase in biological process control.'
Water Res., 12 pp 1009-1016.

72. GOODMAN, B.L., ENGLANDE, A.J., (1974).
'A unified model of the activated sludge process.'
J. Water Pollut. Control Fed., 46 No. 2 pp 312-332.

73. GOTO, M., ANDREWS, J.F., (1985).
'On-line estimation of oxygen uptake rate in the activated sludge process.'
In "Instrumentation and control of water and wastewater treatment and transport systems", Proc. 4th IAWPRC Workshop, Houston & Denver, pp 465-472.

74. GRADY, C.P.L., ROPER, R.E., (1974).
'A model for the bio-oxidation process which incorporates the viability concept.'
Water Res. 8 pp 471-83.

75. GRADY, C.P., WILLIAMS, D.R., (1975).
'Effects of influent substrate concentration on the kinetics of natural microbial populations.'
Water Res. 9 No 2 pp 171-180.

76. GRAU, P., DOHANYOS, M., CHUDOBA, J., (1975).
'Kinetics of multi-component substrate removal by activated sludge.'
Water Res. 9 No 7 pp 637-642.

77. GUJER, W., JENKINS, D., (1975).
'The contact stabilization activated sludge process-oxygen utilization, sludge production and efficiency.'
Water Res., 9 pp 533-560.

78. GUJER (1977).
'Design of nitrifying activated sludge process with the aid of dynamic simulation.'
Prog. Water Technol. 9 pp 323-336

79. GUSTAVSSON, I. (1975).
'Survey of applications of identification in chemical and physical processes.'
Automatica 11, pp 3-24.

80. HAAS, C.N, (1979).
'Oxygen uptake rate as an activated sludge control parameter.'
J. Water Pollut. Control Fed., 51 No. 5 pp 938-943.

81. HALL, E.R., MURPHY, K.L., (1980).
'Estimation of nitrifying biomass and kinetics in wastewater.'
Water Res. 14 pp 297-304.

82. HANDLEY, J., (1974).
'Sedimentation: An introduction to solids flux theory.'
Water Pollut. Control 73 pp 230-240.

83. HIBBERT, R.L., JONES, W.F., (1974).
'The design and operation of activated sludge final settling tanks.'
Water Pollut. Control 73 pp 14-29.

84. HIGBIE, R., (1935).
'The rate of absorption of pure gas into a still liquid during short periods of exposure.'
Trans. Am. Inst. Chem. Eng. 31 pp 365.

85. HIRAOKA, M., TSUMURA, K., TERAO, Y., OTA, M., (1985).
'Systematic approach to the control of an activated sludge wastewater treatment plant.'
In 'Instrumentation and Control of Water and Wastewater Treatment and Transport Systems', Proc. 4th IAWPRC Workshop, Houston & Denver, pp 661-664.

86. HOLMBERG, A., (1981).
'Microprocessor-based estimation of oxygen utilization in the activated sludge wastewater treatment process.'
Int. J. Systems Sci., 12 No. 6 pp 703-718.

87. HOLMBERG, A., (1982).
'Modelling of the activated sludge process for microprocessor-based state estimation and control.'
Water Res., 16 pp 1233-1246.

88. HOLMBERG, A., RANTA, J., (1982).
'Procedures for parameter and state estimation of microbial growth process models.'
Automatica, 18 No. 2 pp 181-193.

89. HOWELL, J.A., YUST, L.J., REILLY, P., (1984).
'On-line measurement of respiration and mass transfer rates in the activated sludge aeration tank.'
J. Water Pollut. Control Fed., 56 No. 4 pp 319-324.

90. HOYLAND, G., (1979).
'Mass-transfer model for aeration. Prog. Water Technol. 11 No. 3 pp 237-246.

91. HUANG, J.Y.C., SHEIKHOLESLAMI, B., (1982).
'Metal inhibition of nitrification.'
Proc. 37th Ind. Waste Conf., Purdue Univ., pp 85.

92. HUANG, J.Y.C., DREW, D.M., (1985).
'Investigation of the removal of organics and nitrogen in an oxidation ditch.'
J. Water Pollut. Control Fed. 57 No.2, pp 151-156.

93. JACOBS, O.L.R., (1974).
'Introduction to Control Theory'.
Clarendon Press, Oxford

94. JACQUART, J.C., LEFORT, D., ROVEL, J.M., (1973).
'An attempt to take account of biological storage in the mathematical analysis of activated sludge behaviour.'
Proc. Int. Conf. Water Pollut. Res., New York, pp 367-375.

95. JAZWINSKI, A.H., (1970).
'Stochastic Processes and Filtering theory.'

Academic Press, New York.

96. JOHNSTONE, D.W.M., (1979).
'Settlement characteristics and settlement-tank performance in the Carrousel activated sludge system.'
Water Pollut. Control, 78 pp 337-353.

97. JOHNSTONE, D.W.M., CARMICHAEL, W.F., (1982).
'Cirencester Carrousel plant : some process considerations.'
Water Pollut. Control, 81 No. 5 pp 587.

98. JOHNSTONE, D.W.M., (1984).
'Oxygen requirements, energy consumption and sludge production in extended-aeration plants.'
Water Pollut. Control 83 pp 100-115.

99. JONES, G.L., (1978).
'A mathematical model for bacterial growth and substrate utilization in the activated sludge process.'
Mathematical models in water pollution control, ed. A. James, a Wiley- Interscience publication.

100. JONES, G.L., PASKINS, A.R., (1980).
'Mathematical model of activated sludge-a comparison of predictions and experimental results.'
Water Research Centre, TR 134.

101. JORGENSEN, S.E., (1983).
'Modelling the ecological processes.'
In 'Mathematical Modelling of Water Quality: Streams, Lakes and Reservoirs', Ed. G.T. Orlob, John Willey & Sons, Chichester.

102. KAYSER, R., ERMEL, G., (1984).
'Control of simultaneous denitrification by a nitrate controller.'
Water Sci. Technol. 16 No 10/11, pp 143-150.

103. KORDES, B., (1985).
'Modelling the energy balance of wastewater treatment plants.'
Environ. Technol. Letters 6 pp 566-575.

104. KO, K.Y.J., McINNIS, B.C., GOODWIN, G.C., (1982).
'Adaptive control and identification of the dissolved oxygen process.'

Automatica, 18 No. 6 pp 727-730.

105. KYNCH, G.J., (1952).
'A theory of sedimentation.'
Trans. Faraday Society 48 pp 166-176.

106. LAWRENCE, A.W., McCARTY, P.L., (1970).
'Unified basic for biological treatment design and operation.'
J. San. Eng. Div. ASCE, 96 SA3, pp 757-778.

107. LECH, R.F., LIM, H.C., GRADY, C.P.L, KOPPEL, L.B., (1978a).
'Automatic control of the activated sludge process- I. Development of a simplified dynamic model.'
Water Res., 12 pp 81-90.

108. LECH, R.F., GRADY, C.P.L., LIM, H.C., KOPPEL, L.B., (1978b).
'Automatic control of the activated sludge process - II. Efficacy of control strategies.'
Water Res., 12 pp 91-99.

109. LEWIS, W.K., WHITMAN, W.C., (1924).
'Principles of gas adsorption.'
Ind. Eng. Chem. 16 pp 1215.

110. LOHMANN, J., SCHLEGEL, S., (1981).
'Measurement and control of the MLSS concentration in activated sludge plants.'

Water Sci. Technol., 13 pp 217-224.

111. LUMBERS, J.P., (1982).
'Future research and objectives for control in the water industry. Water and waste research.'
The way ahead. Science and Engineering research council, Environment committee. Imperial College 17-18 June 1982

112. MARAIS, G.v.R, (1975).
'Aeration devices: basic theory.'
Water Pollut. Control 74 pp 172-173.

113. MARAIS, G.vR., EKAMA, G.A., (1976).
'The activated sludge process. Part I.-Steady state behaviour.'

Water S.A., 2 No.4, pp 164-200.

114. MARRIOT, M.J., (1981).
'Dynamic modelling of the performance of a secondary sedimentation tank.'
MSc. Report, Imperial College, University of London.

115. MARSILI-LIBELLI, S., (1980).
'Reduced-order modelling of the activated sludge process.'
Ecological Modelling 9 pp 15-32.

116. MARSILI-LIBELLI, S., (1982).
'On-line estimation of bioactivities in activated sludge processes.'
Proc. of 1st IFAC workshop on 'Modelling and control of biotechnical processes', Helsinki, August 17-19, 1982 pp 121-126.

117. MARSILI-LIBELLI, S., (1984).
'Activated sludge process control using dissolved oxygen measurements.'
Wat. Sci. Techn. 16, No 5-7, pp 595-611.

118. MASUI, S., SHIOYA, M., OHTO, T., NOGITA, S., (1981).
'Organic load control of the activated sludge process based on predicted daily variation of influent load.'
Water Sci. Technol., 13 pp 387-392.

119. McCARTY, P.L., BECK, L., St AMANT P., (1969).
'Biological denitrification of wastewaters by addition of organic material.'
24th Ind. Waste Conf., Purdue Univ., pp 1271-85.

120. McCARTY, P.L., (1973).
'Nitrification-denitrification by biological treatment.'
Correspondence Conference on Denitrification of Municipal Wastes, Univ. of Massachusetts.

121. McKINNEY, R.E., (1962).
'Mathematics of complete mixing activated sludge.'
J. San. Eng. Div. ASCE 88 SA3, pp 87-113.

122. MEHRA, R.K., (1970).
'On the identification of variances and adaptive Kalman filtering.'
IEEE trans. on Autom. Control, 15 No. 2 pp 175-184.

123. MEISSINGER, H.F., (1960).
'The use of parameter influence coefficients in computer analysis of dynamic systems.'
Proceed. of Western Joint Computer Conf., San Francisco, pp 181-192.

124. METCALF & EDDY INC., (1979).
'Waste Water Engineering: treatment, disposal reuse.'
McGraw-Hill Inc., N. York.

125. MIURA, R., (1981).
'An approach to full-automatic control of activated sludge process.'
Water Sci. Technol., 13 pp 451-457.

126. MONOD, J. (1949).
'The growth of bacterial cultures.'
Ann. Rev. Microbiol. 3 pp 371-94.

127. MONTGOMERY, H.A.C., THOMAS, N.S., COCKBURN, A., (1964).
'J. Applied Chemistry 14 pp 280.

128. MORRIS, J.C., STUMM, W., (1960).
'Colloidal aspects of waste treatment.'
Proc. Rudolphs Res. Conf., Rutgers Univ., New Brunswick, N.J.

129. MUCK, R.E., GRADY, C.P.L., (1974).
'Temperature effects on microbial growth in CSTR's.'
J. Environ. Eng. Div. ASCE, 100 No. EE5, pp 1147-1163.

130. NATIONAL WATER COUNSIL, (1978).
'River water quality. The next stage: review of discharge consent conditions.'
National Water Counsil, London.

131. NOGITA, S., WATANABE, S., MORI, S., (1981).
'Experience of MLSS control of the activated sludge process.'
Water Sci. Technol., 13 pp 421-426.

132. NOGITA, S., HIRAOKA, M., (1981).
'Calculation of sludge reservoir volume for MLSS control.'
Water Sci. Technol., 13 pp 433-438.

133. NOVAK, J.T., EICHELBERGER, M.P., BANERJI, S.K., YAUN, J., (1984).
'Stabilization of sludge from an oxidation ditch.'

J. Wat. Poll. Control Fed., 56, No. 8, pp 950-954.

134. OLSSON G., ANDREWS, J.F., (1978).
'The dissolved oxygen profile-A valuable tool for control of the activated sludge process.'
Water Res. 12 pp 985-1004.

135. OLSSON, G., RUNDQWIST, L., ERIKSSON, L., HALL, L., (1985).
'Self tuning control of the dissolved oxygen concentration in activated sludge systems.'
In 'Instrumentation and Control of Water and Wastewater Treatment and Transport Systems', Proc. 4th IAWPRC Workshop, Houston & Denver, pp 473-480.

136. PAINTER, H.A., (1970).
'A review of literature on inorganic nitrogen metabolism in microorganisms.'
Water Res., 4 pp 393-450.

137. PAINTER, H.A., (1977).
'Microbial transformations of inorganic nitrogen.'
Prog. Water Technol. 8 No. 4/5, pp 3-29.

138. PETTY, C.A., (1975).
'Continuous sedimentation of a suspension with a non-convex flux law.'
Chem. Eng. Sci., 30 pp 1451-1458.

139. PFLANZ, P., (1969).
'Performance of (activated sludge) secondary sedimentation basins.'
Proc. 4th Int. Conf. Water Pollut. Res., pp 569-593.

140. PODUSKA, R.A., ANDREWS, J.F., (1975).
'Dynamics of nitrification in the activated sludge process.'
J. Water Pollut. Control Fed. 47 pp 2599-2619.

141. RACHWAL, A.J., JOHNSTONE, D.W.M., HANBURY, M.J., CARMICHAEL, W.F., (1983).
'An intensive evaluation of the Carrousel system.'
In 'Oxidation Ditches in Wastewater Treatment', Pitman, London, pp 132- 172.

142. RINALDI, S., SONCINI-SESSA, R., STEHFEST, H., TAMURA, H., (1979).
'Modelling and Control of River Quality.'

McGraw-Hill Inc., N. York.

143. ROSENBROCK, H.H., (1960).
'An automatic method for finding the greatest or least value of a function.'
The Computer Journal 3 pp 175-184.

144. SCHROEDER, E.D., IRVINE, R.L., (1979).
'Parameter choice for process control.'
J. Environ. Eng. Div. ASCE, 105 No. EE2, pp 217-229.

145. SEKINE, T., IWAHORI, K., FUJIMOTO, E., INAMORI, Y., (1985).
'Advanced control strategies for the activated sludge process.'
In 'Instrumentation and Control of Water and Wastewater Treatment and Transport Systems', Proc. 4th IAWPRC Workshop, Houston & Denver, pp 269-276.

146. SHAH ALAM, A.B., ANGELBECK, D.I., (1976).
'Optimal control of activated sludge system: Laboratory model study.'
Proc. 31st Ind. Waste Conf., Purdue Un., pp 713-732.

147. SHANNON, P.T., TORY, E.M., (1965).
'Settling of slurries.'
Ind. & Eng. Chemistry 57 No 2 pp 18-25.

148. SHARMA, B., AHLERT, R.C., (1977).
'Nitrification and nitrogen removal.'
Water Res., 11 pp 897-925.

149. SHEFFER, S.M., TSUMURA, K., HIRAOKA, M., (1981).
'A new computerised control system for the activated sludge process in transient states.'
Water Sci. Technol., 13 pp 381-386.

150. SHEFFER, M.S., HIRAOKA, M., TSUMURA, K., (1984).
'Flexible modelling of the activated sludge system - theoretical and practical aspects.'
Water Sci. Technol., 17 pp 247-258.

151. SIDWICK, J.M., BONNICK, A.S., (1981).
'Instrumentation, control and automation equipment systems.'
Wat. Sci. Tech. 13, No 8, pp 49-54.

152. SINCIC, D., BAILEY, J.E., (1978).
'Optimal periodic control of activated sludge processes- I. Results for the base case with Monod/decay kinetics.'
Water Res., 12 pp 47-53.

153. STEHFEST, H., (1984).
'An operational dynamic model of the final clarifier.'
Trans. Inst. Measurement and Control 6 No 3 pp 160-164.

154. STEHFEST, H., (1985).
'Optimal periodic control of the steep-feed activated sludge plant.'
Environ. Technol. Letters 6 pp 556-565.

155. STENSTROM, M.K., ANDREWS, J.F., (1979).
'Real time control of activated sludge process.'
J. Environ. Eng. Div. ASCE 105 No. EE2, pp 245-260.

156. STENSTROM, M.K., PODUSKA, R.A., (1980).
'The effect of dissolved oxygen concentration on nitrification.'
Water Res. 14 pp 643-649.

157. STENSTROM, M.K., ANDREWS, J.F., (1980).
'Cost interactions in activated sludge systems.'
J. Environ. Eng. Div. ASCE, 106 No. EE4, pp 787-795.

158. STENSTROM, M.K., BROWN, L.C., HWANG, H.J., (1981).
'Oxygen transfer parameter estimation.'
J. Environ. Eng. Div. ASCE, 107 No. EE2, pp 379-397.

159. SUIDAN, M.T., SAUNDERS, F.M., GODFREY, C.S., STEWART, H.T., (1983).
'Wastewater treatment: sensitivity analysis.'
J. Environ. Eng. Div. ASCE, 109 No. 1 pp 120-138.

160. SYKES, R.B., (1981).
'Limiting nutrient concept in activated sludge models.'
J. Water Pollut. Control Fed., 53 No. 7 pp 1213-1218.

161. SYKES, R.M., (1982).
'Hydraulic regime and activated sludge performance.'
J. Environ. Eng. Div. ASCE, 108 No EE2, pp 286-296.

162. TAKASE, I., MIURA, R., (1985).
'Sludge flow control for activated sludge processes.'
In 'Instrumentation and Control of Water and Wastewater Treatment and Transport Systems', Proc. 4th IAWPRC Workshop, Houston & Denver, pp 675-678.

163. TANTHAPANICHAKOON,W., HIMMELBLAU, D.M., (1981).
'Simulation of a time dependent activated sludge wastewater treatment plant.'
Water Res. 15 pp 1185-1195.

164. TANUMA, M., KASHIWAGI, M., TUCHIYA, N., KASAI, T., (1981).
'Total sludge quantity control for activated sludge process.'
Water Sci. Technol., 13 pp 427-432.

165. TERASHIMA, Y., ISHIKAWA, M., (1985).
'The kinetic analysis of BOD and nitrogen removal in an oxidation ditch.'
Water Sci. Technol. 17 No 2/3, pp 291-302.

166. THAMES WATER, (1979).
'River water quality - The next stage: review of discharge consent conditions.'
Report, Feb. 1979.

167. TOMLINSON, E.J., CHAMBERS, B., (1979).
'The effect of longitudinal mixing on the settleability of activated sludge.'
Tech. Rep. Water Res. Centre, 122 Stevenage laboratory.

168. TRACY, K.D., KEINATH, R.M., (1973).
'Dynamic model for thickening of activated sludge.'
Am. Inst. Chem. Eng., Symposium series: Water, pp 291-309.

169. TRUESDALE, G.A., DOWNING, A.L., LOWDEN, G.F., (1955).
J. Applied Chemistry 5 pp 53.

170. TSUNO, H., GODA, T., (1978).
'Kinetic model of activated sludge metabolism and its application to the response of qualitative shock load.'
Water Res., 12 pp 513-522.

171. TUNTOOLAVEST, M., GRADY, C.P., (1982).
'Effect of activated sludge operational conditions on sludge thickening characteristics.'

J. Water Pollut. Control Fed. 54 No 7 pp 1112-1117.

172. VANDEVENNE, L., ECKENFELDER, W.W., (1980).
'A comparison of models for completely mixed activated sludge treatment design and operation.'
Water Res., 14 pp 561-566.

173. VESILIND, P.A., (1968).
'Theoretical considerations:Design of prototype thickeners from batch settling tests.'
Water & Sew. Works 115 p 302.

174. von JESZENSZKY,T., DUNN, I.J., (1976).
'Dynamic modelling and control simulation of a biological wastewater process.'
Water Res., 10 pp 461-467.

175. VOSLOO, P.B.B., (1973).
'Oxygen requirements the activated-sludge process.'
Water Pollut. Control, 72 pp 209-212.

176. WALKER, L.F., (1971).
'Hydraulically controlling solids retention time in the activated sludge process.'
J. Water Pollut. Control Fed. 43 pp 30-39.

177. WANG, L.K., POON, C.P.C., WANG, M.H., (1976).
'Control tests and kinetics of activated sludge process.'
Proc. 31st Ind. Waste Conf., Purdue Un., pp 501-524.

178. WESTBERG, N., (1969).
'An introductory study of regulation in the activated sludge process.'
Water Res. 3 pp 613-621.

179. WHITE, M.J.D., (1975).
'Settling of activated sludges.'
Tech. Rep. Water Res. Centre, TR 11.

180. WHITE, S.F., (1981).
'Requirements and application of control and automation systems in wastewater treatment - A critical review.'
Wat. Sci. Tech. 13, No 8, pp 41-48.

181. WILD, H.E., SAWER, C.N., McMAHON, T.C., (1971).
'Factors affecting nitrification kinetics.'
J. Water Pollut. Control Fed. 43 pp 1845-54.

182. WILLIAMSON McCARTY (1975).
'Rapid measurements of Monod half-velocity coefficients.'
Biotechnol. Bioengng. 17, pp 915-924.

183. WINKLER, M.A., THOMAS, A., (1978).
'Biological treatment of aqueous wastes.'
In 'Topics in Enzyme and Fermentation Biotechnology',(ed.) Wiesman A., Ellis Horwood 2 pp 200-279.

184. WINKLER, M.A., (1981).
'Biological Treatment of Waste-Water.'
Ellis Horwood Ltd. Publishers, Chichester, England.

185. WISHART, S.J. (1986).
'Dynamic modelling of oxidation ditch solids.'
MSc. Report, Imperial College, University of London.

186. WRC, CIRIA, (1981).
'Sewage treatment optimization model, user manual and description.'
Tech. Rep. Water Res. Centre 144.

187. YEUNG, S.Y.S., SINCIC, D., BAILEY, J.E., (1980).
'Optimal periodic control of activated sludge processes: II. Comparison with conventional control for structured sludge kinetics.'
Water Res., 14 pp 77-83.

188. YOUNG, J.C., (1981).
'Specific oxygen demand as an operating parameter for activated sludge processes.'
Water Sci. Technol., 13 pp 397-403.

189. YUST, L.J., STEPHENSON, J.P., MURPHY, K.L., (1981).
'Dynamic step feed control for organic carbon removal in a suspended growth system.'
Water Sci. Technol., 13 pp 729-736.

190. YUST, L.J., STEPHENSON, J.P., MURPHY, K.L., (1984).
'Control of the specific oxygen utilization rate from the step feed activated-process.'
Trans. Inst. Measurement & Control 6 No 3 pp 165-172.

APPENDICES

APPENDIX 1

The main determinants chosen to describe the performance of a model and characterise the goodness of fit to the observations, are given below with their definitions :

A. Determinants of residual error

1. Prediction error sequence
$$e_i = X_{ob}(i) - X_{pr}(i)$$
2. Mean of error
$$\bar{e} = \frac{1}{N} \sum e_i$$
3. Variance of error
$$s_e^2 = \frac{1}{N-1} \sum (e_i - \bar{e})^2$$
4. Root mean square error
$$RMS = \sum \frac{e_i^2}{N}$$
5. Sum of square error
$$SQE = \sum e_i^2$$

B. Determinants of a population

6. Mean of a population
$$\bar{X} = \frac{1}{N} \sum X_i$$
7. Standard deviation of a population
$$s_x = \frac{1}{N} \sum (\bar{X}_i - X)^2$$
8. Variance of a population
$$s^2 = \frac{1}{N-1} \sum (X_i - \bar{X})^2$$
9. Coefficient of variation
$$c_{var} = \frac{s_x}{\bar{X}}$$
10. Skewness coefficient
$$a_3 = \frac{1}{N-1} \sum (X_i - \bar{X})^3 / e^3$$
11. Kurtosis coefficient
$$a_4 = \frac{1}{N-1} \sum (X_i - \bar{X})^4 / e^4$$

12. Correlation coefficient between two series
$$R = \frac{\sum (\bar{X}_i - \bar{X}) \cdot (\bar{Y}_i - \bar{Y})}{[\sum (X_i - \bar{X})^2] \cdot [\sum (Y_i - \bar{Y})^2]}$$

13. Coefficient of determination between observed and predicted series
$$COD = 1 - \frac{\sum (X_{ob}(i) - X_{pr}(i))^2}{\sum (X_{ob}(i) - \bar{X})^2}$$

where; N : number of data in the series,
$\sum(*)$: denotes the sum for all values in the series,
X_i, Y_i : population sequences,
e_i : error sequence,
$X_{ob}(i)$: observed variable,
$X_{pr}(i)$: predicted variable.

APPENDIX 2

The Kalman Filter algorithm

A brief description of the Kalman Filter equations and its application for combined state and parameter estimation in the general case of a non-linear model is given below.

The continuous/discrete time system can be written in the following form :

$$\begin{aligned} \frac{d\underline{x}(t)}{dt} &= f(\underline{x}(t), \underline{u}(t), t) + \underline{\xi}(t) \\ \underline{y}(t_k) &= h(\underline{x}(t_k), \underline{u}(t_k), t_k) + \underline{\eta}(t_k) \end{aligned}$$

where; f, h : non-linear functions (system, measurement function),
$\underline{x}$: augmented state/parameter vector,
$\underline{u}$: deterministic input vector,
$\underline{y}(t_k)$: observation vector,
$\underline{\xi}, \underline{\eta}$: system disturbances and measurement noise respectively.

The system equations must be linearized so that the Kalman filter algorithm can be applied. The linearization is carried out via 1st- order Taylor series expansion around a deterministic nominal trajectory of the states. The following system of linear differential equations is subsequently obtained describing the dynamic variation of small perturbations about the reference trajectory (Beck, 1979).

$$\begin{aligned} \delta\dot{\underline{x}}(t) &= F'(\bar{\underline{x}}(t), \bar{\underline{u}}(t), \delta t) \cdot \delta\underline{x}(t) + G'(\bar{\underline{x}}(t), \delta\bar{\underline{u}}(t), t) \cdot \underline{u}(t) + \underline{\xi}(t) \\ \delta\underline{y}(t_k) &= H'(\bar{\underline{x}}(t_k), \bar{\underline{u}}(t_k), t_k) \cdot \delta\underline{x}(t_k) + \underline{\eta}(t_k) \end{aligned}$$

where;

$$\begin{aligned} F'(\bar{\underline{x}}(t), \bar{\underline{u}}(t), t)_{i,j} &= \frac{\partial f_i(\bar{\underline{x}}(t), \bar{\underline{u}}(t), t)}{\partial x_j(t)} \\ G'(\bar{\underline{x}}(t), \bar{\underline{u}}(t), t)_{i,j} &= \frac{\partial f_i(\bar{\underline{x}}(t), \bar{\underline{u}}(t), t)}{\partial u_j(t)} \\ H'(\bar{\underline{x}}(t_k), \bar{\underline{u}}(t_k), t_k)_{i,j} &= \frac{\partial h_i(\bar{\underline{x}}(t_k), \bar{\underline{u}}(t_k), t_k)}{\partial x_j(t_k)} \end{aligned}$$

$$\begin{aligned} \delta\underline{x}(t) &\equiv \underline{x}(t) - \bar{\underline{x}}(t) \\ \delta\underline{u}(t) &\equiv \underline{u}(t) - \bar{\underline{u}}(t) \\ \delta\underline{y}(t_k) &\equiv \underline{y}(t_k) - \bar{\underline{y}}(t_k) \end{aligned}$$

The vectors $\bar{\underline{x}}(t)$ and $\bar{\underline{u}}(t)$ represent the reference trajectory so that :

$$\dot{\bar{\underline{x}}}(t) = f(\bar{\underline{x}}(t), \bar{\underline{u}}(t), t)$$

and $\underline{\bar{y}}(t_k) \equiv h(\underline{\bar{x}}(t_k), \underline{\bar{u}}(t_k), t_k)$ is the reference measurement trajectory.

The algorithm progresses iteratively through the data and at each iteration updates the parameters and state variables. In this case of combined state/parameter estimation the parameters are considered as additional states and the following augmented state vector is obtained.

$$X^* = [\frac{X}{\beta}] = [x_1(t), x_2(t), .., x_N(t), \beta_1(t), \beta_2(t), ..., \beta_q(t)]^T$$

where; X : the state vector,
β : the parameter vector.

The dynamics of the parameters are generally unknown and commonly they are assumed to vary stochastically (Cook et al. 1984) :

- (i) Non-dynamic
  $\dot{\underline{\beta}}(t) = 0$
- (ii) Random walk
  $\underline{\beta}(t_{k+1}) = \underline{\beta}(t_k) + \underline{\varsigma}(t_k)$ or $\dot{\underline{\beta}}(\tau) = \underline{\varsigma}(\tau)$
  where, $\underline{\varsigma}(t_k)$ is a Gaussian white noise process.
- (iii) Gauss-Markov
  $\underline{\beta}(t_{k+1}) = a \cdot \underline{\beta}(t_k) + \underline{\varsigma}(t_k)$ where $-1 < a < 1$

Now the equations of the Extended Kalman filter algorithm can be formally presented (Jazwinski 1970, Beck 1980).

(a) Prediction stage (between observations)

Predicted state $\underline{\hat{x}}(t_{k+1}/t_k)$.

$$\underline{\hat{x}}(t_{k+1}/t_k) = \underline{\hat{x}}(t_k/t_k) + \int_{t_k}^{t_{k+1}} f(\underline{\hat{x}}(\tau/t_k), \underline{u}(\tau), \tau) \cdot d\tau \qquad (1)$$

Predicted error covariance, $\hat{P}(t_{k+1}/t_k)$.

$$\begin{aligned} \hat{P}(t_{k+1}/t_k) = \; & \Phi(t_k, t_{k+1}, \underline{\hat{x}}(t_k/t_k), \underline{\bar{u}}(t_k)) \cdot P(t_k/t_k) \cdot \\ & \Phi^T(t_k, t_{k+1}, \underline{\hat{x}}(t_k/t_k), \underline{\bar{u}}(t_k)) + Q \end{aligned} \qquad (2)$$

where the transition matrix (of the linearized system) is :

$$\Phi(t_k, t_{k+1}, \underline{\hat{x}}(t_k/t_k), \underline{\bar{u}}(t_k)) = exp\{\int_{t_k}^{t_{k+1}} F'(\underline{\bar{x}}(\tau/t_k), \underline{\bar{u}}(\tau), \tau) \cdot d\tau\}$$

where Q is the variance-covariance matrix of the system noise $\underline{\xi}(t)$.

(b) Correction stage (at t_{k+1})

When the observation vector $\underline{y}(t_{k+1})$ is received the following corrections are made.

Kalman gain, $K(t_{k+1})$.

$$K(t_{k+1}) = P(t_{k+1}/t_k) \cdot H'^T(t_{k+1}) \cdot [(H'(t_{k+1}) \cdot P(t_{k+1}/t_k) \cdot H'^T + R]^{-1} \tag{3}$$

Corrected states, $\hat{\underline{x}}(t_{k+1}/t_{k+1})$.

$$\hat{\underline{x}}(t_{k+1}/t_{k+1}) = \hat{\underline{x}}(t_{k+1}/t_k) + K(t_{k+1}) \cdot [\underline{y}(t_{k+1}) - h(\hat{\underline{x}}(t_{k+1}/t_k), \underline{u}(t_k), t_{k+1})] \tag{4}$$

Corrected covariance, $P(t_{k+1}/t_{k+1})$.

$$\begin{aligned} P(t_{k+1}/t_{k+1}) \;=\; & [I - K(t_{k+1}) \cdot H'(t_{k+1})] \cdot P(t_{k+1}/t_k) \cdot [I - K(t_{k+1}) \cdot H'(t_{k+1})]^T + \\ & K(t_{k+1}) \cdot R \cdot K^T(t_{k+1}) \end{aligned} \tag{5}$$

where R is the variance-covariance matrix of the measurement noise.

Limitations of the algorithm

Since the Kalman filter is a recursive algorithm it requires a set of initial values at time t_0 for the augmented state vector $\hat{\underline{x}}(t_0/t_0)$ and their associated error variances $P(t_0/t_0)$. Usually the uncertainty in the initial state values is accompanied by a sufficiently large variance-covariance matrix P. However large deviations of the initial values from the reference trajectory would make the linearization as an invalid approximation. According to Jazwinski (1970), we expect the dynamics of the linearized system to be a good approximation if the matrices Q and $P(t_0)$ are sufficiently small.

Thus, in the case of nonlinear system dynamics the initial state values should be specified with a high degree of confidence, and the unknown disturbances should be minimal in order that the filter retains its optimality.

The Kalman filter is designed to give optimal estimates of states or parameters at any step with respect to a number of criteria such as minimum variance, least square error and maximum likelihood. However lack of optimality will occur (Cook et al. 1984), when :

- the functions f, h are not well approximated by 1st-order Taylor series expansion and/or the 2-nd and higher order terms are large.
- the initial augmented state vector is biased (especially in the case of nonlinear system dynamics).
- the error matrices P, Q and R are incorrectly specified.
- the error sequence $[\underline{y}(t_k) - H'(t_k) \cdot \hat{\underline{x}}(t_k)]$ is not Gaussian white noise process (Mehra, 1970).

The matrices $h\{*\}$ and $H'\{*\}$ of the linearized system are required only in the computation of the covariances in eq. 2, 5 and for the gain matrix in eq. 3. This is because at each iteration the reference trajectory is substituted by the "current" state estimate (Beck, 1980). So for the evaluation of H' the following substitution is made:

$$\bar{\underline{x}}(t_{k+1}) = \hat{\underline{x}}(t_{k+1}/t_k)$$

and for the evaluation of h,

$$\bar{\underline{x}}(t_k) = \hat{\underline{x}}(t_k/t_k)$$

which enables us to use the original nonlinear system function $f\{*\}$ and $h\{*\}$.

APPENDIX 3

Sensitivity analysis of system

The sensitivity coefficient (S_{ij}) of a state X_i with respect to the parameter β_j can be simply expressed by the relative change in the variable caused by a change in the parameter :

$$S_{ij} = \frac{\Delta X_i / \bar{X}_i}{\Delta \beta_j / \bar{\beta}_j}$$

where; $\bar{X}_i$: nominal value of state X_i,
$\bar{\beta}_j$: nominal value of parameter β_j,
$\Delta \beta_j$: small variation in parameter around $\bar{\beta}_j$,
ΔX_i : resulting variation in the state value.

In the general case of a non-linear, continuous dynamic system with the following state-space representation,

$$\frac{dX_i}{dt} = F_i\{X_1, X_2, ..., X_N, t, \beta_1, \beta_2, ..., \beta_q\}$$

where; $X_1, .., X_N$: state variables,
$\beta_1, .., \beta_q$: system parameters,
F_i : general non-linear functions.

the sensitivity coefficients $S_{ij}(t)$, of the state X_i to parameter β_j can be calculated from the following set of differential equations (Beck, 1983b) :

$$\frac{dS_{ij}(t)}{dt} = [\frac{dFi\{.\}}{dX_1}]_x \cdot S_{1j} + [\frac{dF_i\{.\}}{dX_2}]_x \cdot S_{2j} + ... + [\frac{dF_i\{.\}}{dX_N}]_x \cdot S_{Nj} + [\frac{dF_i\{.\}}{d\beta_j}]_x$$

for $i = 1, 2, .., N$ and $j = 1, 2, ..., q$.

where, $[*]_x$ indicates that all partial derivatives are computed at the nominal value of the state and parameter vector.

In the case of q parameters there will be q-differential equations to be solved simultaneously, for each one of the state variables. The initial conditions of the above system are:

$$S_{ij\ (0)} = [\frac{dX_{i\ (0)}}{d\beta_j}] = 0,$$

provided that the initial conditions of the state vector $X_{i\ (0)}$ are not considered as model parameters.

After the sensitivity coefficients have been calculated, the perturbed solution of the system for small variations in the parameters around their nominal value is given by :

$$\underline{X}(t,\underline{\beta}) \approx \underline{\bar{X}}(t,\underline{\beta}) + \underline{S}(t,\underline{\beta}) \cdot (\underline{\beta} - \underline{\bar{\beta}})$$